

**Beetles going underground -
morphological adaptations linked with subterranean habits**

Dissertation

zur Erlangung des akademischen Grades „doctor rerum naturalium“

(Dr. rer. nat.)

**vorgelegt dem Rat der Fakultät für Biowissenschaften
der Friedrich-Schiller-Universität Jena**

von

M. Sc. Xiaozhu Luo

geboren am 15.11.1992 in Guizhou, China

Gutachter:

1. Prof. Rolf G. Beutel, Jena
2. Prof. Ján Kodada, Bratislava
3. PD Dr. Hans Pohl, Jena

Tag der öffentlichen Verteidigung: 26.04.2022

This page intentionally left blank

Table of Contents

1 Introduction	1
1.1 Subterranean systems and organisms	1
1.2 Origin and evolution of subterranean organisms	3
1.3 Beetles living underground	5
1.4 Motives and objectives of this study	9
2 Material and methods	11
2.1 Studied species	11
2.2 Morphological examination	13
2.3 Terminology	14
2.4 Phylogenetic reconstruction	15
3 Publications	16
3.1 Study I: The cephalic morphology of the troglobiontic cholevine species <i>Troglocharinus ferreri</i> (Coleoptera, Leiodidae)	18
3.2 Study II: Profound head modifications in <i>Claviger testaceus</i> (Pselaphinae, Staphylinidae, Coleoptera) facilitate integration into communities of ants.....	34
3.3 Study III: In the twilight zone-The head morphology of <i>Bergrothia saulcyi</i> (Pselaphinae, Staphylinidae, Coleoptera), a beetle with adaptations to endogean life but living in leaf litter	49
3.4 Study IV: Structural megadiversity in leaf litter predators - the head anatomy of <i>Pselaphus heisei</i> (Pselaphinae, Staphylinidae, Coleoptera).....	68
3.5 Study V: Evolution of cephalic structures in extreme myrmecophiles: a lesson from Clavigeritae (Coleoptera: Staphylinidae: Pselaphinae).....	90
3.6 Study VI: The thoracic morphology of the troglobiontic cholevine species <i>Troglocharinus ferreri</i> (Coleoptera, Leiodidae)	134
3.7 Study VII: The specialized thoracic skeletomuscular system of the myrmecophile <i>Claviger testaceus</i> (Pselaphinae, Staphylinidae, Coleoptera)	147
3.8 Study VIII: Subterranean or blind beetles (Leiodidae) have no improved antennal sensory equipment compared to their epigean or sighted relatives.....	167
4 Discussion	186

4.1 Entangled ecological classifications of subterranean animals	186
4.2 Morphological modifications of subterranean beetles	188
4.3 Effects of environmental factors on subterranean adaptation.....	196
4.4 Success of Coleoptera dwelling underground	199
4.5 Conclusions and outlook.....	202
5 Summary	204
6 Zusammenfassung.....	206
7 References	209
8 Appendixes	224
9 Acknowledgements	232
10 Curriculum Vitae.....	234
11 Ehrenwörtliche Erklärung.....	236

1 Introduction

1.1 Subterranean systems and organisms

1.1.1 Cave environment and cavernicolous organisms

In the perspective of explorers, “cave” usually refers to a natural opening of rocks, which is large enough for humans to enter it; however, it appears more suitable to use the definition “a natural opening in solid rock with areas of complete darkness and larger than a few millimeters in diameter”, which is suitable to function as habitat of organisms (White & Culver 2019; Culver & Pipan 2019). Although they can be influenced by outside seasonal change, caves are habitats with permanent darkness, and with relatively stable temperature, humidity, and air flow (Gunn 2004). Along with the easily defined and stable climate, cave communities are simple and can be well studied. These characteristics make caves a natural laboratory of organisms (Poulson & White 1969).

The French word “biospéologie” was first proposed by Viré (1904), but the history of humans exploring cave organisms goes way back to ancient periods (White & Culver 2019). Moreover, subterranean faunas have been intensely explored in countries like Slovenia, France, and the USA since the beginning of 19th century (Gunn 2004). On the other side of the planet, this goes even back to the Ming Dynasty of China. The well-known explorer and traveler Xu Xiake (1586-1641) has contributed greatly to the knowledge of caves during his travels around China. He recorded more than 300 sites in his travel diary “Xu Xiake Youji”, which covered size, type, hydrology, and troglobiotic animals of the places he has visited (Yang 1983). In the memory of his work, scientists have named cave species after him, for example: *Sinaphaenops xuxiakei* Deuve & Tian (Carabidae, Coleoptera, Insecta) and *Hyleoglomeris xuxiakei* Liu & Wynne (Glomeridae, Diplopoda) (Deuve & Tian 2014; Liu & Wynne 2019).

Since the first description of a cave-dwelling animal, *Proteus anguinus* Laurenti 1768, also known as “human fish”, cave organisms (Fig. 1) started to intrigue scientist by their characteristic features, clearly distinguishing them from their surface-living relatives (Moldovan 2012; Vandel 1965). However, the underground environment has been considered as a marginal habitat for animals until the first cave beetle *Leptodirus hochenwartii* Schmidt was found in the Postojna cave in Slovenia and described by Ferdinand Schmidt in 1832 (see Polak 2005). From then till now, biospeologists have found that numerous organisms inhabit this fragile ecosystem all over the world (Vandel 1965). Recently, in addition to cave systems a with long tradition of exploration in the USA and Europe (Faille & Deharveng 2021; Niemiller et al. 2021), more and more subterranean sites in Asia have turned

out as intriguing spots of biodiversity (Eberhard & Howarth 2021; Huang et al. 2021).

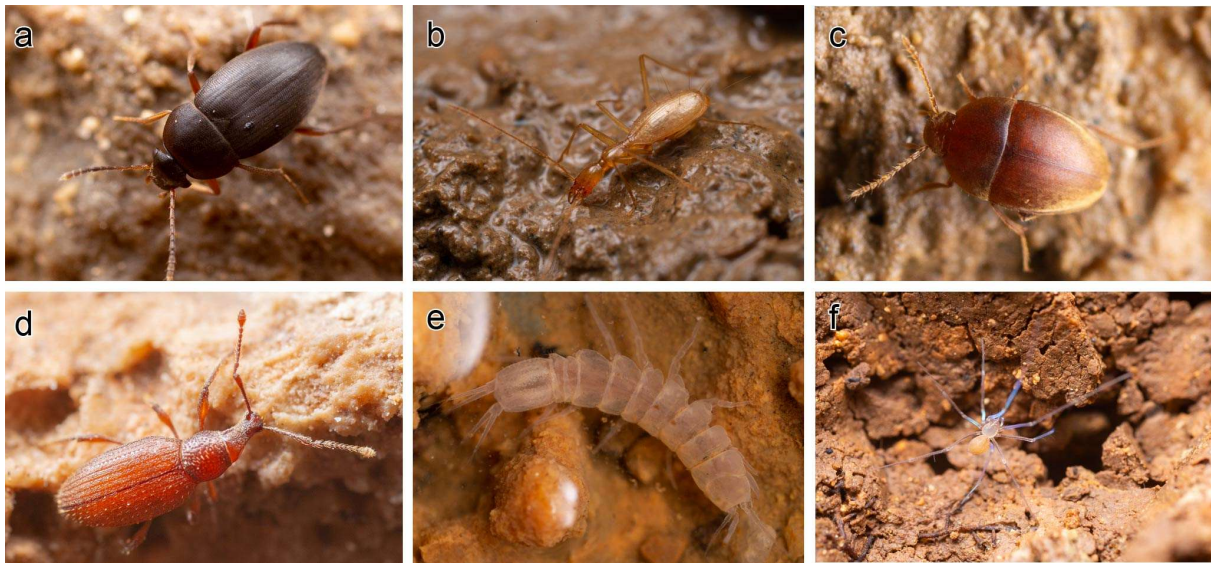


Fig. 1 Photographs of cave-dwelling organisms. **a.** *Anemadus acicularis* (Kraatz, 1852) (Leiodidae); **b.** *Aphaenops cerberus* (Dieck, 1869) (Carabidae); **c.** *Speonomus infernus* (Dieck, 1869) (Leiodidae); **d.** *Trogloorhynchus raffaldii* Alziar, 1977 (Curculionidae); **e.** *Stenasellus virei* Dollfus, 1897 (Isopoda); **f.** *Leptoneta* sp. (Araneae) (The figure plate was produced with permission from Sunbin Huang [Muséum National d'Histoire Naturelle, Paris])

With the continuous efforts of exploration by generations of biospeologists, the hypogean environment has been recorded as a habitat with events of diversification in many groups, ranging from protozoans to various metazoan lineages including nematodes, crustacean, arachnids, myriapods, insects, vertebrates, and others (Romero 2009). Although various categorizations of cave-dwelling animals have been introduced (e.g. Schiødte 1849; Joseph 1882), the most accepted one is the “Schiner-Racovitza classification”, which was proposed by Racovitza (1907), distinguishing three groups of subterranean animals: (1) Trogloxenes: visitors only occasionally or accidentally appearing in caves, and rarely showing subterranean specialization; (2) Troglaphiles: organisms which are able to live and reproduce in surface areas but also in caves, and in some cases show modifications related to dark environments; (3) Troglobites: animals which are only able to inhabit underground environments, usually in deep parts of caves, and displaying highly specialized morphological traits clearly correlated with cave life.

Even though many studies were published on different aspects of terrestrial organisms of the underground, the depth of the investigations is still far behind research on aquatic animals. Cave fish, for instance, became the most thoroughly studied group of hypogean animals in the last decades. Accumulated solid

experimental data on the cellular and molecular level allow researchers to address and answer evolutionary problems with more and more convincing evidence. The species *Astyanax mexicanus* (De Filippi) (Characidae) has been used as a model organism in numerous projects. It has provided extensive information that made it possible to test evolutionary hypotheses and even revealed mechanisms of diseases (Jeffery 2001, 2019; Niemiller et al. 2019a; Rohner et al. 2013; Yamamoto & Jeffery 2000; Yamamoto et al. 2004).

1.1.2 Other subterranean habitats and their organisms

Even though cave systems arguably attracted most attention, other varieties of lightless environments are also important in the context of organisms going underground. The subterranean world, which provides multiple habitats for various groups of organisms, was divided into two main categories, more or less dry substrates or liquid media (Racovitza 1907). Vandel (1965) provided a comprehensive introduction into these habitats: (1) solid media including both rocks and soil, (2) liquid media such as subterranean streams and ground water. More or less deep layers of soil are not always considered as subterranean environment, but obviously should be included (Culver & Pipan 2019). Soil is a multiphase system, composed of mineral materials, organic matters such as roots or decaying parts of plants, water and also gases. Giachino & Vailati (2010) divided the interconnected soil environment into three categories: (1) epigeal, (2) endogean environment (=edaphic), and (3) hypogean (includes the crevices in bedrock, and caves) environments. It obviously provides a suitable environment for a very broad spectrum of organisms, including successful groups like for instance nematode worms, and also immatures and adults of numerous groups of arthropods (Bardgett 2005; Burgers & Raw 1967). Soil-dwelling beetles show different specializations to this environment, and more advanced permanent underground dwellers of deeper layers display far-reaching modifications (e.g. Crowson 1981). In addition, myrmecophiles and termitophiles belong to a special group of animals of the underground, and some of them share specialized morphological characteristics with more or less closely related cavernicolous organisms (Vandel 1965).

1.2 Origin and evolution of subterranean organisms

Subterranean animals first caught the attention of scientists by their bizarre morphology, which is one of the hallmarks of these organisms (Fišer 2019). Observations of their behavior and physiological studies followed and also

intrigued the curiosity of researchers (Gunn 2004). Investigations of nearly two centuries have revealed valuable but still fragmentary information related to evolutionary processes in the context of cavernicolous animals. Essential questions are still insufficiently solved, how exactly species invaded and colonized subterranean habitats and in which ways they evolved as cave specialists.

1.2.1 Invasion

Although evolutionary models related to cave-dwelling animals have been explored by generations of biospeologists, no single concept could be confirmed as generally valid. Danielopol & Rouch (2012) distinguished two main categories of subterranean colonization: (1) active and (2) passive invasion. The former is mainly related to environmental cues, whereas passive invasion is either caused by force or chance of environmental dynamics. Among the proposed hypotheses, the most well-known is probably the “climatic-relict” model: this suggests that surface-dwelling organisms colonized a cave during a period with drastic environmental change, and that the ones which were unable to adapt to the new habitat became extinct later. Besides, both the “adaptive-shift” and “active colonization” models proposed the possibility of “preadapted” animals, able to colonize the underground habitat without periods of environmental stress. Additionally, some models suggest that the speciation of cave-dwelling beetles requires two steps: (1) local diversification in deep soil; (2) isolation in nearby caves (Barr 1968). The chief ancestral habitats of terrestrial cave-dwelling species likely consist of leaf litter, moss, and mostly rocky terrains (Howarth 2009). In short, various other hypotheses were suggested, but most of them were never subjected to strict scientific tests (Danielopol & Rouch 2012).

1.2.2. Evolution

Hypotheses on how hypogean organisms evolved and adapted to lightless environments have been discussed for a long time (e.g. Culver et al. 1995), mainly focused on the question whether the driving force is “natural selection” or whether “neutral mutation” played the main role? Darwin (1859), obviously fascinated by cave-dwelling organisms, suggested that the elongated antennae and palpi are compensations for blindness. Endler (1986) proposed that repeated independent evolutionary transformations in similar environments but different sites (even continents) can be explained by natural selection. The supporters of this hypothesis argued that “adaptation” is the major evolutionary force, while the proponents of “neutral mutation” emphasize the importance of random genetic

drift (Trontelj 2012). Alternatively, Protas et al. (2007) argued that the actual question is how important neutral mutation is compared to natural selection in shaping the evolutionary history of subterranean organisms. It was estimated that adaptive troglomorphic traits might take approximately 100,000 years for a new cave invader to evolve its specific features (Culver et al. 1995).

1.3 Beetles living underground

The megadiverse beetles (Coleoptera) contain several groups with successful radiations in subterranean environments. Cave dwelling species of various families are widely distributed from tropical to temperate areas of all continents except for Antarctica. The majority of cave-dwellers is described from the Palearctic regions, but this may be an artefact due to an uneven degree of cave exploration (Deharveng & Bedos 2018; Faille 2019; Gunn 2004; Romero 2009). Since the discovery of the leiodid *Leptodirus hochenwartii*, a species with extremely specialized body shape (see Fig. 2 in Moldovan 2012), cave beetles have fascinated numerous of biospeologists around the world. Species of at least 18 families of the order Coleoptera have been found in caves, inhabiting terrestrial or aquatic environments (Romero 2009), and 14 families include strictly subterranean species (Gunn 2004). Of the two dominant radiations of cave beetles (containing over 80% of the species found in the subterranean environment), Carabidae belongs to the suborder Adephaga, and Leiodidae to the megadiverse suborder Polyphaga (Culver & Pipan 2019). The specific habitats of cave beetles comprise a wide spectrum: caves, networks of cracks, the MSS (“Milieu Souterrain Superficiel” in French and “Mesovoid Shallow Substratum” in English, also called the Superficial Underground Compartment), lava tubes, wells, springs, and subterranean water systems. The range of temperatures ranges between 1°C and 25 °C, at nearly 100% humidity (Gunn 2004). Like other subterranean organisms, hypogean beetles are well-known for conspicuous morphological traits compared to their epigeal relatives. Among them, the most distinct and common features are as follows: (1) reduction or complete loss of eyes; (2) slender and elongated body and appendages; (3) depigmentation of the cuticle (Moldovan 2012; Romero 2009; Faille 2019).

1.3.1 Terrestrial cave-dwelling fauna

According to Decu & Juberthie (1998), 1180 carabid species, 599 leiodid species, and 110 staphylinid species were described by that time from all around the world. These three families, two of them megadiverse, in total account for 98% of the

cavernicolous beetles. During the next twenty years, numerous new species have been discovered and described in different world regions (e.g. Tian et al. 2017; Pellegrini & Ferreira 2011). In the summary of Faille (2019), the rank of the three largest families stays the same: (1) Carabidae is the family which accounts for 60% of all cave beetles, and 14 out of 33 subfamilies contain species found in caves (Casale et al. 1998). The dominant Trechinae show the most impressive adaptation among 12 subfamilies of Carabidae, including “anophthalmic” and “aphaenopsian” morphological types; it consists of approximately 2000 species, among them more than 1000 troglobites (Gunn 2004). Trechini, the most diverse tribe, includes the most advanced cave carabids, and is widely distributed in Europe, Asia, and North America (Faille 2019). It is reported that many species have been found in limited regions or even only in one particular cave. One of the most well-known trechine genera is the North American *Pseudanophthalmus* Jeannel, which includes over 200 species, each of them restricted to an isolated belt of karst area (Holsinger 2012). (2) The family with the second largest diversity of cave beetles is Leiodidae, which contains around 31% of the subterranean species. Among cave leiodids, Leptodirini is the most diverse tribe, which comprises 900 species and is mostly distributed in the Western Palearctic. In contrast, the tribe Ptomaphagini is more common in North America. Species of Leiodidae with a subterranean life style are informally categorized into four morphotypes: (a) the “bathyscioid” type, the ancestral body shape, with an ovoid body and short appendages; (b) the intermediate “pholeuonoid” type, with longer appendages and a more slender body; and (c, d) the highly specialized “leptodiroid” and “scaphoid” types, both with extremely long appendages and narrow head and thorax, but with the abdomen distinctly swollen in the former and narrow in the latter (Moldovan et al. 2018); (3) With up to 200 species, Staphylinidae (including Pselaphinae and Scydmaeninae) is ranked as the third largest subterranean radiation, accounting for roughly 5% (Gunn 2004) of cave beetles. Among them, the subfamily Pselaphinae (formerly Pselaphidae) comprises more than 80% of the total number of subterranean species. Some species of the polyphagan families Histeridae (Hydrophiloidea) and Curculionidae (Phytophaga) are also found in caves, and some species are also troglomorphic (Gunn 2004). However, as a whole they play only a marginal role in the context of subterranean lifestyle. It is noteworthy that the cave-dwelling Carabidae and Leiodidae are quite unbalanced on the tribal level: Trechini and Leptodirini are doubtlessly the largest cave radiations, respectively, whereas other tribes contain significantly less specialized species (Faille 2019).

Feeding habits of hypogean terrestrial coleopteran species are similar to those of the epigean relatives in most cases: cave carabids are usually predators of other small invertebrates, but some of them show trophic specialization, for instance,

Neaphaenops tellkampfi (Erichson) and *Rhadine subterranea* (Van Dyke) feeding on orthopteran eggs (Gunn 2004; Romero 2009). The subterranean leiodids are scavengers (Deharveng & Bedos 2018) and found also feeding on “moonmilk” (a precipitate produced by microbiological reactions) in the caves (Romero 2009). On the other hand, the population size is very different between the major families: detritivorous leiodids usually have much larger population comparing to carnivorous carabids. It was estimated that 30,000 to 50,000 Leptodirini individuals occur in caves and interstitial systems in the Pyrenees (Gunn 2004), and the overall population size of three troglobitic species of *Speonomus* Jeannel in the “Grotte de Ramioul” (Belgium) as around 44,000 individuals (Tercafs & Brouwir 1991). In contrast, the microphthalmic carabid *Laemostenus schreibersi* Küster in a cave near Villach (Austria) was estimated at constantly around 80 to 100 individuals (Rusdea 1994).

1.3.2 Aquatic cave-dwelling fauna

Aquatic beetles are apparently much rarer in caves than terrestrial coleopteran species, forming only 2% of all known cave-dwellers (Moldovan 2012). Even though this comparatively low species diversity, aquatic cave beetles cover four families, the adaphagan Dytiscidae and Noteridae, and the polyphagan Elmidae and Hydrophilidae (Moldovan 2018). None of the four families are closely related with each other.

Dytiscidae, is doubtlessly the most successful group in terms of subterranean specialization (Romero 2009). The first hypogean dytiscid *Sieltitia balsentensis* Abeille de Perrin was already discovered in 1904 in southern France (Abeille de Perrin 1904). Today it is known that diving beetles are highly diversified in subterranean aquifers of Australia, but still remains species-poor in hypogean waters of other areas. In other regions, only few species showing typical cave specializations have been recorded so far (Faille 2019), whereas at least 99 stygobiotic dytiscid species have been described from Australia. These aquatic stygobiotic forms show different degrees of eye reduction from normal size to ocular vestiges to complete loss (Watts & Humphreys 2009). Despite being overshadowed by the cave fish as objects of research, aquatic cave beetles have still attracted attention due to some unique features (Humphreys 2008; Langille et al., 2019, 2021). Subterranean species of Dytiscidae and Noteridae are very likely predators like their epigeal relatives (e.g. Crowson 1981). In contrast the saprophagous adults of Hydrophilidae and Elmidae have to rely on organic materials brought in from the surface (Crowson 1981) as no photosynthesis can take place in complete darkness.

1.3.3 Endogean fauna

As pointed out above, caves are not the only habitat of subterranean animals. Endogean beetles (“soil-inhabitants”) also show a considerable and probably vastly underestimated diversity (Andújar et al. 2017; Andújar & Grebennikov 2021; Bardgett 2005). The groups best represented in deeper soil layers are as follows: Carabidae, Staphylinidae (mainly Pselaphinae and Scydmaeninae), Leiodidae, and Curculionidae (Vandel 1965). The endogean environment shows some similarities to hypogean habitats, such as darkness and environmental stability, but also differs from them by containing rich and varied food resources (Sket 2004). Additionally, the myrmecophiles and termitophiles were also considered as “solid media-related” subterranean arthropods (Vandel 1965). It is noteworthy that the morphology of endogean animals also includes cuticular depigmentation and the reduction or absence of wings and eyes. However, these animals do not appear slender, and they lack elongated appendages (Culver & Pipan 2019). Although endogean species shows some differences compared to hypogean life forms, many members of the former group live in the entrance area of caves. Therefore, a strict distinction between them could be delicate in many cases (Vandel 1965).

As the soil is stratified and the fauna affected by this vertically, Eisenbeis & Wichard (1987) proposed a classification of soil-dwelling life forms which includes: (1) the euedaphic soil arthropods have a round more or less worm-like body, and they are small, photophobic and depigmented, with reduced or missing eyes; usually they have adapted their sensory perception towards subterranean life; (2) the epedaphic species live in the leaf litter layer, and are restricted to the area close to the surface and larger soil cavities; they are strongly pigmented, with more or less well-developed eyes, long filamentous antennae, great mobility, and diurnal activity rhythms; (3) the hemiedaphon is often a temporary form of life, adopted by epedaphic arthropods occupying burrows in the soil. All three life forms of soil-dwelling arthropods occur in Coleoptera.

The available food in the soil substrate consists of plant roots, fungi, small animals, and various other organic materials, providing diverse energy sources for beetles with different feeding habits, not only including carnivores (e.g. Carabidae, Staphylinidae [partim]), but also root-feeders (e.g. Elateridae, Galerucinae) and species relying on fungi and humus-like substrates (Crowson 1981). The term “endogean” (adapted from French “endogène”) is used for species which spend their entire cycles beneath the ground (Crowson 1981).

1.3.4 Myrmecophilous fauna

Myrmecophilous beetles have also fascinated scientists for a long time (see Hermann 1979). Symbiotic associations have been found in at least 35 coleopteran families, and myrmecophilous beetles exhibit very diverse behavioral patterns and also morphological adaptations to their hosts (Mynhardt 2013). Species of several coleopteran groups are frequently found in ant nests. Important myrmecophilous radiations occurred in the adepagan Paussinae (Carabidae) and in the polyphagan Aleocharinae, Pselaphinae, Scydmaeninae (Staphylinidae) and Histeridae (e.g. Crowson 1981; Parker 2016). Interestingly, Paussinae are the only myrmecophilous group in the megadiverse and mostly predacious Carabidae. The tribe Paussini is the largest clade of exclusively myrmecophilous beetles, with over 600 known species and displaying a very advanced form of myrmecophily as larvae and adults (Erwin 1979; Nagel 1979; Parker 2016). Morphological adaptations in beetles associated with ants include strongly modified compact antennae, the presence of trichomes (tufts of setae associated with exocrine glands), a reddish body color, and often modified mouthparts and legs (Wheeler 1910).

1.4 Motives and objectives of this study

Bizarre cave organisms have captured the interest of many researchers, with recently more than 200 studies on subterranean biology published every year (Culver & Pipan 2019). The investigation of subterranean beetles has a very long and fruitful history: various researchers (e.g. Jeannel 1926; Juberthie & Massoud 1977) have contributed valuable morphological information on subterranean species of different families. More recently, the phylogenetic relationships of taxa with subterranean species have been addressed (e.g. Ribera et al. 2010; Faille et al. 2010, 2013, 2015), and cave beetles even became a model for studying the impact of past and predicted climatic changes on biodiversity (Sánchez-Fernández et al. 2016).

Morphological and anatomical studies are critical to understand the adaptation and evolution of organisms (e.g. Beutel et al., 2014). However, at present, comparative morphological studies of subterranean beetles from different specific habitats are still rare. Vandel (1965) stated that “it would be naive to believe that there is clear-cut demarcation between the subterranean and surface environments.” Therefore, it is necessary to conduct comparative studies of cavernicolous organisms and inhabitants of other types of subterranean habitats. Surprisingly, studies dealing with the latter are even scarcer than those on true cave species. Consequently, the investigation of their morphological features should have high priority.

Our research from Study I to Study VII aims to explore the cephalic and thoracic morphology of beetles with different degrees of subterranean adaptations, including also species associated with ants. The anatomical results are compared with conditions found in relatives inhabiting less specialized environments. Different character transformations in the head and thorax are documented, and correlations with the invasion of underground habitats are discussed. To provide thorough documentations of external and internal features, established methods like scanning electron microscopy (SEM) and histology are combined with modern techniques such as Micro-CT and three-dimensional reconstruction.

Study VIII addresses a widely accepted evolutionary hypothesis concerning subterranean Leiodidae, suggesting that the length and density of hair-like antennal sensilla increases in cave dwelling species. To test this, a relatively large number of leiodid representatives of various ecological groups were chosen. Types, number, and density of antennal sensilla of 38 species were examined and analyzed based on a molecular phylogenetic background.

2 Material and methods

2.1 Studied species

The list of studied species is shown in Table 1. For details of collection information, see “Material and methods” chapters in the studies included in the dissertation.

Table 1 Studied beetle species

Species	Studies
Family: Leiodidae	
<i>Adelopsella bosnica</i> (Reitter, 1884)	VIII
<i>Anemadus hajeki</i> Růžička & Perreau 2017	VIII
<i>Anillochlamys bueni</i> Jeannel, 1909	VIII
<i>Aphaobius haraldi</i> Faille, Ribera & Fresneda 2016	VIII
<i>Baronniesia delioti</i> Fresneda, Bourdeau & Faille, 2009	VIII
<i>Bathysciola aubei</i> (Kiesenwetter, 1850)	VIII
<i>Bathysciola derosasi</i> Jeannel, 1914	VIII
<i>Bathysciola grandis</i> (Fairmaire, 1857)	VIII
<i>Bathysciola lapidicola simplex</i> Coiffait, 1959	VIII
<i>Bathysciola ovata</i> (Kiesenwetter, 1850)	I, VIII
<i>Bathysciola pusilla</i> (Motschulsky, 1840)	VIII
<i>Bathysciotes khewenhuelleri khewenhuelleri</i> Miller 1852	VIII
<i>Besuchetiola priapus</i> Rampini & Zoia, 1991	VIII
<i>Cansiliella servadeii</i> Paoletti 1980	VIII
<i>Catops picipes</i> Fabricius, 1787	VIII
<i>Cytodromus dapsoides</i> (Abeille de Perrin, 1875)	VIII
<i>Halbherria zorzii</i> (Ruffo, 1950)	VIII
<i>Josettekia mendizabali</i> (Bolívar, 1921)	VIII
<i>Karadeniziella omodeoi</i> Casale & Giachino, 1989	VIII
<i>Leptodirus hochenwartii</i> Schmidt, 1832	I, VIII
<i>Machaeroscelis infernus cagiranus</i> Coiffait, 1955	VIII
<i>Neobathyscia mancinii</i> Jeannel, 1924	VIII
<i>Notidocharis calabrezi</i> Giachino & Salgado, 1989	VIII
<i>Paraspeonomus vandeli</i> Coiffait, 1952	VIII
<i>Parvospeonomus delarouzei catalonicus</i> (Jeannel, 1910)	VIII

<i>Patriziella sardoa</i> Jeannel, 1956	VIII
<i>Pholeuon gracile</i> Frivaldszky, 1861	VIII
<i>Platycholeus hamatus</i> Kilian & Mađra 2015	VIII
<i>Platycholeus opacellus</i> Fall, 1909	I
<i>Ptomaphagus pyrenaeus</i> Jeannel, 1934	VIII
<i>Ptomaphagus troglodytes</i> Blas & Vives, 1983	I, VIII
<i>Quaestus longicornis</i> Salgado, 1989	VIII
<i>Speonemadus bolivari</i> (Jeannel, 1922)	VIII
<i>Speonomidius crotchi crotchi</i> (Sharp, 1872)	VIII
<i>Speonomus longicornis longicornis</i> Saulcy, 1872	VIII
<i>Speophyes lucidulus</i> Delarouzee, 1860	VIII
<i>Tismanella chappuisi chappuisi</i> Jeannel, 1928	VIII
<i>Troglocharinus ferreri</i> (Reitter, 1908) ^a	I, VI
<i>Troglocharinus orcinus orcinus</i> (Jeannel, 1910)	VIII
<i>Troglodromus bucheti</i> Sainte-Claire Deville, 1898	VIII
<i>Zearagytodes maculifer</i> (Broun, 1880)	VI
Family: Staphylinidae	
<i>Articerodes syriacus</i> (Saulcy, 1865)	II
<i>Batrisodes venustus</i> (Reichenbach, 1816)	II, VII
<i>Bergrothia saulcyi</i> (Reitter, 1877) ^a	III
<i>Brachygluta fossulata</i> (Reichenbach, 1816)	II, VII
<i>Bryaxis bulbifer</i> (Reichenbach, 1816)	II, VII
<i>Cerylambus reticulatus</i> (Raffray, 1895)	II, V
<i>Claviger apenninus</i> Baudi di Selve, 1869	II
<i>Claviger longicornis</i> Müller, 1818	II, V
<i>Claviger testaceus</i> Preyssler, 1790 ^a	II, VII
<i>Diartiger fossulatus</i> Sharp, 1883	II
<i>Diartiger kubotai</i> Nomura, 1997 ^a	V
<i>Disarthricerus integer</i> Raffray, 1895	II, V
<i>Euplectus karstenii</i> (Reichenbach, 1816)	II, VII

<i>Novoclaviger gibbiventris</i> (Raffray, 1910)	V
<i>Pararticerus latus</i> (Raffray, 1910)	V
<i>Pselaphus heisei</i> Herbst, 1792 ^a	II, IV, VII
<i>Tiracaleda minuta</i> Hlaváč, Parker, Maruyama & Fikáček, 2021	V
<i>Tiracerus</i> sp.	V
<i>Tiraspirus tabulates</i> Hlaváč, Parker, Maruyama & Fikáček, 2021	V
<i>Trichonyx sulcicollis</i> (Reichenbach, 1816)	II, VII
<i>Tyrus mucronatus</i> (Panzer, 1803)	II
<i>Zuluclavodes briantaylori</i> Hlaváč, 2007	V
Family: Carabidae	
<i>Sinaphaenops wangorum</i> Ueno et Ran 1998 ^{a, b}	/
<i>Trechiotes perroti</i> Jeannel 1954 ^{a, b}	/
<i>Bembidion</i> sp. ^{a, b}	/

Note: a. species was scanned using micro-CT and three-dimensional reconstruction models were generated; b. information on the species was extracted from Luo et al. (2018a, b) and involved in the general discussion.

2.2 Morphological examination

Light microscopy

Specimens were cleaned following the protocols recommended in the Schneeberg et al. (2017) and subsequently dried in air or a critical point dryer. Besides, some dissected body parts were cleared briefly in 10% aqueous solution of sodium hydroxide, dehydrated in isopropanol and mounted in Canada balsam. Different microscopes and cameras were used in taking images (Please see “Materials and methods” parts in Study I to VIII for more details of image acquirement and processing)

Scanning electron microscopy

Prior to scanning electron microscopy (SEM), dried samples were sputter-coated with gold, and attached either to a rotatable specimen holder (Pohl 2010) or to small sample holders. SEM observation and imaging was performed in Jena (Germany) and Wrocław (Poland). For the equipment used in the studies, please see Table 2. Images were processed using CorelDraw Graphic Suite 2017 (Corel

Corporation, Ottawa, Canada), Adobe Photoshop CC and Illustrator CS6 (Adobe Inc., California, USA).

Table 2 Sputter-coaters and scanning electron microscopes used in the studies.

Study	Sputter-Coater	SEM	References
I	Emitech K500	FEI (Philips) XL 30 ESEM	Luo et al. 2019b
II	Leica EM ACE600	Helios Nanolab 450HP	Jałoszyński et al. 2020
III	Emitech K500	FEI (Philips) XL 30 ESEM	Luo et al. 2021a
IV	[Uncoated]	Helios Nanolab 450HP	Beutel et al. 2021
V	[Uncoated]	Helios Nanolab 450HP	Jałoszyński et al. subm.
VI	Emitech K500	FEI (Philips) XL 30 ESEM	Luo et al. 2019a
VII	Emitech K500	FEI (Philips) XL 30 ESEM	Luo et al. 2021b
VIII	Emitech K500	FEI (Philips) XL 30 ESEM	Luo et al. in prep.

Histological serial sections

Specimens were embedded in araldite CY 212® (Agar Scientific, Stansted/Essex, UK). Subsequently sections were cut at 1 µm intervals using a microtome HM 360 (Microm, Walldorf, Germany) equipped with a glass knife, and stained with toluidine blue and pyronin G (Waldeck GmbH and Co.KG/Division Chroma, Münster, Germany). The sections are stored in the collection of the Phyletisches Museum.

Micro Computer-Tomography (µCT) and three-dimensional reconstruction

Specimens were transferred to acetone and then dried at the critical point (Emitech K850, Quorum Technologies Ltd., Ashford, UK). Scans were conducted at the Zoological Research Museum Alexander Koenig (Bonn, Germany) with a Skyscan 1272 scanner (Bruker, Knotich, Belgium), Max-Planck-Institut for the Science of Human History (Jena, Germany) with a SkyScan 2211 X-ray nanotomograph (Bruker, Knotich, Belgium). The CT-scan data were stored in the collection of the Phyletisches Museum Jena. Amira 6.1.1 (Thermo Fisher Scientific, Waltham, USA) and VG studio Max 2.0.5 (Volume Graphics, Heidelberg, Germany) were used for the three-dimensional reconstruction and volume rendering.

2.3 Terminology

Beutel et al. (2014) was used for general morphological terminology. Cephalic muscles were designated following the terminology of v. Kéler (1963), with the

exception of *Mm. compressores epipharyngis* (*Mm. III*). For this muscle we followed Belkaceme (1991). Muscles are also homologized according to Wipfler et al. (2011), with corresponding abbreviations added in parentheses after the designation of v. Kéler (1963); for example, *M7-M. labroepipharyngalis* (0lb5). Thoracic muscles were designated following Larsén (1966), but the muscular terms introduced by Friedrich & Beutel (2008) (see also Beutel et al. [2014]) were added. Different nomenclatorial systems for thoracic muscles were compared and aligned by Friedrich et al. (2009). Muscles not mentioned in the morphological description are absent. The terminology related to subterranean biology followed different sources in the literature (Table 3).

Table 3 Definition of terms related to subterranean biology in the studies.

Terms	Definition	References
trogomorphy	Evolutionary changes of morphology associated with subterranean life	Christiansen (1962)
troglobite	Animals which are only able to inhabit underground environments, usually in deep parts of caves, and displaying highly specialized morphological traits clearly correlated with cave life	Racovitza (1907)
troglophile	Organisms which are able to live and reproduce in surface areas but also in caves, and in some cases show modifications related to dark environments	Racovitza (1907)
trogloxene	Only occasionally or accidentally appearing in caves, and rarely showing subterranean specialization	Racovitza (1907)
subterranean	All types of environments that lie closely beneath the surface organic matter of living vegetation and loose plant material and woody debris (e.g. leaf litter)	Wong & Guénard (2017)
endogean	Species which permanently inhabit deep soil layers during their entire life cycle	Andújar & Grebennikov (2021)

2.4 Phylogenetic reconstruction

The phylogenetic reconstruction was based on morphological data in Study V (Jałoszyński et al. *subm.*) and on molecular data in Study VIII (Luo et al. *in prep.*). For detailed methods, please see part “Phylogenetic analysis” of the manuscripts.

3 Publications

Study I: Luo, X.-Z., Antunes-Carvalho, C., Wipfler, B., Ribera, I., Beutel, R.G., (2019). The cephalic morphology of the troglobiontic cholevine species *Troglocharinus ferreri* (Coleoptera, Leiodidae). *J. Morphol.* 280, 1207–1221.

Significance in the present thesis: This study on *Troglocharinus ferreri* is first detailed treatment of the cephalic anatomy of a cave-dwelling leiodid. The observed features are compared with conditions found in other species of Leptodirini and also in species of Ptomaphagini.

Study II: Jałoszyński, P., Luo, X.-Z., Beutel, R.G., (2020). Profound head modifications in *Claviger testaceus* (Pselaphinae, Staphylinidae, Coleoptera) facilitate integration into communities of ants. *J. Morphol.* 281, 1072–1085.

Significance in the present thesis: This study on the myrmecophilous beetle *Claviger testaceus* provides the first detailed documentation of external and internal head structures (including skeleton, muscles, nervous system, and glands etc.) of a pselaphine species and of a beetle closely associated with ants. A special focus is on modifications of mouthparts related to highly specialized feeding habits in ant nests.

Study III: Luo, X.-Z., Hlavac, P., Jałoszyński, P., Beutel, R.G., (2021). In the twilight zone-The head morphology of *Bergrothia saulcyi* (Pselaphinae, Staphylinidae, Coleoptera), a beetle with adaptations to endogean life but living in leaf litter. *J. Morphol.* 282, 1170–1187.

Significance in the present thesis: *Bergrothia saulcyi* is a species living in leaf litter but also occurs in deeper soil layer. Therefore, it is a potential model for transitions from superficial layers to subterranean habitats.

Study IV: Beutel, R.G., Luo, X.-Z., Yavorskaya, M., Jałoszyński, P., (2021). Structural megadiversity in leaf litter predators - the head anatomy of *Pselaphus heisei* (Pselaphinae, Staphylinidae, Coleoptera). *Arthropod Syst. Phylogeny* 79, 443–463.

Significance in the present thesis: *Pselaphus heisei* was studied as an example of a less specialized pselaphine species living in leaf litter. A special focus was on predacious feeding habits, presumably an ancestral feature in the subfamily.

Study V: Jałoszyński, P., Luo, X.-Z., Beutel, R.G., [Submitted]. Evolution of cephalic structures in extreme myrmecophiles: a lesson from Clavigeritae (Coleoptera: Staphylinidae: Pselaphinae)

Significance in the present thesis: This study provides a formal analysis of transformations of head structures in the myrmecophilous Clavigeritae, and more widely in the species-rich Pselaphinae. This illuminates changes possibly associated with underground life but especially with myrmecophilous habits. Internal and external head structures of the ant-associated *Diartiger kubotai* were documented to allow a detailed comparison with the related *Claviger* and other pselaphines.

Study VI: Luo, X.-Z., Antunes-Carvalho, C., Ribera, I., Beutel, R.G., (2019). The thoracic morphology of the troglobiotic cholevine species *Troglocharinus ferreri* (Coleoptera, Leiodidae). *Arthropod Struct. Dev.* 53, 100900.

Significance in the present thesis: This is the first study on the thoracic morphology of a cave-dwelling carabid beetles. The effect of subterranean life on the skeleto-muscular system is evaluated.

Study VII: Luo, X.-Z., Jałoszyński, P., Stoessel, A., Beutel, R.G., (2021). The specialized thoracic skeletomuscular system of the myrmecophile *Claviger testaceus* (Pselaphinae, Staphylinidae, Coleoptera). *Org. Divers. Evol.* 21, 317–335.

Significance in the present thesis: The thoracic morphology of a pselaphine beetle and of a myrmecophilous species was examined for the first time. The observed features are evaluated with respect to living underground and in association with ants.

Study VIII: Luo, X.-Z., Gabelaia, M., Faille A., Beutel, R.G., Ribera I., Wipfler B. [In preparation]. Subterranean or blind beetles (Leiodidae) have no improved antennal sensory equipment compared to their epigean or sighted relatives.

Significance in the present thesis: Antennal sensillar patterns of 38 species of Leiodidae were compared. In contrast to a widely accepted interpretation, the loss of eyes and life underground does not enhance the sensorial apparatus, i.e. the length or density of sensilla.

3.1 Study I

The cephalic morphology of the troglobiontic cholevine species *Troglocharinus ferreri* (Coleoptera, Leiodidae)

Xiao-Zhu Luo, Caio Antunes-Carvalho, Benjamin Wipfler, Ignacio Ribera, Rolf G. Beutel

2019. *J. Morphol.* 280, 1207–1221. <https://doi.org/10.1002/jmor.21025>

Abstract: Leiodidae are the second largest subterranean radiation of beetles at family rank. To explore morphological trends linked with troglobiontic habits and characters with potential phylogenetic significance, the head of the cave-dwelling species *Troglocharinus ferreri* (Cholevinae, Leptodirini) was examined in detail. Overall, the general pattern is similar to what is found in *Catops ventricosus* (Cholevini). Shared apomorphic features include a fully exposed anterolateral concavity containing the antennal socket, a distinct bead above this depression, a bilobed lip-like structure anterad the labrum, a flat elevated portion of the ventral mandibular surface, and a ventral process at the proximomesal edge of this mandibular area. The tentorial structures are well-developed as in *C. ventricosus*, with a large laminatentorium and somewhat shortened dorsal arms. The mouthparts are largely unmodified, with the exception of unusually well-developed extrinsic maxillary muscles. Features of *T. ferreri* obviously linked with subterranean habits are the complete lack of compound eyes, circumocular ridges, and optic lobes. A series of characters is similar to conditions found in other genera of Leptodirini: the head capsule completely lacks a protruding ocular region, a distinct neck is missing, the transverse occipital crest is indistinct, and the antennae are elongate and lack a distinct club. Two different trends of cephalic transformations occur in troglobiontic Leptodirini, with some genera like *Troglocharinus* and *Leptodirus* having elongated head capsules and antennae, and others having broadened, more transverse heads. In contrast, the modifications are more uniform in the closely related Ptomaphagini, with a pattern distinctly differing from Leptodirini: the head is transverse, with a distinctly protruding ocular region, a distinct transverse occipital crest, and a very narrow neck region.

Conceptualization: X.Z. Luo, C. Antunes-Carvalho, B. Wipfler, I. Ribera, R. G. Beutel

Visualization: X.Z. Luo, B. Wipfler

Writing-original draft: X.Z. Luo, C. Antunes-Carvalho, R. G. Beutel


Writing-review & editing: X.Z. Luo, C. Antunes-Carvalho, B. Wipfler, I. Ribera, R. G. Beutel

Funding acquisition: X.Z. Luo, I. Ribera

Estimated own contribution: 80%

RESEARCH ARTICLE

The cephalic morphology of the troglobiontic cholevine species *Troglocharinus ferreri* (Coleoptera, Leiodidae)

Xiao-Zhu Luo^{1,2}  | Caio Antunes-Carvalho³ | Benjamin Wipfler⁴ | Ignacio Ribera² | Rolf G. Beutel¹

¹Institut für Zoologie und Evolutionsforschung, Friedrich-Schiller-Universität Jena, Jena, Germany

²Institut de Biologia Evolutiva (CSIC-Universitat Pompeu Fabra), Barcelona, Spain

³Departamento de Biologia Geral, Instituto de Biologia, Universidade Federal Fluminense, Outeiro de São João Batista, Niterói, Brazil

⁴Center of Taxonomy and Evolutionary Research, Zoological Research Museum Alexander Koenig, Bonn, Germany

Correspondence

Xiao-Zhu Luo, Institut für Zoologie und Evolutionsforschung, Friedrich-Schiller-Universität Jena, Erbertstrasse 1, 07743 Jena, Germany.
Email: xiaozhu.luo@uni-jena.de

Funding information

AEI/FEDER, UE, Grant/Award Number: CGL2013-48950-C2; China Scholarship Council, Grant/Award Number: 201708440281

Abstract

Leiodidae are the second largest subterranean radiation of beetles at family rank. To explore morphological trends linked with troglobiontic habits and characters with potential phylogenetic significance, the head of the cave-dwelling species *Troglocharinus ferreri* (Cholevinae, Leptodirini) was examined in detail. Overall, the general pattern is similar to what is found in *Catops ventricosus* (Cholevini). Shared apomorphic features include a fully exposed anterolateral concavity containing the antennal socket, a distinct bead above this depression, a bilobed lip-like structure anterad the labrum, a flat elevated portion of the ventral mandibular surface, and a ventral process at the proximomesal edge of this mandibular area. The tentorial structures are well-developed as in *C. ventricosus*, with a large laminatentorium and somewhat shortened dorsal arms. The mouthparts are largely unmodified, with the exception of unusually well-developed extrinsic maxillary muscles. Features of *T. ferreri* obviously linked with subterranean habits are the complete lack of compound eyes, circumocular ridges, and optic lobes. A series of characters is similar to conditions found in other genera of Leptodirini: the head capsule completely lacks a protruding ocular region, a distinct neck is missing, the transverse occipital crest is indistinct, and the antennae are elongate and lack a distinct club. Two different trends of cephalic transformations occur in troglobiontic Leptodirini, with some genera like *Troglocharinus* and *Leptodirus* having elongated head capsules and antennae, and others having broadened, more transverse heads. In contrast, the modifications are more uniform in the closely related Ptomaphagini, with a pattern distinctly differing from Leptodirini: the head is transverse, with a distinctly protruding ocular region, a distinct transverse occipital crest, and a very narrow neck region.

KEYWORDS

3D-reconstruction, micro-CT, musculature, subterranean beetle, troglomorphy

1 | INTRODUCTION

With about 4,135 described species arranged in 374 genera, 18 tribes and 6 subfamilies, Leiodidae is the second largest family of the megadiverse Staphylinoidea (Newton, 2016). Their distribution is world-wide, with the exception of Antarctica. Leiodidae accounts for

31% of the currently known cave beetles (Moldovan, 2012). The family and its subterranean tendencies have attracted the attention of many scientists, especially in North America and Europe, since *Leptodirus hohenwartii* Schmidt, 1832 was discovered in Slovenia as the first cave dwelling invertebrate (Polak, 2005; Schmidt, 1832). This species is included in Leptodirini, a tribe of Cholevinae with

more than 800 species and 181 genera (Newton, 2016). The tribe represents one of the most successful radiations of beetles in subterranean environments, and is therefore a suitable model to study cave adaptations.

In recent years, biospeleologists have not only kept describing new species on the morphological level, but have also used molecular data to explore the evolutionary history of this group (Latella, Sbordon, & Allegrucci, 2018; Njunjić et al., 2018; Ribera et al., 2010; Rizzo, Comas, Fadrique, Fresneda, & Ribera, 2013; Rizzo, Sánchez-Fernández, Alonso, Pastor, & Ribera, 2017). Such analyses of molecular data are valuable as a highly efficient toolset for beetle systematics (e.g., McKenna, 2016; McKenna et al., 2015). Nevertheless, morphological characters still play an important role in reconstructing the phylogeny and evolution of Leiodidae and other groups, and are important in their own right for understanding evolutionary patterns. Jeannel (1911, 1936, 1958) provided detailed morphological treatments of several groups, and Newton (1998) produced a monograph of world Leiodidae based on morphological features. Morphological data were also used in the phylogenetic analysis of Fresneda, Grebennikov, and Ribera (2011), even though only 28 characters of 15 species were included, while an earlier phylogenetic study of Leptodirini (Fresneda, Salgado, & Ribera, 2007) was mainly focused on genitalia and with 32 described characters. More recently, Antunes-Carvalho, Ribera, Beutel, and Gnaspini (2019) presented a phylogeny of Cholevinae with a representative taxonomic sampling (93 species) and 97 morphological characters which included 23 cephalic features. However, the internal morphology of Leiodidae has been rarely investigated since an early study by Packard (1888). For example, Larsen, Booth, Perks, and Gundersen (1979) studied the brain of the eyeless *Glacivicola bathyscioides* Westcott, 1968 (Catopocerinae: Glacivicolini), and a detailed reconstruction of the cephalic morphology of *Catops ventricosus* (Weise, 1877; Cholevini) was presented by Antunes-Carvalho et al. (2017), including descriptions of the skeleton, musculature, digestive tract, and nervous system. The internal morphology of the head of *Agathidium mandibulare* Sturm, 1807 (Leiodinae, Agathidiini) was partly described in a study with a main focus on Staphylinidae (Weide & Betz, 2009; Weide, Thayer, & Betz, 2014). Although numerous investigations have dealt with subterranean adaptations of beetles, a detailed and complete documentation of the head morphology of cave-dwelling species of Leiodidae was not available so far.

Species of Leiodidae with a subterranean life style are informally categorized into four morphotypes: (a) the “bathyscioid” type, the ancestral body shape, with an ovoid body and short appendages; (b) the intermediate “pholeuonoid” type, with longer appendages and a more slender body; and (c, d) the highly specialized “leptodiroid” and “scaphoid” types, both with extremely long appendages and narrow head and thorax, but with the abdomen distinctly swollen in the former and narrow in the latter (Moldovan, Kováč, & Halse, 2018). As a representative of the “pholeuonoid” type, we chose the troglobiontic *Troglocharinus ferreri* (Reitter, 1908) for our study. To achieve a detailed documentation of skeletal elements and internal soft parts, we applied a broad spectrum of traditional (e.g., histological sectioning) and modern techniques (e.g., micro-computed

tomography). In order to evaluate the morphological modifications toward a subterranean life style of this species, the observed features were compared to conditions found in the free-living *C. ventricosus* (Cholevini; Antunes-Carvalho et al., 2017) and also to selected species of the tribes Leptodirini and Ptomaphagini, which are characterized by a trend toward life in deeper substrate levels or subterranean habits. Additionally, the highly cave-adapted carabid beetle *Sinaphaenops wangorum* Uéno & Ran, 1998 (Luo et al., 2018) is taken into consideration for discussion of general trends of adaptation toward life in caves.

2 | MATERIALS AND METHODS

2.1 | Studied species

Specimens of *T. ferreri* were collected by J. Pastor in the Avenc d'en Roca, Cervelló, Barcelona, Spain (April 22, 2013). All individuals used in this study were preserved in 100% ethanol. In addition to material of *T. ferreri*, we used scanning electron microscopy (SEM) images of other species of Leptodirini and Ptomaphagini, which include *Platycholeus opacellus* Fall, 1909, *Ptomaphagus troglodytes* Blas & Vives, 1983, *Bathysciola ovata* Kiesenwetter 1850, and *L. hochenwartii*.

2.2 | Micro-computed tomography (micro-CT) and microtome sections

Specimens were transferred to acetone and then dried at the critical point (Emitech K850, Quorum Technologies Ltd., Ashford, UK). One dried specimen was scanned at the Zoological Research Museum Alexander Koenig, Bonn, Germany with a Skyscan 1272 scanner (Bruker, Knotich, Belgium) with the following parameters: 25 kV voltage, 190 μ A current, 2,700 ms exposure time, 2,400 projections over 360° (rotation steps of 0.15°), frame averaging of 7, random movement of 15, and no filter. Projections were reconstructed with NRecon (Bruker, Knotich, Belgium) into BMP files with a spatial resolution of 0.850006 μ m. The CT-scan is stored in the collection of the Phyletisches Museum Jena and the Zoological Research Museum Alexander Koenig, Bonn (for access, please contact XZL or BW). Amira 6.1.1 (Thermo Fisher Scientific, Waltham) and VG studio Max 2.0.5 (Volume Graphics, Heidelberg, Germany) were used for the three-dimensional reconstruction and volume rendering.

For microtome sectioning, one specimen of *T. ferreri* was embedded in Araldite CY 212 (Agar Scientific, Stansted/Essex, UK). Subsequently sections were cut at 1 μ m intervals using a microtome HM 360 (Microm, Walldorf, Germany) equipped with a glass knife, and stained with toluidine blue and pyronin G (Waldeck GmbH and Co. KG/Division Chroma, Münster, Germany). The sections are stored in the collection of the Phyletisches Museum.

2.3 | Light and scanning electron microscopy

We followed the protocol introduced by Schneeberg, Bauernfeind, and Pohl (2017) to clean specimens: transfer from 100% ethanol into

70% ethanol; from this to 5% KOH, then glacial acetic acid followed by distilled water (Aqua dest.), and finally 70% ethanol. Subsequently, specimens were dehydrated and dried in an Emitech K850 critical point dryer. A Keyence VHX-2000 digital microscope (Keyence Corporation, Osaka, Japan) was used for taking photographs with different depths of field (z-stacking); these z-stacks were assembled to a single sharp image using Helicon Focus (Helicon Soft Ltd., Kharkov, Ukraine). Prior to SEM, samples were sputter-coated with gold (Emitech K500; Quorum Technologies Ltd., Ashford, UK) and attached to a rotatable specimen holder (Pohl, 2010). SEM observation and imaging was performed with an FEI (Philips) XL 30 ESEM at 10 kV. Final figure plates were assembled and arranged with Adobe Photoshop CC and Illustrator CS6 (Adobe, Inc., CA).

2.4 | Terminology

Cephalic muscles were designated following the terminology of K  ler (1963), with the exception of Mm. compressores epipharyngis (Mm. III). For this muscle, we followed Belkaceme (1991). Muscles are also homologized according to Wipfler, Machida, M  ller, and Beutel (2011), with homolog abbreviations added in parentheses after the designation of K  ler (1963); for example, M7 - M. labroepipharyngalis (0lb5). Muscles not mentioned in the morphological description are absent. Beutel, Friedrich, Ge, and Yang (2014) was used for general morphological terminology.

3 | RESULTS

3.1 | External head structures

The head (Figure 1) is prognathous; the neck region is not distinctly narrowed; a curved, transverse occipital crest (occr; Figures 2a and 9c) is present but indistinct; the ridge separates a largely smooth and glabrous posterior area from the rest of the head capsule; the posteriormost part of the head is retracted into the prothorax; a

broad M-shaped incision (Figure 1a) at the posterodorsal edge is covered by the pronotum in the normal retracted position of the head. The head capsule is about 1.5 times as long as the maximum width. Its coloration is light-brown, whereas the labrum, maxillae, submentum, prementum, and labial palps are yellowish. The dorsal surface (Figure 2a) is densely covered with medium-length setae (ca. 0.15 mm); a microreticulation resembling a fingerprint pattern is only visible under high magnification; a few short setae are distributed on the area posterior to the occipital crest; the ventral surface (Figure 2b) is also setose but the density is lower than on the dorsal side; a microreticulation is visible on the gular region but setae are missing; only the anterior area of the gena (ge; Figure 2b,c) is sparsely setose, while the posterior region displays a dense microreticulation. The internal frontoclypeal strengthening ridge ("epistomal suture") is distinct and complete, visible through the semitransparent cuticle as a dark brown line (Figure 1a); it is nearly straight medially and slightly curved anterad toward the lateral clypeal margin; an external furrow is missing (Figure 2a). The medium-sized clypeus (cl; Figure 2a) is subhexagonal; the ratio of maximum width/length is about two; a distinct, broad bead is present along the nearly straight anterior and lateral margin; the anterolateral corners are rounded and the lateral edges slightly oblique. The anterior tentorial groove is not visible externally. The clypeal bead is continuous with a narrower bead, which extends posterolaterally above the fully exposed and concave antennal insertion area; it meets the anterolateral ends of the transverse occipital crest posterolaterally. The concave oblique antennal insertion area is extended posteriorly, covering the erstwhile ocular region; its surface is largely smooth and glabrous dorsally and posteriorly. The compound eyes are completely reduced, and ocelli of the frontal region are also absent. Triangular genal extensions normally covering the posterior side of the compound eyes and a postocular constriction of the head capsule are absent. The gula (gu; Figure 2b) is subtrapezoidal, with its slightly concave posterior edge about two times as long as the anterior margin; the distinct

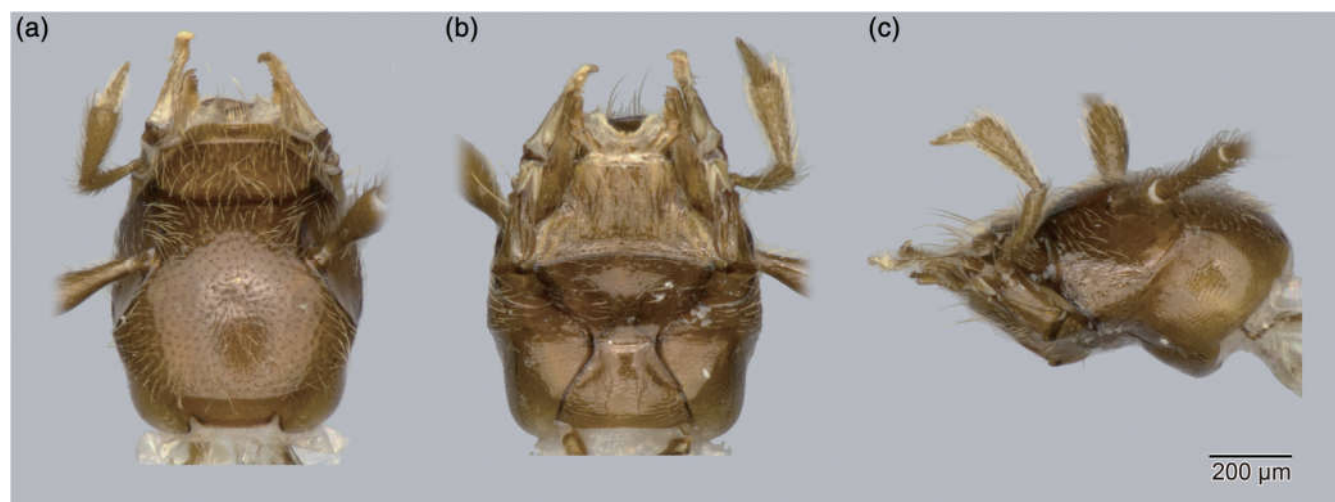


FIGURE 1 Head habitus of *Troglucharinus ferreri*. (a) Dorsal view. (b) Ventral view. (c) Lateral view

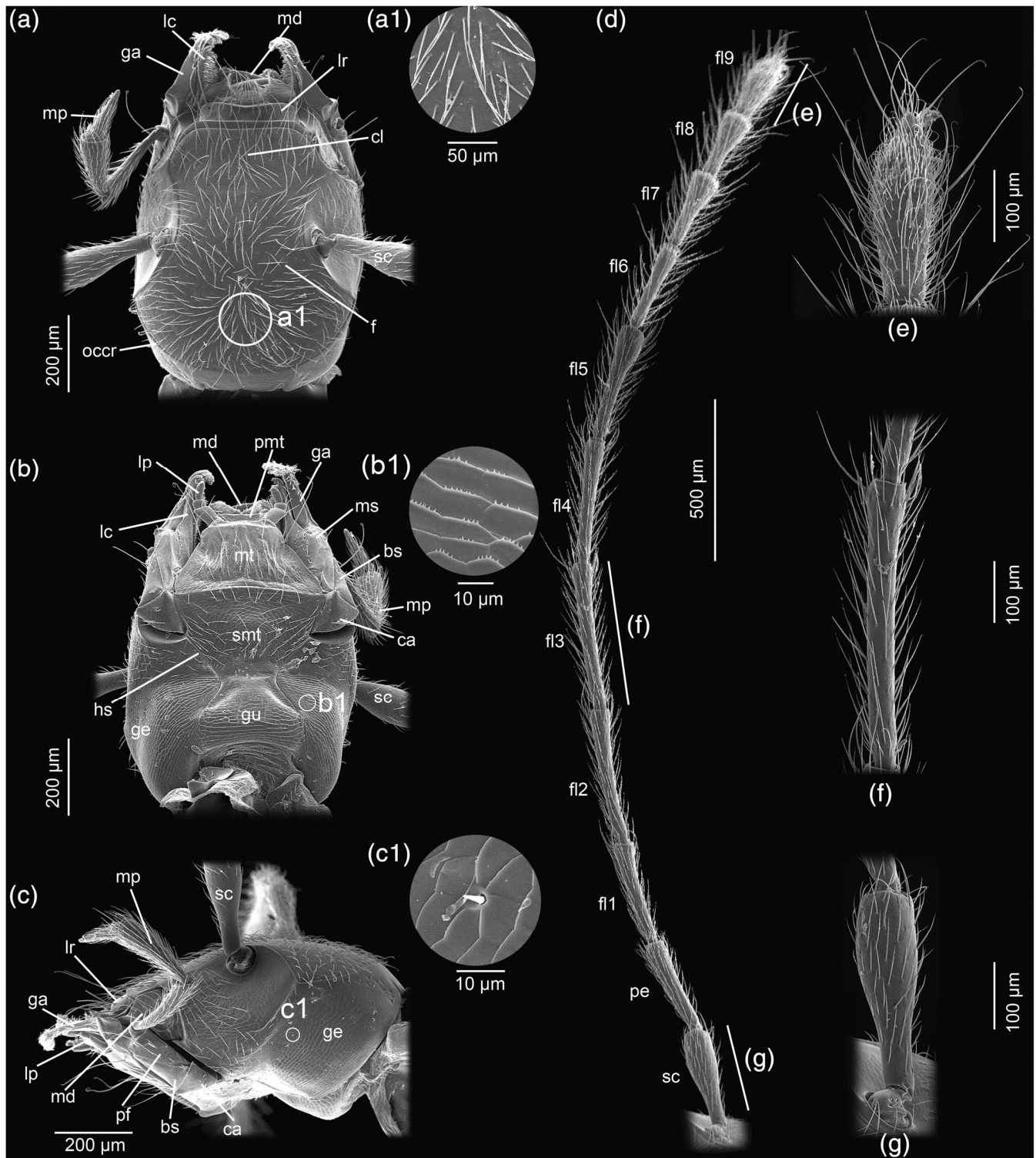


FIGURE 2 Scanning electron microscopy images of the head (a–c) and antenna (d–g). (a) Dorsal view. (b) Ventral view. (c) Lateral view. (d–g) Dorsal view. Abbreviations: bs, basistipes; ca, cardo; cl, clypeus; f, frons; fl, flagellomere; ga, galea; ge, gena; gu, gula; hs, hypostomal suture; lc, lacinia; lp, labial palp; lr, labrum; md, mandible; mp, maxillary palp; ms, mediostipes; mt, mentum; occr, occipital crest; pe, pedicellus; pf, palpifer; pmt, prementum; sc, scapus; smt, submentum

dark-brown gular sutures are distinctly curved; they are widely separated posteriorly and anteriorly converging before they meet the lateral submental edge; the gula-submental border is indicated by a shallow transverse furrow. The hypostomal suture (hs; Figure 2b) is

well-developed and clearly visible; it originates anteriorly from the maxillary groove and extends posteriorly to connect with the gular suture. Posterior tentorial grooves are not visible externally.

3.2 | Internal skeletal structures

An extensive internal frontoclypeal ridge stabilizes the anterodorsal part of the head capsule. Posterior, dorsal, and anterior tentorial arms are present. The strongly developed anterior arms (ata; Figure 3a,b) extend from the central tentorial body upward to the anterolateral edges of the frons, close to the antennal foramen. The nearly vertically oriented dorsal arms (dta; Figure 3a) are weakly developed and short, directed toward the middle region of the frons but not attached to it. The posterior arms are fused with the gular ridges (gur; Figure 3a,b), which form two wall-like structures diverging toward the postoccipital ridge. A thin and anteriorly arched tentorial bridge (tb; Figure 3a,b) is formed posteriorly between these walls; in dorsal view, it appears W-shaped. The anterior, dorsal, and posterior arms are connected in the middle region of the head, thus forming the laminatentorium; this massive structure (lt; Figure 3b) consists of two parts: a flat horizontal plate and a vertical plate; the latter is ventrally attached to the horizontal plate along the median line and posteriorly continuous with the central tentorial body (ctb; Figure 3b); the vertical plate protrudes anteriorly beyond the anterior edge of the horizontal plate. Circumantennal

ridges are present but internal circumocular ridges are completely missing. The postoccipital ridge is well-developed and slightly widening ventrolaterally.

3.3 | Labrum

The sclerotized part of the labrum (lr; Figures 2a,c, and 4c) is transverse, with a shallow median emargination at the anterior edge. The exposed part in dorsal view is about five times as wide as long; its lateral edges are nearly straight and subparallel. The cuticle of the dorsal surface is largely smooth. Ten setae of medium-length and six long setae are symmetrically arranged on the dorsal surface, and six additional setae are inserted close to the anterior margin. A pale and membranous bilobed lip-like structure is present in front of the sclerotized plate-like part of the labrum; it is densely set with short marginal setae. On the ventral surface of the labrum, that is, the anteriormost epipharynx, mesally oriented microtrichia of medium length (Figure 4d1) are present, with anterolateral areas with a high density separated by a median glabrous region.

Musculature (Figure 5): M7 - *M. labroepipharyngalis* (Olb5), many fibers, O: dorsal wall of labrum, I: anteriormost epipharynx, that is, unsclerotized ventral wall of labrum.

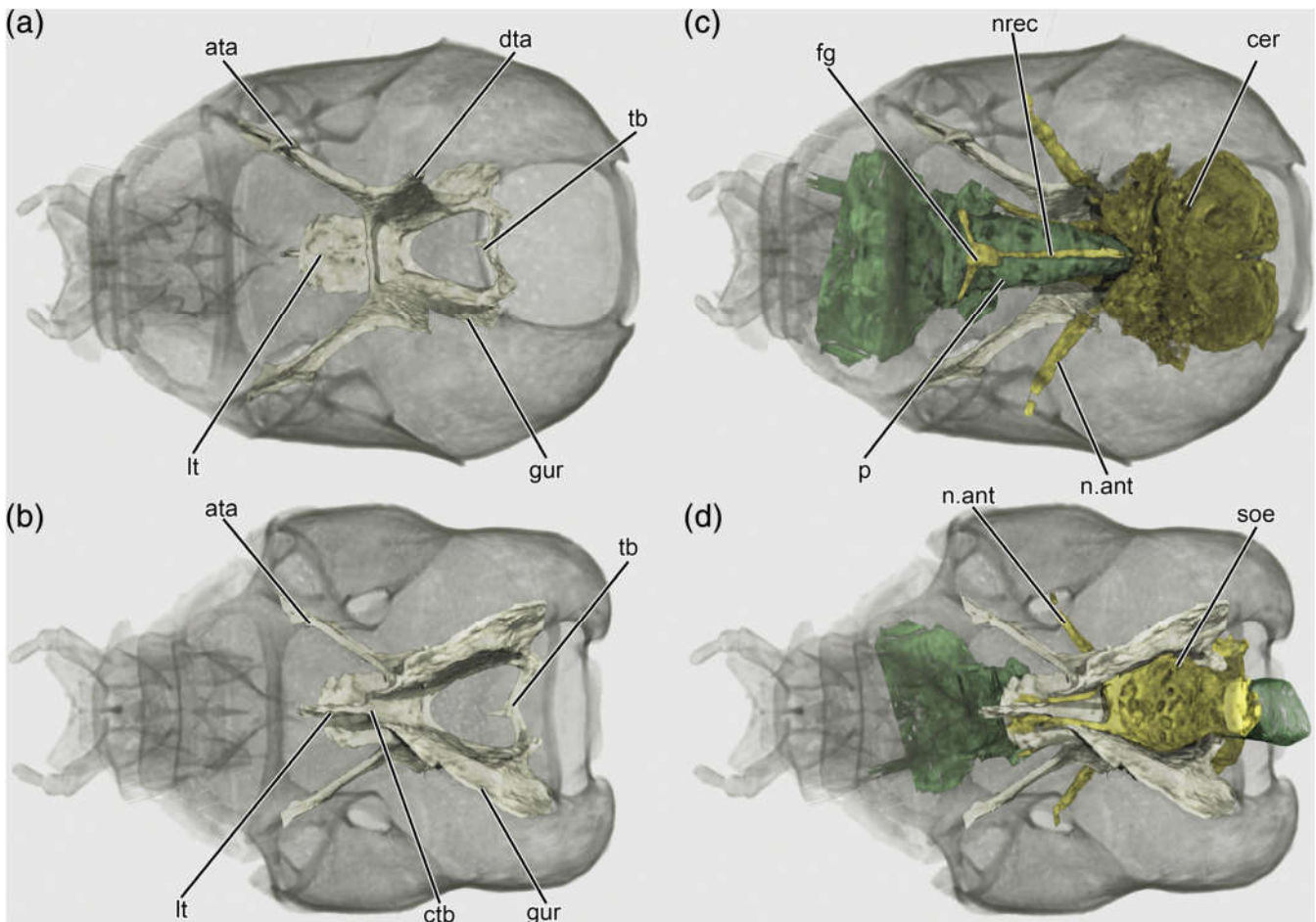


FIGURE 3 Three-dimensional reconstructions of the tentorium (a,b), digestive and nervous system (c,d). (a) and (c) dorsal view. (b) and (d) ventral view. Abbreviations: ata, anterior tentorial arm; cer, cerebrum; ctb, central tentorial body; dta, dorsal tentorial arm; fg, frontal ganglion; gur, gular ridge; lt, laminatentorium; n.ant, antennal nerve; nrec, nervus recurrens; p, pharynx; soe, subesophageal ganglion; tb, tentorial bridge

3.4 | Antennae

The slender filiform antenna (Figure 2d) is 11-segmented. At about 3.67 mm, it is almost as long as the total body length without appendages. The oval antennal foramen is fully exposed in dorsal view; it is anterolaterally oriented and located in the extensive anterolateral concavity of the head capsule (Figure 2a,c); it is enclosed by a distinctly raised circumantennal ridge. All antennomeres are densely setose. The scapus (sc; Figure 2d,g) is bipartite, with a distinct proximal constriction almost suggesting a short basal segment; the short globular basal part, which articulates with the head capsule, bears several short setae inserted in shallow depressions; the distal part is elongate and club-shaped, moderately widening in its middle region and slightly narrowing apically. The pedicellus (pe; Figure 2d) is slightly shorter and narrower than the scapus. The flagellomeres are elongate and slender; 2–5 are slightly longer than the pedicellus (fl3; Figure 3d, f); the distal flagellomeres slightly decrease in length and slightly widen distally; a distinct antennal club is not developed. A circle of short smooth bottle-like sensilla is present on the distal area of flagellomeres 6–9, sparse on flagellomere 6 but more densely arranged on flagellomeres 7–9; the tip of flagellomere 9 is peg-like.

Musculature (Figure 6a): M1 - *M. tentorioscapalis anterior* (Oan1), O: dorsal surface of horizontal plate of laminatentorium, I: ventrally on condyle of scapus; M2 - *M. tentorioscapalis posterior* (Oan2), O: lateral

surface of dorsal tentorial arm, I: posterodorsally on condyle of scapus; M4 - *M. tentorioscapalis medialis* (Oan4), O: dorsal tentorium arm and anterodorsal area of gular ridge, I: medioventrally on basal margin of scapus; M5 - *M. scapopedicellaris lateralis* (Oan6), O: dorsomesal wall of scapus, I: dorsally on pedicellar base; M6 - *M. scapopedicellaris medialis* (Oan7), O: ventromesal wall of scapus, I: ventrally on pedicellar base.

3.5 | Mandibles

The mandibles slightly project anteriorly beyond the labral margin in their resting position, rendering only the distalmost part visible in dorsal and ventral view (md; Figure 2a,b); a larger mandibular area is visible in lateral view (md; Figure 2c). The mandibles are largely symmetrical and roughly triangular, with a length/basal width ratio of about 1.25. The flattened lateral edge is almost evenly rounded (Figure 4a,b). The relatively slender distal half of the mandible is curved inwards; a pointed apical tooth (ai; Figure 4a,b) is followed proximally by a distinct, acuminate subapical incisor (sai; Figure 4a,b); several small and rounded teeth are present between these two structures. Proximal to the subapical incisor, the middle section of the mesal edge is evenly concave and bears a densely arranged row of microtrichia of medium length (ca. 50 μm); a membranous lobe-like prostheca (prst; Figure 4a,b) with dense microtrichia is present; a retinaculum is missing. A single long

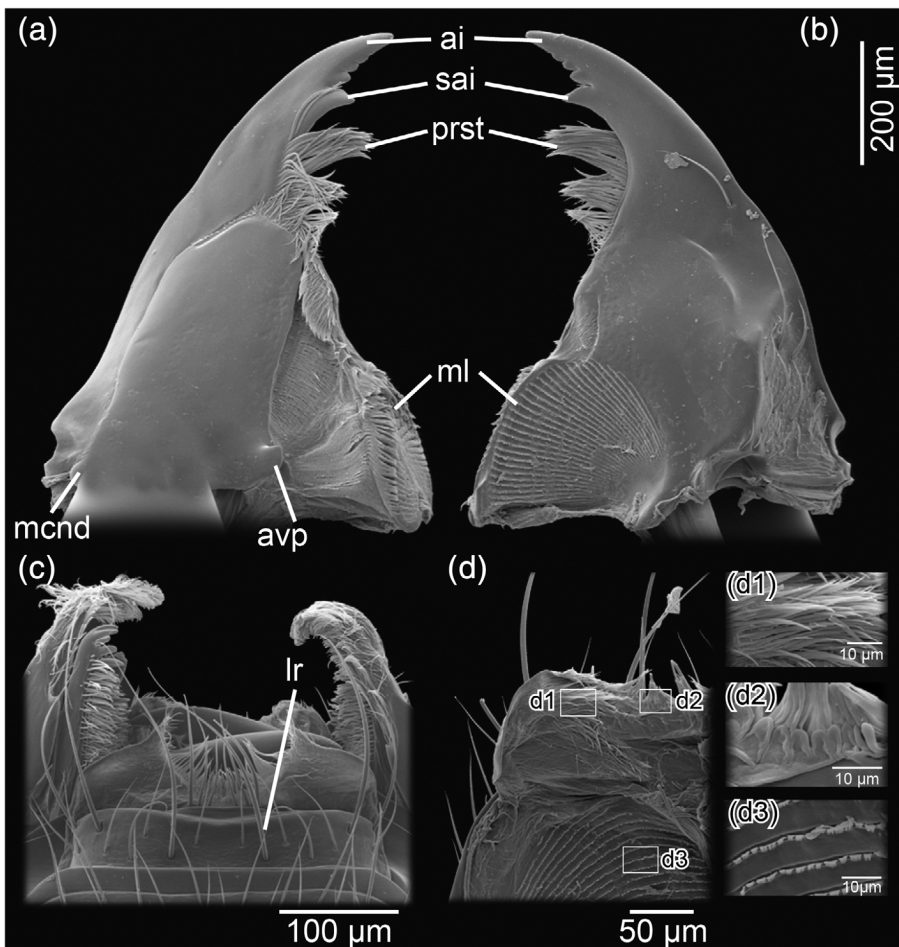


FIGURE 4 Scanning electron microscopy images of mandible (a,b) and labrum (c,d). (a, d) ventral view. (b,c) Dorsal view. Abbreviations: ai, apical incisor; avp, mandibular accessory ventral process; lr, labrum; mcnd, mandibular condyle; ml, mola; prst, prostheca; sai, subapical incisor

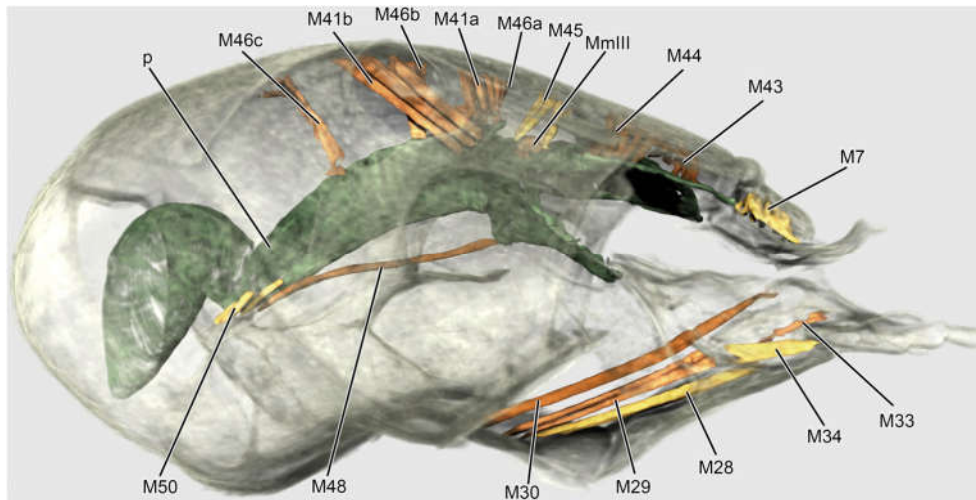


FIGURE 5 Three-dimensional reconstructions of labral, pharyngeal, and hypopharyngeal muscles, lateral view. Abbreviations: p, pharynx. Muscles: M7, *M. labroepipharyngalis* (Olb5); M28, *M. submentopraementalis* (Ola8); M29, *M. tentoriopraementalis inferior* (Ola5); M30, *M. tentoriopraementalis superior* (Ola6); M33, *M. praementopalpalis internus* (Ola13); M34, *M. praementopalpalis externus* (Ola14); M41, *M. frontohypopharyngalis* (Ohy1); M43, *M. clypeopalpalis* (Oci1); M44, *M. clypeobuccalis* (Obu1); M45, *M. frontobuccalis anterior* (Obu2); M46, *M. frontobuccalis posterior* (Obu3); M48, *M. tentoriobuccalis anterior* (Obu5); M50, *M. tentoriobuccalis posterior* (Obu6); MmIII, *Mm. compressores epipharyngis*

seta is inserted on the anterolateral area of the dorsal side of the mandible. Most areas of the dorsal surface are smooth, except for the mola and the lateral scrobe; the cuticular surface of the latter is scale-like and several setae are inserted on this area, increasing in length distally. The scrobe is delimited by a longitudinal edge from the main part of the ventral mandibular surface; a strongly curved edge is present at its anterior end, extending more than half way toward the concave part of the mesal mandibular margin. A large mola (ml; Figure 4a,b) at the mesal mandibular base bears numerous equidistant dense rows of posteriorly oriented microtrichia on its dorsal side; its mesal edge appears flattened. A small mesal concavity with a somewhat irregular surface is present distad the mola in dorsal view; it bears rather indistinct posteriorly directed microtrichia. A small, round and plate-like process is present on the dorsal posteromedial area of the mandible, with a scrobe on its lateral region. Most parts of the ventral mandibular surface are smooth except for the molar region. Setae are lacking. A large plate-like middle part of the proximal half of the ventral side is slightly elevated, delimited by distinct, nearly straight mesal and lateral edges; the unevenly curved anterior edge is set with relatively long microtrichia mesally and extremely short bristles laterally; a small group of short microtrichia is also present at the mesal edge. A ventral accessory process (avp; Figure 4a) is present mesally at the base of the ventral mandibular surface, and a mandibular condyle (mcnd; Figure 4a) laterally. The ventral molar surface (ml; Figure 4a) of the right mandible is subdivided into an anterior and posterior part, the former with a field of horizontally arranged and posteromesally oriented microtrichia, and the latter area with a nearly vertical brush-like arrangement of microtrichia; a narrow transitional area with a rough surface is recognizable between both regions. The ventral molar surface of the left mandible shows some differences compared to the right one; it is less convex and smoother, with rows of densely arranged microtrichia on the posterior and mesal areas.

Musculature (Figure 6c): M11 - *M. craniomandibularis internus* (Omd1), O: several bundles on lateral, dorsal and ventral areas of head capsule, I: mesal mandibular base with strongly developed tendon; M12 - *M. craniomandibularis externus* (Omd3), O: two bundles along lateral margin of head capsule, subcomponent a: dorsal, almost reaching foramen occipitale; subcomponent b: ventral, anterior part of head, I: lateral mandibular base with tendon; M13 - *M. hypopharyngomandibularis* (Omd4), thin, O: dorsal surface of laminatentorium, exact point not clearly recognizable due to common attachment site with other muscles; I: mesal area of mandibular base, near insertion of M11.

3.6 | Maxillae

The maxillary groove is bordered by the lateral submental edge and the anterior edge of the gena (Figure 2b,c). The transverse, subtriangular cardo (ca; Figures 2b,c and 7a,b) is mostly smooth except for its posterior area, which is sparsely striated and bears several short setae; the basal cardinal process (cp; Figure 7a) is well-developed and divided into a mesal and lateral branch. The subtriangular basistipes (bs; Figures 2b,c and 7a,b) is connected to the anterior cardinal margin, the mediostipes (ms; Figures 2b and 7b) and palpifer (pf; Figures 2c and 7a,b) to its mesal and lateral edges, respectively. The galea (ga; Figures 2a-c and 7a,b) is subtriangular, with triangular scales on a protruding basal area of the dorsal side; a brush of mesally oriented setae is present on the anterior region of both the dorsal and ventral surface; the posterior area of the galea is largely smooth and glabrous. The lacinia (lc; Figures 2a,b and 7a,b) is narrow and located mesad the galea; a mesally oriented digitiform structure formed by five short and finger-like elements with blunt tips is present on its distal surface; rows of setae are present on the mesal edge of the lacinia; its posteromesal area is membranous and covered with slightly-protruding narrow stripes. The palpifer

(pf; Figures 2c and 7a,b) is laterally adjacent to the lateral edge of the basistipes, and anteromesally connected with the mediostipes; it is composed of mesal smooth areas and a striated region with several setae laterally. The maxillary palp (mp; Figures 2a-c and 7a,b) is four-segmented; palpomere 1 is short, with a long seta on the distal area and a short one on the basal region; the slender palpomere 2 is the longest palpomere, with setae evenly distributed from the mesal to the distal region; palpomere 3 is widest and club-shaped, bearing medium-sized setae; the cone-shaped palpomere 4 bears a cluster of smooth and short sensilla on the ventral surface of its basal region (Figure 7b1); a sensilla complex is

present on the tip of this palpomere (Figure 7a1). Small round fields of pores are present on palpomeres 3 and 4.

Musculature (Figure 6d): M15 - *M. craniocardinalis externus* (Omx1), O: posteroventral area of head capsule, I: with tendon on lateral branch of cardinal process; M17 - *M. tentoriocardinalis* (Omx3), three bundles, subcomponent a: posterior area of laminatentorium, close to base of anterior tentorium, I: mesal branch of cardinal process; subcomponent b: O: along outer surface of gular ridge, I: same as 17a; subcomponent c: thin, O: anterolateral tip of horizontal plate of laminatentorium; I: inner

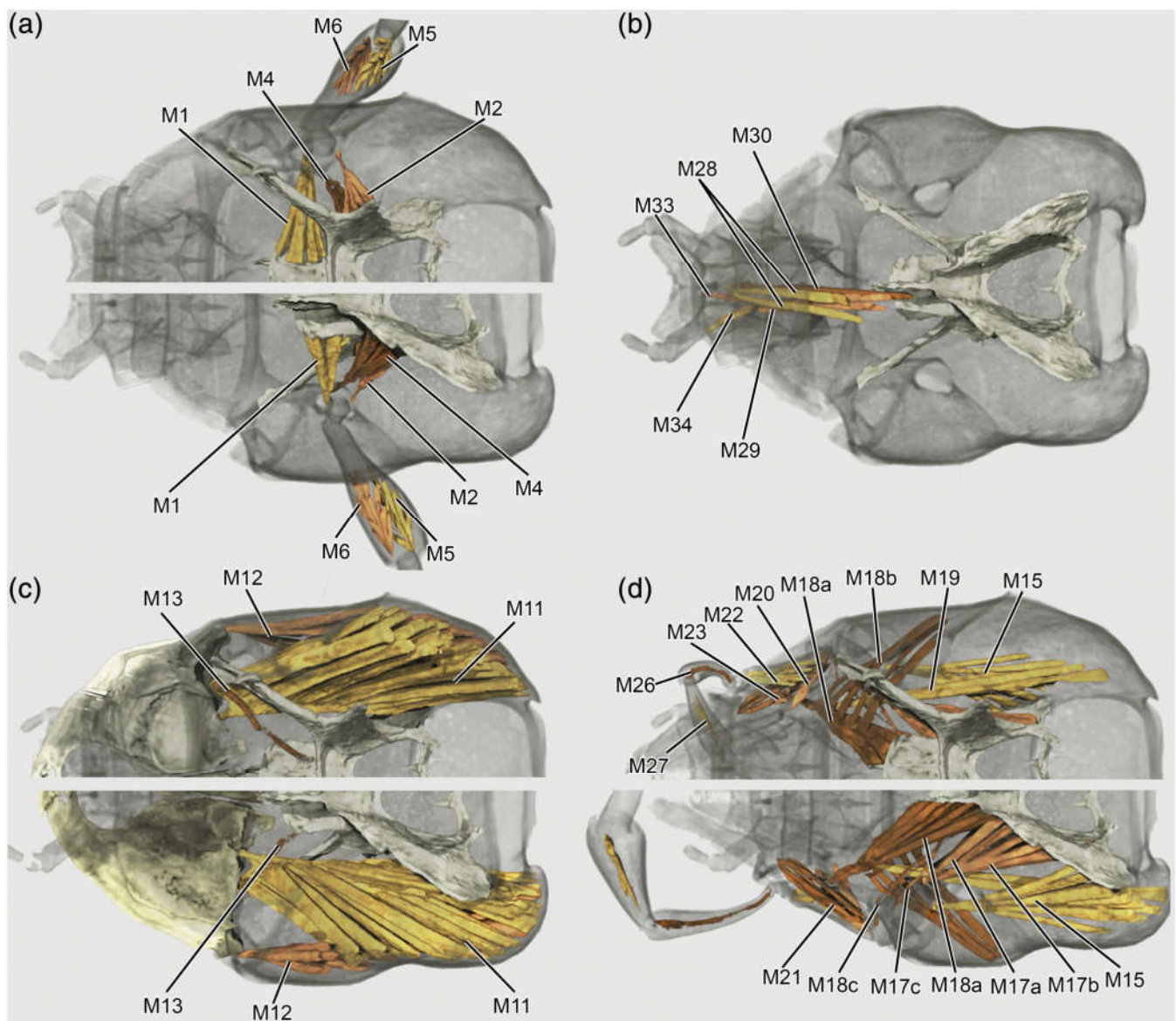


FIGURE 6 Three-dimensional reconstructions of antennal (a), labial (b), mandibular (c), maxillary (d) muscles. (a, c, and d) Upper half is in dorsal view, lower half is in ventral view. (b) Ventral view. Muscles: M1, *M. tentorioscapalis anterior* (Oan1); M2, *M. tentorioscapalis posterior* (Oan2); M4, *M. tentorioscapalis medialis* (Oan4); M5, *M. scapopedicellaris lateralis* (Oan6); M6, *M. scapopedicellaris medialis*, (Oan7); M11, *M. craniomandibularis internus* (Omd1); M12, *M. craniomandibularis externus* (Omd3); Man-M13, *M. hypopharyngomandibularis* (Omd4); M15, *M. craniocardinalis externus* (Omx1); M17, *M. tentoriocardinalis* (Omx3); M18, *M. tentoriostipitalis* (Omx4/Omx5); M19, *M. craniolacinialis* (Omx2); M20, *M. stipitolacinialis* (Omx6); Max-M21, *M. stipitogalealis* (Omx7); M22, *M. stipitopalpalis externus* (Omx8); M23, *M. stipitopalpalis internus* (Omx10); M26, *M. palpopalpalis tertius* (Omx14); M27, *M. palpopalpalis quartus* (Omx15)

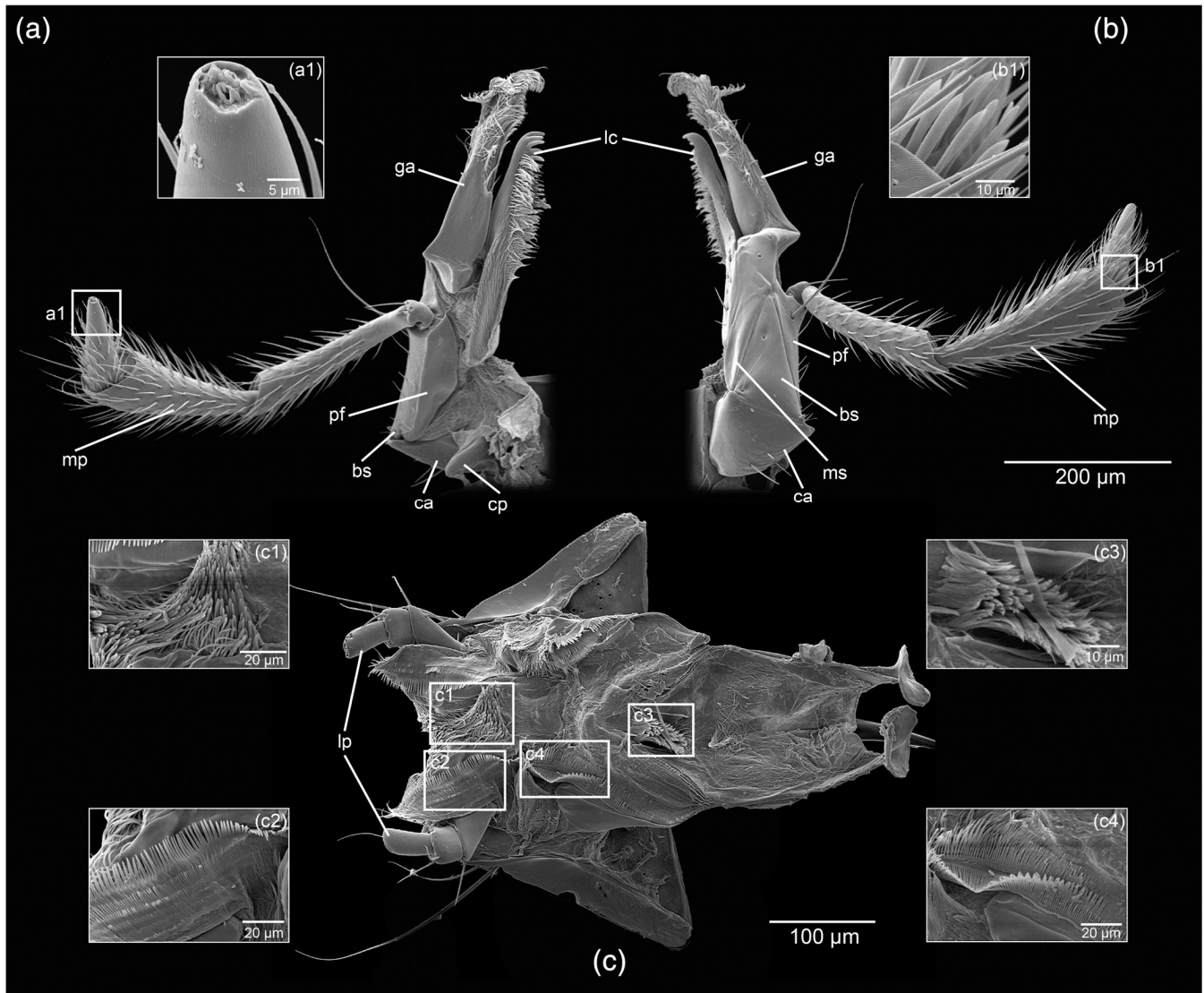


FIGURE 7 Scanning electron microscopy images of maxillae (a,b) and hypopharynx (c). (a,c) dorsal view. (b) Ventral view. Abbreviations: bs, basistipes; ca, cardo; cp, cardinal process; ga, galea; lc, lacinia; mp, maxillary palp; ms, mediostipe; pf, palpifer

surface of cardo; M18 - *M. tentoriostipitalis* (0mx4/0mx5), three major bundles, subcomponent a: larger, O: large parts of laminatentorium; subcomponent b: several separate thin bundles, O: ventrolateral area of head capsule; l: membrane of stipital base; subcomponent c, O: lower area of laminatentorium; l: basal area of basistipes; M19 - *M. craniolacinalis* (0mx2), O: two bundles on posteriormost ventrolateral region of head capsule, l: membranous area posterior to base of lacinia; M20 - *M. stipitolacinalis* (0mx6), O: basal margin of stipes, l: base of lacinia; M21 - *M. stipitogalealis* (0mx7), O: basal wall of basistipes, l: basal margin of galea; M22 - *M. stipitopalpalis externus* (0mx8), O: base of dorsal plate of palpifer, l: laterally on base of palpomere 1; M23 - *M. stipitopalpalis internus* (0mx10), short vertical muscle, O: mediostipes, l: palpifer; M26 - *M. palpopalpalis tertius* (0mx14), O: lateral wall of palpomere 2, l: mesally on palpomere 3; M27 - *M. palpopalpalis quartus* (0mx15), O: lateral wall of palpomere 3, l: mesally on palpomere 4.

3.7 | Labium

The short transverse prementum (pmt; Figure 2b) is partly concealed by the mentum; it bears several minute setae and shallow pits on its surface; a pair of divergent ligular lobes is present apically; two rather long setae and densely arranged short microtrichia are present on the anterior area. The large and plate-like trapezoid mentum (mt; Figure 2b) is narrowing apically and its anterior margin is slightly sinuated; the anteriorly converging lateral edges are adjacent to the mediostipes; four long setae are inserted on the anterior area of the mentum; the surface of the posterior region shows a striated pattern and more than 10 shorter and thinner setae are inserted on it. The submentum (smt; Figure 2b) is about as large as the mentum and separated from it by a slightly curved transverse suture; numerous thin setae are present on its striated surface, with a slightly higher density than on the mentum; a transverse shallow furrow separates the submentum from the gula (see above). The widely separated palpigers, which bear the three-segmented labial

palps (lp; Figures 2b,c and 7c), are partly concealed by the anterior part of the mentum; palpomere 1 is directed outward and the widest of the three segments; its distal edge is slightly oblique and bears two setae anteromesally and anterolaterally, respectively; palpomere 2 is less than half as long as 1; it bears two setae on the anterolateral area; palpomere 3 is almost as long as 1 but narrower and apically rounded; its apical part bears a complex of numerous short, smooth and sensilla with blunt tips.

Musculature (Figures 5 and 6b): M28 - *M. submentopraementalis* (Ola8), two bundles close to each other, O: medial area of ventral head capsule, in front of M29, I: membranous area between prementum and mentum; M29 - *M. tentoriopraementalis inferior* (Ola5), two bundles, O: medial area of ventral head capsule, I: on the sclerotized lateral process of the lateral wall of prementum; M30 - *M. tentoriopraementalis superior* (Ola6), O: medially on submentum, I: medially on border region between anterior and posterior hypopharynx; M33 - *M. praementopalpalis internus* (Ola13), O: sclerotized lateral process of the lateral wall of prementum, closely attach to the origin of M34, I: near mesal margin of base of palpomere 1 (note: could not be clearly identified, and the homologization remains ambiguous); M34 - *M. praementopalpalis externus* (Ola14), O: sclerotized lateral process of the lateral wall of prementum, I: basal margin of palpomere 1.

3.8 | Epipharynx and hypopharynx

The middle region of the epipharynx (Figure 4d), posterad the unsclerotized ventral wall of the labrum, is medially divided by a dense, posteriorly narrowing triangular group of microtrichia (see Anton & Beutel, 2004; Anton, Yavorskaya, & Beute, 2016: lep [longitudinal epipharyngeal process]); large paired areas with rows of posteriorly oriented microtrichia are present posterolaterad this structure, placed in shallow depressions of the lateral epipharyngeal surface. The largely semimembranous hypopharynx (Figure 7c) forms a structural and functional unit with the dorsal prementum; lamellae with several dense comb-like rows of microtrichia extend along its lateral edges, from the anterior to the posterior region (Figure 7c2,c4); two dense tufts of hairs are present on the anteromesal and posteromesal areas, the anterior one on a distinct elevation (Figure 7c1,c3; see Anton & Beutel, 2004; Anton et al., 2016; lhp [longitudinal hypopharyngeal process]); two strongly developed plate-like posterolateral apodemes are muscle attachment sites. The posteriormost parts of the epipharynx and hypopharynx are laterally fused, thus forming a short prepharynx anterad the anatomical mouth opening.

Musculature (Figure 5): M41 - *M. frontohypopharyngalis* (Ohy1), two subcomponents, posterior bundle longer than anteromesal one, O: anterior frontal area, I: posterolateral hypopharyngeal apodeme, laterally at anatomical mouth opening; M43 - *M. clypeopalpalis* (Oci1), O: mesally on clypeus, I: epipharyngeal wall; M44 - *M. clypeobuccalis* (Obu1), O: mesally on clypeus, behind M43, I: posterior area of epipharynx; MmIII-Mm. compressores epipharyngis, numerous transverse bundles on posterior epipharynx.

3.9 | Prepharynx and pharynx

The anatomical mouth is marked by the position of the frontal ganglion and the insertion of M45 (Figures 3c and 5). A short prepharynx, formed by lateral fusion of the posterior epipharynx and hypopharynx, is shaped like a transverse oval in cross section. The pharynx (Figures 3c,d and 5) gradually descends toward the tentorial bridge, where it forms a narrow loop. It is continuous with the oesophagus, which widens and enters the postoccipital foramen. The pharyngeal lumen appears oval in cross section. Longitudinal pharyngeal folds are recognizable but indistinct.

Musculature (Figure 5): M45 - *M. frontobuccalis anterior* (Obu2), O: anterior area of frons, I: dorsal pharyngeal wall at anatomical mouth; M46 - *M. frontobuccalis posterior* (Obu3), several longitudinally arranged paired bundles, O: middle region of frons, I: successively on dorsal pharyngeal wall; M48 - *M. tentoriobuccalis anterior* (Obu5), a single bundle: O: anterodorsally on tentorial bridge, I: ventromesally on anterior pharynx; M50 - *M. tentoriobuccalis posterior* (Obu6), short, O: anteriorly on tentorial bridge, I: ventral wall of posterior pharynx.

3.10 | Nervous system

The brain (cer; Figure 3c) is medium-sized in relation to the head capsule and located in the posterior cephalic region. Two protruding lobes are present on the anterior protocerebral surface. Optic neuropils are completely absent, but antennal nerves (n. ant; Figure 3c,d) are present and relatively thick. The frontal ganglion (fg; Figure 3c,d) is located above the anatomical mouth opening. The nervus recurrens (nrec; Figure 3c) lies medially above the pharynx; it originates posteromedially from the frontal ganglion and reaches the hypocerebral ganglion posteriorly. The circumoesophageal connectives, originating from the tritocerebral lobes, enclose the pharynx and connect with the suboesophageal ganglion (soe; Figure 3d), which is located between the gular ridges, entirely within the head capsule.

3.11 | Glands and neurohemal organs

Loose gland-like material in the occipital region above the oesophagus and laterad the pharyngo-oesophageal loop probably represents parts of the retrocerebral complex. Paired round and compact structures, probably corpora cardiaca, are present laterad the posteriormost pharynx and immediately posterad the posterior protocerebral surface (connection with brain recognizable on microtome sections). Numerous unicellular glands are attached to the lateral walls of the middle region of the labio-hypopharyngeal complex. Similar cells are also present in the basal mandibular region, partly attached to the mandibular wall in a single layer, but partly forming a compact conglomerate.

3.12 | Fat body

Fat body tissue is widely distributed in the lumen of the head capsule. A thin layer extends along the inner wall of the posterior gula. Paired

lobes extend from the region between brain and the dorsomesal part of *M. craniomandibularis internus* (M. 11) toward the distal portion of this muscle and into the lumen of the mandibles; this complex is also continuous with lobes adjacent to the concave anterolateral wall of the head capsule, and around the strongly developed anterior tentorial arms. An elongated unpaired fat body lobe is present above the anterior pharynx and along the entire epipharynx, the anterior part close to the clypeal wall. Another unpaired portion encloses the distal part of *M. tentoriopraementalis superior* (M30) in the middle region of the labio-hypopharyngeal complex.

3.13 | Tracheal system

Two main tracheal trunks enter the head between the oesophagus and the suboesophageal complex, and turn downward between *M. tentoriomandibularis internus* (M. 11) and the tentorial extrinsic maxillary muscles (M. 17, 18). Smaller branches originating from these large trachea extend into the dorsal, dorsolateral, and ventral cephalic regions, mainly supplying muscles of the paired mouthparts with oxygen. The entire configuration of the cephalic tracheal system appears quite asymmetrical and may vary between individuals.

3.14 | Circulatory system

The dorsal aorta does not enter the head.

4 | DISCUSSION

Even though the head of *T. ferreri* is obviously affected by troglobiotic habits, the observed characters have to be seen in a phylogenetic context. The sister group relationship between the Nearctic genus *Platycholeus* and the rest of Leptodirini (i.e., the Palearctic branch) was revealed by Fresneda et al. (2011). More recently, a phylogenetic affinity of the tribe with the endogean genus *Sciaphyes* was suggested based on morphological characters, and also a close relationship with Ptomaphagini (Antunes-Carvalho et al., 2019, figure 25), which also include species in hypogean environments. A suitable outgroup within Cholevinae is *Catops*, a genus of Cholevini with epigeal species. A distant outgroup is the trechine cave-dwelling carabid species *S. wangorum* (Luo et al., 2018). It can be assumed that derived features shared between this species and the ones under consideration here have evolved independently as a result of similar selective pressures.

A head as it is found in *C. ventricosus*, described in great detail in Antunes-Carvalho et al. (2017), is likely close to the groundplan of Cholevinae in many aspects (Antunes-Carvalho et al., 2019). The head capsule of this species is about as long as wide, with a distinctly protruding lateral ocular region, a distinct transverse occipital crest (see character 20 in Antunes-Carvalho et al., 2019), and a distinctly narrowed posterior neck region. A distinct bead is present along the lateral clypeal edges and still recognizable anterolaterally. The antenna is inserted in an oblique and fully exposed concavity on the lateral side of the head, arguably a synapomorphy of Cholevinae or a more

inclusive group of Leiodidae. The largely glabrous area anterad the compound eyes of *Catops* is dorsally delimited by a distinct bead, which is posteriorly continuous with a supraocular bead, which is again posteriorly connected with the transverse occipital crest. The dorsal vestiture of medium length setae is dense in *C. ventricosus*.

The head of *T. ferreri* differs distinctly from the presumably plesiomorphic cholevine pattern. The head capsule is longer than wide and completely lacks compound eyes and a protruding ocular region. The neck region is scarcely narrowed and the transverse occipital crest is indistinct. The concave antennal insertion area is extended posteriorly, and the triangular genal extension is absent, both features apparently linked with the complete loss of eyes. The dorsolateral bead is distinct and anteriorly continuous with a bead of the clypeus, also distinct and broad along the anterior edge. The density of the setation on the dorsal side is similar to the pattern observed in *C. ventricosus*.

The trend of troglobitic transformation reaches a maximum in *L. hohenwartii*, which has a strongly elongated head without any recognizable neck region or occipital crest. In its general shape, the head of *Leptodirus* resembles the condition described for the trechine carabid *Sinaphaenops* (Luo et al., 2018). The concave antennal insertion area of *Leptodirus* is still recognizable but the dorsolateral bead is obliterated; only the bead along the anterior clypeal margin is distinct. Interestingly, the elongate head capsule is nearly glabrous; the vestiture of setae on the dorsal side is sparse. In contrast, the head capsule of species of *Platycholeus* is about as broad as long, and distinct but relatively small compound eyes are present (Figure 9); the transverse occipital crest is slightly more distinct than in *Troglocharinus* but less pronounced than in *Catops*, and a slightly narrowed neck region is present.

The partial reduction of the neck region and occipital crest are arguably apomorphies linking *Sciaphyes* and *Platycholeus* with the Palearctic Leptodirini, although the phylogenetic position of *Sciaphyes* is still uncertain (Fresneda et al., 2011). In contrast to these more or less constant features, the head shape varies strongly within the tribe. Differing from the moderately elongated head of *T. ferreri* and the strongly elongated condition in *L. hohenwartii* (Figure 8a), the head is distinctly broadened in *B. ovata* (Figures 8b and 9e) and to a slightly lesser degree

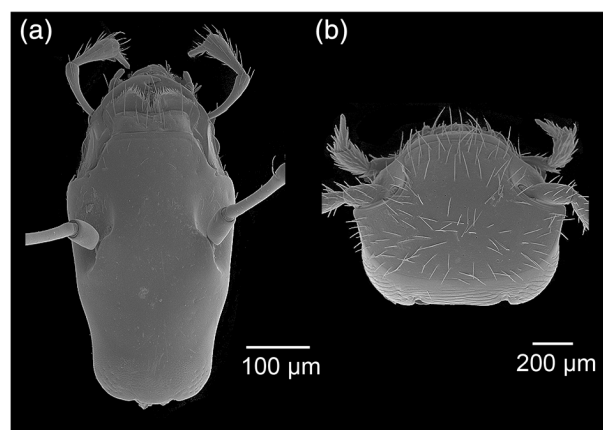


FIGURE 8 Scanning electron microscopy images of the head of (a) *Leptodirus hohenwartii*; (b) *Bathysciola ovata*

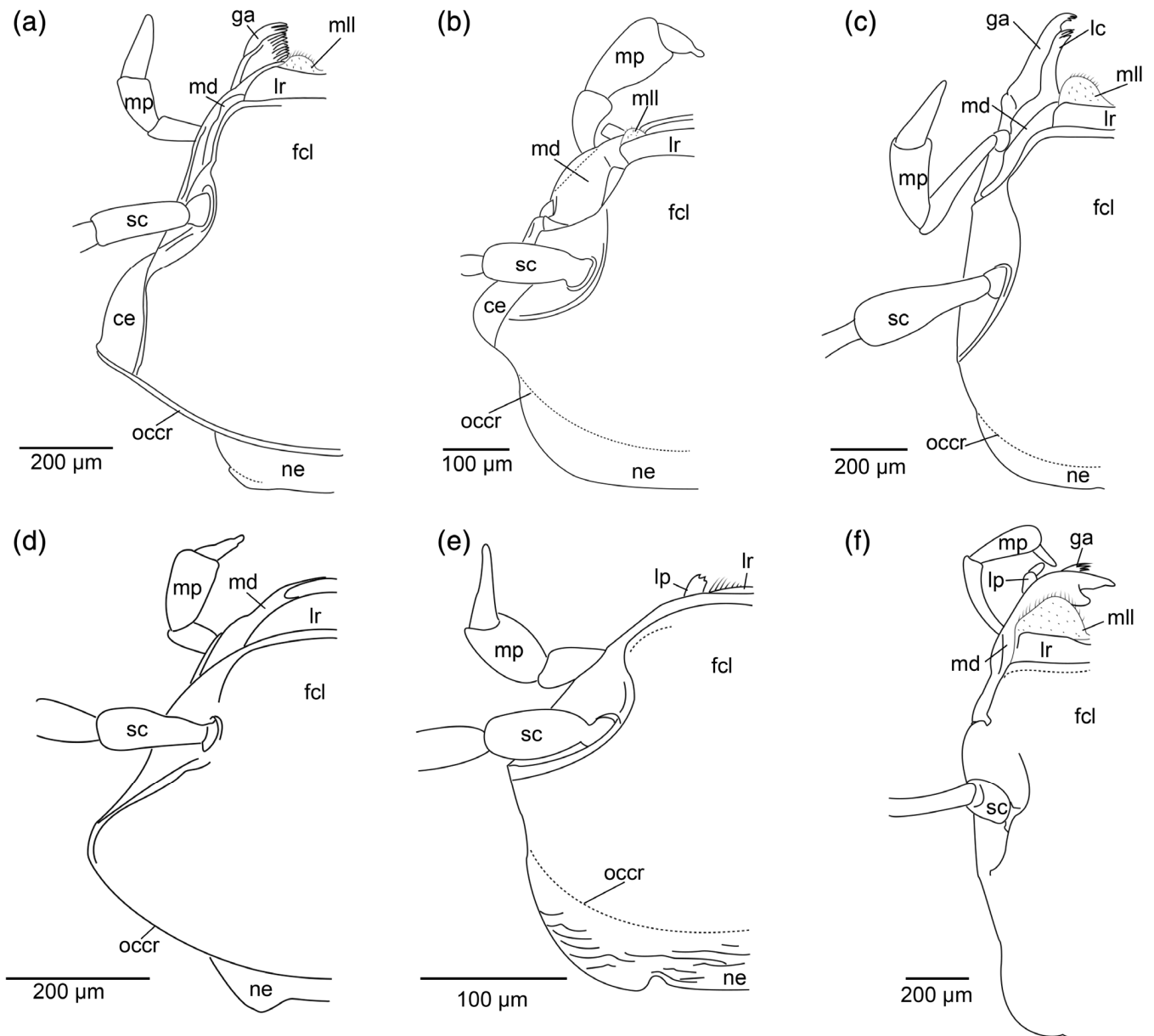


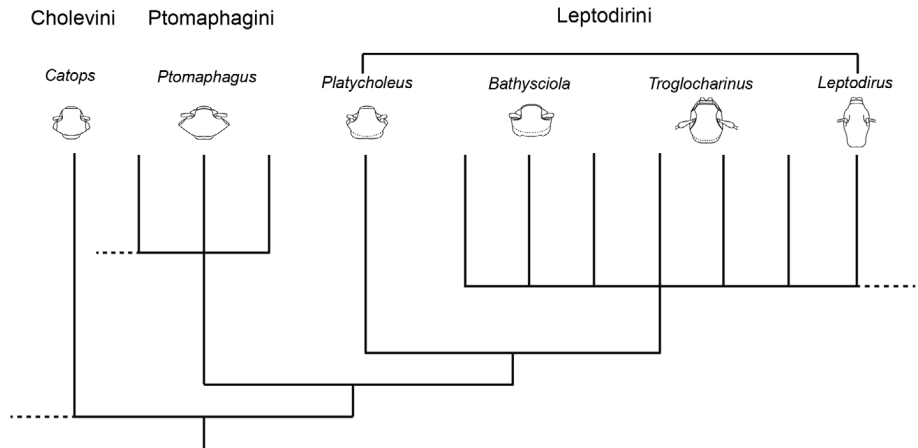
FIGURE 9 Line drawings of the head of (a) *Catops ventricosus*; (b) *Platycholeus opacellus*; (c) *Troglocharinus ferreri*; (d) *Ptomaphagus troglodytes*; (e) *Bathysciola ovata*; (f) *Leptodirus hochenwartii*. Abbreviations: ce, compound eye; fcl, frontoclypeus; ga, galea; lc, lacinia; lp, labial palp; lr, labrum; md, mandible; mll, membranous lobe of labrum; mp, maxillary palp; ne, neck; occr, occipital crest; sc, scapus

in other species of this and closely related genera. The anterior clypeal bead is broad in *B. ovata* and the concavity of the antennal insertion area unusually transverse. The dorsal setation is distinctly less dense than in *Catops* or *Troglocharinus*.

Interestingly, Ptomaphagini, which are closely related with Leptodirini (Antunes-Carvalho et al., 2019) and also include some subterranean species, have evolved different cephalic modifications. The head of *Ptomaphagus troglodytes* appears more transverse than in *Catops*, with distinctly protruding ocular regions despite of lacking compound eyes; the occipital crest is distinct, and the neck region narrow compared to the maximum width of the head. Similar conditions are also found in species illustrated in Jeannel (1936) and Fresneda et al. (2011, figures 26, 27).

Well-developed posterior and anterior tentorial arms as they are present in *T. ferreri* are ancestral for Leiodidae and for the entire Staphyliniformia (Anton & Beutel, 2004; Antunes-Carvalho et al., 2017; Beutel, Anton, & Jäch, 2003). The dorsal arm is short in contrast to *C. ventricosus*, where it is long and thin (Antunes-Carvalho et al., 2017). A medially fused laminatentorium as it is present in *T. ferreri* and *C. ventricosus* (Antunes-Carvalho et al., 2017) is also described for Hydraenidae and Hydrophiloidea (Anton & Beutel, 2004; Beutel et al., 2003), suggesting that this is a groundplan feature of Staphyliniformia. Even though the cephalic anatomy of other cave dwelling leiodids is unknown, the condition found in *T. ferreri* suggests that endoskeletal structures are not affected by subterranean habits, except for the loss of the internal ocular ridges.

FIGURE 10 Head evolution of several groups within subfamily Cholevinae based on the phylogenetic tree of Antunes-Carvalho et al. (2019)



The movable labrum of the examined leiodid species differs in shape but is likely not affected by cave-dwelling habits. It seems to be generally shorter and more rounded in forms with a more transverse head, as for instance in *P. troglodytes* or *B. ovata*. A phylogenetically and functionally interesting feature is the bilobed lip-like labral extension, distinctly developed in *Catops* and other genera including *Troglocharinus* and *Leptodirus*. The presence is obviously a derived feature as this structure is missing in other groups of Coleoptera (e.g., Anton & Beutel, 2004; Beutel et al., 2003). A precise phylogenetic interpretation is not possible at present as the character is not well-documented among different groups of Leiodidae. However, there is apparently a trend to extend these flexible structures with increasing elongation of the head, with extensive lobes present in the cave dwelling *L. hohenwartii* (Figures 8a and 9f). The lobes are well-developed in *C. ventricosus* (Figure 9a), but indistinct or not visible in cave-dwelling forms with a strongly transverse head (Figures 9 and 10). The character should be considered with some caution. The condition of the unsclerotized structure may depend on the fixation and the apparent degree of exposure on the angle of view.

The antennae of species of *Catops* (Antunes-Carvalho et al., 2017), *Ptomaphagus* (Jeannel, 1936), *Platycholeus* and *Sciaphyes* (Fresneda et al., 2011, figures 2, 20) are at most half as long as the body excluding legs. A weak to distinct 5-segmented club is present. This is likely a groundplan condition of Cholevinae and also Leiodidae (Newton, 2016; Peck, 2001). In clear contrast to this, the antennae of *T. ferreri* are about as long as the body, and even longer in *L. hohenwartii*. In both cases, a club is not developed, likely linked with the general elongation of the antennomeres. The slender distal antennomeres are only slightly extended toward their apex. Considering the long and slender antennae of *S. wangorum* and other cave-dwelling trechine carabids, it appears plausible to assume that this is correlated with hypogean habits. However, this link is not consistent within Leiodidae, as indicated by the short antennae of troglobiontic species of Ptomaphagini (Jeannel, 1936), and also of cave-dwelling leptodirine species of *Bathysciola* (e.g., Salgado & Fresneda, 2000). An unusual antennal feature of *T. ferreri* is the elongate shape of flagellomere 6, which is narrower but not shorter than flagellomeres 5 and 7. This is in contrast to the typical condition in Leiodidae, with flagellomere 6 both shorter and narrower than the adjacent segments (Newton, 2016).

The morphology of the mandibles of *T. ferreri* is similar to what is described for *C. ventricosus* (Antunes-Carvalho et al., 2017). The presence of a well-developed and complex mola, an apical part with several teeth, a mesal brush, and a flexible setiferous prostheca are likely groundplan features of Cholevinae. *Troglocharinus ferreri* and *C. ventricosus* also share a flat elevated portion of the ventral mandibular surface, and a ventral process at the proximomesal edge of this area (Figure 4a; Antunes-Carvalho et al., 2017, figure 3b). However, as in the case of the labral extensions, the documentation of leiodid mandibular features is too fragmentary at present for a reliable interpretation. The distal part of the mandibles of *T. ferreri* appears slightly elongated compared to the condition found in *C. ventricosus* (Antunes-Carvalho et al., 2017, figure 3a, b). A stronger degree with distinctly projecting mandibles occurs in *L. hohenwartii*, resembling conditions found in cave-dwelling carabids (Luo et al., 2018). It is likely that mandibular elongation is linked with the general shape of the head, but not with cave dwelling habits.

The maxillae of *T. ferreri* are similar to those of *C. ventricosus* (Antunes-Carvalho et al., 2017) in their general configuration and the presence of pore plates on the preapical palpomeres. Projecting sensilla on the base of the apical palpomere are a synapomorphy shared by the genera of Leptodirini (Antunes-Carvalho et al., 2019). Moldovan, Jalzic, and Erichsen (2004) examined mouthparts of several subterranean species of Cholevinae, and their observations confirmed that modifications of shapes and structures are diverse among the group, with changes in structural details likely linked with feeding habits. The elongation of the galea and lacinia in *T. ferreri* and *L. hohenwartii* is likely correlated with the elongation of the head and other appendages. Long distal maxillary parts may be advantageous in a lightless environment, as in *S. wangorum* and other troglobiontic trechine carabids (Luo et al., 2018). However, elongation of maxillary endite lobes is definitely not a general feature of cave-dwelling cholevines (e.g., Fresneda et al., 2011; Jeannel, 1936). The general configuration of the maxillary muscles of *T. ferreri* is similar to the condition described for *C. ventricosus* (Antunes-Carvalho et al., 2017). However, M17 (*M. tentoriocardinalis*-Omx3), M18 (*M. tentoriostipitalis*-Omx4/Omx5), and M19 (*M. craniolacinalis*-Omx2) consist of several subcomponents

with different sites of origin and insertion. The unusually complex arrangement of bundles likely results in an improved control and efficiency of maxillary movements, but a link with subterranean habits is uncertain.

The labium of *T. ferreri* does not differ distinctly from that of *C. ventricosus* (Antunes-Carvalho et al., 2017). As in the case of the maxillary lobe, the ligular lobes of the prementum appear moderately enlarged. The complex epi- and hypopharyngeal structures are largely consistent with the general staphyliniform pattern (e.g., Anton & Beutel, 2004; Antunes-Carvalho et al., 2017; Beutel et al., 2003; Weide et al., 2014; Weide & Betz, 2009; Yavorskaya, Beutel, & Polilov, 2017). A derived feature of *T. ferreri* compared to *C. ventricosus* and other staphyliniform beetles is the loss of a cranial muscle laterally attached to the hypopharynx (Anton & Beutel, 2004, Mx). Apomorphic features of the digestive tract are the far-reaching reduction of the longitudinal pharyngeal folds, and the pharyngeal loop in the occipital region. The corresponding plesiomorphic conditions are found in *C. ventricosus* (Antunes-Carvalho et al., 2017). However, the micro-CT data used in that study did not reveal fine details of the anatomy of the digestive tract (Antunes-Carvalho et al., 2017, figure 4). Presently, the data on the digestive organs of Leiodidae are extremely sparse.

Compound eyes are missing in *T. ferreri* as in other subterranean species of Leptodirini and Ptomaphagini (e.g., Gunn, 2004; Jeannel, 1936). This is obviously linked with the subterranean habits, and a trend toward reduction may have been triggered by a preference for deeper soil layers in Leptodirini (Newton, 1998). Along with the light sense organs, the optic lobes are completely absent in *T. ferreri*, as in *G. bathyscioides* (Larsen et al., 1979) and the trechine *S. wangorum* (Luo et al., 2018); this is likely generally the case in eyeless beetles. Interestingly, unusually thick antennal nerves are present in *T. ferreri*, in contrast to *S. wangorum* (Luo et al., 2018). Presently, no information on this character in other subterranean leiodids is available.

5 | CONCLUSIONS

It is conceivable that the appearance of troglobiontic habits took place independently several times within Leptodirini and Ptomaphagini, with different degrees of morphological specialization. Aside from the reduction of eyes, our study reveals a broad spectrum of cephalic modifications in Cholevinae, in contrast to predaceous troglobiontic carabid beetles, which are uniform in their habitus. Whereas Ptomaphagini are generally characterized by a broad head and a compact body, with appendages of normal length, conditions vary strongly in Leptodirini. A distinct trend toward elongation affects the head and appendages in some genera of this tribe, with a maximum reached in *L. hohenwartii*, similar to conditions found in cave-dwelling trechine carabids (Luo et al., 2018). In clear contrast to this, a broad head and comparatively short antennae and legs are maintained in troglobiontic species of *Bathysciola* and similar genera. Our study showed that the cephalic morphology of *Troglocharinus* is consistent with several features described in *Catops*, a non-troglocharinid outgroup representative. Many characteristics of the head of *Troglocharinus* were not affected by the evolution of the

subterranean life-style. However, comparisons with *S. wangorum* also revealed changes clearly associated with the subterranean habits, as the loss of eyes, circumocular ridges, and the optic lobes. Our study underlines the scarcity of anatomical documentation for an important group of staphyliniform beetles. More morphological studies may yield new phylogenetic insights and help to understand evolutionary patterns in the group.

ACKNOWLEDGMENTS

The authors are very grateful to Dr. Hans Pohl (FSU Jena) for his assistance with the SEM samples, and to Brendon Boudinot (University of California at Davis) for linguistic improvements and many suggestions, which greatly helped to improve this manuscript. Very helpful comments by two anonymous reviewers are also gratefully acknowledged, and we are also grateful to Karolin Engelkes (University of Hamburg, Germany) for generously providing the image output script for Amira. The first author wants to express thanks to CSC (No. 201708440281). Our work was also partly funded by project CGL2013-48950-C2 (AEI/FEDER, UE).

ORCID

Xiao-Zhu Luo  <https://orcid.org/0000-0002-5253-267X>

REFERENCES

- Anton, E., & Beutel, R. G. (2004). On the head morphology and systematic position of *Helophorus* (Coleoptera: Hydrophiloidea: Helophoridae). *Zoologischer Anzeiger*, 242, 313–346.
- Antunes-Carvalho, C., Ribera, I., Beutel, R. G., & Gnaspini, P. (2019). Morphology-based phylogenetic reconstruction of Cholevinae (Coleoptera: Leiodidae): A new view on higher-level relationships. *Cladistics*, 35, 1–41.
- Antunes-Carvalho, C., Yavorskaya, M., Gnaspini, P., Ribera, I., Hammel, J. U., & Beutel, R. G. (2017). Cephalic anatomy and three-dimensional reconstruction of the head of *Catops ventricosus* (Weise, 1877) (Coleoptera: Leiodidae: Cholevinae). *Organisms Diversity & Evolution*, 17, 199–212.
- Anton, E., Yavorskaya, M. I., & Beutel, R. G. (2016). The head morphology of Clambidae and its implications for the phylogeny of Scirtoidea (Coleoptera: Polyphaga). *Journal of morphology*, 277, 615–633.
- Belkaceme, T. (1991). Skelet und Muskulatur des Kopfes und Thorax von *Noterus laevis* Sturm: ein Beitrag zur Morphologie und Phylogenie der Noteridae (Coleoptera: Adephaga). *Stuttgarter Beiträge Zur Naturkunde Serie A (Biologie)*, 462, 1–94.
- Beutel, R. G., Anton, E., & Jäch, M. A. (2003). On the evolution of adult head structures and the phylogeny of Hydraenidae (Coleoptera, Staphyliniformia). *Journal of Zoological Systematics and Evolutionary Research*, 41, 256–275.
- Beutel, R. G., Friedrich, F., Ge, S. Q., & Yang, X. K. (2014). *Insect morphology and phylogeny: A textbook for students of entomology*. Berlin, Germany: De Gruyter.
- Fresneda, J., Grebennikov, V. V., & Ribera, I. (2011). The phylogenetic and geographic limits of Leptodirini (Insecta: Coleoptera: Leiodidae: Cholevinae), with a description of *Sciaphyes shestakovi* sp. n. from the Russian Far East. *Arthropod Systematics & Phylogeny*, 69, 99–123.
- Fresneda, J., Salgado, J. M., & Ribera, I. (2007). Phylogeny of western Mediterranean Leptodirini, with an emphasis on genital characters (Coleoptera: Leiodidae: Cholevinae). *Systematic Entomology*, 32, 332–358.

- Gunn, J. (2004). *Encyclopedia of cave and karst science*. New York, NY: Taylor & Francis Group.
- Jeannel, R. (1911). Biospeologica XIX. Révision des Bathysciinae (Coléoptères Silphides). Morphologie, distribution géographique, systématique. *Archives de Zoologie Expérimentale et Générale*, 7, 1–641.
- Jeannel, R. (1936). Monographie des Catopidae (Insectes Coléoptères). *Mémoires du Muséum National d'Histoire Naturelle*, 1, 1–433.
- Jeannel, R. (1958). Sur la famille des Camiaridae Jeannel lignée paléantarctique. *Revue Française d'Entomologie*, 25, 5–15.
- Kéler, S. von (1963). *Entomologisches Wörterbuch*. Berlin, Germany: Akademie Verlag.
- Larsen, J. R., Booth, G., Perks, R., & Gundersen, R. (1979). Optic neuropiles absent in cave beetle *Glacivicolia bathyscioides* (Coleoptera, Leiodidae). *Transactions of the American Microscopical Society*, 98, 461–464.
- Latella, L., Sbordoni, V., & Allegrucci, G. (2018). Three new species of *Bathysciola* Jeannel, 1910 (Leiodidae, Cholevinae, Leptodirini) from caves in Central Italy, comparing morphological taxonomy with molecular phylogeny. *Insect Systematics & Evolution*, 49, 409–442.
- Luo, X. Z., Wipfler, B., Ribera, I., Liang, H. B., Tian, M. Y., Ge, S. Q., & Beutel, R. G. (2018). The cephalic morphology of free-living and cave-dwelling species of trechine ground beetles from China (Coleoptera, Carabidae). *Organisms Diversity & Evolution*, 18, 125–142.
- McKenna, D. D. (2016). Molecular systematics of Coleoptera. In R. A. B. Leschen & R. G. Beutel (Eds.), *Handbook of Zoology Vol. 1: Morphology and systematics* (2nd ed., pp. 23–34). Berlin, Germany: Walter de Gruyter.
- McKenna, D. D., Wild, A. L., Kanda, K., Bellamy, C. L., Beutel, R. G., Caterino, M. S., ... Farrell, B. D. (2015). The beetle tree of life reveals that Coleoptera survived end-Permian mass extinction to diversify during the cretaceous terrestrial revolution. *Systematic Entomology*, 40, 835–880.
- Moldovan, O. T. (2012). Beetles. In D. C. Culver & W. B. Williams (Eds.), *Encyclopaedia of caves* (pp. 54–62). Oxford, England: Elsevier Academic Press.
- Moldovan, O. T., Jalzic, B., & Erichsen, E. G. I. L. (2004). Adaptation of the mouthparts in some subterranean Cholevinae (Coleoptera, Leiodidae). *Natura Croatica*, 13, 1–18.
- Moldovan, O. T., Kováč, L., & Halse, S. (2018). *Cave ecology*. Basel, Switzerland: Springer International Publishing.
- Newton, A. F. (1998). Phylogenetic problems, current classification and generic catalog of world Leiodidae (including Cholevinae). *Museo Regionale di Scienze Naturali di Torino Atti*, 8, 41–177.
- Newton, A. F. (2016). Leiodidae Fleming, 1821. In R. G. Beutel & R. A. B. Leschen (Eds.), *Handbook of Zoology Vol. 1. Morphology and Systematics* (2nd ed., pp. 364–376). Berlin, Germany: De Gruyter.
- Njunjić, I., Perrard, A., Hendriks, K., Schilthuizen, M., Perreau, M., Merckx, V., ... Deharveng, L. (2018). Comprehensive evolutionary analysis of the *Anthroherpon* radiation (Coleoptera, Leiodidae, Leptodirini). *PLoS One*, 13, e0198367.
- Packard, A. S. (1888). The cave fauna of North America, with remarks in the anatomy of brain and the origin of blind species. *Memoirs of the National Academy of Sciences*, 4, 1–156.
- Peck, S. B. (2001). Leiodidae. In R. H. Arnett & M. C. Thomas (Eds.), *American beetles* (Vol. 1, pp. 250–258). Boca Raton, FL: CRC Press.
- Pohl, H. (2010). A scanning electron microscopy specimen holder for viewing different angles of a single specimen. *Microscopy Research and Technique*, 73, 1073–1076.
- Polak, S. (2005). Importance of discovery of the first cave beetle *Leptodirus hochenwartii* Schmidt, 1832. *Endins: Publicació d'Espeleologia*, 28, 71–80.
- Ribera, I., Fresneda, J., Bucur, R., Izquierdo, A., Vogler, A. P., Salgado, J. M., & Cieslak, A. (2010). Ancient origin of a Western Mediterranean radiation of subterranean beetles. *BMC Evolutionary Biology*, 10, 29.
- Rizzo, V., Comas, J., Fadrique, F., Fresneda, J., & Ribera, I. (2013). Early Pliocene range expansion of a clade of subterranean Pyrenean beetles. *Journal of Biogeography*, 40, 1861–1873.
- Rizzo, V., Sánchez-Fernández, D., Alonso, R., Pastor, J., & Ribera, I. (2017). Substratum karstificability, dispersal and genetic structure in a strictly subterranean beetle. *Journal of Biogeography*, 44, 2527–2538.
- Salgado, J. M., & Fresneda, J. (2000). *Bathysciola diegoi* sp. n. (Coleoptera: Cholevinae: Leptodirinae) de Navarra (España). *Elytron*, 14, 183–189.
- Schmidt, F. (1832). *Leptodirus hochenwartii* n. g., n. sp. *Illyrisches Blatt*, 21, 9.
- Schneeberg, K., Bauernfeind, R., & Pohl, H. (2017). Comparison of cleaning methods for delicate insect specimens for scanning electron microscopy. *Microscopy Research and Technique*, 80, 1199–1204.
- Weide, D., & Betz, O. (2009). Head morphology of selected Staphylinoidae (Coleoptera: Staphyliniformia) with an evaluation of possible groundplan features in Staphylinidae. *Journal of Morphology*, 270, 1503–1523.
- Weide, D., Thayer, M. K., & Betz, O. (2014). Comparative morphology of the tentorium and hypopharyngeal-premental sclerites in sporophagous and non-sporophagous adult Aleocharinae (Coleoptera: Staphylinidae). *Acta Zoologica*, 95, 84–110.
- Wipfler, B., Machida, R., Müller, B., & Beutel, R. G. (2011). On the head morphology of Grylloblattodea (Insecta) and the systematic position of the order, with a new nomenclature for the head muscles of Dicondylia. *Systematic Entomology*, 36, 241–266.
- Yavorskaya, M., Beutel, R. G., & Polilov, A. (2017). Head morphology of the smallest beetles (Coleoptera: Ptiliidae) and the evolution of sporophagy within Staphyliniformia. *Arthropod Systematics & Phylogeny*, 75, 417–434.

How to cite this article: Luo X-Z, Antunes-Carvalho C, Wipfler B, Ribera I, Beutel RG. The cephalic morphology of the troglobiontic cholevine species *Troglocharinus ferrei* (Coleoptera, Leiodidae). *Journal of Morphology*. 2019;280: 1207–1221. <https://doi.org/10.1002/jmor.21025>

3.2 Study II

Profound head modifications in *Claviger testaceus* (Pselaphinae, Staphylinidae, Coleoptera) facilitate integration into communities of ants

Paweł Jałoszyński, **Xiao-Zhu Luo**, Rolf Georg Beutel

2020. *J. Morphol.* 281, 1072–1085. <https://doi.org/10.1002/jmor.21232>

Abstract: Clavigeritae is a group of obligate myrmecophiles of the rove beetle subfamily Pselaphinae (Staphylinidae). Some are blind and wingless, and all are believed to depend on ant hosts through feeding by trophallaxis. Phylogenetic hypotheses suggest that their ancestors, as are most pselaphines today, were free-living predators. Morphological alterations required to transform such beetles into extreme myrmecophiles were poorly understood. By studying the cephalic morphology of *Claviger testaceus*, we demonstrate that profound changes in all mouthpart components took place during this process, with a highly unusual connection of the maxillae to the hypopharynx, and formation of a uniquely transformed labium with a vestigial prementum. The primary sensory function of the modified maxillary and labial palps is reduced, and the ventral mouthparts transformed into a licking/‘sponging’ device. Many muscles have been reduced, in relation to the coleopteran groundplan or other staphylinoids. The head capsule contains voluminous glands whose appeasement secretions are crucial for the beetle survival in ant colonies. The brain, in turn, has been shifted into the neck region. The prepharyngeal dilator is composed of an entire series of bundles. However, the pharynx does not show any peculiar adaptations to taking up liquid food. We demonstrate that far-reaching cephalic modifications characterize *C. testaceus*, and that the development of appeasement glands and adaptation of the mouthparts to trophallaxis determine the head architecture of this extreme myrmecophile.

Conceptualization: P. Jałoszyński, R. G. Beutel

Visualization: P. Jałoszyński, **X. Z. Luo**

Writing-original draft: P. Jałoszyński, **X. Z. Luo**, R. G. Beutel

Writing-review & editing: P. Jałoszyński, **X. Z. Luo**, R. G. Beutel

Funding acquisition: P. Jałoszyński

Estimated own contribution: 25%

Profound head modifications in *Claviger testaceus* (Pselaphinae, Staphylinidae, Coleoptera) facilitate integration into communities of ants

Paweł Jałoszyński¹  | Xiao-Zhu Luo²  | Rolf Georg Beutel²

¹Museum of Natural History, University of Wrocław, Wrocław, Poland

²Institut für Zoologie und Evolutionsforschung, Friedrich-Schiller-Universität Jena, Jena, Germany

Correspondence

Paweł Jałoszyński, Museum of Natural History, University of Wrocław, Sienkiewicza 21, 50-335 Wrocław, Poland.
Email: scydaenus@yahoo.com

Funding information

AEI/FEDER, UE, Grant/Award Number: CGL2013-48950-C2

Abstract

Clavigeritae is a group of obligate myrmecophiles of the rove beetle subfamily Pselaphinae (Staphylinidae). Some are blind and wingless, and all are believed to depend on ant hosts through feeding by trophallaxis. Phylogenetic hypotheses suggest that their ancestors, as are most pselaphines today, were free-living predators. Morphological alterations required to transform such beetles into extreme myrmecophiles were poorly understood. By studying the cephalic morphology of *Claviger testaceus*, we demonstrate that profound changes in all mouthpart components took place during this process, with a highly unusual connection of the maxillae to the hypopharynx, and formation of a uniquely transformed labium with a vestigial prementum. The primary sensory function of the modified maxillary and labial palps is reduced, and the ventral mouthparts transformed into a licking/'sponging' device. Many muscles have been reduced, in relation to the coleopteran groundplan or other staphylinoids. The head capsule contains voluminous glands whose appeasement secretions are crucial for the beetle survival in ant colonies. The brain, in turn, has been shifted into the neck region. The prepharyngeal dilator is composed of an entire series of bundles. However, the pharynx does not show any peculiar adaptations to taking up liquid food. We demonstrate that far-reaching cephalic modifications characterize *C. testaceus*, and that the development of appeasement glands and adaptation of the mouthparts to trophallaxis determine the head architecture of this extreme myrmecophile.

KEYWORDS

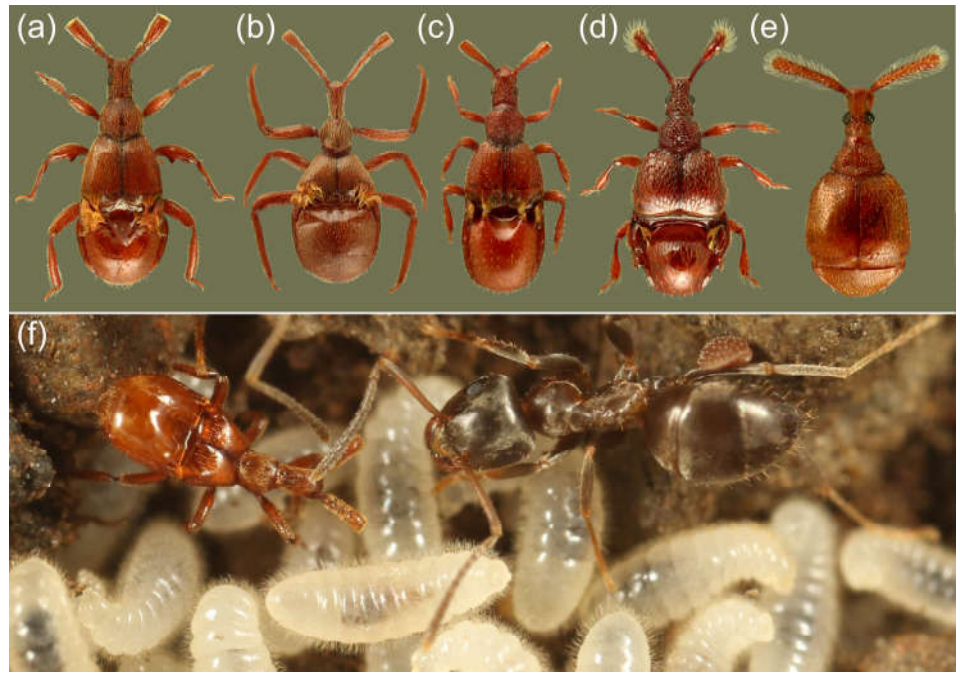
3D reconstruction, cephalic anatomy, micro-CT, obligate myrmecophily, trophallaxis

1 | INTRODUCTION

An estimated 10,000 arthropod species exploit resources associated with ant communities (Elmes, 1996). Among the most successful myrmecophiles are some lineages within Pselaphinae, a subfamily of rove beetles (Staphylinidae). Pselaphines exceed 10,000 described species (Thayer (2005), and later publications), and have an evolutionary history at least as long as that of ants (Parker, 2016a; Barden, 2017: ca. 100 million years; Yin, Parker, Cai, Huang, & Li, 2018; Yin,

Kurbatov, Cuccodoro, & Cai, 2019). They fulfil the synergistic ancestral preconditions for myrmecophily defined by Parker (2016b): predatory diet; microhabitats shared with ants; defensive morphology; a small body size; and an exposed abdomen with glandular structures. Pselaphines show also a great diversity of body forms and structures, reflecting their ecological plasticity (see Figures S1 and S2), which enabled them to reach remarkable abundance and species richness in terrestrial ecosystems. The supertribe Clavigeritae (Figure 1) of Pselaphinae comprises species that are all believed to be obligate

FIGURE 1 Diversity of extreme Clavigeritae myrmecophiles. (a) *Diartiger fossulatus* Sharp; (b) *Claviger apenninus* Baudi di Selve; (c) *Articerodes syriacus* (Saulcy); (d) *Cerylambus reticulatus* (Raffray); (e) *Disarthricerus integer* Raffray; and (f) *Claviger testaceus* Preysslér interacting with host *Lasius* sp. ant worker in larval chamber



myrmecophiles, and which developed the most intimate relationships with their hosts (Parker, 2016b). Some Clavigeritae are able to disperse actively; they have large eyes and long wings (Nomura, Sakchoowong, & Abd Ghani, 2008). Others, counted among the most extreme myrmecophiles, are blind, wingless, and helpless outside of ant colonies (Parker, 2016b). All clavigerite pselaphines share the 'myrmecophilous' groundplan (Figure 1a–f): mouthparts specialized to feed by trophallaxis (i.e., to take up liquid food regurgitated by ants); abdominal tergites IV–V fused and bearing specialized groups of setae (trichomes) associated with glands that secrete host appeasement compounds and trophallaxis stimulants; protective morphology that includes simplified and thickened antennae, partially reduced palps and tarsi; and a compound abdominal tergite that is heavily sclerotized to withstand the ant's grip whenever the beetle is carried by workers. The most thoroughly studied species is the European *C. testaceus* Preysslér (Figure 1f), well known to manipulate the host ant's behaviour to stimulate workers to regurgitate contents of their crops (Cammaerts, 1974, 1992). This species can be regarded as a model extreme myrmecophile.

Despite many scrupulous experiments and observations (Cammaerts, 1974, 1991, 1992, 1995, 1996, 1999), the modified mouthparts of *C. testaceus* were never studied in detail. Free-living pselaphine species are predatory on springtails or mites (e.g., Park, 1947; Engelmann, 1956; Schomann, Afflerbach, & Betz, 2008; see also Chandler (2001) for a summary), although scavenging on dead arthropods also seems possible (Figure S2e). They usually have elongate and dentate mandibles, long (often conspicuously so) maxillary palps and well-developed labial palps (e.g., Schomann et al., 2008; see also Figures S3 and S4). This is also the case in *Protopselaphus*, the sister group of Pselaphinae (Newton & Thayer, 1995), and is therefore clearly the plesiomorphic condition. Parker and Grimaldi ((2014), Figure 4a) place

Clavigeritae among the 'higher Pselaphinae', as sister group of Arhytodini + Pselaphini, with these two tribes sister to the 'tyrine lineage'. Pselaphini and tyrines are predatory (e.g., Schomann et al., 2008), Arhytodini are poorly investigated and their biology is not known. Later Parker (2016a) resolved Clavigeritae nested within Pselaphitae. The consistent clustering of Clavigeritae with the predominantly predatory Pselaphitae suggests that predatory habits are the ancestral condition, and that trophallaxis is a specialized adaptation. This also clearly conforms with conditions observed in *Protopselaphus* (Newton & Thayer, 1995).

In order to elucidate how intimate relationships between obligate clavigerite myrmecophiles and their host ants evolved, it is essential to understand functional morphology of inquiline. Behavioural interactions with host ants, including transport (Cammaerts, 1999; Leschen, 1991) and feeding (Cammaerts, 1992, 1996; Park, 1932), and chemical camouflage (Akino, 2002) of Clavigeritae attracted some attention. However, although the appeasement glands of *Claviger* were discovered over a century ago (Krüger, 1910; Wasmann, 1903), and later studied in detail (Cammaerts, 1974), no other internal cephalic structures have been described and illustrated for Clavigeritae. Even the mouthparts, frequently illustrated in taxonomic studies related to many other pselaphines (mostly because of a great diagnostic value of often conspicuously long and elaborate maxillary palps), for Clavigeritae are usually illustrated in undissected specimens, with only their externally exposed components visible (e.g., Baňar & Hlaváč, 2014; Hlaváč & Nakládal, 2016; Nomura et al., 2008). In one case, dissected mouthparts were illustrated, but only as line drawings, and did not include the epi- and hypopharyngeal structures (Besuchet, 1991). Using modern techniques, including μ -CT, we provide the first insight into the architecture of musculature, cephalic central nervous system, glands, alimentary canal and

skeletal structures of a pselaphine species, *C. testaceus*. Our study is focused on adaptations to trophallaxis, clearly a derived morphological, behavioural and physiological adaptation to life among ants. We compare mouthparts of *C. testaceus* with those of selected free-living pselaphines, and we identify structures whose function can be linked directly with trophallaxis, and in consequence, with myrmecophily. Because of an enormous morphological diversity, a large number of genera and tribes included in Pselaphinae, and the still poorly understood phylogeny, we do not attempt a detailed and formal reconstruction of the pselaphine morphological groundplan. Instead, we compare structures found in *C. testaceus* to the coleopteran groundplan (e.g., Beutel & Yavorskaya, 2019) and conditions found in less specialized staphylinoid beetles (e.g., Weide & Betz, 2009) including *Protopselaphus*, wherever relevant in the context of specialized feeding adaptations.

2 | MATERIALS AND METHODS

2.1 | Studied specimens

The species studied in detail is a blind obligate myrmecophile, *C. testaceus* Preyssl (Insecta: Coleoptera: Staphylinidae: Pselaphinae: Clavigeritae), an inquiline that is not naturally found outside ant colonies. Numerous beetles were collected near Prudnik ad Opole (SW Poland) in May 2019, in colonies of *Lasius* sp. found under stones by the first author. Specimens were preserved in FAE (10 ml 35% formalin, 5 ml glacial acetic acid, 85 ml absolute ethanol), and some in 75% ethanol. Dry-mounted specimens of the following Clavigeritae were examined by light microscopy, as examples of morphological diversity: *Articerodes syriacus* (Saulcy) (Israel), *Cerylambe reticulatus* (Raffray) (Vietnam), *Claviger apenninus* Baudi di Selve (Italy), *Claviger longicornis* Müller (Poland), *Diartiger fossulatus* Sharp (Japan), *Disarthricerus integer* Raffray (Malaysia), and several undetermined clavigerite species from South Africa, Madagascar, and New Caledonia (deposited in the Museum of Natural History, University of Wrocław, Poland, and in the private collection of the first author, Wrocław, Poland). Dissected mouthparts in transparent microscope slides of seven free-living Pselaphinae species were examined, illustrated and compared with exoskeletal structures found in *C. testaceus*: *Euplectus karstenii* (Reichenbach), *Trichonyx sulcicollis* (Reichenbach), *Brachygluta fossulata* (Reichenbach), *Bryaxis bulbifer* (Reichenbach), *Batrisodes venustus* (Reichenbach), *Tyrus mucronatus* (Panzer), and *Pselaphus heisei* Herbst (all collected in Poland; specimens deposited in the collection of the first author). Additionally, taxonomic literature was screened for illustrations of mouthparts of other Clavigeritae, to allow for more general conclusions.

2.2 | μ -CT and microtome sections

Beetles were transferred to acetone and then dried in a critical point dryer (Emitech K850, Quorum Technologies Ltd., Ashford, UK). μ -CT

scans were made at the Max Planck Institute für Menschheitsgeschichte (Jena, Germany) using a SkyScan 2211 (Bruker, Knotich, Belgium), with the following parameters: 70 kV voltage, 300 μ A current, 3.600 ms exposure time, rotation step 0.150, frame averaging on, random movement off, and filter assembly open. Projections were reconstructed by NRecon (Bruker) into JPG files with a voxel size of 0.68 μ m. Amira 6.1.1 (Thermo Fisher Scientific, Waltham, MA) and VG studio Max 2.0.5 (Volume Graphics, Heidelberg, Germany) were used for three-dimensional reconstructions and volume rendering. For microtome sectioning, one specimen of *Claviger* was embedded in araldite CY 212 (Agar Scientific, Stansted/Essex, UK). Sections were cut at 1 μ m intervals using a microtome HM 360 (Microm, Walldorf, Germany) equipped with a diamond knife, and stained with toluidine blue and pyronin G (Waldeck GmbH and Co.KG/Division Chroma, Münster, Germany). The sections are stored in the collection of the Phyletisches Museum, Jena, Germany. The μ -CT dataset is archived at the same institution and available upon request.

2.3 | Light microscopy

Specimens were observed under a Nikon SMZ1500 stereomicroscope. Dissected mouthparts, cleared briefly in 10% aqueous solution of sodium hydroxide, dehydrated in isopropanol and mounted in Canada balsam, were observed with a Nikon Eclipse Ni compound microscope. Photographs were taken with a Nikon Coolpix 4500 camera (habitus images; as stacks processed with Helicon Focus v. 6.8.0 (HeliconSoft Ltd.)), transparent structures were photographed with a Nikon D7500 camera mounted respectively on the stereo- and compound microscope. A Nikon Eclipse Ni compound microscope was also used to observe an undissected head of a freshly killed *C. testaceus* in a droplet of water, in dark field. Living pselaphines were photographed with a Canon 7D Mark II camera with a MP-E 65 mm lens, and an Olympus C-750UZ digital camera with a Raynox MSN-202 close-up lens; photographs are from archives of the first author.

2.4 | Scanning electron microscopy

Beetles were transferred from 75% to 99% ethanol for 15 min and air-dried. Some of them were macerated for 20–60 min in a warm 10% aqueous solution of NaOH, thoroughly washed in distilled water and dissected; isolated mouthparts were dehydrated in 99% ethanol and air-dried. Five beetles were dissected in order to make sure that the observed fusion of the maxillae with the hypopharynx is not an artefact. Entire beetles and dissected parts were mounted on scanning electron microscopy (SEM) stubs with carbon tabs, sputter-coated (Leica EM ACE600) with 20 nm of carbon and examined using a Helios Nanolab 450HP scanning electron microscope (FEI, Hillsboro, OR). Images were processed using CorelDraw Graphic Suite 2017; the following adjustments were made: overall brightness and contrast enhanced; background manually replaced with black; selected structures highlighted with manually applied colour.

2.5 | Terminology and measurements

Cephalic muscles were designated following the terminology of von K  ler (1963), with the exception of Mm. compressores epipharyngis (Mm. III). For this muscle, we followed Belkaceme (1991). Muscles are also homologized according to Wipfler, Machida, M  ller, and Beutel (2011), with homolog abbreviations added in parentheses after the designation of von K  ler (1963); for example, M44 - M. clypeobuccalis (Obu1). Muscles not mentioned in the morphological description are lacking. The length of the head capsule is measured in dorsal view, from the anterior clypeal margin to the posterior margin of vertex; width of head is maximum width of the anterior (exposed) part.

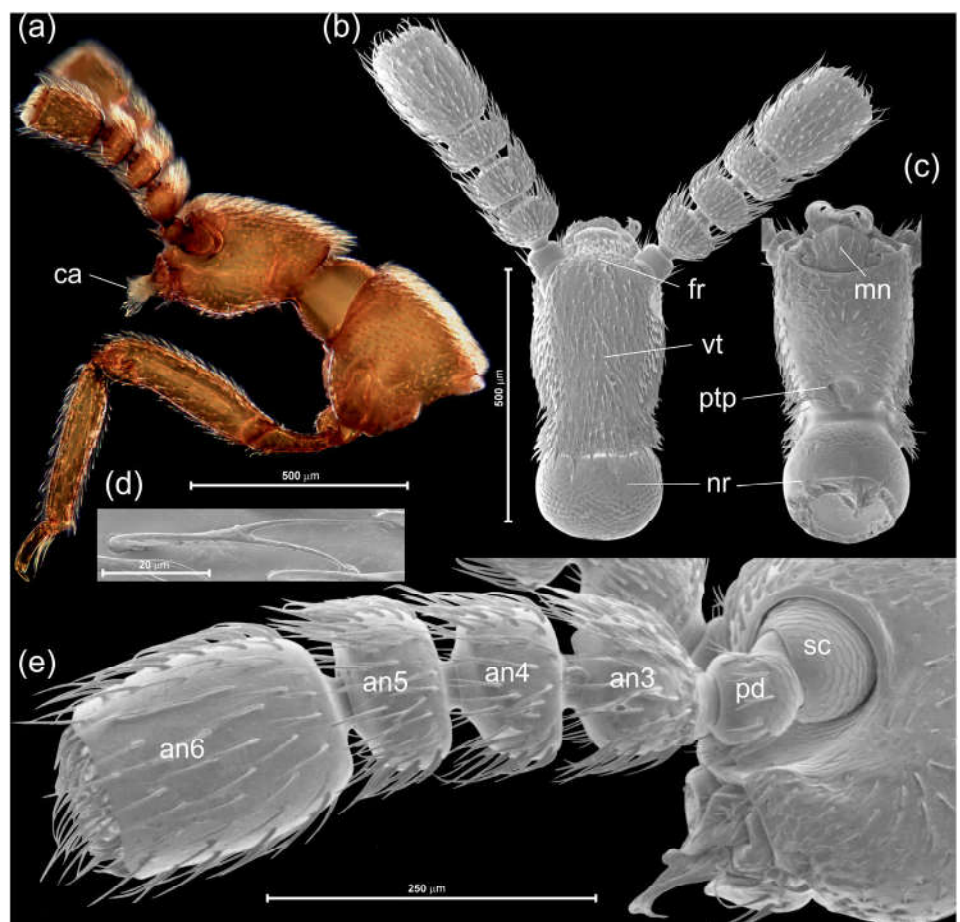
3 | RESULTS

3.1 | External head structures of *C. testaceus*

The head capsule (Figure 2a-c) is about 0.4 mm long and the maximum width is 0.25 mm. The coloration is light brown. The head is prognathous and appears cork-shaped in dorsal view (Figure 2b), truncated anteriorly with scarcely protruding mouthparts; it is distinctly bulging on the ventral side, but the main part is almost cylindrical; a

nearly hemispherical neck region is present posteriorly. Any traces of ecdysial sutures are lacking on the dorsal side; a clypeofrontal strengthening ridge is not recognizable externally; gular sutures are largely reduced and sutures delimiting the submentum are also missing. Dorsal foveae and ocelli are absent. The compound eyes are completely reduced, without recognizable external or internal traces. The clypeal region is almost vertically sloping between the anterior edges of the large antennal fossae, which are enclosed by a distinct smooth bead except for the anterolateral margin; a slightly concave oblique smooth area anterolaterad the antennal fossa is continuous with the anterolateral clypeal region; the anterior margin of the clypeus is a sharp edge, separating it very distinctly from the labrum. A broad and short anteromedian emargination accommodates the prelabium (i.e., mentum and vestigial prementum) on the ventral side of the head (Figure 2c); a distinct smooth bead is present along its margin and continues anterolaterally. Dorsally and laterally the neck region is separated from the main cephalic part by a sharp occipital crest, which is obliterated ventrolaterally. The head capsule is slightly constricted laterally anterior to the crest; paired ventral foveae are present in this cephalic region; they appear like invagination sites laterally and are nearly confluent anteromedially. The main part of the head bears a relatively regular vestiture of medium-length bifurcate setae (ca. 30 μm) (Figure 2d); the length and density increases at the postoccipital crest; the surface between the setae appears shiny. The

FIGURE 2 Cephalic morphology of *C. testaceus*, black field light micrograph (a) and scanning electron microscopy (SEM) images (b-e). (a) Head and prothorax in lateral view (preparation in water, showing projecting capillary mouthpart structures); (b) head in dorsal view; (c) head in ventral view; (d) bifurcate setae on vertex; (e) left antenna in lateral view. an3-6, antennomere 3-6; ca, capillary apparatus; fr, frons; mn, mentum; nr, neck region; pd, pedicel; ptp, posterior tentorial pit; sc, scape; vt, vertex



posteroventral and posterolateral regions of the main cephalic part are smooth and glabrous; the hemispherical 'neck' region lacks setae; most parts of its surface display a distinct reticulate pattern, but it is smooth posteroventrally. Short fissure-shaped vestiges of gular sutures are recognizable ventrolaterally at the posterior cephalic margin.

3.2 | Internal skeletal structures

The tentorium (Figure 5a) is distinctly reduced, with only a pair of stick-like arms arising in the posterior contracted area of the head capsule; the areas of origin of these structures comprising the posterior and dorsal arms are almost adjacent to each other on the ventral side, but they diverge anteriorly to insert on the dorsolateral head region, thus forming a V-shaped structure; the dorsal arms are apically fused with the dorsal wall of the head capsule; the areas of fusion are visible as shallow dorsolateral depressions (reduced 'vertexal foveae' of Chandler (2001)). The ventral posterior tentorial pits (gular foveae of Chandler (2001)) appear as a medially fused invagination site. Anterior tentorial grooves, anterior arms, the tentorial bridge and gular ridges are absent. The circum-antennal ridges are strongly developed and form round and deep antennal fossae. Circumocular ridges are absent.

3.3 | Antennae

The club-shaped antennae (Figure 2a,b,e) comprise only six compact and wide segments; articulatory membranes are not visible. With about 0.35 mm, the antennae are subequal to the total head length. The dorsomesal part of the oblique antennal foramen is visible in dorsal view, and also a small part of the scapus, which is short and hemispherical and inserted into the foramen in a ball-and-socket manner; the surface structure is scaly; setae are lacking. The pedicellus has a curved basal part and a more or less cylindrical distal part, which is about as wide as long; the surface of the basal portion is scaly; a ring of double setae is present at the border between both regions. The four flagellomeres are distinctly enlarged, with a smooth and fairly narrow basal peduncle and a strongly widened distal part. Flagellomeres 1–3 are distinctly wider than long; a vestiture of simple setae is present on the outer surface whereas the nearly flat apical surface is glabrous; the setae are slightly longer than those of the head capsule. The cylindrical apical antennomere is slightly shorter than the three preceding ones combined; it also bears a regular vestiture of setae; the truncate apex is densely covered with setae.

Musculature (Figure 5b,c) (for a list of all cephalic muscles of *C. testaceus* and their functions, see Table 1; for comparison to previously studied species of Staphylinodea see Table S1): M1 - *M. tentorioscapalis anterior* (0an1), origin (O): large area of the lower tentorial region, insertion (I): anteroventral margin of the scapus; M2 - *M. tentorioscapalis posterior* (0an2), O: anterodorsal wall of the head capsule, directly in front of the tentorium, I: posterodorsal margin

of the scapus; M4 - *M. tentorioscapalis medialis* (0an4), O: upper region of the tentorium and anterodorsal wall of the head capsule, in front of the tentorium, laterad m2, I: medioventrally on the basal scapal margin; M5 - *M. scapopedicellaris lateralis* (0an6), O: mesal wall of the scapus, I: dorsal margin of the pedicellar base; M6 - *M. scapopedicellaris medialis* (0an7), O: lateral wall of the scapus, I: ventrally on the median margin of the pedicellar base.

3.4 | Labrum

The labrum (Figure 3a–c), which is distinctly separated from the clypeus, is only about one-third as wide as the strongly pronounced anterior clypeal edge; viewed from above it appears transverse and short, with rounded anterolateral edges; however, the anterior edge is strongly extended ventrad, thus forming a large shield-like structure, slightly concave and covered with fairly large-scale-like surface structures. Setae are absent from the strongly sclerotized dorsal surface, the anterior edge, and the shield-like part, which is only visible in frontal view; however, a pair of very strongly developed setae are inserted on the ventral side in an anterolateral notch. Long apodeme-like tormae with apical muscle discs originate from the posterolateral labral edges.

Musculature (Figure 5h): M7 - *M. labroepipharyngalis* (0lb5); O: dorsal wall of the labrum, I: anteriormost area of the epipharynx.

3.5 | Mandibles

A heavily sclerotized shield-like structure formed by the mandibles (Figures 3a–c and 4c,d) and labrum covers the ventral mouthparts. The mandibles are characterized by a weakly developed apical region and a distinctly simplified molar area; only a single small and blunt apical tooth is present, followed by a simple, slightly rounded subapical edge. The ventral surface is almost entirely flat; the small ventral part of the molar area is mesally delimited by a rounded furrow; a dense fringe of medium-length microtrichia (ca. 20 µm) is present along the mesal edge; the surface of the ventral side is entirely smooth and glabrous. The dorsal part of the molar area is a slightly concave field densely covered with medium-length microtrichia. A somewhat irregular prominent elevation of the lateral dorsal surface is anterolaterally followed by a deep concavity with several very stout setae of about 25 µm length. The dorsal mandibular base is deeply emarginated. A distinct rounded process of the internal face of the lateralmost clypeal region overlaps with the mandibular base laterally. The adductor and abductor tendons are well developed and attached very close to the mesal and lateral edges of the mandibular base, respectively.

Musculature (Figure 5d,e): M11 - *M. craniomandibularis internus* (0md1), O: middle region of the lateral wall of the head capsule, anterior to the tentorium, I: close to the mesal mandibular base with the adductor tendon; M12 - *M. craniomandibularis externus* (0md3), O: ventral area of the head capsule, ventrad the origin of m11 and laterad the ventral tentorial base; I: with the abductor tendon on the

TABLE 1 Cephalic muscles of *C. testaceus*

Muscle	Symbol	Function
M. tentorioscapalis anterior	M1 (0an1)	Depressor and rotator of antenna
M. tentorioscapalis posterior	M2 (0an2)	Levator, retractor and rotator of antenna
M. tentorioscapalis medialis	M4 (0an4)	Depressor of antenna
M. scapopedicellaris lateralis	M5 (0an6)	Extensor and levator of flagellum
M. scapopedicellaris medialis	M6 (0an7)	Flexor and depressor of flagellum
M. labroepipharyngalis	M7 (0lb5)	Levator of epipharynx
M. craniomandibularis internus	M11 (0md1)	Adductor of mandible
M. craniomandibularis externus	M12 (0md3)	Abductor of mandible
M. hypopharyngomandibularis	M13 (0md4)	Proprioreceptor
M. craniocardinalis externus	M15 (0mx1)	Extensor of cardo
M. tentoriocardinalis	M17 (0mx3)	Flexor of cardo and entire maxilla
M. tentoriestipitalis	M18 (0mx4/0mx5)	Adductor of stipes and lacinia
M. craniolacinalis	M19? (0mx2)	Adductor of stipes and lacinia, retractor of maxilla
M. tentoriopraementalis superior	M30 (0la6)	Retractor of prementum
M. frontohypopharyngalis	M41 (0hy1)	Levator of hypopharynx, dilator of anatomical mouth opening
M. clypeopalatalis	M43 (0ci1)	Dilator of prepharynx
M. clypeobuccalis	M44 (0bu1)	Dilator of posteriormost prepharynx and anatomical mouth
M. frontobuccalis anterior	M45 (0bu2)	Dorsal dilator of anatomical mouth and anterior pharynx
M. frontobuccalis posterior	M46 (0bu3)	Dorsal dilator of middle section of pharynx
M. tentoriobuccalis anterior	M48 (0bu5)	Ventral dilator of prepharynx
M. tentoriobuccalis posterior	M50 (0bu6)	Ventral dilator of anterior pharynx
Mm. compressores epipharyngis	MmIII	Compressors of epipharynx

lateral mandibular base; M13 - M. hypopharyngomandibularis (0md4), very thin, O: ventral base of the tentorium, I: mesal area of the mandibular base, close to the adductor tendon.

3.6 | Maxillae

The maxillary groove (= fossa maxillaris; see, e.g., Dressler & Beutel, 2010; Beutel & Yavorskaya, 2019) is lacking; the small maxillae (Figures 3a–c and 4e) are inserted between the lateral base of the mentum and the lateral edge of the anteromedian emargination of the ventral wall of the head capsule. The well-developed cardo is roughly semicircular and bears a distinct internal process with a lateral and a mesal branch; setae are absent. The stipes is small and a subdivision is not recognizable; a conspicuous protuberance close to the lateral base bears a seta; an additional single seta is inserted proximad the base of the galea. The small palp (Figure 4e,f) appears undivided and S-shaped, with a wide-meshed reticulate surface structure, a strongly developed apical appendage, and three long apical digitiform sensilla; a transverse sclerite possibly representing a palpifer is recognizable in dorsal view; an additional elongate and curved structure is present mesad this sclerite. The lacinia is a

relatively large, roughly triangular structure and very distinctly separated from the stipes; along its mesal margin, it bears a very dense fringe of long flexible setae of about 70 µm length; the lacinia is ventrally connected to the hypopharynx (Figure 4h). The galea is connected to the distal stipital edge; it is also well-developed, elongate and quadrangular, and equipped with a dense fringe of long setae along its distal margin.

Musculature (Figure 5f,g): M15 - M. craniocardinalis externus (0mx1), O: anterolateral area of the ventral capsule; I: lateral branch of the cardinal process; M17 - M. tentoriocardinalis (0mx3), O: anterolateral area of the ventral head capsule, in front of the ventral tentorial base; I: mesal branch of the cardinal process; M18 - M. tentoriestipitalis (0mx4/0mx5), O: ventral side of basal tentorial part; I: basal area of stipes; M19? - M. craniolacinalis (0mx2), O: ventral wall of head capsule, in front of the ventral tentorial base; I: likely on a membrane attached to the lacinial base, but precise insertion site not recognizable on available data sets.

3.7 | Labium

The submentum is completely fused with the ventral wall of the head capsule. The large, plate-like mentum (Figures 3c and 4g) is inserted

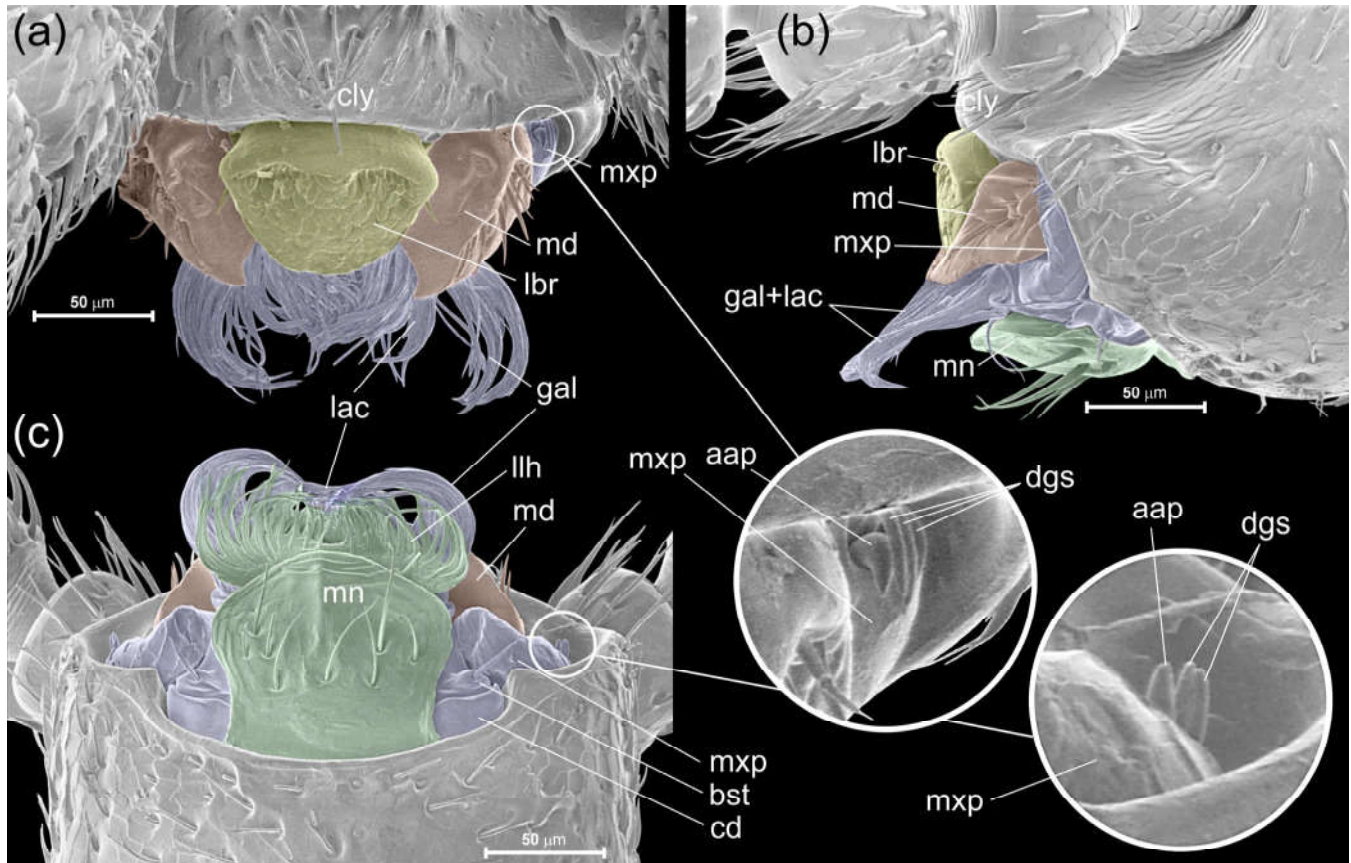


FIGURE 3 Cephalic morphology of *C. testaceus*, scanning electron microscopy (SEM) images of undissected mouthparts in anterodorsal (a), lateral (b), and ventral (c) view. aap, apical appendage; bst, basistipes; cd, cardo; cly, clypeus; dgs, digitiform sensilla; gal, galea; lac, lacinia; lbr, labrum; llh, lateral lobes of hypopharynx; md, mandible; mn, mentum; mxp, maxillary palp

into the anteromedian emargination and internally connected with the submental region by a membranous fold; it is slightly diverging anteriorly, with rounded anterolateral margins; the anterior margin is distinctly convex. The largely concealed prementum is vestigial and lacks labial palps.

Musculature (Figure 5e,h): M30 - *M. tentoriopraementalis superior* (Ola6), O: median area of the vestigial submentum, I: parasagittally on the dorsal region of the prelabium (Figure 5h,e) (precise site not recognizable with available data).

3.8 | Epipharynx and hypopharynx

The anteriormost epipharynx (Figure 4a,b), that is, the ventral side of the labrum, is sclerotized, smooth and glabrous; two distinct transverse ridges are present laterally, one of them long and one short; a spindle-shaped distinctly delimited median region bears a pair of sensorial papillae, each of them with a distinct pore. The middle epipharyngeal region, which forms the roof of the laterally open cibarium, is anteriorly delimited by a semicircular sclerotized bead; it is flat, semimembranous, and bears a regular and dense vestiture of short microtrichia (ca. 5 μm); a distinct median bulge or process with longer microtrichia is absent; posteriorly this

epipharyngeal section is delimited by a posteriorly directed semi-circular sclerotized bar, between the basal region of the tormae; the sclerotized area is slender laterally; the broader median part bears three deep pits with setae inserted in them; a median group of longer microtrichia (ca. 8 μm) is present at the posterior margin. The posterior epipharynx is laterally fused with the posterior hypopharynx thus forming the roof of an elongate prepharyngeal tube. The anterior hypopharynx (Figure 4h) forms a structural and functional unit with the prelabium; its anteromedian region forms a pair of lateral hypopharyngeal lobes densely set with long trichia.

Musculature (Figure 5h): M41 - *M. frontohypopharyngalis* (Ohy1), O: posterodorsal area of the head capsule, anterior to the neck region, I: laterad the anatomical mouth; M43 - *M. clypeopalatalis* (Oci1), two subcomponents, M43a with two bundles, M43b with a long series of bundles, O: on the anterodorsal wall of the head capsule (M43a) and on the frontal area including the median region between the antennal sockets (M43b), I: dorsal wall of middle epipharyngeal region (M43a) and dorsal wall of prepharyngeal tube (M43b); M44 - *M. clypeobuccalis* (Obu1), three closely adjacent bundles immediately anterior to the anatomical mouth, between insertion sites of M41, O: posterior area of the frontal region, I: dorsally on the prepharynx immediately anterad the anatomical mouth.

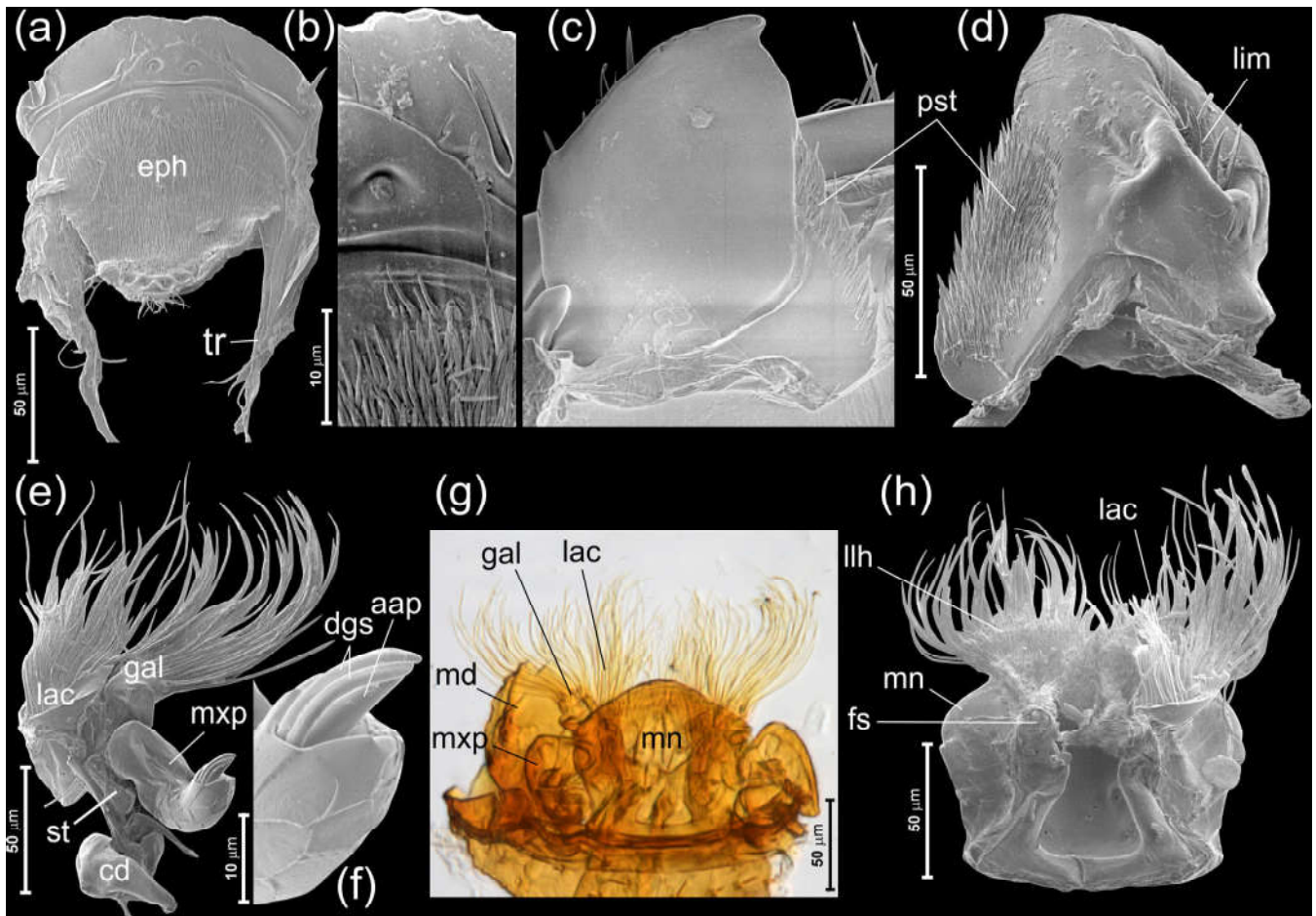


FIGURE 4 Cephalic morphology of *C. testaceus*, scanning electron microscopy (SEM) images (a–f,h) and light micrograph (g) of dissected mouthparts. (a) Labrum in ventral view; (b) anterior sublateral area of epipharynx; right mandible in ventral (c) and dorsal (d) views; (e) left maxilla in dorsal view; (f) apex of left maxillary palp in ventral view; labium, mandible and maxilla in ventral view; (g) labio-maxillary complex and right mandible in ventral view; (h) labio-maxillary complex in ventral view, with right maxilla torn off. aap, apical appendage; cd, cardo; dgs, digitoform sensilla; eph, epipharyngeal microtrichial field; fs, fusion site of lacinia; gal, galea; lac, lacinia; lim, lateral impression; llh, lateral lobe of hypopharynx; mn, mentum; mxp, maxillary palp; pst, microtrichial field on prostheca; st, stipes; tr, torva

3.9 | Prepharynx and pharynx

The anatomical mouth, that is, the border between the prepharynx and the pharynx (e.g., Beutel, Friedrich, Yang, & Ge, 2013), is marked by the position of the frontal ganglion. An elongate, closed prepharyngeal tube is formed by lateral fusion of the posterior epipharynx and hypopharynx. In cross section, this prepharynx appears heart-shaped; it is ventrally rounded and sclerotized, and a median invagination (for muscular insertion) is present on the flexible dorsal side. The pharynx (Figure 5h) is mostly enclosed by the cerebrum and suboesophageal complex, and posteriorly distinctly narrowed. The pharyngeal lumen appears round to oval in cross section. Longitudinal pharyngeal folds are recognizable but indistinct.

Musculature (Figure 5h): M45 - *M. frontobuccalis anterior* (Obu2), vertically oriented, O: middle region of the dorsal wall of the head capsule, I: dorsal pharyngeal wall; M46 - *M. frontobuccalis posterior* (Obu3), O: middle region of the vertex, posterior to M45 and laterad M41, I: dorsal pharyngeal wall; M48 - *M. tentoriobuccalis anterior*

(Obu5) (for a discussion of the homology of this muscle and *M. tentoriohypopharyngalis* (M42), see Beutel, Kristensen, and Pohl (2009)), O: ventral tentorial base, I: ventral prepharyngeal wall; M50 - *M. tentoriobuccalis posterior* (Obu6), vertically oriented, O: ventrally on the middle region of the head capsule, I: ventral wall of the precerebral pharynx; MmIII-Mm. compressores epipharyngis, numerous transverse bundles on the posterior epipharynx.

3.10 | Nervous system

The brain (Figure 6a,b) is of medium size compared to the entire volume of the head and located in the posterodorsal cephalic area, occupying a large portion of the neck region; it is constricted in the area of the occipital crest; anteriorly it almost reaches the tentorial arms. The ventral side of the suboesophageal complex (Figure 6a,b) is very close to the ventral wall of the head capsule; the posterior part is distinctly enlarged and protrudes from the cephalic lumen. The protocerebrum lacks optic neuropils,

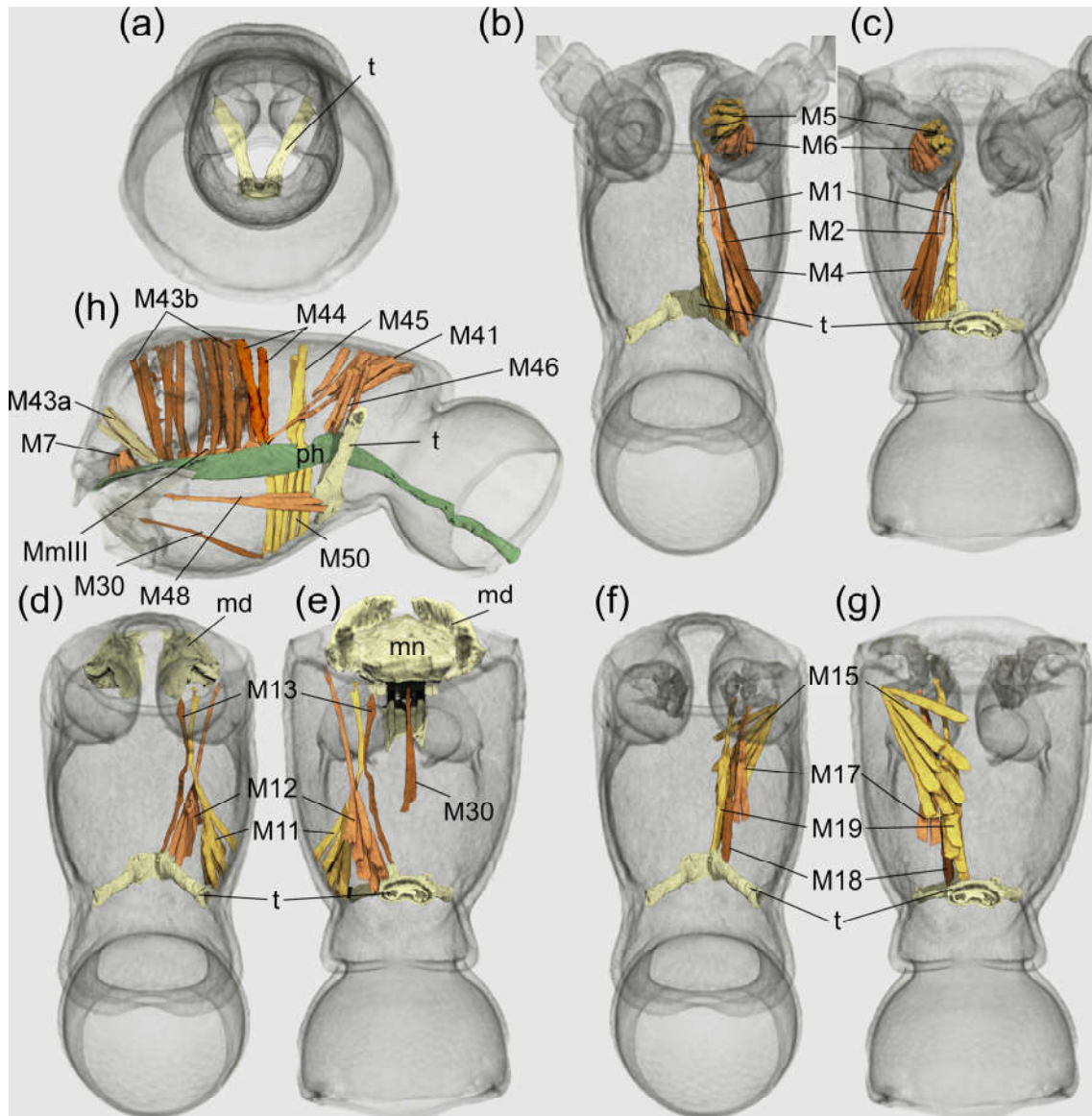


FIGURE 5 Cephalic morphology of *C. testaceus*, microcomputed tomography (μ -CT) reconstructions of tentorium in caudal view (a); antennal muscles in dorsal (b) and ventral (c) views; mandibular muscles in dorsal view (d); mandibular and labial muscles in ventral view (e); maxillary muscles in dorsal (f) and ventral (g) view; epi- and hypopharyngeal musculature, and muscles associated with cephalic section of alimentary tract in lateral view (h). M1, M. tentorioscapalis anterior; M2, M. tentorioscapalis posterior; M4, M. tentorioscapalis medialis; M5, M. scapopedicellaris lateralis; M6, M. scapopedicellaris medialis; M7, M. labroepipharyngalis; M11, M. craniomandibularis internus; M12, M. craniomandibularis externus; M13, M. hypopharyngomandibularis; M15, M. craniocardinalis externus; M17, M. tentoriocardinalis; M18, M. tentoriostipitalis; M19, M. craniolacinalis; M30, M. tentoriopraementalis superior; M30, M. tentoriopraementalis superior; M41, M. frontohypopharyngalis; M43, M. clypeopalatalis; M44, M. clypeobuccalis; M45, M. frontobuccalis anterior; M46, M. frontobuccalis posterior; M48, M. tentoriobuccalis anterior; M50, M. tentoriobuccalis posterior; md, mandible; MmIII, Mm. compressores epipharyngis; mn, mentum; t, tentorium

whereas the deutocerebral antennal nerves are well developed. The frontal ganglion is located in the middle region of the head; it is posteriorly connected to the brain by the frontal connectives.

3.11 | Glands

Tubular glands (Figure 6c,d; and schematically in Figure 6e) are strongly developed in the anterior region of the head and occupy a considerable

portion of this area. Several pairs extend from the middle cephalic region in front of the tentorial arms to the base of the maxillae and hypopharynx. Connecting ducts open in a pair of anterior labral impressions and in the lateral impression on each mandible (Figure 6e).

4 | DISCUSSION

It was long known that individuals of *C. testaceus* accept food directly from ant workers, and that regurgitation is triggered by a

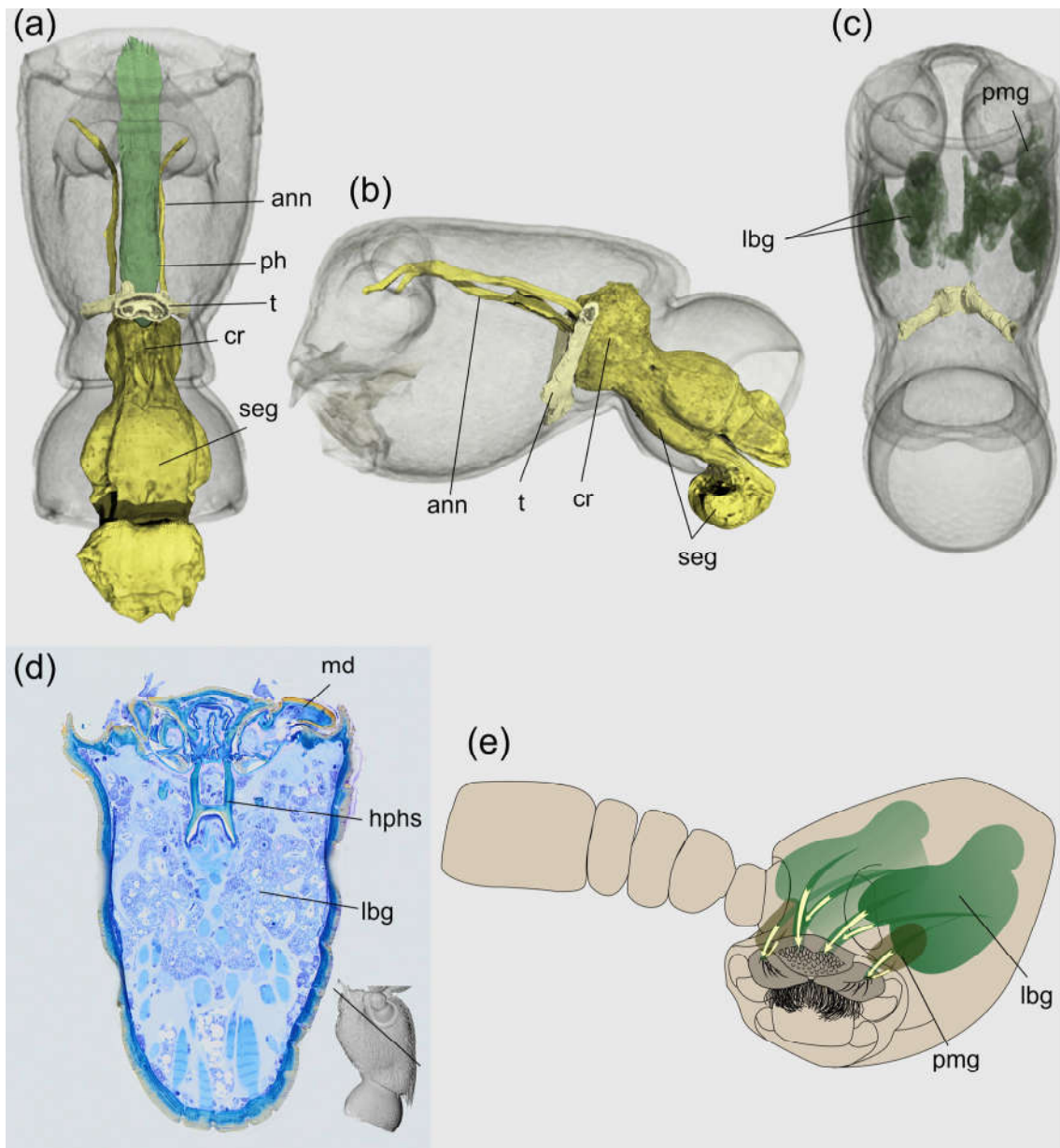


FIGURE 6 Cephalic morphology of *C. testaceus*, microcomputed tomography (μ -CT) reconstructions of central nervous system and pharynx (a,b), and cephalic glands (c–e); histological section of head (inlet showing the plane of section) (d); schematic arrangement of appeasement glands and their connecting ducts, combined from our results and Cammaerts (1974) (e). ann, antennal nerve; cr, cerebrum (brain); hphs, hypopharyngeal suspensorium; lbg, clusters of labral glands; md, mandible; ph, pharynx; pmg, clusters of postmandibular glands; seg, suboesophageal ganglia; t, tentorium

physical contact between beetles and ants, made possible by secretions produced by cephalic and abdominal glands of the beetles (Cammaerts, 1991, 1992, 1995, 1996). Many small beetles evolved special protective mechanisms to reduce contacts with aggressive predators, for instance size reduction of the head (Corylophidae: Polilov and Beutel (2010)), or modifications that allow to conceal the head on the ventral side of the body or to retract it into the prothorax (Clambidae: (Anton, Yavorskaya, & Beutel, 2016); some Leiodidae: (Park, Leschen, & Ahn, 2014); some Scydmaeninae: (Jałoszyński, 2013); and Histeridae, including

myrmecophiles, e.g., Parker, 2016b). In contrast, the elongate head of *Claviger* is exposed to contacts with ants. All pselaphines and *Protopselaphus* (Newton & Thayer, 1995) have exposed heads, except for a short part of the neck region that is retracted into the prothorax. Among Pselaphini, which include taxa phylogenetically close to Clavigeritae, the head is distinctly elongate (examples are shown in Figure S1b,c). *Claviger* clearly uses variations of the subfamily groundplan, with many modifications to facilitate trophallaxis.

Our results demonstrate that the mouthparts of *Claviger* are well adapted to frequent contacts with the sharp mandibles of ants, as

there are no projecting components that could be accidentally damaged during feeding. This is in clear contrast to most other Pselaphinae, which have large, exposed mandibles, tetramerous and long maxillary palps (e.g., Figures S1c, S3, and S4), and dimerous labial palps inserted on a well-developed prementum (e.g., Figures S3b,d,g and S4b,d). The mouthparts of *Claviger* strongly deviate from those of free-living beetles (e.g., Antunes-Carvalho et al., 2017; Beutel & Yavorskaya, 2019; Newton & Thayer, 1995), and also from those of myrmecophilous non-Clavigeritae pselaphines. The labrum bears a pair of openings for the labral glands, whose secretion was previously found to attract ants and to trigger regurgitation (Cammaerts, 1974). The scale-like microsculpture likely facilitates spreading of the secretion onto the entire anterior labral surface by means of capillary forces. As the labral musculature consists of only internal bundles, the entire structure can be moved only passively. We interpret the shape and structure of the labrum as being well suited to present the glandular secretion to approaching ants and to transfer liquids into the oral cavity, by capillary forces created by the microtrichial field on the anterior epipharynx.

The mandibles form a functional complex with the labrum: together they form a heavily sclerotized shield that covers the more delicate ventral mouthparts and presumably protects them during the frequent contacts with ants' mandibles. The lateral mandibular impressions bear glandular openings and deliver appeasement secretions to ants (as demonstrated by Cammaerts, 1974, 1992). The microtrichial fields of the prostheca suggest that liquids can be also transferred into the oral cavity in this manner. The mandibles of *Claviger* are conspicuously short and their muscles weakly developed. Even the adductor (M11), typically the most voluminous and most powerful muscle of the head in Coleoptera (e.g., Antunes-Carvalho et al., 2017; Dressler & Beutel, 2010; Weide & Betz, 2009), is strikingly small in *Claviger* and composed of only few bundles. In predatory pselaphines, the long and often toothed mandibles (Figures S3a,c,e and S4a,c,e,g), when closed, strongly project from under the labrum and overlap or cross in the median line (e.g., Schomann et al., 2008). In *Claviger*, the labrum covers most of their mesal edges, even when the mandibles are extended. The primary function in beetles with sharp mesal mandibular edges, that is, cutting, is clearly obsolete in *Claviger*.

The maxillary palps are strongly transformed, each composed of one only segment, and resting permanently in a lateral concavity of the buccal region. In *Protopselaphus* (Newton & Thayer, 1995, figure 4) and predatory pselaphines, the long maxillary palps are four-segmented (Figures S3b,d,f and S4b,d,f,g), and in some species participate in catching springtails, as demonstrated by Schomann et al. (2008). They also show a tendency to extreme elongation, for instance in members of Pselaphini (Figures S1b,c and S4g). It is plausible that once the ancestor of *Claviger* shifted from predatory feeding to trophallaxis, involvement of the palps in catching prey was no longer required. It has been proposed that myrmecophilous habits promote shortening of the maxillary palps to prevent possible damage during contacts with aggressive ants (Parker, 2016b). Even though the palps of *Claviger* have become the most vestigial known among beetles, their sensory function has been at least partly preserved. The palps

are recurved exposing the sensory apical appendage and digitiform sensilla, and when directed forward they are able to receive tactile or chemical stimuli. However, while the maxillary palps are long-range sense organs in free-living pselaphines, they have been transformed into short-range sensors in *Claviger*, strategically situated near the mandibular glandular impressions that are crucial for the trophallaxis. The maxilla is equipped with a set of only four muscles that adduct the cardo, stipes, and lacinia, and protract, adduct and retract the entire maxilla. Muscles of the endite lobes are missing, for instance M20, but their loss is common among many unrelated non-myrmecophilous beetles (Anton & Beutel, 2004, 2006, 2012; Antunes-Carvalho et al., 2017; Dressler & Beutel, 2010; Weide & Betz, 2009), and also all palp muscles. The function of the maxillae is integrated with that of the labrum and mandibles. The extremely long and dense distal setae of the lacinia and galea, projecting far beyond the mandibles, form a licking/'sponging' capillary apparatus, which is lacking in all beetles with predacious or fungivorous feeding habits (Beutel & Yavorskaya, 2019). A small ventral area of the lacinia is fused with the hypopharynx, a modification unknown in any other beetles (e.g., Beutel & Yavorskaya, 2019). Dissections of seven free-living pselaphine species (illustrated in Figures S3 and S4) revealed in each case that the lacinia is not fused or connected with the hypopharynx. This unique fusion in *Claviger* may align all the capillary elements in a certain arrangement, even when the maxillae are moved in relation to other structures, to ensure efficient uptake of liquids. Moreover, the site of fusion located on a relatively small and flexible membranous area creates an additional fulcrum. This presumably changes the lever system of sclerotized maxillary structures and modulates their movements. A mechanical modelling study may be required to address this interesting question.

The labium of *Claviger* is highly modified. The palps are absent and the prementum is vestigial, recognizable only by the presence of M30, which in beetles inserts on the prementum and functions as one of its retractors (e.g., Anton & Beutel, 2004; Weide & Betz, 2009). The only other muscle indirectly associated with the labium in *Claviger* is the hypopharyngeal levator and dilator of the anatomical mouth opening (M41). In contrast to this, three or four pairs of labial muscles are usually present in Coleoptera that have a fully developed labium (e.g., Anton & Beutel, 2004; Antunes-Carvalho et al., 2017; Weide & Betz, 2009), underlining the profoundness of the modifications in *Claviger*. The extremely long setae of the lateral lobes of the hypopharynx are probably suitable for taking up regurgitates. This setal complex of the mouthparts is best visible in Figure 2a; the flexible fringes of the maxillae and the lateral hypopharyngeal lobes project far beyond the mandibles. The mouthparts of the recently discovered early Eocene (50–52 Ma) *Protoclaviger*, assigned to stem-group Clavigeritae, look similar in lateral view (illustrated in Parker and Grimaldi (2014)), demonstrating that this morphological modification has a long evolutionary history.

Far-reaching modifications of the anterior section of the alimentary tract were described in some beetles that take up liquid food in large quantities. An example is the system of pharyngeal valves found in larvae of *Cephennium* (Staphylinidae: Scydmaeninae), which feed on

liquefied tissues of mites. This innovation may play a role in synchronizing the transfer of food from each pharyngeal section into the next one (Jałoszyński & Beutel, 2012). In *Claviger*, we found only one peculiarity in this region: the prepharyngeal dilator *M. clypeopalatalis* is distinctly increased in size compared to other staphylinoid beetles (Weide & Betz, 2009, figure 1; Antunes-Carvalho et al., 2017); it is composed of an entire series of bundles. Aside from this, the prepharynx and pharynx do not show specializations facilitating the transport of liquid food. Modifications are also lacking in adults of *Cephennium*, which feed in the same manner as the larvae. This shows that an efficient transfer of liquids can be maintained without major changes to the anterior digestive tract (Jałoszyński & Beutel, 2012). Similarly, it seems that no changes of the pharyngeal complex were required in the ancestral lineage of Clavigeritae to adopt trophallaxis.

It appears that the reduced primary sensory functions of the palps of Clavigeritae are partly compensated by adaptations of the antennae. The antennae of Clavigeritae are always strongly modified, apically broadening, and with only three to six antennomeres (Parker, 2016b), somewhat similar to conditions occurring in the myrmecophilous paussines of Carabidae (e.g., Geiselhardt, Peschke, & Nagel, 2007). In contrast, filiform antennae with 11 antennomeres belong to the groundplan of crown-group Coleoptera and Pselaphinae (Beutel & Hörnschemeyer, 2008; Newton & Thayer, 1995). The scape and pedicel of *Claviger*, segments crucial for antennal movements, are the smallest. The scape is subglobose and only a small portion is exposed, whereas it is most commonly elongate and largely exposed in other pselaphines and also in *Protopselaphus* (Newton & Thayer, 1995, figure 6). The flagellomeres of *Claviger*, although reduced in number, are enlarged, which increases their sensory surface covered with sensilla trichodea. Additionally, the modified apex of the terminal segment bears a large sensory/glandular setose field enhancing the sensorial apparatus. Despite of the small size of the scapus and the reduced number of flagellomeres, the movability of the antennae is fully retained, with a well-developed set of three extrinsic muscles, and two additional intrinsic bundles moving the pedicel.

Since they live inside ant colonies, and specialized on trophallaxis, *Claviger* beetles do not need to detect escaping prey or test surrounding objects for their edibility, which are typical functions of maxillary and labial palps in beetles. As the conditions inside ant colonies promoted the far-reaching reduction of palps, it is likely that the eyeless *Claviger* mostly relies on the antennae to recognize ants as food donors, in order to stimulate the regurgitation at the right moment. The set of detectors (antennae), stimulators (glands), and food uptake devices (the capillary mouthpart complex) constitute the core of myrmecophilous adaptations of the head of *Claviger*.

Cammaerts (1974) found several separate pairs of exocrine glands inside the head of *Claviger*: mandibular, mandibulo-maxillary, external and internal labral, and postantennal clusters. The most important in stimulating trophallaxis are the labral glands that discharge onto the anterior surface of the labrum, and, to a lesser extent, the lateral concavities of the mandibles (Cammaerts, 1992). We found interconnected groups of tubular glands that almost completely fill the

space between other organs in the anterior head region, making it difficult to define individual clusters. The general arrangement is similar to that found by Cammaerts (1974), with the largest volume occupied by the labral-postmandibular clusters, which discharge (via connecting ducts) their secretions onto the labrum and mandibles. No reservoirs were found that would allow secretions to be stored until needed and discharged in large quantities. This may explain the large size of the glands, enabling them to produce enough secretion to satisfy ants, and why the abdominal glands serve the same purpose, that is, to co-stimulate regurgitation, even though ants regurgitate onto the beetle's abdomen, as observed by Cammaerts (1992). An ant licking the abdominal trichomes, even if initially regurgitating onto a wrong place, remains interested long enough to eventually get in a close contact with the beetle's head and repeat the regurgitation into its mouth. We postulate that both the cephalic and abdominal glands are necessary to ensure sufficient production of the stimulants (which cannot be stored in large quantities), and that the labral and mandibular glandular openings direct the regurgitation into the beetle's mouth.

The glands in *Claviger* occupy a considerable space inside the head capsule. The brain is shifted posterior to the tentorium. A similar arrangement was found in males of some scydmaenine beetles, which have an anterodorsal cavity serving as a reservoir for secretions produced by a very large cephalic gland, and the brain shifted to the neck region (Jałoszyński, Hünefeld, & Beutel, 2012). In contrast, the brain of scydmaenines without cephalic glands is located in the pre-tentorial lumen of the head (Jałoszyński et al., 2012). The development of cephalic glands in *Claviger*, crucial for its integration into ant communities, may be the reason for the posterior shift of the brain. A similar shift in other beetles (and larvae) to the 'neck' or even into the prothorax, is usually associated with a small relative size of the head (e.g., Polilov and Beutel (2010)). However, the head of *Claviger* is large in relation to the prothorax and it is unlikely that miniaturization played an important role in the observed architecture and placement of the brain.

5 | CONCLUSIONS

In order to achieve a full integration with ant communities, pselaphines of certain lineages fundamentally changed their diet and considerably transformed their mouthparts to take up ants' regurgitate as food. This was not possible without an earlier development or re-programming of existing (epidermal?) glands to produce secretions that manipulate the ants' behaviour to an extreme extent, with hosts not only tolerating the beetles in their brood chambers, but also feeding them upon request. A reduction of most projecting components of the mouthparts, with their sensorial apparatus so important in the context of feeding in free-living beetles, suggests physical aggression from ants as a driving factor in the evolution of Clavigeritae. Evolution of mouthparts was determined by adopting to trophallaxis, which involved shortening and simplification of the mandibles, shortening of the maxillary palp, a hypertrophy of capillary structures, a unique connection between the lacinia and hypopharynx, and reduction of the

prementum, labial palps, and different muscles. The development of conspicuously enlarged cephalic glands producing specific secretions made it possible to chemically manipulate the host ants' behaviour. Loss of optic neuropils and eyes, along with reduction of wings, sealed the fate of extreme myrmecophiles as dependent on ants not only in feeding but also for dispersal.

ACKNOWLEDGEMENTS

Our work was partly funded by project CGL2013-48950-C2 (AEI/FEDER, UE). The first author is indebted to Miłosz Mazur (University of Opole, Poland) for organizing a field trip on which numerous individuals of *C. testaceus* were collected, and Rafał Ruta (University of Wrocław, Poland) for his help in collecting the beetles. Anna Siudzińska (Laboratory of Electron Microscopy, PORT Polish Center for Technology Development, Wrocław) is acknowledged for taking the SEM images. Great thanks are also due to Adrian Richter (FSU Jena) for conducting the μ -CT scan and to Dr Alexander Stoessel for providing access to the equipment at the MPI für Menschheitsgeschichte (Jena). Alfred Newton (The Field Museum of Natural History, Chicago, IL), Peter Hlaváč (Prague, Czech Rep.), and Rostislav Bekchiev (National Museum of Natural History, Sofia, Bulgaria) provided help in finding rare literature. Finally, the authors thank an anonymous reviewer and Donald S. Chandler (University of New Hampshire) for many helpful comments, which helped greatly to improve this manuscript.

CONFLICT OF INTERESTS

The authors declare no conflicts of interest.

AUTHOR CONTRIBUTIONS

Paweł Jałoszyński designed the research, carried out SEM study, and drafted the manuscript to which Xiao-Zhu Luo and Rolf Georg Beutel contributed; Xiao-Zhu Luo and Rolf Georg Beutel conducted the μ -CT and 3D reconstructions.

DATA AVAILABILITY STATEMENT

The data that support the findings of this study are available from the corresponding author upon request.

ORCID

Paweł Jałoszyński  <https://orcid.org/0000-0003-2973-1803>

Xiao-Zhu Luo  <https://orcid.org/0000-0002-5253-267X>

REFERENCES

- Akino, T. (2002). Chemical camouflage by myrmecophilous beetles *Zyras comes* (Coleoptera: Staphylinidae) and *Diaritiger fossulatus* (Coleoptera: Pselaphidae) to be integrated into the nest of *Lasius fuliginosus* (Hymenoptera: Formicidae). *Chemoecology*, 12, 83–89.
- Anton, E., & Beutel, R. G. (2004). On the head morphology and systematic position of *Helophorus* (Coleoptera: Hydrophiloidea: Helophoridae). *Zoologischer Anzeiger*, 242, 313–346.
- Anton, E., & Beutel, R. G. (2006). On the head morphology of Lepiceridae (Coleoptera: Myxophaga) and the systematic position of the family and suborder. *European Journal of Entomology*, 103, 85–95.
- Anton, E., & Beutel, R. G. (2012). The head morphology of *Dascillus* (L.) (Dascilloidea: Dascillidae) and *Glaresis* Erichson (Scarabeoidea: Glaresidae) and its phylogenetic implications. *Arthropod Structure and Development*, 70, 3–42.
- Anton, E., Yavorskaya, M. I., & Beutel, R. G. (2016). The head morphology of Clambidae and its implications for the phylogeny of Scirtoidea (Coleoptera: Polyphaga). *Journal of Morphology*, 277, 615–633.
- Antunes-Carvalho, C., Yavorskaya, M., Gnaspini, P., Ribera, I., Hammel, J. U., & Beutel, R. G. (2017). Cephalic anatomy and three-dimensional reconstruction of the head of *Catops ventricosus* (Weise, 1877) (Coleoptera: Leiodidae: Cholevinae). *Organisms Diversity & Evolution*, 17(1), 199–212.
- Bañař, P., & Hlaváč, P. (2014). The Pselaphinae (Coleoptera: Staphylinidae) of Madagascar. III. Additional description of *Andasibe sahondrae* Hlaváč & Baňař, 2012 based on males. *Zootaxa*, 3861, 170–176.
- Barden, P. (2017). Fossil ants (Hymenoptera: Formicidae): Ancient diversity and the rise of modern lineages. *Myrmecological News*, 24, 1–30.
- Belkaceme, T. (1991). Skelet und muskulatur des kopfes und thorax von *Noterus laevis* Sturm: ein Beitrag zur morphologie und phylogenie der Noteridae (Coleoptera: Adephaga). *Stuttgarter Beiträge Zur Naturkunde Serie A (Biologie)*, 462, 1–94.
- Besuchet, C. (1991). Révolution chez les Clavigerinae (Coleoptera, Pselaphidae). *Revue Suisse de Zoologie*, 98, 499–515.
- Beutel, R. G., Friedrich, F., Yang, X. K., & Ge, S. Q. (2013). *Insect morphology and phylogeny: A textbook for students of entomology*. Berlin, Germany: Walter de Gruyter.
- Beutel, R. G., & Hörschemeyer, T. (2008). On the head morphology of *Tetraphalerus*, the phylogeny of Archostemata and the basal branching events in Coleoptera. *Cladistics*, 24, 270–298.
- Beutel, R. G., Kristensen, N. P., & Pohl, H. (2009). Resolving insect phylogeny: The significance of cephalic structures of the Nannomecoptera in understanding endopterygote relationships. *Arthropod Structure & Development*, 38(5), 427–460.
- Beutel, R. G., & Yavorskaya, M. (2019). Structure and evolution of mouthparts in Coleoptera. In H. Krenn (Ed.), *Insect mouthparts* (pp. 387–418). Cham, Switzerland: Springer.
- Cammaerts, R. (1974). Le système glandulaire tégumentaire du coléoptère myrmécophile *Claviger testaceus* Preyßler, 1790 (Pselaphidae). *Zeitschrift für Morphologie und Ökologie der Tiere*, 77, 187–219.
- Cammaerts, R. (1991). Interactions comportementales entre la Fourmi *Lasius flavus* (Formicidae) et le Coléoptère myrmécophile *Claviger testaceus* (Pselaphidae). I. Ethogramme et modalités des interactions avec les ouvriers. *Bulletin et Annales de La Société Royale Belge d'entomologie*, 127, 155–190.
- Cammaerts, R. (1992). Stimuli inducing the regurgitation of the workers of *Lasius flavus* (Formicidae) upon the myrmecophilous beetle *Claviger testaceus* (Pselaphidae). *Behavioural Processes*, 28, 81–96.
- Cammaerts, R. (1995). Regurgitation behaviour of the *Lasius flavus* worker (Formicidae) towards the myrmecophilous beetle *Claviger testaceus* (Pselaphidae) and other recipients. *Behavioural Processes*, 34, 241–264.
- Cammaerts, R. (1996). Factors affecting the regurgitation behaviour of the ant *Lasius flavus* (Formicidae) to the guest beetle *Claviger testaceus* (Pselaphidae). *Behavioural Processes*, 38, 297–312.
- Cammaerts, R. (1999). Transport location patterns of the guest beetle *Claviger testaceus* (Pselaphidae) and other objects moved by workers of the ant, *Lasius flavus* (Formicidae). *Sociobiology*, 34, 433–475.
- Chandler, D. S. (2001). *Biology, morphology and systematics of the ant-like litter beetle genera of Australia* (Coleoptera: Staphylinidae: Pselaphinae). *Memoirs on Entomology, International 15*. Gainesville, FL: Associated Publishers.
- Dressler, C., & Beutel, R. G. (2010). The morphology and evolution of the adult head of Adephaga (Insecta: Coleoptera). *Arthropod Systematics & Phylogeny*, 68, 239–287.
- Elmes, G. W. (1996). Biological diversity of ants and their role in ecosystem function. In H. B. Lee, T. H. Kim, & B. Y. Sun (Eds.), *Biodiversity research and its perspectives in the East Asia* (pp. 33–48). Korea: Chonbuk National University.

- Engelmann, M. D. (1956). Observations on the feeding behavior of several pselaphid beetles. *Entomological News*, 67, 19–24.
- Geiselhardt, S. F., Peschke, K., & Nagel, P. (2007). A review of myrmecophily in ant nest beetles (Coleoptera: Carabidae: Paussinae): Linking early observations with recent findings. *Naturwissenschaften*, 94(11), 871–894.
- Hlaváč, P., & Nakládal, O. (2016). The Pselaphinae (Coleoptera: Staphylinidae) of Madagascar. IV. Contribution to the knowledge of subtribes Hoplitoxenina and Dimerometopina with description of a new species of *Hadrophorus* Fairmaire, 1898. *Zootaxa*, 4105, 274–284.
- Jałoszyński, P. (2013). A new species of the putatively myrmecophilous genus *Plaumanniola* Costa Lima, with notes on the systematic position of Plaumanniolini (Coleoptera: Staphylinidae: Scydmaeninae). *Zootaxa*, 3670, 317–328.
- Jałoszyński, P., & Beutel, R. G. (2012). Functional morphology and evolution of specialized mouthparts of Cephenniini (Insecta, Coleoptera, Staphylinidae, Scydmaeninae). *Arthropod Structure and Development*, 41, 593–607.
- Jałoszyński, P., Hünefeld, F., & Beutel, R. G. (2012). The evolution of “deformed” brains in ant-like stone beetles (Scydmaeninae, Staphylinidae). *Arthropod Structure and Development*, 41, 17–28.
- Kéler, S. V. (1963). *Entomologisches Wörterbuch mit besonderer Berücksichtigung der morphologischen Terminologie* (3rd ed.). Berlin, Germany: Akademie Verlag.
- Krüger, E. (1910). Beiträge zur anatomie und biologie des *Claviger testaceus* Preyss. *Zeitschrift für Wissenschaftliche Zoologie*, 95, 327–381.
- Leschen, R. A. B. (1991). Behavioral observations on the myrmecophile *Fustiger knausii* (Coleoptera: Pselaphidae: Clavigerinae) with a discussion of grasping notches in myrmecophiles. *Entomological News*, 102, 215–222.
- Newton, A. F., & Thayer, M. K. (1995). *Protopselaphinae new subfamily for Protopselaphus new genus from Malaysia, with a phylogenetic analysis and review of the Omaliine Group of Staphylinidae including Pselaphidae (Coleoptera). Biology, Phylogeny, and Classification of Coleoptera: Papers Celebrating the 80th Birthday of Roy A. Crowson* (pp. 219–320). Warszawa: Muzeum i Instytut Zoologii PAN.
- Nomura, S., Sakchoowong, W., & Abd Ghani, I. (2008). A taxonomic revision of the Clavigerine genus *Cerylambus* (Insecta, Coleoptera, Staphylinidae, Pselaphinae). *Bulletin of the National Museum of Nature and Science, Tokyo Series A*, 34, 123–140.
- Park, O. (1932). The myrmecocoles of *Lasius umbratus mixtus aphidicola* Walsh. *Annals of the Entomological Society of America*, XXV, 77–88.
- Park, O. (1947). Observations on *Batrisodes* (Coleoptera: Pselaphidae), with particular reference to the American species east of the Rocky Mountains. *Bulletin of the Chicago Academy of Sciences*, 8, 45–132.
- Park, S.-J., Leschen, R. A. B., & Ahn, K.-J. (2014). Phylogeny of the Agathidiini Westwood (Coleoptera: Leiodidae) and implications for classification and contractile morphology. *Systematic Entomology*, 39, 36–48.
- Parker, J. (2016a). Emergence of a superradiation: Pselaphine rove beetles in mid-cretaceous amber from Myanmar and their evolutionary implications. *Systematic Entomology*, 41, 541–566.
- Parker, J. (2016b). Myrmecophily in beetles (Coleoptera): Evolutionary patterns and biological mechanisms. *Myrmecological News*, 22, 65–108.
- Parker, J., & Grimaldi, D. A. (2014). Specialized myrmecophily at the ecological dawn of modern ants. *Current Biology*, 24, 2428–2434.
- Polilov, A. A., & Beutel, R. G. (2010). Developmental stages of the hooded beetle *Sericoderus lateralis* (Coleoptera: Corylophidae) with comments on the phylogenetic position and effects of miniaturization. *Arthropod Structure & Development*, 39, 52–69.
- Schomann, A., Afflerbach, K., & Betz, O. (2008). Predatory behaviour of some central European pselaphine beetles (Coleoptera: Staphylinidae: Pselaphinae) with descriptions of relevant morphological features of their heads. *European Journal of Entomology*, 105, 889–907.
- Thayer, M. K. (2005). Staphylinidae Latreille, 1802. In R. G. Beutel & R. A. B. Leschen (Eds.), *Handbuch der zoologie/handbook of zoology, Vol. IV (Arthropoda: Insecta), part 38 Coleoptera, beetles. Volume 1: Morphology and systematics (Archostemata, Adephaga, Myxophaga, Polyphaga partim)* (pp. 296–344). Berlin, Germany: Walter de Gruyter.
- Wasmann, E. (1903). Zur näheren Kenntnis des echten Gastverhältnisses (Symphilie) bei den Ameisen und Termitengästen. *Biologisches Zentralblatt*, 28, 63–72.
- Weide, D., & Betz, O. (2009). Head morphology of selected Staphylinidae (Coleoptera: Staphyliniformia) with an evaluation of possible groundplan features in Staphylinidae. *Journal of Morphology*, 270(12), 1503–1523.
- Wipfler, B., Machida, R., Müller, B., & Beutel, R. G. (2011). On the head morphology of Grylloblattodea (Insecta) and the systematic position of the order, with a new nomenclature for the head muscles of Dicondylia. *Systematic Entomology*, 36, 241–266.
- Yin, Z.-W., Kurbatov, S. A., Cuccodoro, G., & Cai, C.-Y. (2019). *Cretobrachygluta* gen. nov., the first and oldest Brachyglutini in mid-cretaceous amber from Myanmar (Coleoptera: Staphylinidae: Pselaphinae). *Acta Entomologica Musei Nationalis Pragae*, 59, 101–106.
- Yin, Z.-W., Parker, J., Cai, C.-Y., Huang, D.-Y., & Li, L.-Z. (2018). A new stem bythinine in cretaceous Burmese amber and early evolution of specialized predatory behaviour in pselaphine rove beetles (Coleoptera: Staphylinidae). *Journal of Systematic Palaeontology*, 16, 531–541.

SUPPORTING INFORMATION

Additional supporting information may be found online in the Supporting Information section at the end of this article.

How to cite this article: Jałoszyński P, Luo X-Z, Beutel RG. Profound head modifications in *Claviger testaceus* (Pselaphinae, Staphylinidae, Coleoptera) facilitate integration into communities of ants. *Journal of Morphology*. 2020;281: 1072–1085. <https://doi.org/10.1002/jmor.21232>

3.3 Study III

In the twilight zone-The head morphology of *Bergrothia saulcyi* (Pselaphinae, Staphylinidae, Coleoptera), a beetle with adaptations to endogean life but living in leaf litter

Xiao-Zhu Luo, Peter Hlaváč, Paweł Jałoszyński, Rolf Georg Beutel

2021. *J. Morphol.* 282, 1170–1187. <https://doi.org/10.1002/jmor.21361>

Abstract: The pselaphine *Bergrothia saulcyi* shows features seemingly linked with life in deep soil layers, such as greatly reduced and non-functional compound eyes, a sensorium of long tactile setae, long appendages, and flightlessness. However, the tiny beetles occur in forest leaf litter, together with a community of beetles with wings and well-developed eyes. We hypothesize that *B. saulcyi* moves into deep soil under dry conditions, and returns to upper layers when humidity increases again. Despite the evolutionary cost of a reduced dispersal capacity, this life strategy may be more efficient and less hazardous than moving to different habitats using flight and the visual sense in an environment periodically drying out. We also discuss cephalic features with potential phylogenetic relevance. Plesiomorphies of *B. saulcyi* include the presence of anterior tentorial arms, well-developed labral retractors, and a full set of extrinsic maxillary and premental muscles. Apomorphic cephalic features support clades Protopselaphinae + Pselaphinae, and Pselaphinae. A conspicuous derived condition, the clypeo-ocular carina, is a possible synapomorphy of Batrisitae and genera assigned to Goniaceritae. A complex triple set of cephalic glands found in *B. saulcyi* is similar to a complex identified in the strict myrmecophile *Claviger testaceus* (Clavigeritae). It is conceivable that glands linked with food uptake in free-living pselaphines were genetically re-programmed in ancestors of inquilines, to enable them to appease the host ants. We suggest that behavioral studies are necessary to understand the poorly known life habits of *B. saulcyi*. Additional information is required to explain why a species with irreversibly reduced visual sense and other adaptations typical of endogean or cave-dwelling beetles was only collected from the upper leaf litter layer.

Conceptualization: X. Z. Luo, P. Hlaváč, R. G. Beutel

Visualization: X. Z. Luo, P. Jałoszyński

Writing-original draft: X. Z. Luo, P. Hlaváč, P. Jałoszyński, R. G. Beutel

Writing-review & editing: X. Z. Luo, P. Hlaváč, P. Jałoszyński, R. G. Beutel

Funding acquisition: X. Z. Luo, P. Hlaváč

Estimated own contribution: 75%

RESEARCH ARTICLE

In the twilight zone—The head morphology of *Bergrothia saulcyi* (Pselaphinae, Staphylinidae, Coleoptera), a beetle with adaptations to endogean life but living in leaf litter

Xiao-Zhu Luo¹  | Peter Hlaváč² | Paweł Jałoszyński³  | Rolf Georg Beutel¹

¹Institut für Zoologie und Evolutionsforschung, Friedrich-Schiller-Universität Jena, Jena, Germany

²Department of Entomology, National Museum, Natural History Museum, Prague, Czech Republic

³Museum of Natural History, University of Wrocław, Wrocław, Poland

Correspondence

Xiao-Zhu Luo, Institut für Zoologie und Evolutionsforschung, Friedrich-Schiller-Universität Jena, Erbertstrasse 1, 07743 Jena, Germany.

Email: xiaozhu.luo@uni-jena.de

Funding information

China Scholarship Council, Grant/Award Number: 201708440281; Ministry of Culture of the Czech Republic, National Museum, Grant/Award Numbers: DKRVO 2019–2023/5.l.c., 00023272

Abstract

The pselaphine *Bergrothia saulcyi* shows features seemingly linked with life in deep soil layers, such as greatly reduced and non-functional compound eyes, a sensorium of long tactile setae, long appendages, and flightlessness. However, the tiny beetles occur in forest leaf litter, together with a community of beetles with wings and well-developed eyes. We hypothesize that *B. saulcyi* moves into deep soil under dry conditions, and returns to upper layers when humidity increases again. Despite the evolutionary cost of a reduced dispersal capacity, this life strategy may be more efficient and less hazardous than moving to different habitats using flight and the visual sense in an environment periodically drying out. We also discuss cephalic features with potential phylogenetic relevance. Plesiomorphies of *B. saulcyi* include the presence of anterior tentorial arms, well-developed labral retractors, and a full set of extrinsic maxillary and premental muscles. Apomorphic cephalic features support clades Protopselaphinae + Pselaphinae, and Pselaphinae. A conspicuous derived condition, the clypeo-ocular carina, is a possible synapomorphy of Batrisitae and genera assigned to Goniaceritae. A complex triple set of cephalic glands found in *B. saulcyi* is similar to a complex identified in the strict myrmecophile *Claviger testaceus* (Clavigeritae). It is conceivable that glands linked with food uptake in free-living pselaphines were genetically re-programmed in ancestors of inquilines, to enable them to appease the host ants. We suggest that behavioral studies are necessary to understand the poorly known life habits of *B. saulcyi*. Additional information is required to explain why a species with irreversibly reduced visual sense and other adaptations typical of endogean or cave-dwelling beetles was only collected from the upper leaf litter layer.

KEYWORDS

3D reconstruction, micro/anophthalmy, micro-CT, musculature, rove beetles

This is an open access article under the terms of the Creative Commons Attribution-NonCommercial-NoDerivs License, which permits use and distribution in any medium, provided the original work is properly cited, the use is non-commercial and no modifications or adaptations are made.

© 2021 The Authors. *Journal of Morphology* published by Wiley Periodicals LLC.

1 | INTRODUCTION

An estimated 95% of all insects is at least temporarily associated with the soil at various life stages (Kühnelt, 1963). The capacities to see and to fly are massive evolutionary advantages, enabling efficient dispersal, avoiding enemies and searching for food and partners for reproduction. Nevertheless, insect species in different groups have adapted to life in deep mineral soil layers, and lost their wings and eyes in the process. Subterranean habitats clearly offer advantages that justify this spectacular evolutionary trade-off. The benefits are usually identified as more stable conditions, access to new resources, reduced competition and predation, and possibly also decreased threats of parasites or parasitoids (e.g., Giller, 1996). Of all insects, beetles seem to predominate in such unusual habitats, with many blind, wingless, miniaturized and often depigmented species known mainly among rove beetles, ground beetles, or weevils (e.g., Faille et al., 2013; Fancello et al., 2009; Grebennikov et al., 2009; Hlaváč et al., 2006, 2008, 2017; Jeannel, 1957; Morrone et al., 2001; Morrone & Hlaváč, 2017; Osella, 1977).

Among large taxonomic groups showing a tendency to shift from upper soil layers to endogean microhabitats, or from the forest floor to deep caves (both subterranean environments presumably colonized from leaf litter), the rove beetle subfamily Pselaphinae is a prime example. Comprising over 10,000 described species (Yin et al., 2019) and showing astounding morphological diversity, pselaphines have conquered a plethora of terrestrial habitats. They are most abundant in the upper soil layers (Chandler, 2001; Park, 1942, 1947), but many groups have adapted to highly specialized conditions of deep soil (e.g., all Mayetiini and Imirini, some Bythinoptectini, Trichonychini, Trogastrini, Bythinini and Amauropini; Besuchet, 1980; Coiffait, 1955, 1958; Jeannel, 1948), caves (e.g., all Thaumastocephalini, many Batrisitae, and some Metopiasini, Goniaceritae and Tyrini; Asenjo et al., 2017; Carlton, 2012; Hlaváč et al., 2019; Yin, 2020), or the similarly unique and demanding environment of ant colonies (all Clavigeritae, and many species in most tribes; e.g., Jałoszyński et al., 2020; Luo et al., 2021). Among Pselaphinae, there are also highly interesting, relatively small lineages that include beetles morphologically rather uniform, and yet showing apparently various degrees or stages of adaptation to life in deeper soil layers and caves. The batrisite Amauropini are a good example of such a group. The tribe includes over 170 species and subspecies, classified in 12 genera and distributed predominantly in the Mediterranean area, Balkans and Caucasus, with only one genus known to occur in North America (P. Hlaváč, personal database). The tribe has never been a subject of a comprehensive phylogenetic study and its monophyly has been recently questioned by Parker (2016) based on morphological evidence. This issue was raised again, when the first DNA-based analyses suggested that Amauropini have evolved from within Batrisini (Parker & Owens, 2018). However, the latter study was based on a limited taxon sampling, and only the Nearctic *Arianops* of Amauropini was included.

Species of Amauropini inhabit upper soil layers (i.e., leaf litter), deep soil (i.e., the mineral layers), from which they can be collected by soil washing techniques (Hlaváč et al., 2019), and also caves (e.g., Hlaváč et al., 1999, 2008; Nonveiller & Pavicevic, 2002). Despite

this ecological diversity, all Amauropini show a similar morphology (examples are shown in Figure 1), with a slender body often with distinctly reduced pigmentation, elongate appendages with long sensory setae, absent or strongly reduced eyes usually with variously shaped adjacent ocular spines, and reduced wings. The only exception is the presumably most ancestral genus *Protamaurops*, which can have well-developed eyes as well as wings (Bekchiev & Hlaváč, 2020). Even a single and morphologically uniform genus, as for instance *Bergrothia*, can include troglobitic species like *Bergrothia barbakadzei* Maghradze, Faille, Barjadze & Hlaváč (Maghradze et al., 2019), whereas others are commonly collected by sifting moist leaf litter accumulated on the surface. This also includes *Bergrothia saulcyi* (Reitter) known to occur in Turkey and Georgia. Feeding habits of Amauropini remain unknown, although their mouthparts resemble those of closely related and morphologically similar Batrisini, well-known to be predators that feed on springtails and mites (e.g., Park, 1947).

The most extreme adaptations to troglobitic and myrmecophilous specializations among various beetles attracted some attention. Anatomical modifications resulting from dwelling in caves were investigated in detail in specialized species of Carabidae (Luo et al., 2018a, 2018b) and Leiodidae (Larsen et al., 1979; Luo, Antunes-Carvalho, Ribera, & Beutel, 2019; Luo, Antunes-Carvalho, Wipfler, et al., 2019), and morphological adaptations to extreme myrmecophily were studied by Jałoszyński et al. (2020) and Luo et al. (2021). These modern studies included not only traditionally examined (and yet still far from being well-known) exoskeletal structures, but also the musculature and other internal organs. Only this approach makes it possible to understand the functional morphology, and later, by adding results of phylogenetic analyses, reconstruct the succession of multiple transformations that led to puzzling and often bizarre specialized character

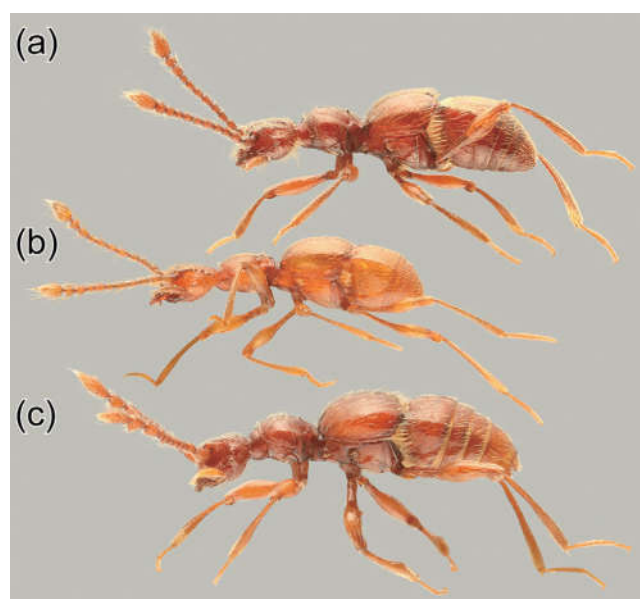


FIGURE 1 Habitus of three species of the tribe Amauropini in lateral view. (a) *Bergrothia solodovnikovi* Hlaváč; (b) *Paramaurops sardous* (Saulcy); (c) *Zoufalia nobilis* (Holdhaus)

systems observed in extant subterranean, troglobitic or myrmecophilous beetles.

Previous studies mentioned above were focused on far-reaching, extreme adaptations to endogean, troglobitic or myrmecophilous life styles. The leaf litter-inhabiting *B. saulcyi* offers an opportunity to understand presumably early, not yet fully developed morphological transformations to endogean habits. By studying this species in detail, and comparing its cephalic structures with those of advanced troglobionts and obligatorily subterranean beetles, we attempt to understand possible pre-conditions to reductions and gains of novel features, required to live in less hospitable niches of deep soil or caves. We use micro-computed tomography (μ -CT), histological techniques and computer-based 3D reconstructions to characterize the cephalic morphology of *B. saulcyi*, and to address the question which transformations are irreversible, and how advanced this species is on the road to life in the complete darkness of subterranean ecosystems already achieved by closely related species.

2 | MATERIALS AND METHODS

2.1 | Studied species

Specimens of *B. saulcyi* were collected by Petr Baňar, Peter Hlaváč, Eteri Maghradze and Shalva Barjadze in Borjomi-Kharagauli NP, Rkinis Jvari, 1793 m a.s.l., N41°54'47.7", E43°10'34.1", Imereti, Georgia (August 25, 2019). All individuals used in this study were preserved in 70% ethanol.

2.2 | Micro-computed tomography

Specimens were dehydrated with an ascending series of ethanol (70%–80%–90%–95%–100%), stained in iodine solution, transferred to acetone and then dried at the critical point (Emitech K850, Quorum Technologies Ltd., Ashford, United Kingdom). One of the dried specimens was scanned at the MPI for the Science of Human History (Jena, Germany) with a SkyScan 2211 X-ray nanotomograph (Bruker, Knotich, Belgium) with an image spatial resolution of 0.30 μ m (isotropic voxel size) using the following parameters: 60 kV, 250 μ A, 4300 ms exposure time, 0.20° rotation steps, frame averaging on (2), and using no filter. Projections were reconstructed by NRecon (Bruker, Knotich, Belgium) into JPG files. The μ CT-scan is stored in the collection of the Phyletisches Museum Jena. Amira 6.1.1 (Thermo Fisher Scientific, Waltham, United States) and VG studio Max 2.0.5 (Volume Graphics, Heidelberg, Germany) were used for the three-dimensional reconstruction and volume rendering.

2.3 | Scanning electron microscopy

The protocol recommended by Schneeberg, Bauernfeind, and Pohl (2017) for cleaning was used with minor modifications: the

specimens were transferred from 70% ethanol to 0.5% Triton X100 (14 h), followed by 5% KOH (14 h), glacial acetic acid (3×15 min), distilled water (multiple times until the specimens appeared clean), and finally 70% ethanol. Subsequently, they were dehydrated and air-dried. Prior to scanning electron microscopy (SEM), samples were attached to a rotatable specimen holder (Pohl, 2010) or small sample holders, then sputter-coated with gold (Emitech K500; Quorum Technologies Ltd., Ashford). SEM observation and imaging were performed with an FEI (Philips) XL 30 ESEM at 10 kV. Final figure plates were assembled and arranged with Adobe Photoshop CC and Illustrator CS6 (Adobe Inc., California, United States).

2.4 | Terminology

Cephalic muscles were named following the terminology of v. Kéler (1963), with the exception of Mm. compressores epipharyngis (Mm. III). For this muscle we followed Belkaceme (1991). Muscles are also homologized according to Wipfler et al. (2011), with abbreviations added in parentheses after the designations of v. Kéler (1963), for example, M7-M. labroepipharyngalis (Olb5). Muscles not mentioned in the morphological description are absent. Beutel, Friedrich, Ge, and Yang (2014) was used for general morphological terminology.

3 | RESULTS

3.1 | External head structures

The head is prognathous and partly retracted into the prothorax. Most areas of the surface are covered with a dense vestiture of unmodified setae of different lengths (~20–150 μ m); long erect setae are concentrated on the posteroventral and posterolateral cephalic areas (Figure 2a–c). The head capsule is longer than wide, with a ratio of length/maximum width of about 1.5; the length between the anterior edge of the labrum and the posterior end of the head is about 600 μ m, the maximum width about 400 μ m. The frontoclypeal rostrum is inconspicuous. The clypeofrontal strengthening ridge is absent and a hypostomal suture not recognizable. Dorsal ecdysial lines and dorsal foveae are also completely missing (Chandler, 2001: frontal foveae, vertexal sulcus). The median area of the posterior frontal region (around 1/3 of the head width) between the vestigial compound eyes (Figure 2b) is distinctly elevated as a broad, anterolaterally rounded bulge. The anterolaterally oriented antennal foramina are hidden below an anterolateral ridge and thus not visible in dorsal view; a distinct antennal tubercle is not developed and dorsal postantennal pits (Chandler, 2001) are also absent; the surface below the antennal insertion areas is slightly concave, smooth and glabrous. The clypeus (Figure 3d,f) is gently sloping toward the hind margin of the labrum; an anteromedian incision or notch is absent; the rounded anterior edge bears a distinct high bead or ridge, the clypeo-ocular ridge (Chandler, 2001: mandibulo-ocular ridge), which continues on the lateral surface of the head capsule and reaches the compound

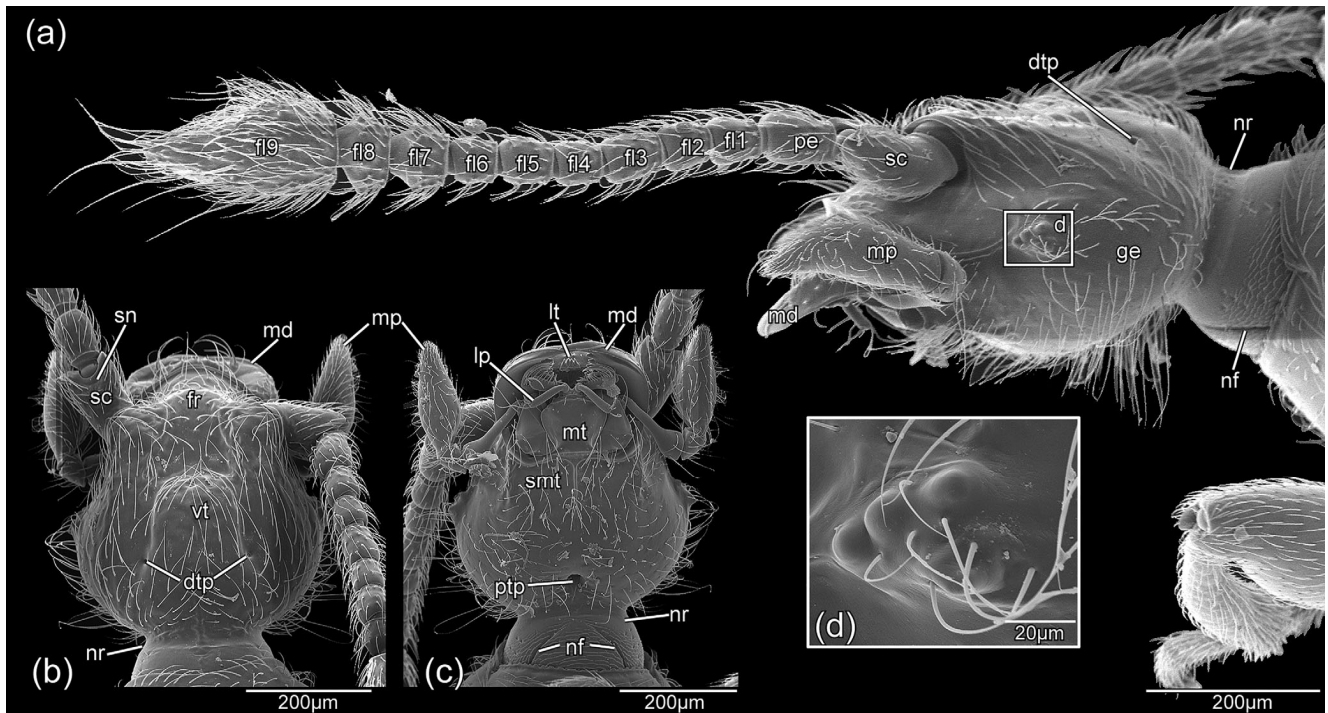


FIGURE 2 *Bergrothia saulcyi*, scanning electron micrographs of the head. (a) Lateral view; (b) dorsal view; (c) ventral view. (d) vestige of compound eyes. Dtp, dorsal tentorial pit; fl1-9, the 1st-9th flagellomere; fr, frontal region; ge, gena; lp, labial palp; lt, labial teeth; md, mandible; mp, maxillary palp; mt, mentum; nf, fissure of neck; nr, neck region; pe, pedicellus; ptp, posterior tentorial pit; sc, scapus; smt, submentum; sn, notch of scapus; vt, vertex

eyes posteriorly; the vertical frontal face of this structure is anteriorly followed by a short, smooth area, which is connected with the posterior labral margin by an articular membrane. The compound eyes are strongly reduced, externally visible as three indistinctly delimited convex cornea lenses, arranged in an obliquely longitudinal row, with several medium length setae (~80 µm) inserted between them; the area directly ventrad the posteriormost lens forms a subtriangular projection (“ocular spine”), well visible in dorsal and ventral view (Figure 2a,d). The ommatidia below the lenses are almost completely reduced but contain small amounts of pigment; a distinctly developed retinula and a lamina ganglionaris are lacking. The long postocular tempora appear evenly, strongly rounded in dorsal view; they are covered with particularly long and erect setae. A deep constriction at the posterior third of the head capsule demarcates a rounded neck region; the anteriormost area of this cephalic region is smooth, and short setae are sparsely distributed on the reticulate surface of its posterior area; the reticulation covers the median and posterior surface and is composed of strongly transverse, scaly meshes. Two posterolaterally diverging fissures are present on the ventral surface of the neck region, the external vestiges of the gular sutures. The small anterior tentorial pits are located lateroventrad the antennal sockets; two distinct but small dorsal tentorial pits (dtp, Figure 2b; Chandler, 2001: vertexal foveae) are located laterad the posterior region of the median bulge and visible in both lateral and dorsal view; the ventral posterior tentorial pit (ptp, Figure 2c) (Chandler, 2001: gular fovea) is a deep unpaired median invagination slightly anterad the ventral neck region; it separates the small gular region on the ventral side of the neck from

the extensive submental area; internally it forms the shared ventral base of the posterior tentorial arms.

3.2 | Internal skeletal structures

The tentorium is mainly formed by a V-shaped vertical structure, comprising the dorsal and posterior arms, which are flattened and slightly widening dorsally (ts, Figures 3e–f); it is located anterior to the occipital constriction of the head capsule; ventrally it originates from a solid unpaired base, which corresponds with the invagination site of the posterior tentorial arms, that is, the posterior tentorial pits; dorsally the diverging paired arms end in the distinct dorsal tentorial pits. The filament-like anterior tentorial arms (ata, Figure 3f) are long and slender; they originate anterolaterally from the minute anterior tentorial pits and merge with the lower third of the vertical structure formed by the dorsal and posterior arms. The tentorial bridge and a laminatentorium are missing; internal gular ridges are also absent. Circumocular ridges are absent, whereas internal circumantennal ridges are distinct. The postoccipital ridge is well-developed dorsally and laterally; a fairly low transverse gular bulge is present at the ventral margin of the foramen occipitale (Figure 3f).

3.3 | Antennae

The articulation between the proximal portion of the scapus and the head capsule is not visible externally (Figure 2a). The densely

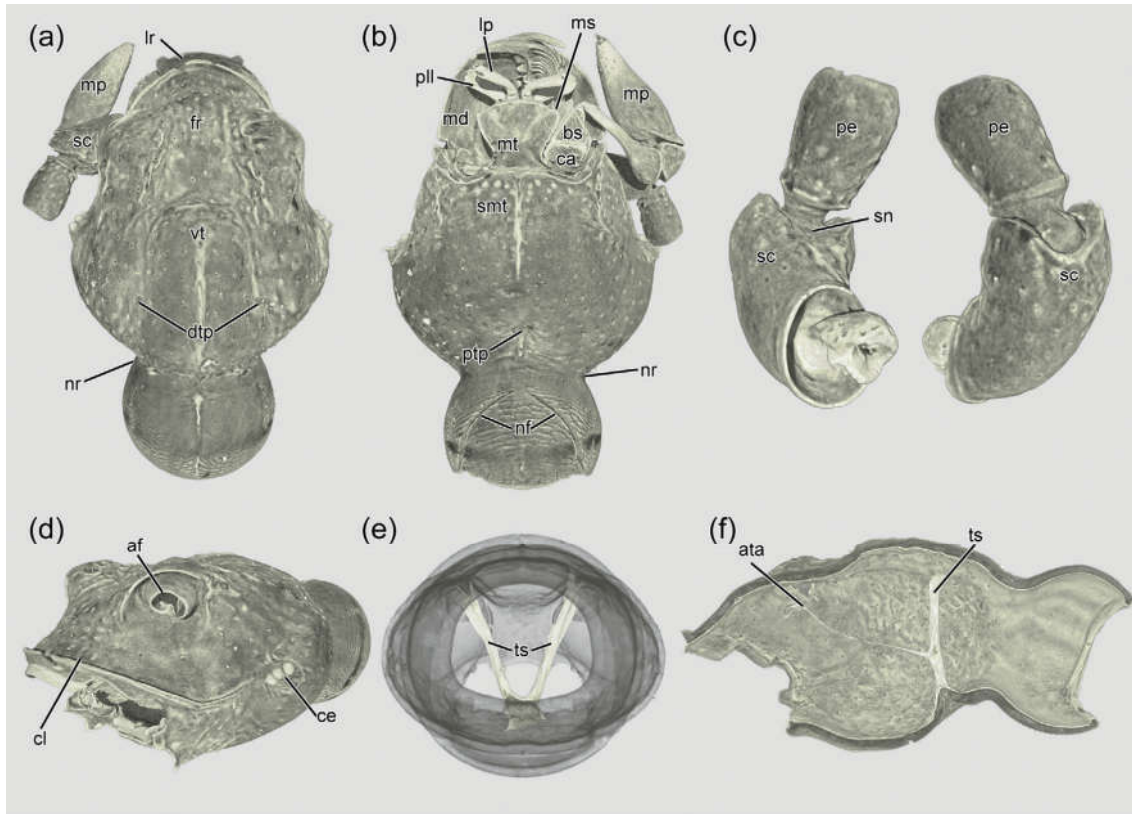


FIGURE 3 *Bergrothia saulcyi*, three-dimensional reconstructions. (a) Head, dorsal view; (b) head, ventral view; (c) scapus and pedicellus; (d) head, anterolateral view; (e) head capsule (semi-transparent) and dorsoventral main component of tentorium (white), posterior view; (f) head capsule (dark) and tentorium (white), sagittal view. af, antennal foramen; ata, anterior tentorial arm; bs, basistipes; ca, cardo; ce, compound eye; cl, clypeus; dtp, dorsal tentorial pit; fr, frons; lp, labial palp; lr, labrum; md, mandible; mp, maxillary palp; ms, mediostipes; mt, mentum; nf, fissure of the neck; nr, neck region; pe, pedicellus; pll, plate-like lobe; ptp, posterior tentorial pit; sc, scapus; smt, submentum; sn, notch of the scapus; ts, tentorial stick; vt, vertex

setose 11-segmented antenna is almost twice as long as the head capsule (~1 mm; Figures 2a and 4a). The scapus (sc, Figure 4a) is markedly bipartite; a small, strongly curved and distally narrowing basal articulatory piece reaches into a deep basal concavity of the large distal scapal portion (Figure 3c), which is enclosed by a distinct bead; the distal portion of the scapus is roughly cylindrical but distinctly curved, widened proximally and slightly narrowing distally; the distal part is covered with medium length setae (~50 μ m) like the other antennomeres (Figure 4a,b); in contrast, the proximal part bears only few minute sensilla (probably proprioceptors; Böhm's sensilla [e.g., Faucheux, 2011]) inserted in shallow depressions on the concave posterior side (Figure 4c); the apical region of the scapus bears a deep U-shaped notch anteriorly and posteriorly, each enclosed by a smooth, glabrous and flat bead (Figures 2a and 3c); these concavities allow the pedicellus to be bent anterad and posterad, and keep this segment plus the flagellum in two defined positions. The pedicellus (pe, Figure 4a) is about half as long as the entire scapus, and only slightly narrower than the widened proximal portion of the distal scapal portion; proximally it bears a small, globular, glabrous articulatory piece, which forms a ball-and-socket joint with the apical articulatory area of the scapus; this is followed by a

short, cup-shaped sub-segment, which is again followed by the nearly cylindrical main portion of the 2nd antennomere (Figure 4a); it is slightly widening distally, and in contrast to the basal parts equipped with the regular vestiture of setae. Each of flagellomeres 1–6 is shorter than the pedicellus but similar in shape and vestiture of setae; they vary slightly in length, flagellomeres 1, 3 and 5 are slightly longer than the others (Figures 2a and 4a). The apical three segments (Figures 2a and 4a) form a loose club; flagellomeres 7 and 8 are distinctly wider than the proximal ones; their ring-shaped setose main part is distinctly separated from a smooth, conical distal portion; the terminal flagellomere 9 is significantly larger than all other segments; its smooth basal part is flat and disc-shaped; the large spindle-shaped main part bears a regular vestiture with slightly increased density, interspersed with some long setae (up to ~150 μ m).

Musculature (Figures 5a and 6a–g): M1–M. tentorioscapalis anterior (Oan1)/M4–M. tentorioscapalis medialis (Oan4), two flat bundles, O: along the middle area of the dorsal tentorial arm (M1/4a on the lateral side and M1/4b on the medial side), I, ventral margin of the scapus; M2–M. tentorioscapalis posterior (Oan2), O: upper area of the dorsal tentorial arm, dorsal to M1, I: posterior margin of the

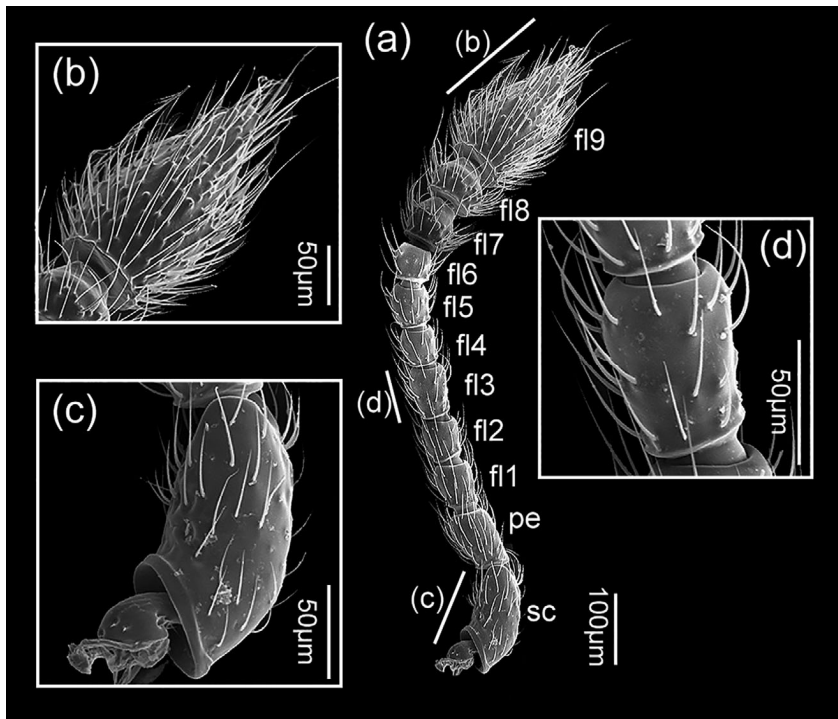


FIGURE 4 *Bergrothia saulcyi*, scanning electron micrographs of antenna. (a) Whole view; (b) 9th flagellomere; (c) scapus; (d) 3rd flagellomere. fl1–9, 1st–9th flagellomere; pe, pedicellus; sc, scapus

scapus; M5–M. scapopedicellaris lateralis (0an6), O: dorsal wall of the scapus, I: lateral margin of pedicellar base; M6–M. scapopedicellaris medialis (0an7), O: ventral wall of the scapus, I: median margin of pedicellar base.

3.4 | Labrum

The labrum (lr, Figures 3a and 7a), which is separated from the clypeus by a fold and internal connecting membrane, is distinctly narrower than the anterior clypeal edge. A transverse M-shaped labral region is visible in dorsal view, with sharp anterolateral angles and a slightly sinuated anterior edge; this exposed part is evenly covered with short setae on its median area and bears several long setae on the lateral edge. Four well-developed peg-like sensilla (Figures 2c and 7b) are present in the middle area of the ventral side of the anterior labrum. Short but well-developed tormae are present posterolaterally.

Musculature (Figures 6a and 9): M7–M. labroepipharyngalis (0lb5), O: dorsal wall of the labrum, very close to posterior margin, I: anterior area of the epipharynx; M9–M. frontoepipharyngalis (0lb2), O: anterolaterally on the head capsule, anterad the dorsomedian bulge, I: tormae at posterolateral corner of the labrum.

3.5 | Mandibles

The roughly triangular mandibles (Figure 8a–d) are largely symmetrical and mostly smooth. They articulate in a typical dicondylic manner; the large rounded and smooth condyle of the primary (ventral) joint is

located at the lateral mandibular base, separated from the lateral edge by a deep incision; a wide concavity of the dorsal margin of the mandibular base forms the socket of the secondary (dorsal) joint. A long and pointed apical tooth is bent toward the median line; six or seven smaller triangular subapical teeth are decreasing in size toward mandibular base. A prostheca is not present. The dorsal surface is convex, fitting with the surface of the epipharynx; a field of ~20 anteriorly directed short setae (~10 μm) is present proximolaterally, widely spaced and each inserted in a distinct socket; a whip-like, flattened and long seta (~100 μm) is inserted on the distal 3rd of the mandible, close to the lateral margin. A shallow oblique ridge is present mesad the row of subapical teeth; a distinct, rounded proximomesal ridge delimits a shallow mola with a finely tuberculate surface. The ventral mandibular surface is largely flat, smooth and glabrous; a distinct curved ridge extends from the ventral condyle along the basal margin, then bends distad, continues close to the mesal mandibular margin, and obliterates mesad the proximal subapical teeth; it separates the elevated proximal and proximomesal areas from the slightly lowered main area of the ventral side of the mandible. The strongly developed adductor tendon is attached to the mesal mandibular base, ~40 μm from the proximal end of the molar area; the less distinct adductor tendon attaches to the base of the lateral protuberance.

Musculature (Figures 5c and 6c–g): M11–M. craniomandibularis internus (0md1), largest cephalic muscle, O: extensive area of the lateral wall of the head capsule, between the vestigial compound eyes and the occipital constriction; I: with a tendon on the mesal mandibular base; M12–M. craniomandibularis externus (0md3), distinctly smaller than M11, O: lateral surface of the capsule, anterolaterad M11; I: with a tendon on the lateral mandibular base.

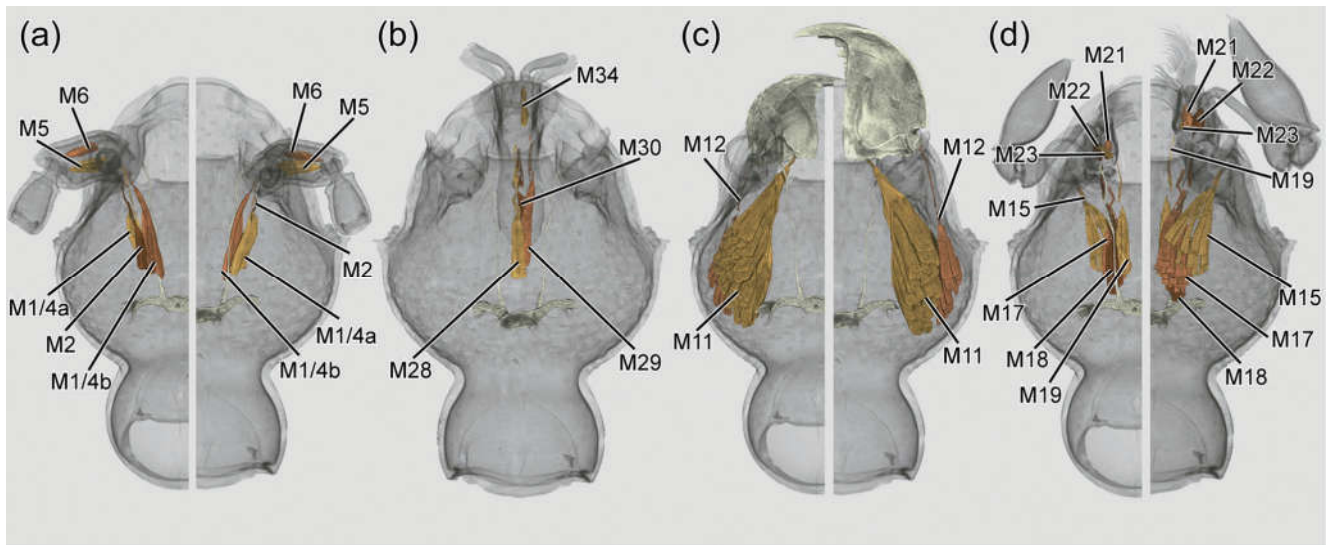


FIGURE 5 *Bergrothia saulcyi*, three-dimensional reconstructions of antennal (a), labial (b) and mandibular (c) and maxillary (d) muscles. (a), (c) and (d): Left half is in dorsal view, right half is in ventral view; (b): Ventral view. Abbreviations of muscles: M1—M. tentorioscapalis anterior (Oan1)/M4—M. tentorioscapalis medialis (Oan4); M2—M. tentorioscapalis posterior (Oan2); M5—M. scapopedicellaris lateralis (Oan6); M6—M. scapopedicellaris medialis (Oan7); M11—M. craniomandibularis internus (Omd1); M12—M. craniomandibularis externus (Omd3); M15—M. craniocardinalis externus (Omx1); M17—M. tentoriocardinalis (Omx3); M18—M. tentoriostipitalis (Omx4/Omx5); M19—M. craniolacinalis (Omx2); M21—M. stipitogalealis (Omx7); M22—M. stipitopalpalis externus (Omx8); M23—M. stipitopalpalis internus (Omx10); M28—M. submentopraementalis (Ola8); M29—M. tentoriopraementalis (Ola5); M30—M. tentoriopraementalis superior (Ola6); M34—M. praementopalpalis externus (Ola14)

3.6 | Maxillae

The maxillary grooves are well-defined, medially bordered by the lateral edge of the mentum and posteriorly by an anterior bead of the submentum. The roughly semicircular cardo (ca, Figure 7h) has a transverse orientation, a straight anterior edge and a rounded posterior margin; at its base it bears an articular process with a distinct branch pointing laterad; the external surface of the cardo is mostly glabrous except for a short seta on the lateral area; a circular structure formed by densely arranged minute pores is present posterior to the seta. The trapezoidal basistipes (bs, Figure 7h) has a straight basal edge connected with the cardo, a short lateral margin, a rounded anterolateral corner, a straight and oblique distal edge, and a straight mesal edge dividing the main part of the maxilla diagonally; the mesal edge is connected with the elongate triangular mediostipes; only a single short seta is inserted on the lateral edge of the basistipes; the slightly concave anterior edge of the mediostipes (ms, Figure 7h) bears a distinct narrow incision close to its mesal margin, possibly marking the border between this sclerite and the lacinia; the contour of the mesal edge is somewhat irregular, with a shallow convexity proximally; distally it is firmly fused with the lacinia. The galea (ga, Figures 7g,h and 8e) and lacinia (lc, Figures 7g,h and 8e) are both flattened, short and broad; the anterior and posterior portions of both endite lobes are wider than the constricted middle area. The galea is inserted on the distal edge of the mediostipes; its rounded distal edge bears a very dense brush of curved, spine-like setae; its ventral basal edge is concealed by the distal margin of the mediostipes; its straight basal edge on the dorsal side is laterally adjacent with the distal

edge of the palpifer. The lacinia is about 1.5 times as long as the galea but of similar shape; on the dorsal side it is completely fused with the mediostipes; distally it bears a dense brush similar to that of the galea and aligned with it; on the dorsal side the lateral and basal margins are free, like the basal edge only connected with the articulary membrane. The large, nearly cylindrical palpifer (pf, Figures 7g and 8e) is inserted on the dorsal side, between the dorsomesal edge of the lacinia and the basistipes. The palp (mp, Figures 2a–c, 3a,b, 7g,h, and 8e) is four-segmented; the strongly curved, short palpomere 1, inserted on the apical articulary area of the palpifer (Figure 8e,i), is the smallest segment; palpomere 2 is clavate, and about five times as long as palpomere 1; its distal area is distinctly widened, slightly curved and sparsely covered with few setae; palpomere 3 appears triangular in dorsal and ventral view, and is slightly longer and distinctly wider than palpomere 1; palpomere 4 is sub-fusiform and the longest and widest segment; it is about 1.5 times as long as palpomere 2; the setae distributed on the surface have a higher density on the distal area. The entire area from the distal surface of palpomere 2 to the apex of palpomere 4 is densely setose; palpomere 4 bears three well-defined sensilla (Figure 8f) on the anterolateral area and a cone-like, elongate apical sensory appendage.

Musculature (Figures 5d and 6b–g): M15—M. craniocardinalis externus (Omx1), O: anterolateral area of the ventral wall of the head capsule, I: lateral branch of the cardinal articulary process; M17—M. tentoriocardinalis (Omx3), O: ventral surface of the head capsule, laterad the common base of the dorsoventral tentorial arms and posterior to the origin of M15, I: mesally on the cardinal process; M18—M.

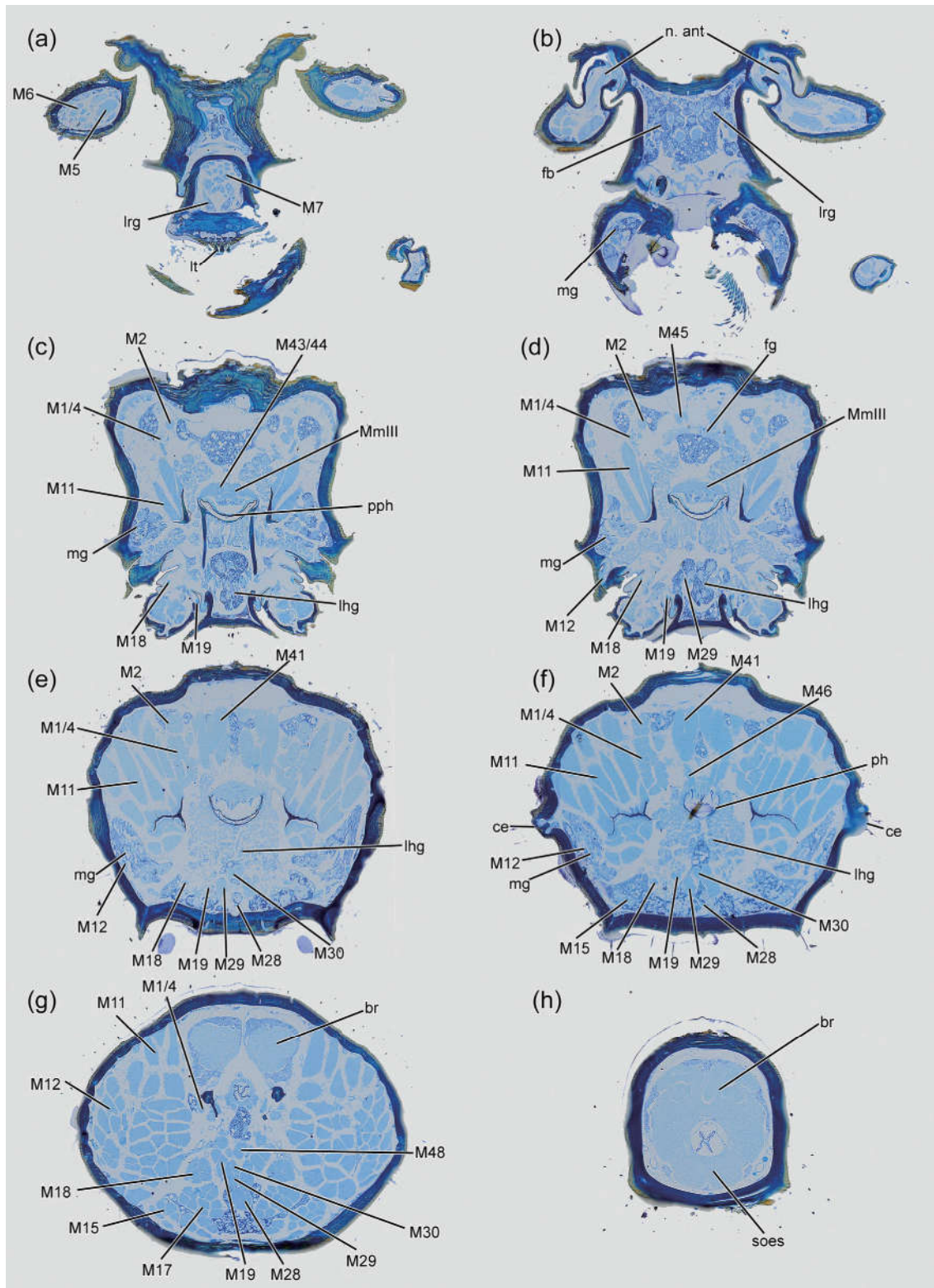


FIGURE 6 *Bergrothia saulcyi*, histological sections. br, brain; fg, frontal ganglion; n. ant, antennal nerve; lhg, labio-hypopharyngeal glands; lt, labral teeth; lrg, labral glands; mg, mandibular glands; ph, pharynx; pph, prepharynx; soes, suboesophageal ganglion. Abbreviations of muscles: M1–M. tentorioscapalis anterior (Oan1)/M4–M. tentorioscapalis medialis (Oan4); M2–M. tentorioscapalis posterior (Oan2); M11–M. craniomandibularis internus (Omd1); M12–M. craniomandibularis externus (Omd3); M15–M. craniocardinalis externus (Omx1); M17–M. tentoriocardinalis (Omx3); M18–M. tentoriostipitalis (Omx4/Omx5); M19–M. craniolacinalis (Omx2); M28–M. submentopraementalis (Ola8); M29–M. tentoriopraementalis (Ola5); M30–M. tentoriopraementalis superior (Ola6); M41–M. frontohypopharyngalis (Ohy1); M43–M. clypeopalatalis (Oci1)/M44–M. clypeobuccalis (Obu1); M45–M. frontobuccalis anterior (Obu2); M46–M. frontobuccalis posterior (Obu3); M48–M. tentoriobuccalis anterior (Obu5); MmIII–Mm. compressores epipharyngis

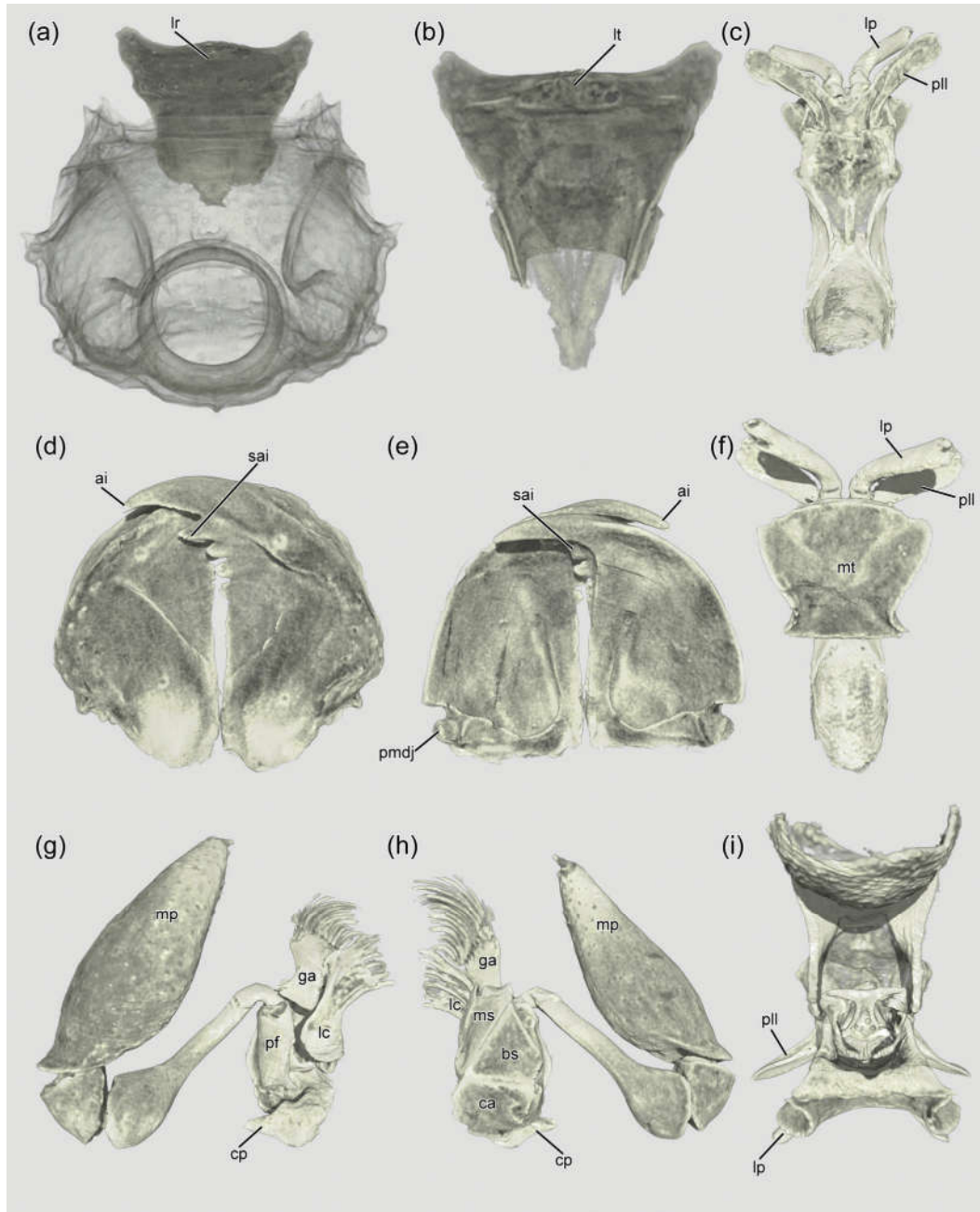


FIGURE 7 *Bergrothia saulcyi*, three-dimensional reconstructions of mouthparts. (a) Labrum, anterodorsal view; (b) labrum, ventral view; (c) labium, dorsal view; (d) mandibles, dorsal view; (e) mandibles, ventral view; (f) labium, ventral view; (g) maxilla, dorsal view; (h) maxilla, ventral view; (i) labium, posterior view. ai, apical incisor; bs, basistipes; ca, cardo; cp, cardinal process; ga, galea; lc, lacinia; lp, labial palp; lr, labrum; lt, labral teeth; mp, maxillary palp; ms, mediostipes; mt, mentum; pll, plate-like lobe; pmdj, primary mandibular joint; sai, subapical incisor

tentoriostipitalis (0mx4/0mx5), O: ventral surface of the head capsule, laterad the common base of the dorsoventral tentorial arms, I: mesal margin of the palpifer; M19–M. craniolacinialis (0mx2), O: ventral head capsule, anterior to the ventral tentorial base, I: lacinial base; M21–M. stipitogalealis (0mx7), O: base of basistipes, I: base of galea; M22–M. stipitopalpalis externus (0mx8), O: base of dorsal plate of palpifer, I: laterally on the base of palpomere 1; M23–M. stipitopalpalis internus (0mx10), O: base of basistipes, I: mesal margin of palpifer.

3.7 | Labium

The submentum is completely fused with the ventral head capsule posteriorly and laterally, but distinctly separated from the mentum anteriorly; a low and narrow longitudinal ridge is present anteromedially (Chandler, 2001: gular carina) and a distinct bead along the anterior submental margin; the lateral portion of the anterior edge is adjacent to the maxillary stipes. The trapezoidal mentum is smooth and largely glabrous, with only short setae on the anterior area; the posterior margin is straight

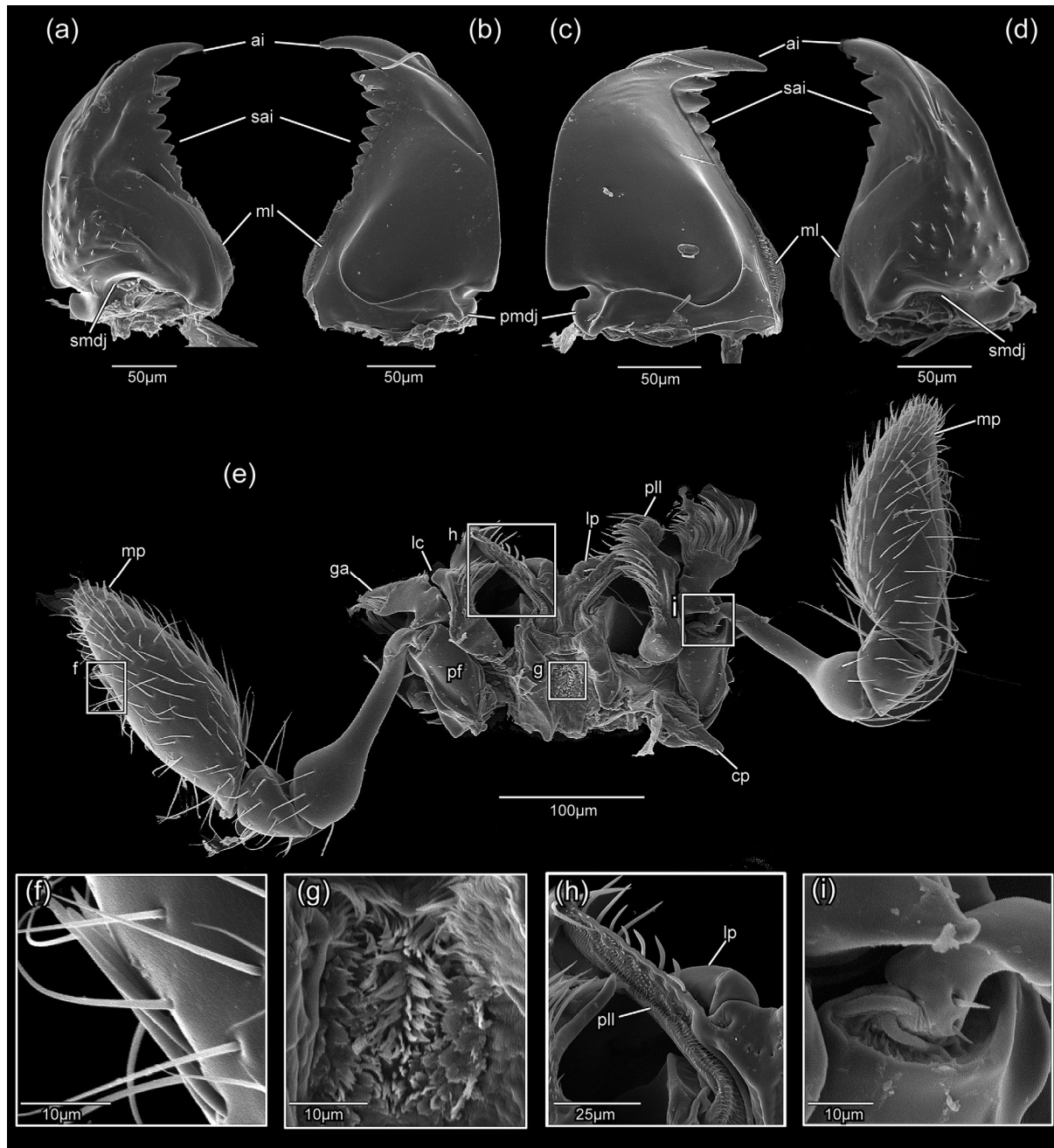


FIGURE 8 *Bergrothia saulcyi*, scanning electron micrographs of mandibles, maxillae and labium. (a) Left mandible, dorsal view; (b) left mandible, ventral view; (c) right mandible, ventral view; (d) right mandible, dorsal view; (e)–(i) maxillae and labium, dorsal view. ai, apical incisor; cpc, cardinal process; ga, galea; lc, lacinia; lp, labial palp; ml, mola; mp, maxillary palp; pf, palpifer; pll, plate-like lobe; pmdj, primary mandibular joint; sai, subapical incisor; smdj, secondary mandibular joint

and shorter than the slightly rounded anterior edge; a distinct constriction is present between the proximal third and the anterior portion of the mentum. The prementum is membranous and concealed below the anterior mentum; anteriorly it is connected with the short, semi-cylindrical palpiger; the laterally directed, cylindrical labial palps appear one-segmented (lp, Figures 2c, 3b, 7f, and 8e) but each is in fact composed of three palpomeres; the entire structure is more than five times longer than the palpiger; palpomere 1 is extremely short and anelliform; palpomere 2 is slender, subcylindrical, with a largely glabrous surface but with two

long setae on the rounded apex; palpomere 3 is setiform and obscured by the apical setae of palpomere 2. A pair of narrow, distally divergent plate-like lobes (pll, Figure 8e,h); resembling paraglossae is present laterad the palps; short, vertically oriented setae are evenly distributed on their mesal edge; the ventral surface is densely covered with microtrichia. Median endite lobes or glossae are absent.

Musculature (Figures 5b, 6d–g, and 9): M28–M. submento-praementalis (Ola8), O: median area of ventral head capsule, in front of the ventral tentorial base, I: membrane anterior to the mentum; M29–M.

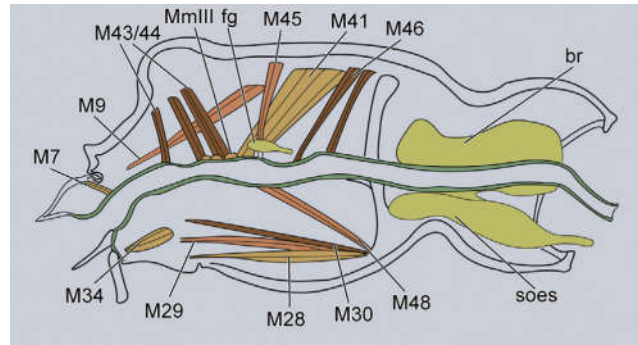


FIGURE 9 *Bergrothia saulcyi*, line drawing of labral, pharyngeal and hypopharyngeal muscles of *B. saulcyi*, sagittal view. br, brain; fg, frontal ganglion; soes, suboesophageal ganglion. Abbreviations of muscles: M7—M. labroepipharyngalis (Olb5); M9—M. frontoepipharyngalis (Olb2); M28—M. submentopraementalis (Ola8); M29—M. tentoriopraementalis (Ola5); M30—M. tentoriopraementalis superior (Ola6); M34—M. praementopalpalis externus (Ola14); M41—M. frontohypopharyngalis (Ohy1); M43—M. clypeopalatalis (Oci1)/M44—M. clypeobuccalis (Obu1); M45—M. frontobuccalis anterior (Obu2); M46—M. frontobuccalis posterior (Obu3); M48—M. tentoriobuccalis anterior (Obu5); MmIII—Mm. compressores epipharyngis

tentoriopraementalis (Ola5), O: anterior to the ventral tentorial base, I: lateral wall of the palpiger; M30—M. tentoriopraementalis superior (Ola6), O: anterior to the ventral tentorial base, I: dorsal wall of the prementum; M34—M. praementopalpalis externus (Ola14), O: inner surface of the palpiger, I: ventral base of palpomere 1.

3.8 | Epipharynx and hypopharynx

The unsclerotized ventral wall of the labrum forms the anterior epipharynx. The anterior part of the hypopharynx consists of a triangular median glabrous area flanked by lateral lobes densely covered with microtrichia (Figure 8e,g,h). The middle epipharyngeal region includes an anterior rectangular portion densely set with microtrichia, glabrous lateral areas, and a median depression very densely covered with short microtrichia. The posteriormost part of the hypopharynx is laterally fused with epipharynx, thus forming a short prepharyngeal tube. Suspensorial sclerotizations or apodemes for attachment of M. frontohypopharyngalis are not recognizable.

Musculature (Figures 6c–g and 9): M41—M. frontohypopharyngalis (Ohy1), O: anterior area of frons, I: laterally on anatomical mouth; M43—M. clypeopalatalis (Oci1)/ M44—M. clypeobuccalis (Obu1), a series of bundles, O: mesally on the anterodorsal wall of the head capsule; I: anteriorly on the epipharyngeal wall and posteriorly dorsal pharyngeal wall at the mouth opening; MmIII—Mm. compressores epipharyngis, numerous transverse bundles above the posteriormost epipharynx, directly anterad the anatomical mouth opening.

3.9 | Prepharynx and pharynx

The short, laterally closed prepharynx (pph, Figure 6c) appears compact and heart-shaped in cross section, with a sclerotized, convex ventral wall and a medially concave dorsal side. The anatomical mouth,

separating the prepharyngeal tube from the pharynx is marked by the frontal ganglion (fg, Figure 6d) and the insertion sites of M. frontopharyngalis anterior (M45) and M. frontohypopharyngalis (M41). The pharynx (ph, Figure 6f) and the cephalic portion of the esophagus are more than 2/3 as long as the entire head; the cephalic esophageal portion between the main part of the tentorium and the occipital foramen is tightly enclosed by the cerebrum and suboesophageal complex (soes, Figure 6h) in the narrowed neck region; the cephalic digestive tract posterior to the anatomical mouth is narrowing posteriorly and appears approximately round to oval in cross section; the longitudinal folds of the pharyngeal part for attachment of dilators are very distinct.

Musculature (Figures 6d–g and 9): M45—M. frontobuccalis anterior (Obu2), O: middle region of the frontal area, I: obliquely inserted on the anteriormost dorsal pharyngeal wall; M46—M. frontobuccalis posterior (Obu3), two widely separated bundles, O: frontal area, distinctly posterior to M45, I: dorsal pharyngeal wall; M48—M. tentoriobuccalis anterior (Obu5), a single bundle, moderately ascending toward its insertion site below the anatomical mouth opening; O: directly in front of the ventral tentorial base, I: ventromesally on the anterior pharynx, just below the insertion of M45. The muscle identified as M50 (M. tentoriobuccalis posterior) in *Claviger testaceus* Preyßler (Jatoczyński et al., 2020) is in fact M48 (M. tentoriobuccalis anterior) with an atypical, nearly vertical orientation; this homology assessment is clearly supported by the insertion directly opposed to the attachment site of M45, below the anatomical mouth.

3.10 | Nervous system

The elongate brain (br, Figure 6g,h and 9) and suboesophageal ganglion (soes, Figure 6h) are located in the posterior third of the head, between the main body of the tentorium and the foramen occipitale. The entire complex is distinctly narrowed at the posterior constriction of the head capsule; the larger posterior portion of the entire unit fills

out almost the entire lumen of the neck region; the anterior third of the brain is rather narrow but it is distinctly widening posterad the constriction. The upper portion of the protocerebrum is strongly bent backwards, almost reaching the foramen occipitale posteriorly. The optic lobes with the optic neuropils are entirely lacking, and even a thin optic nerve is not preserved; in contrast, a well-developed olfactory nerve (nervus antennalis) originates from the anterior deutocerebral region. A separate tritocerebral commissure is present. The suboesophageal ganglion appears flattened and is almost as broad as the posterior portion of the brain; it reaches the posterior gular edge posteriorly and is continuous with the paired first connective entering the prothorax. The well-developed transverse frontal ganglion (fg, Figure 6d) above the anatomical mouth opening releases the frontal connectives laterally and the unpaired nervus recurrens posteriorly.

3.11 | Glands

Three well-developed glandular clusters of Cammaert's (1974) multicellular type A are present in the head (clearly recognizable in histological sections and μ -CT data): (1) the labral glands (lrg, Figure 6a,b), extending between the anterior labral region anteriorly and the anterior margin of the brain; it is divided into a large median subunit, a small intermediate portion close to *M. frontohypopharyngalis* (*M. 41*), and a larger flat lateral lobe above bundles of *M. craniomandibularis internus* (*M11*); the tissue is rather loose, somewhat resembling the fat body, but contains thin and distinct ducts with cuticular lining; the openings could not be precisely localized but secretions are likely released through pores on the anterior labral edge. (2) (ii) large paired mandibular glands (mg, Figure 6b,c–f), also type A, but differing structurally from the former, with more solid subunits; they lie mostly outside of the mandibles in the lateral preocular head region, but enter the mandibular lumen and likely release their secretions through pores on the mandibles. (3) the large labio-hypopharyngeal glands (lhg, Figure 6c,d) of type A fill out large areas of the ventral head lumen; they reach far back as a sheath enclosing *M. tentoriobuccalis* (*M. 48*) and anteriorly they enter the prementum; they release their secretions at the base of the labial palps (salivary material according to Cammaerts, 1974 in *Claviger*).

4 | DISCUSSION

Taxonomic studies of Pselaphinae and the exploration of the diversity of the group are thriving, with an impressive number of new extant and extinct species from different world regions described in the last years (e.g., Hlaváč et al., 2019; Huang et al., 2018; Nakládal & Hlaváč, 2018; Park & Chandler, 2017; Parker, 2016; Yin et al., 2019). However, the investigation of the systematic relationships within the highly diverse subfamily is still in a preliminary stage, despite substantial contributions of Jeannel (1950), Newton and Thayer (1995), Chandler (2001), Kurbatov (2007), Kurbatov et al. (2007), Kurbatov and

Cuccodoro (2019), Kurbatov and Sabella (2008, 2015), Parker (2016) and others. In addition, the anatomical knowledge of this group is minimal at present, impeding in depth phylogenetic evaluations based on morphology. It is in fact restricted to one study on the head (Jałoszyński et al., 2020) and one on the thorax (Luo et al., 2021), both on a species of the highly specialized genus *Claviger* of the obligatorily myrmecophilous Clavigeritae. An additional issue is the morphological terminology used in recent pselaphine studies, outlined in detail in Chandler (2001). There is no doubt that this system has its merits in a taxonomic context, especially in a group of beetles with an unparalleled structural diversity, often with bizarre morphological variations (e.g., Asenjo et al., 2017; Besuchet, 1991: figure 1; Hlaváč et al., 2013; Jałoszyński et al., 2020; Parker & Maruyama, 2013). However, it is somewhat detached from the modern morphological nomenclature used for other beetles (e.g., Anton & Beutel, 2004; Antunes-Carvalho et al., 2017; Beutel & Komarek, 2004; Lawrence et al., 2011) and insects of other orders (e.g., Beutel et al., 2014), for instance using vertexal foveae for the dorsal tentorial pits, or gular carina (Chandler, 2001) for a highly variable ridge or even plate-like elevation on the submental area. In the present study, like in Jałoszyński et al. (2020), we attempt to “align” pselaphine morphological terminology as defined in Chandler (2001) with a general nomenclature for insect structures, and also a provisional phylogenetic assessment of structural features. The latter is clearly preliminary as detailed morphological information on pselaphine beetles is extremely scarce, and almost non-existent concerning internal structures. In the last part of the discussion, we address subterranean tendencies and adaptations in *Bergrothia*, in comparison with cavernicolous species in other groups of Pselaphinae and also in other families.

4.1 | Cephalic features and their potential phylogenetic implications

A discussion on the potential phylogenetic value of characters observed in *Bergrothia* and the previously studied *Claviger* is hampered by an exceptionally poor knowledge of the morphology, especially concerning internal structures. Already Newton and Thayer (1995) noticed a high level of homoplasy in various units of the Omaliinae group of Staphylinidae, to which Pselaphinae belong, and assumed multiple events of parallel evolution. With unparalleled morphological diversity and many bizarre adaptations, it seems possible to find exceptionally shaped structures in any presently recognized subgroup. Therefore, even diagnoses of higher-level taxonomic units are still unclear. Although the current state of morphological knowledge may seem insufficient for such a discussion, we nevertheless attempt to indicate some potentially important features, as a starting point for future discussions.

Bergrothia displays all cephalic apomorphies assigned to the groundplan of Pselaphinae or Pselaphinae + Protopselaphinae in previous studies (Jałoszyński et al., 2020; Newton & Thayer, 1995). An antenna with a club usually formed by three abruptly widened antennomeres 9–11 (Figure 4a,b) is a potential synapomorphy of both

subfamilies (Chandler, 2001; Jałoszyński et al., 2020; Jeannel, 1950; Newton & Thayer, 1995: figure 6), implying that gradually widened distal antennomeres occurring in some Faronitae (Jeannel, 1950: figure 2b) and occasionally in other tribes are due to reversal. The gular ridges are obliterated in *B. saulcyi*, like in *Claviger* (Jałoszyński et al., 2020) and other pselaphine taxa (Nomura, 1991: figure 1d), and probably also in *Protopselaphus* (Newton & Thayer, 1995: gular sutures indicated only over short distance posteriorly). The unpaired posterior tentorial grooves (Chandler, 2001: gular foveae) are another potential synapomorphy of Pselaphinae and *Protopselaphus* (Newton & Thayer, 1995: figure 3). Posterior pits apparently separated in *Nornalup afoveatus* Park et Chandler of Faronitae (Park & Chandler, 2017: figure 3b), in Euplectitae (e.g., Jałoszyński & Nomura, 2021), and also in at least some Goniaceritae (Kurbatov & Sabella, 2015: figures 1–12), are arguably due to character reversal. A V-shaped main part of the tentorium (Figure 3e,f), comprising the posterior and dorsal arms, is also likely a groundplan apomorphy of the two subfamilies, and also the fusion of the dorsal arms with the dorsal wall of the head capsule, externally visible as distinct pits (Figure 2b; Jeannel, 1950: figure 1a; Chandler, 2001: vertexal foveae [in fact located on the frontal region]; Newton & Thayer, 1995: figures 1–3). This condition differs clearly from what is found in other groups of Staphylinoidea (e.g., Antunes-Carvalho et al., 2017; Weide et al., 2014; Weide & Betz, 2009). Whether a tentorial bridge occurs in any species of Pselaphinae as suggested by Nomura (1991: figure 1d) is uncertain. It is missing in the groups with detailed anatomical data. The structure addressed as tentorial bridge in Newton and Thayer (Newton & Thayer, 1995: figure 2) lies far posterad the V-shaped main tentorial body.

A condyle-like, semi-globular neck region as it is present in *B. saulcyi* (Figures 2a–c and 3a,b) is likely an autapomorphy of Pselaphinae. The postocular cephalic portion of *Protopselaphus* is also rounded laterally, but does not form a distinctly defined neck (Newton & Thayer, 1995: figures 2 and 3). A neck region similar to that of pselaphines is also found in Scydmaeninae except for Cephenniitae (e.g., Jałoszyński, 2018). However, as this subfamily is not included in the Omaliinae group of rove beetles, this is certainly a result of parallel evolution. A groundplan apomorphy of Pselaphinae may be a four-segmented maxillary palp (e.g., Parker, 2016), with a short and often triangular palpomere 3, and a large, club-shaped palpomere 4 with (or without) a minute sensorial “pseudosegment” (Figures 2c, 7g,h, and 8e; Chandler, 2001; Jeannel, 1950; Schomann et al., 2008: figure 24). Such a condition is present in *Faronus* Aubé (Jeannel, 1950: figure 5a), *B. saulcyi* (Figures 7h and 8e) and many others (e.g., Chandler, 2001). However, the pselaphine maxillary palps are the most variable among all subfamilies of Staphylinidae, apparently many times undergoing far-reaching and often bizarre modifications, whose functions remain unknown. Palpomere 4 can be almost as small as 3 and oval in Mayetiini, (e.g., Novoa & Baselga, 2002), and small and subconical in Hybocephalini (e.g., Nomura, 1989). In contrast to the suggested groundplan condition, palpomere 3 of Tychini is often strongly elongate and club-like (e.g., Nomura, 1996). Another potential autapomorphy of Pselaphinae is the shift of the brain into

the neck region and the rather compact mass formed with the sub-oesophageal ganglion, a condition found both in leaf-litter dwelling *B. saulcyi* (Figure 6h and 9) and in a highly specialized myrmecophilous *Claviger* (Jałoszyński et al., 2020). However, the condition in *Protopselaphus* and in the vast majority of pselaphines is yet unknown.

Bergrothia differs distinctly in its cephalic anatomy from other taxa previously examined (e.g., Jałoszyński et al., 2020; Jeannel, 1950; Nomura, 1991), notably displaying a series of plesiomorphic features. In contrast to Clavigeritae and many other pselaphines, a frontal rostrum (Chandler, 2001) is not developed (or obsolete; Figures 2a,b and 3a). The clypeus, often steep in Pselaphinae (Jeannel, 1950: “le plus souvent fortement déclive”; Jałoszyński et al., 2020), is evenly sloping in *Bergrothia* (Figures 2a and 3d). This is likely a plesiomorphic feature, as this condition is also found in *Protopselaphus* (Newton & Thayer, 1995) and other groups of Staphylinidae (e.g., Blackwelder, 1936; Thayer, 2016; Thayer & Newton, 1979; Weide & Betz, 2009). Another plesiomorphy is the presence of thin but complete anterior tentorial arms, like in *Protopselaphus* (Newton & Thayer, 1995: figure 2) and *Mipselytrus levini* Chandler (2001), but in contrast to *Claviger* (Jałoszyński et al., 2020), and probably also *Batrisopslisus* (Nomura, 1991: figure 1) and other pselaphine groups. Other plesiomorphies compared to the clavigerite species examined by Jałoszyński et al. (2020) are the presence of a movable labrum with well-developed fronto-epipharyngeal retractors (Figure 9), antennal muscles exclusively originating from the tentorium (Figure 5a), strongly developed mandibles with distinct teeth and a narrow but distinct mola (Figures 7d,e and 8a–d), a full set of extrinsic maxillary and premental muscles (Figures 5b and 9), moderately-sized prepharyngeal dilators (M43, M44), and a slightly ascending M. tentoriobuccalis anterior (M48). A comparison with the cephalic muscle system of several species of Staphylinidae and one species of Leiodidae is shown in Table S1. The interpretation of the presence of an entire series of subapical mandibular teeth is difficult. This condition occurs in *Bergrothia* (Figure 8a–d) and other genera of Batrisitae (e.g., Yin et al., 2010: figure 6), and also in other groups such as for instance Brachyglutini (Kurbatov & Sabella, 2015: figures 19–27) (see also Chandler, 2001) and Euplectini (e.g., Jałoszyński & Nomura, 2021). Subapical teeth are missing in *Protopselaphus* (Newton & Thayer, 1995: figure 8) and also in *Faronus* (Jeannel, 1950: figure 5b), but as they are present in other representatives of Faronitae (Park & Carlton, 2015a), they are likely part of the groundplan feature of Pselaphinae.

The absence of a median frontal impression (Chandler, 2001: frontal fovea) is an ambivalent character, and also the complete absence of a vertexal sulcus sensu Chandler (2001) (in fact located on the frontal region) and of vestiges of dorsal ecdysial sutures (Figures 2b and 3a,d). A distinct frontal fovea is present in many groups including Faronitae (e.g., Chandler, 2001: figure 31; Park & Carlton, 2015b: figures 3l,m), and this is arguably a groundplan apomorphy of the subfamily, suggesting secondary loss in *Bergrothia* and some other pselaphines. The vertexal sulcus is well-developed in many pselaphine species and demarcating an inversely U-shaped median head region laterally and anteriorly (e.g., Jałoszyński & Nomura, 2021). This median area can be flat as in Euplectitae, but is

usually elevated in Batrisitae, and not demarcated by a vertexal sulcus, or this groove is at least shallow and barely discernible (e.g., Nomura, 1991). The latter condition is also found in *Bergrothia*, possibly a plesiomorphic condition in Pselaphinae. The absence of dorsal postantennal pits and of distinct antennal tubercles are also likely plesiomorphic conditions. A feature requiring further documentation among pselaphine taxa is the presence of a flexible, whip-like seta on the distal lateral margin of the mandible (Figure 8a,b; see also Schomann et al., 2008: figure 19a). Another potentially useful character observed in *Bergrothia* is the presence of a group of stiff setae on the lateral area of the ultimate maxillary palpomere (Figure 8f; Maghradze et al., 2019: figure 10a). Presently, a detailed documentation of the mouthparts is lacking in most taxonomic studies on Pselaphinae, impeding a phylogenetic interpretation of these features.

An autapomorphy of Batrisitae suggested by Kurbatov (2007) is the presence of a group of four stout setae or peg-like sensilla on the ventral side of the labrum, also well-developed in *Bergrothia* (Figure 2c; see also Yin et al., 2010: figure 4). Whether the presence of two similar pegs on the labrum of Brachyglutini (Kurbatov & Sabella, 2015: figures 28–39) is a preceding stage of this derived condition is uncertain. Another apomorphic feature of Batrisitae is the distinct anterolateral expansion of the labrum (Figure 8a,h; Kurbatov, 2007: figures 6 and 52–75). Like the previous feature this condition also occurs in species of Brachyglutini, even though quite variable and indistinct or absent in some genera (Kurbatov & Sabella, 2015: figures 28–39). A conspicuous derived condition is the presence of a clypeo-ocular ridge or carina (Figure 3d; Chandler, 2001: mandibulo-ocular carina). This feature does not only occur in Batrisitae, but also in Goniaceritae including the fossil *Cretobrachygluta* (Yin et al., 2019: figures 1b and 2d). This tentatively suggests a closer relationship between both supertribes, even though the monophyly of the latter is very uncertain (e.g., Chandler, 2001).

An unusual antennal feature shared by *Bergrothia* (Figure 5c) and most other pselaphines is a basal articulatory piece deeply countersunk in the main cylindrical scapal portion (Figure 4c; Jeannel, 1950: figure 1). Interestingly, this apomorphic condition is missing in Faronitae according to Jeannel (1950), and is also absent in *Protopselaphus* (Newton & Thayer, 1995: figure 6). Even though a more detailed documentation among pselaphine taxa is required for a reliable interpretation, this highly unusual feature may turn out as phylogenetically important. Another unusual antennal feature is the presence of an anterior and posterior incision at the apical scapal margin (Figure 3c; Chandler, 2001: figure 10; Kurbatov, 2007; Yin et al., 2010: figure 2), a mechanism fixing the remaining antenna in two defined positions. Even though this condition also occurs in some Scydmaeninae, it appears to be absent in extinct and extant pselaphines outside of Batrisitae (e.g., Chandler, 2001: figures 7, 9 and 31; Jałoszyński et al., 2020; Jeannel, 1950: figure 2; Parker, 2016: figures 2f and 3g; Yin et al., 2019). Consequently, this is an additional potential autapomorphy of this supertribe, even though it may have also evolved outside this group, in members of Proterini and in the *Morana-Nipponobythus* group of genera of Iniocyphini (Kurbatov, 2007; but see Yin, 2020: figure 2b). Another derived feature compared to *Protopselaphus*

(Newton & Thayer, 1995) and non-pselaphine staphylinids (Blackwelder, 1936; Thayer, 2016; Weide et al., 2010; Weide & Betz, 2009) is the presence of a median longitudinal submental ridge (Chandler, 2001: gular carina [but not reaching the gular plate posteriorly]). This structure is distinct in *Bergrothia* (Figure 3b) and also present in other pselaphines (e.g., Jeannel, 1950: figure 1b), but is missing in Clavigeritae (Jałoszyński et al., 2020: figure 3c) and also in Faronitae and Pselaphitae (Chandler, 2001; Park & Chandler, 2017: figure 3b). Even though this feature may vary strongly (e.g., in Brachyglutini; Chandler, 2001), it should be considered as a potential synapomorphy of a large subgroup of Pselaphinae including Batrisitae.

4.2 | Glands and their function

Cephalic integumental glands of pselaphine larvae and their use in prey capture were described by De Marzo (1988) (see also Schomann et al., 2008). The larval glandular tissue appears to be present in various groups of the subfamily (De Marzo, 1985, 1988), with the noteworthy exception of Faronitae (Newton, 1991). Maxillary palps of adults of *Bryaxis* Klug containing gland tissues and used for capturing prey were described by Schomann et al. (2008). A complex and voluminous system of cephalic glands of adults of Pselaphinae was described and documented in a study on *Claviger testaceus* (Jałoszyński et al., 2020: figure 6d,e). It is known that secretions are crucial for appeasing ants in their colonies by the myrmecophile species (Cammaerts, 1974, 1992). However, a similar set of labral, mandibular and labiohypopharyngeal glands is present in *B. saulcyi*. As all glandular subunits likely release their secretions into the preoral space, it appears likely that they are related with preoral digestion in *Bergrothia*, and probably also in other pselaphines not associated with ants. It is obvious that more data, especially on chemical compounds, are required for a reliable interpretation. As such information is presently completely lacking, there is ample room for speculation. It is conceivable that cephalic gland secretions are used for preoral digestion in the groundplan of Pselaphinae (or at least a large clade that includes Clavigeritae and Batrisitae), and substances of specialized subunits for prey capture in some cases (Schomann et al., 2008). Under strong selective pressure in ant colonies, genetic re-programming may have taken place, enabling at least some of the subunits to produce secretions attractive for ants. It is well-established that secretions of glands associated with abdominal trichomes (tergites IV–V) induce ants to regurgitate contents of their crops to supply clavigerite inquilines, and this is also likely for the labral and mandibular glands of the myrmecophile beetles (Cammaerts, 1974, 1992).

4.3 | Adaptations to subterranean habits

A derived character state of *B. saulcyi* is the greatly reduced condition of the compound eyes. This is likely an autapomorphy of the genus, even though reduction of light sense organs occurs frequently in

Pselaphinae, especially in cave-dwelling species and inquilines (e.g., Asenjo et al., 2017; Hlaváč et al., 2019; Jajoszyński et al., 2020). Despite being an inhabitant of leaf litter, the species shows features commonly found among endogean or troglobitic pselaphines, including Batrisitae, and especially other Amauropini, but normally not in species associated with upper, organic layers of soil. Apparent exceptions are some montane pselaphines and also carabids in tropical Africa, where conditions (humidity and temperature) in altitudes between 2000 and 2900 m are similar to those found in caves in the Mediterranean region (Jeannel & Leleup, 1952; Leleup, 1952).

The external elements of the compound eyes of *B. saulcyi* are strongly reduced, with only three cuticular lenses and small amounts of pigment. Moreover, a functional retina and optic neuropils (or even a thin optic nerve) are completely missing. A similar condition, at least concerning external structures, is found in the recently described cavernicolous *B. barbakadzei*. However, pigmentation is apparently lacking completely in this cave-dwelling species (Maghradze et al., 2019). Despite the presence of externally observable cornea lenses, *B. saulcyi* is obviously blind considering internal structures. The morphological modifications are so far-reaching that this condition is likely irreversible. A gradual impairment of vision might have started with a reduction of the number of functional ommatidia and the amount of optically-active pigments. However, a point of no return was reached with the reduction of the optic lobes and neuropils.

Other features likely linked with the ability of *B. saulcyi* to penetrate into deeper layers are the long antennae and a beard-like dense vestiture of long and thin setae on the posterior cephalic region. Long tactile hairs on different body regions are a typical feature of cave beetles, presumably compensating for the reduction or loss of the optical reception of stimuli (e.g., Luo et al., 2018a, 2018b; Luo, Antunes-Carvalho, Ribera, & Beutel, 2019; Luo, Antunes-Carvalho, Wipfler, et al., 2019). This sensorium appears even enhanced in the cavernicolous *B. barbakadzei* (Maghradze et al., 2019: figure 9). Additionally, the antenna of this species is more than twice as long as the head capsule, which is typical of cavernicolous pselaphine species, but only 1.8 times as long in *B. saulcyi* (Figure 2a). This also resembles conditions found in cave dwelling beetles of other families (e.g., Luo et al., 2018a; Luo, Antunes-Carvalho, Wipfler, et al., 2019). However, this character varies in morphologically similar species of Pselaphinae, and is not necessarily linked with subterranean habits. *Acanthanops bambuseti* Jeannel of eastern Africa, for instance, is likely dwelling in leaf litter but has distinctly elongated antennae (Jeannel & Leleup, 1952).

B. saulcyi apparently shows a set of morphological adaptations typical of endogean or cavernicolous beetles. This is, however, in contrast with frequent collecting of this species from upper layers of leaf litter (Hlaváč, 1999). It is conceivable that *Bergrothia* is adapted to occasional or periodical life in deep soil layers or crevices. Almost nothing is known about the natural history of this genus, except for preferences of each species to dwell in leaf litter, deep soil or in caves. A periodical search for more suitable and stable microhabitats by leaf litter-dwelling beetles in areas where the upper soil layers dry up during arid seasons seems a probable mechanism. For instance, the

common Iberian scydmaenine *Palaeostigus palpalis* (Latreille) (Mastigitae) is normally found in humid, shaded places, often near streams that tend to completely dry out in summer. This species was used as an indicator of hidden entrances to caves, as it shows a tendency to enter shallow cave chambers, where the microclimate is more stable (Pérez Fernández et al., 2013). The incomplete reduction of eyes may enable certain species of Amauropini to inhabit moist leaf litter layers, where conditions are not as inhospitable as those in deep soil, with abundant potential prey, and where sight may offer a considerable advantage. As the example of the blind *B. saulcyi* demonstrates, even a complete loss of optic nerves and neuropils does not mean a permanent life in deep soil. In areas where climatic factors periodically decide whether leaf litter environment is still viable, being adapted to quick moves deeper into the zone of complete darkness may determine the survival of the population and species. The slender body with long antennae and long sensory setae of *Bergrothia* is typical of subterranean beetles. It enables the beetles to persist in the locality in deeper, lightless layers and to “resurface” to leaf litter when the moisture increases. Stouter beetles with large eyes and a less developed setal sensorium must rely on their wings to leave their previously suitable dwellings and find other, still sufficiently humid, but possibly distant places. This strategy requires more energy and is more hazardous than simply moving into deeper layers of soil. Similarly, the return of non-endogean species during moist seasons will be delayed in relation to those taxa that do not need to disperse into distant suitable sites, but simply move closer to the surface, following a zone of optimum humidity. Such a strategy saves time and energy and offers advantage in competition with non-endogean insects. There is evidence that micro- and anophthalmous species of Pselaphinae (e.g., Jeannel & Leleup, 1962; Leleup, 1952) and beetles of other families (notably Carabidae: Trechinae, and Leiodidae: Choleviinae: e.g.; Bisio et al., 2012; Giachino, 1992) do occur in the leaf litter layer in montane regions, but this phenomenon is poorly understood. Behavioral observations are necessary to test our interpretation, or at least attempts to collect *Bergrothia* during arid seasons from deep soil (using a soil washing technique, for instance). This may also concern other taxa traditionally classified as leaf litter-dwellers but showing an “endogean” suite of features, as some carabids and leiodids. Such a scenario seems at least plausible, taking into account morphological adaptations observed in *B. saulcyi*.

5 | CONCLUSIONS

The morphological variability of Pselaphinae reaches an unusually high level. Nevertheless, detailed morphological investigations facilitated by modern technology (e.g., μ -CT), will likely improve the understanding of the phylogeny and evolution of the group. The present study supports the monophyly of Batrisitae and possible phylogenetic affinities with genera assigned to Goniaceritae. *B. saulcyi* has preserved an entire series of plesiomorphies of the head and its appendages and internal structures. However, the far-reaching reduction of the compound eyes and loss of optic lobes,

long antennae, and a sensorium of long setae are obviously adaptations to dark environments, such as deeper soil layers. Yet, the irreversible loss of optic nerves and neuropils does not necessarily mean a complete loss of eyes, as vestigial ommatidia are still present in blind *B. saulcyi*. Moreover, morphological adaptations to endogean life, including the loss of sight, do not confine a species to permanent life in deep soil or caves. The ability to move into zones of complete darkness under dry seasonal conditions may be an advantage of *B. saulcyi* and related species, a life strategy possibly more efficient and less hazardous than moving to different habitats using flight. This may compensate for the evolutionary costs of a reduced dispersal capacity. A large complex of cephalic glands found in *Bergrothia* and showing similarities to appeasement glands of myrmecophilous *Claviger* may be crucial to understand the processes of genetic re-programming of glandular secretions. The glands in *Bergrothia* seem to play a role in food intake or processing, while those in *Claviger* are crucial to manipulate behavior of ant hosts. We hypothesize that structurally similar glands may be a part of groundplan features of Pselaphinae (or a group including Clavigeritae and Batrisitae within Pselaphinae), and novel functions have evolved in myrmecophiles as adaptations to life with ants.

ACKNOWLEDGMENTS

We express great thanks to PD. Dr Hans Pohl (FSU Jena) for his assistance with the preparation of SEM samples, and also to Adrian Richter (FSU Jena) for conducting the μ CT scan and to Dr Alexander Stoessel for providing access to the equipment at the MPI für Menschheitsgeschichte (Jena). Valuable information on deep soil beetles was provided by Dr Vasily V. Grebennikov (Agriculture Canada), which is also gratefully acknowledged. We are also grateful for valuable comments made by Dr Arnaud Faille (Museum für Naturkunde Stuttgart) and two anonymous reviewers. The first author wants to express his thanks to CSC (No. 201708440281). The work of the second author was supported by the Ministry of Culture of the Czech Republic (DKRVO 2019–2023/5.I.c, National Museum, 00023272). Open Access funding enabled and organized by Projekt DEAL.

CONFLICT OF INTEREST

The authors declare no conflict of interest.

AUTHOR CONTRIBUTIONS

Xiao-Zhu Luo: Conceptualization; funding acquisition; visualization; writing-original draft; writing-review & editing. **Peter Hlaváč:** Conceptualization; funding acquisition; resources; writing-original draft; writing-review & editing. **Paweł Jałoszyński:** Conceptualization; visualization; writing-original draft; writing-review & editing. **Rolf Beutel:** Conceptualization; supervision; validation; visualization; writing-original draft; writing-review & editing.

DATA AVAILABILITY STATEMENT

The data that support the findings of this study are available from the corresponding author upon request.

ORCID

Xiao-Zhu Luo  <https://orcid.org/0000-0002-5253-267X>

Paweł Jałoszyński  <https://orcid.org/0000-0003-2973-1803>

REFERENCES

- Anton, E., & Beutel, R. G. (2004). On the head morphology and systematic position of *Helophorus* (Coleoptera: Hydrophiloidea: Helophoridae). *Zoologischer Anzeiger*, 242, 313–346.
- Antunes-Carvalho, C., Yavorskaya, M., Gnaspini, P., Ribera, I., Hammel, J. U., & Beutel, R. G. (2017). Cephalic anatomy and three-dimensional reconstruction of the head of *Catops ventricosus* (Weise, 1877) (Coleoptera: Leiodidae: Cholevinae). *Organisms Diversity & Evolution*, 17, 199–212.
- Asenjo, A., Ferreira, R. L., & Zampaulo, R. D. A. (2017). Description of *Metopiellus painensis* sp. nov. (Coleoptera, Staphylinidae), first troglobitic Pselaphinae from Brazil. *Zootaxa*, 4269, 115–123.
- Bekchiev, R., & Hlaváč, P. (2020). Endogean and Cavernicolous Coleoptera of the Balkans. XX. Notes on the genus *Protamaurops* J. Müller, 1944 (Coleoptera: Staphylinidae: Pselaphinae) with the description of a new species from Bulgaria. *Zootaxa*, 4779, 367–378.
- Belkaceme, T. (1991). Skelet und Muskulatur des Kopfes und Thorax von *Noterus laevis* Sturm: ein Beitrag zur Morphologie und Phylogenie der Noteridae (Coleoptera: Adephaga). *Stuttgarter Beiträge zur Naturkunde Serie A (Biologie)*, 462, 1–94.
- Besuchet, C. (1980). Le genre *Imirus* Reitt. (Coleoptera, Pselaphidae). *Nouvelle Revue d'Entomologie*, 10, 51–58.
- Besuchet, C. (1991). Révolution chez les Clavigerinae (Coleoptera, Pselaphidae). *Revue Suisse de Zoologie*, 98, 499–515.
- Beutel, R. G., Friedrich, F., Ge, S. Q., & Yang, X. K. (2014). *Insect morphology and phylogeny: A textbook for students of entomology*. Walter De Gruyter.
- Beutel, R. G., & Komarek, A. (2004). Comparative study of thoracic structures of adults of Hydrophiloidea and Histeroidea with phylogenetic implications (Coleoptera, Polyphaga). *Organisms Diversity & Evolution*, 4, 1–34.
- Bisio, L., Negro, M., & Allegro, G. (2012). I Coleotteri Carabidi della Valle di Gressoney (Valle d'Aosta) (Coleoptera Carabidae). *Revue Valdôtaine d'Histoire Naturelle*, 66, 5–43.
- Blackwelder, R. E. (1936). Morphology of the coleopterous family Staphylinidae. *Smithsonian Miscellaneous Collections*, 94, 1–102.
- Cammaerts, R. (1974). Le système glandulaire tégumentaire du coléoptère myrmécophile *Claviger testaceus* Preyssl, 1790 (Pselaphidae). *Zeitschrift für Morphologie der Tiere*, 77, 187–219.
- Cammaerts, R. (1992). Stimuli inducing the regurgitation of the workers of *Lasius flavus* (Formicidae) upon the myrmecophilous beetle *Claviger testaceus* (Pselaphidae). *Behavioural Processes*, 28, 81–96.
- Carlton, C. E. (2012). First records of troglobitic beetles from Arkansas: Two new species of *Speleochus* Park (Coleoptera: Staphylinidae: Pselaphinae: Bythinini), and synonymy of *Subterrochus* Park with *Speleochus*. *Coleopterists Bulletin*, 66, 177–186.
- Chandler, D. S. (2001). *Biology, morphology, and systematics of the ant-like litter beetle genera of Australia (Coleoptera: Staphylinidae: Pselaphinae)* (Vol. 15). Associated Publishers.
- Coiffait, H. (1955). Révision des *Mayetia* Muls. et Rey. *Revue Française d'Entomologie*, 22, 9–31.
- Coiffait, H. (1958). Les Coléoptères du sol. *Vie et Milieu, Supplément*, 7, 1–204.
- De Marzo, L. (1985). Organi erettili e ghiandole tegumentali specializzate nelle larve di *Batrisodes oculatus* Aubé: studio morfo-istologico (Coleoptera, Pselaphidae). *Entomologica (Bari)*, 20, 125–146.
- De Marzo, L. (1988). Comportamento predatorio nelle larve di *Pselaphus heisei* Herbst (Coleoptera, Pselaphidae). *Atti del XV Congresso Nazionale Italiano di Entomologia 1988, L'Aquila*, pp. 817–824.
- Faille, A., Casale, A., Balke, M., & Ribera, I. (2013). A molecular phylogeny of alpine subterranean Trechini (Coleoptera: Carabidae). *BMC Evolutionary Biology*, 13, 248.

- Fancello, L., Hernando, C., & Leo, P. (2009). The endogean beetle fauna of the Marganai-Oridda-Valle del Leni area (SW Sardinia), with description of seven new species of Staphylinidae Leptotyphlinae (Coleoptera). *Zootaxa*, 2318, 317–338.
- Faucheux, M. J. (2011). Antennal sensilla of the yellow longicorn beetle *Phoracantha recurva* Newman, 1840: Distribution and comparison with *Phoracantha semipunctata* (Fabricius, 1775) (Coleoptera: Cerambycidae). *Bulletin de l'Institut Scientifique*, 33, 19–29.
- Giachino, P. M. (1992). La distribuzione dei generi *Binaghtites* e *Bathysciola* nelle Alpi Occidentali (Coleoptera: Carabidae e Cholevidae). *Biogeographia*, XVI, 401–424.
- Giller, P. S. (1996). The diversity of soil communities, the 'poor man's tropical rainforest'. *Biodiversity and Conservation*, 5, 135–168.
- Grebennikov, V. V., Bulirsch, P., & Magrini, P. (2009). Discovery of *Anti-reicheia* in Cameroon with description of four new species and discussion on phylogeny and distribution of endogean Reicheiina (Coleoptera: Carabidae: Scaritinae: Clivinini). *Zootaxa*, 2292, 1–14.
- Hlaváč, P. (1999). Description of new *Bergrothia* from Turkey and notes on Amauropini (Coleoptera: Staphylinidae: Pselaphinae). *Entomological Problems*, 30, 49–53.
- Hlaváč, P., Baňaf, P., & Parker, J. (2013). The Pselaphinae of Madagascar. II. Redescription of the genus *Semiclaviger* Wasmann, 1893 (Coleoptera: Staphylinidae: Pselaphinae: Clavigeritae) and synonymy of the subtribe Radamina Jeannel, 1954. *Zootaxa*, 3736, 265–276.
- Hlaváč, P., Kodada, J., & Koval, A. (1999). A new cavernicolous species of *Seracamaurops* Winkler, 1925 (Coleoptera: Staphylinidae: Pselaphinae) from Caucasus. *Revue Suisse de Zoologie*, 106, 241–248.
- Hlaváč, P., Bregović, P., & Jalžić, B. (2019). Endogean and cavernicolous Coleoptera of the Balkans. XVIII. Strong radiation in caves of the central Dinarides: Seven new species of *Thaumastocephalus* Poggi et al., 2001 (Staphylinidae: Pselaphinae). *Zootaxa*, 4559, 90–110.
- Hlaváč, P., Oromi, P., & Bordoni, A. (2006). Catalogue of troglobitic Staphylinidae (Pselaphinae excluded) of the world. *Subterranean Biology*, 4, 19–28.
- Hlaváč, P., Ozimec, R., & Pavičević, D. (2008). Catalogue of the troglobitic Pselaphinae. *Institute for Nature Conservation of Serbia, Monograph*, 22, 307–328.
- Hlaváč, P., Perreau, M., & Čeplik, D. (2017). *The subterranean beetles of the Balkan Peninsula* (p. 267). ČZU.
- Huang, M. C., Li, L. Z., & Yin, Z. W. (2018). Eleven new species and a new country record of *Pselaphodes* (Coleoptera: Staphylinidae: Pselaphinae) from China, with a revised checklist of world species. *Acta Entomologica Musei Nationalis Pragae*, 58, 457–478.
- Jajoszyński, P. (2018). World genera of Mastigitae: Review of morphological structures and new ecological data (Coleoptera: Staphylinidae: Scydmaeninae). *Zootaxa*, 4453, 1–119.
- Jajoszyński, P., Luo, X. Z., & Beutel, R. G. (2020). Profound head modifications in *Claviger testaceus* (Pselaphinae, Staphylinidae, Coleoptera) facilitate integration into communities of ants. *Journal of Morphology*, 281, 1072–1085.
- Jajoszyński, P., & Nomura, S. (2021). A new species of *Leptoplectus* Casey from Ryukyu Islands, Japan, with comments on morphology of integumental structures in Euplectitae (Coleoptera, Staphylinidae, Pselaphinae). *Zootaxa*, 4915, 411–423.
- Jeannel, R. (1948). Révision des *Amaurops* et genres voisins (Pselaphidae). *Revue Française d'Entomologie*, 15(1), 1–19.
- Jeannel, R. (1950). Coleoptères Pselaphides. *Faune de France*, 53, iii +, 421.
- Jeannel, R. (1957). Révision des bembidiides endogés d'Afrique et de Madagascar (Anillini, Coleoptera Caraboidea). *Annales du Musée Royal du Congo Belge*, 52, 1–68.
- Jeannel, R., & Leleup, N. (1962). L'évolution souterraine dans la région méditerranéenne et sur les montagnes du Kivu. *Notes Biospéologiques*, 7, 7–13.
- Kéler, S. v. (1963). *Entomologisches Wörterbuch*. Akademie Verlag.
- Kühnelt, W. (1963). Soil-inhabiting arthropoda. *Annual Review of Entomology*, 8, 115–136.
- Kurbatov, S. A. (2007). Revision of the genus *Intestinarius* gen. N from Southeast Asia, with notes on a probable autapomorphy of Batrisitae (Coleoptera Staphylinidae: Pselaphinae). *Russian Entomological Journal*, 16, 281–295.
- Kurbatov, S. A., & Cuccodoro, G. (2019). Notes on *Iniocyphus iheringi* Raffray, 1912 (Coleoptera: Staphylinidae: Pselaphinae). *Zootaxa*, 4586, 171–179.
- Kurbatov, S. A., Cuccodoro, G., & Löbl, I. (2007). Revision of *Morana* sharp and allied genera (Coleoptera: Staphylinidae: Pselaphinae). *Annales Zoologici*, 57, 591–720.
- Kurbatov, S. A., & Sabella, G. (2008). Revision of the genus *Atychodea* Reitter with a consideration of the relationships in the tribe Tychini (Coleoptera, Staphylinidae, Pselaphinae). *Transactions of the American Entomological Society*, 134, 23–68.
- Kurbatov, S. A., & Sabella, G. (2015). A revision of the Chilean Brachyglutini. Part. 1. Some taxonomic changes in Brachyglutini and preliminary diagnosis of *Achilia* Reitter, 1890 (Coleoptera: Staphylinidae: Pselaphinae). *Revue Suisse de Zoologie*, 122, 297–306.
- Larsen, J. R., Booth, G., Perks, R., & Gundersen, R. (1979). Optic neuropiles absent in cave beetle *Glacivicola bathyscioides* (Coleoptera, Leiodidae). *Transactions of the American Microscopical Society*, 98, 461–464.
- Lawrence, J. F., Ślipiński, A., Seago, A. E., Thayer, M. K., Newton, A. F., & Marvaldi, A. E. (2011). Phylogeny of the Coleoptera based on morphological characters of adults and larvae. *Annales Zoologici*, 61, 1–217.
- Leleup, N. (1952). Réflexions sur l'origine probable de certains Arthropodes troglobies. *Revue de Zoologie et de Botanique Africaines*, 45(3–4), 210–221.
- Luo, X. Z., Antunes-Carvalho, C., Wipfler, B., Ribera, I., & Beutel, R. G. (2019). The cephalic morphology of the troglobiontic cholevine species *Troglocharinus ferrerii* (Coleoptera, Leiodidae). *Journal of Morphology*, 280, 1207–1221.
- Luo, X. Z., Antunes-Carvalho, C., Ribera, I., & Beutel, R. G. (2019). The thoracic morphology of the troglobiontic cholevine species *Troglocharinus ferrerii* (Coleoptera, Leiodidae). *Arthropod Structure & Development*, 53, 100900.
- Luo, X. Z., Jajoszyński, P., Stoessel, A., & Beutel, R. G. (2021). The specialized thoracic skeletomuscular system of the myrmecophile *Claviger testaceus* (Pselaphinae, Staphylinidae, Coleoptera). *Organisms Diversity & Evolution*. <https://doi.org/10.1007/s13127-021-00484-1>
- Luo, X. Z., Wipfler, B., Ribera, I., Liang, H. B., Tian, M. Y., Ge, S. Q., & Beutel, R. G. (2018a). The cephalic morphology of free-living and cave-dwelling species of trechine ground beetles from China (Coleoptera, Carabidae). *Organisms Diversity & Evolution*, 18, 125–142.
- Luo, X. Z., Wipfler, B., Ribera, I., Liang, H. B., Tian, M. Y., Ge, S. Q., & Beutel, R. G. (2018b). The thoracic morphology of cave-dwelling and free-living ground beetles from China (Coleoptera, Carabidae, Trechinae). *Arthropod Structure & Development*, 47, 662–674.
- Maghradze, E., Faille, A., Barjadze, S., & Hlaváč, P. (2019). A new cavernicolous species of the genus *Bergrothia* Reitter, 1884 (Coleoptera, Staphylinidae, Pselaphinae) from Georgia. *Zootaxa*, 4608, 371–379.
- Morrone, J., Osella, G., & Zuppa, A. M. (2001). Distributional patterns of the relictual subfamily Raymondionyminae (Coleoptera: Eriirhinidae): A track analysis. *Folia Entomologica Mexicana*, 40, 381–388.
- Morrone, J. J., & Hlaváč, P. (2017). Checklist of the micro- and anophthalmic soil-dwelling weevils of the world (Coleoptera: Curculionidae). *Zootaxa*, 4239, 1–102.
- Nakládal, O., & Hlaváč, P. (2018). New species and records of Clavigeritae (Coleoptera: Staphylinidae: Pselaphinae) from Africa and Asia. *Zootaxa*, 4402, 595–600.
- Newton, A. F. (1991). Pselaphidae (Staphylinidae). In F. W. Stehr (Ed.), *Immature insects* (Vol. 2, pp. 353–355). Kendall/Hunt.
- Newton, A. F., & Thayer, M. K. (1995). Protopselaphinae new subfamily for *Protopselaphus* new genus from Malaysia, with a phylogenetic analysis and review of the Omaliine Group of Staphylinidae including Pselaphidae (Coleoptera). In *Biology, phylogeny, and classification of*

- Coleoptera: papers celebrating the 80th birthday of Roy A. Crowson*. Muzeum i Instytut Zoologii PAN, Warszawa, pp. 219–320.
- Nomura, S. (1989). Description of a new species of *Apharinodes* (Coleoptera, Pselaphidae) from Okinawa Island, Japan. *Japanese Journal of Entomology*, 57, 278–282.
- Nomura, S. (1991). Systematic study on the genus *Batrisoplisus* and its allied genera from Japan (Coleoptera, Pselaphidae). *Esekia*, 30, 1–462.
- Nomura, S. (1996). A revision of tychine pselaphids (Coleoptera, Pselaphidae) of Japan and its adjacent regions. *Elytra*, 24, 245–278.
- Nonveiller, G., & Pavicevic, D. (2002). Une nouvelle espèce de *Pseudamaurops* Jeannel, 1948 du Monténégro, et remarques sur les genres voisins (Coleoptera: Pselaphinae: Amauropini). *Annales de la Société Entomologique de France*, 38, 435–442.
- Novoa, F., & Baselga, A. (2002). A new *Mayetia* Mulsant and Rey (Coleoptera: Staphylinidae: Pselaphinae) from Galicia (Northwest Spain). *The Coleopterists Bulletin*, 56, 541–546.
- Osella, G. (1977). Revisione della sottofamiglia Raymondionyminae (Coleoptera, Curculionidae). *Memorie del Museo Civico di Storia Naturale di Verona, 2 serie. Sezione Scienze della Vita*, 1, 1–162.
- Park, O. (1942). A study in neotropical Pselaphidae. In *Northwestern University studies in the biological sciences and medicine* (1st ed., p. 403). Northwestern University, x + 21 pls.
- Park, O. (1947). Observations on *Batrisodes* (Coleoptera: Pselaphidae), with particular reference to the American species east of the Rocky Mountains. *Bulletin of the Chicago Academy of Sciences*, 8, 45–132.
- Park, J. S., & Carlton, C. E. (2015a). *Aucklandea* and *Leschenea*, two new monotypic genera from New Zealand (Coleoptera: Staphylinidae: Pselaphinae), and a key to New Zealand genera of the supertribe Faronitae. *Annals of the Entomological Society of America*, 108(4), 634–640.
- Park, J. S., & Carlton, C. E. (2015b). *Brounea*, a new genus (Coleoptera: Staphylinidae: Pselaphinae) from New Zealand, with descriptions of nine new species. *Zootaxa*, 3990, 551–566.
- Park, J. S., & Chandler, D. S. (2017). *Nornalup*, a new genus of pselaphine beetle from southwestern Australia (Coleoptera, Staphylinidae, Pselaphinae, Faronitae). *ZooKeys*, 695, 111–121.
- Parker, J. (2016). Emergence of a superradiation: Pselaphine rove beetles in mid-cretaceous amber from Myanmar and their evolutionary implications. *Systematic Entomology*, 41(3), 541–566.
- Parker, J., & Maruyama, M. (2013). *Jubogaster towai*, a new Neotropical genus and species of Trogastrini (Coleoptera: Staphylinidae: Pselaphinae) exhibiting myrmecophily and extreme body enlargement. *Zootaxa*, 3630, 369–378.
- Parker, J., & Owens, B. (2018). *Batriscydmaenus* Parker and Owens, new genus, and convergent evolution of a “reductive” ecomorph in socially symbiotic Pselaphinae (Coleoptera: Staphylinidae). *The Coleopterists Bulletin*, 72, 219–229.
- Pérez Fernández, T., Pérez Ruiz, A., Pérez Fernández, J., & García Román, F. (2013). *Palaeostigus palpalis* (Latreille, 1804) (Col., Staphylinidae, Scydmaeninae) como bioindicador espeleológico. *e-insecta*, 1, 31–35.
- Pohl, H. (2010). A scanning electron microscopy specimen holder for viewing different angles of a single specimen. *Microscopy Research and Technique*, 73, 1073–1076.
- Schneeberg, K., Bauernfeind, R., & Pohl, H. (2017). Comparison of cleaning methods for delicate insect specimens for scanning electron microscopy. *Microscopy Research and Technique*, 80, 1199–1204.
- Schomann, A., Afflerbach, K., & Betz, O. (2008). Predatory behaviour of some central European pselaphine beetles (Coleoptera: Staphylinidae: Pselaphinae) with descriptions of relevant morphological features of their heads. *European Journal of Entomology*, 105, 889–907.
- Thayer, M. K. (2016). Staphylinidae Latreille, 1802. In R. G. Beutel & R. A. B. Leschen (Eds.), *Handbook of Zoology, Vol. IV Arthropoda: Insecta, part. 38 Coleoptera, Vol. 1: Morphology and systematics (Archostemata, Adephaga, Myxophaga, Polyphaga (partim))*. (2nd ed., pp. 394–442). Walter De Gruyter.
- Thayer, M. K., & Alfred, F. N. (1979). Revision of the south temperate genus *Glypholoma* Jeannel, with four new species (Coleoptera: Staphylinidae: Omaliinae). *Psyche*, 85, 25–63.
- Wipfler, B., Machida, R., Mueller, B., & Beutel, R. G. (2011). On the head morphology of Grylloblattodea (Insecta) and the systematic position of the order, with a new nomenclature for the head muscles of Di-condylia. *Systematic Entomology*, 36, 241–266.
- Weide, D., & Betz, O. (2009). Head morphology of selected Staphylinidae (Coleoptera: Staphyliniformia) with an evaluation of possible groundplan features in Staphylinidae. *Journal of Morphology*, 270, 1503–1523.
- Weide, D., Thayer, M. K., Newton, A. F., & Betz, O. (2010). Comparative morphology of the head of selected sporophagous and non-sporophagous aleocharinae (Coleoptera: Staphylinidae): Musculature and hypopharynx-prementum complex. *Journal of Morphology*, 271, 910–931.
- Weide, D., Thayer, M. K., & Betz, O. (2014). Comparative morphology of the tentorium and hypopharyngeal-premental sclerites in sporophagous and non-sporophagous adult Aleocharinae (Coleoptera: Staphylinidae). *Acta Zoologica*, 95, 84–110.
- Yin, Z. W. (2020). New species of karst-dwelling Pselaphinae from southwestern China (Coleoptera: Staphylinidae). *Acta Entomologica Musei Nationalis Pragae*, 60, 163–168.
- Yin, Z. W., Kurbatov, S. A., Cuccodoro, G., & Cai, C. Y. (2019). *Cretobrachygluta* gen. Nov., the first and oldest Brachyglutini in mid-cretaceous amber from Myanmar (Coleoptera: Staphylinidae: Pselaphinae). *Acta Entomologica Musei Nationalis Pragae*, 59, 101–106.
- Yin, Z. W., Li, L. Z., & Zhao, M. J. (2010). *Araneibatrus gracilipes* gen. et sp. n., a remarkable Batrisitae (Coleoptera, Staphylinidae, Pselaphinae) from PR China. *ZooKeys*, 69, 53.

SUPPORTING INFORMATION

Additional supporting information may be found online in the Supporting Information section at the end of this article.

How to cite this article: Luo X-Z, Hlaváč P, Jałoszyński P, Beutel RG. In the twilight zone—The head morphology of *Bergrothia saulcyi* (Pselaphinae, Staphylinidae, Coleoptera), a beetle with adaptations to endogean life but living in leaf litter. *Journal of Morphology*. 2021;1–18. <https://doi.org/10.1002/jmor.21361>

3.4 Study IV

Structural megadiversity in leaf litter predators - the head anatomy of *Pselaphus heisei* (Pselaphinae, Staphylinidae, Coleoptera)

Rolf Georg Beutel, **Xiao-Zhu Luo**, Margarita I. Yavorskaya, Paweł Jałoszyński

2021. *Arthropod Syst. Phylogeny* 79, 443–463. <https://doi.org/10.3897/asp.79.e68352>

Abstract: The head anatomy of *Pselaphus heisei* (Pselaphitae) is described and documented. The structural features are evaluated in comparison with findings presented in earlier studies on the subfamily, with a special focus on correlations with predacious habits and the groundplan of Pselaphinae. We found the tentorium, labrum, maxillary palps, shape of head, and a system of dorsal pits and sulci highly variable within the subfamily, reflecting multiple transformations, including many homoplasious changes. The following major characters are identified as groundplan features of Pselaphinae: falciform mandibles; small mola; semiglobular neck; ventrolateral antennal articulation; steep clypeal region; setiform labial palpomere 3; tentorium with nearly vertical main branches and lacking laminatentoria; separation of tentorial bridge from tentorial arms; fusion of dorsal tentorial arms with the head capsule; large brain placed in the posterior third of the head; and a triple cluster of well-developed cephalic glands. The last feature supports a hypothesis that multiple and independent cases of adaptations to myrmecophilous habits observed in various lineages of Pselaphinae were possible by re-programming already existing glands to produce appeasement secretions. The cephalic muscle apparatus of *P. heisei* is similar to what is found in other staphylinoid groups, with some exceptions, whereas it is strongly modified in the myrmecophile *Claviger testaceus*. We propose that the unparalleled structural megadiversity in Pselaphinae is primarily linked with life in the upper soil layers combined with specialized carnivorous habits, with small and agile or mechanically protected arthropods as prey. Within the group, various specialized life habits have evolved, including myrmecophily, termitophily, and also life in deep soil or caves, each with unique morphological adaptations.

Conceptualization: R. G. Beutel, P. Jałoszyński

Visualization: X. Z. Luo, P. Jałoszyński

Writing-original draft: R. G. Beutel, X. Z. Luo, M. I. Yavorskaya, P. Jałoszyński

Writing-review & editing: R. G. Beutel, M. I. Yavorskaya, P. Jałoszyński

Funding acquisition: P. Jałoszyński

Estimated own contribution: 25%



Structural megadiversity in leaf litter predators - the head anatomy of *Pselaphus heisei* (Pselaphinae, Staphylinidae, Coleoptera)

Rolf Georg Beutel¹, Xiao-Zhu Luo¹, Margarita I. Yavorskaya², Paweł Jałoszyński³

1 Institut für Zoologie und Evolutionsforschung, Friedrich-Schiller-Universität Jena, Erbertstrasse 1, 07743 Jena, Germany [rolf.beutel@uni-jena.de]

2 Universität Tübingen, Institut für Evolution und Ökologie, Auf der Morgenstelle 28E, 72076 Tübingen, Germany

3 Museum of Natural History, University of Wrocław, Wrocław, Poland [scydmaenus@yahoo.com]

<http://zoobank.org/AB5CCA9B-032D-4040-A49B-0AFD7FAB6ABA>

Corresponding author: Margarita I. Yavorskaya (margarita.yavorskaya@uni-tuebingen.de)

Received 6 May 2021

Accepted 17 July 2021

Published 11 August 2021

Academic Editors André Nel, Marianna Simões

Citation: Beutel RG, Luo X-Z, Yavorskaya M, Jałoszyński P (2021) Structural megadiversity in leaf litter predators – the head anatomy of *Pselaphus heisei* (Pselaphinae, Staphylinidae, Coleoptera). Arthropod Systematics & Phylogeny 79: 443–463. <https://doi.org/10.3897/asp.79.e68352>

Abstract

The head anatomy of *Pselaphus heisei* (Pselaphitae) is described and documented. The structural features are evaluated in comparison with findings presented in earlier studies on the subfamily, with a special focus on correlations with predacious habits and the groundplan of Pselaphinae. We found the tentorium, labrum, maxillary palps, shape of head, and a system of dorsal pits and sulci highly variable within the subfamily, reflecting multiple transformations, including many homoplasious changes. The following major characters are identified as groundplan features of Pselaphinae: falciform mandibles; small mola; semiglobular neck; ventrolateral antennal articulation; steep clypeal region; setiform labial palpomere 3; tentorium with nearly vertical main branches and lacking laminatentoria; separation of tentorial bridge from tentorial arms; fusion of dorsal tentorial arms with the head capsule; large brain placed in the posterior third of the head; and a triple cluster of well-developed cephalic glands. The last feature supports a hypothesis that multiple and independent cases of adaptations to myrmecophilous habits observed in various lineages of Pselaphinae were possible by re-programming already existing glands to produce appeasement secretions. The cephalic muscle apparatus of *P. heisei* is similar to what is found in other staphylinoid groups, with some exceptions, whereas it is strongly modified in the myrmecophile *Claviger testaceus*. We propose that the unparalleled structural megadiversity in Pselaphinae is primarily linked with life in the upper soil layers combined with specialized carnivorous habits, with small and agile or mechanically protected arthropods as prey. Within the group, various specialized life habits have evolved, including myrmecophily, termitophily, and also life in deep soil or caves, each with unique morphological adaptations.

Keywords

Glands, micro-CT, musculature, pselaphine beetles, 3D-reconstruction.

1. Introduction

Pselaphinae, also known as short-winged mold beetles or ant beetles, are a group with small brownish adults, often with a cryptic lifestyle (e.g. Park 1947a; Chandler 2001). Nevertheless, they have attracted a lot of attention among coleopterists, also including numerous amateur collectors and taxonomists. Despite their small size and often obscure existence in soil and leaf litter, they are a very successful subgroup of rove beetles, with over 1,200 genera and more than 10,000 described species (Thayer 2016, with later additions). Based on their unusual morphology, they were previously considered as a separate family of Staphylinioidea (e.g. Latreille 1802; Jeannel 1950; De Marzo and Vovlas 1989; see also Newton and Chandler 1989), but are now assigned subfamily rank within Staphylinidae (e.g. Thayer 2016). Pselaphine beetles play an important ecological role in their microhabitats. Park (1947a) stated that they are not a predominant influence in any specific task or in any given community, but that “despite of this lack of drama” they play an essential role in forest floor litter. Aside from rather unspecialized predacious species of upper soil levels, like for instance *Pselaphus heisei* Herbst, 1792 or species of *Bryaxis* Kugelann, 1794 (Schomann et al. 2008), a remarkable spectrum of specialized life styles has evolved within the group, including myrmecophiles, termitophiles and cave dwelling species (e.g. Besuchet 1991; Hlaváč et al. 1999; Chandler 2001; Parker and Grimaldi 2014; Parker 2016a; Jałoszyński et al. 2021; Luo et al. 2021a, 2021b). Aside from the enormous taxonomic and ecological diversity, Pselaphinae are probably unparalleled in Staphylinioidea (if not in Coleoptera) in the extreme variability of structures and shapes of different body regions, with a plethora of specialized structural modifications unknown in other groups of beetles (e.g. De Marzo and Vovlas 1989; Chandler 2001; Parker 2016a, 2016b; Jałoszyński et al. 2020; Luo et al. 2021a, 2021b).

The external aspects of the structural megadiversity were treated in several substantial contributions, for instance Jeannel (1950), De Marzo and Vovlas (1989), Chandler (2001) and Parker (2016). However, as pointed out in Jałoszyński et al. (2021) and Luo et al. (2021a, 2021b), the presently available information on the anatomy is basically restricted to a study on the highly specialized myrmecophile genus *Claviger* Preyssler, 1790 (Clavigeritae) (Jałoszyński et al. 2020; Luo et al. 2021b), and one on a nearly eyeless species of *Bergrothia* Reitter, 1884 (Batrisitae) (Luo et al. 2021a). The already documented structures provided important insight into some aspects of evolution, especially those related to obligatory myrmecophily or the loss of sight, while some unexpectedly discovered features remain puzzling, like for instance the presence of large cephalic glands in non-myrmecophiles (Luo et al. 2021a). It can be expected that studying internal structures of other tribes will substantially increase chances to clarify the currently poorly understood phylogeny, and also factors that triggered a megadiation within rove beetles. Consequently, the aim

of the present contribution is a detailed documentation of external and internal head structures of a less specialized representative of Pselaphinae. For this purpose, we chose the type genus of the subfamily, *Pselaphus* Herbst, 1792 of the supertribe Pselaphitae, represented by its predacious type species, *Pselaphus heisei*. The genus comprises 79 extant species and has a Holarctic, Oriental, Afrotropical (incl. Madagascar), Southern Pacific (New Zealand) and Caribbean (Jamaica) distribution (Newton and Chandler 1989, and later additions). To investigate and document the cephalic anatomy, we used a combination of well-established and modern morphological techniques, notably scanning electron microscopy (SEM), μ -computed tomography (μ -CT), and computer-based 3D reconstruction. The morphological results are compared with observations made in other pselaphines, especially *Claviger testaceus* Preyssler, 1790 (Jałoszyński et al. 2021) and *Bergrothia saulcyi* (Reitter, 1877) (Luo et al. 2021a), but also other members of the subfamily and species of related groups.

2. Material and methods

2.1. Studied species

Pselaphitae: *Pselaphus heisei*; beetles collected from leaf litter in Turze Pole ad Brzozów, SE Poland, by Dariusz Twardy. Specimens were preserved in 75% ethanol.

2.2. Micro-computed tomography (μ -CT) and microtome sections

Specimens were dehydrated with an ascending series of ethanol (70%–80%–90%–95%–100%), stained in iodine solution, transferred to acetone and then dried at the critical point (Emitech K850, Quorum Technologies Ltd., Ashford, UK). One of the dried specimens was scanned at the MPI for the Science of Human History (Jena, Germany) with a SkyScan 2211 X-ray nanotomograph (Bruker, Knotich, Belgium) with an image spatial resolution of 0.30 μ m (isotropic voxel size) using the following parameters: 50 kV, 300 μ A, 4600 ms exposure time, 0.16° rotation steps, frame averaging on (2), and using Filter (0.5 mm Ti). Projections were reconstructed by NRecon (Bruker, Knotich, Belgium) into TIFF files. AMIRA 6.1.1 (Thermo Fisher Scientific, Waltham, USA) and VG studio Max 2.0.5 (Volume Graphics, Heidelberg, Germany) were used for the three-dimensional reconstruction and volume rendering. The μ -CT-scan is stored in the collection of the Phyletisches Museum Jena (for access, please contact X.-Zh. Luo).

For microtome sectioning, one specimen of *P. heisei* was embedded in araldite CY 212® (Agar Scientific, Stansted/Essex, UK). Sections were cut at 1 μ m intervals using a microtome HM 360 (Microm, Walldorf, Germany) equipped with a diamond knife, and stained with tolu-

idine blue and pyronin G (Waldeck GmbH and Co.KG/ Division Chroma, Münster, Germany). The sections are stored in the collection of the Phyletisches Museum.

2.3. Scanning electron microscopy

Specimens were cleared in a warm 10% aqueous solution of KOH for 20–60 min, thoroughly washed in distilled water and dissected; isolated body parts were transferred from 75% to 99% ethanol for 15 min and air-dried, mounted on SEM stubs with carbon tabs and examined uncoated using a Helios Nanolab 450HP scanning electron microscope (FEI, Hillsboro, USA). Images were processed using CorelDraw Graphic Suite 2017; the following adjustments were made: overall brightness and contrast enhanced, and background manually replaced with black.

2.4. Terminology

The nomenclature of v. Kéler (1963) for cephalic muscles was used. Designations introduced by Wipfler et al. (2011) for the entire Neoptera are added in parentheses, for example M7-M. labroepipharyngalis (0lb5).

3. Results

3.1. External head structures

The distinctly prognathous head (Figs 1, 2A, C) is about 0.5 mm long, and the maximum width at the ocular region is ca. 0.3 mm; it is divided into three well-defined regions: (1) a distinctly developed anterior frontal rostrum (fr; Fig. 1A) (ca. 0.13 mm) bearing the antennae and mouthparts (Figs 3A, B, 4A–C); (2) a widened middle area with the laterally placed semiglobular compound eyes (ce; Figs 1A–C, 2A, C, 5A–E, G, 6A, B, 7A–F, 8B–C) and an evenly narrowing postocular region; and (3) a nearly hemispherical neck. The neck region (nr, Figs 1B–C, 2C, 5A, C, E, G) is distinctly retracted into the prothorax, especially on the dorsal side, and demarcated from the anterior portion of the head by a distinct occipital constriction (occ; Fig. 1A). The median region is flattened, with the highest elevation between and behind the compound eyes; the dorsal surface of the anterior region in front of the eyes is distinctly lower than the postocular area. The coloration of the cuticle is brown; it is smooth on most areas of the head capsule, but displays an irregular pattern of meshes separated by narrow, low cuticular ridges on the lateral and ventral areas of the rostrum; a vestiture of long, rather widely spaced setae (ca. 70–100 µm long) is present but mostly confined to the dorsal and lateral areas; median furrows (mf; Figs 1A, 5A) on the anterior and posterior frontal areas, and also the entire neck region are glabrous. No vestiges of dorsal ecdysial sutures

are present; the areas of the posterior frons, vertex (vt; Figs 1A, 5A) and genae (ge; Figs 1C, 5E) are completely confluent; an external division between the clypeus (cl; Fig. 5A) and the anterior frontal region is present; this low clypeofrontal ridge (cfr; Fig. 5A) is clearly visible in dorsal view. The well-developed, raspberry-shaped compound eyes are strongly protruding laterally; each is composed of 24 large ommatidia with strongly convex cornea lenses (diameter ca. 20 µm); setae or microtrichia between the lenses are absent; a row of four widely spaced setae is present posteroventrad the slightly emarginated posteroventral margin of the compound eyes; a group of similar setae is inserted in a supraocular groove, and two setae in a smaller concavity above them.

Ocelli are absent. The frontal region is strongly differentiated; widely spaced long and curved setae are inserted on different areas, except for the smooth and glabrous median furrows. The posterior frontal part between the compound eyes is medially divided by a deep furrow, ca. 20 µm wide anteriorly, narrowing posteriorly, and obliterating at the level of the posterior ocular margins; the posterior frontal portion is demarcated from the frontal roof of the rostrum by a deep semicircular emargination, which contains the large openings (diameter ca. 30 µm) of deep frontal pouches (fp; Figs 1A, 5A, 6A) reaching towards the compound eyes; a very dense circle of basally slightly flattened setae secludes the lumen of the pouches, which is filled with very homogenous, unrecognizable substrate, from the outside world. The rostrum formed by the anterior frontal region and the clypeus is dorsomedially divided by a broad furrow (ca. 30 µm), delimited by a very distinctly defined edge, sub-parallel anteriorly, but strongly widening posteriorly towards the lateral margin of the opening of the frontal pouches. Two large frontoclypeal supraantennal lobes (fcl; Figs 1A, 3A, 5A) (ca. 70 µm long and wide) form the anterior part of the frontoclypeal rostrum; they are evenly rounded laterally and anteriorly, and medially separated by a deep (ca. 35 µm), roughly triangular incision; widely spaced long setae are present on the dorsal and ventral side; the dorsal surface is smooth, whereas the lateral and ventral areas display a pattern of roughly pentagonal meshes with raised margins; the large antennal fossae are located on the ventral side of the lobes; a triangular distal clypeal area arises narrowly below the median incision and widens evenly towards the apical clypeal margin; this distinctly delimited flat triangular area and the ventral surface of the supra-antennal lobes have a reticulate surface sculpture; one pair of long setae is inserted on the middle region of the vertical clypeal part and three pairs very close to the apical margin.

The ventral side of the neck region (nr; Figs 1B, 2C, 5C) has a smooth surface on its lateral and anterior areas; a large median region with a reticulate surface structure represents the posterior gula; it is enclosed by indistinct, curved longitudinal furrows, the vestigial gular sutures (gs; Figs 1B, 2C). An extensive ventral region between the occipital constriction and the posterior tentorial pits, the anterior gular portion, is confluent with the adjacent ventrolateral genal areas; the entire region including the

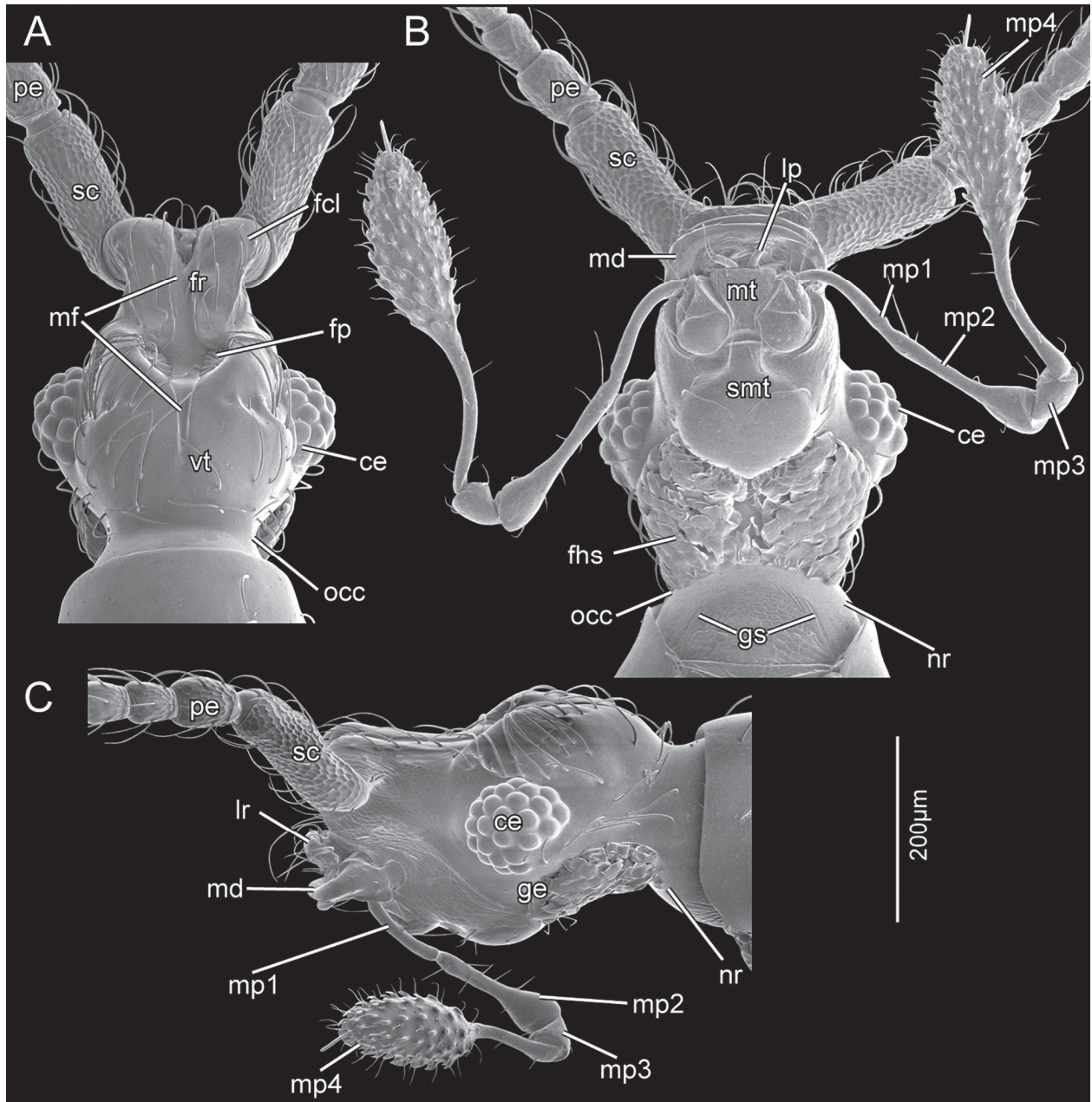


Figure 1. SEM images, head of *Pselaphus heisei*. (A) dorsal view; (B) ventral view; (C) lateral view. Abbreviations: ce, compound eye; fcl, frontoclypeal lobe; fhs, flattened hyaline setae; fp, frontal pouch; fr, frons; ge, gena; gs, gular sutures; lp, labial palp; lr, labrum; md, mandible; mf, median furrow; mp1–4, maxillary palpomere 1–4; mt, mentum; nr, neck region; occ, occipital constriction; pe, pedicellus; sc, scapus; smt, submentum; vt, vertex.

large and medially separated posterior tentorial pits (ptp; Fig. 6B) is covered with flattened hyaline setae (fhs; Fig. 1B), with the socket of each accompanied by a tiny glandular pore (gp; Fig. 2D, hyalinous seta removed, pore shown in close up). A fairly large and roughly circular portion of the ventral wall of the head, anterior to the posterior tentorial pit, is elevated and has a smooth surface (width ca. 0.14 mm); it is of submental origin, but laterally fused with the lateral walls of the rostrum. Two pairs of long setae are inserted on the sides of this bulging region, near the anterior third and on the anterior margin.

3.2. Internal skeletal structures

The main part of the tentorium (t; Figs 5B, I, 6D, 7A, 8D) is a nearly vertically oriented paired structure, comprising the posterior and dorsal arms. Anterior tentorial arms are missing and anterior tentorial pits are not recognizable externally. A tentorial bridge (tb; Fig. 5I) is present as curved sclerotized branches arising at the foramen occipitale, at the border between the gula and the low postoccipital bridge; it is interrupted medially. The large posterior pits (ptp; Fig. 6B) are widely separated from the bridge and also distinctly separated from each other medially. The nearly parallel main tentorial arms are dorsally fused with deep invaginations of the head capsule, externally

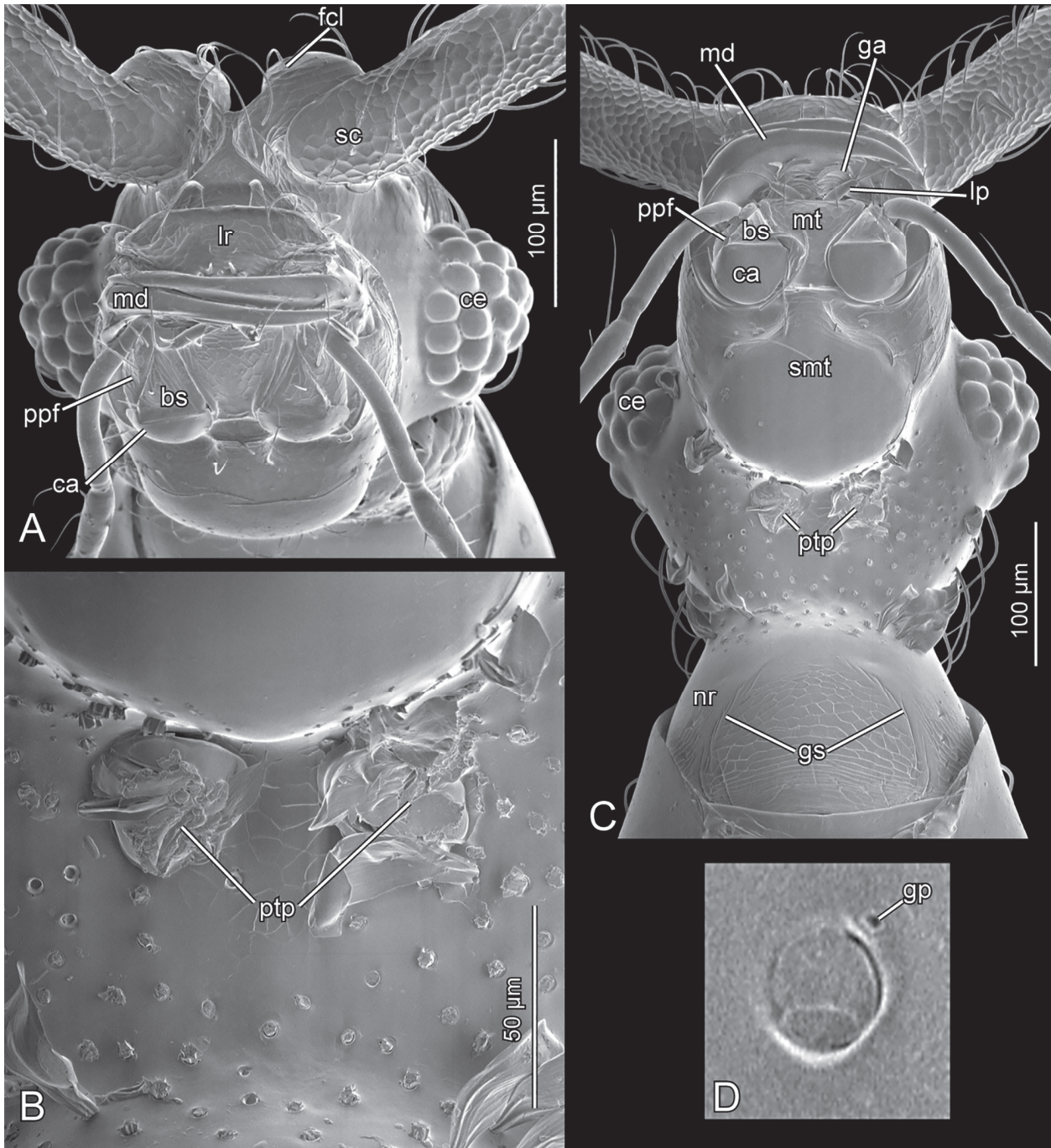


Figure 2. SEM images, head of *P. heisei*, (A) frontal view; (B–D) ventral view, flattened hyaline setae removed. Abbreviations: bs, basistipes; ca, cardo; ce, compound eye; ga, galea; gp, glandular pore; gs, gular suture (vestigial); lp, labial palp; lr, labrum; md, mandible; mt, mentum; nr, neck region; ppf, palpifer; ptp, posterior tentorial pit; sc, scapus; smt, submentum.

visible as frontal pouches (fp; Figs 6A, C–D), resulting in deeply countersunk dorsal tentorial pits (indicated as dorsal attachments of tentorium, dat, in Fig. 6C) (Chandler 1991: vertexal foveae).

3.3. Labrum

The labrum (lr; Figs 1C, 2A, 4C, 5A, E, 8A) is distinctly developed even though unusually shaped, short and only visible in frontal and lateral views. In lateral view the labrum has a rounded and elevated dorsal surface, resem-

bling a broad transverse bead, with several pairs of long and anteriorly curved setae (likely homologous to medio-dorsal or anterodorsal transverse row of setae of pse-laphines with an unmodified labrum); the strongly sclero-tized anterior area in front of these setae appears like an almost vertical ‘battering ram’ and overhangs the distal labral margin; it displays a somewhat irregular reticulate pattern of oblique to transverse cuticular scales, and a pair of short setae (ca. 7 μm) is inserted on the middle region, close to the median line; the thickened distal margin of the labrum bears a fixed, apically rounded median tooth, a pair of more pointed paramedian teeth, and a pair of stout,

curved setae (ca. 20 μm) posterior to the latter. The lateral margin is rounded; a tightly arranged group of three long brachyplumose microtrichia is present in the anterolateral corner, two long curved setae laterally (ca. 80 μm), and an additional pair of long setae posterolaterally. A pair of short (ca. 15 μm) but strongly developed tormae (width ca. 6 μm) is present at the base of the labrum, distinctly separated from the lateral edge, with a bifurcated, laterally directed process at the base.

Musculature (Fig. 7G): M7, *M. labroepipharyngalis*, O: posterior area of the dorsal wall of the labrum, close to the median line, I: anterior area of the epipharynx; M9, *M. frontoepipharyngalis*, O: anterior clypeofrontal area, close to the midline, anterior to the origin of M45, I: tormae at the posterolateral labral corner.

3.4. Antennae

The antennae are inserted on the ventral side of the rounded frontoclypeal supraantennal lobes (fcl; Figs 1A, 3A, 5A). They are ca. 1 mm long, eleven-segmented, and bear a three-segmented distal club. The roughly cylindrical scapus (sc; Figs 1A–C, 2A, 3A, 5A) is strongly elongate and subequal in length to antennomere 11 (both nearly 0.2 mm); it has a strongly curved short proximal region, and the visible basal edge has an approximately parallel orientation to the longitudinal antennal axis; the antennal articulation with the head capsule is not visible externally; the distal articulatory scapal portion is countersunk in a proximal concavity of the main part of the segment, whereas the proximal part lies within the lumen of the supra-antennal lobe; the remaining exposed surface of the scapus displays a pattern of deep pentagonal cells resembling hammered metal; about two dozens of long setae are evenly distributed over the surface. The pedicellus (pe; Figs 1A–C, 3A) is ca. 75 μm long and subcylindrical; a short, smooth basal pedestal is delimited from the distal portion of the segment by a slightly raised ring; the surface pattern of the distal cylindrical part is similar to that of the scapus; less than ten setae are inserted on the pedicellar surface in its middle region. Flagellomere 1 (fl1; Fig. 3A) is slightly shorter than the pedicellus and slightly longer than each of the three following segments; it slightly widens towards its apex after a short, smooth basal part; the cuticular microsculpture is less distinct than that on the scapus and pedicellus; five or six setae are inserted on the surface in the middle region. Flagellomeres 2–6 (fl2–6; Fig. 3A) are very similar, only 5 is slightly longer. The apical three segments (fl7–9, Fig. 3A) are slightly asymmetrical and form a loose but distinct club; the proximal club segment is slightly longer and broader than the pedicellus; it is distinctly widened distally, but the apical articulatory area is not wider than those of the other flagellomeres; like on the following two antennomeres, the density of the setae is distinctly increased; the surface microsculpture is largely obliterated on all three club segments, but still distinct on the basal areas; the penultimate antennomere is similar to the preceding one but shorter and stout; the apical segment is by far the largest, slightly

longer than the scapus, fusiform, and strongly widened in its middle region; the setation is also dense, and strongly concentrated on the apical region.

Musculature (Figs 7A–B): M1, *M. tentorioscapalis anterior*, O: ventral half of the dorsal tentorial arm; I: antero-ventral margin of the scapal base; M2, *M. tentorioscapalis posterior*, O: dorsalmost region of the dorsal tentorial arm, I: posterodorsal margin of the scapal base; M4, *M. tentorioscapalis medialis*, O: upper half of the dorsal tentorial arm, between the areas of origin of M1 and M2, I: medio-ventral area of the scapal base; M5, *M. scapopedicellaris anterior*, O: laterodorsal wall of the scapus, I: dorsolaterally on the basal margin of the pedicellus; M6, *M. scapopedicellaris posterior*, O: dorsolateral wall of the scapus, I: ventromedially on the basal margin of the pedicellus.

3.5. Mandibles

The slightly asymmetrical, broadly falciform mandibles are largely concealed below the labrum in their resting position, but well-developed and prominent when extended. They are mostly flat but a large, conspicuous protuberance (mpb; Fig. 4A) is present on the dorsal side of the basal portion. The surface is smooth; only few setae are present on the proximal region, close to the lateral margin. The articulation is dicondylic, with a very large dorsal condyle articulating with the head capsule, thus forming the secondary (dorsal) joint (smdj; Fig. 4A). The basal mandibular half is roughly parallel-sided and ca. 80 μm wide; a flat lamella (lml; Fig. 4A) is present proximolaterally. The distal mandibular part is strongly curved inwards, with a rounded outer edge; a curved longitudinal concavity (clc; Fig. 4B) is present on the ventral side of the bending area. The sharp mandibular apical tooth (at; Fig. 4A–B) is followed by two or three medium sized subapical teeth (sat; Fig. 4A) and two small teeth; the latter are continuous with the straight mesal edge of the proximal mandibular portion. The number and shape of preapical teeth were found to vary among individuals (two different beetles are shown in Figs 3A and 3B), and between the left and right mandible. A prostheca and mola are missing.

Musculature (Figs 7C–D): M11, *M. craniomandibularis internus*, largest cephalic muscle, O: large area of the lateral wall of the head capsule but posteriorly not reaching the neck region; I: with a tendon on the mesal mandibular base; M12, *M. craniomandibularis externus*, distinctly smaller than M11, consisting of two separate bundles with a shared a tendon, O: ventrolateral area of the capsule, M12a in front of the ventral base of the tentorium, M12b posterolaterad the ventral tentorial base, between bundles of M11; I: with a tendon on the lateral mandibular base.

3.6. Maxillae

The maxillary groove is very shallow; a smooth peristomal concavity is present laterad the basal half of the maxilla, delimited by a distinct, rounded ridge. The cardo

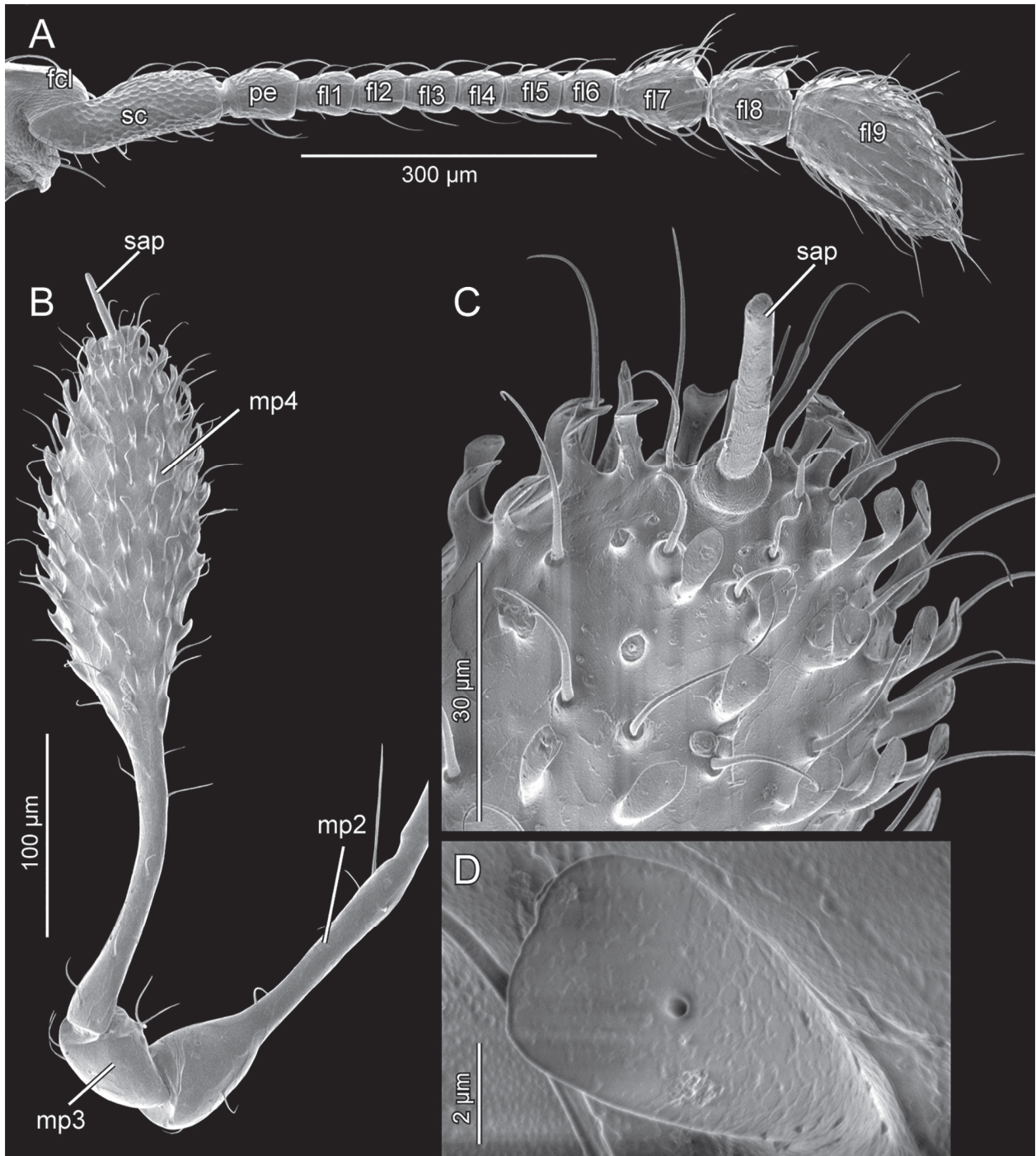


Figure 3. SEM images, antenna (A), maxillary palp (B), apical region of palpomere 4 (C), and spatulate projection on apical region of palpomere 4 (D) of *P. heisei*. Abbreviations: fcl, frontoclypeal lobe; fl1–9, flagellomeres 1–9; mp2–4, maxillary palpomeres 2–4; pe, pedicellus; sap, sensory appendage; sc, scapus.

(ca; Fig. 2A, C, 4B, 5G) is large in comparison to the remaining maxillary body, hemispherical, largely smooth and glabrous, except for one long seta inserted on the outer basilateral region. The largely glabrous stipes forms an angle of ca. 45° relative to the horizontal longitudinal axis of the head; the triangular basistipes (bs; Fig. 2A, C, 4B, 5G) is broadly connected with the distal margin of the cardo; a pattern of meshes with raised borders is present but faint; two short setae are inserted on the outer lateral margin; the narrow mediostipes (Fig. 4B) is laterally connected with the mesal basistipital edge; it bears

a pattern of longitudinal furrows and its mesal apex is strongly pointed; its oblique apical edge and the apical part of the palpifer enclose the base of the galea (ga; Fig. 2C); mesally it is fused with the lacinia. The galea is composed of a short, sclerotized basigaleomere with a lateral concavity, and a very dense tuft of long and curved bristles. A sharply pointed hook-shaped structure is present on the apex of the lacinia, and bristles similar to those on the galea are inserted along the mesal edge. The large palpifer (ppf; Fig. 2A, C, 4B, 5G) is broadly connected with the lateral basistipital edge and proximally also with

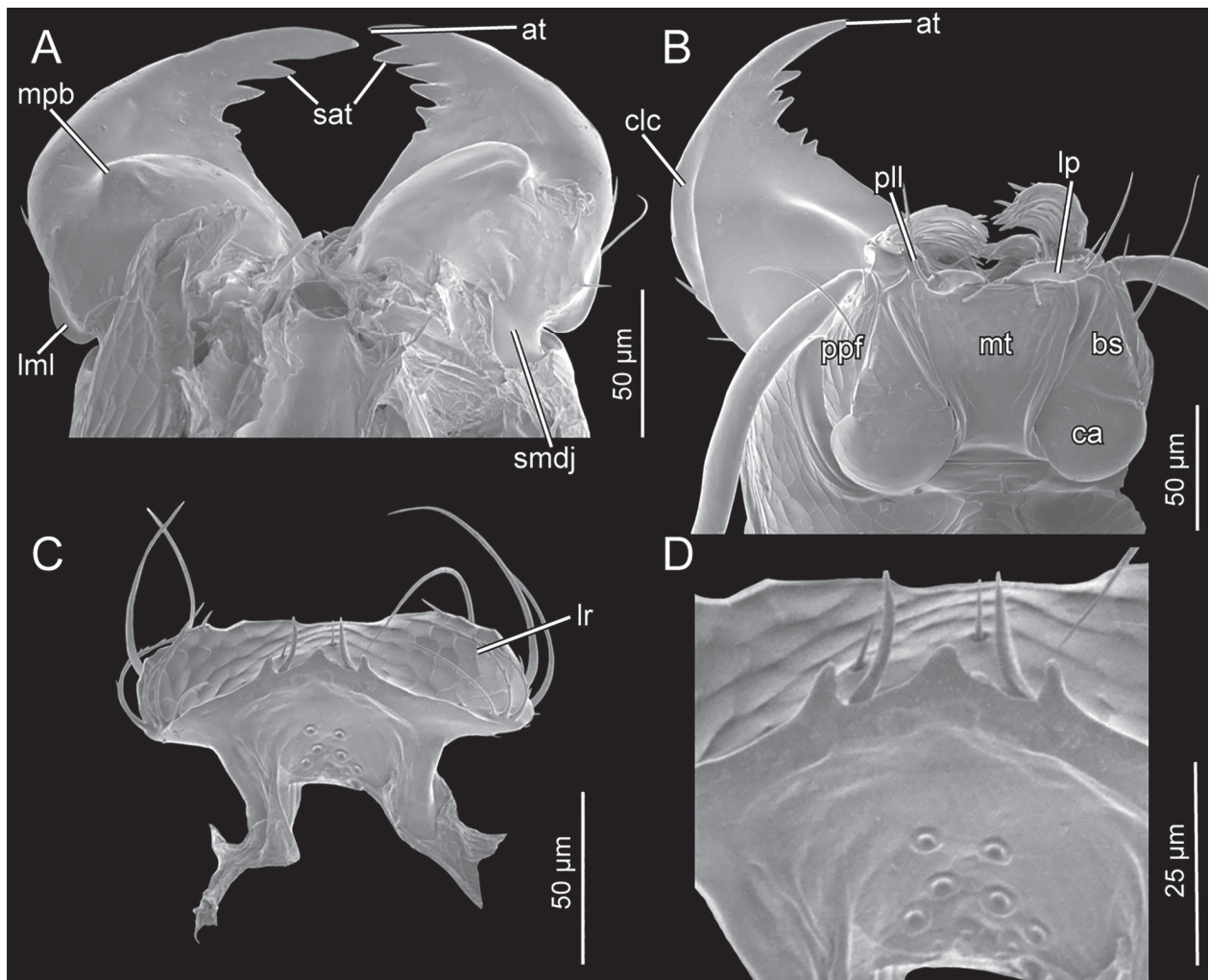


Figure 4. SEM images, mouthparts of *P. heisei*. (A) mandibles, dorsal view; (B) right mandible, mentum and part of maxilla, ventral view; (C–D) labrum-epipharynx, ventral view. Abbreviations: at, apical tooth; bs, basistipes, ca, cardo; clc, curved longitudinal concavity; lml, lamella; lp, labial palp; lr, labrum; mpb, mandibular protuberance; mt, mentum; pll, plate-like lobe; ppf, palpifer; sat, subapical tooth; smdj, secondary mandibular joint.

the oblique lateral part of the distal cardinal margin; its surface bears a distinct pattern of meshes and a long seta in the middle region (ca. 50 µm) and a short seta (ca. 15 µm) distally. The long and four-segmented maxillary palp is inserted on the oblique apical articulatory area of the palpifer; the extremely elongate basal palpomere (mp1; Fig. 1C) is cylindrical, over six times as long as broad and slightly curved; the articulation with palpomere 2 is only vaguely recognizable on the surface as an indistinct and broad constriction (clearly visible in transparent slides); palpomere 2 (mp2; Figs 1C, 3B) is nearly 1.3 times as long as 1 and its proximal 2/3 are subcylindrical, indistinctly broader than palpomere 1 and straight, and its distal part is distinctly widening distally, almost club-shaped, with distal articulating surface oblique in relation to the long axis of the palpomere; few thin setae are inserted on its smooth surface, by far the longest of them close to the base (ca. 70 µm); a short (ca. 60 µm) palpomere 3 (mp3; Figs 1B, C, 3B) is obliquely attached to the apical articulatory area of the preceding segment; it has an evenly rounded outer margin and a much shorter, nearly straight mesal edge, and a slightly oblique distal articulatory area;

four thin setae are inserted on the distal half, two on the outer and two on the mesal surface; its apical articulatory area is distinctly widened; palpomere 4 (mp4; Figs 1B–C, 3B) is ca. 0.37 mm long and by far the largest segment; the basal half is slender, cylindrical, slightly curved and smooth, with only few thin setae inserted on its surface; the distal half is conspicuously widened, fusiform, with a maximum width of ca. 80 µm; it bears a rich array of various surface structures, including many unmodified setae of ca. 25 µm length, sensilla campaniformia of different size, and specifically shaped cuticular projections (ca. 15 µm), curved, distally broadened and flattened, with a spatulate distal part which bears a single pore; the very slender, smooth and glabrous sensory appendage on apex of palpomere 4 (length ca. 40 µm, basal width ca. 4 µm) is inserted on a globular papilla; it is slightly narrowing distally and rounded apically.

Musculature (Figs 7E–F): M15, *M. craniocardinalis*, a moderately sized muscle, O: anterolateral area of the ventral wall of the head capsule, I: lateral branch of the cardinal process; M17, *M. tentoriocardinalis*, two separate bundles, O: both from the anterolateral area of the ventral wall

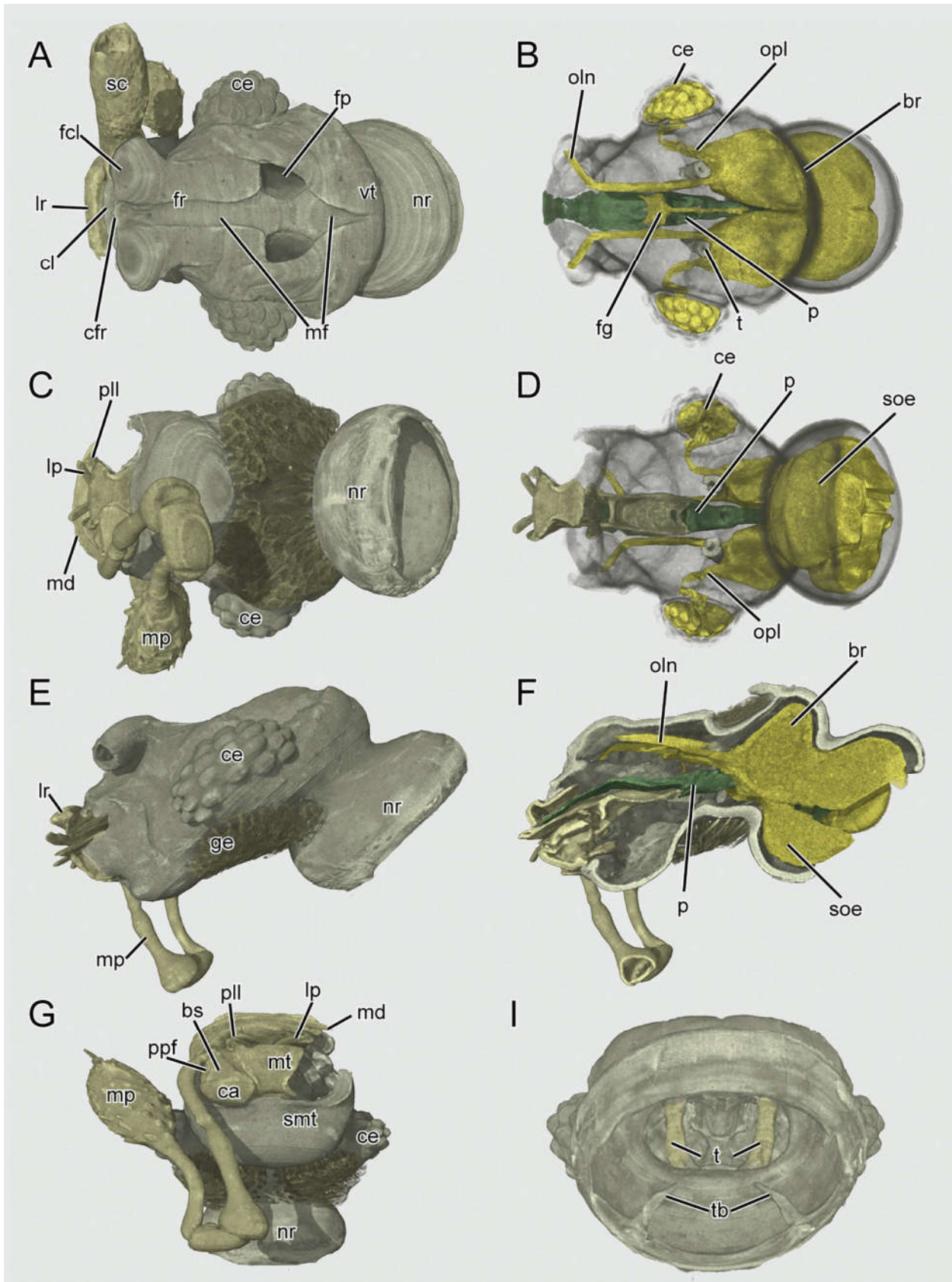


Figure 5. 3D reconstruction, head of *P. heisei*. (A) head, dorsal view; (B) nervous and digestive system, head capsule rendered transparent, dorsal view; (C) head, ventral view; (D) nervous and digestive system, head capsule rendered transparent, ventral view; (E) head, lateral view; (F) nervous and digestive system, head capsule rendered transparent, sagittal view; (G) head with right maxillary palp, ventral view; (I) head, posterior view. Abbreviations: br, brain; bs, basistipes; ca, cardo; ce, compound eye; cfr, clypeofrontal ridge; cl, clypeus; fcl, frontoclypeal lobe; fg, frontal ganglion; fp, frontal pouch; fr, frons; ge, gena; lp, labial palp; lr, labrum; md, mandible; mf, median furrow; mp, maxillary palp; mt, mentum; nr, neck region; oln, olfactory nerve; opl, optic lobe; p, pharynx; pll, plate-like lobe; ppf, palpifer; sc, scapus; smt, submentum; soe, suboesophageal ganglion; t, tentorium; tb, tentorial bridge; vt, vertex.

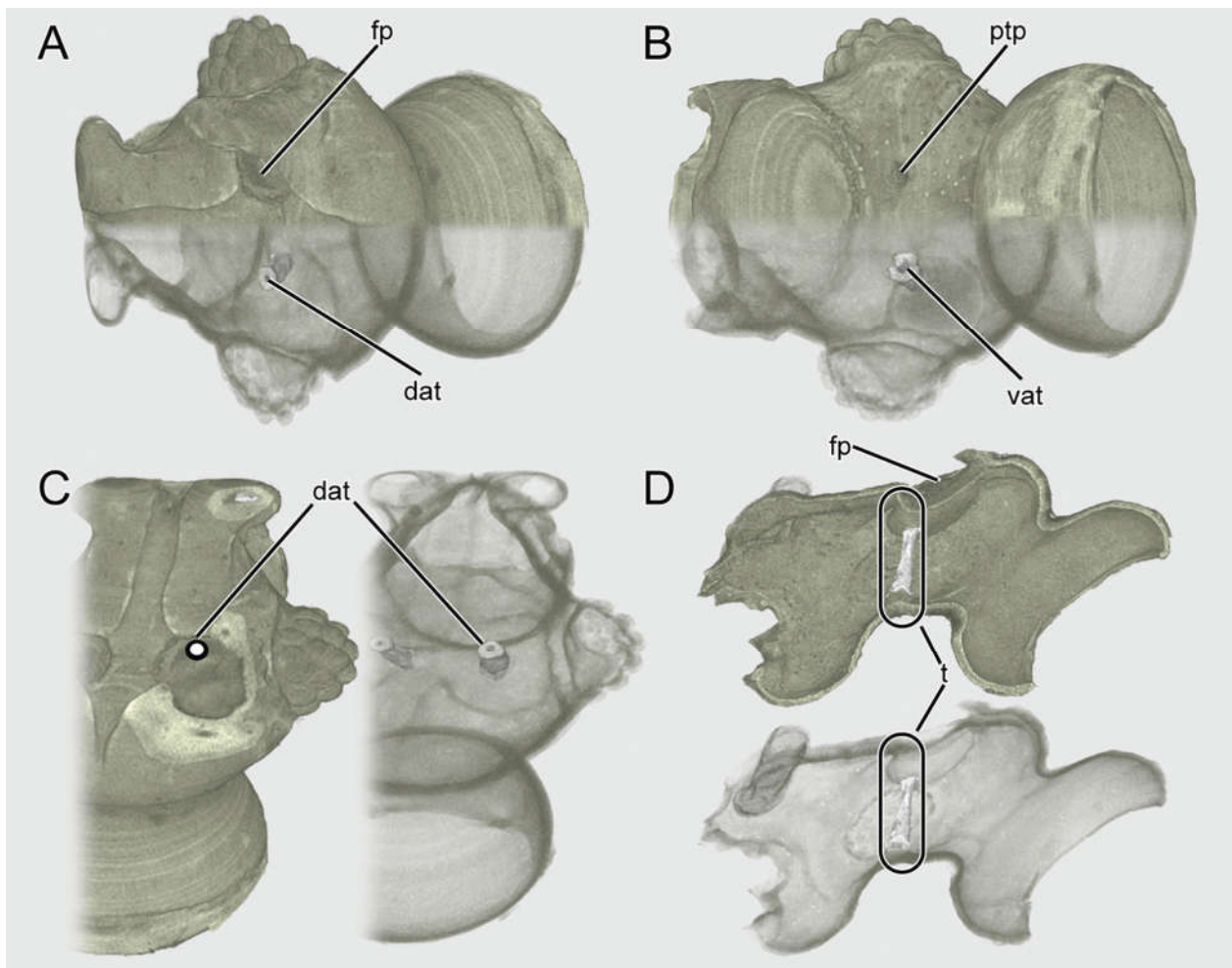


Figure 6. 3D reconstruction, head of *P. heisei*, tentorium. (A) dorsal view; (B) ventral view, flattened hyalinous setae removed, (A–B) upper half with intransparent cuticle, lower half with transparent cuticle; (C) dorsal view, uppermost part of frontal pouch cut off, cuticle intransparent on left side, transparent on right side; (D) sagittal view, upper half with cuticle intransparent, lower half with transparent cuticle. Abbreviations: dat, dorsal attachment of tentorium; fp, frontal pouch; ptp, posterior tentorial pouch; t, tentorium; vat, ventral attachment of the tentorium.

of the head capsule, I: separately on the mesal branch of the cardinal process, M17a on the typical attachment area on the mesal margin of the cardinal process, and M17b laterad this insertion site; M18, *M. tentoriostipitalis*, O: in front of the ventral base of the tentorium, I: with a tendon on the mediostipital base; M19, *M. craniolacinalis*, O: in front of the ventral tentorial base, I: with a thin tendon on the lacinal base; M21, *M. stipitogalealis*, O: base of the basistipes, I: basal area of the galea; M22, *M. stipitopalpalis externus*, O: base of the dorsal plate of the palpifer, I: laterally on the base of palpomere 1; M23, *M. stipitopalpalis internus*, O: base of the basistipes, I: basal margin of the palpifer; M26, *M. palpopalpalis tertius*, O: anterior-most wall of palpomere 2, I: basal margin of palpomere 3; M27, *M. palpopalpalis quartus*, O: along the ventral wall of palpomere 3, I: basal margin of palpomere 4.

3.7. Labium

The submentum (smt; Figs 1B, 2B) is completely fused with the adjacent areas of the ventral wall of the head

capsule; its large and smooth, nearly circular posterior region is distinctly elevated and convex; several long setae are inserted close to its posterior margin, a very long pair laterad the lateral margin, and one pair anteriorly; the raised anteromedian submental region is anteriorly connected with the mentum by an internalized membranous fold; the very indistinctly convex anterior margin is slightly thickened; the anterolateral submental region is slightly concave and forms a part of the shallow fossa maxillaris with its anterior margin. The large mentum (mt; Fig. 1B, 2C, 4B, 5G) (length ca. 70 μm) is inserted between the maxillae; a short and steep proximal portion is demarcated from the much larger anterior region by a transverse bulge; the anterior part is distinctly widening anteriorly, with a straight anterior margin (ca. 70 μm); a somewhat irregular bulge is present along the lateral edge; the anterolateral corners are rounded; the anterior portion completely covers the prementum; an indistinct pattern of meshes is present and a pair of setae is inserted close to the anterior margin. In contrast to the main body of the prementum, the labial palps are externally visible (lp; Figs 1B, 2C, 4B, 5G); the small palpomere 1 is al-

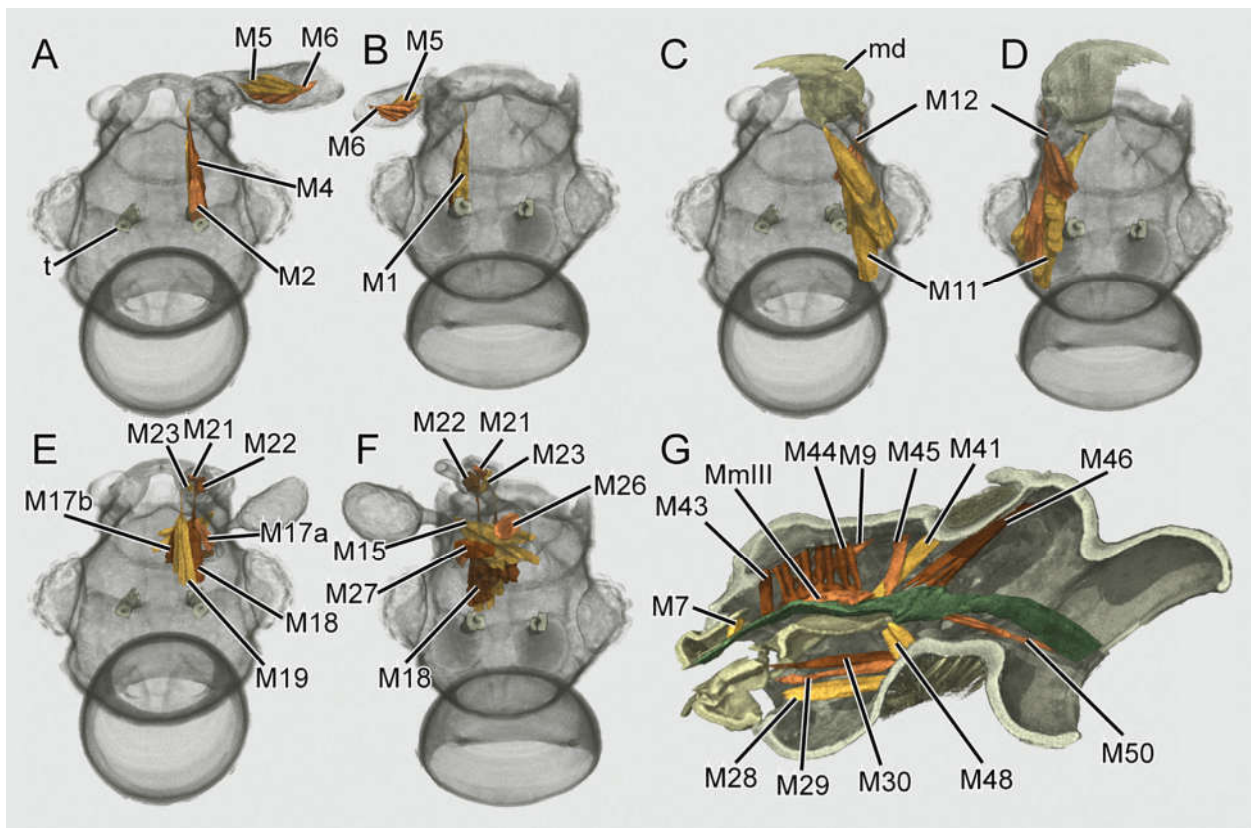


Figure 7. 3D reconstruction, head of *P. heisei*. (A–B) antennal muscles; (C–D) mandibular muscles; (E–F) maxillary muscles; (G) labral-epipharyngeal, pharyngeal and labio-hypopharyngeal muscles; (A), (C) and (E) dorsal view, (B), (D) and (F) ventral view, (G) sagittal view. Abbreviations: M1 – M. tentorioscapalis anterior (0an1); M2 – M. tentorioscapalis posterior (0an2); M4 – M. tentorioscapalis medialis (0an4); M5 – M. scapopedicellaris lateralis (0an6); M6 – M. scapopedicellaris medialis (0an7); M7 – M. labroepipharyngalis (0lb5); M9 – M. frontoepipharyngalis (0lb2); M11 – M. craniomandibularis internus (0md1); M12 – M. craniomandibularis externus (0md3); M15 – M. craniocardinalis externus (0mx1); M17a, M17b – M. tentoriocardinalis (0mx3); M18 – M. tentoriostipitalis (0mx4/0mx5); M19 – M. craniolacinalis (0mx2); M21 – M. stipitogalealis (0mx7); M22 – M. stipitopalpalis externus (0mx8); M23 – M. stipitopalpalis internus (0mx10); M26 – M. palpopalpalis tertius (0mx14); M27 – M. palpopalpalis quartus (0mx15); M28 – M. submentopraementalis (0la8); M29 – M. tentoriopraementalis (0la5); M30 – M. tentoriopraementalis superior (0la6); M41 – M. frontohypopharyngalis (0hy1); M43 – M. clypeopalpalis (0ci1); M44 – M. clypeobuccalis (0bu1); M45 – M. frontobuccalis anterior (0bu2); M46 – M. frontobuccalis posterior (0bu3); M48 – M. tentoriobuccalis anterior (0bu5); M50 – M. tentoriobuccalis posterior (0bu6); MmIII – Mm. compressores epipharyngis; md, mandible; t, tentorium.

most completely concealed; the slender palpomere 2 is spindle-shaped and ca. 30 μm long; a very long seta (ca. 40 μm) longer than palpomere 2 is inserted on its apex; a very slender, setiform palpomere 3 (ca. 15 μm) is inserted subapically on palpomere 2; it is more than 8 times as long as wide and has a smooth surface. Setiferous plate-like lobes (pll; Figs 4B, 5G) resembling paraglossae (Jeannel 1950: fig. 4, “languette”) are visible externally, laterad the palps, but inconspicuous (pll; Fig. 4B). It is likely that these structures are extensions of the anterior hypopharynx rather than true labial structures (see Luo et al. 2021a: figs 2c, 3b, 7c).

Musculature (Fig. 7G): M28, M. submentopraementalis, a seemingly unpaired median muscle, O: ventral wall of the head capsule, anterior to the tentorial base, I: ventromedially on the hind margin of the prementum; M29, M. tentoriopraementalis inferior, O: ventral wall of the head capsule, directly posterad M28, I: posterolaterally on the prementum; M30, M. tentoriopraementalis superior, O: ventral wall of the head capsule, posterolaterad

M29, I: dorsally on the posterior margin of the prementum; M34, not visible, probably absent.

3.8. Epipharynx and hypopharynx

The anteriormost epipharynx, i.e. the ventral side of the labrum (Fig. 4C–D), is sclerotized, smooth and glabrous; it lacks any microtrichia but two short, curved rows of three round pores with a distinctly elevated margin are present on the posterior portion. The posterior epipharynx, which forms the roof of a closed prepharyngeal tube, has a smooth surface and is distinctly sclerotized (Figs 8B–C). The anterior hypopharynx, which forms a structural unit with the anterior labium, is not visible externally (Figs 4B, 7G), with the possible exception of the plate-like lobes (pll; Fig. 4B). The posterior hypopharynx is laterally fused with the posterior epipharynx, thus forming the weakly sclerotized floor of the prepharynx (pph; Fig. 8B–C). Suspensorial sclero-

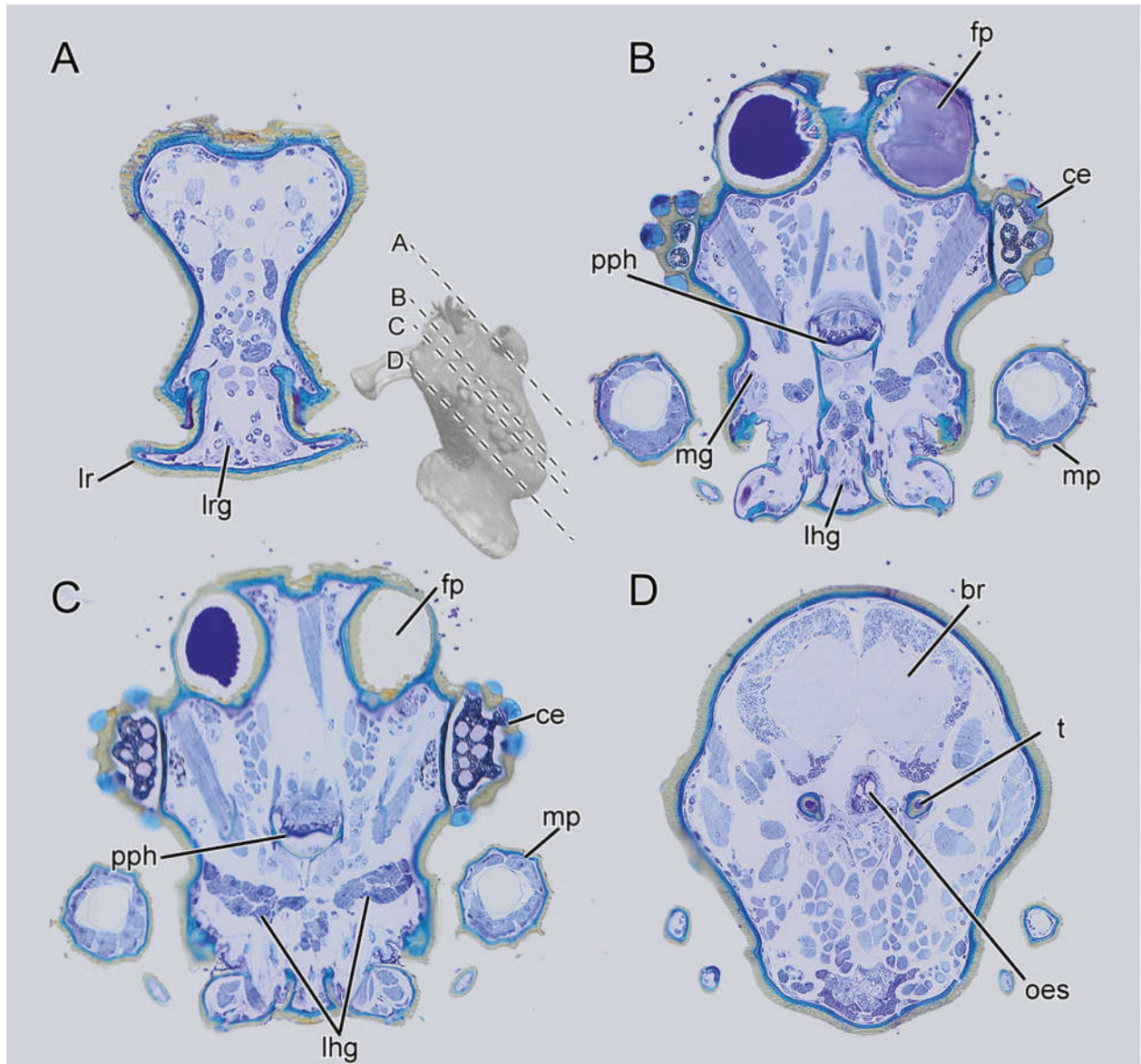


Figure 8. Histological sections of *P. heisei*. (A) labral region; (B–C) middle frontal region; (D) posterior frontal region (see inserted figure with dotted lines indicating position and orientation of sections). Abbreviations: br, brain; ce, compound eye; fp, frontal pouch; lhg, labiohypopharyngeal gland; lr, labrum; lrg, labral gland; mg, mandibular gland; mp, maxillary palp; oes, oesophagus; pph, prepharynx; t, tentorium.

tizations are not recognizable (microtome sections and μ -CT data).

Musculature (Fig. 7G): M41, *M. frontohypopharyngalis*, well-developed, moderately flattened muscle, O: central frontal region, posterolaterad M45 (see below), I: posterior edge of prepharyngeal tube, laterad the functional mouth and below the frontal ganglion; M43, *M. clypeopalatalis*, bipartite muscle complex formed by a single anterior pair and a series bundles, O: clypeofrontal region close to the median line; I: anterior bundle to the middle region of the epipharynx, the series of bundles on the epipharyngeal wall of the prepharyngeal tube; M44, *M. clypeopalatalis*, a single pair between the last bundle of the posterior subunit of M43 and M45; O: I: dorsal wall of the prepharyngeal tube, directly anterior to the anatomical mouth opening; MmIII, *M. buccalis transversalis*, a strong transverse bundle anterior to the anatomical

mouth; additionally thin transverse muscles are present between bundles of M43 and M44.

3.9. Prepharynx and pharynx

The closed prepharyngeal tube (pph; Fig. 8C) is fairly broad anteriorly, but narrower and higher posteriorly, almost heart-shaped in cross section where it connects with the anatomical mouth below the frontal ganglion. The pharynx (p, Figs 5B, D, F) is fairly wide anteriorly but distinctly narrowed between the brain and suboesophageal complex; the folds for attachment of dilator muscles are indistinct.

Musculature (Fig. 7G): M45, *M. frontobuccalis* anterior, O: central region of the frontal area, I: dorsally on the anteriormost pharynx, directly behind the anatomical

mouth opening; M46, M. frontobuccalis posterior, two long oblique bundles, O: frontal region, posterior to M41 and M45, I: dorsal pharyngeal wall, anterior to the brain; M48, M. tentoriobuccalis anterior, two short, stout bundles, almost vertically oriented, O: between the tentorial bases, I: ventrally on the anteriormost pharynx, directly posterior to the anatomical mouth, opposed to M45; M50, M. tentoriobuccalis posterior, O: from the apical part of the medially interrupted tentorial bride, I: ventrally on the precerebral pharynx, below the insertion of M46.

3.10. Nervous system

The brain (br; Figs 5B, F) and suboesophageal ganglion (soe; Figs 5D, F) are large in relation to the head size, occupying a large proportion of the lumen of the posterior half of the head, and almost completely filling out the narrowed neck region. The upper portion of the two protocerebral hemispheres is strongly inclined posterad, thus reaching the foramen occipitale; the lower protocerebral region and the deutocerebrum are slightly broader than the protocerebral portion in the neck region, and separated from it by a distinct constriction, corresponding with the occipital constriction of the head capsule. The optic lobes (opl; Fig. 5B) originate from the protocerebrum anterolaterally; they are distinctly developed but fairly thin and elongated, forming a conspicuous loop around M. craniomandibularis (M11) internus; the optic neuropils are indistinct; the thick olfactory nerves (oln; Figs 5B, F) are similar in diameter to the optic lobes and separated from them by the dorsal tentorial arms; they originate from the anterolateral deutocerebral region and enter the antennal lobes and scapus. The compact suboesophageal ganglion lies in the ventral half of the neck region. The unusually long, almost quadrangular frontal ganglion above the anatomical mouth releases an indistinct, short nervus procurrens anteromedially and a distinct nervus recurrens posteromedially; the frontal connectives originate anterolaterally.

3.11. Glands

Three well-developed glandular clusters are present in the head, unpaired labral and labiohypopharyngeal glands, and paired mandibular glands. The relatively small labral glands (lrg; Fig. 8A) are located within and posterad the labrum, the mandibular glands (mg; Fig. 8B) within the mandibular lumen and posterior to the mandibles. The labiohypopharyngeal cluster (lhg; Fig. 8B–C) is the largest; it extends from the tentorial base to the prementum and reaches its greatest width in the postocular region, where it almost reaches the lateral walls of the head capsule.

A rather diffuse tissue is present in the apical antennomere. However, an unambiguous interpretation as gland is not possible with the material at hand.

4. Discussion

Even though the present contribution on the unspecialized predacious *Pselaphus heisei* adds information on external and internal head structures, the available morphological data for Pselaphinae are still too limited for a formal character evaluation. Internal soft parts of crucial taxa are completely unknown, notably of *Protopselaphus* Newton and Thayer, 1995, the sister taxon of Pselaphinae, and also of Faronitae, probably the sister group of all remaining pselaphine supertribes (Newton and Thayer 1995; Parker 2016b). In the following we discuss different head structures with respect to their functional or phylogenetic significance (or both). The first part is focused on features likely linked with predaceous habits, the second part on characters where such a functional background is lacking or not apparent.

4.1. Predacious habits as ancestral condition

It was pointed out by Park (1947a) that the leaf mold carpet of forest floor, the typical pselaphine habitat, is inhabited by “imponderable numbers” of small animals, including for instance earthworms, millipedes, isopods, springtails (Collembola), insect larvae and mites. He suggested that the small predacious pselaphines feed on a variety of prey they can overpower with their forelegs and mandibles, and that mites may play a special role as food source. The predaceous habits of pselaphine species of several supertribes were investigated by Engelmann (1956), and later Schomann et al. (2008) using springtails as prey. The authors observed the role of different appendages in the process, notably the antennae in detection and the fore legs and mandibles in capture, but also the maxillary palps supporting detection and seizure. Park (1947b) described that certain species of *Batrisodes* Reitter, 1882 feed on armoured mites (Oribatida) under natural conditions, confirmed also by laboratory experiments. Alternative feeding on earthworms by species of the same genus was reported by the same author. Feeding on living springtails was observed many times under laboratory conditions by the senior author (PJ) for members of Euplectini, Brachyglutini, Iniocyphini, Bythinini, and Pselaphini.

That predaceous habits belong to the groundplan of Pselaphinae is clearly indicated by one feature found in *P. heisei* and many other species (e.g. Schomann et al. 2008: fig. 19A; Luo et al. 2021a), falcate mandibles with several sharp subapical teeth. As this condition is also found in Faronitae (Park and Carlton 2014, 2015a: fig. 2d), it is likely a groundplan apomorphy of the subfamily. In contrast, the mandibles of *Protopselaphus* display only an apical tooth, are rather triangular than falcate, and bear a dense elongate brush of microtrichia along their mesal edge (Newton and Thayer 1995: figs 8, 9). The loss of the brush is arguably another autapomorphy of Pselaphinae, although it is developed in Clavigeritae (Jałoszyński et al.

2020), as a part of an elaborate capillary apparatus to feed on a liquid regurgitate of ant workers. The presence of a small mola is probably part of the groundplan of the subfamily, like for instance in Faronitae (Park and Carlton 2014, 2015a: fig. 2d) or in *Bergrothia* (Luo et al. 2021a), and the complete absence like in *P. heisei* (Figs 4A–B) is a derived condition. The atrophied condition of the mandibles of *Claviger* (Jałoszyński et al. 2020) is obviously correlated with myrmecophilous habits, with adults being fed by the host ants. That a mandibular mola belongs to the groundplan of Staphyloidea and Staphylinidae is clearly indicated by the presence in some rove beetle subfamilies and in Leiodidae and related groups (e.g. Betz et al. 2003; Antunes-Carvalho et al. 2017).

Schomann et al. (2008: fig. 3) observed a distinct rise of the anterior body and a downward movement of the head during the predatory strike. The semiglobular neck, likely another autapomorphy of Pselaphinae, probably functions like a ball-and-socket joint with the anterior prothoracic foramen, thus facilitating the orientation of the mouthparts towards the prey. The strongly pronounced neck region is present in *P. heisei* and all other groups of pselaphines including the myrmecophilous Clavigeritae (Chandler 2001; Jałoszyński et al. 2020). In contrast, it is indistinct in *Protopselaphus* (Newton and Thayer 1995: fig. 2) and also indistinct or absent in many other groups of Staphylinidae (e.g. Blackwelder 1936).

The role of the antennae in prey detection and capture in different pselaphine species was described by Engelmann (1956) and Schomann et al. (2008). Specific antennal features are shared by Pselaphinae and *Protopselaphus* (Newton and Thayer 1995), including a moderately distinct three-segmented club, an enlarged apical segment, pedunculate antennomeres, and a rich array of sensilla. The proximal antennomeres of many pselaphines appear disproportionately thick in relation to the size of the anterior portion of the head (Fig. 2A; Jałoszyński et al. 2020; Luo et al. 2021a). However, this is a gradual modification and depends on the width of the anterior frontal region. The articulation of the antenna is highly unusual in *P. heisei* as compared to other beetles (e.g. Anton and Beutel 2004; Antunes-Carvalho et al. 2017), on the ventral side of distinctly developed supraantennal frontal lobes of the frontal rostrum (Fig. 1A). A shifted antennal insertion is apparently a gradual modification in Pselaphinae, with various intermediate stages. A ventrolateral articulation as it is found in *Bergrothia* (Luo et al. 2021a: figs 2a, b) and the extinct Cretaceous †*Burmagluta* Yin and Cai, 2021 (Yin et al. 2019) is possibly a groundplan apomorphy of Pselaphinae. The functional significance of this feature is rather unclear. The modified articulation possibly facilitates screening the underground with the antenna, movements relevant in the context of prey detection. Glands in the apical antennomere were identified in different species of Batrisini by De Marzo and Vít (1983). However, the secretions likely play no role in prey capture, but rather function as female attractants, as such glands are known only in males (De Marzo and Vít 1983).

The German common name “Palpenkäfer” (palp beetles) refers to another complex autapomorphy of Pselaph-

inae, the greatly modified (and extremely diverse) maxillary palps. This appendage is usually characterized by a short and often triangular palpomere 3, a large, terminal club-shaped palpomere 4, and a peg-like sensorial apical ‘pseudosegment’ (e.g. Schomann et al. 2008: fig. 24; Luo et al. 2021a). The palp with its well-developed muscles can be involved in prey detection and capture as described in detail in Schomann et al. (2008), even involving secretion of viscous substances in species of *Bryaxis*. The maxillary palps of *P. heisei* are enormously elongate, which is a typical feature of Pselaphini (e.g. Chandler 2001). Not only palpomeres 2 and 4 are remarkably long, but also palpomere 1. This is in very clear contrast to other groups of Pselaphinae, where the basal segment is very short and inconspicuous, very likely a groundplan feature of the subfamily, and also of the entire Staphylinidae.

The long range of the palps is certainly important for the small predacious species of Pselaphinae. Palpomere 4 of *Pselaphus* displays an unusually dense array of various sensilla and hair-like structures, including curved and apically spatulate cuticular projections, presumably with glandular openings (Figs 3B–C). It was suggested by Schomann et al. (2008) that elusive prey like springtails is entangled between various cuticular surface structures of the palps of *P. heisei*. Similar structures are known in other Pselaphini, with various modifications. Additionally, plumose and erect setae with glandular openings at their insertion sites can be found on palpomeres of many species of Goniaceritae (Jałoszyński, unpublished obs.). Consequently, the “entangling mechanism” of prey capture may be common in this group, and realized by different morphological modifications. The elaborate, conspicuous, and variously modified maxillary palps have been extensively used for taxonomic purposes, as their unique structure offers unambiguous diagnostic features for genera and tribes. No other subfamily among the megadiverse Staphylinidae shows a comparable degree of diversity in the structure and shape of these appendages.

The documentation of the labrum of Pselaphinae is sparse, as this structure is usually partly concealed (e.g. Luo et al. 2021a: fig. 1). However, it is likely that it plays a role in prey capture in various group. The known broad morphological diversity of labrum may reflect particular prey preferences or feeding techniques. A group of four stout labral setae (peg-like sensilla) has been identified as an autapomorphy of Batrisitae by Kurbatov (2007). It is conceivable that these large structures, apart from providing sensorial information, help to fix prey in the preoral space, combined with prominent lateral labral regions often projecting anterolaterad (Kurbatov 2007: figs 26–51). It is likely that three non-articulated spines at the apical margin of the labrum of *P. heisei* (Figs 4C–D) fulfil a similar function, as this is also known from predacious beetle larvae of different groups (e.g. Beutel 1993, 1999). The labral structure of *Pselaphus* supports the close relationship between Pselaphitae and Clavigeritae (Parker 2016b): the anterior surface of the labrum is nearly vertical in both supertribes, forming a bulldozer-like structure, and distinctly microreticulate. As this large vertical labral surface is obviously not unique for myrmecophilous Clav-

igeritae, it very likely represents a feature inherited from a common ancestor. The labrum of the distantly related *Bergrothia* (Luo et al. 2021a: fig. 6b) gradually and weakly declines anterad, and lacks a microsculpture. As its shape and orientation resemble a condition found in many unspecialized Staphyloidea (e.g. Weide and Betz 2009), it is likely plesiomorphic and part of the groundplan of Pselaphinae. In other large groups within Staphylinidae (or Staphyloidea), the labrum is relatively uniform, and not as diverse as in Pselaphinae (e.g. Blackwelder 1936; Antunes-Carvalho et al. 2017). An example is Scydmaeninae, a subfamily of rove beetles of over 5,500 described species with exoskeletal structures very well studied at the genus level (data in more than 200 studies by Jałoszyński). Their mandibles display a remarkable morphological diversity, reflecting various specialized prey-capture techniques. In contrast, the labrum is typically a transverse, weakly declining and slightly convex structure, with rounded sides and a straight, convex or dentate anterior margin, and a setose dorsal surface. In contrast to Pselaphinae, deviations from this general scheme are relatively minor in Scydmaeninae.

A typical pselaphine feature is a very steep clypeus, strongly declining from the anterior region of the frontal rostrum. This condition is present in *P. heisei* (Fig. 2A) and *Claviger* (Jałoszyński et al. 2020), and many other pselaphines including species of Faronitae (Chandler 2001; Park and Carlton 2015b: figs 2, 3L–M; Park and Chandler 2017: figs 2G–L, 3a), but not in *Bergrothia* (Luo et al. 2021a: fig. 1a) and many other Batrisitae. The condition in basal Faronitae suggests that a steep clypeal region is a groundplan apomorphy of Pselaphinae, with reversal in some groups including *Bergrothia*. It is likely that the derived configuration helps to fix agile prey like springtails between the mandibles, labrum and wide antennal bases.

The cephalic digestive tract of *P. heisei* is similar to what is found in other beetles in its general configuration (e.g. Anton and Beutel 2004; Dressler and Beutel 2010; Antunes-Carvalho et al. 2017). A feature of the preoral space distinguishing the hitherto examined species of Pselaphinae from other staphyliniform groups (e.g. Beutel et al. 2003; Anton and Beutel 2004; Antunes-Carvalho et al. 2017) is the absence of longitudinal epipharyngeal and hypopharyngeal lobes with dense arrays of microtrichia. The presence of these structures is likely linked with feeding on small particles such as fungal spores (Yavorskaya et al. 2017). Their absence in Pselaphinae may be an additional adaptation to secondarily acquired predacious habits.

4.2. Evolution of cephalic features within the group

An intriguing and characteristic but puzzling character system of Pselaphinae is the presence of furrows, foveae, non-foveal pits, and other cephalic (and also thoracic and abdominal) surface structures, and also various modes of ‘deformation’ of the head capsule (e.g. Chandler 2001).

These structural modifications are clearly absent in the groundplan of Staphyloidea and Staphylinidae (e.g. Blackwelder 1936; Beutel et al. 2003; Thayer 2016; Antunes-Carvalho et al. 2017; Yavorskaya et al. 2017). A more or less elongate frontal rostrum with anterolateral supraantennal lobes is present in *P. heisei* and many other groups, including some representatives of Faronitae (Chandler 2001: fig. 32). However, this feature is extremely variable in most supertribes and often indistinct or not recognizable (e.g. *Bergrothia*; Luo et al. 2021a: fig. 1b), rendering it problematic on a higher taxonomic level. Similarly, a V- or U-shaped frontal fovea or groove (Chandler 2001: vertexal sulcus) is very widespread among the supertribes. This structural modification is very characteristic for the subfamily and unknown in other groups of Staphylinidae. Nevertheless, its extreme variability and frequent absence renders it highly problematic for phylogenetic reconstructions. Moreover, the function of this dorsal modification of the head capsule is completely unclear, although it is conceivable that at least various sulci or grooves increase the rigidity of the head capsule. Interestingly, this system of pits and grooves is lacking or vestigial in Clavigeritae (Jałoszyński et al. 2020).

The presence of a very distinct longitudinal median frontal furrow is arguably a derived groundplan feature of Pselaphinae. This structure is absent in Protopselaphinae (Newton and Thayer 1995) but present in Faronitae (e.g. Chandler 2001; Park and Carlton 2015b: fig. 3l–m; Park and Chandler 2015b, 2017) and many other pselaphines (e.g. Chandler 2001) including *P. heisei* (Fig. 1A). The furrow may be a result of narrowing the anterior region of the head, with supraantennal tubercles becoming approximate, and a large and weakly concave anteromedian frontal area becoming squeezed to form a longitudinal groove. Consequently, a primary narrowing and secondary widening of the anterior head region may cause the median furrow to develop and become obliterated. Both processes might have occurred independently in various lineages, as the shape of the head varies greatly within some supertribes. Therefore, this feature is another problematic character system for phylogenetic reconstruction.

A conspicuous feature observed in *P. heisei* (Fig. 1) is the presence of very deep foveae situated anteromedially to the compound eyes, secluded from the outside world by a very dense rosette of flattened setae and filled with very homogenous material. These unusual structural modifications are missing in *Bergrothia* (Luo et al. 2021a) and *Claviger* (Jałoszyński et al. 2020), and also in *Protopselaphus* (Newton and Thayer 1995). However, densely setose pits combined with pouches occur in different groups of Pselaphinae (e.g. Chandler 2001: classified as ‘non-foveate pits’ [p. 26]). For instance, pouches of some species of *Euplectops* Reitter, 1882 (Euplectitae) are extending back as far as the cervical region, or taking up half of the cephalic lumen in some male *Bunoderus* Raffray, 1904 (Goniaceritae) (Chandler 1983, 2001). The distinct enlargement in males of the latter genus suggests a role in a sexual context. However, the function is still elusive, and also the phylogenetic significance. Various shapes, placements, and setal arrangements of these pits

and pouches, and their unknown contents and function(s) make it almost impossible to assess the homology between tribes and genera. Remarkably, similar pouches do not only occur in various subgroups of Pselaphinae, but also on other body regions in non-related staphylinid subfamilies, Scydmaeninae and Dasycerinae (Jałoszyński, pers. obs.), or even in certain species of Coccinellidae (e.g. Jałoszyński and Ślipiński 2014).

A potential synapomorphy of *Protopselaphus* and Pselaphinae is the V- or U-shaped tentorium, with nearly vertical main branches, each comprising the posterior and dorsal arm, and lacking laminatentoria completely. This is in clear contrast to the presumably ancestral condition found in other staphylinid beetles (Weide et al. 2014: fig. 3; Antunes-Carvalho et al. 2017). Another potential synapomorphy is the separation of the tentorial bridge from these structures. It is placed right in front of the foramen occipitale, a condition also found in Scydmaeninae, another group of Staphylinidae with well-developed and demarcated neck region (e.g. Jałoszyński 2020). The bridge is complete in *Protopselaphus* (Newton and Thayer 1995) like in other staphylinid and staphylinid beetles (e.g. Blackwelder 1936; Antunes-Carvalho et al. 2017), clearly an ancestral condition. It is present but medially interrupted in *P. heisei* (Fig. 5I), and absent in *Bergrothia* (Luo et al. 2021a) and *Claviger* (Jałoszyński et al. 2020). The hypopharyngeal retractor, M. tentoriopharyngalis anterior (M50), arises from the tentorial bridge in *P. heisei* (Fig. 7G) and many other beetles (e.g. Anton and Beutel 2004; Weide et al. 2010; Antunes-Carvalho et al. 2017), but from the ventral head capsule in *Bergrothia* (Luo et al. 2021a) and *Claviger* (Jałoszyński et al. 2020). The dorsal tentorial pits are another potential synapomorphy of *Protopselaphus* and Pselaphinae, indicating a firm fusion of the dorsal arms with the head capsule. This is usually not the case in beetles (e.g. Antunes-Carvalho et al. 2017), although a fusion not marked externally by pits occurs in some species of Scydmaeninae (Jałoszyński, unpublished obs.). Anterior arms, usually an important attachment site for antennal muscles, are present in *Protopselaphus* (Newton and Thayer 1995: fig. 2) and *Bergrothia* (Luo et al. 2021a: fig. 5f). In contrast, they are completely reduced in *Pselaphus* and *Claviger* (Jałoszyński et al. 2020), and probably in many other pselaphines (e.g. Nomura 1991), being a part of the remarkable morphological diversity of head structures in Pselaphinae.

An unusual feature of *P. heisei*, possibly an autapomorphy of the genus, is a dense vestiture of broadened and flattened hyaline setae on the anterior gular region. The arrangement of these structures is so dense that they form a continuous mass covering a large ventral area of the head. Mechanical removal of the setae revealed small pores, presumably glandular openings, at each setal insertion. Similar setae densely cover the ventral precoxal region of the prothorax, a large anterior area of the mesoventrite, and the first exposed abdominal sternite. The massive, bulging submental region of the head seen in anterior view (Figs 1B–C) may have a protective function for this setal cover that otherwise would be prone to abrasion during moving forward among soil particles,

or during feeding. The setae could function as an evaporation apparatus for glandular secretions. However, their ventral and rather hidden placement does not support this explanation; neither the simple shape and dense, overlapping coverage appear well-suited to increase evaporation. It seems more likely that these specialized setal patches are rendered hydrophobic by glandular secretions deposited on the scaly setae, and help surviving periodical flooding of habitats where *P. heisei* can be found. This species inhabits *Sphagnum* cushions and other mosses on water edges, marshes and moist meadows, and leaf litter in such places (Jałoszyński, pers. obs.). The ventral cephalic, pro- and mesothoracic, and abdominal hydrophobic surfaces may help surviving flooding, when the beetles are trapped inside moss cushions. Behavioural observations are needed to verify this hypothesis. Patches of similar hyaline setae are not known among Batrisitae and Clavigeritae.

A very unusual, apparently derived antennal feature observed in *P. heisei* and other pselaphine genera (e.g. Jeannel 1950; Luo et al. 2021a: fig. 3c) is a basal articulatory piece of the scapus countersunk in the cylindrical distal part of the antennomere. This is clearly absent in the groundplan of Staphyloidea and Staphylinidae (Blackwelder 1936; Beutel et al. 2003; Thayer 2016; Antunes-Carvalho et al. 2017). Interestingly, a plesiomorphic condition is found in *Faronus lafertei* Aubé, 1844 (Jeannel 1950: fig. 2b), like in *Protopselaphus* (Newton and Thayer, 1995: fig. 6) and other staphylinid beetles (e.g. Antunes-Carvalho et al. 2017). Consequently, this is a potential synapomorphy of Pselaphinae excluding Faronitae (“higher Pselaphinae” of Parker 2016b). The functional significance of this feature in free-living pselaphines is unclear. It is possibly related with the unusual articulation with the supraantennal lobes. In myrmecophile pselaphines this modification likely increases the protection of the short and very compact antennae (Jałoszyński et al. 2020). However, it is evident that this was rather a pre-adaptation, and not a specialized transformation unique for inquilines.

In contrast to the maxillae and especially the maxillary palps, the prementum of pselaphine beetles is inconspicuous, more or less retracted, and not visible externally at all in *P. heisei* (Fig. 2) and *Claviger* (Jałoszyński et al. 2020). This is clearly a derived condition compared to a distinctly exposed prementum in other groups of Staphyloidea (Blackwelder 1936; Antunes-Carvalho et al. 2017). A setose appendage of the prementum or anterior hypopharynx (Jeannel 1950: “languette”) is inconspicuous in *P. heisei* (pll, Fig. 4B) but prominent in *Bergrothia* (Luo et al. 2021a: fig. 4e, h, pll) and *Claviger* (Jałoszyński et al. 2020: figs 3c, 4h). The labial palps in Pselaphinae (and *Protopselaphinae*) are modified in a very different manner than those of the maxillae. Newton and Thayer (1995) coded palpomere 3 for *Protopselaphus* and all pselaphine terminal taxa as “represented only by elongate hyaline process” in their matrix. Indeed, the terminal palpomere in these groups is slender, strongly elongate, rod-like and aetose. However, in *Protopselaphinae*, this structure is easily recognizable as a palpomere, about as thick as its

intrinsic maxillary muscles, three premental retractors, and a standard set of hypopharyngeal, prepharyngeal and pharyngeal muscles. Derived features are the absence of the hypopharyngeal mandibular muscle (M13), which occurs as a very thin bundle in various groups of beetles (e.g. Dressler and Beutel 2010; Antunes-Carvalho et al. 2017; Yavorskaya et al. 2017), the obsolete condition or absence of the muscle of the labial palp, and the absence of *M. verticopharyngalis*. The latter muscle is missing in many groups of Coleoptera (e.g. Weide and Betz 2009), notably in all examined small species with the brain shifted posteriorly (Yavorskaya et al. 2017). Interestingly, the dorsal prepharyngeal dilators (M43, M44) are strongly developed in *Claviger*, moderately in *Pselaphus*, and rather weakly in *Bergrothia* (Fig. S1).

The extrinsic and intrinsic antennal muscles are also well-developed in *Bergrothia saulcyi* (Luo et al. 2021a: fig. 7a), and the former even unusually large in the obligatory myrmecophile *Claviger* (Jałoszyński et al. 2020). The extrinsic bundles originate on the dorsal arms of the tentorium in *Pselaphus* and *Bergrothia*, instead of the anterior arms as in most adult beetles (e.g. Beutel et al. 2001, 2003; Anton and Beutel 2004, Antunes-Carvalho et al. 2017). In contrast, the areas of origin are partly shifted to the head capsule in *Claviger* (Jałoszyński et al. 2020: fig. 5b–c), demonstrating a considerable variability, even within such a limited sample of Pselaphinae. The sites of origin of extrinsic antennal muscles differ in *Claviger* and *Pselaphus*, genera recovered as closely related in a recent combined morphological and molecular analysis, while they are similar in *Pselaphus* and *Bergrothia*, the latter genus belonging to Batrisitae, found to be phylogenetically distant from Pselaphitae and Clavigeritae (Parker 2016a: fig. 6b). It is very likely that the latter condition, i.e. exclusive origin on the tentorium, is plesiomorphic within the subfamily.

In contrast to other staphyliniform beetles (e.g. Anton and Beutel 2004; Antunes-Carvalho et al. 2017; Yavorskaya et al. 2017), *M. craniobasimaxillaris* (Mx) is absent in all hitherto examined pselaphines. A plesiomorphic feature of *P. heisei* compared to *Bergrothia* and *Claviger* is the origin of *M. tentoriopharyngalis* (M50) on the interrupted tentorial bridge, instead of the ventral wall of the head capsule. Derived features of the highly specialized species of *Claviger* include the loss of the extrinsic labral muscle (M9), the origin of parts of the extrinsic antennal muscles on the head capsule, the modest size of the mandibular flexor (M11), the reduction of intrinsic maxillary muscles, notably of the muscles of the palp, and the loss of two out of three premental retractors (Jałoszyński et al. 2020).

An intriguing character system documented in *P. heisei*, *Claviger* (Jałoszyński et al. 2020) and *Bergrothia* (Luo et al. 2021a) is a triple cluster of well-developed cephalic glands. This configuration is not present in other groups of Staphylinioidea (e.g. Beutel et al. 2003; Antunes-Carvalho et al. 2017; Yavorskaya et al. 2017). It was demonstrated that these organs, or at least a part of them, are involved in appeasing ants in *Claviger* (Cammaerts 1974, 1992; see also Luo et al. 2021a). Even though this

likely applies to myrmecophilous taxa like Clavigeritae, this is obviously not the case in the less specialized predacious *P. heisei* and *Bergrothia* (Luo et al. 2021a). It is conceivable that these glands are associated with digestion in some way as they open in the preoral region (Luo et al. 2021a). However, the precise function of each of the differentiated subunits is yet unknown, and also the evolutionary transformation leading to the appeasement function in myrmecophilous species. The tripartite cluster of labral, mandibular and labiohypopharyngeal glands are possibly a groundplan apomorphy of Pselaphinae. However, it is unknown whether they are present in Faronitae, and data are also lacking for Protopselaphinae and other groups of the omaliine lineage. It is possible that these glands were a part of a set of pre-adaptations to myrmecophily (other than those recognized by Parker 2016a). Re-programming of their secretions to function as appeasement compounds for ants may explain why specialized myrmecophilous habits evolved independently so many times in each large lineage of Pselaphinae.

The presently available morphological information of Pselaphinae is not even remotely sufficient for a formal character analysis. However, an overwhelming morphological diversity of head structures is obvious, by far surpassing what is found in related groups of staphylinid beetles (e.g. Blackwelder 1936; Naomi 1987; Weide and Betz 2009; Weide et al. 2014; Thayer 1978, 1987, 2016). It is an intriguing question, which circumstances in the life history or microhabitats of Pselaphinae resulted in an enormously increased phenotypic plasticity, with an extreme structural diversity including rampant homoplasy. It is likely that life in soil combined with predatory habits, often specialized on small agile or armoured arthropods like springtails or mites, has played an important role. Even though the connection of some features with predatory behaviour is not obvious or non-existent, this is still quite clear in many other cases. It is noteworthy that the ecologically similar but phylogenetically distant staphylinid subfamily Scydmaeninae also comprises small-sized soil predators with diverse feeding adaptations (Jałoszyński 2012a, b, 2018; Jałoszyński and Olszanowski 2013, 2015, 2016), yet showing far less morphological diversity.

5. Conclusions

The study of cephalic structures of the free-living and predacious *P. heisei* made it possible to compare presumably unspecialized conditions with features previously described for the extreme myrmecophile *Claviger testaceus* and the blind *Bergrothia saulcyi*, the latter presumably adopted to periodic shifts into deep soil layers. These species belong in three different supertribes of Pselaphinae, and although such a small sample out of over 10,000 known species is insufficient to draw general conclusions, we identify possible groundplan features of the subfamily: falciform mandibles with several sharp subapical teeth and a vestigial mola but lacking a mesal microtrichial

brush (secondarily developed in specialized, liquid-feeding Clavigeritae); a semiglobular neck; a ventrolateral articulation of the antennae below supraantennal frontal lobes; a steep clypeal region; a setiform labial palpomere 3; V- or U-shaped tentorium, with nearly vertical main branches, each comprising the posterior and dorsal arm, and lacking laminatentoria; separation of the tentorial bridge from the tentorial arms; a firm fusion of dorsal tentorial arms with the head capsule, with fusion sites usually visible externally as dorsal tentorial pits; functional compound eyes with a limited number of ommatidia; a very large brain placed in the posterior third of the head; a constriction separating the anterior protocerebral part from the posterior portion (linked with the development of the occipital constriction); a triple cluster of well-developed cephalic glands. A strongly modified, largely vertical labrum is a possible synapomorphy of Pselaphitae and Clavigeritae. The shape of the head capsule, especially of its preocular region, the dorsal system of foveae and sulci, the shape and orientation of the labrum, and especially the maxillary palps were all found very variable within only three examined pselaphine species, documenting an enormously high morphological diversity, likely including frequent homoplasious transformations. To explore the genetic background of the structural megadiversity in Pselaphinae will be an intriguing target of future investigations, screening genomes or transcriptomes of pselaphines and other staphylinid beetles to detect changes enabling accelerated evolution of morphological structures.

6. Acknowledgements

Our work was partly funded by project CGL2013-48950-C2 (AEI/FED-ER, UE). We are indebted to Dariusz Twardy (Brzozów, Poland) who collected specimens used in our study; Anna Siudzińska (PORT Polish Center for Technology Development, Wrocław) is acknowledged for taking the SEM images; and Peter Hlaváč (Prague, Czech Rep.) kindly provided rare literature and valuable data on the taxonomy of Pselaphinae.

7. References

- Anton E, Beutel RG (2004) On the head morphology and systematic position of *Helophorus* (Coleoptera: Hydrophiloidea: Helophoridae). *Zoologischer Anzeiger* 242: 313–346. <https://doi.org/10.1078/0044-5231-00107>
- Anton E, Yavorskaya MI, Beutel RG (2016) The head morphology of Clambidae and its implications for the phylogeny of Scirtoidea (Coleoptera: Polyphaga). *Journal of morphology* 277(5): 615–633. <https://doi.org/10.1002/jmor.20524>
- Antunes-Carvalho C, Yavorskaya M, Gnaspini P, Ribera I, Hammel JU, Beutel RG (2017) Cephalic anatomy and three-dimensional reconstruction of the head of *Catops ventricosus* (Weise, 1877) (Coleoptera: Leiodidae: Cholevinae). *Organisms Diversity and Evolution* 17: 199–212. <https://doi.org/10.1007/s13127-016-0305-3>
- Besuchet C (1991) Révolution chez les Clavigerinae (Coleoptera, Pselaphidae). *Revue Suisse de Zoologie* 98(3): 499–515.
- Betz O, Thayer MK, Newton AF (2003) Comparative morphology and evolutionary pathways of the mouthparts in spore-feeding Staphylinoida (Coleoptera). *Acta Zoologica* 84(3): 179–238. <https://doi.org/10.1046/j.1463-6395.2003.00147.x>
- Beutel RG (1993) Phylogenetic analysis of Adephaga (Coleoptera) based on characters of the larval head. *Systematic Entomology* 18: 127–147. <https://doi.org/10.1111/j.1365-3113.1993.tb00658.x>
- Beutel RG (1999) Morphology and evolution of the larval head structures of Hydrophiloidea and Histeroidea (Coleoptera: Staphylinidae). *Tijdschrift voor Entomologie* 142: 9–30.
- Beutel RG, Anton E, Bernhard D (2001) Head structures of adult *Spercheus*: their function and possible significance to staphyliniform phylogeny. *Annales Zoologici* 51(4): 473–484.
- Beutel RG, Anton E, Jäch MA (2003) On the evolution of adult head structures and the phylogeny of Hydraenidae (Coleoptera, Staphyliniformia). *Journal of Zoological Systematics and Evolutionary Research* 41: 256–275. <https://doi.org/10.1046/j.1439-0469.2003.00224.x>
- Beutel RG, Haas A (1998) Larval head morphology of *Hydroscapha natans* (Coleoptera, Myxophaga) with reference to miniaturization and the systematic position of Hydroscaphidae. *Zoomorphology* 118(2): 103–116.
- Beutel RG, Haas F (2000) Phylogenetic relationships of the suborders of Coleoptera (Insecta). *Cladistics* 16(1): 103–141.
- Blackwelder RE (1936) Morphology of the coleopterous family Staphylinidae. *Smithsonian Miscellaneous Collections* 94(13): 1–102.
- Cammaerts R (1974) Le système glandulaire tégumentaire du coléoptère myrmécophile *Claviger testaceus* Preyssl, 1790 (Pselaphidae). *Zeitschrift für Morphologie und Ökologie der Tiere* 77: 187–219.
- Cammaerts R (1992) Stimuli inducing the regurgitation of the workers of *Lasius flavus* (Formicidae) upon the myrmecophilous beetle *Claviger testaceus* (Pselaphidae). *Behavioural Processes* 28: 81–95. [https://doi.org/10.1016/0376-6357\(92\)90051-E](https://doi.org/10.1016/0376-6357(92)90051-E)
- Chandler DS (1983) A revision of *Bunoderus* (Coleoptera: Pselaphidae). *Brenesia* 21: 203–227.
- Chandler DS (2001) Biology, morphology, and systematics of the ant-like litter beetle genera of Australia (Coleoptera: Staphylinidae: Pselaphinae). Vol. 15. Associated Publishers, Gainesville, Florida.
- Clarke DJ, Grebennikov VV (2009) Monophyly of Euaesthetinae (Coleoptera: Staphylinidae): phylogenetic evidence from adults and larvae, review of austral genera, and new larval descriptions. *Systematic Entomology* 34: 346–397. <https://doi.org/10.1111/j.1365-3113.2009.00472.x>
- De Marzo L, Vit S (1983) Contributo alla conoscenza delle Batrisinae paleartiche (Coleoptera, Pselaphidae). Le ghiandole antennali nei maschi di *Batrisus* Aubè e *Batrisodes* Reitter: variazioni morfologiche, istologia e valore tassonomico. *Entomologica* 18: 77–110.
- De Marzo L, Vovlas N (1989) Strutture ed organi esoscheletrici in *Batrisodes oculatus* (Aubé) (Coleoptera, Pselaphidae). *Entomologica* 24: 113–125.
- Dressler C, Beutel RG. (2010) The morphology and evolution of the adult head of Adephaga (Insecta, Coleoptera). *Arthropod Systematics and Phylogeny* 68: 239–287.
- Engelmann MD 1956. Observations on the feeding behavior of several pselaphid beetles. *Entomological News* 67: 19–24.
- Evans MEG (1965) A comparative account of the feeding methods of the beetles *Nebria brevicollis* (F.) (Carabidae) and *Philonthus decorus* (Grav.) (Staphylinidae). *Transactions of the Royal Society of Edinburgh* 64: 91–109.

- Grebennikov VV, Beutel RG (2002) Morphology of the minute larva of *Ptinella tenella*, with special reference to effects of miniaturisation and the systematic position of Ptiliidae (Coleoptera: Staphylinidae). *Arthropod Structure and Development* 31: 157–172. [http://dx.doi.org/10.1016/S1467-8039\(02\)00022-1](http://dx.doi.org/10.1016/S1467-8039(02)00022-1)
- Hlaváč P (2009). Taxonomic notes on the *Bryaxis splendidus* species group (Coleoptera: Staphylinidae: Pselaphinae), with the description of a new species from the Ukraine. *Acta Entomologica Musei Nationalis Pragae* 49(2): 651–659.
- Hlaváč P, Kodada J, Koval A (1999) A new cavernicolous species of *Seracamaurops* Winkler, 1925 (Coleoptera: Staphylinidae: Pselaphinae) from Caucasus. *Revue suisse de Zoologie* 106(1): 241–248.
- Jałoszyński P (2012a) Adults of European ant-like stone beetles (Coleoptera: Staphylinidae: Scydmaeninae) *Scydmaenus tarsatus* Müller and Kunze and *S. helwigii* (Herbst) prey on soft-bodied arthropods. *Entomological Science* 15: 35–41. <https://doi.org/10.1111/j.1479-8298.2011.00479.x>
- Jałoszyński P (2012b) Observations on cannibalism and feeding on dead arthropods in *Scydmaenus tarsatus* Müller and Kunze. *Genus* 23(1): 25–31.
- Jałoszyński P (2018) World genera of Mastigitae: review of morphological structures and new ecological data (Coleoptera: Staphylinidae: Scydmaeninae). *Zootaxa* 4453(1): 1–119. <https://doi.org/10.11646/zootaxa.4453.1.1>
- Jałoszyński P (2020) *Himaloconnus* Franz and *Nogunius* gen. n. of Japan (Coleoptera: Staphylinidae: Scydmaeninae). *Zootaxa* 4822(3): 334–360. <http://dx.doi.org/10.11646/zootaxa.4822.3.2>
- Jałoszyński P, Luo XZ, Beutel RG (2020) Profound head modifications in *Claviger testaceus* (Pselaphinae, Staphylinidae, Coleoptera) facilitate integration into communities of ants. *Journal of Morphology* 281(9): 1072–1085. <https://doi.org/10.1002/jmor.21232>
- Jałoszyński P, Olszanowski Z (2013) Specialized feeding of *Euconnus pubicollis* (Coleoptera: Staphylinidae, Scydmaeninae) on oribatid mites: prey preferences and hunting behaviour. *European Journal of Entomology* 110(2): 339–353. <http://dx.doi.org/10.14411/eje.2013.047>
- Jałoszyński P, Olszanowski Z (2015) Feeding of *Scydmaenus rufus* (Coleoptera: Staphylinidae, Scydmaeninae) on oribatid and uropodine mites: prey preferences and hunting behaviour. *European Journal of Zoology* 112(1): 151–164. <http://dx.doi.org/10.14411/eje.2015.023>
- Jałoszyński P, Olszanowski Z (2016) Feeding of two species of Scydmaeninae ‘hole scrapers’, *Cephenonium majus* and *C. ruthenum* (Coleoptera: Staphylinidae), on oribatid mites. *European Journal of Entomology* 113: 372–386. <http://dx.doi.org/10.14411/eje.2016.048>
- Jałoszyński P, Ślipiński A (2014) *Ruthmuelleria*, a new genus of Carinodulini (Coleoptera: Coccinellidae: Microweiseinae) from South Africa. *Zootaxa* 3784(3): 275–280. <https://dx.doi.org/10.11646/zootaxa.3784.3.7>
- Jeannel R (1950) Faune de France, 53. Coleoptères Pselaphides. Lechevalier, Paris, 421 pp.
- Kéler S (1963) Entomologisches Wörterbuch. Akademie Verlag, Berlin.
- Kurbatov SA (2007) Revision of the genus *Intestiniarius* gen. n. from southeast Asia, with notes on a probable autapomorphy of Batrisitae (Coleoptera: Staphylinidae: Pselaphinae). *Russian Entomological Journal* 16(3): 281–295.
- Latreille PA (1802) Histoire Naturelle, Générale et Particulière des Crustacés et des Insectes. Volume 3. Familles Naturelles des Genres. Dufart, Paris, 387 pp.
- Luo, X-Z, Hlaváč P, Jałoszyński P, Beutel RG (2021a) In the twilight zone – the head morphology of *Bergrothia saulcyi* (Pselaphinae, Staphylinidae, Coleoptera), a beetle with adaptations to endogean life but living in leaf litter. *Journal of Morphology* 1-18 <https://doi.org/10.1002/jmor.21361>.
- Luo X-Z, Jałoszyński P, Stöbel A, Beutel RG (2021b) The specialized thoracic skeletomuscular system of the myrmecophile *Claviger testaceus* (Pselaphinae, Staphylinidae, Coleoptera). *Organism Diversity and Evolution* 1–19. <https://doi.org/10.1007/s13127-021-00484-1>
- Naomi S (1987) Comparative morphology of the Staphylinidae and the allied groups (Coleoptera, Staphylinidae): I. Introduction, head sutures, eyes and ocelli. *Kontyû* 55(3): 450–458.
- Newton AF, Chandler DS (1989). World catalog of the genera of Pselaphidae (Coleoptera). *Fieldiana: Zoology (New Series)* 53: 1–93.
- Newton AF, Thayer MK (1995) Protopselaphinae new subfamily for *Protopselaphus* new genus from Malaysia, with a phylogenetic analysis and review of the Omaliine Group of Staphylinidae including Pselaphidae (Coleoptera). *Biology, phylogeny, and classification of Coleoptera: papers celebrating the 80th birthday of Roy A. Crowson*. Muzeum i Instytut Zoologii PAN, Warszawa, 219–320.
- Meyer-Rochow VB (1999) Compound eye: circadian rhythmicity, illumination, and obscurity. *Atlas of arthropod sensory receptors*. Springer. Tokyo, Berlin, New York, 97–124.
- Nomura S (1991) Systematic study on the genus *Batrisoplisus* and its allied genera from Japan (Coleoptera, Pselaphidae). *Esekiya* 30: 1–462.
- Park O (1947a) The pselaphid at home and abroad. *The Scientific Monthly* 65(1): 27–42.
- Park O (1947b) Observations on *Batrisodes* (Coleoptera: Pselaphidae), with particular reference to the American species east of the Rocky Mountains. *Bulletin of the Chicago Academy of Sciences* 8: 45–132.
- Park JS, Carlton CE (2014) *Pseudostenosagola*, a new genus from New Zealand (Coleoptera: Staphylinidae: Pselaphinae: Faronitae). *Annals of the Entomological Society of America* 107(4): 734–739. <https://doi.org/10.1603/AN14025>
- Park JS, Carlton CE (2015a) *Aucklandea* and *Leschenea*, two new monotypic genera from New Zealand (Coleoptera: Staphylinidae: Pselaphinae), and a key to New Zealand genera of the supertribe Faronitae. *Annals of the Entomological Society of America* 108(4): 634–640. <https://doi.org/10.1093/aesa/sav033>
- Park JS, Carlton CE (2015b) *Brounea*, a new genus (Coleoptera: Staphylinidae: Pselaphinae) from New Zealand, with descriptions of nine new species. *Zootaxa* 3990(4): 551–566. <https://doi.org/10.11646/zootaxa.3990.4.4>
- Park JS, Chandler DS (2017) *Nornalup*, a new genus of pselaphine beetle from southwestern Australia (Coleoptera, Staphylinidae, Pselaphinae, Faronitae). *ZooKeys* 695: 111–121. <https://dx.doi.org/10.3897/zookeys.695.19906>
- Parker J (2016a) Myrmecophily in beetles (Coleoptera): Evolutionary patterns and biological mechanisms. *Myrmecological News* 22: 65–108.
- Parker J (2016b) Emergence of a superradiation: pselaphine rove beetles in mid-Cretaceous amber from Myanmar and their evolutionary implications. *Systematic Entomology* 41(3): 541–566. <https://doi.org/10.1111/syen.12173>
- Parker J, Grimaldi DA (2014) Specialized myrmecophily at the ecological dawn of modern ants. *Current Biology* 24(20): 2428–2434. <https://doi.org/10.1016/j.cub.2014.08.068>
- Polilov AA, Beutel RG (2009) Miniaturization effects in developmental stages of *Mikado* sp. (Coleoptera: Ptiliidae), one of the smallest

- free-living insects. *Arthropod Structure and Development* 38: 247–270. <https://doi.org/10.1016/j.asd.2008.11.003>
- Schomann A, Afflerbach K, Betz O (2008) Predatory behaviour of some Central European pselaphine beetles (Coleoptera: Staphylinidae: Pselaphinae) with descriptions of relevant morphological features of their heads. *European Journal of Entomology* 105(5): 889–907. <http://dx.doi.org/10.14411/eje.2008.117>
- Thayer MK (1987) Biology and phylogenetic relationships of *Neophonus bruchi*, an anomalous south Andean staphylinid (Coleoptera). *Systematic Entomology* 12(3): 389–404. <https://doi.org/10.1111/j.1365-3113.1987.tb00209.x>
- Thayer MK (2016) 14.7. Staphylinidae Latreille, 1802. In: Beutel RG, Leschen RAB (Eds) *Handbook of Zoology, Vol. IV Arthropoda: Insecta. Part 38. Coleoptera, Vol. 1: Morphology and Systematics (Archostemata, Adephaga, Myxophaga, Polyphaga (partim). Second Edition.* Walter De Gruyter, Berlin, New York, 394–442.
- Thayer MK, Newton AF (1978) Revision of the south temperate genus *Glypholoma* Jeannel, with four new species (Coleoptera: Staphylinidae: Omaliinae). *Psyche: A Journal of Entomology* 85(1): 25–63. <http://dx.doi.org/10.1155/1978/29756>
- Weide D, Betz O (2009) Head morphology of selected Staphylinoida (Coleoptera: Staphyliniformia) with an evaluation of possible groundplan features in Staphylinidae. *Journal of Morphology* 270: 1503–1523. <http://dx.doi.org/10.1002/jmor.10773>
- Weide D, Thayer MK, Newton AF, Betz O (2010) Comparative morphology of the head of selected sporophagous and non-sporophagous aleocharinae (Coleoptera: Staphylinidae): Musculature and hypopharynx-prementum complex. *Journal of Morphology* 271(8): 910–931. <https://dx.doi.org/10.1002/jmor.10841>
- Weide D, Thayer MK, Betz O (2014) Comparative morphology of the tentorium and hypopharyngeal-premental sclerites in sporophagous and non-sporophagous adult Aleocharinae (Coleoptera: Staphylinidae). *Acta Zoologica* 95: 84–110. <http://dx.doi.org/10.1111/azo.12011>
- Wipfler B, Machida R, Mueller B, Beutel RG (2011) On the head morphology of Grylloblattodea (Insecta) and the systematic position of the order, with a new nomenclature for the head muscles of Dicondylia. *Systematic Entomology* 36: 241–266. <http://dx.doi.org/10.1111/j.1365-3113.2010.00556.x>
- Yavorskaya M, Beutel RG, Polilov A (2017) Head morphology of the smallest beetles (Coleoptera: Ptiliidae) and the evolution of sporophagy within Staphyliniformia. *Arthropod Systematics and Phylogeny* 75: 417–434.
- Yin ZW, Kurbatov SA, Cuccodoro G, Cai CY (2019) *Cretobrachygluta* gen. nov., the first and oldest Brachyglutini in mid-Cretaceous amber from Myanmar (Coleoptera: Staphylinidae: Pselaphinae). *Acta Entomologica Musei Nationalis Pragae* 59(1): 101–106.

Supplementary material

File 1

Authors: Beutel RG, Luo X-Z, Yavorskaya M, Jałoszyński P (2021)

Data type: .pdf

Explanation note: **Figure S1.** Comparison of pharyngeal, labral-epipharyngeal and labial-hypopharyngeal muscles of *Claviger testaceus*, *Begrothia saulcyi*, *Pselaphus heisei*, in sagittal view.

Copyright notice: This dataset is made available under the Open Database License (<http://opendatacommons.org/licenses/odbl/1.0>). The Open Database License (ODbL) is a license agreement intended to allow users to freely share, modify, and use this Dataset while maintaining this same freedom for others, provided that the original source and author(s) are credited.

Link: <https://doi.org/10.3897/asp.79.e68352.suppl1>

3.5 Study V

Evolution of cephalic structures in extreme myrmecophiles: a lesson from Clavigeritae (Coleoptera: Staphylinidae: Pselaphinae) [Submitted]

Paweł Jałoszyński, **Xiao-Zhu Luo**, Rolf Georg Beutel

Abstract: Pselaphinae is a large subfamily, comprising about 10,000 species of the megadiverse polyphagan Staphylinidae (rove beetles). A remarkable feature is the extreme structural diversity of different body regions, especially the head and its appendages. Within the group, Clavigeritae stand out as a clade of highly specialized myrmecophiles. In the present study we examined internal and external head structures of the clavigerite species *Diartiger kubotai* Nomura, using state-of-the-art techniques. The cephalic morphology indicates that the loss of eyes in some Clavigeritae was the youngest of major evolutionary transformations. We compiled the largest set of morphological data ever scored for the subfamily, comprising 155 characters of the head. Parsimony analyses and Bayesian inference yielded a similar phylogenetic pattern for Pselaphinae, also largely congruent with previously published results. Our analyses retrieved Pselaphinae as a clade, and Faronitae as sister to the remaining subfamily. Faronitae is followed by a ‘Euplectitae grade’ and non-monophyletic Goniaceritae, Batrisitae and Pselaphitae. Clavigeritae are clearly monophyletic, but has evolved within the pselaphite grade. The enigmatic *Colilodion* Besuchet, recently shifted from Clavigeritae to (paraphyletic) Pselaphitae, was placed as sister to extant clavigerites based on an array of cephalic synapomorphies. We conclude that the current classification of Pselaphinae is unstable and deep changes should be made maintaining only monophyletic units, while most of the currently recognized supertribes are paraphyletic. As shown in previous studies, characters of the head, with a concentration of mouthparts, sensory structures, and essential parts of the digestive tract and the nervous system, are highly informative phylogenetically. Study of internal structures, presently still at a very preliminary stage, is obviously essential for understanding the evolution of Pselaphinae. Future genetic investigations may reveal mechanisms behind the unique structural megadiversity in this exceptional group of rove beetles.

Conceptualization: P. Jałoszyński, R. G. Beutel

Visualization: P. Jałoszyński, **X. Z. Luo**

Writing-original draft: P. Jałoszyński, **X. Z. Luo**, R. G. Beutel

Writing-review & editing: P. Jałoszyński, R. G. Beutel

Funding acquisition: P. Jałoszyński

Estimated own contribution: 10%

Evolution of cephalic structures in extreme myrmecophiles: a lesson from Clavigeritae (Coleoptera: Staphylinidae: Pselaphinae)

Paweł Jałoszyński^{a*}, Xiao-Zhu Luo^b, Rolf Georg Beutel^b

^aMuseum of Natural History, University of Wrocław, Sienkiewicza 21, 50-335 Wrocław, Poland. ^bInstitut für Zoologie und Evolutionsforschung, Friedrich-Schiller-Universität Jena, Erbertstrasse 1, 07743 Jena, Germany

*Corresponding author. E-mail: scydmaenus@yahoo.com

Short running title: Evolution of cephalic structures in Clavigeritae

Acknowledgements

The first author is indebted to Hiroyuki Yoshitomi (Entomological Laboratory, Ehime University), who made it possible to collect specimens of *D. kubotai* during a trip to Shikoku. Anna Siudzińska (Laboratory of Electron Microscopy, PORT Polish Center for Technology Development, Wrocław) is acknowledged for taking the SEM images. TNT software was made available with the sponsorship of the Willi Hennig Society.

Abstract

Pselaphinae is a large subfamily, comprising about 10,000 species of the megadiverse polyphagan Staphylinidae (rove beetles). A remarkable feature is the extreme structural diversity of different body regions, especially the head and its appendages. Within the group, Clavigeritae stand out as a clade of highly specialized myrmecophiles. In the present study we examined internal and external head structures of the clavigerite species *Diartiger kubotai* Nomura, using state-of-the-art techniques. The cephalic morphology indicates that the loss of eyes in some Clavigeritae was the youngest of major evolutionary transformations. We compiled the largest set of morphological data ever scored for the subfamily, comprising 155 characters of the head. Parsimony analyses and Bayesian inference yielded a similar phylogenetic pattern for Pselaphinae, also largely congruent with previously published results. Our analyses retrieved Pselaphinae as a clade, and Faronitae as sister to the remaining subfamily. Faronitae is followed by a 'Euplectitae grade' and non-monophyletic Goniaceritae, Batrisitae and Pselaphitae. Clavigeritae are clearly monophyletic, but has evolved within the pselaphite grade. The enigmatic *Colilodion* Besuchet, recently shifted from Clavigeritae to (paraphyletic) Pselaphitae, was placed as sister to extant clavigerites based on an array of cephalic synapomorphies. We conclude that the current classification of Pselaphinae is unstable and deep changes should be made maintaining only monophyletic units, while most of the currently recognized supertribes are paraphyletic. As shown in previous studies, characters of the head, with a concentration of mouthparts, sensory structures, and essential parts of the digestive tract and the nervous system, are highly informative phylogenetically. Study of internal structures, presently still at a very preliminary stage, is obviously essential for understanding the evolution of Pselaphinae. Future genetic investigations may reveal mechanisms behind the unique structural megadiversity in this exceptional group of rove beetles.

Key words: Coleoptera head, myrmecophily, Pselaphinae, Clavigeritae, evolution

Introduction

Pselaphinae is a large subfamily of the megadiverse Staphylinidae (rove beetles), informally classified within the 'Omaliine Group' (Newton and Thayer, 1995). They currently include more than 10,000 species (Hlaváč et al., 2021) and show an astounding morphological diversity (e.g., Chandler, 2001). Most pselaphines inhabit moist leaf litter where these small (~1–5 mm) predators feed on tiny invertebrates, such as springtails or mites (Park, 1947; Engelmann, 1956; Schomann et al., 2008). In nearly all major lineages within Pselaphinae, strong and clearly independent evolutionary trends lead to a development of myrmecophilous habits, including obligatory dependence on the ant hosts (Parker, 2016a). Predatory adaptations were recognized as ancestral for the subfamily (Beutel et al., 2021), and consequently a shift toward myrmecophily required transformations that allowed for breaching defensive mechanisms of ants, i.e., entering the nests and living with hosts that aggressively protect their offspring and resources. Such a shift required adaptations related to all aspects of life, most notably feeding, reproduction, and dispersal into new ant nests. Various patterns of relationships have evolved, from occasional scavenging and predation to obligatory myrmecophily (for review, see Parker, 2016a). Within Pselaphinae, the latter phenomenon is common, and this subfamily includes the most spectacular cases of extreme dependence of inquiline species on ant hosts. The supertribe Clavigeritae (Fig. 1), comprising ~370 nominal species distributed worldwide, is believed to include exclusively such extreme obligatory myrmecophiles (Hlaváč et al., 2021). These beetles are supposedly unable to live outside ant colonies. They manipulate their hosts' behavior, they are fed by worker ants, transported by them to new nests, and their integration into the ant colonies is regarded as most advanced (Parker, 2016a).

Such a tight association with ants required revolutionary transformations that involved not only changes in body structures, but also in physiology. Clavigeritae have been model subjects of experiments and observations that demonstrated how they utilize chemical camouflage (Akino, 2002), and how their glandular secretions manipulate the hosts' behavior (Cammaerts, 1974, 1991, 1992, 1995, 1996, 1999). The appeasement glands direct the attention of the ants, diverting their mandibles toward strictly defined regions of the beetle's body. This reduces the chance of injury including the loss of vulnerable structures, and leads to regurgitation by workers onto the inquiline's mouthparts (Cammaerts, 1992). Jałoszyński et al. (2020) provided the first detailed anatomical description of the strongly transformed head of a clavigerite beetle, *Claviger testaceus* Preissler, including profound alterations of the associated musculature. The previously popular view of "reduced" mouthparts in Clavigeritae was revised, as some structures responsible for the capillary mechanism of fluid uptake show in fact a hypertrophy compared to those in predatory pselaphines. Moreover, very large cephalic glands release their secretions directly onto the modified mandibles and labrum, through externally visible openings (Jałoszyński et al., 2020). Also "reductions" in the antennal structure should be regarded rather as highly specialized adaptations that have re-

engineered the entire cuticular sensorium and glandular apparatus to optimize them for functional requirements inside ant colonies.

The hitherto published results of phylogenetic evaluations of Pselaphinae and related groups show a considerable heterogeneity. If any consensus can be agreed upon, such a scenario would most likely place Faronitae as sister to the rest of the subfamily. However, the branching sequence within the remaining, so called “higher Pselaphinae” remains unclear (Parker and Grimaldi, 2014), and also the systematic position among supposedly related groups of rove beetles. Newton and Thayer (1995) resolved a topology Neophoninae + (Dasycerinae + (Protopselaphinae + Pselaphinae)). Parker (2016b), in an analysis not including the very rare Protopselaphinae, obtained (Dasycerinae + Neophoninae) + Pselaphinae. Yin et al. (2021) suggested (Protopselaphinae + Pselaphinae) + (Neophoninae + Dasycerinae). Previous phylogenetic reconstructions of Pselaphinae, especially including those specifically focused on Clavigeritae, were based on a very limited selection of characters. Specifically, features of the head, usually the most informative tagma in a phylogenetic context (e.g. Beutel et al., 2011), were not well represented. In the presently largest and most conclusive study of Hlaváč et al. (2021), only 22 cephalic characters were included (out of a total of 82 characters). Parker (2016b) in his analysis of all major supertribes of Pselaphinae scored 26 cephalic features (out of a total of 57). Yin et al. (2021) focused on Dasycerinae, but included 15 members of Pselaphinae as part of the outgroup sampling. Their analysis included 33 cephalic characters (out of a total of 84).

In the course of detailed studies of head structures (including the muscles, brain and the alimentary tract) of single representatives of Clavigeritae, Batrisitae and Pselaphitae (Jałoszyński et al., 2020; Luo et al., 2021a; Beutel et al., 2021), we demonstrated that even within such a tiny sample the diversity of cephalic exoskeletal elements is astounding, and that based on the head alone it may be possible to propose testable hypotheses regarding ancestral characters of these groups. Moreover, even though only three pselaphine species were studied so far using advanced morphological techniques, especially micro-computed tomography, results proved to be fundamental to understand the evolution of Clavigeritae. For instance, it was demonstrated that large clusters of cephalic glands found in *Claviger* and opening onto the mouthparts to release appeasement secretions, were not unique for myrmecophiles. A similar arrangement of cephalic glands was found in *Bergrothia saulcyi* (Reitter) (Batrisitae) and *Pselaphus heisei* Herbst (Pselaphitae), free-living predatory species only remotely related to *Claviger* Preyssler. This finding suggests that the “myrmecophilous shift” might have been achieved by re-programming already existing glands, possibly related to food digestion, to produce secretions manipulating the behavior of the ant hosts.

A group possibly essential in understanding the evolution of Clavigeritae is the monogeneric Colilodionini (Besuchet, 1991), which was included in the supertribe until very recently. *Colilodion* Besuchet displays a great array of bizarre autapomorphic characters, including particularly odd head modifications. Its life habits remain unknown, but based on morphological structures it is considered

as a myrmecophile (for a review see Hlaváč et al., 2021). It has “reduced”, i.e. distinctly modified mouthparts and antennae, and a general body form resembling those of other members of Clavigeritae. Besuchet (1991) hypothesized that *Colilodion* is a genus of this supertribe that has retained some ancestral characters typical of extant Pselaphitae, possibly the sister group. He placed Colilodionini as one of three tribes within Clavigerinae, then a subfamily of Pselaphidae. His view, not supported by a formal analysis, was that Colilodionini is the sister group of all remaining clavigerite tribes. This notion was partly supported by Parker and Grimaldi (2014: fig. 3), who limited this conclusion to “Colilodionini sister to all extant Clavigeritae”, as they found a Cretaceous *Protoclaviger* Parker and Grimaldi that was resolved as sister to *Colilodion* + other Clavigeritae. Hlaváč et al. (2021) resolved *Colilodion* as sister group of Arhytodini of Pselaphitae, and both as sister to Clavigeritae. Even though the support was low, they transferred *Colilodion* to Pselaphitae. In this context, it should be noted that Pselaphitae are paraphyletic without Clavigeritae in Hlaváč et al. (2021), and this is also the case in Parker and Grimaldi (2014), Parker (2016b), and Yin et al. (2021). Clearly, the “*Colilodion* problem” is still unsolved, and it is likely a crucial issue in the context of phylogenetic relationships and evolutionary transformations of Pselaphitae and Clavigeritae.

The current study builds upon and expands our previous findings. So far, we demonstrated that exoskeletal oddities (interpreted as adaptations to extreme myrmecophily) in blind *Claviger* beetles profoundly affect the musculature and other internal head organs. By studying in detail internal cephalic structures in another clavigerite species, *Diartiger kubotai* Nomura, a beetle with large eyes, we aim to understand how the presence and loss of sight influenced the evolution of cephalic structures. This is an intriguing question, as even though extreme myrmecophiles live permanently in the darkness of ant colonies and are believed to be dispersed by their host ants, a complete sight loss is a surprisingly rare phenomenon within this group. We compare the external and internal head structures in *Diartiger* and the previously studied *Claviger*, in order to identify the limits of cephalic transformations in inquiline, i.e. to address the question which structures can be further modified, and which have likely reached a terminal point.

In order to provide a solid framework for evaluating character evolution, we studied in detail external cephalic features in a large selection of Pselaphinae that covers Faronitae, Euplectitae, Batrisitae, Goniaceritae, Pselaphitae and Clavigeritae. We scored and include over 150 characters of the head in a phylogenetic analysis. This approach allows us to identify traits strictly associated with the “myrmecophilous shift” from free predatory to inquiline life, and features that are variable within extreme myrmecophiles and therefore may have evolved by a “morphological drift” under weak selection, as recently postulated by Hlaváč et al. (2021). Moreover, by using such an expanded character matrix, we are able to propose for the first time a diagnosis of Clavigeritae that includes novel character states, and to re-visit the “*Colilodion* problem”. The extensive character set is also a step towards future in depth analyses of Pselaphinae, which may lead to a solid phylogenetic concept and subsequently to a better understanding of patterns of structural megadiversity.

Material and methods

Specimens

The species studied in detail is an obligate myrmecophile, *Diartiger kubotai* Nomura (Insecta: Coleoptera: Staphylinidae: Pselaphinae: Clavigeritae: Clavigerini), an inquiline that is not naturally found outside ant colonies. Beetles were collected from rotten deciduous wood inhabited by *Lasius* (Fabricius) sp. ants by the first author, near Toon-shi, Ehime Pref., Japan, in May 2018. Specimens were preserved in 75% ethanol. For comparative purposes, cephalic structures of nine Clavigeritae species (representing nine genera and three tribes) were examined and documented by scanning electron microscopy; the list of species, depositories, and countries of origin is compiled in Appendix S1.

Micro-computed tomography (μ -ct)

Specimens of *D. kubotai* were transferred to acetone and then dried in a critical point dryer (Emitech K850, Quorum Technologies Ltd., Ashford, UK). Micro-CT scans were made at the Max Planck Institute für Menschheitsgeschichte (Jena, Germany) using a SkyScan 2211 (Bruker, Knotich, Belgium), with the following parameters: 70 kV voltage, 300 μ A current, 3.600 ms exposure time, Rotation Step 0.150, frame averaging on, random movement off, and filter assembly open. Projections were reconstructed by NRecon (Bruker, Knotich, Belgium) into JPG files with a voxel size of 0.68 μ m. Amira 6.1.1 (Thermo Fisher Scientific, Waltham, USA) and VG studio Max 2.0.5 (Volume Graphics, Heidelberg, Germany) were used for three-dimensional reconstructions and volume rendering. The μ -CT data set is archived at the Phyletisches Museum, Jena, Germany and available upon request.

Scanning electron microscopy (SEM)

Beetles were transferred from 75% to 99% ethanol for 15 min and air-dried. One specimen of *D. kubotai* was macerated for 60 min in a warm 10% aqueous solution of NaOH, thoroughly washed in distilled water and dissected; isolated mouthparts were dehydrated in 99% ethanol and air-dried. Entire beetles and dissected parts were mounted on SEM stubs with carbon tabs and examined uncoated using a Helios Nanolab 450HP scanning electron microscope (FEI, Hillsboro, USA). Images were processed using CorelDraw Graphic Suite 2017; the following adjustments were made: overall brightness and contrast enhanced, and background manually replaced with black.

Terminology and measurements

Cephalic muscles were designated following the terminology of Kéler (1963), with the exception of Mm. compressores epipharyngis (Mm. III), which was named following Belkaceme (1991). Homolog

abbreviations of Wipfler et al. (2011) were added in parentheses after the designation of Kéler (1963); for example, M44 - *M. clypeobuccalis* (0bu1). Muscles not mentioned in the morphological description are lacking.

Phylogenetic analysis

Phylogenetic analysis was based on 155 (numbered from 0) non-additive and unordered adult cephalic exoskeletal characters; inapplicable character states were assigned a gap value ("–") and treated equivalent to missing data ("?"). The character states were scored for 71 Pselaphinae species selected to represent supertribes Faronitae, Euplectitae, Batrisitae, Goniaceritae, Pselaphitae, and Clavigeritae, including 13 species of Clavigeritae representing Clavigerini, Disarthricerini and Tiracerini. As outgroups, ten species of Staphylinidae were selected, representing subfamilies Dasycerinae, Micropeplinae, Omaliinae, Proteininae (together with Pselaphinae traditionally included in the Omaliine Group), and more remotely related Staphylininae. Protopselaphinae were not included due to a lack of suitable material. A complete list of taxa can be found in Appendix S1; an illustrated list of characters and character states in Appendix S2. The data matrix was assembled in Nexus Data Editor for Windows v. 0.5.0 (Page, 2001) (Appendix S3; nexus version in Appendix S4). Parsimony analysis was conducted in TNT v.1.5 (Goloboff et al., 2008) under implied weighting, at the weighting function $K = 9$, using the 'traditional search' strategy; the analysis was rooted with *Ocypus* Leach. The tree bisection reconnection swapping algorithm was applied, with 1000 replicates and 100 trees saved per replication. Symmetric resampling (Goloboff et al., 2003) ($P=33$, 1000 replicates) was also conducted in TNT, and character mapping was performed in WinClada v. 1.00.08 (Nixon, 1999–2002). Trees were exported from TNT, adjusted in Mesquite v. 3.2 (Maddison and Maddison, 2017) and annotated in CorelDraw Graphic Suite 2017. The Bayesian analysis was conducted using MrBayes v. 3.2.6 (Ronquist et al., 2012) on the CIPRES Science Gateway v. 3.3 (phylo.org), with four chains of 2 runs each. The Mkv model of character evolution was used with a gamma distribution, to allow for variation in the rate of evolution between characters, considered to be more realistic given the wide range of variability seen between morphological structures. Default priors were used, except for 'temp=0.05' to improve mixing of the chains, and 30 million generations. Convergence was assessed in Tracer v1.7.2 (Rambaut et al., 2014) and using PSRF and average standard deviation of split frequencies values in the MrBayes output.

Results

Head structures of Diartiger kubotai

Head capsule. The head is prognathous and subcylindrical (Fig. 2A–C), strongly elongate and higher than broad; the highest site is situated between the compound eyes and antennal insertions. Nearly

the entire dorsal and lateral surfaces of the anterior, exposed portion of the head capsule are covered with shallow alveolate impressions; these densely arranged concavities appear irregular in shape and are separated by narrow septa; the clypeus, lateral postantennal impressions and anterior gula + submentum are smooth; areas around the antennal fossae are covered with reticulate microsculpture. Setae on the head are sparse, long and suberect, and brachyplumose (barbed); a large portion of the ventral surface is nearly aseptose. The neck region (Fig. 2B, C; *nr*) is subglobose and much longer ventrally than dorsally, anteriorly demarcated by the shallow occipital constriction (Fig. 2C; *occ*); its ventral surface is microreticulate. The vertex (Fig. 2A, B; *vt*) and tempora (Fig. 2A, B; *tm*) are confluent and much longer than the eyes; the tempora are subparallel, and the vertexal region transverse and slightly flattened medially. The occipital crest delimiting the vertex and tempora posteriorly is present; it reaches the ventrolateral head region and is continuous with an indistinct rounded furrow, which delimits the neck region on the ventral side. Dorsal tentorial pits (Fig. 2A, B, D; *dtp*) are present and distinct, circular and aseptose, situated dorsolaterally posterodorsad the compound eyes. The compound eyes, each with 23 ommatidia with strongly convex cornea lenses, are kidney-shaped, convex anteriorly and concave posteriorly. The frons (Fig. 2A, B, D; *fr*) is posteriorly confluent with the vertex, elongate and weakly narrowing anterad; its extensive dorsal surface is weakly convex, its short anterior region steeply declining between the antennal insertions towards the clypeus. The broad and transverse clypeal region is medially steep (Fig. 2D; *cl*), but its sides nearly horizontal. An elongate, impressed and smooth postantennal-supraocular region forms an antennal sulcus (Fig. 2B, D; *ans*), which receives the proximal portion of the antennal flagellum when the antennae are directed lateroposterad. An elongate buccal bulge (Fig. 2B, D; *bub*), i.e. a lateral convex area extending from the oral fossa to the compound eye is present; in lateral view its dorsal margin is delimited by a ventrally concave, rounded edge. The ventral post-tentorial region of the head is weakly impressed; gular sutures are only recognizable as rather indistinct furrows on the posterior region of the gular plate (Fig. 2C; *gp*). Posterior tentorial pits (Fig. 2C; *ptp*) are present, large and circular, broadly separated medially. The anterior gular (pretentorial) - submental region is convex; a demarcated submentum is not recognizable.

Labrum. The labrum (Figs 2, 3A–C, 4A; *lbr*) is distinctly separated from the clypeus, nearly vertical, approximately lentiform, broadest near its proximal 1/3 and narrowing both posterad and anterad. Its distal edge bears a shallow median emargination. A pair of submedian glandular openings (Fig. 3B; *glo*) is present with poorly developed scale-like microsculpture in front of them; each side bears a short sensillum, and similar sensilla are inserted on the dorsal surface near the distal margin. Musculature (Fig. 5I): M7 - M. labroepipharyngalis (Olb5), O: dorsal wall of the labrum, I: anteriormost area of the epipharynx.

Antennae. The club-shaped, tetramerous antenna is ~1.2 times as long as the head and only ~0.2 times as long as the body (Fig. 1C); the articular membranes are not visible. The short and hemispherical scapus (Figs 3E, 5A; *sc*) is inserted in a ball-and-socket manner; its surface structure is reticulate; setae are absent; it is largely hidden inside the antennal foramen and subdivided into a short proximal articular region, which distally is countersunk into the slightly concave base of the large distal scapal portion. The pedicellus (Figs 3E, 5A; *pd*) is short and subcylindrical, with a smooth basal articular part and a reticulate pattern on the remaining surface; a short seta is inserted on the mesal and lateral edge. Antennomere 3 (Fig. 3E; *f1*) is more than three times as long as the pedicellus and slightly widening distad; the surface except for a short smooth basal portion displays a dense pattern of large punctures, most of them with a minute sensillum in the middle; sparse setae of medium length are distributed on the distal half, all weakly barbed. The terminal antennomere 4 (Fig. 3E; *f2*) is nearly twice as long as 3 and strongly widening distad; the surface pattern of a short basal portion is similar to that of antennomere 3 but the remaining surface is smooth and sparsely covered with setae of medium length, some weakly barbed, some unmodified. The antennal apex (Fig. 3E, F) is round in cross-section and truncated; its distal surface is sunken and surrounded by a strongly elevated, smooth rim, and bears densely arranged digitiform, pointed sensilla. Musculature (Fig. 5C, D): M1 - M. tentorioscapalis anterior (0an1), O: large area of the lower region of the tentorium, I: anteroventral margin of the scapus; M2 - M. tentorioscapalis posterior (0an2), O: anterodorsal wall of the head capsule, directly in front of the tentorium, I: dorsal margin of the scapus; M4 - M. tentorioscapalis medialis (0an4), O: large area of the upper region of the tentorium, I: medially on the scapal margin; M5 - M. scapopedicellaris lateralis (0an6), O: mesal wall of the scapus, I: dorsal margin of the base of the pedicellus; M6 - M. scapopedicellaris medialis (0an7), O: lateral wall of the scapus, I: ventrally on the median margin of the pedicellar base.

Mandibles. The mandibles (Figs 2D, 3A–D, 4A; *mnd*) are well-developed and largely exposed, but their apices do not overlap in the flexed position. They are articulated in a dicondylic manner, and slightly inclined in relation to the longitudinal axis of the head. They appear approximately triangular in dorsal view and wedge-shaped in lateral view, robust at the base and gradually decreasing in thickness towards the apex. A seta is inserted on the lateral face, just behind and slightly above a large and deep glandular opening (Fig. 3B; *glo*). The dorsal surface is slightly concave; a seta is inserted close to the anterior clypeal margin; this part of the mandible is separated from the rounded lateral surface by a distinct edge, which obliterates on the apical part. The short but acuminate mandibular apex is followed by several slightly shorter densely arranged mesal preapical teeth. A prosthema (Fig. 3E; *pst*) is present, with long and densely arranged microtrichia. A mola is not developed. The ventral mandibular surface (Fig. 3E) is largely flat and smooth. Musculature (Fig. 5E, F): M11 - M. craniomandibularis internus (0md1), O: posterolateral area of the head capsule, posterior to the tentorium, I: with the adductor tendon on the mesal mandibular base; M12 - M.

craniomandibularis externus (0md3), O: ventral wall of the head capsule, posterior M17; I: with the abductor tendon on the lateral mandibular base; M13 - M. hypopharyngomandibularis (0md4), very thin, O: ventrally on the basal portion of the tentorium, I: mesal area of the mandibular base, close to the tendon of M11.

Maxillae. A maxillary groove is missing. The cardo (Fig. 3D; *cd*) is large and almost quadrangular. The basistipes (Fig. 3D; *bst*) is stout, its basal bulging portion bears a long, modified seta, which is broadened and flattened distally; the distal portion of the basistipes and the entire mediostipes are hidden below the mentum. The lacinia (Fig. 4B; *lac*) and galea are very short and strongly flattened, both in natural position hidden between the mandibles and mentum, except for conspicuously long setal fringes protruding anterad beyond the remaining mouthparts (Fig. 3A–D). The maxillary palp (Figs 3B, D, 4B–D; *mxp*) is strongly reduced, in resting position hidden in a deep lateral palpal cavity (Fig. 3B; *ppc*); the only recognizable palpomere is clavate, curved near the base and covered with an irregular microreticulation; one submedian seta is visible on its mesal surface (which in resting position in the palpal cavity is exposed anteriorly); a sensory appendage (Fig. 4D; *sap*) is present but shifted onto the subapical lateral surface and curved in such a way that its apex is directed anterodorsad in the resting position (Fig. 4C, D); the sensory appendage is accompanied by a pair of long digitiform sensilla (Fig. 4D; *dgs*). The apex of the maxillary palp is modified, developed as a short papilla bearing a group of slender setiform apical sensilla (Fig. 4D; *aps*). Musculature (Fig. 5G, H): M15 - M. craniocardinalis externus (0mx1), O: anterolateral area of the ventral wall of the head capsule; I: lateral branch of the cardinal process; M17 - M. tentoriocardinalis (0mx3), O: anterolateral area of the ventral wall of the head capsule, in front of the ventral tentorial base; I: mesal branch of the cardinal process; M18 - M. tentoriostipitalis (0mx4/0mx5), O: ventral side of the basal portion of the tentorium; I: basal area of the stipes; M19 - M. craniolacinalis (0mx2), O: anterior to the ventral base of the tentorium; I: base of the lacinia.

Labium. The large shield-like mentum (Fig 3D; *mn*) is strongly sclerotized and smooth; four strongly developed setae inserted at about half length form an irregular transverse row. The prementum is not visible externally and the palps are reduced. Musculature (Fig. 5 I): M28 – M. submentopraementalis (0la4), O: ventral wall of the head capsule, anterior to the tentorium, I: ventrally on the posterior premental border (Fig. 5I); M30 - M. tentoriopraementalis superior (0la6), O: tentorial base, I: dorsolaterally on the posterior premental border.

Internal skeletal structures. The tentorium (Fig 5B–H; *t*) is partially reduced, lacking the tentorial bridge, laminatentoria and anterior arms. The strongly developed and nearly vertical tentorial arms originate from two shallow pits on the posteroventral area of the head capsule, and are attached to dorsolateral wall behind the compound eyes. Circumocular ridges are present.

Epipharynx and hypopharynx. The anterior epipharynx (i.e., the ventral labral region; Fig. 4A; *lbr*) is largely smooth, lacking microtrichia, with only one pair of lateral setae and one pair of lateral structures resembling campaniform sensilla; a group of densely arranged similar circular sensilla is present behind fine transverse ridge. The anterior hypopharynx bears a pair of lateral hypopharyngeal lobes (Fig. 4B; *lhh*) with anterior fringes of conspicuously long and dense trichia. The posterior epipharyngeal and hypopharyngeal lateral margins are fused, thus forming an elongate prepharyngeal tube. Musculature (Fig. 5I): M41 - *M. frontohypopharyngalis* (0hy1), O: posterodorsal area of the head capsule, anterior to the neck region, I: laterad the anatomical mouth; M43 - *M. clypeopalatalis* (0ci1), O: mesally on the anterodorsal area of the head capsule, I: epipharyngeal wall; M44 - *M. clypeobuccalis* (0bu1), O: anterior frontal area, posterad the antennal sockets, I: dorsal pharyngeal wall at the anatomical mouth.

Prepharynx and pharynx. The sclerotized hypopharyngeal ventral wall of the laterally closed prepharynx appears evenly curved in cross-section. The intima of the pharynx is unusually strongly developed, forming tooth like structures resembling elements of a proventriculus within the head. Musculature (Fig. 5I): M45 - *M. frontobuccalis anterior* (0bu2), O: middle frontal region, I: obliquely inserted on the dorsal pharyngeal wall; M46 - *M. frontobuccalis posterior* (0bu3), O: frontal region posterior to M45 and laterad M41, I: dorsal pharyngeal wall; M48 - *M. tentoriobuccalis anterior* (0bu5), O: ventral wall of the head in front of the tentorial base, I: ventral prepharyngeal wall; MmIII-Mm. *compressores epipharyngis*, numerous transverse bundles on the posterior epipharynx.

Nervous system. The brain (Fig. 6A, C; *br*) is of medium size compared to the entire volume of the head and located in the posterodorsal cephalic area, occupying a large portion of the neck region; it is constricted in the area of the occipital crest; anteriorly it almost reaches the tentorial arms. The ventral side of the suboesophageal complex (Fig. 6B, C; *soe*) is very close to the ventral wall of the head capsule; the posterior part is distinctly enlarged and protrudes from the cephalic lumen. The protocerebral optic lobes (Fig. 6A, B; *opl*) and deutocerebral antennal nerves (Fig. 6A–C, *ann*) are well-developed, the former originating on the lateral protocerebral extensions dorsolaterad the latter. The connection of the optic neuropils to the compound eyes (Fig. 6A–C; *ce*) is apparently thin and not recognizable on the μ -CT data. The frontal ganglion (Fig. 6A; *fg*) is located in the middle region of the head; it is posteriorly connected to the brain by the frontal connectives.

Glands. Tubular glands are strongly developed in the anterior region of the head and occupy a considerable portion of the lumen in this area (Fig. 6D; *g/c*). Several pairs extend from the middle cephalic region in front of the tentorial arms to the base of the maxillae and hypopharynx. Connecting ducts open into a pair of anterior labral impressions and on the lateral impression on each mandible.

Variability of external head structures within Clavigeritae

Within the studied species representing three tribes of Clavigeritae, the head capsule shows a considerable variability in shape and size, compared to the pronotum and the rest of the body (Fig. 1, Fig. S1–3). The most elongate head, and longest in relation to the body, occurs in *Claviger* (Fig. 1B), *Diartiger* Sharp (Fig. 1C), *Zuluclavodes* Hlaváč (Fig. 1F) (all Clavigerini), *Disarthricerus* (Fig. 1G) (Disarthricerini), and *Tiraspirus* Hlaváč, Parker, Maruyama et Fikáček (Fig. 1J) (Tiracerini). In contrast the shortest and stoutest head can be found in *Tiracaleda* Hlaváč, Parker, Maruyama et Fikáček (Tiracerini) (Fig. 1H). The general form of the anterior (exposed) portion of the head can be narrowing anterad (*Cerylambus* Newton et Chandler, Fig. 7A; *Tiracaleda*, Fig. 7G), subparallel (*Diartiger*, Fig. 2A; *Novoclaviger* Wasmann, Fig. 7C; *Pararticerus* Jeannel, Fig. 7D; *Tiracerus* Besuchet, Fig. 7H; *Tiraspirus*, Fig. 7I), or widening anterad (*Claviger*, Fig. 7B; *Zuluclavodes*, Fig. 7E; *Disarthricerus* Raffray, Fig. 7F). The difference between the highest and the lowest site of the head in lateral view is also highly variable; the smallest difference can be seen in *Tiracaleda* (Fig. 7G), and the greatest in *Disarthricerus* (Fig. 7F) and *Tiraspirus* (Fig. 7I). The sculpture of the head is extremely variable, ranging from virtually none in *Claviger* (Fig. 7B) and *Tiracaleda* (Fig. 7G) to variously large and dense punctures in the remaining genera, with the largest alveolate impressions densely covering the head in *Cerylambus* (Fig. 7A), *Novoclaviger* (Fig. 7C), and *Tiracerus* (Fig. 7H).

The dorsal tentorial pits can be well-marked (e.g., *Diartiger*, Fig. 2A; *Novoclaviger*, Fig. 7C; *Zuluclavodes*, Fig. 7E) or completely obliterated (e.g., *Cerylambus*, Fig. 7A, and all studied Tiracerini, Fig. 7G–I). The ventral tentorial pits are either widely separated (e.g., *Diartiger*, Fig. 2C; *Cerylambus*, Fig. 7A; *Tiracaleda*, Fig. 7G), or approximate or nearly fused (e.g., *Claviger*, Fig. 7B; *Disarthricerus*, Fig. 7F).

The occipital crest limiting the vertex and tempora posteriorly can be inconspicuous (e.g., *Diartiger*, Fig. 2A; *Claviger*, Fig. 7B; *Zuluclavodes*, Fig. 7E), or forming a temporal denticle, well visible in dorsal and ventral view (e.g., *Cerylambus*, Fig. 7A, *Novoclaviger*, Fig. 7C; *Pararticerus*, Fig. 7D). The postantennal region on the side of the head is in some cases developed as a smooth impression with well-defined margins, forming an antennal sulcus (e.g., *Diartiger*, Fig. 2B; *Novoclaviger*, Fig. 7C), or such an impression can be lacking (e.g., *Claviger*, Fig. 7B; *Tiraspirus*, Fig. 7I).

The mouthparts (Figs 8, 9, and Figs S4, 5) show little variability, restricted to minor differences in shape, sculpture, setation and arrangement of glandular openings on the labrum and mandibles. Most notably, Tiracerini (Fig. 8G–I) have the oral fossa markedly narrower in relation to the head width than in all remaining studied Clavigeritae. In *Tiracaleda* an unusual sexual dimorphism occurs that strongly affects the arrangement of the mouthparts; in males, the mentum is extremely elongate and narrowing anterad into a pointed, slender apex (Figs 8G, 9G, and Figs S5G, S6A, C, D). This hypertrophy causes the labrum to adopt a more horizontal orientation than in all remaining species

(Fig. S6C). In contrast, mouthparts of females do not protrude anterad and the mentum is not modified (Fig. 1H, Fig. S6B).

Profound differences can be found in the antennal structure (Figs 1, 3E, 10, Fig. S7). The variability primarily affects the flagellum, which can be composed of only one flagellomere (*Cerylambus*, Fig. 10A; *Disarthricerus*, Fig. 10F; and all studied Tiracerini, Fig. 10G–I), two (*Diartiger*, Fig. 3E; *Novoclaviger*, Fig. 10C; *Pararticerus*, Fig. 10D), or four (*Claviger*, Fig. 10B; and *Zuluclavodes*, Fig. 10E). The flagellum is circular in cross-section (most genera) or strongly flattened (*Tiraspirus*, Fig. 10I). The antennal apex in most genera forms a sensory plate either oblique (*Cerylambus*, Fig. 10A; *Tiracaleda*, Fig. 10G; *Tiraspirus*, Fig. 10I) or transverse (Clavigerini other than *Cerylambus*, Figs 3F, 10B–E; and *Tiracerus*, Fig. 10H) in relation to the longitudinal axis of the antenna. Such a plate is missing in *Disarthricerus* (Fig. 10F, Fig. S7F), which has the antennal apex broadly rounded and not demarcated by a rim.

Phylogeny

The multiple runs of the Bayesian analysis converged before 30 million generations; at the end of the analysis, all PRSF values were approaching 1.000 and the average standard deviation of split frequencies reached 0.004. Pselaphinae were resolved as a monophylum strongly supported by the posterior probability (PP) value 1 (Fig. 11A). Dasycerinae were resolved as a sister group to Pselaphinae, also with a strong support (PP 0.99). Within Pselaphinae, the pattern Faronitae + all remaining Pselaphinae was strongly supported (PP 1). However, the currently recognized supertribes Euplectitae, Goniaceritae, and Pselaphitae were resolved as non-monophyletic. Within Pselaphitae, a well-supported (PP 0.98) clade composed of Tyrini, Phalepsini, Tmesiphorini and Ctenistini was retrieved, but none of the tribes represented by more than one terminal was monophyletic. Also, the three Pselaphini species included in the analysis were obtained as a strongly supported (PP 0.99) monophylum, and a well-supported (PP 0.94) pattern Pselaphini + (Colilodionini + Clavigeritae) was found. Colilodionini + Clavigeritae is a strongly supported (PP 1) monophylum, and likewise monophyletic Clavigeritae are strongly supported (PP 1). Within Clavigeritae, however, Tiracerini form a basal grade, followed by *Disarthricerus* and monophyletic but very poorly supported (PP 0.66) Clavigerini.

The parsimony analysis (TNT) retrieved two most parsimonious trees, the strict consensus is shown in Fig. 11B (tree length, L = 579; consistency index, Ci = 0.38; retention index, Ri = 0.77). The general topology is similar to that of the Bayesian tree, also with Dasycerinae resolved as sister to Pselaphinae (but with a moderate symmetric resampling (SR) support value 88). The monophyletic Pselaphinae are strongly supported (SR 100), and the basal branching pattern also includes first Faronitae, and then the 'Euplectitae grade'. Euplectitae, Goniaceritae, Batrisitae, and Pselaphitae are not monophyletic. The clade composed of Tyrini, Phalepsini, Tmesiphorini and Ctenistini is weakly supported (SR 76), whereas Pselaphini are well-supported (SR 98). The topology Pselaphini +

(Colilodionini + Clavigeritae) was also found, but very poorly supported (SR 59). However, Colilodionini + Clavigeritae (SR 99) and Clavigeritae (SR 100) form strongly supported monophyla. Non-monophyletic Tiracerini were also retrieved as the basal grade within Clavigeritae, but Clavigerini are paraphyletic in relation to Disarthricerini. Internal relationships in Clavigeritae are poorly supported or not supported at all.

The monophyly of Pselaphinae is supported by the following cephalic characters (Fig. 12A) (character number and states in brackets): [10(0)] neck region prominent, subglobose or barrel-shaped, broadest behind occipital constriction; [11(0)] occipital constriction deep (but reversed in Clavigeritae); [31(0)] dorsomedian inversely U- or V-shaped region delimited by sulcus or in a step-wise manner present (reversed in some groups, incl. Clavigeritae); [52(1)] antennal insertions close to sides of frons and lateroventral; [53(1)] antennal fossae moderately broadly separated by distance 1.5-3 times as broad as scape; [55(0)] clypeus steeply declining anterad; [80(1)] posterior tentorial pits subcircular; [104(2)] labial palpomere 2 strongly elongate, subcylindrical, with truncate apex; [130(0)] apical sensory appendage of maxillary palp present; [133(0)] galea broad and flat, with setal fringe on mesal and distal margins; [137(0)] mesal mandibular margin with several pre-apical teeth (reversed in some Clavigeritae); [139(0)] prostheca with slender microtrichia absent (but secondarily developed in Clavigeritae); [145(0)] approximate median peg-like sensilla on anterior labral margin present, two (but modified in Batrisitae, Pselaphitae and Clavigeritae). The 'higher Pselaphinae'. i.e., Pselaphinae excluding Faronitae, share a unique and constant feature: the basal portion of scapus countersank in the base of the distal portion [147(1)].

The monophyly of Colilodionini + Clavigeritae (Fig. 12B) is supported by: [70(1)] anterolateral cavities in oral fossa present to hide maxillary palps; [101(1)] prementum reduced, with indiscernible and lacking palps; [109(1)] maxillary palpifer largely or entirely concealed in ventral view; [110(1)] basistipes stout, with bulging transverse basal portion, partly concealed under side of mentum; [111(1)] maxillary palp strongly reduced, composed of one palpomere; [132(1)] sensory appendage of maxillary palp subapical, strongly oblique to long axis of palpomere; [135(1)] setal fringes of lacinia and galea longer than lobes of lacinia and galea and strongly projecting anterad beyond labrum; [136(1)] mandibles strongly shortened, subtriangular and not falcate, in closed position at most apices overlapping.

The monophyly of Clavigeritae (Fig. 12B) is supported by: [11(1)] occipital constriction shallow; [141(4)] labrum conspicuously small, approximately lentiform or rhomboidal, with posterior and anterior margins convex and surface subvertical; [148(1)] distal portion of scapus with its basal half or more concealed inside antennal cavity; [149(2)] distal portion of scapus subglobose, conspicuously short; [150(1)] pedicellus distinctly bent at an obtuse angle between proximal articulating portion and exposed distal part.

Discussion

Phylogeny of Pselaphinae based on cephalic structures

Despite of great attention attracted by Clavigeritae as morphologically bizarre and ecologically fascinating extreme myrmecophiles, morphological structures of this group are still exceptionally poorly studied. The most recently emended diagnosis of the supertribe reveals how problematic it is to define this group. Hlaváč et al. (2020) defined Clavigeritae as having the following set of characters: (1) reduced number of antennomeres (three to eight; but *Colilodion*, excluded from Clavigeritae and placed within Pselaphitae by the same authors, has 3–4-segmented antennae, and 6–11-segments are present in the remotely related *Plagiophorus* Motschulsky of Goniaceritae [Nomura and Sugaya, 2007; Sugaya et al., 2004]); (2) terminal antennomere “usually longest” (but not in the clavigerite genus *Thysdariella* Hlaváč); (3) apex of terminal antennomere either truncate or “simply rounded”; (4) mouthparts reduced and barely visible (same in *Colilodion*); (5) buccal cavity transverse (as in fact in nearly all groups of Staphylinioidea) “with or without lateral cavities for the accommodation of maxilla” (in fact, the maxillae in Clavigeritae are not hidden inside lateral cavities, but largely concealed between a broad mentum and mandibles; the lateral cavities accommodate only modified maxillary palps, as is also the case in *Colilodion*); (6) abdominal tergites IV–VI free or fused; (7) elytra and abdomen with trichomes (but entirely lacking in one tribe); (8) legs with elongate meso- and metatrochanters (also in *Colilodion*, Pselaphini and others); (9) tarsomere 3 longer than 1–2 combined (again, as in *Colilodion*; according to Chandler (2001), tarsomere 3 is also about as long as 1–2 combined in Pselaphitae, and this state may overlap with conditions observed in Clavigeritae); (10) tarsus with a single tarsal claw (as in *Colilodion* and all Arhytodini and Pselaphini, according to Chandler (2001)). It is evident that not a single character in this list is unique for Clavigeritae and occurs in all species of this supertribe.

Is it then possible to define Clavigeritae by characters restricted solely to the head, including structures unknown or ignored by previous authors? Among species examined in the present study, only Clavigeritae have a clearly marked but at the same time shallow occipital constriction; a uniquely shaped, small and subvertical labrum; the distal portion of the scapus with its basal half concealed inside the antennal fossa, and its distal portion subglobose and conspicuously short; and the pedicellus distinctly bent at an obtuse angle between the proximal articulating portion and the exposed distal part (the latter illustrated in Appendix S2, character 150(1)). Even though our selection is limited and does not include the enigmatic tribes Mastigerini, Lunillini, and the extinct Protoclavigerini, at least the specifically modified labrum, the shortened, partly concealed scapus, and the angulate (and also shortened) pedicellus seem to be unique for Clavigeritae. All three features can be associated with the most conspicuous ecological trait of Clavigeritae - myrmecophily. The labrum is part of a functional-morphological system that allows Clavigeritae to feed by trophallaxis (Jałoszyński et al., 2020). As the cephalic appeasement glands open on the mouthparts (Jałoszyński et al., 2020, and present results) and consequently the ants’ attention is directed toward

the anterior head region, where the antennal bases are inserted, it seems reasonable to interpret also the very compact structure of the proximal antennomeres and the way the scapus and its basal articulation are protected as adaptations to life as inquilines. Despite myrmecophilous habits of pselaphines belonging to other supertribes (e.g., *Saulcyella schmidtii* (Märkel), *Batrisodes unisexualis* Besuchet, *Batrisus formicarius* Aubé, *Ctenistes* sp., *Tmesiphorus crassicornis* (Sharp), among those included in the phylogenetic analysis), none of them shows the traits identified here as synapomorphies of Clavigeritae. Consequently, a detailed morphological examination identifies diagnostic and also phylogenetically relevant features overlooked in previous, more general studies.

This raises the question whether phylogenetic reconstruction based solely on cephalic characters agree with results based on whole-body morphological and molecular analyses carried out so far? Newton and Thayer (1995) in a morphological analysis recovered the topology Neophoninae + (Dasycerinae + (Protopselaphinae + Pselaphinae); Parker (2016b) in a study based on both morphological and molecular data proposed (Neophoninae + Dasycerinae) + Pselaphinae, and Yin et al. (2021) in a morphological study resolved (Protopselaphinae + Pselaphinae) + (Neophoninae + Dasycerinae). Our analysis lacks the rare Neophoninae and Protopselaphinae, but the relationship Dasycerinae + Pselaphinae should be regarded as close to the previously published results. Hlaváč et al. (2021) included only *Dasycerus* Brongniart as an outgroup for Pselaphinae. The largest number of representative Pselaphinae terminals were included in analyses published by Parker and Grimaldi (2014) and Parker (2016b). These authors, using morphological and molecular data, resolved Faronitae as the most basal branch, and a similar result was also obtained by Parker and Maruyama (2013) and Yin et al. (2021). This early branching event is further corroborated by our study, and strongly supported both in Bayesian and parsimony analyses. For the first time we identify a remarkable unique innovation that marks the emergence of the 'higher Pselaphinae' (excluding Faronitae) - a modification of the scapal base that has differentiated into two sharply delimited portions, with the basal one countersunk in the proximal one (illustrated in Appendix S2, character 147(1)). Our analysis also yielded the non-monophyly of Euplectitae, which were resolved as 'Euplectitae grade'. This term was proposed by Parker (2016b), who obtained terminals belonging in this currently recognized supertribe as a series of clades sequentially branching off the pselaphine backbone directly after Faronitae. In the earlier results of Parker and Maruyama (2013) (focused on placing a new genus of Trogastrini) Euplectitae were also not monophyletic. Parker (2016b) retrieved Goniaceritae as non-monophyletic, and additionally paraphyletic in relation to Batristitae (but even inclusion of Batristitae into Goniaceritae would not render the latter monophyletic). The author suggested that Amauropini should be synonymized with Batrisini, and the paraphyly of Batrisini in relation to Amauropini was further corroborated by Parker and Owens (2018). We included one member of the Batristitae tribe Amauropini and seven Batrisini and, in agreement with those previous results, resolved Batrisini paraphyletic in regard to Amauropini. Nevertheless, we regard our and

other available phylogenies of Pselaphinae as preliminary, so we refrain from taking formal taxonomic or nomenclatural actions at this early stage.

There is already a growing body of evidence (morphological and molecular) that Clavigeritae have evolved from within paraphyletic Pselaphitae (Parker and Grimaldi, 2014; Parker, 2016b; Hlaváč et al., 2021). Moreover, the enigmatic, morphologically bizarre genus *Colilodion* Besuchet was initially considered as the sister group of all extant Clavigeritae (Besuchet, 1991; Parker and Grimaldi, 2014: fig. 3C). In contrast, in the most recent study (Hlaváč et al., 2021) it was resolved as part of a pselaphite subunit placed as sister to Clavigeritae. For this reason, Hlaváč et al. (2021) formally transferred Colilodionini from Clavigeritae to Pselaphitae. This action, however, did not solve any problems related to the apparent paraphyly of Pselaphitae in relation to Clavigeritae, found also by other authors. Parker and Grimaldi (2014, fig. 4) resolved the topology (Arhytodini + Pselaphini) + Clavigeritae; Parker (2016b) either a polytomous Arhytodini-Clavigeritae clade within a polytomous branch that included other Pselaphitae (in morphology-based results; Parker (2016b: fig. 6A)), or Clavigeritae + Pselaphini (in the combined morphological and molecular results; Parker (2016b: fig. 6B)). Hlaváč et al. (2021: fig. 1) resolved (*Colilodion* + Arhytodini of Pselaphitae) + Clavigeritae, but this entire clade was sister to Pselaphini. Yin et al. (2021: fig. 10), in turn, resolved Pselaphini as sister to the clade Clavigeritae + (Tyrini + Ctenistini). Both Tyrini and Ctenistini currently also belong in Pselaphitae. Consequently, all available evidence strongly suggests that Clavigeritae may have evolved from within Pselaphitae. Our analysis, based solely on cephalic features, resolved Pselaphini + Clavigeritae within Pselaphitae, and further corroborates this view.

Colilodion is an extremely rare genus, whose bizarre morphology is still poorly studied. Besuchet (1991) illustrated dissected mouthparts, and Nomura and Sugaya (2007) added high-quality scanning electron micrographs showing the undissected head and related structures in several views. These illustrations clearly show that the proximal antennomeres have a structure typical of Pselaphini, and not Clavigeritae (i.e., the distal portion of the scapus is exposed, and the proximal articulating element of the pedicellus is in a straight axis with the distal portion). Moreover, the labrum is not of the Clavigeritae form, but closely resembles that in all terminal taxa included in our analysis that are currently placed in Pselaphitae. We argue, however, that all these features are plesiomorphic conditions, compared to what is found in Clavigeritae, and thus phylogenetically irrelevant. In contrast, several character states are very likely derived and shared between *Colilodion* and Clavigeritae: a) the general structure of the oral fossa, with the lateral palpal cavities, b) the stout mandibles with long prothecae, c) reduced maxillary palps, d) each with a subapical group of sensilla, e) conspicuously long setal fringes on the short lacinia and galea, and f) a transformed mentum (lacking prementum and palps). All these conditions documented for *Colilodion* closely resemble features observed in Clavigeritae, but not in the 'true' Pselaphitae. Additionally, antennae of *Colilodion* have a reduced number of flagellomeres, and the most distal one resembles that in *Disarthricerus* of Clavigeritae. In our analysis, character states listed here placed *Colilodion* as sister

to Clavigeritae, with very good support both in Bayesian and parsimony analyses. One may argue that this could be a result of parallel evolution, and adaptations to a similar life style and similar selective pressure. However, there are no published observations that could support the broadly accepted hypothesis that *Colilodion* is a myrmecophile; in contrast, all known specimens have been collected from leaf litter like predacious pselaphines. The mandibles of *Colilodion*, although resembling more those of Clavigeritae, are nonetheless larger, but still much shorter than those e.g., in the predatory *Pselaphus* (Beutel et al., 2021: fig. 4A, B), and their pre-apical teeth are as small and blunt as those in e.g., *Diartiger*. Although clearly reduced compared to mandibles of Pselaphitae, their mesal edges partly overlap in a closed position (Nomura and Sugaya, 2007: fig. 3E), and may presumably be used for cutting, or at least ‘pinching’ the larval cuticle of ants. Hypertrophied capillary structures of the maxillae and a strongly reduced labium were identified as important components of the apparatus for liquid food uptake in *Claviger* (Jałoszyński et al. 2020). Intriguingly, these structures look almost identical in *Colilodion*. This suggests that *Colilodion* is also fed by ants by trophallaxis. Also, the reduced maxillary palp with its subapical sensorium and the palpal cavity to retract and protect from contacts with ants’ mandibles are very similar in Clavigeritae and *Colilodion*. Consequently, the cephalic morphology seems to support the hypothesis of *Colilodion* being a myrmecophile, even though glandular openings on its labrum and mandibles are not visible and likely absent. Despite the results of Hlaváč et al. (2021), our view is that Besuchet’s original placement of *Colilodion* as sister to all extant Clavigeritae should not be rejected without further, detailed characterization of the external and internal morphology of Colilodionini, and including more genera of Pselaphitae in morphological and molecular analyses. Our results, based on a limited character system, cannot be used to support a formal taxonomic action, and therefore we retain Colilodionini as a part of the non-monophyletic Pselaphitae, and Clavigeritae as separate from Pselaphitae. However, the need for a deep reclassification of Pselaphinae was already clearly demonstrated by results of all hitherto published phylogenetic results, including the one presented here.

The internal classification of Clavigeritae is also problematic. Hlaváč et al. (2021) found seven former subtribes as non-monophyletic and merged them with Clavigerini. Hlaváč et al. (2021) included in their analysis members of three largest tribes, and resolved the topology Tiracerini as the basal branch + (Mastigerini + Clavigerini). Parker and Grimaldi (2014: fig. 4) analyzed over 30 species of Clavigeritae. Although *Tiracerus* (Tiracerini) was also the basal branch, the direct subsequent branching events included genera of Clavigerini, and the latter tribe was paraphyletic in relation to Mastigerini. Based solely on cephalic structures, we also resolved members of the currently recognized Tiracerini as the most basal branches within Clavigeritae, albeit as a paraphyletic grade. Clavigerini were resolved as a poorly supported clade in Bayesian analysis, but paraphyletic in relation to Disarthricerini in the parsimony analysis. Therefore, cephalic structures alone may not be sufficient to reconstruct deep divergences within Clavigeritae, although the basal

position of Tiracerini genera, in agreement with Hlaváč et al. (2021), underlines the importance of features of the head in the evolution of this supertribe.

Evolution of cephalic structures within Clavigeritae

It was suggested by Hlaváč et al. (2021) that “characters postulated to be involved in beetle-ant communication are amongst the most invariant, and least convergent”, and that morphological diversity may not be truly adaptive, but be a result of a “morphological drift” under weak selective pressure. Indeed, once the structures (and physiological pathways) crucial for integration into ant colonies have developed, these might have remained conserved, and further modifications might have not increased the fitness. Stable conditions inside ant colonies, and the established dependence on ants in feeding and dispersal, might have not exerted further selective pressure on the already ‘optimized’ body structures. Under such conditions, the current diversity seen in particular body features might have indeed evolved as a result of the postulated “morphological drift”. This raises the question which cephalic structures are most variable within Clavigeritae and which are most stable. It is also an intriguing question whether these extreme myrmecophiles have retained a potential to further modify (reduce?) any head structures in their future evolution.

The term “reduced mouthparts” is still broadly used to describe Clavigeritae (e.g., Hlaváč et al., 2021). However, if regarded as one functional entity (which they undoubtedly are), the clavigerite mouthparts represent a model example of a complex structure, with some components reduced and others hypertrophied compared to ancestral traits. Beutel et al. (2021) attempted to identify groundplan features of Pselaphinae. They interpreted the following character states of the mouthparts as ancestral for the subfamily: a labrum anteriorly broadened and weakly declining anterad; and long, falciform and multidentate mandibles lacking a protheca but with a partially reduced but recognizable mola. Fully developed maxillae with tetramerous maxillary palps, and the labium with a well-developed prementum and trimerous labial palps can also be regarded as parts of the pselaphine groundplan. A shift from a predatory life to feeding by trophallaxis in Clavigeritae involved a strong transformation of the labrum, which decreased in size and was transformed into a heavily sclerotized shield with its dorsal surface facing anterad, exposing glandular openings that present the appeasement secretions to ant workers. The openings are not easily observable in all studied Clavigeritae (see Fig. S5), and in some cases they were scored as absent. These openings can be fairly obvious, developed as large and deep impressions with several pores inside (as in *Diartiger*; Fig. 3B, or *Tiraspirus*; Fig. S5I), or as a few scattered tiny pores partly obscured by deep microsculpture (e.g., as in *Pararticerus*; Fig. S5D). The cases where we did not recognize any such openings may in fact be artifacts of preparation, as the solidified secretion might have blocked and obscured tiny pores. The mandibles in Clavigeritae join the labrum in secretory functions, as they also bear openings to release the products of cephalic glands (Fig. S5). The mandibular pores also show a similar variability as those on the labrum, with *Pararticerus* (Fig. S5D) as an example of large,

easily observable pores, which are less pronounced or obscured by microsculpture or setae in other genera. This secretion-releasing labral-mandibular system is conspicuously similar in all studied Clavigeritae (Fig. S5), and it is also linked with similar transformations of the musculature. The labral musculature in *Diartiger* and the previously studied *Claviger* (Jałoszyński et al., 2020) does not differ in any fundamental features from that in free-living predatory pselaphines (Beutel et al., 2021; Luo et al., 2021a); it consists only of short intrinsic bundles. However, the mandibular muscles in Clavigeritae are distinctly less voluminous than those in their predatory relatives (Beutel et al., 2021; Luo et al., 2021a). Consequently, the main function of the mandibles in Clavigeritae is to cooperate with the labral secretory action and to participate in the liquid food uptake, via strongly developed, dense trichia of the prostheca. Among pselaphines, such prosthecae are known only in Clavigeritae and *Collodion*, which is a secondary modification of the ancestral prostheca lost by other pselaphines (Beutel et al., 2021). Therefore, the labro-mandibular system can be recognized as largely conserved within the supertribe, as its function is related to manipulating the worker ants' behavior and feeding, crucial to survival. The labio-maxillary complex, in turn, has largely or completely lost the prementum and labial palps, and the maxillary palp has been strongly reduced. At the same time, the adaptation to trophallaxis has caused far-reaching innovations. The most spectacular one is the hypertrophy of setal fringes on the lacinia and galea, and the trichia on the lateral lobes of the hypopharynx. These structures are nearly identical in *Diartiger* and *Claviger*, and examination of externally visible elements of the mouthparts in all remaining studied Clavigeritae did not reveal any deviations from this capillary device, perfectly suited to transfer liquid food into the oral cavity. An unexpected and surprising finding, however, is that the dilator of the prepharynx (*M. clypeopalatalis*, M43) in *Diartiger* is composed of a markedly smaller number of bundles than in the otherwise similar *Claviger*. A strongly developed M43 may be explained as a component of a prepharyngeal pump optimized to take up liquid food. However, the remarkable difference in the development of this muscle between *Claviger* and *Diartiger* indicates that at least some Clavigeritae rely on a different mechanism to transfer the food from the oral cavity into the pharynx, or that the capillary action of the mouthparts and action of a moderately sized M43 and the remaining dilators (M41, M44, M45, M46, M48) provide a sufficient mechanism. No other significant differences were found in the head musculature between *Diartiger* and *Claviger*.

Among the most variable cephalic characters of Clavigeritae are: the general shape (especially the length in relation to the rest of the body) of the head capsule; its sculpture; the presence or absence of the dorsal tentorial pits; the presence or absence of the lateral antennal sulci; and the size and mutual proximity of the posterior tentorial pits. These structures are not related to feeding and indeed may change through the “morphological drift” mechanism postulated by Hlaváč et al. (2021). It is conceivable that they do not evolve under a strong selective pressure, but arguably as a result of a genetic drift.

Two cephalic structures deserve a special attention: antennae and eyes. Both are important sensory devices in almost all insects, and profound modifications usually mean strict and narrow specialization. Antennae composed of 11 antennomeres belong to the groundplan of crown-group Coleoptera and also Staphylinidae and Pselaphinae (Beutel and Hörnschemeyer, 2008; Newton and Thayer, 1995). Although reductions are not uncommon among pselaphines (e.g., Sugaya et al., 2004), the lowest numbers of segments are clearly reached in Clavigeritae. The peculiar modification of the scapus and pedicellus (discussed in previous paragraphs) and the compact and thickened flagellum (discussed in Jałoszyński et al. (2020)) can be interpreted as adaptations to myrmecophily. Reducing the length of antennae, increasing their thickness, and, first of all, reducing the number of vulnerable articulations between segments might have been beneficial for beetles that live among aggressive ants. The thickening of the flagellum was interpreted as a way to increase its surface, and therefore to increase the number of chemical and tactile sensilla, crucial for life in ant colonies (Jałoszyński et al., 2020). However, the present study shows that the antennae in Clavigeritae are one of the structures that show the greatest evolutionary plasticity. They are compact and relatively short in most Clavigeritae, but in addition to the variability illustrated in Fig. 10, Parker and Grimaldi (2014) and Hlaváč et al. (2021) show examples of taxa with antennae even more shortened in relation to the body length (e.g., genera *Radama* Raffray, *Semiclaviger* Wasmann, *Pseudacerus* Raffray, *Theocerus* Raffray, *Longacerus* Hlaváč, *Antalaha* Jeannel), or elongate and even slightly exceeding half of body length (e.g., *Dzumaca* Hlaváč et al., *Ziweia* Hlaváč et al.). The number of antennomeres in extant Clavigeritae ranges from three to six (examples of trimerous, tetramerous and hexamerous antennae are given in Fig. 10), and they can be circular in cross-section or strongly flattened. The flagellum can be widening, but also somewhat narrowing distad. In some cases, apparently secondarily, the antennae are nearly filiform, except for a short clavate terminal antennomere (in *Tiramieua* Hlaváč et al.). The density of antennal sensilla trichodea is highly variable in the examples illustrated here (Fig. 10). However, it should be noted that the antennal apex, independently of the general antennal shape and density of setae on lateral surfaces of the antennomeres, is always densely covered with either setae or/and digitiform sensilla, most commonly concentrated on a delimited, flat and somewhat sunken plate surrounded by a rim. Even if the specialized apical sensory plate is not differentiated, as in *Disarthricerus* (Figs 10F, S7F), the apex is densely covered with sensilla trichodea. It is likely that the moderately reduced number of six antennal articulations (as in *Cerylambus*; Fig. 10E) is sufficiently protecting against damage. Was the further reduction in other genera necessary? Was it an important factor in competition between various inquilines exploiting the same ant species? Or has a genetic mechanism of anarthrogenesis, once initiated, continued to reduce the antennae to merely three segments in some lineages? It is beyond the scope of the present study to address these intriguing questions that may require genetic investigations. However, it is important to note that in some groups within Clavigeritae, there is apparently still room for further antennal reduction. The example of trimerous antennae in many

members of the supertribe suggests that a mechanism of losing or fusing flagellomeres played an important role in the evolution of the clade.

Although Clavigeritae are considered as obligatory myrmecophiles, and consequently they spend all their life in a darkness of ant nests under stones, under bark, or deep in soil or hollow trunks, surprisingly few genera have completely lost the eyes. *Claviger testaceus*, an exemplary blind Clavigeritae species, studied in detail previously (Jałoszyński et al., 2020), has no ommatidia, optic nerves and optic neuropils. As it was demonstrated that the presence of externally observable cornea lenses does not mean that the eyes are functional (see Luo et al., 2021a), anatomical study is necessary to obtain a complete picture of the reduction of the visual sense. In the case of *Diartiger*, the large compound eyes are accompanied by well-recognizable optic lobes, and therefore the organs of sight are very likely fully functional. The architecture of the muscle system (except for some elements associated with the alimentary tract), brain, suboesophageal ganglion, cephalic portion of the fore gut, large glands and the tentorium do not differ between *Claviger* and *Diartiger*. It appears that the presence or absence of eyes does not affect the architecture of other internal cephalic structures or only to a very limited degree. Both blind species of *Claviger* included in the present phylogenetic analysis were resolved within branches composed of taxa with large eyes. The loss of eyes in *Claviger* was therefore a secondary process and it took place when already all important internal cephalic structures of Clavigeritae were developed and arranged as those in *Diartiger*. The loss of eyes in some Clavigeritae can be regarded as chronologically the latest and most extreme body transformation. This was very likely linked with loss of the flight capacity, as the blind *Claviger* has vestigial, non-functional wings and reduced flight musculature (Luo et al., 2021b).

An obvious question in this context is why then the great majority of Clavigeritae have large, well-developed and clearly functional eyes. It is conceivable that the view of a strict dependence on ants for dispersal is false, and that at least some clavigerite species can spend some time outside ant colonies to actively find another nest. As a matter of fact, some species have well-developed wings, and *Cerylambus reticulatus* (Raffray) (Fig. 1A) was collected not only by sifting leaf litter, but also using a flight intercept trap (Nomura et al., 2008). Hlaváč et al. (2021) also mention that some tropical Clavigeritae can be collected by flight intercept traps or at UV light. Such winged species with large eyes may actively disperse and utilize visual clues in navigation, and antennal sensilla to find an ant colony. On the other hand, the genus *Diartiger*, common in Japan, includes some winged species, which nonetheless have never been collected in flight intercept traps or at light (Shûhei Nomura, e-mail to the first author dated 19.03.2021). Ecological and behavioral observations are too scarce (in fact, non-existent for most Clavigeritae species) to explain this phenomenon. It is well-known, however, that blind and wingless European species of *Claviger* are associated with different species of *Lasius* ants and can be found in colonies under stones, in rotten wood or under bark. These beetles are never found outside ant colonies (Franz, 1992; Hlaváč and Lackner, 1998; Hlaváč et al., 2007), and some of their host species are microphthalmous (e.g., *Lasius flavus* (Fabricius)). Even

though the colonies of *Lasius* spp. do not seem to offer any peculiar conditions unique only for this genus, among Eurasian Clavigeritae only *Claviger* is blind, showing the most profound dependence on its hosts.

Interestingly, even though *Claviger* has reached a level of myrmecophily that apparently excludes dispersal assisted by visual clues (not directly observed, but also not excluded for *Diartiger* and all other taxa with large eyes), it has not reached the most extreme antennal reduction and has maintained four flagellomeres. In contrast, the North American *Adranes* LeConte, another example of a genus with blind species, has only one flagellomere (Akre and Hill, 1973). This genus has arguably reached a peak in the evolution of Clavigeritae, displaying the most profoundly reduced cephalic structures among all known species.

Conclusions

As shown in previous studies (e.g. Beutel et al. 2011), characters of the head, with a concentration of mouthparts, sensory structures, and essential parts of the digestive tract and the nervous system, are highly informative phylogenetically. Even though the phylogenetic results presented here should be regarded as preliminary, strong evidence could be provided for the monophyly of various branches in the phylogeny of Pselaphinae. Study of internal structures of members of the subfamily is at a very preliminary stage. However, it is evident that covert morphology is essential for understanding the evolution of Pselaphinae (and also other groups).

Among Clavigeritae, the cephalic morphology of *Diartiger kubotai* shows a moderate level of morphological reductions, including for instance tetramerous antennae. The well-developed, functional eyes are clearly plesiomorphic. Although its head structures are very similar to those of the previously studied blind *Claviger*, a remarkable difference in the size of M43 (dilator of the prepharynx) was found, which is much less developed in *Diartiger*. This demonstrates that some degree of variability in the musculature can be expected among externally similar taxa of Clavigeritae, and that liquid food uptake may not strictly depend on an exceptionally strong prepharyngeal pump. The loss of eyes in *Claviger* is identified as a young event in the evolution of Clavigeritae that took place after a full integration into ant colonies was already achieved.

Our phylogenetic analysis based solely on cephalic characters resolved Pselaphinae as a monophylum, and the internal branching pattern is similar to that obtained by other authors, both using morphological and molecular data. Faronitae is sister to the remaining Pselaphinae, followed by the 'Euplectitae grade' and non-monophyletic Goniaceritae, Batrisitae and Pselaphitae. Clavigeritae are (again) resolved as a monophylum that has evolved from within Pselaphitae. The enigmatic *Collodion*, previously included in Clavigeritae but later removed to (paraphyletic) Pselaphitae, was placed as sister to extant Clavigeritae based on an array of cephalic synapomorphies. We conclude that the current classification of Pselaphinae is unstable and deep

changes should be made maintaining only monophyletic units, while most of the currently recognized supertribes are paraphyletic.

References

- Akino, T., 2002. Chemical camouflage by myrmecophilous beetles *Zyras comes* (Coleoptera: Staphylinidae) and *Diaritiger fossulatus* (Coleoptera: Pselaphidae) to be integrated into the nest of *Lasius fuliginosus* (Hymenoptera: Formicidae). *Chemoecol.* 12, 83–89.
- Akre, R.D. and Hill, W.B., 1973. Behavior of *Adranes taylori*, a myrmecophilous beetle associated with *Lasius sitkaensis* in the Pacific Northwest (Coleoptera: Pselaphidae; Hymenoptera: Formicidae). *J. Kansas Entomol. Soc.* 46, 526–536.
- Belkaceme, T. 1991. Skelet und Muskulatur des Kopfes und Thorax von *Noterus laevis* Sturm: ein Beitrag zur Morphologie und Phylogenie der Noteridae (Coleoptera: Adephaga). *Stuttgarter Beitr. Naturk. Ser. A (Biol.)* 462,1–94.
- Besuchet, C., 1991. Révolution chez les Clavigerinae (Coleoptera, Pselaphidae). *Rev. suisse Zool.* 98, 499–515.
- Beutel, R.G. and Hörschemeyer, T., 2008. On the head morphology of *Tetraphalerus*, the phylogeny of Archostemata and the basal branching events in Coleoptera. *Cladistics* 24, 270–298.
- Beutel, R.G., Luo, X.-Z., Yavorskaya, M.I., and Jałoszyński, P., 2021. Structural megadiversity in leaf litter predators -the head anatomy of *Pselaphus heisei* (Pselaphinae, Staphylinidae, Coleoptera). *Arthr. Syst. Phyl.* 79, 443–463.
- Cammaerts, R., 1974. Le système glandulaire tégumentaire du coléoptère myrmécophile *Claviger testaceus* Preyssl, 1790 (Pselaphidae). *Z. Morph. Ökol. Tiere* 77, 187–219.
- Cammaerts, R., 1991. Interactions comportementales entre la Fourmi *Lasius flavus* (Formicidae) et le Coléoptère myrmécophile *Claviger testaceus* (Pselaphidae). I. Ethogramme et modalités des interactions avec les ouvrières. *Bull. Ann. Soc. R. Belge entomol.* 127, 155–190.
- Cammaerts R. 1992. Stimuli inducing the regurgitation of the workers of *Lasius flavus* (Formicidae) upon the myrmecophilous beetle *Claviger testaceus* (Pselaphidae). *Behavioural Processes* 28: 81–96.
- Cammaerts, R., 1995. Regurgitation behaviour of the *Lasius flavus* worker (Formicidae) towards the myrmecophilous beetle *Claviger testaceus* (Pselaphidae) and other recipients. *Behav. Proc.* 34, 241–264.
- Cammaerts, R., 1996. Factors affecting the regurgitation behaviour of the ant *Lasius flavus* (Formicidae) to the guest beetle *Claviger testaceus* (Pselaphidae). *Behav. Proc.* 38, 297–312.
- Cammaerts, R., 1999. Transport location patterns of the guest beetle *Claviger testaceus* (Pselaphidae) and other objects moved by workers of the ant, *Lasius flavus* (Formicidae). *Sociobiol.* 34, 433–475.
- Chandler, D.S., 2001. Biology, morphology, and systematics of the ant-like litter beetle genera of Australia (Coleoptera: Staphylinidae: Pselaphinae). Vol. 15. Associated Publishers, Gainesville, Florida, 560 pp.
- Engelmann, M.D., 1956. Observations on the feeding behavior of several pselaphid beetles. *Entomol. News* 67, 19–24.
- Franc, V., 1992. Myrmecophilous beetles of Slovakia with special reference to their endangerment and perspectives for protection. *Acta Univ. Carolinae biol.* 36, 299–324.

- Goloboff, P.A., Farris, J.S., Källersjö, M., Oxelman, B., Ramírez, M.J. and Szumik, C.A., 2003. Improvements to resampling measures of group support. *Cladistics* 19, 324–332.
- Goloboff, P., Farris, J. and Nixon, K., 2008. TNT, a free program for phylogenetic analysis. *Cladistics* 24, 774–786.
- Hlaváč, P., Bekchiev, R., Růžička, J. and Lackner, T., 2007. Contribution to the knowledge of myrmecophilous beetles (Coleoptera) of Bulgaria. *Acta Soc. Zool. Bohem.* 71: 131–136.
- Hlaváč, P. and Lackner, T., 1998. Contribution to the knowledge of myrmecophilous beetles of Slovakia. *Entomofauna carpatica* 10, 1–9.
- Hlaváč, P., Parker, J., Maruyama, M. and Fikáček, M., 2021. Diversification of myrmecophilous Clavigeritae beetles (Coleoptera: Staphylinidae: Pselaphinae) and their radiation in New Caledonia. *Syst. Entomol.* 46: 422–452.
- Jałoszyński, P., Luo, X.-Zh., Beutel, R.G., 2020. Profound head modifications in *Claviger testaceus* (Pselaphinae, Staphylinidae, Coleoptera) facilitate integration into communities of ants. *J. Morph.* 281, 1072–1085.
- Kéler, S. v., 1963. *Entomologisches Wörterbuch*. Akademie Verlag, Berlin, 679 pp.
- Luo, X.-Zh., Hlaváč, P., Jałoszyński, P. and Beutel, R.G., 2021a. In the twilight zone – the head morphology of *Bergrothia saulcyi* (Pselaphinae, Staphylinidae, Coleoptera), a beetle showing adaptations to endogean life but living in leaf litter. *J. Morph.* 1–18. <https://doi.org/10.1002/jmor.21361>
- Luo, X.-Zh., Jałoszyński, P., Stoessel, A. and Beutel, R.G. 2021b. The specialized thoracic skeletomuscular system of the myrmecophile *Claviger testaceus* (Pselaphinae, Staphylinidae, Coleoptera). *Org. Div. Evol.* 21, 317–335. <https://doi.org/10.1007/s13127-021-00484-1>
- Maddison, W.P. and Maddison, D.R., 2017. Mesquite: a modular system for evolutionary analysis. Version 3.2, [WWW document]. URL <http://mesquiteproject.org>.
- Newton, A.F. and Thayer, M.K., 1995. Protopselaphinae new subfamily for *Protopselaphus* new genus from Malaysia, with a phylogenetic analysis and review of the Omaliine Group of Staphylinidae including Pselaphidae (Coleoptera). *Biology, phylogeny, and classification of Coleoptera: papers celebrating the 80th birthday of Roy A. Crowson*. Muzeum i Instytut Zoologii PAN, Warszawa, 219–320.
- Nomura, S. and Sugaya, H., 2007. A new species of the genus *Colilodion* Besuchet (Coleoptera: Staphylinidae: Pselaphinae) from Vietnam. *Ann. Soc. Entomol. France (n.s.)* 43, 333–339.
- Nomura, S., Sakchoowing, W., Abd Ghani, I., 2008. A taxonomic revision of the cleverigerine genus *Cerylambus* (Insecta, Coleoptera, Staphylinidae, Pselaphinae). *Bull. Nat. Mus. Nat. Sci., Ser. A* 34, 123–140.
- Park, O., 1947. Observations on *Batrisodes* (Coleoptera: Pselaphidae), with particular reference to the American species east of the Rocky Mountains. *Bull. Chicago Acad. Sci.* 8, 45–132.
- Parker, J., 2016a. Emergence of a superradiation: pselaphine rove beetles in mid-Cretaceous amber from Myanmar and their evolutionary implications. *Syst. Entomol.* 41, 541–566.
- Parker, J., 2016b. Myrmecophily in beetles (Coleoptera): evolutionary patterns and biological mechanisms. *Myrmecol. News* 22, 65–108 .
- Parker, J. and Grimaldi, D.A., 2014. Specialized myrmecophily at the ecological dawn of modern ants. *Curr. Biol.* 24, 2428–2434.

- Parker, J. and Maruyama, M., 2013. *Jubogaster towai*, a new Neotropical genus and species of Trogastrini (Coleoptera: Staphylinidae: Pselaphinae) exhibiting myrmecophily and extreme body enlargement. *Zootaxa* 3630, 369–378.
- Parker, J. and Owens, B., 2018. *Batriscydmaenus* Parker and Owens, new genus, and convergent evolution of a “reductive” ecomorph in socially symbiotic Pselaphinae (Coleoptera: Staphylinidae). *Coleopt. Bull.* 72, 219–229.
- Rambaut, A., Suchard, M.A., Xie, D. and Drummond, A.J., 2014. Tracer v1.6 457 <http://beast.bio.ed.ac.uk/Tracer>.
- Ronquist, F., Teslenko, M., Van Der Mark, P., Ayres, D.L., Darling, A., Höhna, S., Larget, B., Liu, L., Suchard, M.A. and Huelsenbeck, J.P., 2012. MrBayes 3.2: efficient Bayesian phylogenetic inference and model choice across a large model space. *Syst.* 61, 539–542.
- Schomann, A., Afflerbach, K., Betz, O., 2008. Predatory behaviour of some Central European pselaphine beetles (Coleoptera: Staphylinidae: Pselaphinae) with descriptions of relevant morphological features of their heads. *Eur. J. Entomol.* 105, 889–907.
- Sugaya, H., Nomura, S. and Burckhardt, D., 2004. Revision of the East Asian *Plagiophorus hispidus* species group (Coleoptera: Staphylinidae, Pselaphinae, Cyathigerini). *Can. Entomol.* 136, 143–167.
- Wipfler, B., Machida, R., Mueller, B. and Beutel, R.G. 2011. On the head morphology of Grylloblattodea (Insecta) and the systematic position of the order, with a new nomenclature for the head muscles of Dicondylia. *Syst. Entomol.* 36, 241–266.
- Yin, Z.-W., Yamamoto, S., Thayer, M., Newton, A.F. and Cai, Ch.-Y., 2021. Dasycerine rove beetles: Cretaceous diversification, phylogeny and historical biogeography (Coleoptera: Staphylinidae: Dasycerinae). *Cladistics* 37, 185–210.

Figure plates

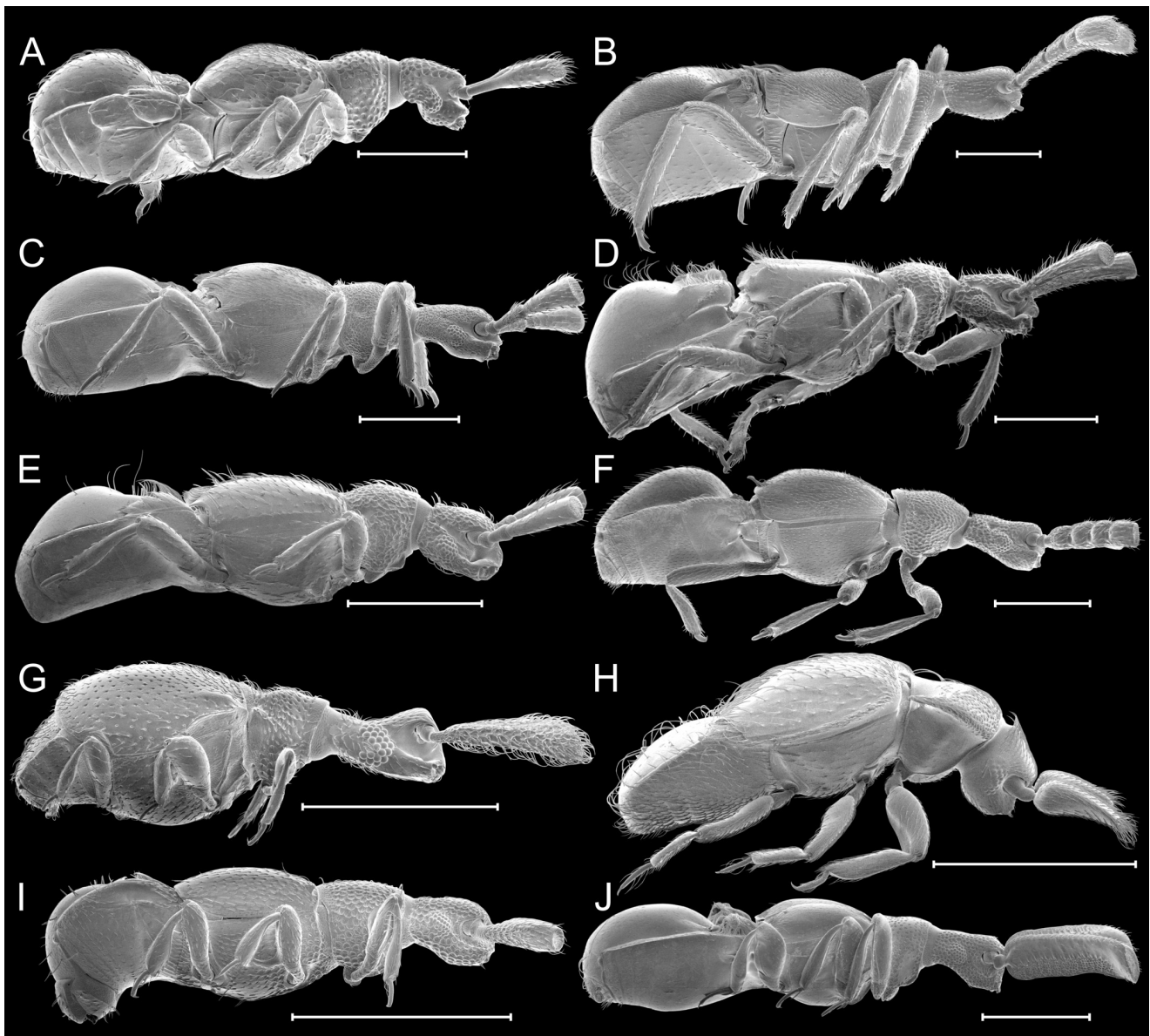


Figure 1. Examples of studied Clavigeritae, scanning electron micrographs, lateral view. A-F, Clavigerini: A, *Cerylambus reticulatus*; B, *Claviger longicornis*; C, *Diartiger kubotai*, D, *Novoclaviger gibbiventris*, E, *Pararticerus latus*; F, *Zuluclavodes briantaylori*; G, Disarthricerini: *Disarthricerus integer*; H-J, Tiracerini: H, *Tiracaleda minuta*; I, *Tiracerus* sp.; J, *Tiraspirus tabulatus*. Scale bars: 500 μ m.

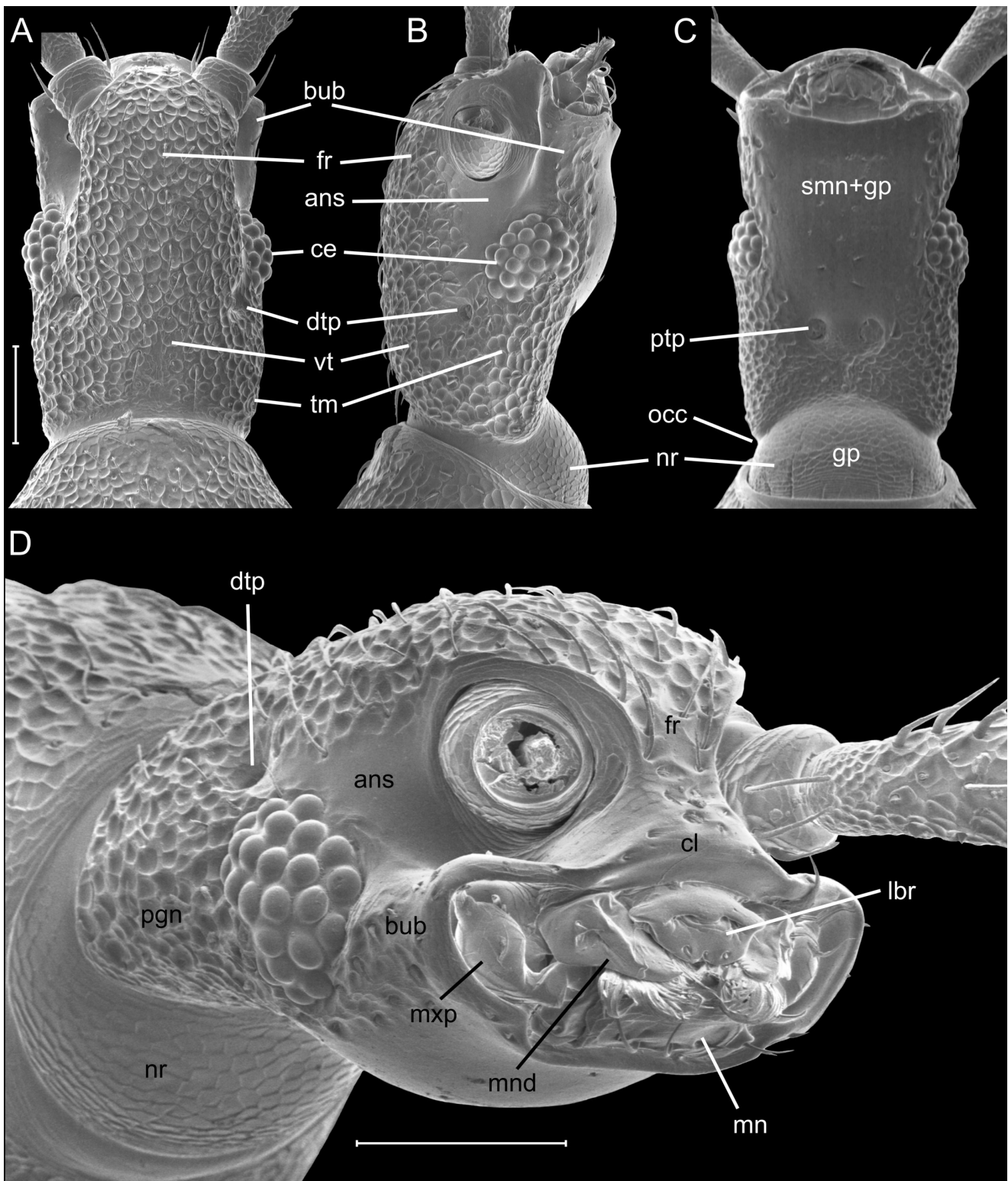


Figure 2. Head morphology of *Diartiger kubotai*, scanning electron micrographs. Head in dorsal (A), lateral (B), ventral (C), and anterolateral (D) views. Abbreviations: ans, antennal sulcus; bub, buccal bulge; ce, compound eye; cl, clypeus; dtp, dorsal tentorial pit; fr, frons; gp, posterior (post-tentorial) gular plate; lbr, labrum; mn, mentum; mnd, mandible; mxp, maxillary palp; nr, neck region; occ, occipital constriction; pgn, postgena; ptp, posterior

tentorial pit; smn+gp, submentum and anterior (pretentorial) gular plate; tm, temple; vt, vertex. Scale bars: 100 μ m.

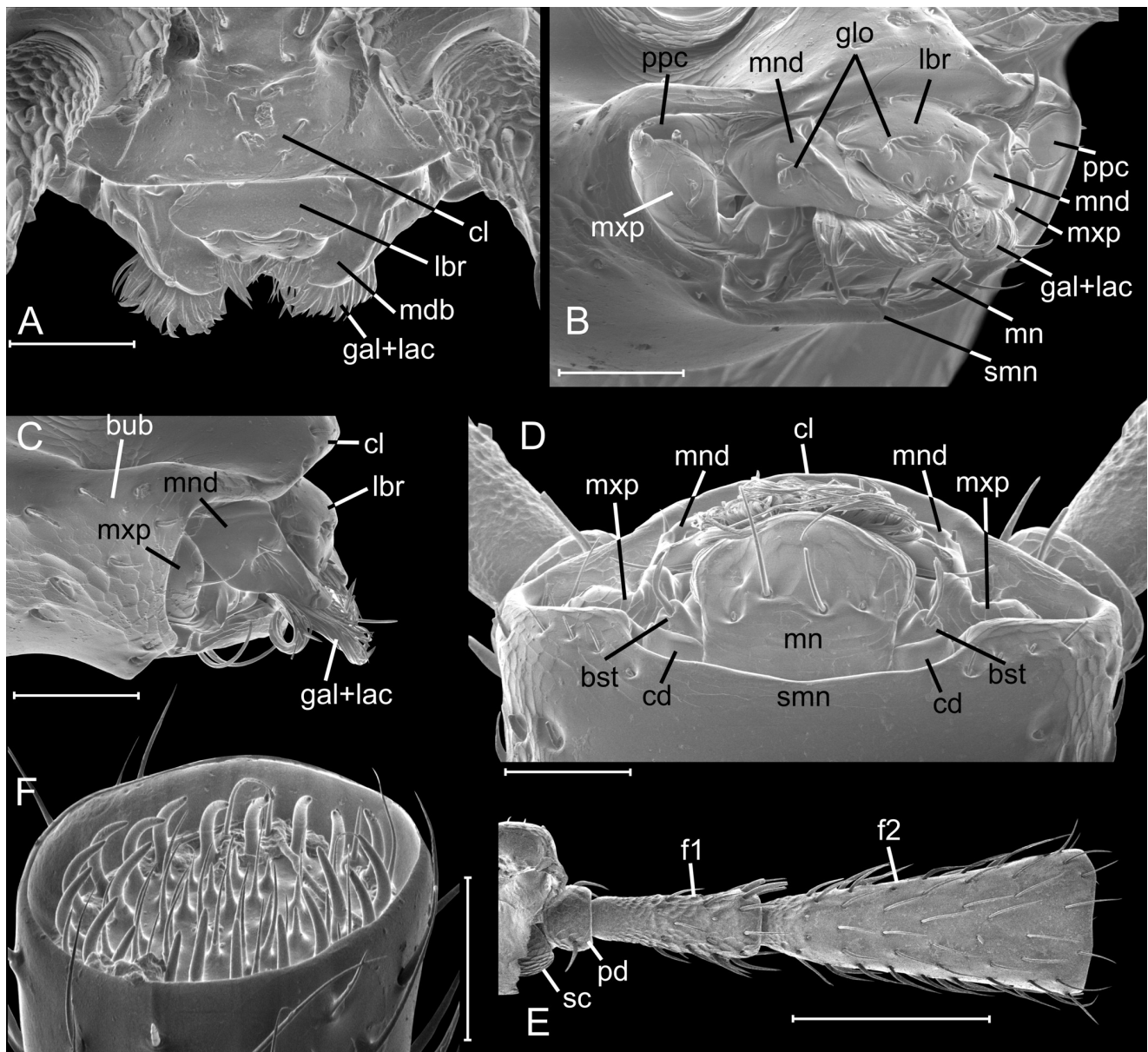


Figure 3. Head morphology of *Diartiger kubotai*, scanning electron micrographs. Mouthparts in dorsal (A), anterolateral (B), lateral (C), and ventral (D) views; E, left antenna in ventral view; F, antennal apex in lateroapical view. Abbreviations: bub, buccal bulge; bst, basistipes; cd, cardo; cl, clypeus; f1-2, flagellomere 1-2; gal+lac, setal fringes of galea and lacinia; glo, glandular opening; lbr, labrum; mdb, mandible; mn, mentum; mxp, maxillary palp; pd, pedicellus; ppc, palpal cavity; sc, scapus; smn, submentum. Scale bars: A-D, F: 50 µm; E: 200 µm.

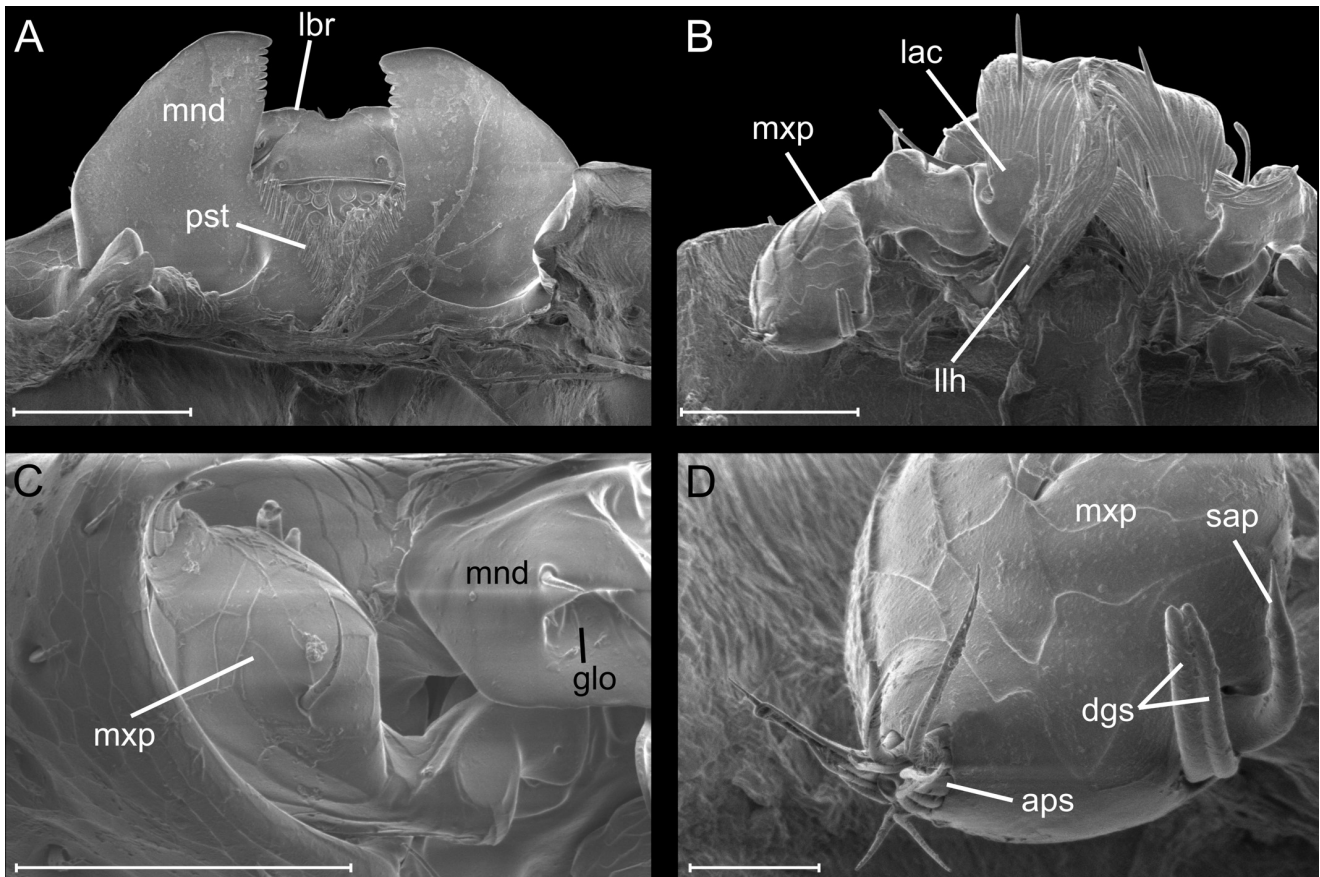


Figure 4. Head morphology of *Diartiger kubotai*, scanning electron micrographs. A, mandibles and labrum in ventral view; B, labium in dorsal view; C, palpal cavity with maxillary palp in anterolateral view; D, distal half of maxillary palp. Abbreviations: aps, apical sensilla; dgs, digitiform sensilla; glo, glandular opening; lac, lacinia; lbr, labrum; llh, lateral lobe of hypopharynx; mnd, mandible; pst, prostheca; sap, sensory appendage. Scale bars: A-C: 50 μ m; D: 10 μ m.

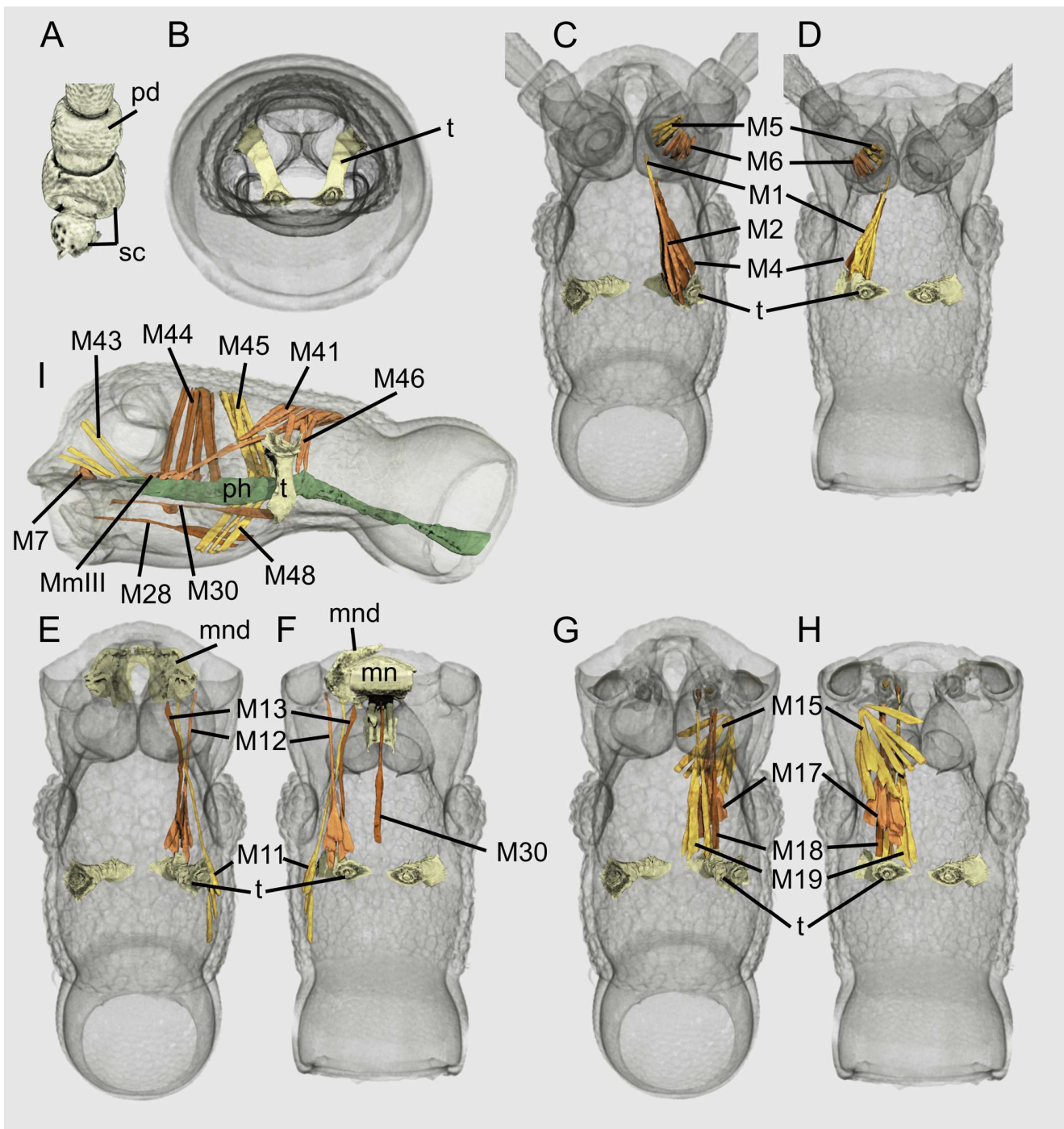


Figure 5. Head morphology of *Diartiger kubotai*, μ -CT reconstructions. A, scapus and pedicellus in lateral view; B, head capsule in posterior view; antennal musculature in dorsal (C) and ventral (D) views; mandibular and labial musculature in dorsal (E) and ventral (F) views; maxillary musculature in dorsal (G) and ventral (H) views; I, epi- and hypopharyngeal musculature, and muscles associated with cephalic section of alimentary tract in lateral view. Abbreviations: M1, M. tentorioscapalis anterior (0an1); M2, M. tentorioscapalis posterior (0an2); M4, M. tentorioscapalis medialis (0an4); M5, M. scapopedicellaris lateralis (0an6); M6, M. scapopedicellaris medialis (0an7); M7, M. labroepipharyngalis (0lb5); M9, M.

frontoepipharyngalis (0lb2); M11, M. craniomandibularis internus (0md1); M12, M. craniomandibularis externus (0md3); M15, M. craniocardinalis externus (0mx1); M17a, M17b, M. tentoriocardinalis (0mx3); M18, M. tentoriotipitalis (0mx4/0mx5); M19, M. craniolacinialis (0mx2); M21, M. stipitogalealis (0mx7); M22, M. stipitopalpalis externus (0mx8); M23, M. stipitopalpalis internus (0mx10); M26, M. palpopalpalis tertius (0mx14); M27, M. palpopalpalis quartus (0mx15); M28, M. submentopraementalis (0la8); M29, M. tentoriopraementalis (0la5); M30, M. tentoriopraementalis superior (0la6); M41, M. frontohypopharyngalis (0hy1); M43, M. clypeopalatalis (0ci1); M44, M. clypeobuccalis (0bu1); M45, M. frontobuccalis anterior (0bu2); M46, M. frontobuccalis posterior (0bu3); M48, M. tentoriobuccalis anterior (0bu5); M50, M. tentoriobuccalis posterior (0bu6); MmIII, Mm. compressores epipharyngis; mn, mentum; mnd, mandible; pd, pedicellus; ph, pharynx; sc, scapus; t, tentorium.

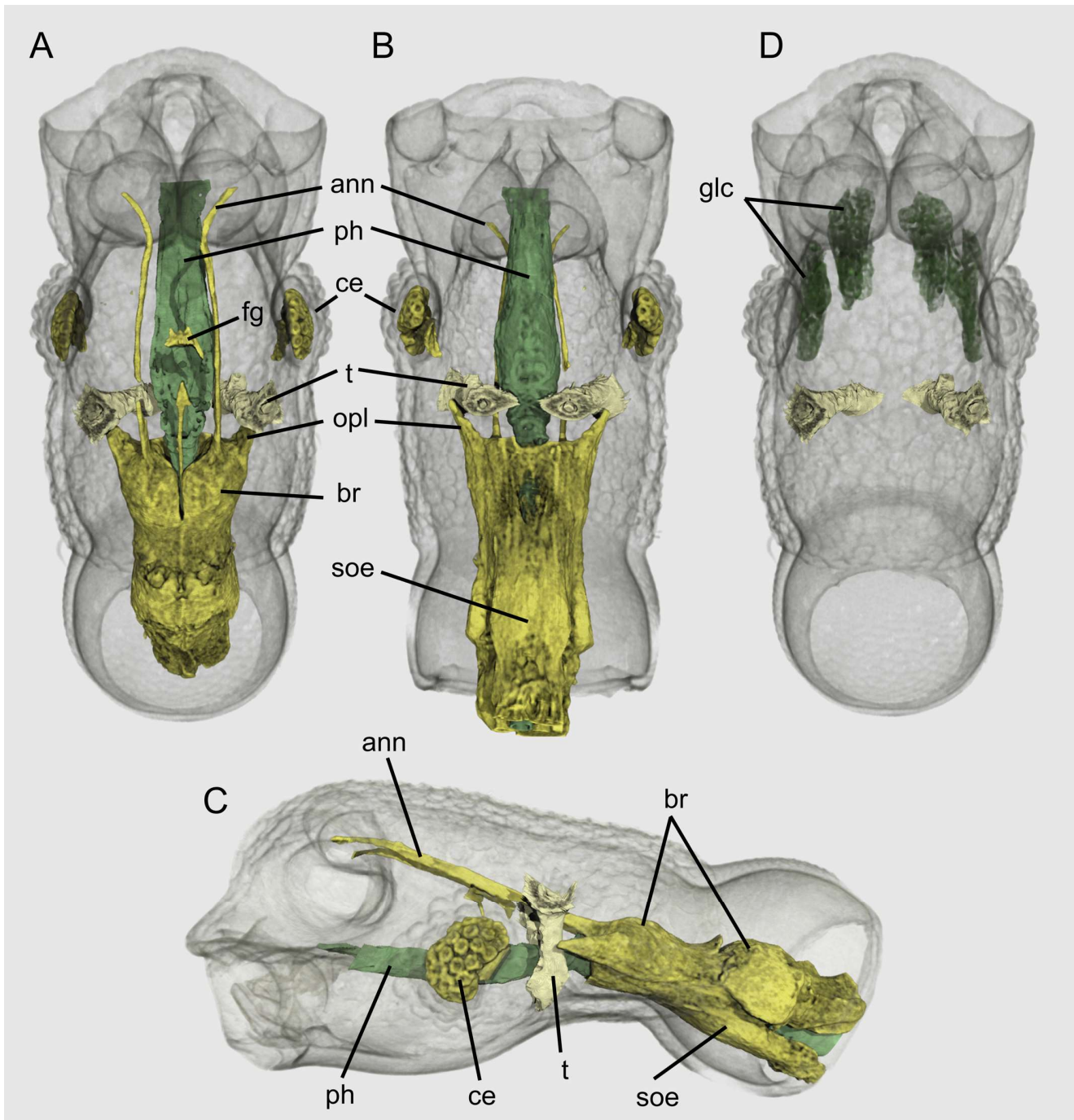


Figure 6. Head morphology of *Diartiger kubotai*, μ -CT reconstructions. Central nervous system and alimentary tract in dorsal (A), ventral (B), and lateral (C) views; D, cephalic glands in dorsal view. Abbreviations: ann, antennal nerve; br, brain; ce, compound eye; glc, glandular cluster; opl, optic lobe; ph, pharynx; soe, suboesophageal ganglion; t, tentorium.

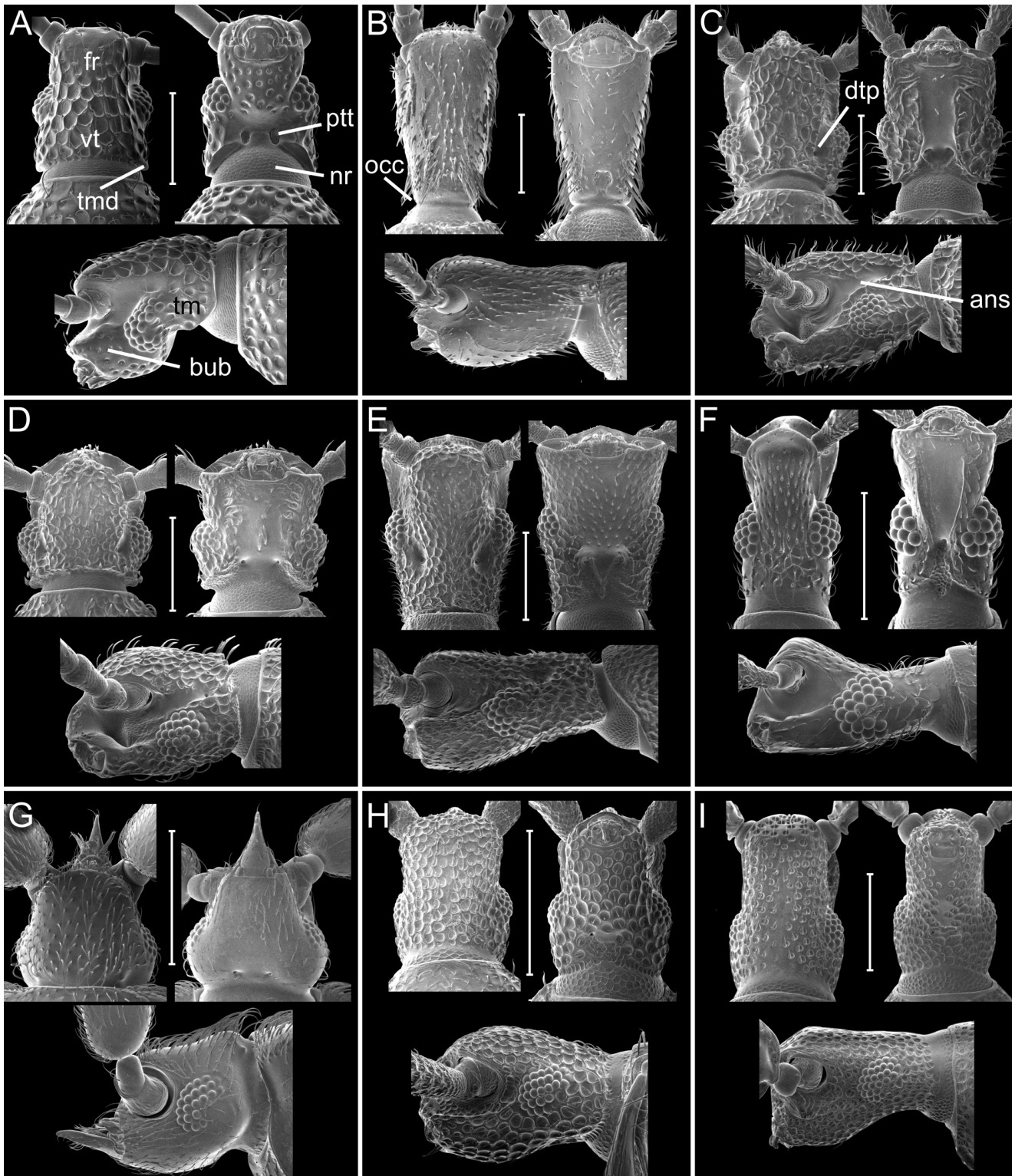


Figure 7. Heads of Clavigeritae, scanning electron micrographs, dorsal, ventral, and lateral views for each species. A, *Cerylambus reticulatus*; B, *Claviger longicornis*; C, *Novoclaviger gibbiventris*; D, *Pararticerus latus*; E, *Zuluclavodes brianaylori*; F, *Disarthricerus integer*; G, *Tiracaleda minuta*; H, *Tiracerus* sp.; I, *Tiraspirus tabulatus*. Abbreviations: ans, antennal sulcus; bub, buccal bulge; dtp, dorsal tentorial pit; fr, frons; nr, neck region; occ, occipital

constriction; ptt, posterior tentorial pit; tm, temple; tmd, temporal denticle; vt, vertex. Scale bars: 200 μm .

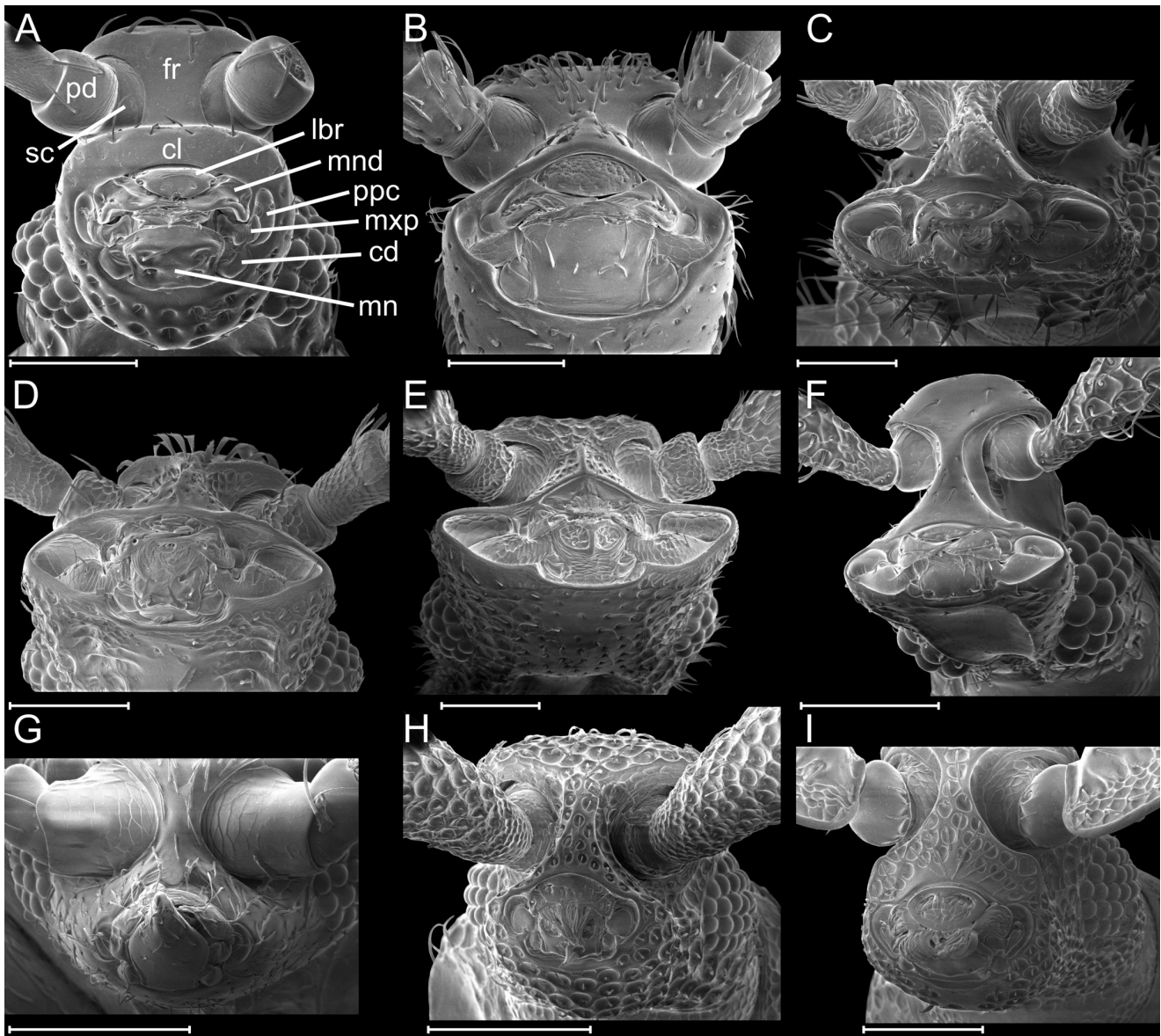


Figure 8. Heads of Clavigeritae, scanning electron micrographs, approximately anterior views. A, *Cerylambus reticulatus*; B, *Claviger longicornis*; C, *Novoclaviger gibbiventris*; D, *Pararticerus latus*; E, *Zuluclavodes briantaylori*; F, *Disarthricerus integer*; G, *Tiracaleda minuta*; H, *Tiracerus* sp.; I, *Tiraspirus tabulatus*. Abbreviations: cd, cardo; cl, clypeus; fr, frons; lbr, labrum; mn, mentum; mnd, mandible; mxp, maxillary palp; pc, palpal cavity; pd, pedicellus; sc, scapus. Scale bars: 100 μ m.

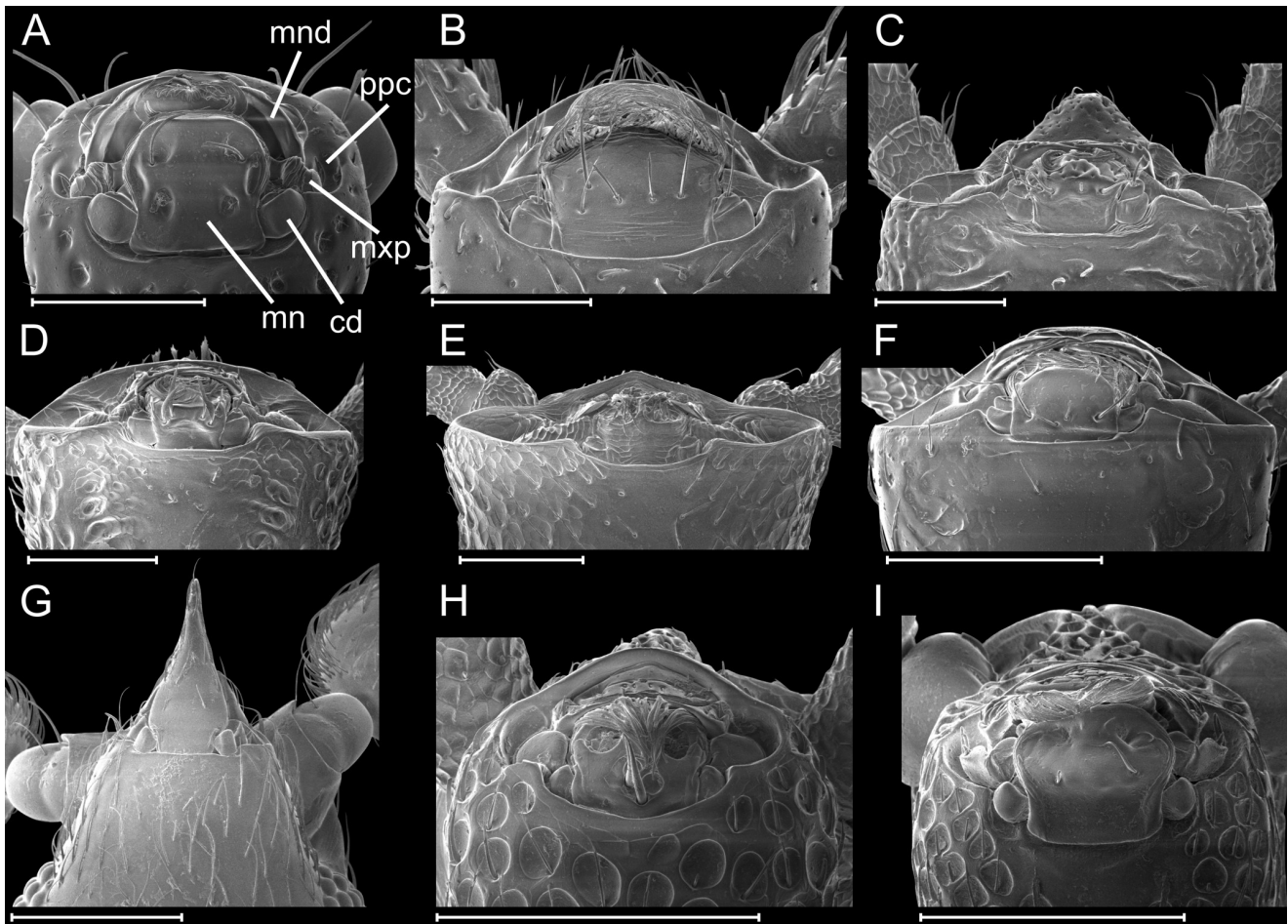


Figure 9. Heads of Clavigeritae, scanning electron micrographs, ventral views. A, *Cerylambus reticulatus*; B, *Claviger longicornis*; C, *Novoclaviger gibbiventris*, D, *Pararticerus latus*; E, *Zuluclavodes briantaylori*; F, *Disarthricerus integer*; G, *Tiracaleda minuta*; H, *Tiracerus* sp.; I, *Tiraspirus tabulatus*. Abbreviations: cd, cardo; mn, mentum; mnd, mandible; mxp, maxillary palp; pc, palpal cavity. Scale bars: 100 μ m.

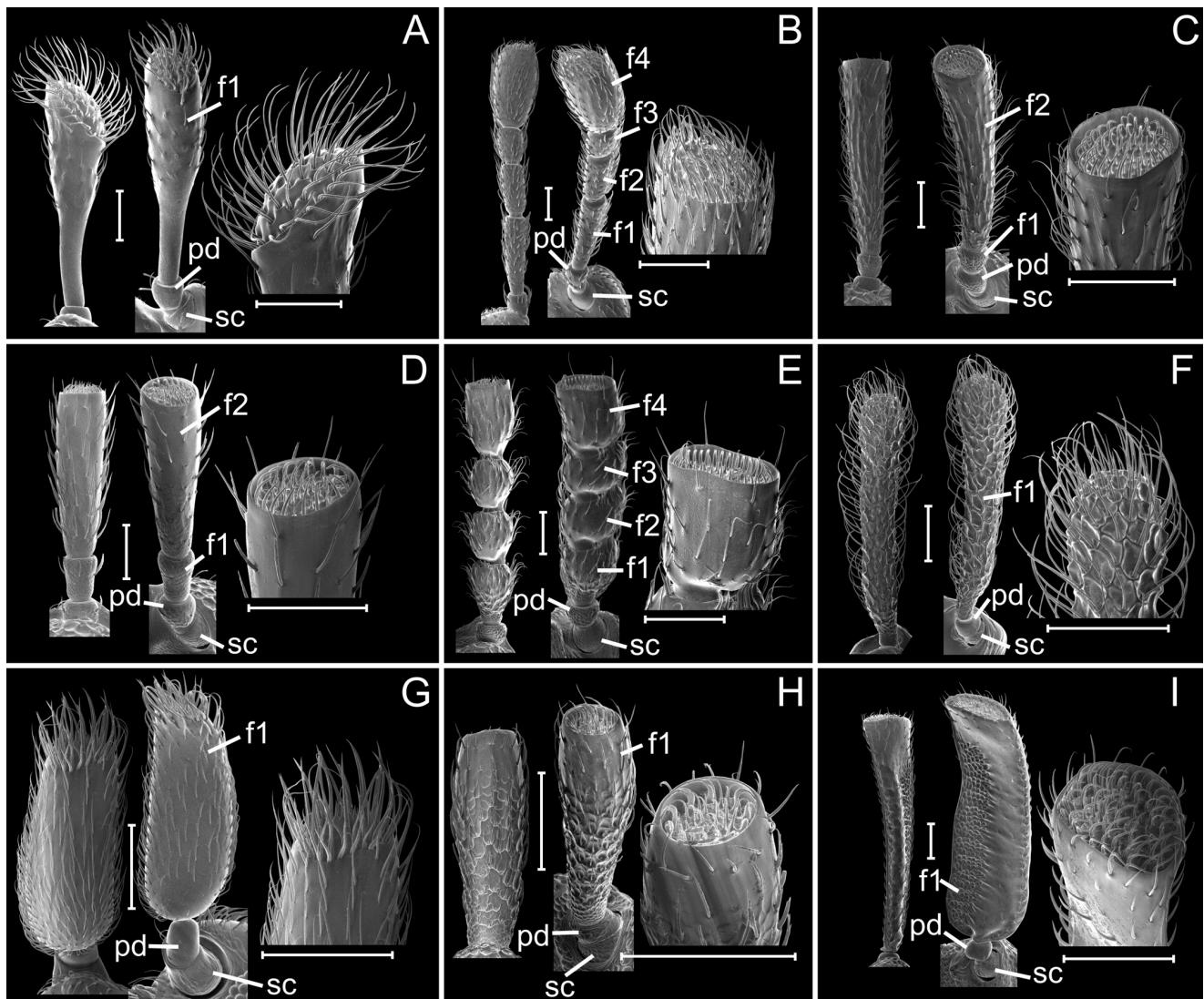


Figure 10. Antennae of Clavigeritae, scanning electron micrographs, in dorsal and external lateral view (whole antenna) and antennal apex is shown for each species. A, *Cerylambus reticulatus*; B, *Claviger longicornis*; C, *Novoclaviger gibbiventris*, D, *Pararticerus latus*; E, *Zuluclavodes briantaylori*; F, *Disarthricerus integer*; G, *Tiracaleda minuta*; H, *Tiracerus* sp.; I, *Tiraspirus tabulatus*. Abbreviations: f1-4, flagellomeres 1-4; pd, pedicellus; sc, scapus. Scale bars: 100 μm.

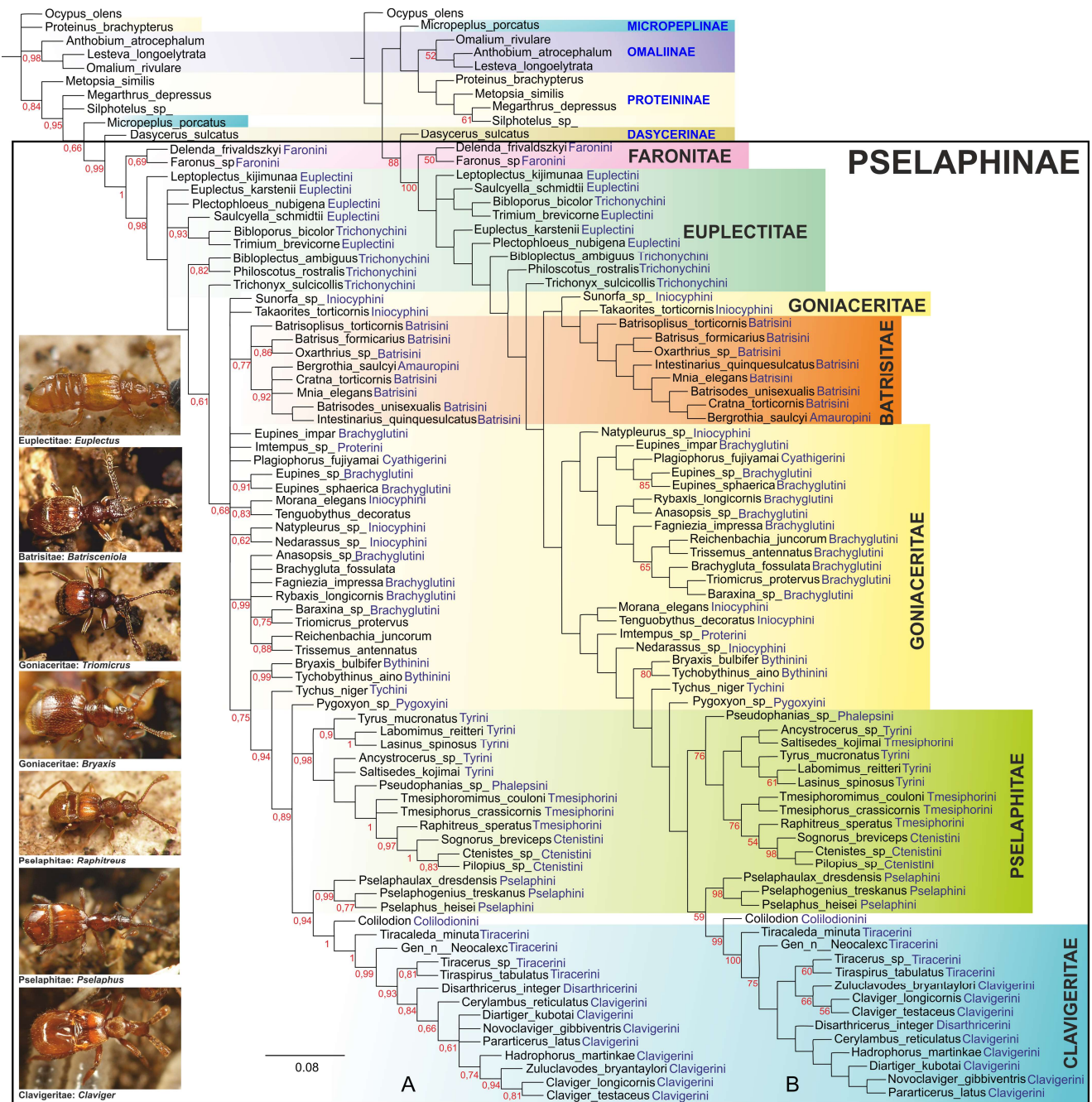


Figure 11. Results of phylogenetic analysis of Pselaphinae focused on cephalic characters. A, Consensus (50% majority rule) tree obtained in Bayesian analysis; posterior probability values higher than 0.5 given at nodes; B, strict consensus tree obtained in parsimony analysis, symmetric resampling support values higher than 50 given at nodes.

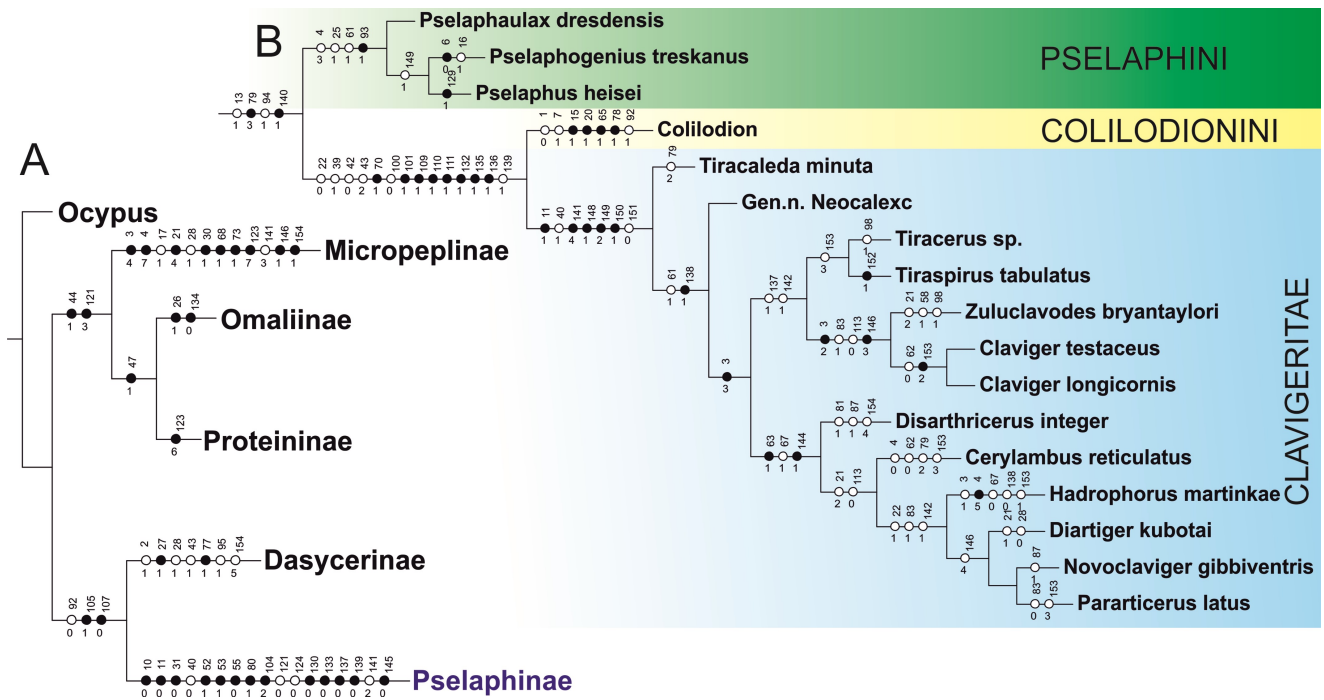


Figure 12. Results of the parsimony analysis of the phylogenetic relationships within Pselaphinae. One of two most parsimonious trees with unambiguously optimized character changes plotted along the internodes. A, characters supporting monophyly of Pselaphinae and sister outgroup; B, characters supporting monophyly of Clavigeritae and their sister-group relatives. Black circles indicate unique character changes; white circles indicate parallelisms or reversals; character numbers are above, character states below circles.

SUPPORTING INFORMATION

Appendix S1. Terminal taxa included in phylogenetic analysis of Pselaphinae based on cephalic exoskeletal structures.

Appendix S2. Characters and character states, with selected structures illustrated.

Appendix S3. Morphological data matrix for phylogenetic analysis of Pselaphinae based on cephalic exoskeletal characters.

Appendix S4. Character matrix in nexus format.

Appendix S5. Character matrix - script for MrBayes.

Figure S1. Heads of Clavigeritae, scanning electron micrographs, dorsal views. A, *Cerylambus reticulatus*; B, *Claviger longicornis*; C, *Novoclaviger gibbiventris*, D, *Pararticerus latus*; E, *Zuluclavodes briantaylori*; F, *Disarthricerus integer*; G, *Tiracaleda minuta*; H, *Tiracerus* sp.; I, *Tiraspirus tabulatus*.

Figure S2. Heads of Clavigeritae, scanning electron micrographs, ventral views. A, *Cerylambus reticulatus*; B, *Claviger longicornis*; C, *Novoclaviger gibbiventris*, D, *Pararticerus latus*; E, *Zuluclavodes briantaylori*; F, *Disarthricerus integer*; G, *Tiracaleda minuta*; H, *Tiracerus* sp.; I, *Tiraspirus tabulatus*.

Figure S3. Heads of Clavigeritae, scanning electron micrographs, lateral views. A, *Cerylambus reticulatus*; B, *Claviger longicornis*; C, *Novoclaviger gibbiventris*, D, *Pararticerus latus*; E, *Zuluclavodes briantaylori*; F, *Disarthricerus integer*; G, *Tiracaleda minuta*; H, *Tiracerus* sp.; I, *Tiraspirus tabulatus*.

Figure S4. Mouthparts of Clavigeritae, scanning electron micrographs, anterior view. A, *Cerylambus reticulatus*; B, *Claviger longicornis*; C, *Novoclaviger gibbiventris*, D, *Pararticerus latus*; E, *Zuluclavodes briantaylori*; F, *Disarthricerus integer*; G, *Tiracaleda minuta*; H, *Tiracerus* sp.; I, *Tiraspirus tabulatus*.

Figure S5. Mouthparts of Clavigeritae, scanning electron micrographs, anterior view, magnified. A, *Cerylambus reticulatus*; B, *Claviger longicornis*; C, *Novoclaviger gibbiventris*, D, *Pararticerus latus*; E, *Zuluclavodes briantaylori*; F, *Disarthricerus integer*; G, *Tiracaleda minuta*; H, *Tiracerus* sp.; I, *Tiraspirus tabulatus*. Abbreviations: glo, glandular opening; lbr, labrum; mn, mentum; mnd, mandible.

Figure S6. Unusual sexual dimorphism in *Tiracaleda minuta*, scanning electron micrographs. A, head of male in lateral view; B, head of female in lateral view; C. mouthparts of male in dorsal view; D. mouthparts of male in lateral view. Abbreviations: lac, lacinia; lbr, labrum; mn, hypertrophied mentum; mnd, mandible.

Figure S7. Antennal apices of Clavigeritae, scanning electron micrographs. A, *Cerylambus reticulatus*; B, *Claviger longicornis*; C, *Novoclaviger gibbiventris*, D, *Pararticerus latus*; E, *Zuluclavodes briantaylori*; F, *Disarthricerus integer*; G, *Tiracaleda minuta*; H, *Tiracerus* sp.; I, *Tiraspirus tabulatus*.

Figure S8. Comparison of head musculature in four species of Pselaphinae, lateral view; μ -CT reconstructions. A, *Claviger testaceus* (Clavigeritae); B, *Diartiger kubotai* (Clavigeritae); C, *Pselaphus heisei* (Pselaphitae); *Bergrothia saulcyi* (Batrisitae). Abbreviations: M7, M. labroepipharyngalis (0lb5); M9, M. frontoepipharyngalis (0lb2); M28, M. submentopraementalis (0la8); M29, M. tentoriopraementalis (0la5); M30, M. tentoriopraementalis superior (0la6); M41, M. frontohypopharyngalis (0hy1); M43, M. clypeopalatalis (0ci1); M44, M. clypeobuccalis (0bu1); M45, M. frontobuccalis anterior (0bu2); M46, M. frontobuccalis posterior (0bu3); M48, M. tentoriobuccalis anterior (0bu5); M50, M. tentoriobuccalis posterior (0bu6); MmIII, Mm. compressores epipharyngis; p, pharynx; t, tentorium.

3.6 Study VI

The thoracic morphology of the troglobiontic cholevine species *Troglocharinus ferreri* (Coleoptera, Leiodidae)

Xiao-Zhu Luo, Caio Antunes-Carvalho, Ignacio Ribera, Rolf Georg Beutel

2019. *Arthropod Struct. Dev.* 53, 100900. <https://doi.org/10.1016/j.asd.2019.100900>

Abstract: The thoracic morphology of the troglobiontic leiodid species *Troglocharinus ferreri* (Cholevinae, Leptodirini) is described and documented in detail. The features are mainly discussed with respect to modifications linked with subterranean habits. *Troglocharinus* is assigned to the moderately modified pholeuonoid morphotype. The body is elongated and slender compared to epigeic leiodids and also cave-dwelling species of Ptomaphagini. The legs are elongated, especially the hindlegs, though to a lesser degree than in the most advanced troglobiontic species. The prothorax is moderately elongated but otherwise largely unmodified. Its muscular system is strongly developed, with more muscle bundles than in free-living staphylinoid or hydrophiloid species. The pterothorax is greatly modified, especially the metathoracic flight apparatus. The meso- and metathoracic elements of the elytral locking device are well-developed, whereas the other notal parts are largely reduced. The mesonotum is simplified, with the triangular scutellar shield as the only distinctly developed part. The mesothoracic musculature is strongly reduced, with only 6 muscles compared to 12 or 13 in free-living staphylinoid or hydrophiloid species. The metanotum is greatly reduced, without a recognizable subdivision into prescutum, scutum and scutellum. It is strongly narrowing laterally and lacks notal wing processes and other wing-related elements, but well-developed alacristae are present. The wings are reduced to small membranous flap-like structures inserted at the posterior end of the metanotum. A metapostnotum is not developed. Like in the case of the head, cave dwelling species of the related Ptomaphagini and Leptodirini show different trends of adaptations, with a compact ovoid or navicular body shape in the former, and a distinct trend towards elongation of the body and appendages in the latter tribe. Structural affinities of the thoraces of *T. ferreri* and the troglobiontic trechine carabid *Sinaphaenops wangorum* are mainly due to the reduced flight apparatus. The degree of muscle reduction in the pterothorax is very similar in both species.

Conceptualization: X.Z. Luo, C. Antunes-Carvalho, I. Ribera, R. G. Beutel

Visualization: X.Z. Luo, R. G. Beutel

Writing-original draft: X.Z. Luo, R. G. Beutel

Writing-review & editing: X.Z. Luo, C. Antunes-Carvalho, I. Ribera, R. G. Beutel

Funding acquisition: X.Z. Luo, I. Ribera

Estimated own contribution: 75%



The thoracic morphology of the troglobiontic cholevine species *Troglocharinus ferreri* (Coleoptera, Leiodidae)

Xiao-Zhu Luo^{a, b, *}, Caio Antunes-Carvalho^c, Ignacio Ribera^b, Rolf Georg Beutel^a

^a Institut für Zoologie und Evolutionsforschung, Friedrich-Schiller-Universität Jena, Erbertstrasse 1, 07743 Jena, Germany

^b Institut de Biologia Evolutiva (CSIC-Universitat Pompeu Fabra), Passeig Marítim de la Barceloneta 37-49, 08003 Barcelona, Spain

^c Departamento de Biologia Geral, Instituto de Biologia, Universidade Federal Fluminense, Outeiro de São João Batista, s/n Centro, 24020-141 Niterói, Brazil

ARTICLE INFO

Article history:

Received 4 August 2019

Received in revised form

15 October 2019

Accepted 18 October 2019

Keywords:

Subterranean beetle

Thoracic anatomy

3D-reconstruction

Micro-CT

Troglocharinus

ABSTRACT

The thoracic morphology of the troglobiontic leiodid species *Troglocharinus ferreri* (Cholevinae, Leptodirini) is described and documented in detail. The features are mainly discussed with respect to modifications linked with subterranean habits. *Troglocharinus* is assigned to the moderately modified pholeuonoid morphotype. The body is elongated and slender compared to epigeal leiodids and also cave-dwelling species of Ptomaphagini. The legs are elongated, especially the hindlegs, though to a lesser degree than in the most advanced troglobiontic species. The prothorax is moderately elongated but otherwise largely unmodified. Its muscular system is strongly developed, with more muscle bundles than in free-living staphylinoid or hydrophiloid species. The pterothorax is greatly modified, especially the metathoracic flight apparatus. The meso- and metathoracic elements of the elytral locking device are well-developed, whereas the other notal parts are largely reduced. The mesonotum is simplified, with the triangular scutellar shield as the only distinctly developed part. The mesothoracic musculature is strongly reduced, with only 6 muscles compared to 12 or 13 in free-living staphylinoid or hydrophiloid species. The metanotum is greatly reduced, without a recognizable subdivision into prescutum scutum and scutellum. It is strongly narrowing laterally and lacks notal wing processes and other wing-related elements, but well-developed alacristae are present. The wings are reduced to small membranous flap-like structures inserted at the posterior end of the metanotum. A metapostnotum is not developed. Like in the case of the head, cave dwelling species of the related Ptomaphagini and Leptodirini show different trends of adaptations, with a compact ovoid or navicular body shape in the former, and a distinct trend towards elongation of the body and appendages in the latter tribe. Structural affinities of the thoraces of *T. ferreri* and the troglobiontic trechine carabid *Sinaphaenops wangorum* are mainly due to the reduced flight apparatus. The degree of muscle reduction in the pterothorax is very similar in both species.

© 2019 Elsevier Ltd. All rights reserved.

1. Introduction

As pointed out by Newton (2016), Leiodidae is the second largest family of the polyphagan superfamily Staphylinoidea, with about 4135 described species, 374 genera, six subfamilies, and a worldwide distribution (with the exception of Antarctica). After the adepagan Carabidae, Leiodidae represents the second largest subterranean radiation in Coleoptera, comprising about 30% of the currently known cave beetles (Moldovan, 2012). *Troglocharinus ferreri* (Reitter, 1908), the species in the focus of the present study, is

included in Leptodirini, a tribe of Cholevinae with ca. 930 species and 195 genera (Kilian and Newton, 2017), and one of the most successful radiations of beetles in subterranean environments (e.g., Fresneda et al., 2007, 2011; Luo et al., 2019). The genus contains 18 species and 19 subspecies, all of them adapted to subterranean habitats (Salgado et al., 2008; Rizzo and Comas, 2015; Luo et al., 2019).

Even though Leiodidae are generally a well-studied group (e.g. Jeannel, 1911, 1936, 1958; Fresneda et al., 2007, 2011; Antunes-Carvalho et al., 2019; see also Newton [1998, 2016] for an overview), internal features, especially soft parts, are almost completely unknown, and not even covered in the monumental works of R. Jeannel. The cephalic anatomy of the unspecialized *Catops ventricosus* (Weise, 1877) and the troglobiontic *T. ferreri* was described recently by Antunes-Carvalho et al. (2017) and Luo et al. (2019),

* Corresponding author. Institut für Zoologie und Evolutionsforschung, Friedrich-Schiller-Universität Jena, Erbertstrasse 1, 07743 Jena, Germany.

E-mail address: xiaozhu.luo@uni-jena.de (X.-Z. Luo).

respectively. However, a detailed study of the thoracic anatomy of any species of the family was so far unavailable. This lack of information induced us to study and document external and internal thoracic structures of *T. ferreri* in the framework of a project on morphological adaptations in cave dwelling beetles (Luo et al., 2018a,b, 2019). The features observed in *T. ferreri* are compared to conditions found in other cave-dwelling and epigeal leiodid species (e.g. Jeannel, 1911, 1936; 1958; Peck, 1986; Fresneda et al., 2011; Newton, 2016; Njunjić, 2016), in epigeal representatives of other staphyliniform families (Larsén, 1966; Beutel and Komarek, 2004; Yavorskaya et al., 2019), and in the troglobiontic trechine carabid *Sinaphaenops wangorum* Ueno et Ran 1998 (Luo et al., 2018a,b). Evolutionary tendencies in Leiodidae, especially in Ptomaphagini and Leptodirini, are discussed, and also general trends linked with subterranean habits in Coleoptera.

2. Materials and methods

2.1. Studied species

Specimens of *T. ferreri* (Cholevinae) were collected by J. Pastor in the Avenc d'en Roca, Cervelló, Barcelona, Spain (22 April 2013). All individuals used in this study were preserved in 100% ethanol. Additionally, specimens of *Zearagytodes maculifer* (Broun, 1880) (Camiarinae) were dissected and used for microtome sectioning. They were collected at Trounson Kauri Park (New Zealand) by R. Leschen in 1997 (ex. *Ganoderma applanata*).

2.2. Micro-computed tomography (micro-CT) and microtome sections

Specimens were transferred to acetone and then dried at the critical point (Emitech K850, Quorum Technologies Ltd., Ashford, UK). One dried specimen was scanned at FSU Jena, Germany with a SkyScan 2211 micro-CT (Bruker, Knotich, Belgium) with the following parameters: 80 kV voltage, 300 μ A current, 3000 ms exposure time, 2400 projections over 360° (rotation steps of 0.20°), frame averaging on, random movement off, and filter assembly open with 0.5 mm Cu. Projections were reconstructed by NRecon (Bruker, Knotich, Belgium) into JPG files with a voxel size of 0.9 μ m. The CT-scan is stored in the collection of the Phyletisches Museum Jena. Amira 6.1.1 (Thermo Fisher Scientific, Waltham, USA) and VG studio Max 2.0.5 (Volume Graphics, Heidelberg, Germany) were used for the three-dimensional reconstruction and volume rendering.

For microtome sectioning, one specimen of *T. ferreri* was embedded in araldite CY 212® (Agar Scientific, Stansted/Essex, UK). Sections were cut at 1 μ m using a microtome HM 360 (Microm, Walldorf, Germany) equipped with a glass knife, and stained with toluidine blue and pyronin G (Waldeck GmbH and Co.KG/Division Chroma, Münster, Germany). The section series is stored in the collection of the Phyletisches Museum.

2.3. Light and scanning electron microscopy

To clean specimens we followed the protocol of Schneberg et al. (2017): transfer from 100% ethanol into 70% ethanol; from this to 5% KOH, then glacial acetic acid, distilled water (Aqua dest.), and finally 70% ethanol. Subsequently, they were dehydrated and dried in an Emitech K850 critical point dryer. A Keyence VHX-1000C digital microscope (Keyence Corporation, Osaka, Japan) was used for photographs with different depths of field (z-stacking). After this they were assembled to a single sharp image with Helicon Focus (Helicon Soft Ltd., Kharkov, Ukraine). Prior to scanning electron microscopy (SEM), samples were sputter-coated with

gold (Emitech K500; Quorum Technologies Ltd., Ashford, UK) and attached to a rotatable specimen holder (Pohl, 2010). SEM observation and imaging was performed with an FEI (Philips) XL 30 ESEM at 10 kV. Final figure plates were assembled and arranged with Adobe Photoshop CC and Illustrator CS6 (Adobe Inc., California, USA).

2.4. Terminology

Thoracic muscles were designated following Larsén (1966), but the muscular terms introduced by Friedrich and Beutel (2008) (see also Beutel et al., [2014]) were added. Different nomenclatures for thoracic muscles were compared and aligned by Friedrich et al. (2009).

3. Results

3.1. General appearance (Fig. 1)

Postcephalic body elongate and slender. Ratio length from anterior pronotal edge to abdominal tip versus maximum width at anterior third of elytra 2.5:1. Forelegs almost as long as postcephalic body, midlegs ca. 10% longer, hindlegs distinctly longer. Coloration light brown. Surface of exposed parts with dense vestiture of very short adpressed setae.

3.2. Prothorax

A pair of distinct boomerang-shaped cervical sclerites is embedded in the cervical membrane ventrolaterally; the wide anterior portion forms a sharp angle with the narrow posterior part. A distinct articulation with the prothorax is missing. The prothorax is moderately elongated, ca. 0.35 times as long as the postcephalic body. The pronotum (n1, Figs. 1–3) is wider than long, with a length/maximum width ratio of 0.72. It is rounded laterally, converging towards the anterior margin, and also converging posteriorly after reaching the maximum width in the middle region, and then again diverging towards the hind margin. It appears evenly convex, without an explanate lateral margin, but with a distinct lateral edge, which appears sinuate in lateral and dorsal view. The anterolateral angles are indistinct; the anterior pronotal edge is slightly concave laterally and slightly convex in the middle region; the anterior collar enclosing the occipital region of the head is narrow; a distinct but narrow bead is present along the anterior pronotal margin and also along the lateral edge. The posterolateral pronotal edges form an angle of less than 90° and slightly rounded apically. An indistinct bead is present along the very slightly concave posterior pronotal margin. The dorsal pronotal surface bears a very dense and regular vestiture of short seta, and a fine microreticulation; long setae, deep grooves, punctures and other surface modifications are absent. The hypomeron (hy, Figs. 1B, C; 3C, E) is broad; it appears bulging anteriorly and concave posteriorly; the surface of the anterior region is sparsely covered with setae whereas the posterior part is glabrous; a deep transverse incision is present at the lateral procoxal margin; posteromesally the hypomeron is continuous with the sclerotized inner surface of the procoxal cavity.

The very short prosternal area (pst, Figs. 1B and 3C) anterior to the procoxal cavity bears a narrow bead along the slightly concave anterior margin. The almost straight notosternal suture reaches about half-length of the segment. A short curved ridge is present anterad the anterolateral edge of the procoxa. Posterolaterally the prosternum reaches the hypomeral incision. The prosternal process (psp, Fig. 1B) is only present as a short triangular projection between the anterior third of the procoxae; it is posteriorly

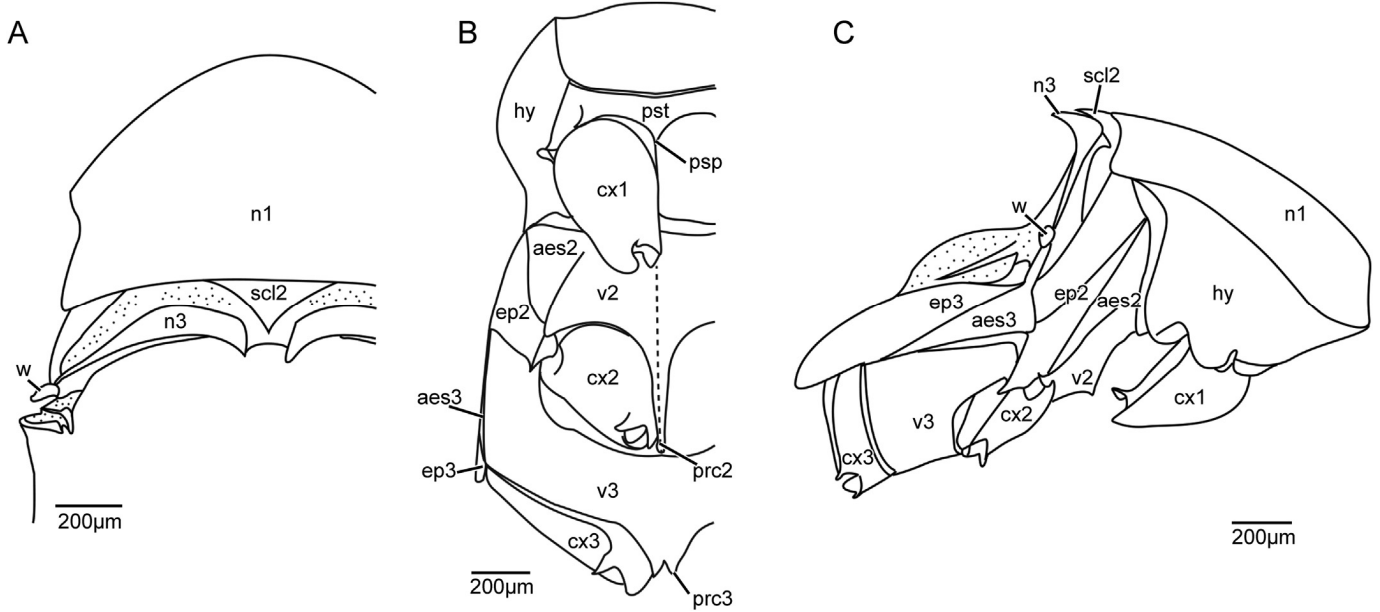


Fig. 1. Line-drawings of *Troglacharinus ferreri*. (A) dorsal view; (B) ventral view; (C) lateral view. Abbreviations: aest2/3, mes-/metanepisternum; cx1/2/3, pro-/meso-/metacoxa; ep2/3, mes-/metepimeron; hy, hypomeron; n1/3, pro-/metanotum; prc2/3, process of meso-/metaventrite; pst, prosternum; scl2, mesoscutellar shield; v2/3, meso-/metaventrite; w, wing.

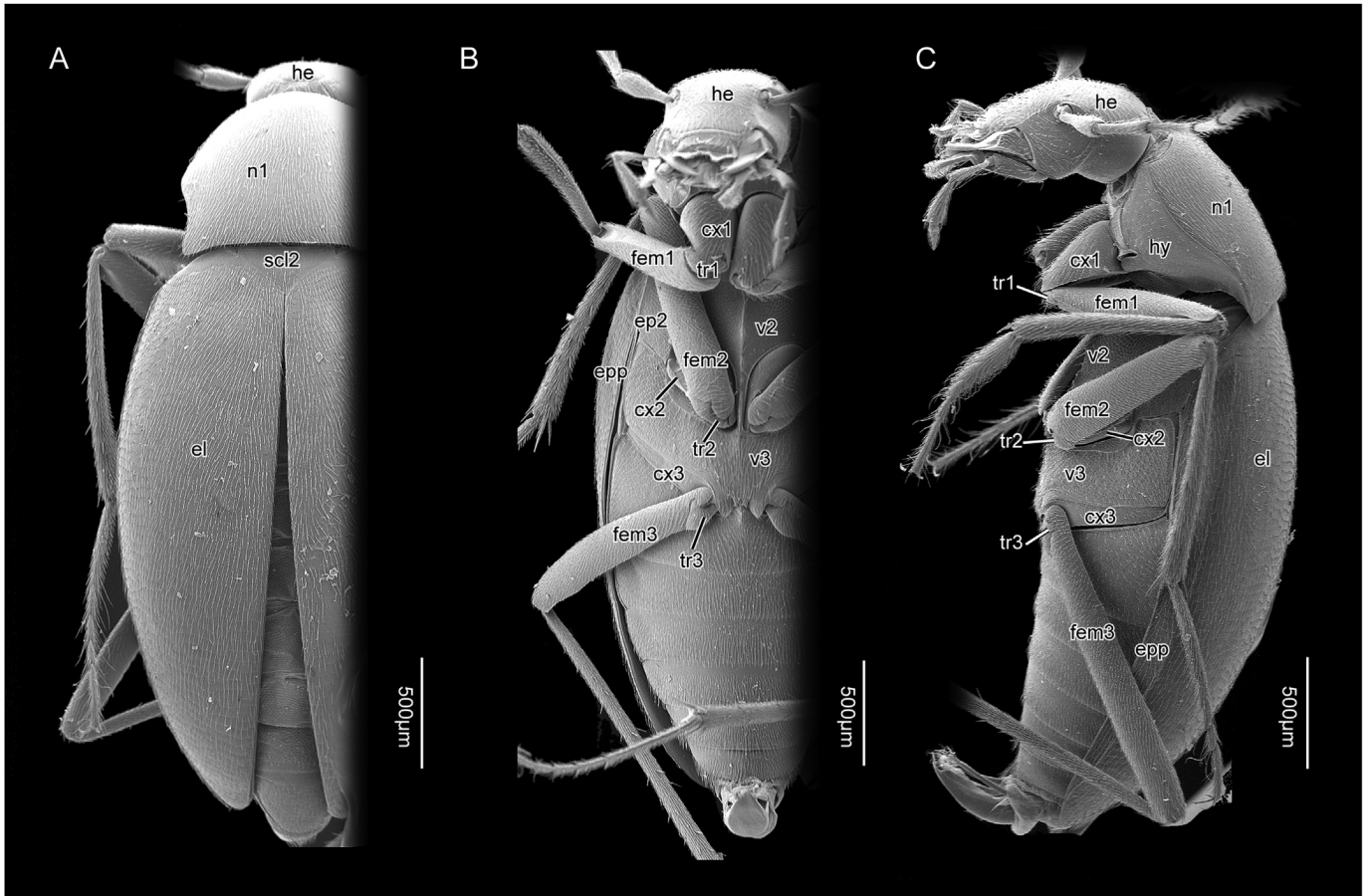


Fig. 2. Scanning electron micrographs of *T. ferreri*. (A) dorsal view; (B) ventral view; (C) lateral view. Abbreviations: cx1/2/3, pro-/meso-/metacoxa; el, elytron; ep2, mesepimeron; epp, epipleuron; fem1/2/3, pro-/meso-/metathoracic femur; he, head; n1, pronotum; scl2, mesoscutellar shield; tr1/2/3, pro-/meso-/metathoracic trochanter; v2/3, meso-/metaventrite.

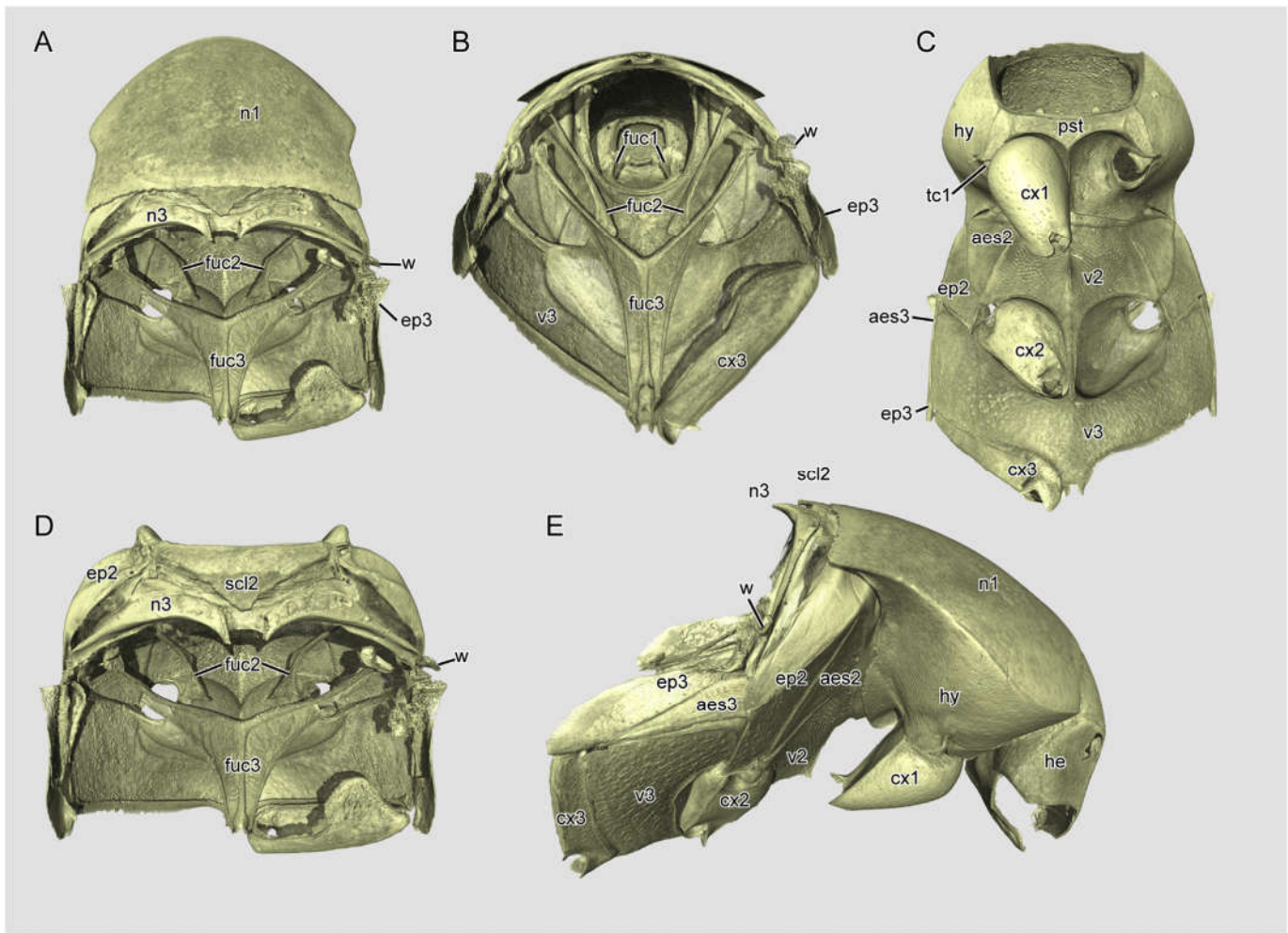


Fig. 3. Three-dimensional reconstructions of *T. ferreri* thorax. (A) dorsal view; (B) posterior view; (C) ventral view; (D) dorsal view (prothorax removed); (E) lateral view. Abbreviations: aest2/3, mes-/metanepisternum; cx1/2/3, pro-/meso-/metacoxa; ep2/3, mes-/metepimeron; fuc1/2/3, pro-/meso-/metafurca; hy, hypomeron; n1/3, pro-/metanotum; pst, prosternum; scl2, mesoscutellar shield; tc1, protrochantin; v2/3, meso-/metaventrite; w, wing.

continuous with a sharp median edge separating the uniperforated procoxal cavities, which are externally closed by hypomeral processes medially connected behind the procoxae; the postcoxal bridge bears a small posteromedian notch.

The distal part of the protrochantin (tc1, Fig. 3C) is partly exposed in the hypomeral incision, whereas its proximal part is concealed and fused with the cryptopleuron. The broad plate-like cryptopleuron is located anterolaterally inside the prothorax and is not fused with the notum. The short and thin plate-like profurcae (fuc1, Fig. 3B) are separated from each other basally and form an angle of nearly 90° with the prosternum. A spina is not present.

The forelegs are about 0.7 times as long as the total body length. The femur/tibia/tarsus ratio is 1.4/1.2/1. The conical procoxae (cx1, Figs. 1B, C; 2B, C; 3C, E) are very prominent and project beyond the posterior prosternal margin in ventral view; the slightly concave posterior surface is separated from the convex main part of the coxa by a distinct edge. The small trochanter (tr1, Fig. 2B, C) is approximately spindle-shaped, with a proximal condylar part articulating with the coxa. The femur (fem1, Figs. 2B, C; 4A) fits into the concavity formed by the posterior procoxal surface and the posterior surface of the hypomeron; it is club-shaped, fairly broad proximally and slightly narrowing towards its apex, which almost reaches the posterior pronotal angle; the anterior surface opposed to the tibia is slightly concave. The cylindrical tibia (tib1, Fig. 4A) is slightly

widening distally and distinctly curved; a row of spines is present along the distal half of its inner margin; the tibial apex bears an irregular crown of spines; the two apical spurs are multi-toothed laterally but lack minute spines. The protarsus (tar1, Fig. 4A) consists of 5 tarsomeres in males (ptm 1–5, Fig. 4D) and only 4 tarsomeres in females (ptm 1–4, Fig. 4E); an adhesive sole with a dense vestiture of tenent setae is present on the ventral surface of the slightly broadened tarsomeres 1–4 of males. Small pore plates are present on the dorsolateral surface of the terminal tarsomere. The protarsus bears a pair of well-developed, flattened curved claws with smooth surface and acute apices; only a single long empodial seta is visible (i.e. the inner one), although a cryptic outer seta is also present. A dense vestiture of very short setae is present on the entire surface of all three pairs of legs.

Musculature (Fig. 5): M1 (M. pronoti primus), O (=origin): posterior part of notum, I (=insertion): dorsolateral part of post-occipital ridge; M2 (M. pronoti secundus), O: lateral area of reduced first phragma, I: dorsolateral part of postoccipital ridge; M4 (M. pronoti quartus), O: anterolateral corner of mesonotum, I: middle-posterior pronotal area; M5 (M. prosterni primus), O: profurcal arm, I: posterior end of cephalic gular ridge; M6 (M. prosterni secundus), O: profurcal arm, I: ventrolateral part of postoccipital ridge; M7 (M. dorsoventralis primus), O: anterior pronotal region, posterior to M9, I: cervical sclerite; M8 (M.

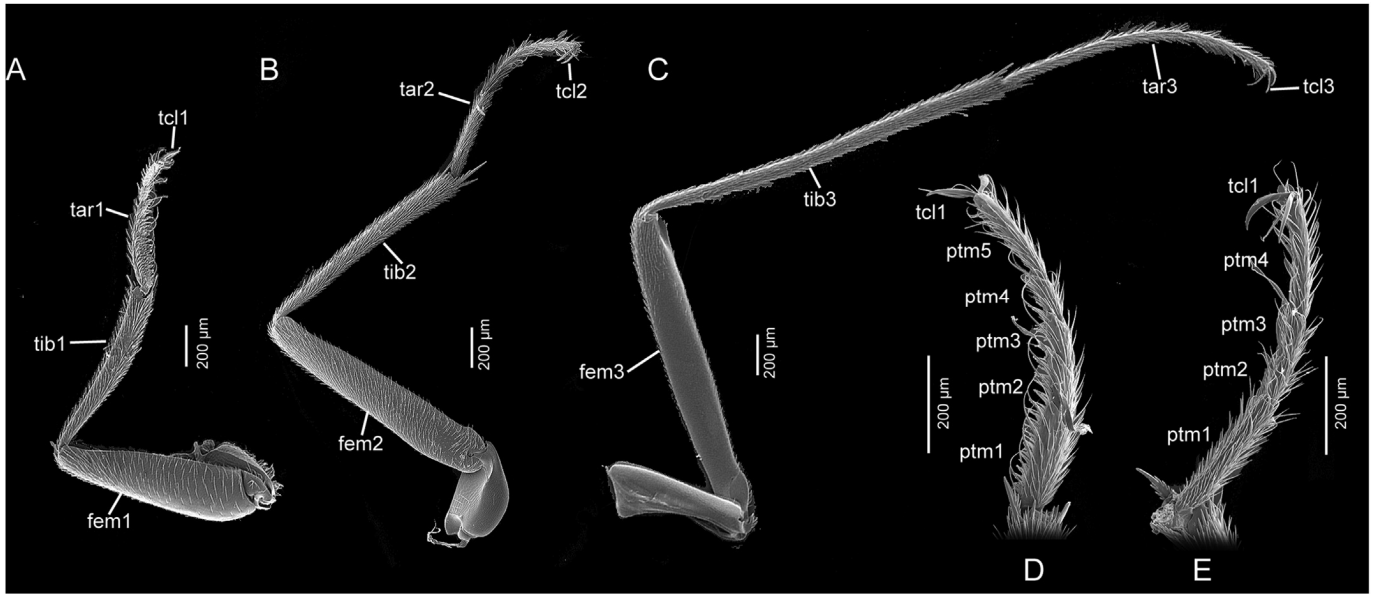


Fig. 4. Scanning electron micrographs, legs of *T. ferreri*. (A) foreleg; (B) midleg; (C) hindleg; (D) protarsus of male individual; (E) protarsus of female individual. Abbreviations: fem1/2/3, pro-/meso-/metafemur; ptm1-5, protarsomere 1-5; tar1/2/3, pro-/meso-/metatarsus; tcl1/2/3, pro-/meso-/metatarsal claw; tib1/2/3, pro-/meso-/metatibia.

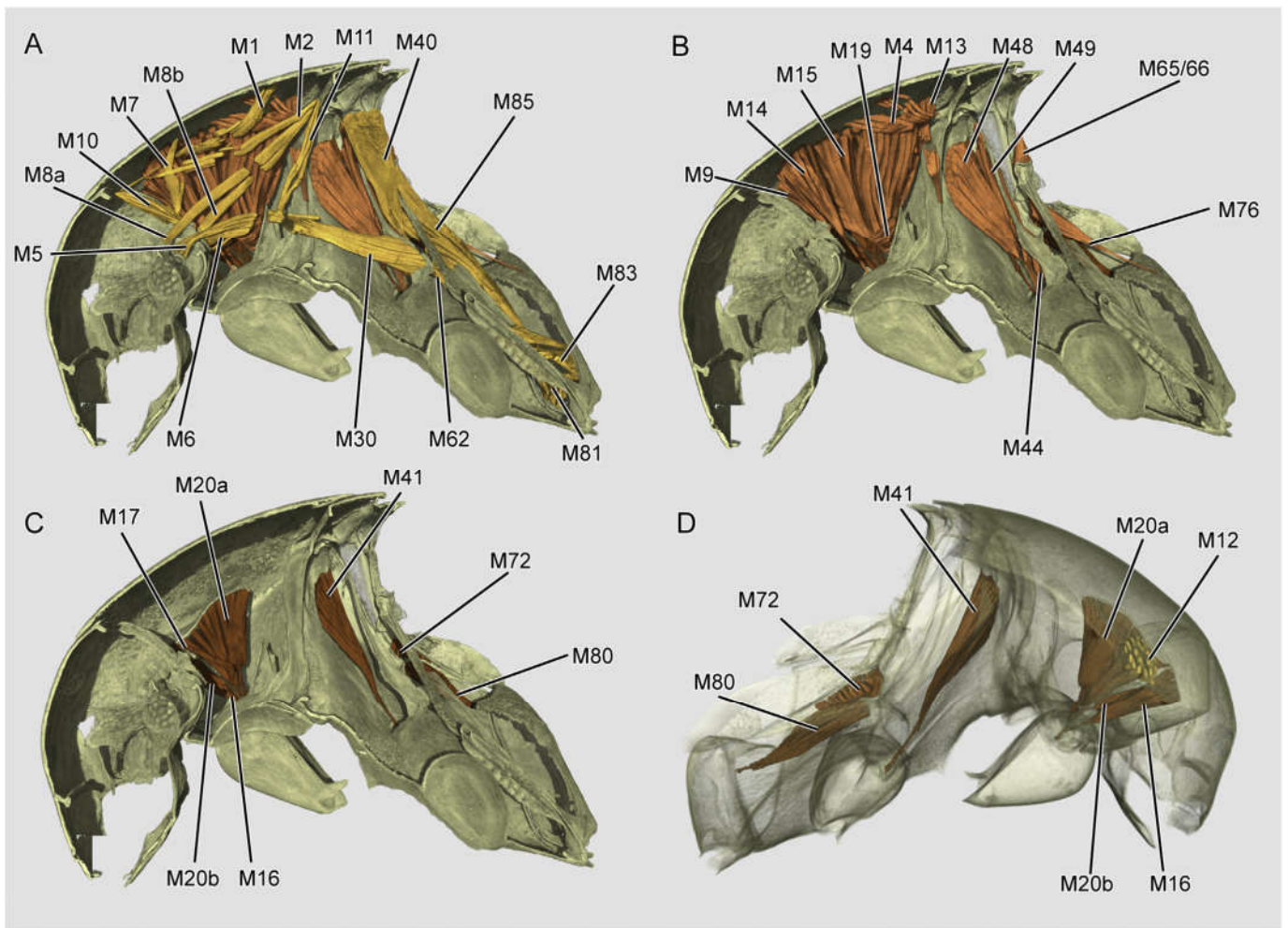


Fig. 5. Three-dimensional reconstructions of thoracic muscles of *T. ferreri*. (A)–(C) mesal view; (D) lateral view. See text for muscle abbreviations.

dorsoventralis secundus): M8a, O: anterolateral corner of mesonotum, I: posterior end of gular ridge; M8b, O: anterolateral corner of mesonotum, I: ventrolateral part of postoccipital ridge; M9 (M. dorsoventralis tertius), O: anterior part of mesonotum, I: cervical sclerite; M10 (M. dorsoventralis quartus), flat bundles, O: anterior part of prosternum, I: dorsal part of postoccipital ridge; M11 (M. dorsoventralis quintus), O: anterolateral corner of mesonotum, I: profurcal arm; M12 (M. noto-pleuralis), O: lateral pronotal margin, I: apical part of cryptopleural ridge; M13 (M. pronotomesepisternalis), O: posterior part of the pronotum, I: intersegmental membrane anterad mesanepisternum; M14 (M. noto-trochantinalis), O: anterior pronotal region, I: trochantin; M15 (M. noto-coxalis), O: large mesonotal area, from anterior to posterior region, I: posterior coxal process; M16 (M. episterno-coxalis), O: anterior part of cryptopleuron, I: lateral rim of coxa; M17 (M. epimero-coxalis), O: anterior part of cryptopleuron, mesad origin of M16, I: tendon shared with M15 and M19, attached to posterior coxal process; M19 (M. furca-coxalis), O: lateral surface of furcal arm, I: tendon shared with M14 and M15, attached to posterior coxal process; M20 (M. pleura-trochanteralis): M20a, O: posterior portion of apical plate of cryptopleuron, I: trochanteral tendon; M20b, O: anterior to M16, I: trochanteral tendon.

3.3. Mesothorax

The mesonotum, which is partly covered by the posterior pronotum, is distinctly simplified. It is formed by the large triangular scutellar shield and a narrow transverse sclerotized stripe anterior to it, presumably homologous with the mesoscutum; the separating line between these two areas is very distinct laterally but obsolete medially. Other scutal or scutellar parts are not recognizable as defined sclerotized elements. The scutellar shield (scl2, Figs. 1A, C; 2A; 3D, E; 6A, C) is exposed between the elytral bases and the posterior pronotal margin; very short setae are densely arranged on most of its surface but the anterior third is glabrous. The anterior mesonotal edge is straight; a transverse sclerotized stripe is well-developed laterally but indistinct medially. Several short setae are inserted in the anterolateral corner of the scutellar region, where a shallow impression is visible. The lateral mesonotal margins are almost straight and form a nearly right angle with the anterior edge. Lateral notal processes are not recognizable. The elements of the elytral articulation are minute.

The anterior margin of the mesoventrite (v2, Figs. 1B, C; 2B-C; 3C, E; 6B, C) is on a slightly higher level than the prothoracic postcoxal bridge. A broad transverse collar (tvc, Fig. 6B, C) is present

along the anteroventral edge of the segment; a few short setae and a shallow impression are present anterolaterally; a low ridge divides the collar medially, and two transverse long anterior impressions are present laterad this longitudinal structure. In lateral view, the mesoventrite appears steeply descending posterior to the collar but horizontal posteriorly; a sharp projection is present between both regions, part of a narrow but distinct median longitudinal carina, which extends posteriorly to form an elongate process separating the mesocoxal cavities; the rounded tip of the process (prc2, Fig. 1B; 6B) projects slightly beyond the posterior coxal edge and overlaps with the anteriormost metaventrite. The nearly straight mesothoracic anapleural suture is distinctly visible on the cuticular surface; it extends anteriorly towards the anterior collar but is obliterated before reaching it. The posterolateral corner of the ventrite forms a smooth and flat triangular process with an acute angle, which delimits the mesocoxal cavity anterolaterally. A narrow bead is present on the anterior edge of the coxal cavity.

The distinct and slightly curved mesothoracic pleural suture extends from the mesocoxal cavity to the anterodorsal edge of the mesopleuron. The sclerotized exposed part of the large mesepimeron (ep2, Figs. 1B, C; 2B; 3C, E; 6B, C) is very broad dorsally and narrowing towards the mesocoxal cavity (cc2, Fig. 6B); its mesal part is nearly parallel-sided; its straight mesal edge, which is about half as long as the anapleural cleft, forms the lateral border of the mesocoxal cavity; the mesal and posterior border form a right angle; the large semimembranosus dorsal part of the mesepimeron has an oblique orientation and is covered by the elytra at rest. The triangular mesanepisternum (aes2, Figs. 1B, C; 3C, E; 6B, C) is largely exposed on the ventral side of the body; it is smaller than the mesepimeron and does not reach the mesocoxal cavity with its pointed posterolateral edge; a few short setae are irregularly distributed on its posterior area.

The mesotrochantin is concealed. The mesofurca (fuc2, Fig. 3A, B, D) consists of two separate and very long rod-like structures, which are relatively wide at the base but narrowed dorsally; the furca extends dorsolaterad, and the dorsal tip is very close to the notum but not fused with it.

The elytra (el, Fig. 2A, C) are about 3 times as long as their maximum width; they cover the dorsal part of the pterothorax except for the mesoscutellar shield and the abdominal dorsum except for the tip of tergum VIII. The humerus forms an obtuse angle. The dorsal surface of the elytra bears a dense, regular vestiture of minute setae, except for a small humeral area, which is overlapped by the posterolateral pronotal corner; the setae are arranged along numerous irregular transverse lines with smooth

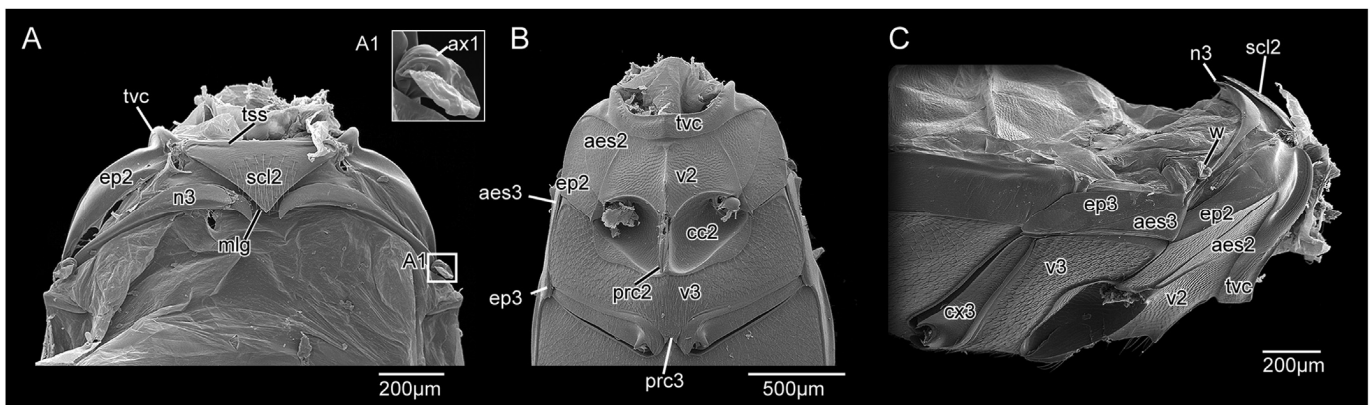


Fig. 6. Scanning electron micrographs, pterothorax of *T. ferreri*. (A) dorsal view; (B) ventral view; (C) lateral view. Abbreviations: aest2/3, mes-/metanepisternum; ax1, axillary sclerite 1; cc2, mesocoxal cavity; ep2/3, mes-/metepimeron; mlg, median longitudinal groove; prc2/3, process of meso-/metaventrite; scl2, mesoscutellar shield; tvc, transverse collar; v2/3, meso-/metaventrite.

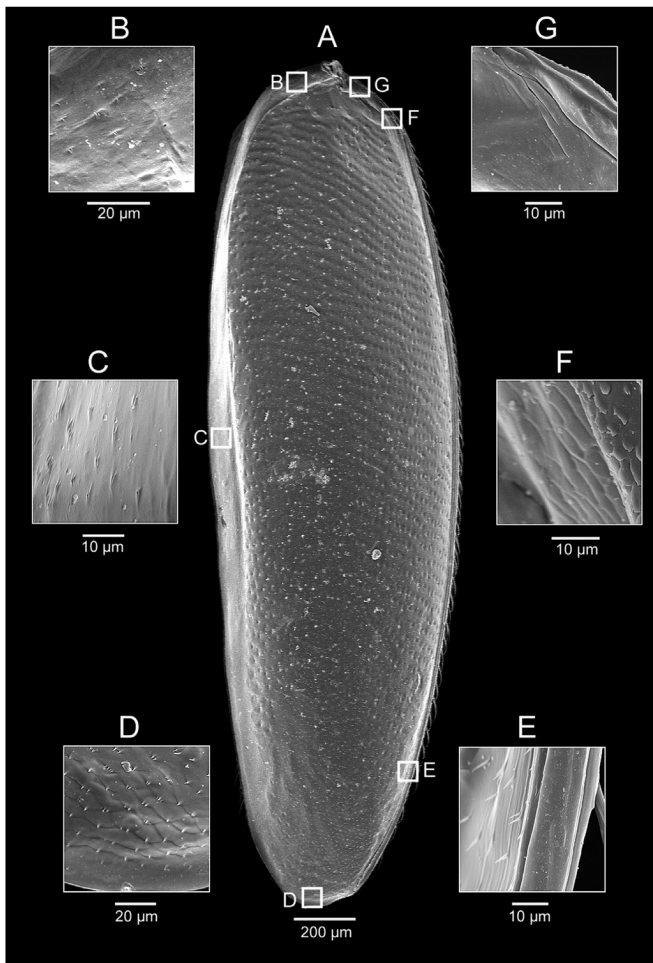


Fig. 7. Scanning electron micrographs, right elytron of *T. ferrei*, ventral view. (A). entire elytron; (B). proximal area of outer rim; (C). outer rim; (D). elytral apex; (E)–(G). inner rim.

areas between them; longitudinal parasutural striae are absent. The proximal area of the ventral surface is largely smooth, with few shallow depressions; the mesal elytral rim displays some scale-like structures anteriorly whereas the posterior area is smooth; the middle region of the ventral surface is covered with scales armed with short microtrichia. The epipleura (epp, Fig. 2B, C) are broad anteriorly and gradually narrowing posteriorly.

The midlegs are slightly longer than the forelegs, ca. 0.8 times of the total body length. The femur/tibia/tarsus ratio of the midlegs is 1.35/1.25/1. The mesocoxa (cx2, Figs. 1B, C; 2B, C; 3C, E) is similar in shape to the procoxa, but slightly transverse, with an oblique orientation and scarcely projecting beyond the surface of the ventral pterothorax. The mesotrochanter (tr2, Fig. 2B, C) is similar to its prothoracic counterpart. The mesofemur (fem, Figs. 2B, C; 4B) is longer than the profemur and less wide proximally. The cylindrical slender tibia (tib2, Fig. 4B) is straight, longer than the protibia, and only very slightly widening distally; two well-developed multi-toothed spurs are present apically. The mesotarsus (tar2, Fig. 4B) is 5-segmented and slender, without expanded tarsomeres and ventral adhesive sole. The pretarsal elements are similar to those of the forelegs, and small pore plates are also present.

Musculature (Fig. 5): M30 (*M. mesoterni primus*), O: mesofurcal arm, I: profurcal arm; M40 (*M. noto-coxalis*), O: posterior notal part, I: posterior coxal rim; M41 (*M. episterno-coxalis*), O: anterior

part of mesanepisternum, I: anterior coxal rim; M44 (*M. furca-coxalis anterior*), O: mesofurcal arm, I: anterior coxal rim; M48 (*M. episterno-trochanteralis*), O: large part of mesanepisternum, I: trochanteral tendon; M49 (*M. epimero-trochanteralis*), O: large part of mesepimeron, I: trochanteral tendon, together with M48.

3.4. Metathorax

The very short metanotum (n3, Figs. 1A, C; 3A, D, E) is distinctly reduced compared to coleopteran species with a well-developed flight apparatus. It is transverse, relatively wide towards the median line but strongly narrowing towards the lateral margin. A prescutum and scutellum are not present as separate areas of the notum. The median longitudinal groove (mlg, Fig. 6A) is short but distinct, enclosed by the distinctly developed alacristae, which form an acute angle posteriorly, and fit with the mesal edge of the elytra base; this median part of the metanotum is partly covered by the mesoscutellar shield. The surface of the median metascutal area is covered with scales, whereas the lateral area is smooth. The anterior, postmedian and posterior notal wing processes are not recognizable, whereas axillary sclerite 1 (ax1, Fig. 6A) is clearly visible. The prealar sclerite is not recognizable and the basalare and its muscle disc and the subalare are absent. A metapostnotum is not developed. A metatergal spine is also missing (Jeannel, 1911: épine métatergale).

The slightly convex metaventrite (v3, Figs. 1B, C; 2B, C; 3C, E; 6B, C) has a scaly surface structure; it is largely covered with evenly-distributed short setae and lacks impressions; the anterolateral angle is slightly elevated and glabrous. An anteromedian bead, which forms the posterior edge of the mesocoxal cavity, is narrow medially but strongly widened laterally. A distinct median longitudinal carina is absent and a lateral suture originating from the lateral side of the mesocoxal cavity is also lacking. A bifid posteromedian process (prc3, Fig. 1B; 6B) is present; the two lobes are sparsely set with small scale-like structures with multiple posteriorly-directed projections, but long setae are lacking. A weakly-developed short transverse suture (“metakatepisternal suture”) is present along the posterior margin of the metaventrite, very close to the metacoxal cavity.

The metepimeron (ep2, Figs. 1B, C; 3A, C, E; 6B, C) and metanepisternum (aes3, Figs. 1B; 3C, E; 6B, C) are scarcely visible in ventral view. The triangular metanepisternum does not reach the metacoxal cavity posteriorly. The metepimeron consists of sclerotized and semi-membranous parts; the anterodorsal corner is densely covered with small, round scales; the posterior area is covered by the anteriormost abdominal pleuron.

The well-developed metafurca (fuc3, Fig. 3A, B, D) consists of a broad basal stalk and two widely separated lateral arms; the dorsal tips of the latter are slightly widened and form plate-like muscle attachment sites.

The membranous hindwings (w, Figs. 1A, C; 3A, B, D, E) are extremely reduced and only present as small flap-like membranous structures.

The hindlegs are elongated, with a femur/tibia/tarsus ratio of 1.1/1.4/1. The metacoxae (cx3, Figs. 1B, C; 2B, C; 3B, C, E) are short and transverse and moderately separated from each other; the coxal plates are weakly-developed. The femur (fem3, Figs. 2B, C; 4C) is flattened, with sub-parallel lateral edges. The tibia (tib3, Fig. 4C) and the five-segmented tarsus (tar3, Fig. 4C) are long and thin. The distal parts of the hindlegs are otherwise very similar to those of the midlegs, and small pore plates are present.

Musculature (Fig. 5): M62 (*M. metasterni primus*), very short, O: metafurcal arm, I: mesofurcal arm; M65/66 (*M. dorsoventralis secundus/M. dorsoventralis tertius*), O: anterior apex of metafurcal arm, I: reduced third phragma; M72 (*M. sterno-episternalis*), O:

lateral margin of ventrite, I: upper part of metanepisternum, below pleural ridge; M76 (M. noto-coxalis posterior), O: lateral notal area, I: posterior coxal rim; M80 (M. sterno-coxalis), O: anterolateral corner of ventrite, I: anterior coxal rim; M81 (M. furca-coxalis lateralis), O: basal part of metafurcal arm, I: anterior coxal rim; M83 (M. furca-coxalis posterior), O: basal part of metafurcal arm, I: posterior coxal rim; M85 (M. furca-trochanteralis), O: furcal arm, I: tendon attached to trochanter.

4. Discussion

Jeannel (1943) categorized subterranean species of Leiodidae into four morphotypes, which were illustrated by Laneyrie (1967) and Njunjić (2016: fig. 2) (see also Moldovan et al. [2018]: fig. 7.6): a) the largely unmodified “bathyscoid” type with an ancestral ovoid body shape with short appendages; b) the intermediate “pholeuonoid” type with moderately elongated appendages and a rather slender body; and c) and d) the highly specialized “leptodiroid” and “scaphoid” types, both with very long appendages and a narrow head. The posterior body comprising the prothorax and abdomen appears distinctly bloated (Njunjić, 2016: pseudo-physogastric) in the former, but slender in the latter morphotype. Even though its head structures are distinctly affected by troglobiotic habits (Luo et al., 2019), *T. ferreri* was assigned to the intermediate “pholeuonoid” category based on its general habitus.

Like most other cave-dwelling beetles (e.g. Jeannel, 1911, 1936), *T. ferreri* shows a distinct degree of depigmentation, which is a typical feature linked with subterranean habits (e.g. Njunjić, 2016). The brownish coloration of the cuticle is distinctly lighter compared to epigeic species, for instance of the cholevine genus *Catops*, or also of representatives of Camiarinae like *Z. maculifer* or *Neopeltops* Jeannel, 1936 (Newton, 2016: fig. 11.4.1), which display depigmented areas or light spots but on a very dark ground color.

A very dense pattern of minute setae on exposed body parts, as present in *T. ferreri*, is unrelated to subterranean habits. A similar vestiture is present in epigeic species of Cholevinae and also Camiarinae. This is arguably a groundplan feature of Leiodidae and Cholevinae, even though glabrous body surfaces also occur within the family (Newton, 2016). Long tactile setae as they occur in cave-dwelling Trechinae (Carabidae) (e.g. Salgado and Ortuño, 1998) are absent in *T. ferreri* and likely generally missing in Leiodidae.

A compact ovoid postcephalic body is likely ancestral for Leiodidae including Leptodirini (e.g. Jeannel, 1911, 1936; Newton, 2016: fig. 11.4.1). A ratio between the length of the postcephalic body and the maximum width at the mid-elytral region of ca. 2:1 is found in species of *Catops* of Cholevinae, and 1.65:1 in *Z. maculifer* of Camiarinae. The postcephalic body of *T. ferreri* is distinctly elongated, with a ratio of approximately 4:1. Elongation of the body is likely linked with subterranean habits (Njunjić, 2016). A length/width ratio of ca. 2.6:1 is found in the troglobiotic *Speoplans giganteus* (J. Müller, 1901) and ca. 4:1 in *Remyella scaphoides* Jeannel, 1931 (Moldovan et al., 2018: fig. 7.6 j, k). The distinctly lower ratio in Leptodirini of the “leptodiroid” type is due to the pseudo-physogastric posterior body (Njunjić, 2016). It is important to note that in contrast to Trechinae an elongation of the body is not a general feature of cave dwelling Leiodidae. In contrast to Leptodirini, subterranean species of the related Ptomaphagini display a compact and more or less ovoid body (e.g. Peck, 1973, 1986), possibly with a trend towards size increase in subterranean species (Peck, 1986).

Elongation of the legs is an almost general trend linked with subterranean habits of beetles, occurring in Carabidae, Leiodidae (Jeannel, 1911, 1926; Luo et al., 2018b), and also Staphylinidae incl. Pselaphinae and Scydmaeninae (Moldovan et al., 2018: fig. 7.6). This feature is apparently less pronounced in subterranean species of

Ptomaphagini, for instance in *Ptomaphagus hirtus* (Tellkamp, 1844) (Peck, 1973: fig. 2). However, a precise analysis of leg lengths is still wanting. Like the antennae (Luo et al., 2019), the legs are distinctly elongated in *T. ferreri*, even though to a lesser degree than in some advanced cave dwellers like for instance *Graciliella ozimeci* Njunjić, Perreau, Hendriks, Schilthuizen & Deharveng, 2016 (Njunjić et al., 2016; Moldovan et al., 2018: fig. 7.6 h). Like in other subterranean species, the degree of elongation is clearly highest in the hindlegs (e.g. Jeannel, 1911).

It is likely that leptodirine troglobiotic species with a slender body and distinctly elongated move freely on the substrate of the floor of caves or relatively large interstices (in relation to their body size). In contrast to this, the compact ovoid body and rather short appendages of Ptomaphagini are better suited for moving through relatively solid substrates accumulated between rocks and in narrow crevices. An elongate cephalo-prothoracic complex and elongated appendages are likely advantageous in the context of predacious habits in the case of Carabidae (e.g. Luo et al., 2019), but also increase the range of the non-visual sensory apparatus (Müller, 1901; Jeannel, 1911). This improves the ability to detect predators in the case of Leptodirini, and possible also facilitates finding suitable food substrates.

Size increase was discussed as a general trend in troglobiotic beetles by Jeannel (1911), even though there are obvious exceptions such as species of *Spelaeobates* J. Müller (1901) or *Remyella* Jeannel, 1931 (Jeannel, 1911; Ćurčić et al., 2013). It was shown by Peck (1986) for *Ptomaphagus* Hellwig, 1795 that the dimensions of the body and appendages do not respond uniformly to selective pressure.

Highly modified leiodids of the leptodiroid or scaphoid morphotypes (e.g. Jeannel, 1911; Njunjić et al., 2016; Moldovan et al., 2018: fig. 6.7 h, I) and troglobiotic Trechinae (e.g. Luo et al., 2018b) are characterized by a very slender and elongated prothorax (Jeannel, 1941: “aphaenopsian” morphological type). In contrast to this, the skeletal morphology of the prothoracic trunk of *T. ferreri* is scarcely modified, except for a moderate degree of elongation, compared for instance with species of Camiarinae, Cholevini or Ptomaphagini (Jeannel, 1911; Peck, 1986; Newton, 2016). The general configuration is similar to what is found in other staphyliniform beetles (e.g. Beutel and Komarek, 2004; Yavorskaya et al., 2019, see also Hlavac, 1972, 1975). The musculature of the prothorax is strongly developed (Table 1), with a total of 18 muscles (excluding the intrinsic leg muscles), two of them bipartite. Sixteen prothoracic muscles are present in the hydrophiloid *Helophorus grandis* Illiger, 1798 (Beutel and Komarek, 2004), 14 in the staphylinid *Creophilus* sp. (Larsén, 1966), 15 in the ptiliid *Nephanes titan* Newman, 1834 (Yavorskaya et al., 2019), and 15 in the subterranean trechine *S. wangorum* (Luo et al., 2018b), and 14 in the silphid *Nicrophorus vespillo* (Linné, 1758) or *N. vespilloides* (Herbst, 1784) (species name abbreviated as “vesp.”; Larsén, 1966). It is apparent that muscles involved with movements of the head and forelegs are not affected by troglobiotic habits, and rather strengthened than reduced.

A plesiomorphic skeletal feature of the prothorax of *T. ferreri* and other cholevines is the narrow external posterior procoxal closure. A very broad procoxal closure as is found in *Anthroherpon* and *Astagobium* (Jeannel, 1911: figs 593, 601) likely increases the movability of the cephalo-prothoracic complex, as it is also the case in carabids with a high grade motility mechanism between the pro- and mesothorax (Hlavac, 1972; Luo et al., 2018b).

In contrast to the prothorax, the prothorax is strongly modified, especially the dorsal parts linked with the elytra and hindwings, and also the muscle apparatus of both segments. Due to complete flightlessness, a general feature of subterranean beetles (e.g. Njunjić, 2016, Luo et al., 2018b; Moldovan et al., 2018), the ability to open the elytra is no longer required. Consequently, the articulatory sclerites at the elytral base can be simplified or reduced

Table 1

Thoracic musculature of several species of Staphyliniformia and the cave-dwelling carabid *Sinaphaenops wangorum*. Muscle numbers refer to Larsén (1966) and Friedrich and Beutel (2008), respectively. "+" = present, "++" = "strongly developed", "-" = absent (muscular data extracted from Beutel and Komarek, 2004; Luo et al., 2018b).

Larsén (1966)	Friedrich and Beutel (2008)	<i>Helophorus aquaticus</i>	<i>Troglocharinus ferreri</i>	<i>Creophilus</i> sp.	<i>Nicrophorus vespillo</i>	<i>Sinaphaenops wangorum</i>
M01	ldlm2	++	+	+	+	+
M02	ldlm1	+	+	+	+	+
M03	ldlm3	+	-	-	-	-
M04	ldlm5	++	+	+	+	+
M05	lvlm3	+	+	+	+	-
M06	lvlm1	+	+	+	+	+
M07	ldvm6	+	+	+	+	+
M08	ldvm8	-	+bipartite	-	-	+
M09	ldvm5	-	+	-	-	-
M10	ldvm2/3	+	+	+	+	+
M11	ldvm10	+	+	+	+	+
M12	ltpm3?	++	+	+	+	+
M13	ltpm6	+	+	+	+	+
M14	ldvm13	++	+	+	+	+
M15	ldvm16/17	++	++	+	+	+
M16	lpcm4	+	+	+	+	+
M17	ldvm18	- (?)	+	-	+	-
M18	lscm1	-	-	-	-	-
M19	lscm2	+	+	-	-	+
M20	lpcm8	++	+bipartite	+	-	+
∑ prothorax		16	18 (+2)	14	14	15
M28	lldlm1	++	-	+	+	-
M29	lldlm2	+	-	+	+	-
M30	lvlm7	++	+	+	+	+
M31	lvlm9	-	-	-	-	-
M32	lldvm8	-	-	+	-	-
M33	lltpm2	+	-	+	+	-
M34	lltpm10?	-	-	-	-	-
M35	lltpm10	-	-	+	-	-
M36	lltpm7/9	+	-	+	+	-
M37	lspm2	+	-	-	+	-
M38	lspm6	-	-	-	-	+
M39	lldvm2	-	-	-	-	+
M40	lldvm5, 4?	++	+	+	+	+
M41	llpcm4	++	+	+	+	+
M42	llpcm3	+	-	+	-	-
M43	lldvm6	-	-	-	-	-
M44	llscm1?	+	+	+	+	+
M45	llscm4	-(?)	-	-	-	-
M46	llscm2	+	-	+	+	+
M47	lldvm7	-	-	-	-	+
M48	llpcm6	++	++	+	+	+
M49	/	-	++	-	-	-
M50	llpcm5	-	-	-	-	-
M51	?	-	-	-	-	-
M52	llscm6	+	-	-	+	-
∑ mesothorax		13	6	13	12	9
M60	llldlm1	++	-	+	+	-
M61	llldlm2	++	-	+	+	-
M62	llvlm3	+	+	+	+	+
M63	llvlm5	-	-	-	-	+
M64	llldvm1	++	-	+	+	-
M65	llldvm8	+	+	+	+	+
M66	llldvm8	+	+	+	+	-
M67	llltpm2	+	-	+	+	-
M68	llltpm6	-	-	-	+	+
M69	llltpm3	+	-	+	+	-
M70	llltpm10	+	-	+	+	-
M71	llltpm7/9	+	-	+	+	-
M72	lllppm1	+	+	+	+	-
M73	lllspm1	++	-	+	+	-
M74	llldvm2	-	-	+	+	-
M75	llldvm4	++	-	+	+	-
M76	llldvm5	+	+	+	+	+
M77	lllpcm4	+	-	+	+	-
M78	lllpcm3	++	-	-	+	-
M79	llldvm6	++	-	+	+	-
M80	llscm7?	-	+	-	-	-
M81	lllscm1	+	+	+	+	+
M82	lllscm4	+	-	+	+	-

(continued on next page)

Table 1 (continued)

Larsén (1966)	Friedrich and Beutel (2008)	<i>Helophorus aquaticus</i>	<i>Troglocharinus ferreri</i>	<i>Creophilus</i> sp.	<i>Nicrophorus vespillo</i>	<i>Sinaphaenops wangorum</i>
M83	IIIscm2	+	+	+	+	+
M84	IIIdvm7	++	–	–	–	–
M85	IIIscm6	++	+	+	+	+
∑ metathorax		22	8	21	23	8
∑ pterothorax		35	14	34	35	17
Total sum		51	32(+2)	48	49	32

as is the case in *T. ferreri*. The usual elytral locking device involving the scutellar shield and the metanotal alacristae is well-developed. An additional clamp mechanism formed by the metanepisterum (Seago et al., 2015) is absent, like in all leiodids outside of Camiarinae. The elytra of epigeal and subterranean leiodids including *T. ferreri* are usually connected along the mesal edges by a groove and spring mechanism like in most beetles (Jeannel, 1911), but medially fused elytra occur in some species (A. Newton, pers. comm.). In contrast to the prothorax, the mesothoracic musculature is strongly reduced (Table 1). Only six muscles are preserved in *T. ferreri*, versus 13 in *H. grandis* (Beutel and Komarek, 2004), *Creophilus* sp. (Larsén, 1966) and *N. titan* (Yavorskaya et al., 2019), 12 in *Nicrophorus* (Larsén, 1966), and nine in the trechine *S. wangorum* (Luo et al., 2018b).

A character which is likely not related with epigeal or subterranean habits is the configuration of the mesocoxae and mesocoxal cavities. The mesocoxae of *T. ferreri* are distinctly separated by an elongate, slender posteromedian process of the mesoventrite. In contrast, the mesocoxal cavities are medially confluent in the related leptodirine *Anthroherpon* (Njunjić, 2016: fig. 14). An association between subterranean habits and the morphology of the ventral tibial spurs is also not supported by any evidence. Multi-toothed meso- and metatibial spurs as described for *T. ferreri* occur in most leptodirines, but are also found in non-subterranean representatives of Anemadini and Cholevini (Antunes-Carvalho et al., 2019). Moreover, the same condition is not present in the cave-dwelling *Ptomaphagus troglodytes* Blas and Vives, 1983 (Ptomaphagini; Fresneda et al., 2011). The drastic reduction of the outer empodial seta of *T. ferreri* is also reported for other leptodirines, also including species of the subtribe Pholeuina such as *Antrocharis querilhaci* (Lespès, 1857), *Notidocharis ovoideus* Jeannel, 1956 and *Speonomus infernus* (Dieck, 1869). However, this feature is very variable within the tribe, without a clear phylogenetic pattern (Antunes-Carvalho and Gnaspini, 2016). The presence of two long empodial setae in the strongly modified cave beetles *Anthroherpon hoermanni* (Apfelbeck, 1889), *Leptodirus hochenwarti* Schmidt (1832) and *R. scaphoides* Jeannel, 1931, for instance, makes any relationship of the empodial setae with the subterranean environment unlikely. The occurrence of pore plates on the terminal tarsomere was confirmed here for *T. ferreri*. This character was recently described and documented for various species of Leptodirini, but not observed in any other group of Leiodidae (Antunes-Carvalho et al., 2019). As its function remains unknown, a connection with a subterranean lifestyle cannot be ruled out yet.

Another feature likely not linked with a specific habitat preference is the presence of a median keel of the mesoventrite. It is absent in *Catops*, *Choleva* (Fresneda et al., 2011) and the troglobiontic genera *Anthroherpon* (Jeannel, 1911) and *Hadesia* Müller, 1901 (Perreau and Pavićević, 2008), but present in other cholevines, such as for instance *Eucatops* Portevin, 1903, an early diverging branch in the subfamily (Antunes-Carvalho et al., 2019), in species of *Ptomaphagus*, and also in *Speonemadus clathratus* (Perris, 1864) and *Quaestus noltei* (Coiffait, 1965) (Fresneda et al., 2011). As a short keel is also present in *Leptinus testaceus* Müller, 1817 (Platypyllinae) and *Agathidium* (Panzer) (Leiodinae) (Fresneda et al., 2011), this is very likely

a groundplan feature of Cholevinae and possibly of Leiodidae. It was pointed out by Jeannel (1911) that the carinae can be enlarged and lamelliform in elongated cave dwelling species and appear rounded or toothed in lateral view. A feature not documented in other taxa and difficult to interpret is the presence of a very strongly developed mesofurca. An increase of the muscle attachment area cannot be the reason, as the muscles originating from the furca are normally developed, or even absent like *M. furca trochanteralis*. Mechanical stabilization of the segment is also unlikely as the distal part of the furca is not connected with pleural or tergal elements.

Except for the strong elongation of the hindlegs, the pterothorax is mainly affected by the reduction of the flight apparatus, as was already described for cavernicolous beetles by Jeannel (1911). Using a scheme developed for Carabidae by Tietze (1963) (see also Darlington, 1936), *T. ferreri* (and other cavernicolous cholevines) belongs to an advanced type, with the metanotum, metaphragma, alae, and wing articulation reduced, but with a metaventrite of normal length in contrast to some flightless carabids (Luo et al., 2019). In contrast to this, the metathoracic flight apparatus is well developed in *Catops* (Jeannel, 1911: fig. 41), in *Ptomaphagus consobrinus* (LeConte, 1853) (Peck, 1973: fig. 7A), and also in the camiarine *Z. maculifer*. Consequently, a normally developed skel-etomuscular system of the metathorax belongs very likely to the groundplan of Leiodidae and Cholevinae.

The dorsal elements of the metathorax are strongly affected by flightlessness, which occurs in about half of all species of Leiodidae and all Old World species of the tribe Leptodirini (Newton, 2016). The metanotal elements, prescutum, scutum and scutellum, form a single undivided transverse structure (Jeannel, 1911: 'bandelette transverse'; see also Peck, 1973: fig. 7), strongly narrowed towards the lateral edge, and completely lacking the notal processes. The latter normally articulate with the axillary sclerites, which are however also missing in *T. ferreri*. Prealar sclerite, basalare, basal muscle disc and subalare are also unrecognizable. The wings are still present as flap like, membranous vestiges as in *Bathysciola damryi* (Abeille, 1881) and as tiny scales in *P. hirtus* (Tellkamp, 1844) (Peck, 1973: fig. 7B), whereas they are entirely absent in other cavernicolous cholevines such as *Apholeuonus nudus* (Apfelbeck, 1889) or *Anthroherpon cylindricolle* (Apfelbeck, 1889) (Jeannel, 1911: figs 52, 53). The only functional part of the metanotum of *T. ferreri* are the short but distinct alacristae, which are part of the elytral locking device. A derived feature occurring within Leptodirini is a more or less distinct elongation of the alacristae. They are slightly extended posteriorly in *Adelopsella bosnica* (Reitter, 1885), and moderately to strongly elongated in some species of *Bathysciola* (Jeannel, 1911: figs 45, 47, 57, 58). The entire metascutal structure bearing the alacristae is reduced to a narrow spine-like structure in *A. nudus* (Jeannel, 1911: fig. 52).

The degree of metanotal reduction in troglobiontic cholevines is very similar to what was described for the cave dwelling trechine *S. wangorum* (Luo et al., 2018a,b: fig. 2A). However, a rudimentary postnotum is still present in that species, whereas it is completely reduced in *T. ferreri* and probably in other cave-dwelling cholevines (Jeannel, 1911: figs 52, 53).

Like in the mesothorax, the muscle system of the metathorax is greatly reduced (Table 1), with only eight muscles preserved (like in

the trechine *S. wangorum*; Luo et al., 2018b) versus 22 in *Helophorus* (Beutel and Komarek, 2004), 17 in *Nephanes* (Yavorskaya et al., 2019), 21 in *Creophilus*, and 23 in *Nicrophorus* (Larsén, 1966). The muscle system of the camiarine *Z. maculifer* was not reconstructed in detail. However, the direct and indirect flight muscles are well-developed in this species, likely reflecting the groundplan condition in the family.

5. Conclusions

As in the case of the head (Luo et al., 2019), the related leiodid tribes Ptomaphagini and Leptodirini show different trends of adaptations to cave-dwelling, with a compact postcephalic body and relatively short appendages maintained in the former, and a distinct tendency towards elongation of both in the latter. The former condition is suitable for pushing through substrates between rocks and in crevices, the latter for moving on the floor of caves or large interstices, with an increased range of the non-visual sensory apparatus. The pattern of reduction of the pterothorax of *T. ferreri* is similar to what is found in the non-related carabid trechine *S. wangorum*, in both cases with strongly simplified tergal elements and drastic reduction of flight-related muscles.

Acknowledgments

We are very grateful to Dr. Hans Pohl (FSU Jena) for his assistance with the SEM samples. The donation of valuable material by Dr. R.A.B. Leschen (New Zealand Arthropod Collection, Landcare Research) is gratefully acknowledged. Great thanks are also due to Adrian Richter (FSU Jena) for conducting the μ CT scan and to Dr. Alexander Stoessel for providing access to the equipment at the MPI für Menschheitsgeschichte (Jena). Our work was partly funded by project CGL2013-48950-C2 (AEI/FEDER, UE). The first author wants to express his thanks to CSC (No. 201708440281).

References

- Antunes-Carvalho, C., Gnaspini, P., 2016. Pretarsus and distal margin of the terminal tarsomere as an unexplored character system for higher-level classification in Cholevinae (Coleoptera, Leiodidae). *Syst. Entomol.* 41, 392–415.
- Antunes-Carvalho, C., Ribera, I., Beutel, R.G., Gnaspini, P., 2019. Morphology-based phylogenetic reconstruction of Cholevinae (Coleoptera: Leiodidae): a new view on higher-level relationships. *Cladistics* 35, 1–41.
- Antunes-Carvalho, C., Yavorskaya, M., Gnaspini, P., Ribera, I., Beutel, R.G., 2017. Cephalic anatomy and three-dimensional reconstruction of the head of *Catops ventricosus* (Weise, 1877) (Coleoptera: Leiodidae: Cholevinae). *Org. Div. Evol.* 17, 199–212.
- Beutel, R.G., Friedrich, F., Ge, S.Q., Yang, X.K., 2014. Insect Morphology and Phylogeny: a Textbook for Students of Entomology. De Gruyter, Berlin.
- Beutel, R.G., Komarek, A., 2004. Comparative study of thoracic structures of adults of Hydrophiloidea and Histeroidea with phylogenetic implications (Coleoptera, Polyphaga). *Org. Div. Evol.* 4, 1–34.
- Ćurčić, S.B., Antić, D.Ž., Ćurčić, N.B., Ćurčić, B.P.M., 2013. *Remyella montenegrina*, a new troglitic leiodid beetle (Coleoptera: Leiodidae: Leptodirini) from Northeastern Montenegro. *Arch. Biol. Sci.* 65, 1217–1222.
- Darlington Jr., P.J., 1936. Variation and atrophy of flying wings of some carabid beetles (Coleoptera). *Ann. Entomol. Soc. Am.* 29 (1), 136–179.
- Fresneda, J., Grebennikov, V.V., Ribera, I., 2011. The phylogenetic and geographic limits of Leptodirini (Insecta: Coleoptera: Leiodidae: Cholevinae), with a description of *Sciaphyes shestakovi* sp. n. from the Russian far East. *Arthropod. Syst. Phylogeny* 69, 99–123.
- Fresneda, J., Salgado, J.M., Ribera, I., 2007. Phylogeny of western Mediterranean Leptodirini, with an emphasis on genital characters (Coleoptera: Leiodidae: Cholevinae). *Syst. Entomol.* 32, 332–358.
- Friedrich, F., Beutel, R.G., 2008. The thorax of *Zorotypus* (Hexapoda, Zoraptera) and a new nomenclature for the musculature of Neoptera. *Arthropod. Struct. Dev.* 37, 29–54.
- Friedrich, F., Farrell, B.D., Beutel, R.G., 2009. The thoracic morphology of Archostemata and the relationships of the extant suborders of Coleoptera (Hexapoda). *Cladistics* 25, 1–37.
- Hlavac, T.F., 1972. The prothorax of Coleoptera: origin, major features of variation. *Psyche* 79, 123–149.
- Hlavac, T.F., 1975. The prothorax of Coleoptera (except Bostrichiformia-Cucujiformia). *Bull. Mus. Comp. Zool.* 147, 137–183.
- Jeannel, R., 1911. Biospeologica XIX. Révision des Bathysciinae (Coléoptères Silphides). Morphologie, distribution géographique, systématique. *Arch. Zool. Exp. Gen.* 7, 1–641 pls. 1–24.
- Jeannel, R., 1926. Monographie des Trechinae. Morphologie comparée et distribution géographique d'un groupe de Coléoptères. *Abeille* 32, 221–550.
- Jeannel, R., 1936. Monographie des Catopidae (Insectes Coléoptères). *Mém. Mus. Nat. Hist. Nat.* 1, 1–433.
- Jeannel, R., 1941. Faune de France. Coléoptères Carabiques I, vol. 39. Lechevalier, Paris.
- Jeannel, R., 1943. Les fossiles vivants des cavernes. Gallimard, Paris.
- Jeannel, R., 1958. Sur la famille des Camiaridae Jeannel lignée paléantarctique. *Rev. Fr. Entomol.* 25, 5–15.
- Kilian, A., Newton, A.F., 2017. Morphology of the immature stages of *Platycholeus* Horn, 1880 (Coleoptera: Leiodidae: Cholevinae: Leptodirini). *Zool. Anz.* 266, 158–168.
- Laneyrie, R., 1967. Nouvelle classification des Bathysciinae. *Ann. Speleol* 22, 585–645.
- Larsén, O., 1966. On the morphology and function of locomotor organs of the Gyrinidae and other Coleoptera. *Opusc. Ent. Suppl* 30, 1–241.
- Luo, X.Z., Wipfler, B., Ribera, I., Liang, H.B., Tian, M.Y., Ge, S.Q., Beutel, R.G., 2018a. The cephalic morphology of free-living and cave-dwelling species of trechine ground beetles from China (Coleoptera, Carabidae). *Org. Div. Evol.* 18, 125–142.
- Luo, X.Z., Wipfler, B., Ribera, I., Liang, H.B., Tian, M.Y., Ge, S.Q., Beutel, R.G., 2018b. The thoracic morphology of cave-dwelling and free-living ground beetles from China (Coleoptera, Carabidae, Trechinae). *Arthropod. Struct. Dev.* 47, 662–674.
- Luo, X.Z., Antunes-Carvalho, C., Wipfler, B., Ribera, I., Beutel, R.G., 2019. The cephalic morphology of the troglitic cholevine species *Troglocharinus ferreri* (Coleoptera, Leiodidae). *J. Morph.* 280, 1207–1221.
- Moldovan, O.T., 2012. Beetles. In: Culver, D.C., William, W.B. (Eds.), *Encyclopaedia of Caves*. Elsevier Academic Press, Oxford, UK, pp. 54–62.
- Moldovan, O.T., Kováč, L., Halse, S., 2018. *Cave Ecology*. Springer International Publishing, Basel, Switzerland.
- Müller, J., 1901. Beitrag zur Kenntniss der Höhlensilphiden. *Verh. Zool. Bot. Ges. Wien* 51, 16–33. +1 pl.
- Newton, A.F., 1998. Phylogenetic problems, current classification and generic catalog of World Leiodidae (including Cholevinae). *Mus. Reg. Sci. Nat. Torino Atti* 8, 41–177, 364–376.
- Newton, A.F., 2016. Leiodidae Fleming, 1821. In: Beutel, R.G., Leschen, R.A.B. (Eds.), *Handbook of Zoology, Coleoptera, Beetles, Morphology and Systematics (Archostemata, Adephaga, Myxophaga, Polyphaga Partim)*, second ed., vol. 1. De Gruyter, Berlin, pp. 364–376.
- Njunjić, I., 2016. Evolution, Adaptation and Speciation in Anthroherpon Reitter, a Genus of Subterranean Coleoptera (Unpubl. PhD dissertation). Muséum National d'Histoire Naturelle, Paris.
- Njunjić, I., Perreau, M., Hendriks, K., Schilthuizen, M., Deharveng, L., 2016. The cave beetle genus *Anthroherpon* is polyphyletic; molecular phylogenetics and description of *Graciliella* n.gen. (Leiodidae, Leptodirini). *Contr. Zool.* 85, 337–359.
- Peck, S.B., 1973. A systematic revision and the evolutionary biology of the *Ptomaphagus* (*Adelops*) beetles of North America (Coleoptera: Leiodidae: Catopinae), with emphasis on cave-inhabiting species. *Bull. Mus. Comp. Zool.* 145, 29–162.
- Peck, S.B., 1986. Evolution of adult morphology and life-history characters in cavernicolous *Ptomaphagus* beetles. *Evol* 40, 1021–1030.
- Perreau, M., Pavičević, D., 2008. The genus *Hadesia* Müller, 1911 and the phylogeny of Anthroherponina (Coleoptera, Leiodidae, Cholevinae, Leptodirini). In: Pavičević, D., Perreau, M. (Eds.), *Advances in the Studies of the Fauna of the Balkan Peninsula. Papers Dedicated to the Memory of Guido Nonveiller*. Institute for Nature Conservation of Serbia, Monograph 22, pp. 215–239.
- Pohl, H., 2010. A scanning electron microscopy specimen holder for viewing different angles of a single specimen. *Microsc. Res. Tech.* 73, 1073–1076.
- Rizzo, V., Comas, J., 2015. A new species of *Troglocharinus* Reitter, 1908 (Coleoptera, Leiodidae, Cholevinae, Leptodirini) from southern Catalonia, with a molecular phylogeny of the related species group. *Zootaxa* 3946, 104–112.
- Salgado, J.M., Blas, M., Fresneda, J., 2008. *Fauna Iberica*, vol. 31. Cholevidae. Consejo Superior de Investigaciones Científicas, Madrid, Coleoptera.
- Salgado, J.M., Ortuño, V.M., 1998. Two new cave-dwelling beetle species (Coleoptera: Carabidae: Trechinae) of the Cantabrian karst (Spain). *Coleopt. Bull.* 52, 351–362.
- Schmidt, F., 1832. *Leptodirus hohenwartii* n. g., n. sp. *Illyrisches Bl.* 21, 9.
- Schneeberg, K., Bauernfeind, R., Pohl, H., 2017. Comparison of cleaning methods for delicate insect specimens for scanning electron microscopy. *Microsc. Res. Tech.* 80, 1199–1204.
- Seago, A.E., Leschen, R.A., Newton, A.F., 2015. Two new high altitude genera of Camiarini (Coleoptera: Leiodidae: Camiarinae) from Australia and New Zealand. *Zootaxa* 3957, 300–312.
- Tietze, F., 1963. Untersuchungen über die Beziehungen zwischen Flügelreduktion und Ausbildung des Metathorax bei Carabiden. *Beitr. Entomol.* 13, 88–167.
- Yavorskaya, M.I., Beutel, R.G., Farisenkov, S.E., Polilov, A.A., 2019. The locomotor apparatus of one of the smallest beetles – the thoracic skeletomuscular system of *Nephanes titan* (Coleoptera, Ptiliidae). *Arthropod. Struct. Dev.* 48, 71–82.

3.7 Study VII

The specialized thoracic skeletomuscular system of the myrmecophile *Claviger testaceus* (Pselaphinae, Staphylinidae, Coleoptera)

Xiao-Zhu Luo, Paweł Jałoszyński, Alexander Stoessel, Rolf Georg Beutel

2021.*Org. Divers. Evol.* 21, 317–335. <https://doi.org/10.1007/s13127-021-00484-1>

Abstract: External and internal structures of the thorax of the myrmecophile beetle *Claviger testaceus* (Clavigeritae, Pselaphinae) were examined and documented with state-of-the-art visualization techniques. Following a general trend in the omaliine lineage (Staphylinidae), the skeletal elements of the pro- and pterothorax in *Claviger* reach a maximum degree of compactness, with largely reduced inter- and intrasegmental sutures and skeletal elements linked with the flight apparatus. The musculature, especially metathoracic direct and indirect flight muscles, also shows a high degree of reduction. Two forms of wings were found among individuals of *C. testaceus*, both non-functional and representing an advanced stage of reduction. However, that wing vestiges are still present and the metanotum, only slightly reduced, suggests that loss of flight in this species is likely the result of a young evolutionary process. Several structures are linked with myrmecophilous habits: small body size facilitates transportation of beetles by ant workers and makes it easier to move inside nest tunnels; the remarkably compact body and mechanically robust appendages make the beetles less vulnerable to attacks by ant mandibles; the improved elytral interlocking mechanism and unusually expanded epipleura enhance the protection of vulnerable dorsal parts of the pterothorax and anterior abdomen; and glands associated with trichomes on the posterolateral elytral angle produce secretions attractive for ants. Various modifications of the thorax and anterior abdomen lead to an optimization of intimate associations with ants. The morphological syndrome enabling these beetles to cope with life in ant colonies evolved in several steps. This is suggested by an increasing solidification of the thoracic skeleton in related non-myrmecophilous groups and also by less modified related clavigerites; for instance, ant-associated tropical species are still able to fly.

Conceptualization: X.Z. Luo, P. Jałoszyński, A. Stoessel, R. G. Beutel

Visualization: X.Z. Luo, P. Jałoszyński, A. Stoessel

Writing-original draft: X.Z. Luo, P. Jałoszyński, R. G. Beutel

Writing-review & editing: X.Z. Luo, P. Jałoszyński, A. Stoessel, R. G. Beutel

Funding acquisition: X.Z. Luo

Estimated own contribution: 70%



The specialized thoracic skeletomuscular system of the myrmecophile *Claviger testaceus* (Pselaphinae, Staphylinidae, Coleoptera)

Xiao-Zhu Luo¹ · Paweł Jałoszyński² · Alexander Stoessel^{1,3} · Rolf Georg Beutel¹

Received: 17 July 2020 / Accepted: 15 January 2021
© The Author(s) 2021

Abstract

External and internal structures of the thorax of the myrmecophile beetle *Claviger testaceus* (Clavigeritae, Pselaphinae) were examined and documented with state-of-the-art visualization techniques. Following a general trend in the omaliine lineage (Staphylinidae), the skeletal elements of the pro- and pterothorax in *Claviger* reach a maximum degree of compactness, with largely reduced inter- and intrasegmental sutures and skeletal elements linked with the flight apparatus. The musculature, especially metathoracic direct and indirect flight muscles, also shows a high degree of reduction. Two forms of wings were found among individuals of *C. testaceus*, both non-functional and representing an advanced stage of reduction. However, that wing vestiges are still present and the metanotum, only slightly reduced, suggests that loss of flight in this species is likely the result of a young evolutionary process. Several structures are linked with myrmecophilous habits: small body size facilitates transportation of beetles by ant workers and makes it easier to move inside nest tunnels; the remarkably compact body and mechanically robust appendages make the beetles less vulnerable to attacks by ant mandibles; the improved elytral interlocking mechanism and unusually expanded epipleura enhance the protection of vulnerable dorsal parts of the pterothorax and anterior abdomen; and glands associated with trichomes on the posterolateral elytral angle produce secretions attractive for ants. Various modifications of the thorax and anterior abdomen lead to an optimization of intimate associations with ants. The morphological syndrome enabling these beetles to cope with life in ant colonies evolved in several steps. This is suggested by an increasing solidification of the thoracic skeleton in related non-myrmecophilous groups and also by less modified related clavigerites; for instance, ant-associated tropical species are still able to fly.

Keywords Beetle · Thorax · Myrmecophile · Ant-associated · 3D

Introduction

With a world-wide distribution and more than 10,000 described species (Yin et al. 2019), Pselaphinae ranks as the second largest subfamily of the megadiverse polyphagan

Staphylinidae (over 64,000 described species, Fikáček et al. 2020). One of the most successful myrmecophilous radiations in Coleoptera took place in this subfamily, with far-reaching morphological modifications (Thayer 2016; Parker 2016a). Extreme morphological specializations, apparently linked with a far-reaching social integration in ant colonies, evolved in Clavigeritae, one of the six pselaphine supertribes with more than 300 described species (Parker and Grimaldi 2014). Bizarre morphological modifications in this clade have attracted attention of different researchers (e.g., Parker and Grimaldi 2014). However, most studies were focused on structural features of the head and abdomen, such as the distinctly reduced mouthparts and specialized armatures of abdominal and elytral trichomes (see Hermann 1982; Parker 2016a; Jałoszyński et al. 2020), and also on appeasement glands (e.g., Cammaerts 1973, 1974). The trichomes on the abdominal tergites are a presumptive synapomorphy of the

✉ Xiao-Zhu Luo
xiao-zhu.luo@uni-jena.de

¹ Institut für Zoologie und Evolutionsforschung,
Friedrich-Schiller-Universität Jena, Erbertstrasse 1,
07743 Jena, Germany

² Museum of Natural History, University of Wrocław, Sienkiewicza
21, 50-335 Wrocław, Poland

³ Max Planck Institute for the Science of Human History, Department
of Archaeogenetics, Kahlaische Strasse 10, 07745 Jena, Germany



group and linked with the association with host ants, which have been recorded to lick on these hair-like structures of several species of Clavigeritae (Hermann 1982; Cammaerts 1992, 1995, 1996).

Like other species of the genus (Parker 2016a), *Claviger testaceus* Preyßler, 1790 displays very advanced morphological specializations, among them the complete loss of eyes and optic neuropils (Jałoszyński et al. 2020) and the reduced and non-functional flight apparatus. Behavioral patterns of *C. testaceus* have been described by Donisthorpe (1927) and Cammaerts (1977) and were summarized by Hermann (1982). The regurgitation behavior of this species in interaction with workers of the host *Lasius flavus* (Fabricius, 1782) has been documented by Cammaerts (1992, 1995, 1996). However, the morphological information about the thorax of *C. testaceus* is still very limited, especially regarding the internal elements of the skeletomuscular system.

In the last two decades, micro-computed tomography (μ -CT) and computer-based 3D reconstruction have been demonstrated as excellent tools for exploring internal structures of beetles and other insects (e.g., Friedrich et al. 2009; Liu et al. 2018; Luo et al. 2018, 2019; Yavorskaya et al. 2019). The cephalic morphology including muscles of selected groups of the highly diversified Staphylinidae was documented in detail in a series of studies by Weide and Betz (2009) and Weide et al. (2010, 2014). In contrast, only very limited information is available on the thoracic anatomy of the family (e.g. Larsén 1966). Detailed studies on the skeletomuscular system of the thorax of Pselaphinae were completely lacking so far. We used various modern techniques to investigate and document thoracic structures of *C. testaceus* and compared the observed features with patterns found previously in less specialized beetles, for instance, Archostemata (Baehr 1975; Friedrich et al. 2009), hydrophiloid beetles capable of flight (Beutel & Komarek 2004), or less specialized species of the staphylinoid families Silphidae and Staphylinidae (Larsén 1966). We also compare thoracic structures of *C. testaceus* with reductional patterns found in adaphagan and staphylinoid species showing cryptic, subterranean life habits (Luo et al., 2018, 2019). The highly modified thoracic anatomy is then interpreted in the context of the specific myrmecophilous life style of Clavigeritae.

Materials and methods

Studied species

Specimens of *Claviger testaceus* were collected by P. Jałoszyński in Klasztorna Góra ad Prudnik, Poland (08.05.2019). All individuals used in this study were preserved in FAE (formaldehyde-acetic acid-ethanol). For comparative purposes, exoskeletal structures of the thorax were

also studied in six free-living, predatory pselaphine species: *Euplectus karstenii* (Reichenbach, 1816) (Euplectitae: Euplectini), *Trichonyx sulcicollis* (Reichenbach, 1816) (Euplectitae: Trichonychini), *Brachygluta fossulata* (Reichenbach, 1816) (Goniaceritae: Brachyglutini), *Bryaxis bulbifer* (Reichenbach, 1816) (Goniaceritae: Bythinini), *Batrisodes venustus* (Reichenbach, 1816) (Batrisitae: Batrisini), and *Pselaphus heisei* Herbst, 1792 (Pselaphitae: Pselaphini). Specimens of these species were collected in various regions of Poland by P. Jałoszyński and preserved dry-mounted.

Light microscopy

Dissected body parts were cleared briefly in 10% aqueous solution of sodium hydroxide, dehydrated in isopropanol and mounted in Canada balsam, except for entire separated wings, which were studied and photographed as temporary mounts in water. Photographs were taken with a Nikon D7500 camera mounted on an Eclipse Ni compound microscope; image stacks were processed using Helicon Focus v. 6.8.0 (HeliconSoft Ltd.).

Micro-computed tomography (μ CT)

Specimens were transferred from FAE to an ascending series of ethanol (70%–80%–90%–95%–100%), stained in iodine solution, transferred to acetone, and then dried at the critical point (Emitech K850, Quorum Technologies Ltd., Ashford, UK). One dried specimen was scanned at the MPI for the Science of Human History (Jena, Germany) with a SkyScan 2211 X-ray nanotomograph (Bruker, Knotich, Belgium) with an image spatial resolution of 0.68 μ m (isotropic voxel size) using the following parameters: 70 kV, 300 μ A, 3600 ms exposure time, 0.15° rotation steps, frame averaging on (3), and using no filter. Projections were reconstructed by NRecon (Bruker, Knotich, Belgium) into JPG files. The μ CT-scan is stored in the collection of the Phyletisches Museum Jena. Amira 6.1.1 (Thermo Fisher Scientific, Waltham, USA) and VG studio Max 2.0.5 (Volume Graphics, Heidelberg, Germany) were used for the three-dimensional reconstruction and volume rendering.

Scanning electron microscopy (SEM)

The protocol recommended by Schneeberg et al. (2017) was modified to clean the beetles: the specimens were transferred from FAE into 70% ethanol, followed by 0.5% Triton X100 (14 h), 5% KOH (14 h), glacial acetic acid (3 \times 15 min), distilled water (multiple times until the specimens appeared clean), and finally 70% ethanol. Subsequently, they were dehydrated and dried in an Emitech K850 at the critical point. Prior to scanning electron microscopy (SEM), samples were

attached to a rotatable specimen holder (Pohl 2010) or small sample holders and then sputter-coated with gold (Emitech K500; Quorum Technologies Ltd., Ashford, UK). SEM observation and imaging were performed with an FEI (Philips) XL 30 ESEM at 10 kV. Final figure plates were assembled and arranged with Adobe Photoshop CC and Illustrator CS6 (Adobe Inc., California, USA).

Terminology

Thoracic muscles were designated following Larsén (1966), but the muscular terms introduced by Friedrich and Beutel (2008) (see also Beutel et al. [2014]) were added. Different nomenclatures for thoracic muscles were compared and aligned by Friedrich et al. (2009).

Results

Two wing variants were found among studied specimens, both vestigial and non-functional, but differing in the degree of reduction: a longer and transversely folded variant I and a shorter variant II. Descriptions of exoskeletal structures are based on a specimen with wing variant I, with differences in relation to variant II indicated. Internal structures are also illustrated and described based on a specimen with variant I.

Prothorax

Skeleton

The subglobose prothorax forms a compact and strongly sclerotized capsule without visible pronoto-hypomeral edge and hypomeral-prosternal boundary. The pronotum (n1, Figs. 1a, c, 2a, 3a–b) is densely covered with apically bifurcated setae (approx. 40 µm long), most of them with a more or less straight posterior orientation, except a few on the posteriormost area, which point posteromesad; the pronotum is slightly longer along the median line than the maximum width in its middle region; an indistinct narrow bead is present anterolaterally; the posterior side is moderately inflected ventrad; a pair of shallow lateral depressions on the posterior third results in a constriction of the pronotum; the lateral pronotal margins are arcuate anterior to the constriction and moderately widening posterior to it; lateral carinae and transverse basal impressions are absent; the largely smooth outer region of the hypomeron (ohy, Figs. 1c, 2b, d, 3c–d) is slightly convex; it is sparsely covered with minute single-tipped setae on the anterior area and longer setae on the posterior region. The inner region of the hypomeron (ihy, Figs. 2b, d) is fused with the prosternum, and notosternal sutures are lacking. Anteriorly, the prosternum (pst, Figs. 2b, d, 3c) bears a distinct smooth collar, which is gradually narrowing laterally; the slightly raised middle region of the prosternum

displays a reticulate surface pattern; anteriorly it connects with the collar, and posterolaterally it forms a distinct and broad bead enclosing the coxal cavities; dorsolaterally it reaches the posterior pronotal area; short setae are sparsely distributed on the surface. No foveae are present on the prosternum. A pronotosternal joint and procoxal fissures are absent. The postcoxal process (pcp, Fig. 2b) is reduced. A mesospiracular peritreme is not developed. The procoxal cavities (cc1, Figs. 2b, 3c) are separated by a short prosternal carina (psc, Fig. 3f) in the midline, and the procoxal sockets are open posteriorly.

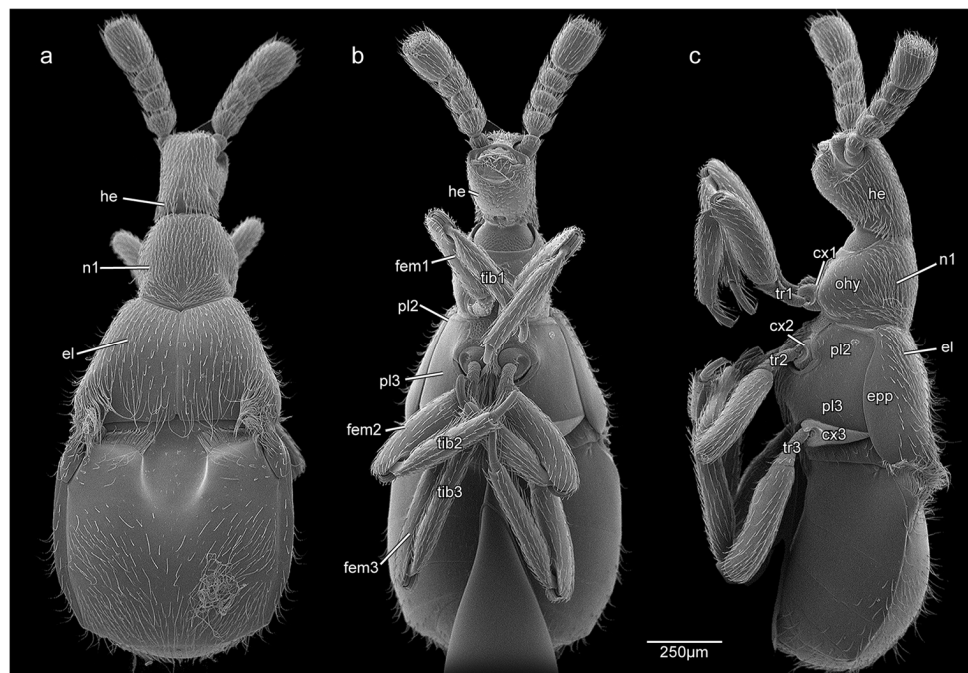
The thin and plate-like profurcal arms (fuc1, Fig. 2d, 3e–f) are vertically emerging from the posterior prosternal margin and basally separated. The protrochantin (fused with cryptopleuron internally) is not exposed and not recognizable as an individual structure. The slightly curved and plate-like cryptopleuron is anterolaterally located within the prothorax; dorsally it reaches only the mid-height of the segment.

The subconical procoxae (cx1, Figs. 1c, 3c) are close to each other medially, with a large concealed lateral extension (ce, Fig. 5d) reaching far into the prothoracic capsule; the proximal area is smooth and the distal part reticulate; a round lateral depression fits with the femur in its elevated position; a lateral keel is missing. The trochanter (tr1, Figs. 1c, 4a) appears bipartite, divided into two regions by a distinct constriction: (1) a glabrous subglobular basal part and (2) a distinctly elongate distal part with several short setae on its reticulate surface. The dorsal and ventral edges of the subparallel femur (fem1, Figs. 1b, 4a) are very slightly curved; its proximal edge articulating with the trochanter is oblique and its distal edge nearly straight, only very slightly rounded; about a proximal third of the femoral surface is reticulate and the remaining distal area smooth; the entire surface bears a regular but sparse vestiture of setae; a distinct distoventral furrow fits with the tibia in its flexed position. The tibia (tib1, Figs. 1b, 4a) is as long as the femur but narrower; it is narrowed and curved proximally, indistinctly narrowed distally, and moderately widened in its middle region; the surface is sparsely setose and lacks robust spines. The tarsus (tar1, Figs. 4a, d) is three-segmented, with the proximal tarsomere (tm1, Fig. 4d) largely hidden below the apical portion of the tibia; the distal tarsomere (tm3, Fig. 4d) is about eight times longer than the middle segment; the tarsomeres bear several long setae, and several additional minute setae are inserted on the distal part of tarsomere 3, which also bears a shallow U-shaped notch distally for the tarsal claw in its abducted position. The single claw (tcl1, Fig. 4d) is short and stout, with a rounded apex. The forelegs excluding the coxa are approximately 1.34-mm long; the ratio of trochanter/femur/tibia/tarsus is 1.67/3.4/3.4/1.

Musculature (Fig. 5)

M1 (M. pronoti primus) [Idlm2], O (= origin): posteromedian pronotal area, right in front of the mesonotum, I (= insertion):

Fig. 1 SEM micrographs of *Claviger testaceus*. **a** dorsal view; **b** ventral view; **c** lateral view. Abbreviations: cx1/2/3, pro-/meso-/metacoxal; el, elytron; epp, epipleuron; fem1/2/3, pro-/meso-/metathoracic femur; he, head; n1, pronotum; ohy, outer region of hypomerion; pl2/3, meso-/metapleuron; tib1/2/3, pro-/meso-/metathoracic tibia; tr1/2/3, pro-/meso-/metathoracic trochanter



dorsolaterally on the cervical membrane; M3 (M. pronoti tertius) [Idlm3], O: anterolateral mesonotal corner, I: dorsolaterally on the cervical membrane, close to the insertion of M1; M4 (M. pronoti quartus) [Idlm5], O: middle pronotal region, I: anterolateral mesonotal corner; M6 (M. prosterni secundus) [Iv1m1], O: dorsal profurcal tip, I: ventrolaterally on the postoccipital ridge; M9 (M. dorsoventralis tertius) [Idvm5], O: lateral pronotal area, mesad the prothoracic hypomerion depression, I: ventrolaterally on the cervical membrane; M10 (M. dorsoventralis quartus) [Idvm2, 3], O: lateral prosternal area, I: dorsolaterally on the postoccipital ridge; M11 (M. dorsoventralis quintus) [Idvm10], O: anterolateral mesonotal corner, I: dorsal area of the profurca; M12 (M. noto-pleuralis) [Itpm3?; homology uncertain] very short, O: anterolateral pronotal area, I: dorsal side of the apical plate of the cryptopleuron; M13 (M. pronotomesepisternalis) [Itpm6], O: posterior pronotal region, I: intersegmental membrane between prothorax and mesothorax; M15 (M. noto-coxalis) [Idvm16, 17], two bundles: M15a, O: posterolateral pronotal area, I: mesal procoxal rim; M15b, O: anterolateral pronotal area, I: dorsolateral tip of the procoxa; M19 (M. furca-coxalis) [Iscm2], O: dorsal profurcal area, I: lateral procoxal rim; M20 (M. pleura-trochanteralis) [Ipcm8], O: ventral side of the apical plate of the cryptopleuron, I: trochanteral tendon.

Pterothorax

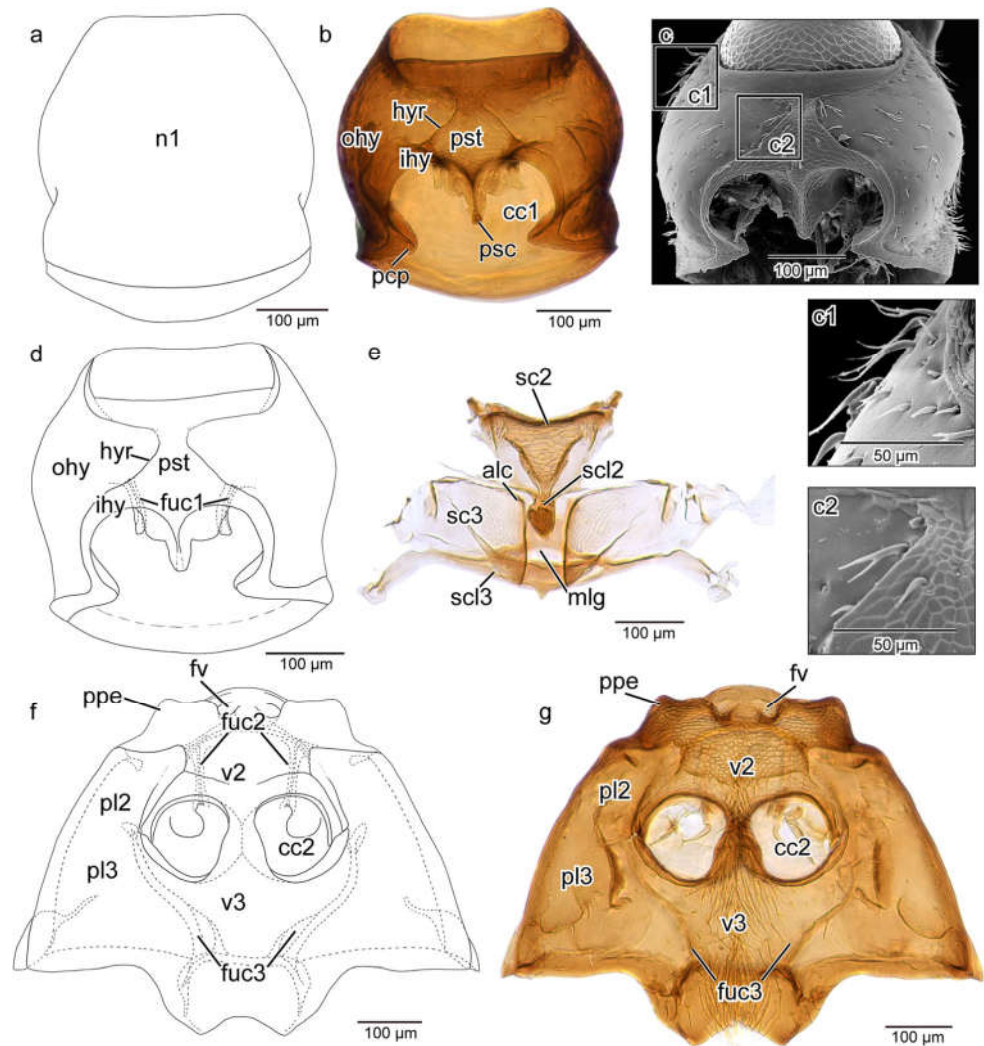
Skeleton

The two pterothoracic segments form an unusually compact structural and functional unit. The lateral and ventral parts of

the meso- and metathorax are rigidly connected, with the anapleural suture separating the ventrites from the anepisternal regions completely obliterated. The pleural sutures separating the anepisternal and epimeral parts are also missing in both segments, and the lateral and ventral segmental borders are also obsolete.

The mesonotum is completely concealed below the elytra. Its main part is a T-shaped sclerite, a product of fusion of the transverse main mesoscutal region (sc2, Figs. 2e, 6a) and the mesoscutellum (sc12, Figs. 2e, 3b) including the posterior triangular mesoscutellar shield; this structure has a scale-like reticular surface; the posterolateral lower mesonotal parts are undifferentiated and unsclerotized, without identifiable notal processes and articulatory elements of the elytra (observation with SEM); the elevated transverse mesoscutal part bears several setae on its anterolateral area; the subtriangular scutellar part forms an acute vertical angle with the remaining sclerite; posteriorly it is elevated just above the median longitudinal groove of the metanotum. The second phragma is vestigial. A short and transverse anterior part of the metanotum is likely the prescutum. The metascutum (sc3, Figs. 2e, 3b, 6a) is by far the largest metanotal element; it is divided by a wide median longitudinal groove (mlg, Figs. 2e, 3b, 6a), delimited by distinct alacristae (alc, Figs. 2e, 3b), which have a scale-like surface structure (Fig. 6a1) and reach the posterior metanotal margin. The short transverse metascutellum (sc13, Figs. 2e, 3b, 6a), separated from the metascutum by a transverse ridge, is medially covered by the alacristae and the enclosed metascutal groove. The third phragma formed by the metapostnotum is present but weakly developed. Axillary sclerites are well-developed and could be clearly identified in “long-winged”

Fig. 2 Line drawings, light-microscopy and SEM images of *C. testaceus*. **a**, prothorax, dorsal view; **b-d** prothorax, ventral view; **e** pterothorax, dorsal view; **f-g**, pterothorax, ventral view. Abbreviations: alc, alacrista; cc1/cc2/cc3, pro-/meso-/metacoxal cavity; cx1/2/3, pro-/meso-/metacoxal; fuc1/2/3, pro-/meso-/metafurca; fv, fovea; he, head; hy, hypomer; hyr, hypomer ridge; ihy, inner region of hypomer; mlg, median longitudinal groove; n1, pronotum; ohy, outer region of hypomer; pcp, postcoxal process; pl2/3, meso-/metapleuron; psc, prosternal carina; pst, prosternum; ppe, prepectus; sc2/3, meso-/metascutum; scl2/3, meso-/metascutellum; v2/3, meso-/metaventrite; w, wing



variant I specimens: axillary sclerite 1 (ax1, Fig. 7a) laterad the anterior notal wing process (anp, Fig. 7a) is posterolaterally attached to axillary sclerite 2 (ax2, Fig. 7a); axillary sclerite 3 (ax3, Fig. 7a) is connected to the posterior notal process (pnp, Fig. 7a). Axillary sclerite 1 (ax1, Fig. 6b) in “short-winged” variant II is similar to that of variant I, whereas axillary sclerite 2 and 3 are not recognizable.

The anteriormost part of the ventral and lateral pterothorax forms a wide prepectus (ppe, Figs. 2f-g, 6c-d) with a reticulated surface pattern. The sclerotized mesopleural region posterior to this collar is largely glabrous and forms a concavity dorsally meeting the elytron. The metanepisternum and metepimeron are fused, but the metapleuron (pl3, Figs. 1b-c, 2f-g, 3c-d, 6c-d) comprises two structurally different portions: (1) a lower part, which is strongly sclerotized and completely visible in ventral view, and (2) an inflected upper part, which is membranous or semimembranous and covered by the elytra. A horizontal lateral plate-like protrusion (Fig. 6d1), densely covered with minute plate-like structures on its ventral side, functions as additional elytral locking device. No external

suture or ridge demarcating the pleuron from the ventrite is visible. The ratio of the length of the mesoventrite (v2, Figs. 2f-g, 3c, 6c) and metaventrite (v3, Figs. 2f-g, 3c, 6c) is approximately 1: 1.5. Setae cover a longitudinal median area, extending to the posteromedian margin of the metaventrite. A pair of oval foveae (fv, Fig. 2f-g) is present in the anteromedian area of the prepectus, and two shallow depressions are situated in front of the mesocoxal cavities; the median area with the reticulate pattern is posteriorly extended to form the anterior margin of the mesocoxal cavities, with a low longitudinal posteromedian carina. The mesocoxal cavities (cc2, Figs. 2f-g, 3c, 6c-d) are distinctly separated medially; a weakly elevated transverse ridge is present on the middle region of the narrowed intercoxal area, which is narrower than the mesocoxal cavity; the mesotrochantin is concealed. The meso- and metaventrite are almost completely fused; a distinct lateral fissure of the middle region of the mesocoxal cavity is possibly a remnant of the segmental border (visible in Fig. 2f). The smooth metaventrite bears few scattered setae laterally and some longer ones on the median area; a pair of obtuse

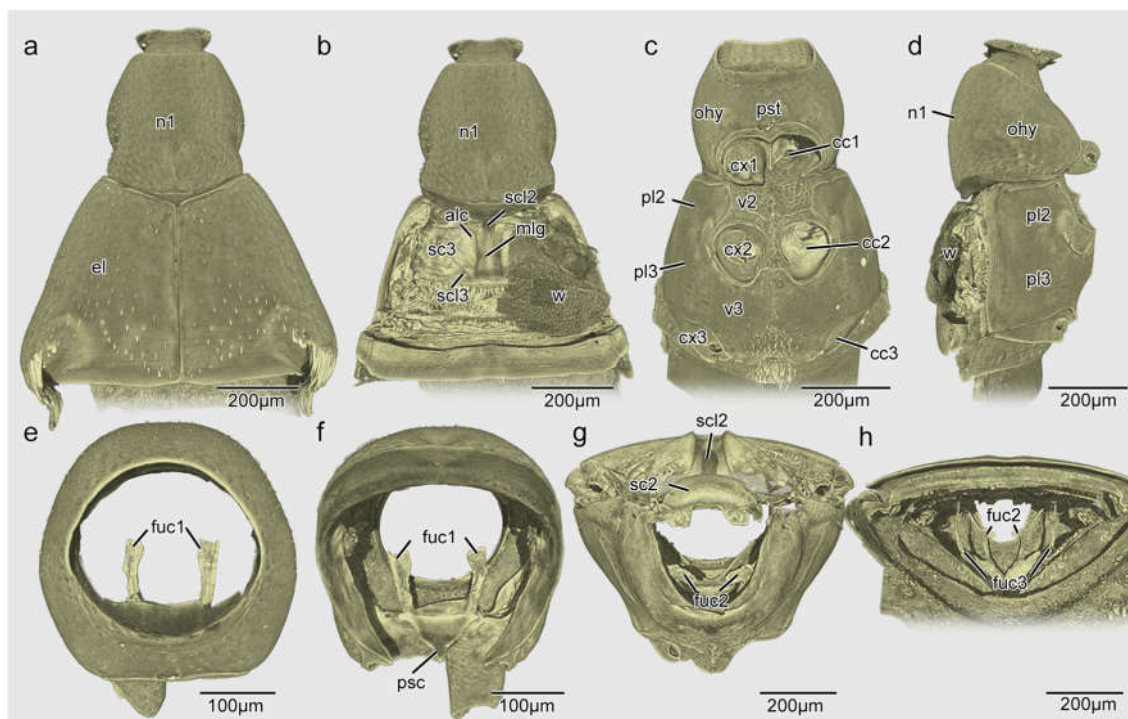


Fig. 3 3D reconstructions of *C. testaceus*. **a** thorax (elytra incl.), dorsal view; **b** thorax (elytra removed), dorsal view; **c** thorax, ventral view; **d** thorax, lateral view; **e** prothorax, anterior view; **f** prothorax, posterior view; **g** pterothorax, anterior view; **h** pterothorax, posterior view. Abbreviations: alc, alacrista; cc1/cc2/cc3, pro-/meso-/metacoxal cavity;

cx1/2/3, pro-/meso-/metacoxxa; el, elytron; fuc1/2/3, pro-/meso-/metafurca; ohy, outer region of hypomerion; mlg, median longitudinal groove; n1, pronotum; pl2/3, meso-/metapleuron; psc, prosternal carina; pst, prosternum; sc2/3, meso-/metascutum; scl2/3, meso-/metascutellum; v2/3, meso-/metaventrte; w, wing

processes on the posteromedian margin forms a reverse V-shaped median emargination. The transverse metacoxal cavities (cc3, Figs. 3c, 6c–d) are distinctly separated from each other.

The well-developed mesofurcal arms (fuc2, Figs. 2f, 3g–h) are basally separated from each other; the basal part is relatively wide and bent anterad; a plate is present in the middle region of each arm; the distal portion of the arms is narrowing towards the dorsolateral region of the segment and ends laterad the mesonotum. The rod-like and sinuate metafurcal arms (fuc3, Figs. 2f–g, 3h) are also basally separated and form a nearly right angle with the ventrite; they taper dorsally and end with a small plate-like tip for muscle attachment close to the metanotum. A low internal anapleural ridge (apr, Fig. 5c) is present laterally; it delimits the boundary between ventrite and pleuron; this structure extends from a site laterad the mesocoxal cavity to the area anterior to the metacoxal cavity.

The trapezoidal elytra (el, Figs. 1a, c, 3a) bear a narrow bead along their anterior margin. Approximately right angles are formed basolaterally (humeral angle) and posteromedially, whereas the posterolateral corner is evenly arcuate and the anteromedian angle obtuse. The elytra are distinctly longer than the pronotum along their mesal edge and also distinctly wider. The setation of the dorsal side of the elytra is less dense than that on the pronotum, and the setae are evenly arranged in longitudinal rows; the setae with bifurcate tips on the anterior

region are distinctly shorter than those with a single tip on the posterior region; the posterolateral corner bears a dense, conspicuous tuft of long setae. No carinae or punctures are present on the dorsal surface, and impunctate impressed striae along the sutural margin are also lacking. The largely glabrous epipleuron (epp, Fig. 1c) is broad and well-visible in ventral view, with a smooth and convex ventral margin; it is gradually widening, reaching the maximum width in the middle area and is then moderately narrowing towards the posterior end; an epipleural keel is missing. The internal surface of the ventral side of the elytra (Fig. 7) is largely smooth and glabrous. The lateral rim is also mostly glabrous, but digitiform structures are present at the anterior corner (Fig. 7f), and low longitudinally arranged ridges (Fig. 7g) are present; the posterior area is covered with scale-like structures, with or without short microtrichia (Fig. 7h, i); the mesal rim is smooth in the middle region but covered with scales on its anterior (Fig. 7k) and posterior (Fig. 7j) areas; a medially protruding lamella (lal, Fig. 7e, 8c, f) originates at the humeral angle; it extends along the lateral rim and is about 2/3 as long; it is inserted onto the membranous inflection of the pleuron. The anteromesal edges of the elytra form a tunnel-shaped cavity covering the mesoscutellar shield.

The hind wings (w, Figs. 3b, 6a, 7b–d) are strongly shortened and non-functional; they show some variability with two distinctly different forms: variant I (Figs. 6a, 7b–d) is a wing

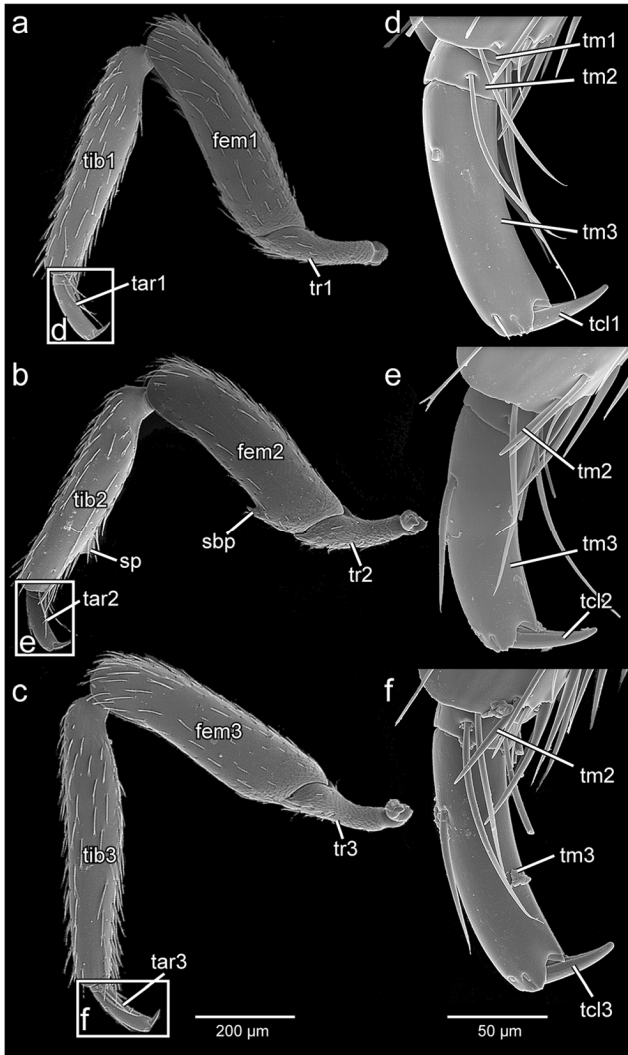


Fig. 4 SEM micrographs, legs of *C. testaceus*. **a** foreleg; **b** midleg; **c** hindleg. Abbreviations: fem1/2/3, pro-/meso-/metathoracic femur; sbp, sub-basal projection; sp, submedian projection; tm1–3, tarsomere 1–3; tar1/2/3, pro-/meso-/metathoracic tarsus; tcl1/2/3, pro-/meso-/metathoracic pretarsal claw; tib1/2/3, pro-/meso-/metathoracic tibia; tr1/2/3, pro-/meso-/metathoracic trochanter

rudiment folded six times transversely, with no longitudinal folds; when folded it is about twice as long as the metanotum (it was not possible to unfold the wing during dissection in water); a relatively large anterior proximal area is sclerotized (Fig. 7c), and the entire wing membrane is very densely covered with long microtrichia, except for two small areas near the wing base; variant II (Fig. 6b1) is barely recognizable as a wing rudiment and shorter than the metanotum; it is irregularly crumpled and folded below the elytron; a proximal sclerotization similar to that of variant I is present; the membranous portion is much shorter but also densely covered with microtrichia.

The general shape of the middle and hind legs (Figs. 1b–c, 4b–c) distad the coxae is similar to that of the forelegs, except for the presence of a ventral sub-basal projection (sbp, Fig. 4b)

on the femur and a ventral submedian projection (sp, Fig. 4b) on the mesotibia of males. The mesocoxa (cx2, Figs. 1c, 3c) is subglobose, without a large internalized part. The middle leg (excluding the coxa) is approximately 1.25-mm long. The ratio of trochanter/femur/tibia/tarsus is around 1.8/3.6/3.8/1. The transverse metacoxae (cx3, Figs. 1c, 3c) bear a well-developed coxal plate with an oblique posterior face. The hind leg (excluding the coxa) is approximately 1.4mm long; the ratio of trochanter/femur/tibia/tarsus is around 1.7/3.3/4.1/1. Tarsomere 1 of the meso- and metatarsi (Figs. 4e, f) appears hidden below the distal tibial margin (in SEM images); tarsomere 1 is well visible (in transparent mounts, not shown here) and similar to that of the protarsus and to tarsomere 2.

Musculature (Fig. 5)

Mesothorax: M28 (*M. mesonoti primus*) [IIdlm1], very weakly developed, O: on the middle region of the highly reduced mesophragma, I: on the prothorax directly laterad the median line; M30 (*M. mesoterni primus*) [IvIm7], O: anterior side of the small mesofurcal plate, I: dorsally on the profurca; M37 (*M. furca-pleuralis*) [IIspm2], very short, O: dorsal tip of the mesofurcal arm, I: on the middle region of the uppermost pleural area; M40 (*M. noto-coxalis*) [IIdvm5, 4?], O: antero-lateral mesonotal corner, I: posterior mesocoxal rim; M41 (*M. episterno-coxalis*) [IIpcm4], O: large part of the mesanepisternal region (anterior pleural area), I: anterior rim of the mesocoxa; M44 (*M. furca-coxalis anterior*) [IIscm1], O: lower part of the mesofurca, posterior to the insertion of M30 on the mesofurcal plate, I: anterior mesocoxal rim; M46 (*M. furca-coxalis posterior*) [IIscm2], O: posterior side of the mesofurcal plate, I: posterior mesocoxal rim; M48 (*M. episterno-trochanteralis*) [IIpcm6] /M49 (*M. epimero-trochanteralis*), O: dorsally on the upper pleural area, I: trochanteral tendon, together with M52; M52 (*M. furca-trochanteralis*) [IIscm6], O: lateral area of the mesofurcal arm, I: trochanteral tendon, together with M48/M49.

Metathorax: M65 (*M. dorsoventralis secundus*)/M66 (*M. dorsoventralis tertius*) [IIIIdvm8], O: posterolateral metanotal area, I: dorsal tip of the metafurcal arm; M71 (*M. pleuralaris*)? [IIItpm9, 7?], O: semimembranous area of the pleural middle region (arguably epimeral part), I: anteriorly close to the wing base (exact attachment site not clearly visible); M72 (*M. sterno-episternalis*) [IIIppm1], wide and flat, O: dorsally along the inflected structure of the largely membranous pleural area (arguably epimeral part), I: ventrally along the internal anapleural ridge; M76 (*M. noto-coxalis posterior*) [IIIIdvm5], O: lateral area of the metanotum, I: posterior metacoxal rim; M77 (*M. episterno-coxalis*) [IIIpcm4], O: inflected sclerotized structure of the pleuron, posterior to the origin of M72, I: anterior metacoxal rim; M81 (*M. furca-coxalis anterior*) [IIIscm1], O: basal metafurcal part, I: anteromedian metacoxal

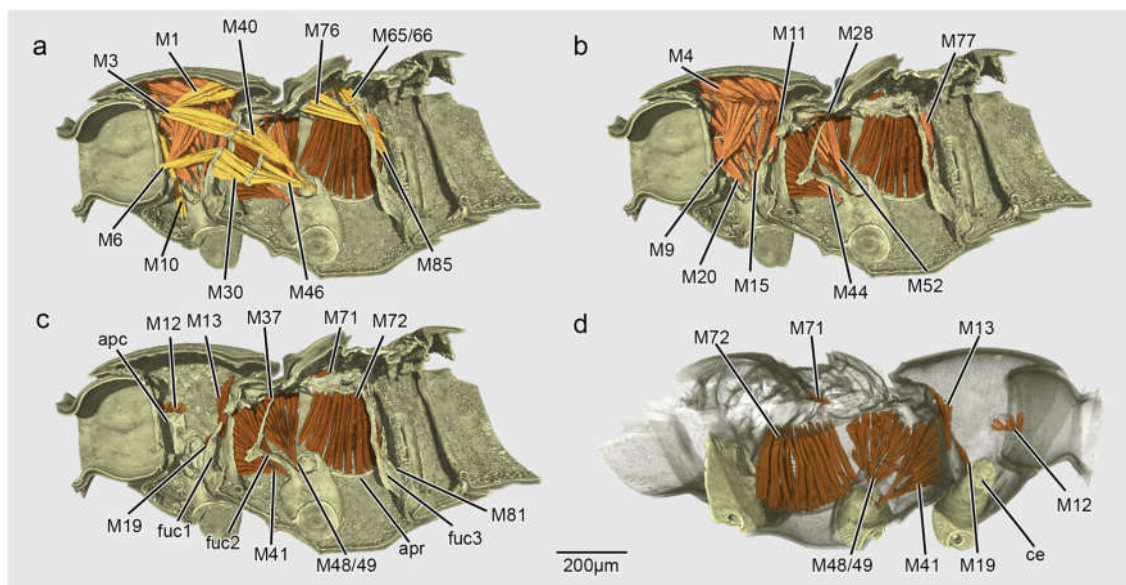


Fig. 5 3D reconstructions of thoracic muscles of *C. testaceus*. **a–c** mesal view; **d** lateral view. Abbreviations: apc, apical plate of the the cryptopleuron; apr, anapleural ridge; ce, concealed lateral extension; fuc1/2/3, pro-/meso-/metafurca. For abbreviations of muscles please see the description

rim; M85 (*M. furca-trochanteralis*) [IIIscm6], O: dorsal tip of the metafurcal arm, I: trochanteral tendon.

Anterior abdominal segments

Skeleton

The abdominal tergites I–III are completely covered by the elytra. Tergites I and II (atI, atII, Fig. 6a) are about equally long and largely membranous; the well-sclerotized tergite III (atIII, Fig. 6a) is distinctly longer than each of them; its anterior part is almost completely covered by low ridges, scales, and short setae, whereas the posterior portion is smooth; a tuft of short setae is present on the lateral margin. Tergite III is posteriorly adjacent with the fused tergites IV–VI. Abdominal sternites I and II are not present as identifiable individual structures, completely membranous and not visible externally. Sternite III (asIII, Fig. 6d) is strongly sclerotized, with an anterior bead forming the posterior margin of the metacoxal cavity; posteriorly it is attached to sternite IV (asIV, Figs. 6d, 8); a dense tuft of long setae is present on the median area of sternite III, and some additional setae are sparsely distributed on the lateral regions.

Musculature (Fig. 9)

All muscles of the anterior abdominal segments described here have a longitudinal orientation; some additional small bundles or fibers are present but could not be clearly identified with our data set. Ma1, O: anterior margin of tergite I; I: fold between tergite I and II; Ma2, O: broadly on the fold between

tergites I and II; I: fold between tergites II and II; Ma3, O: fold between tergites II and III; I: posterior phragma of abdominal tergite III; Ma4, O: along the metafurcal edge, ventrally near the base and dorsally reaching about 2/3 of the entire length of the furca, I: region of the strongly reduced abdominal sternite I; Ma5, O: ventrally on the region of the reduced abdominal sternite I, I: region of the membranous abdominal sternite II; Ma6, O: region of abdominal sternite II, I: posterior margin of abdominal sternite III.

Discussion

Phylogenetic background

Pselaphinae were for a long time regarded as a separate family (e.g., Akre and Hill 1973), but were convincingly identified as a subgroup of the megadiverse Staphylinidae (e.g., Newton and Thayer 1995). Newton and Thayer (1995) presented a comprehensive morphological study of the Omaliine group, one of the major lineages of rove beetles, also including Protopselaphinae and Pselaphinae as sister taxa. They emphasized a high level of homoplasy and events of parallel evolution in different subunits (Table 1). One important apomorphic feature of the Omaliine group is (1) the absence of the suture separating the mesoventrite and mesopleuron (Character 61 of Newton and Thayer 1995 [in the following abbreviated as N&Th]). Several potential synapomorphies of the Pselaphine lineage (i.e., Neophoninae, Dasycerinae, Protopselaphinae, and Pselaphinae), a subunit of the Omaliine group, were suggested by Newton and Thayer

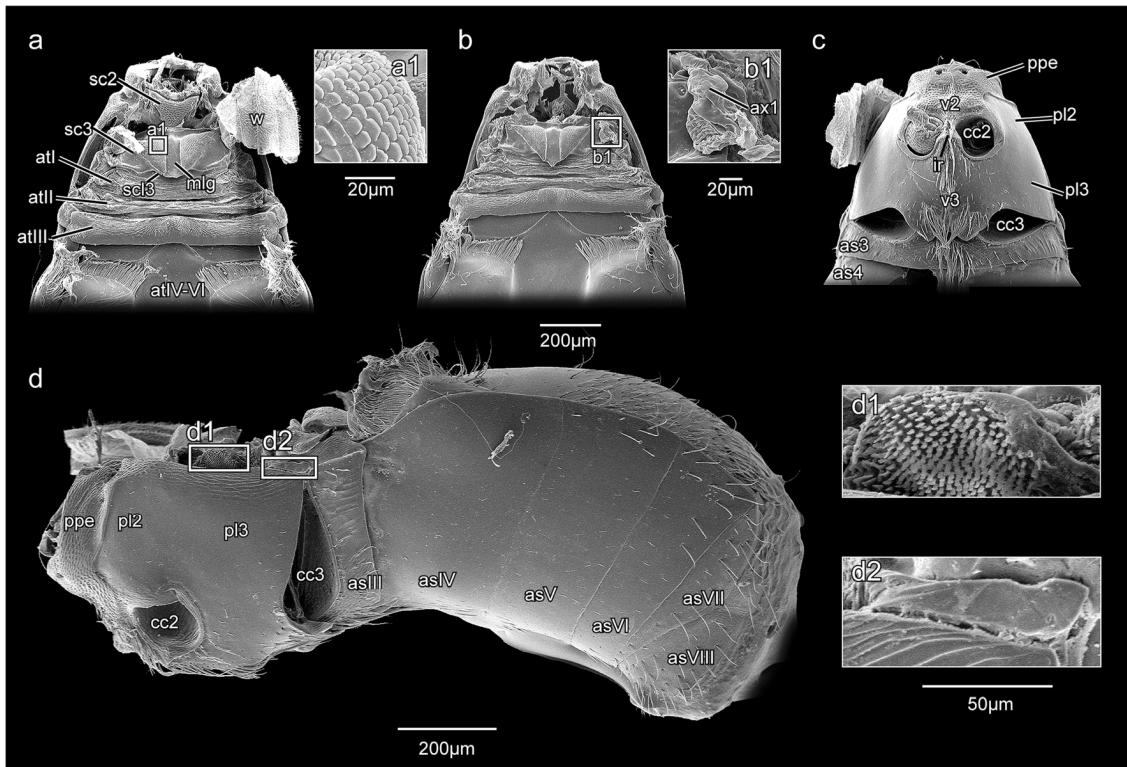


Fig. 6 SEM micrographs, pterothorax of *C. testaceus*. **a** “long-winged” (variant I) individual, dorsal view; **b** “short-winged” (variant II) individual, dorsal view; **c** ventral view; **d** lateral view. Abbreviations: asIII - VIII, abdominal sternite III - VIII; atI - VI, abdominal tergites I - VI; ax1,

axillary sclerite 1; cc2/cc3, pro-/meso-/metacoxal cavity; mlg, median longitudinal groove; pl2/3, meso-/metapleuron; ppe, prepectus; sc2/3, meso-/metascutum; scl2, mesoscutellum; v2/3, meso-/metaventricle

(1995): (2) a reduced or lacking suture laterally separating the meso- and metaventricle (Fig. 2f: complete absence, but a partly developed suture is visible in some pselaphines, e.g., Figs. S3a, b, d) (Ch. 60 N&Th), (3) an external protibial edge without spines (Fig. 4a) (Ch. 78 N&Th), and (4) three-segmented tarsi (Fig. 4) (Ch. 80 N&Th).

A clade strongly supported by thoracic features is Protopselaphinae + Pselaphinae (Newton and Thayer 1995). Potential synapomorphies are the following: (5) the loss of the lateral pronotal carina (Fig. 1c) (Ch. 51 N&Th), (6) the complete absence of the membranous pronoto-prosternal connection (Fig. 1c) (Ch. 55 N&Th), (7) the closed procoxal fissure and completely concealed trochantin (Figs. 2b–d) (Ch. 56 N&Th), (8) procoxae without keel (Fig. 3c) (Ch. 57 N&Th), (9) a strongly reduced or absent postcoxal process (Figs. 2b–d: strongly reduced) (Ch. 58 N&Th), (10) elytra without rows of punctures (Fig. 1a) (Ch. 69 N&Th), and (11) tarsal empodia without setae (Fig. 4) (Ch. 82 N&Th).

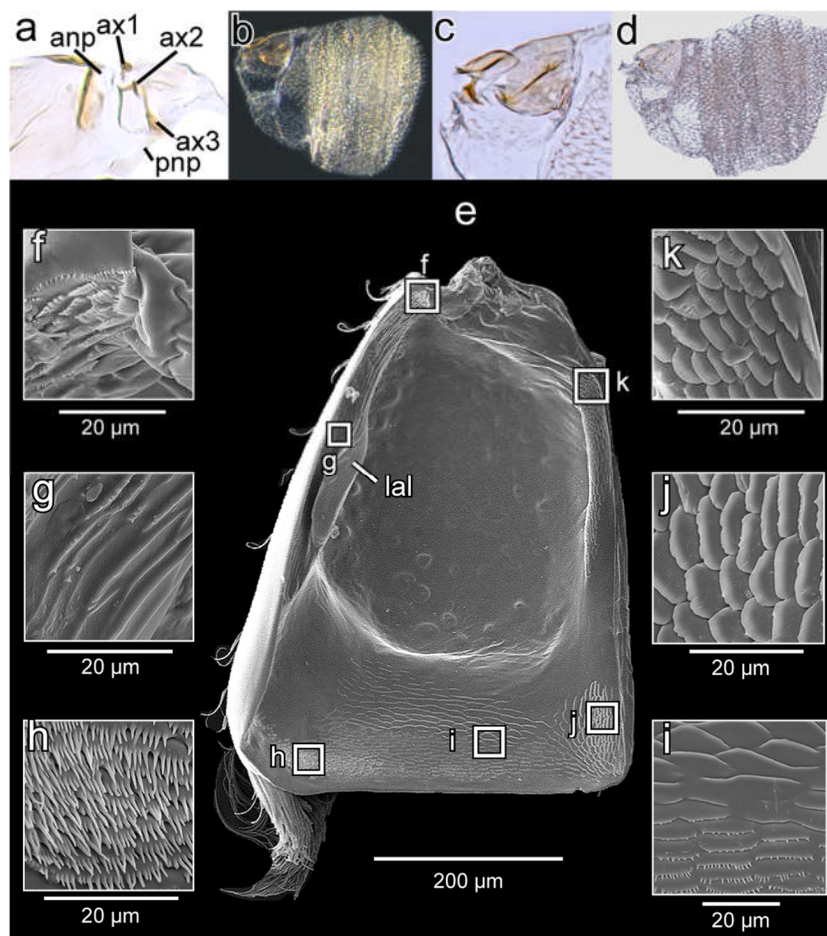
One thoracic apomorphy of the latter group is mentioned by Newton and Thayer (1995): (12) mesoventrite with foveae (Fig. 2f–g) (Ch. 5 N&Th). This feature is also present in Clavigeritae, although the foveae are distinctly reduced in *Claviger* compared with those of other studied pselaphines (cf. Fig. S3), only visible as a pair of shallow concavities on the anteromedian region of the mesoventrite (fv, Fig. 2f, g).

Obviously, several changes that took place in the early evolution of the subfamily do not remain constant in the supertribe Clavigeritae. An additional structural simplification was interpreted as potential synapomorphy of Pselaphinae excluding Faronitae by Newton and Thayer (1995): (13) the absence of the mesopleural ridge (“sulcus”) (Fig. 6d) (Ch. 63 N&Th).

Even though Clavigeritae are obviously highly specialized, the group is not characterized by a single unique and non-homoplasious thoracic apomorphy. Even the conspicuous elytral trichomes can be absent in some members of this group (e.g., Hlaváč 2005). Nevertheless, the monophyly appears well-supported by several derived thoracic features: (16) secondary absence of foveae on the metaventricle (Figs. 1b, 6c) (Ch. 6 N&Th), (17) absence of the transverse antebasal pronotal impression (Fig. 1a) (Ch. 53 N&Th), (18) absence of the suture separating the mesepimeron from the metaventricle (Fig. 6d) (Ch. 65 N&Th), (19) elytra with a straight apex or evenly arcuate near the lateral margin (Fig. 1a, 7e) (Ch. 71 N&Th), (20) the presence of only a single claw (Fig. 4) (Ch. 81 N&Th), and (21) a long mesotrochanter (Fig. 4b) (Ch. 84 N&Th), with the entire femoral base distinctly separated from the coxal cavity.

Characters 55, 56, 60, 61, 63, and 65 of Newton and Thayer (1995) (corresponding to chars. 6, 7, 2, 1, 13, and 18 in the text above and Table 1) are part of an evolutionary trend

Fig. 7 Hind wings of variant I **a–d**, in dorsal view and elytra **e–k**, in ventral view of *C. testaceus*. Abbreviations: anp, anterior notal process; ax1–3, axillary sclerite 1–3; lal, lateral lamella; pnp, posterior notal process



in the Omaliine group, leading to different degrees of fusion and an increasing mechanical stabilization of the thorax in several stages, and apparently reaching a maximum in Clavigeritae. Obviously, these features did not evolve as adaptations to myrmecophily, as they also occur in groups lacking this specialized life style. However, a compact and robust thorax was likely a pre-adaptation for an association with ants. It was obviously advantageous for myrmecophiles, offering improved mechanical protection (Parker 2016a).

An interesting feature of the prothorax is the long and concealed lateral extension of the procoxa (ce, Fig. 5d), a modification that has apparently evolved independently in several pselaphine groups including Clavigeritae and also in other subfamilies of Staphylinidae outside of the Omaliine group (e.g., Steninae, Euaesthetinae, Osoriinae [part.] (Lawrence and Ślipiński 2013; Thayer 2016). It is conceivable that this contributes to the general mechanical protection of the thorax. However, the precise functional background is largely unclear at present.

The ventral prothoracic configuration of *C. testaceus* is similar to what is found in other (free-living and predatory) pselaphines (Fig. S1), with open procoxal cavities and the prosternum fused with the hypomera. However, it differs in

the absence of foveae. The ventral prothoracic foveae occurring in Pselaphinae are typically situated in front of the procoxal cavities and/or on a lateral longitudinal hypomeral groove found in many species (Fig. S3a–e). The hypomeral groove is absent in *Claviger* (Fig. 2b–d) and also in *Pselaphus* (Fig. S1f), a member of Pselaphitae, which in recent phylogenetic analyses consistently clusters together with Clavigeritae (Parker 2016b; Parker and Grimaldi 2014). However, the groove is also absent in Protopselaphinae, arguably in this case a plesiomorphic condition. Apparently, the presence or absence of this concavity varies strongly within the group. It is likely absent in the groundplan of Protopselaphinae + Pselaphinae and may have been acquired and secondarily lost several times in the latter group. A feature of the prothorax of *Claviger* distinguishing it from that of other pselaphines is the expansion of the anterior half of the hypomera towards the midline, thus distinctly narrowing the prosternal area (Fig. 2c–d). As a prosternum fully separated from the hypomera by notosternal sutures (as in Fig. 10a) is part of the groundplan of Coleoptera (e.g., Beutel and Haas 2000) and very likely also of Staphylinidae (Newton and Thayer 1995), a scenario can be proposed to explain transformations leading to the condition observed in *Claviger* (Fig. 10a–d). In the first stage,

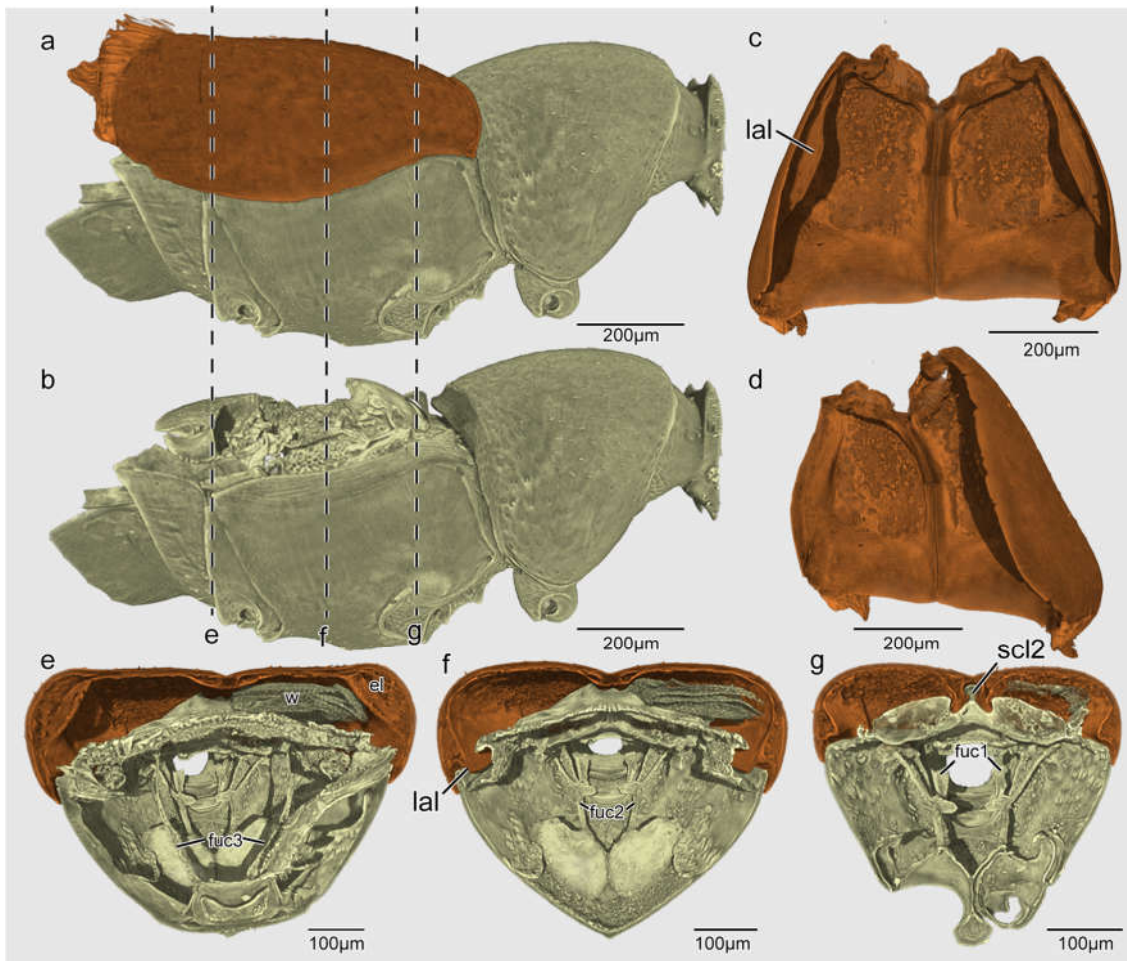


Fig. 8 3D reconstruction of *C. testaceus*. **a–b** thorax, lateral view; **c–d** elytra; **e–g** thorax, posterior view. Abbreviations: el, elytron; fuc1/2/3, pro-/meso-/metafurca; lal, lateral lamella; scl2, mesoscutellum; w, wing

hypomeral ridges develop, which reinforce the prothorax mechanically (Fig. 10b); this process results in a division of the hypomera into an outer part (ohy, Fig. 10b), which is continuous with the lateral and dorsal pronotum, and a narrow longitudinally extending inner part (ihy, Fig. 10b). In the next step, the notosternal sutures (or connecting membranes) are reduced and the prosternum fuses with the inner hypomeral part on both sides (Fig. 10c); this condition is typical for Pselaphinae, but the notosternal sutures are reduced to various degrees, and hypomeral ridges can be also found among non-related scydmaenines (e.g., Jałoszyński 2020); vestiges of notosternal sutures occur in species of both subfamilies, either visible in transparent mounts only (internalized notosternal sutures; irns, Fig. S1a) or as short notches on the anteroventral prothoracic margin (e.g., Jałoszyński 2018). As a final transformation, the mesally expanding hypomera distinctly narrow the prosternal region (Fig. 10d), a process resulting in the unusual condition seen in *C. testaceus* (Figs. 2c–d).

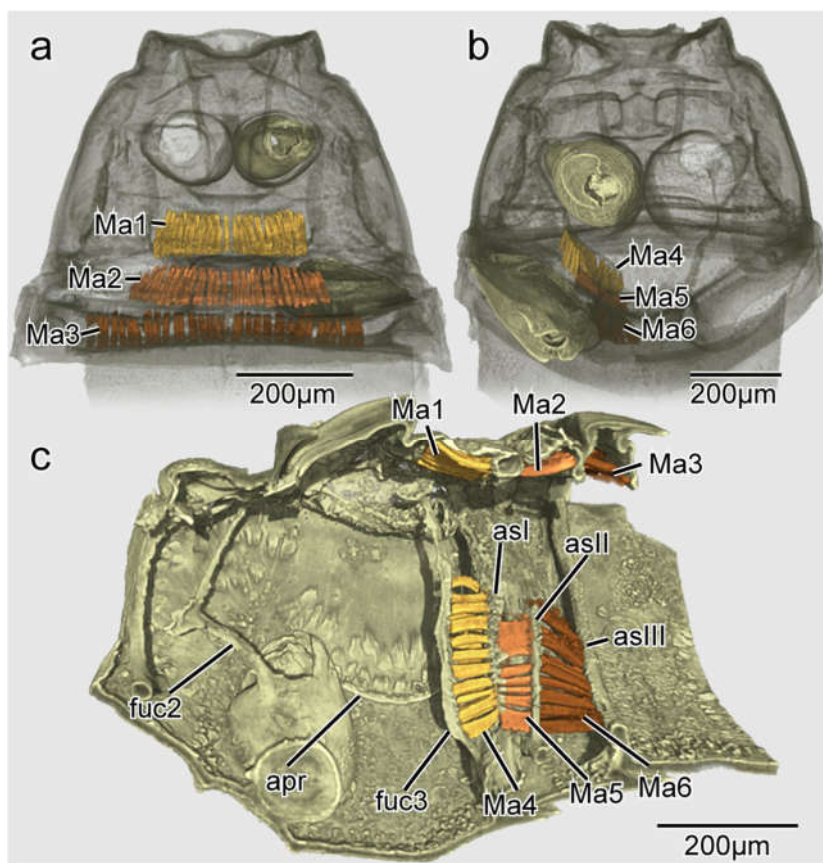
The presently available data on internal skeletal structures and muscles of Pselaphinae are too scarce for a systematic evaluation. Some information on skeletal elements was

provided by Lawrence and Ślipiński (2013). Nomura (1991) described the pro- and mesofurcae in the *Batrisocenus* complex of the supertribe Batrisitae, which are similar to the homologous structures of *C. testaceus*, and therefore possibly close to the groundplan condition in the subfamily. The metafurcae of *Batrisцениоla semipunctulata* (Raffray, 1909) and *Batrisoschema euplectiforme* (Sharp, 1883) were not explicitly described in text but were illustrated with line drawings (Nomura 1991: Fig. 18A, B). As they converge basally and lack a median plate extending from the arms, they differ distinctly from the metafurca of *C. testaceus*. The internal anapleural ridge delimitating the metaventrite and metapleuron was not documented for any pselaphine species so far.

Musculature

This first detailed anatomical investigation of a pselaphine species revealed some interesting traits of the thoracic musculature. It is obvious that multiple muscle losses or partial reductions observed in *C. testaceus* are more or less directly

Fig. 9 3D Reconstruction of longitudinal abdominal muscle. Abbreviations: apr, anapleural ridge; asI - III, abdominal sternite I - III; fuc2/3, meso-/metafurca; For abbreviations of muscles see description



linked to flightlessness, with the exception of the weakly-developed M28 (*M. mesonoti primus*). The homology of the presumptive M71 (*M. pleura-alaris*) remains ambiguous, due to far-reaching skeletal modifications. The almost complete loss of direct flight muscles is obviously linked with profound simplifications of skeletal elements linked with flight, for instance, the absence of the basalar muscle disc or a defined subalare. The presence of a single bundle likely equivalent with combined muscles M65/M66 is a feature shared with the cave-dwelling leiodid *Troglocharinus ferreri* (Reitter, 1908) (Luo et al. 2019), apparently a result of parallel evolution related to flightlessness. It is noteworthy that *C. testaceus* lacks more dorsal and ventral muscles (M2 and M5 in the prothorax, M62 in the metathorax) than *T. ferreri* (Luo et al. 2019). This is arguably linked with the increased mechanical compactness of the prothorax and pterothorax. Another derived feature is the fusion of M48 and M49, likely associated with the fusion of anepisternal and epimeral elements in the mesothorax of *C. testaceus*. A comparison of the thoracic musculature of three species of Staphylinioidea is presented in Table 2, including the cryptic and flightless *C. testaceus* and *T. ferreri* (Leiodidae) (Luo et al. 2019), and the unspecialized, large, diurnal predator *Creophilus maxillosus* (Linnaeus, 1758) (Staphylininae) (Larsén 1966).

Elytral locking system and flightlessness

Elytral fixation mechanisms are a specific and complex characteristic of Coleoptera. The locking devices formed by the mesoscutellar shield and the metanotal alacristae (Klima 1983) are very likely a groundplan feature of the Order (Friedrich et al. 2009). A remarkable array of additional fixation devices has evolved within the group, especially frictional surfaces, a character system evaluated in detail in the family Tenebrionidae (Gorb 1998).

An extreme case of mechanical strengthening of the elytral body cover occurs in the “diabolically ironclad beetle” *Nosoderma diabolicum* LeConte (Zopheridae, Tenebrionoidea) (Rivera et al. 2020). Another unique and enhanced type of locking system has evolved in Pselaphinae, arguably a key feature in the evolution of this successful subfamily. The involved structures of *Batrisocenus* complex (Batrisitae) were documented by Nomura (1991), suggesting a general similarity with the condition observed in the species we examined. The most noteworthy features observed in *C. testaceus* are the following: (1) well-developed lateral elytral lamella (lal, Fig. 7e) interacting with the inflected semimembranous pleural area; (2) a tunnel-shaped structure formed by the mesal elytral bases and enclosing the elevated mesoscutellar shield (Fig. 8g); and (3) the distinct anterolateral

Table 1 Phylogenetically informative thoracic characters of supertribe Clavigeritae extracted from Newton and Thayer (1995), with updated morphological nomenclature. Numbers in round brackets indicate the state of traits in the original text; abbreviations in square brackets: UFC: unique forward change; HFC: homoplasious forward change; HR: homoplasious reversal, forward changes are from state 0 to 1 to 2 and reversal changes follow the opposite order (eg. state 2 to state 1); group numbers I to VII are from higher to lower level of taxonomic categories

Characters	Groups
1. Ch. 61. Suture separating mesoventrite from mesopleuron (“mesanepisternum” in original text) absent or represented at most by a solid suture in posterior region 1/3 (1) [UFC].	I. Omaliine group
2. Ch. 60. Suture separating mesoventrite from metaventrite absent laterally or entirely missing (1) [HFC];	II. Pselaphine lineage
3. Ch. 78. External protibial edge without spines (1) [HFC];	
4. Ch. 80. Tarsi three-segmented (2) [UFC].	
5. Ch. 51. Pronotum without lateral carina (1) [HFC];	III. Protopselaphinae + Pselaphinae
6. Ch. 55. Pronoto-prosternal membranous connection completely absent (2) [HFC];	
7. Ch. 56. Procoxal fissure closed, trochantin completely concealed in ventrolateral view (2) [UFC];	
8. Ch. 57. Procoxae without keel (1) [HFC];	
9. Ch. 58. Pronotal postcoxal process strongly reduced or absent (1) [HFC];	
10. Ch. 69. Elytron without numerous rows of punctures (1) [HFC];	
11. Ch. 82. Tarsal empodia without setae (2) [HFC].	IV. Pselaphinae
12. Ch. 5. Foveae on mesoventrite present (1) [HFC].	V. Pselaphinae excluding Faronitae
13. Ch. 63. Mesopleural ridge (“sulcus”) absent (2) [UFC].	VI. Pselaphitae, Clavigeritae
14. Ch. 66. Metacoxae separated by more than 0.1 coxal width (1) [HFC];	
15. Ch. 68. Elytron without epipleural keel (1) [HFC].	
16. Ch. 6. Foveae on metaventrite absent (0) [HR];	VII. Clavigeritae
17. Ch. 53. Pronotum without transverse antebasal impression (0) [HR];	
18. Ch. 65. Suture separating mesepimeron from metaventrite absent (2) [HFC];	
19. Ch. 71. Elytron with apex straight or evenly arcuate near lateral margin (0) [HR];	
20. Ch. 81. Tarsal claw 1 (2) [HFC];	
21. Ch. 84. Mesotrochanter long, with entire femoral base distinctly separated from coxal cavity (1) [HFC].	

process of the elytra corresponding to the anterior concavity of the dorsal side of the mesothorax (Fig. 7e). We did not observe differences in these features between individuals with the variants I and II of wing reduction. It is very likely that this is due to an advanced stage of flight loss in both cases, when even the less reduced type of wings is non-functional and occupies only a small space below the elytra. The set of elytral locking mechanisms is a complex suite of apomorphies not described in any other groups of beetles so far. However, at present, data for closely related taxa are insufficient for a systematic evaluation.

Loss of flight is a common phenomenon in Coleoptera (Smith 1964). Flightless beetles can show only a simple degeneration of tissue of indirect flight muscles like in Amphizoidae (Beutel 1988), or various muscular reductions (Larsén 1966) and skeletal simplifications, including a complete loss of wings and different associated structures (Luo et al. 2018, 2019). Only few anatomical studies on the thorax of flightless beetles are available. However, it appears that the pattern of muscle losses varies only slightly, with the loss of large indirect flight muscles followed by the reduction of the smaller direct muscles in more advanced forms (Larsén 1966, Luo et al. 2018, 2019). Remarkably, the whirligig beetle *Orectochilus villosus* O.F. Müller shows a high degree of muscle reduction in the metathorax but has retained its ability to fly (Liu et al. 2018).

Wings may be polymorphic within populations of the same species, with the occurrence of macropterous and brachypterous individuals (e.g., Smith 1964; in Pselaphinae see e.g., Nomura 1991). Distinct skeletal simplifications observed in cave-dwelling Carabidae and Leiodidae (e.g., Peck 1973: Fig. 7) indicate irreversibility of the wing reduction (e.g., Luo et al. 2018, 2019). Unlike in the flightless and eyeless *Sinaphaenops wangorum* Ueno & Ran, 1998 (Carabidae) and *Troglocharinus ferreri* (Leiodidae), or in scydmaenines of the tribe Mastigini (Jałoszyński 2018), the metanotum of *C. testaceus*, a crucial element of the flight apparatus, shows only a minor degree of reduction. It is distinctly shortened in relation to the mesonotum and compared with the metanota of winged pselaphines belonging to other supertribes (Fig. 2e vs. Fig. S2a-f) but has still retained most of its structural elements. Other skeletal structures such as the pterothoracic phragmata, metanotal wing processes, and pleural muscle discs are distinctly or completely reduced. Three-dimensional reconstructions of *C. testaceus* revealed a distinctly reduced metathoracic muscle system. According to Hlaváč (2005), anophthalmous species of Clavigeritae of the northern temperate regions are always unable to fly and never actively leave their host’s colonies, in contrast to tropical relatives with functional compound eyes and wings. Consequently, the far-reaching reduction of flight muscles and some skeletal elements of the flight apparatus in *C. testaceus* is not surprising.

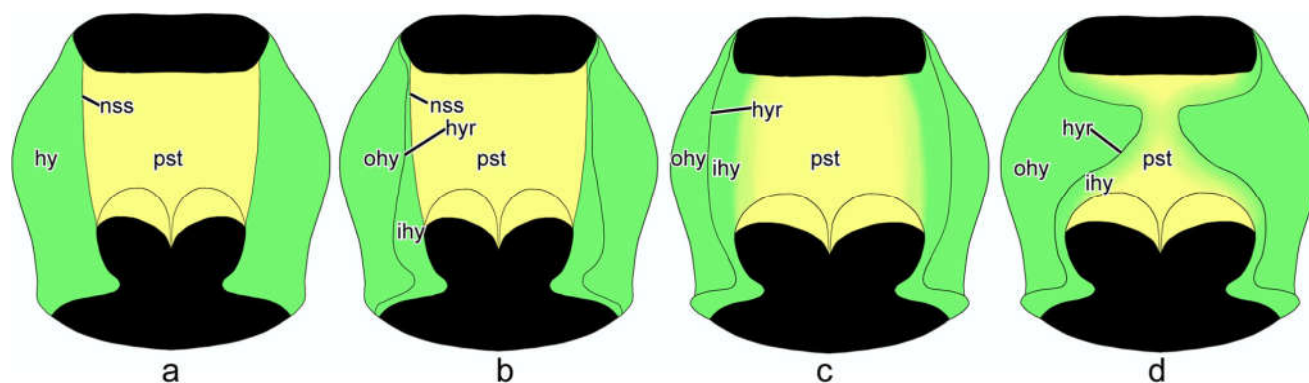


Fig. 10 Hypothetical steps in the evolution of the prothorax in *Claviger*, ventral view. **a** groundplan (prosternum separated from undivided hypomera by complete notosternal sutures); **b** hypomera subdivided by hypomeral ridges (inner portion of hypomeron thickened, reinforces adcoxal region); **c** prosternum fused with hypomera (notosternal sutures

obliterated); **d** *Claviger* (hypomeral ridges strongly bent mesad, prosternum narrowed medially). Abbreviations: hy, hypomeron; hyr, hypomeral ridge; ihy, inner region of hypomeron; nss, notosternal suture; ohy, outer region of hypomeron; pst, prosternum

However, that some flight-related structures remain relatively well-developed, like the metanotum, and that vestigial wings still occur, indicates that the mechanism of reduction is genetically not completely fixed yet and may therefore be the result of a relative young evolutionary process.

Myrmecophilous habits

Due to their greatly reduced mouthparts, *C. testaceus* and related species rely on feeding by host ant workers (Akre and Hill 1973; Hermann 1982). Profound myrmecophilous adaptations related to the mouthparts and other cephalic structures of *Claviger* were a subject of a separate study (Jałoszyński et al., 2020).

Despite of lacking defensive glands, myrmecophilous pselaphine species can permanently live and reproduce in ant colonies (Parker 2016a). One modification facilitating myrmecophilous habits of *C. testaceus* and related species is size reduction. Small or very small body size (usually 1–3 mm in Pselaphinae) can play an important role in association with ant hosts (Parker 2016a), facilitating transportation of eyeless and flightless beetles by workers (Hermann 1982) and making it easier to move inside the ant nest tunnels.

Another character complex is an unusually compact and robust thorax and abdomen. In *C. testaceus* this adaptation includes an internalized prothorax and partially internalized procoxa, the high degree of fusion of the pterothoracic segments, and the lack of sutures separating the lateral pleural sclerites from the ventrites. The lack of thoracic sutures and the highly compacted segments make the beetles less vulnerable to attacks by ant workers using their mandibles. This also applies to the short legs with their thickened cuticle, with flattened tibiae, and shortened tarsi, considered as a common feature in myrmecophilous beetles, likely reducing the risk of losing limbs in interaction with host ants (Parker 2016a). Additionally, the highly complex elytral interlocking

mechanism enhances the protection of the less-sclerotized dorsal parts of the pterothorax and anterior abdomen. Unlike in many other small beetles (e.g., Scydmaeninae), the elytra of *C. testaceus* are not easy to separate from the thorax during dissection. In beetles with strongly convex elytra, pressure applied from above often results in separating the elytra and exposing the delicate dorsal pterothorax and anterior abdomen. The dorsally flattened elytra of *C. testaceus* likely reduce this risk. Not only the interlocking mechanisms are relevant in this context, but also the ventrally deflexed, broad epipleura, which effectively clasp the sides of the thorax. This ensures that the elytra stay in place when an ant grasps this body region, and vulnerable structures beneath them remain well protected. The same function can be ascribed to the heavily sclerotized and fused postelytral abdominal segments, where the attention of host ants is directed by trichomes, from which workers lick appeasement secretions (Hill et al. 1976; Cammaerts 1974, 1977).

Foveae on the surface, which are common in Pselaphinae (e.g., Chandler 2001), are almost entirely absent in *C. testaceus* (except for a pair of somewhat reduced ones on the anteromedian region of the mesoventrite) and also occasionally missing in other pselaphine subgroups (e.g., Parker and Maruyama 2013). The abdomen of species of Clavigeritae is certainly not as flexible as, for instance, in ant-associated Aleocharinae (Parker 2016a: Fig. 4).

We assume that the increased rigidity of the abdomen of Clavigeritae (Jeannel 1950: Fig. 23) provides improved protection against ants. However, it is likely that this is linked with a drastically reduced movability of this unusually short and broad tagma. It was pointed out by Blum (1979) that shortened elytra, correlated with a highly movable abdomen, are a characteristic feature of rove beetles, linked with the presence of diagonally crossed abdominal muscles. He found this condition in different groups of Staphylinidae, with the notable exception of

Table 2 Thoracic musculature of four species of Staphylinidae, one species of Hydrophilidae, one species of Caraboidea. Species names follow by “1” are flightless and “2” are capable of flying. Muscle numbers refer to Larsén (1966) and Friedrich and Beutel (2008), respectively. “+” = present, “-” = absent, “?” = unclear, MFR (“Muscles related to flight reduction”) are muscles where the loss is related with flightlessness according to Larsén (1966) (muscular data extracted from Beutel and Komarek, 2004; Larsén 1966 and Luo et al. 2018, 2019)

	Friedrich and Beutel (2008)	<i>Claviger testaceus</i> ¹	<i>Troglucharinus ferreri</i> ¹	<i>Creophilus maxillosus</i> ²	<i>Nicrophorus vespillo</i> ²	<i>Helophorus aquaticus</i> ²	<i>Sinaphaenops wangorum</i> ¹	Notes
M01 (M. pronoti primus)		+	+	+	+	+	+	
M02 (M. pronoti secundus)	Idm2	-	+	+	+	+	+	
M03 (M. pronoti tertius)	Idm1	+	-	-	-	-	-	
M04 (M. pronoti quartus)	Idm3	+	+	+	+	+	+	
M05 (M. prosterni primus)	Idm5	-	+	+	+	+	+	
M06 (M. prosterni secundus)	Ivlm3	+	+	+	+	+	+	
M07 (M. dorsoventralis primus)	Ivlm1	-	+	+	+	+	+	
M08 (M. dorsoventralis secundus)	Ivlm6	-	+	+	+	+	+	
M09 (M. dorsoventralis tertius)	Idvm8	+	+	-	-	-	-	
M10 (M. dorsoventralis quartus)	Idvm5	+	+	+	+	+	+	
M11 (M. dorsoventralis quintus)	Idvm2, 3	+	+	+	+	+	+	
M12 (M. noto-pleuralis)	Idvm10	+	+	+	+	+	+	
M13 (M. pronotomesepisternalis)	Ipm3?	+	+	+	+	+	+	
M14 (M. noto-trochantinalis)	Ipm6	-	+	+	+	+	+	
M15 (M. noto-coxalis)	Idvm13	+	+	+	+	+	+	
M16 (M. episterno-coxalis)	Idvm16, 17	-	+	+	+	+	+	
M17 (M. epimero-coxalis)	Ipcm4	-	+	+	+	+	+	
M18 (M. sterno-coxalis)	Idvm18	-	+	-	-	- (?)	-	
M19 (M. furca-coxalis)	Iscm1	-	+	-	-	-	-	
M20 (M. pleura-trochanteralis)	Iscm2	+	+	-	-	-	-	
M28 (M. mesonoti primus)	Ipcm8	+	+	+	+	+	+	
M29 (M. mesonoti secundus)	Idlm1	-	-	+	+	+	+	MFR
M30 (M. mesosterni primus)	Idlm2	-	-	+	+	+	+	MFR
M31 (M. mesosterni secundus)	Ivlm7	+	+	+	+	+	+	
M32 (M. dorsoventralis)	Ivlm9	-	-	+	+	+	+	
M33 (M. noto-pleuralis)	Idvm8	-	-	+	+	+	+	
M34 (M. noto-epimeralis)	Itpm2	-	-	-	-	-	-	
M35 (M. epimero-subalaris)	Itpm10?	-	-	+	+	+	+	
M36 (M. pleura-alaris)	Itpm10	-	-	+	+	+	+	
M37 (M. furca-pleuralis)	Itpm7, 9	-	-	+	+	+	+	
M38 (M. profurca-mesepisternalis)	Ispm2	+	-	-	-	-	-	
M39 (M. noto-trochantinalis)	Ispm6	-	-	-	-	-	-	
M40 (M. noto-coxalis)	Idvm2	-	-	-	-	-	-	
M41 (M. episterno-coxalis)	Idvm5, 4?	+	+	+	+	+	+	
M42 (M. coxa-basalaris)	Ipcm4	+	+	+	+	+	+	
M43 (M. coxa-subalaris)	Ipcm3	-	-	+	+	+	+	
M44 (M. furca-coxalis anterior)	Idvm6	-	-	-	-	-	-	
M45 (M. furca-coxalis lateralis)	Iscm1	+	+	+	+	+	+	
M46 (M. furca-coxalis posterior)	Iscm4	-	-	+	+	+	+	
M47 (M. noto-trochanteralis)	Iscm2	+	+	+	+	+	+	
M48 (M. episterno-trochanteralis)	Idvm7	-	-	-	-	-	-	
M49 (M. epimero-trochanteralis)	Ipcm6	+	+	+	+	+	+	
M50 (M. trochantero-basalaris)	? Ipcm5	-	+	-	-	-	-	

Table 2 (continued)

Larsén (1966)	Friedrich and Beutel (2008)	<i>Claviger testaceus</i> ¹	<i>Troglodytes ferrerii</i> ¹	<i>Creophilus maxillosus</i> ²	<i>Nicrophorus vespillo</i> ²	<i>Helophorus aquaticus</i> ²	<i>Sinaphaenops wangorum</i> ¹	Notes
M51 (M. sterno-trochanteralis)	?	-	-	-	-	-	-	
M52 (M. furca-trochanteralis)	Ilscm6	+	-	-	+	+	-	MFR
M60 (M. metanoti primus)	Illdm1	-	-	+	+	+	-	
M61 (M. metanoti secundus)	Illdm2	-	-	+	+	+	-	
M62 (M. metasterni primus)	IvIm3	-	+	+	+	+	+	
M63 (M. metasterni secundus)	IvIm5	-	-	-	-	-	-	
M64 (M. dorsoventralis primus)	Illdvm1	-	-	+	+	+	-	
M65 (M. dorsoventralis secundus)	Illdvm8	+	+	+	+	+	+	
M66 (M. dorsoventralis tertius)	Illdvm8	-	-	+	+	+	-	
M67 (M. pleural-praealaris)	Iltpm2	-	-	+	+	+	-	MFR
M68 (M. noto-pleuralis)	Iltpm6	-	-	+	+	-	+	
M69 (M. noto-basalaris)	Iltpm3	-	-	+	+	+	-	MFR
M70 (M. epimero-subalaris)	Iltpm10	-	-	+	+	+	-	MFR
M71 (M. pleura-alaris)	Iltpm9, 7	+	-	+	+	+	-	MFR
M72 (M. sterno-episternalis)	Ilppm1	+	+	+	+	+	-	
M73 (M. sterno-basalaris)	Ilspm1	-	-	+	+	+	-	
M74 (M. noto-trochantinalis)	Illdvm2	-	-	+	+	-	-	MFR
M75 (M. noto-coxalis anterior)	Illdvm4	-	-	+	+	+	-	MFR
M76 (M. noto-coxalis posterior)	Illdvm5	+	+	+	+	+	-	
M77 (M. episterno-coxalis)	Ilpcm4	+	-	+	+	+	+	
M78 (M. coxa-basalaris)	Ilpcm3	-	-	+	+	+	-	
M79 (M. coxa-subalaris)	Illdvm6	-	-	+	+	+	-	
M80 (M. sterno-coxalis)	Ilscm7?	-	+	-	-	-	-	MFR
M81 (M. furca-coxalis anterior)	Ilscm1	+	+	+	+	+	+	
M82 (M. furca-coxalis lateralis)	Ilscm4	-	-	+	+	+	-	
M83 (M. furca-coxalis posterior)	Ilscm2	-	+	+	+	+	+	
M84 (M. noto-trochanteralis)	Illdvm7	-	-	-	-	+	-	
M85 (M. furca-trochanteralis)	Ilscm6	+	+	+	+	+	+	

Omaliinae, a group with exceptionally long elytra compared with other subfamilies. His sampling did not include members of Pselaphinae, by that time still considered as a separate family. However, even though we did not examine the posterior abdominal segments, our findings suggest that the movability is reduced to a minimum in *Claviger*, and very likely also in related groups. The parallel-sided longitudinal muscles of the proximal abdomen probably allow for limited vertical movements, but torsions of the tagma can be excluded with certainty. Functional consequences outlined by Blum (1979) are the lacking ability to fold and clean the wings using the abdomen. However, this is irrelevant in the case of the flightless *Claviger*. Considering the systematic position of Pselaphinae, it is likely that the high abdominal movability and diagonally crossed muscles were secondarily reduced within the subfamily. It is conceivable this was not the case in Faronitae with a comparatively long abdomen or also in *Protopselaphus*, but anatomical data are completely lacking for these groups. The abdominal muscles remain also unstudied in other staphylinid subfamilies characterized by short or long abdomens, with a limited ability of lateral and dorso-ventral movements (e.g., Micropeplinae or Osoriinae).

Conclusions

In summary, a remarkable degree of morphological modification of the thorax (and other body parts) of Clavigeritae leads to an optimization of intimate associations with ants, keeping the ecological coexistence stable and sustainable. Parts of the morphological syndrome making specialized staphylinid beetles well able to cope with the challenging life in ant colonies evolved in several steps. This occurred long before myrmecophilous habits were established in subordinate groups within the Omaliine lineage.

Supplementary Information The online version contains supplementary material available at <https://doi.org/10.1007/s13127-021-00484-1>.

Acknowledgments We are very grateful to PD. Dr. Hans Pohl (FSU Jena) for his assistance with the preparation of SEM samples. The first author wants to express his thanks to CSC (No. 201708440281). The second author is indebted to Miłosz Mazur (University of Opole, Poland) for organizing a field trip on which *C. testaceus* was collected, and Dr. Rafał Ruta (University of Wrocław, Poland) for his help with collecting the beetles. We are also grateful for helpful comments made by an anonymous reviewer and Prof. Dr. Michael Ohl (Naturkundemuseum Berlin), and to Dr. Margaret Thayer (Field Museum, Chicago) and Prof. Dr. Alexey Polilov (Moscow State University) for providing literature.

Funding Open Access funding enabled and organized by Projekt DEAL. CSC (No. 201708440281).

Data availability The datasets generated during and/or analyzed during the current study are available from the corresponding author on reasonable request.

Compliance with ethical standards

Conflict of interest The authors declare that they have no conflict of interest.

Open Access This article is licensed under a Creative Commons Attribution 4.0 International License, which permits use, sharing, adaptation, distribution and reproduction in any medium or format, as long as you give appropriate credit to the original author(s) and the source, provide a link to the Creative Commons licence, and indicate if changes were made. The images or other third party material in this article are included in the article's Creative Commons licence, unless indicated otherwise in a credit line to the material. If material is not included in the article's Creative Commons licence and your intended use is not permitted by statutory regulation or exceeds the permitted use, you will need to obtain permission directly from the copyright holder. To view a copy of this licence, visit <http://creativecommons.org/licenses/by/4.0/>.

References

- Akre, R. D., & Hill, W. B. (1973). Behavior of *Adranes taylori*, a myrmecophilous beetle associated with *Lasius sitkaensis* in the Pacific northwest (Coleoptera: Pselaphidae; Hymenoptera: Formicidae). *Journal of the Kansas Entomological Society*, 46, 526–536.
- Baehr, M. (1975). Skelett und Muskulatur des Thorax von *Priacma serrata* Leconte (Coleoptera, Cupedidae). *Zeitschrift für Morphologie der Tiere*, 81(1), 55–101.
- Beutel, R. G. (1988). Studies of the metathorax of the trout-stream beetle, *Amphizoa lecontei* Matthews (Coleoptera: Amphizoidae): Contribution towards clarification of the systematic position of Amphizoidae. *International Journal of Insect Morphology and Embryology*, 17(1), 63–81.
- Beutel, R. G., Friedrich, F., Ge, S. Q., & Yang, X. K. (2014). *Insect morphology and phylogeny: A textbook for students of entomology*. Berlin: De Gruyter.
- Beutel, R. G., & Haas, F. (2000). Phylogenetic relationships of the suborders of Coleoptera (Insecta). *Cladistics*, 16(1), 103–141.
- Beutel, R. G., & Komarek, A. (2004). Comparative study of thoracic structures of adults of Hydrophiloidea and Histeroidea with phylogenetic implications (Coleoptera, Polyphaga). *Organisms, Diversity and Evolution*, 4(1–2), 1–34.
- Blum, P. (1979). Zur Phylogenie und ökologischen Bedeutung der Elytrenreduktion und Abdomenbeweglichkeit der Staphylinidae (Coleoptera). Vergleichend-und funktionsmorphologische Untersuchungen. *Zoologische Jahrbücher für Anatomie*, 102, 533–582.
- Cammaerts, R. (1973). Etude histologique du système glandulaire tégumentaire du Coléoptère myrmécophile *Claviger testaceus* Preyssl (Pselaphidae). Proceedings of the 7th international congress of IUSSI, London: 56–61.
- Cammaerts, R. (1974). Le système glandulaire tégumentaire du coléoptère myrmécophile *Claviger testaceus* Herbst, 1792 (Pselaphidae). *Zeitschrift für Morphologie und Ökologie der Tiere*, 77, 187–219.
- Cammaerts, R. (1977). Secretions of a beetle inducing regurgitation in its host ant. *Proceedings of the 8th International Congress of the International Union for the Study of Social Insects*, Wageningen, 295.

- Cammaerts, R. (1992). Stimuli inducing the regurgitation of the workers of *Lasius flavus* (Formicidae) upon the myrmecophilous beetle *Claviger testaceus* (Pselaphidae). *Behavioural Processes*, 28, 81–95.
- Cammaerts, R. (1995). Regurgitation behavior of the *Lasius flavus* worker (Formicidae) towards the myrmecophilous beetle *Claviger testaceus* (Pselaphidae) and other recipients. *Behavioural Processes*, 34, 241–264.
- Cammaerts, R. (1996). Factors affecting the regurgitation behaviour of the ant *Lasius flavus* (Formicidae) to the nest beetle *Claviger testaceus* (Pselaphidae). *Behavioural Processes*, 38, 297–312.
- Chandler, D. S. (2001). *Biology, morphology and systematics of the ant-like litter beetle genera of Australia (Coleoptera: Staphylinidae: Pselaphinae)*. Memoirs on entomology, international volume 15. Gainesville: Florida, Associated Publishers.
- Donisthorpe, H. (1927). *The guests of British ants: Their habits and life histories*. London: George Routledge & Sons.
- Fikáček, M., Beutel, R. G., Cai, C., Lawrence, J. F., Newton, A. F., Solodovnikov, A., Yamamoto, S. (2020). Reliable placement of beetle fossils via phylogenetic analyses—Triassic *Leehermania* as a case study (Staphylinidae or Myxophaga?). *Systematic Entomology*, 45(1), 175–187.
- Friedrich, F., & Beutel, R. G. (2008). The thorax of *Zorotypus* (Hexapoda, Zoraptera) and a new nomenclature for the musculature of Neoptera. *Arthropod Structure & Development*, 37, 29–54.
- Friedrich, F., Farrell, B. D., & Beutel, R. G. (2009). The thoracic morphology of Archostemata and the relationships of the extant suborders of Coleoptera (Hexapoda). *Cladistics*, 25, 1–37.
- Gorb, S. N. (1998). Frictional surfaces of the elytra-to-body arresting mechanism in tenebrionid beetles (Coleoptera: Tenebrionidae): Design of co-opted fields of microtrichia and cuticle ultrastructure. *International Journal of Insect Morphology and Embryology*, 27(3), 205–225.
- Hermann, H. R. (1982). *Social insects volume 3*. New York, San Francisco, London: Academic press.
- Hill, W. B., Akre, R. D., & Huber, J. D. (1976). Structure of some epidermal glands in the myrmecophilous beetle *Adranes taylori* (Coleoptera: Pselaphidae). *Journal of the Kansas Entomological Society*, 49, 367–384.
- Hlaváč, P. (2005). *Thysdariella*, a new genus of the myrmecophilous supertribe Clavigeritae (Coleoptera: Staphylinidae, Pselaphinae) from Madagascar. *The Coleopterists Bulletin*, 59(3), 304–309.
- Jałoszyński, P. (2018). World genera of Mastigitae: Review of morphological structures and new ecological data (Coleoptera: Staphylinidae: Scydmaeninae). *Zootaxa*, 4453(1), 1–119.
- Jałoszyński, P. (2020). *Aenigmaphes* gen. n., a new glandulariine genus of the Australian region (Coleoptera: Staphylinidae: Scydmaeninae). *Zootaxa*, 4731(3), 439–446.
- Jałoszyński, P., Luo, X.-Z., & Beutel, R. G. (2020). Profound head modifications in *Claviger testaceus* (Pselaphinae, Staphylinidae, Coleoptera) facilitate integration into communities of ants. *Journal of Morphology*, 281(9), 1072–1085.
- Jeannel, R. (1950). Coléoptères psélaphides. *Faune de France*, 53, 1–421.
- Klima, J. (1983). Die Gesperre der Käfer-Elytren und deren phylogenetische Bedeutung. *Berichte des naturwissenschaftlichen medizinischen Vereins in Innsbruck*, 70, 155–165.
- Larsén, O. (1966). On the morphology and function of locomotor organs of the Gyrinidae and other Coleoptera. *Opuscula Entomologica Supplementum*, 30, 1–241.
- Lawrence, J. F., & Ślipiński, S. A. (2013). *Australian Beetles* (Vol. 1). Collingwood: CSIRO Publishing.
- Liu, S. P., Wipfler, B., & Beutel, R. G. (2018). The unique locomotor apparatus of whirligig beetles of the tribe Orectochilini (Gyrinidae, Coleoptera). *Journal of Zoological Systematics and Evolutionary Research*, 56(2), 196–208.
- Luo, X. Z., Antunes-Carvalho, C., Ribera, I., & Beutel, R. G. (2019). The thoracic morphology of the troglobiontic cholevine species *Troglocharinus ferreri* (Coleoptera, Leioididae). *Arthropod Structure & Development*, 53, 100900.
- Luo, X. Z., Wipfler, B., Ribera, I., Liang, H. B., Tian, M. Y., Ge, S. Q., & Beutel, R. G. (2018). The thoracic morphology of cave-dwelling and free-living ground beetles from China (Coleoptera, Carabidae, Trechinae). *Arthropod Structure & Development*, 47, 662–674.
- Newton, A. F., & Thayer, M. K. (1995). Protopselaphinae new subfamily for *Protopselaphus* new genus from Malaysia, with a phylogenetic analysis and review of the Omaliine Group of Staphylinidae including Pselaphidae (Coleoptera). In J. Pakaluk & A. Ślipiński (Eds.), *Biology, phylogeny, and classification of Coleoptera: Papers celebrating the 80th birthday of Roy a. Crowson* (pp. 221–320). Warszawa: Muzeum i Instytut Zoologii PAN.
- Nomura, S. (1991). Systematic study on the genus *Batrisoplisus* and its allied genera from Japan (Coleoptera, Pselaphidae). *Esakia*, 30, 1–462.
- Parker, J. (2016a). Myrmecophily in beetles (Coleoptera): Evolutionary patterns and biological mechanisms. *Myrmecological News*, 22, 65–108.
- Parker, J. (2016b). Emergence of a superradiation: pselaphine rove beetles in mid-Cretaceous amber from Myanmar and their evolutionary implications. *Systematic Entomology*, 41, 541–566.
- Parker, J., & Grimaldi, D. A. (2014). Specialized myrmecophily at the ecological dawn of modern ants. *Current Biology*, 24, 2428–2434.
- Parker, J., & Maruyama, M. (2013). *Jubogaster towai*, a new Neotropical genus and species of Trogastrini (Coleoptera: Staphylinidae: Pselaphinae) exhibiting myrmecophily and extreme body enlargement. *Zootaxa*, 3630, 369–378.
- Peck, S. B. (1973). A systematic revision and the evolutionary biology of the *Ptomaphagus* (*Adelops*) beetles of North America (Coleoptera: Leioididae; Catopinae), with emphasis on cave-inhabiting species. *Bulletin of the Museum of Comparative Zoology at Harvard College*, 145, 29–162.
- Pohl, H. (2010). A scanning electron microscopy specimen holder for viewing different angles of a single specimen. *Microscopy Research and Technique*, 73, 1073–1076.
- Rivera, J., Hosseini, M. S., Restrepo, D., Murata, S., Vasile, D., Parkinson, D. Y., Barnard, H. S., Arakaki, A., Zavattieri, P., & Kisailus, D. (2020). Toughening mechanisms of the elytra of the diabolical ironclad beetle. *Nature*, 586(7830), 543–548.
- Schneeberg, K., Bauernfeind, R., & Pohl, H. (2017). Comparison of cleaning methods for delicate insect specimens for scanning electron microscopy. *Microscopy Research and Technique*, 80, 1199–1204.
- Smith, D. S. (1964). The structure and development of flightless Coleoptera: A light and electron microscopic study of the wings, thoracic exoskeleton and rudimentary flight musculature. *Journal of Morphology*, 114(1), 107–183.
- Thayer, M. K. (2016). Staphylinidae Latreille, 1802. In: Beutel, R.G., Leschen, R.A.B. (Volume eds.), Coleoptera, beetles. Volume 1: Morphology and systematics (Archostemata, Adephaga, Myxophaga, Polyphaga partim). In Handbook of Zoology (pp. 394–442). Walter de Gruyter Berlin.
- Weide, D., & Betz, O. (2009). Head morphology of selected Staphylinidae (Coleoptera: Staphyliniformia) with an evaluation of possible groundplan features in Staphylinidae. *Journal of Morphology*, 270, 1503–1523.
- Weide, D., Thayer, M. K., & Betz, O. (2014). Comparative morphology of the tentorium and hypopharyngeal-premental sclerites in sporophagous and non-sporophagous adult Aleocharinae (Coleoptera: Staphylinidae). *Acta Zoologica*, 95, 84–110.
- Weide, D., Thayer, M. K., Newton, A. F., & Betz, O. (2010). Comparative morphology of the head of selected sporophagous and non sporophagous aleocharinae (Coleoptera: Staphylinidae):

- Musculature and hypopharynx prementum complex. *Journal of Morphology*, 271, 910–931.
- Yavorskaya, M. I., Beutel, R. G., Farisenkov, S. E., & Polilov, A. A. (2019). The locomotor apparatus of one of the smallest beetles—the thoracic skeletomuscular system of *Nephanes titan* (Coleoptera, Ptiliidae). *Arthropod Structure & Development*, 48, 71–82.
- Yin, Z. W., Kurbatov, S. A., Cuccodoro, G., & Cai, C. Y. (2019). *Cretobrachygluta* gen. Nov., the first and oldest Brachyglutini in mid-Cretaceous amber from Myanmar (Coleoptera: Staphylinidae: Pselaphinae). *Acta Entomologica Musei Nationalis Pragae*, 59(1), 101–106.

Publisher's note Springer Nature remains neutral with regard to jurisdictional claims in published maps and institutional affiliations.

3.8 Study VIII

Subterranean or blind beetles (Leiodidae) have no improved antennal sensory equipment compared to their epigean or sighted relatives. [In preparation]

Xiao-Zhu Luo, Mariam Gabelaia, Arnaud Faille, Rolf Beutel, Ignacio Ribera, Benjamin Wipfler

Abstract: The subterranean realm is well-known for ecological factors like constant darkness, constant temperature and humidity, and scarcity of resources. It is usually assumed that subterranean animals compensate their lack of eyes with transformations of other sensorial structures, especially the antennae with their rich array of sensilla. To test this hypothesis, 38 species of Leiodidae (Coleoptera) with or without eyes and dwelling in various environments were selected, and types, arrangement and density of antennal sensilla documented and compared. Statistical analyses carried out after correcting effects of body size yielded the following results: (1) the number of sensilla does not differ among different ecological groups; (2) the density of sensilla is lower in blind or hypogean species than in sighted or epigean ones; (3) the length and diameter of antennal sensilla of blind or hypogean species does not differ significantly from sighted or epigean ones. Our finding based on studied leiodid species clearly refutes widely accepted earlier interpretations, showing that sensilla patterns are scarcely affected in subterranean beetles if at all, and even less dense in eyeless species. Our results provide a new facet of evolution toward the darkness in beetles.

Conceptualization: X.Z. Luo, I. Ribera, R. G. Beutel

Visualization: X.Z. Luo, I. Ribera

Measurement and statistical analysis: X.Z. Luo, M. Gabelaia

Writing-original draft: X.Z. Luo, M. Gabelaia, A. Faille, R. G. Beutel, B. Wipfler

Writing-review & editing: X.Z. Luo, M. Gabelaia, A. Faille, R. G. Beutel, B. Wipfler

Funding acquisition: X.Z. Luo, I. Ribera

Estimated own contribution: 60%

Subterranean or blind beetles (Leiodidae) have no improved antennal sensory equipment compared to their epigean or sighted relatives.

Xiao-Zhu Luo^{1,2,§,*}, Mariam Gabelaia^{3,§}, Arnaud Faille⁴, Rolf Beutel¹, Ignacio Ribera^{2,†}, Benjamin Wipfler^{3,*}

¹ Institut für Zoologie und Evolutionsforschung, Friedrich-Schiller-Universität Jena, Jena, Germany

² Institute of Evolutionary Biology (CSIC-Universitat Pompeu Fabra), Barcelona, Spain

³ Zoologisches Forschungsmuseum Alexander Koenig, Adenauerallee 160, 53117 Bonn, Germany

⁴ Department of Entomology, Coleoptera, Stuttgart State Museum of Natural History, Stuttgart, 70191, Germany

* corresponding authors: xiaozhu.luo@uni-jena.de & benjamin.wipfler@leibniz-zfmk.de

§ contributed equally

† the present work is dedicated to the late Ignacio Ribera

Abstract: The subterranean realm is well-known for ecological factors like constant darkness, constant temperature and humidity, and scarcity of resources. It is usually assumed that subterranean animals compensate their lack of eyes with transformations of other sensorial structures, especially the antennae with their rich array of sensilla. To test this hypothesis, 38 species of Leiodidae (Coleoptera) with or without eyes and dwelling in various environments were selected, and types, arrangement and density of antennal sensilla documented and compared. Statistical analyses carried out after correcting effects of body size yielded the following results: (1) the number of sensilla does not differ among different ecological groups; (2) the density of sensilla is lower in blind or hypogean species than in sighted or epigean ones; (3) the length and diameter of antennal sensilla of blind or hypogean species does not differ significantly from sighted or epigean ones. Our finding based on studied leiodid species clearly refutes widely accepted earlier interpretations, showing that sensilla patterns are scarcely affected in subterranean beetles if at all, and even less dense in eyeless species. Our results provide a new facet of evolution toward the darkness in beetles.

Key words: beetles, hypogean, leaf-litter, adaptation

Introduction

Dark and humid subterranean systems are highly specialized habitats for various forms of life [1-3]. The reduced food resources, limited space and overall stability of the cave environment makes the inhabitants of these ecosystems ideal model organisms for various fields of research, including adaptive processes, ecological adaptations, changes in the circadian rhythm, or human diseases such as albinism or autisms [1, 4-7]. Another major reason for the attractiveness of troglobiotic or hypogean animals for solving basic evolutionary and ecological questions are their uniform and widely found adaptations towards the dark and confined environment that comprise reduced or completely absent eyes, the loss of pigmentation, and the elongation of legs and other appendages (in the case of insects and other arthropods the antennae). The cave adaptations that are summarized under the term troglomorphy evolved various times independently in various underground groups of animals [8-11]. To compensate for the loss of visual information, elongate sensory appendages evolved in troglobionts. This can increase the number of tactile and olfactory sensors that help in orientation and in finding food or potential mates. This concept of sensory compensation in blind organisms dates back to Darwin's "On the origin of species" that states that "natural selection will often have affected other changes, such as increase in the length of the antennae or palpi, as a compensation for blindness" [12] and is today common text book knowledge [8-10, 13-17].

The most successful lineage of organisms in terms of the total species number but also troglobiotic specialists are insects [13, 18, 19]. The reduction of the compound eyes in this group is compensated by the elongation of the antennae and an increase and elongation of sensilla on it according to earlier and current interpretations [2, 8, 10, 13, 14]. The antennae of insects are composed of the basal scapus and pedicellus, and the flexible flagellum, which is almost always by far the longest antennal element [20]. The scapus is the only segment with intrinsic muscles and the pedicellus contains a chordotonal organ (Johnston's organ). The flagellum is composed of several or many segments in all adult insects, and usually bears most of the sensorial structures (Fig. 1). The antennal vestiture is usually mostly formed by hair-like structures, articulated setae, but variously shaped sensilla can fulfill different tasks including tactile, olfactory, humidity-sensitive or chemoreceptor functions [21-23]. The assumption that subterranean or hypogean insects have more and longer sensilla on their antennae is widely accepted in text books (e.g. [2, 8-10, 13, 19]), even though only few original studies have investigated this phenomenon in a quantitative way (e.g. [24-26]).

These studies used a limited number of species and did neither correct the retrieved data for body size nor for phylogenetic constraints.

We therefore studied the relations between the length of the antennal segments and their sensory equipment for 38 epigean and hypogean species of round fungus beetles (Leiodidae), and evaluated the retrieved data in a statistical context that also accounts for the body size and phylogeny of the studied animals. With about 800 described subterranean species in various sub-lineages, Leiodidae are the second largest radiation of subterranean insects [13, 27-29] after the ground beetles (Carabidae). They have been used in several studies about morphological, physiological and ecological cave adaptations (e.g. [30-32]).

Materials and methods

Animals: The present study is based on 38 species of Leiodidae from four tribes: Anemadini, Cholevini, Leptodirini and Ptomaphagini. Supplementary table 1 provides a detailed list of the studied species including their source and collection accession number. The body length of the species is provided in supplementary table 2.

Antennal segments and sensilla: Leiodids generally have nine flagellomeres (Fig. 1A), a groundplan feature of Coleoptera (e.g. Beutel et al. 2014). The present study compares the sensilla on the flagellomeres V-VIII (Fig. 1A). These were chosen as the number of sensilla increases on the distal segments [33]; Fig. 1A). We thus expected them to be more informative than the basal ones. The apical flagellomere (IX on Fig. 1A) was excluded as it is so densely covered with setae that the individual sensilla cannot be properly separated. Following Peck [24], who studied the antennal sensilla in the leiodid genus *Ptomaphagus*, we distinguished between furrowed and smooth setae. Furrowed or fluted sensilla bear longitudinal grooves and belong to the general category of sensilla chaetica (blue in Fig. 1) sensu [24]. The second type are sensilla with a smooth surface (red in Fig. 1) that resemble typical sensilla basiconica sensu Peck [24]. The sensilla were identified and counted on flagellomeres V-VIII of all species in the list (all raw data are presented in supplementary table 3). The studied flagellomeres were considered as cylindrical for the surface measurements. For calculating surface areas of the chosen flagellomeres, their lengths and diameters were measured with Adobe Illustrator CS6 (Adobe Inc., California, USA). The lengths were measured between upper and lower middle points of the flagellomeres, the diameters based on the width of the middle part of the segments (all raw data presented in supplementary table 3 and 4). For the assessments of average lengths and basal diameters of the furrowed sensilla, three of them from flagellomeres X of each species were chosen.

Ecological traits: The studied species were categorized into different groups based on (1) the absence or presence of eyes; (2) hypogean (living underground) or epigean habitat (on the surface). The latter also includes edaphic species such as *Bathysciola*, *Besuchetiola* or *Karadeniziella*. Supplementary table 1 provides the coding of these characters for all studied species.

Scanning electron microscopy (SEM): The protocol recommended by Schneeberg et al. [34] for cleaning surfaces was modified for the beetles we used: specimens were transferred from FAE into 70% ethanol, followed by 0.5% Triton X100 (14 h), 5% KOH (14 h), glacial acetic acid (3 × 15 min), distilled water (multiple times until the specimens appeared clean), and finally 70% ethanol. Subsequently, they were dehydrated and dried in an Emitech K850 at the critical point. Prior to scanning electron microscopy (SEM), samples were attached to a rotatable specimen holder [35] or small sample holders, then sputter-coated with gold (Emitech K500; Quorum Technologies Ltd., Ashford, UK). SEM observation and imaging was performed with an FEI (Philips) XL 30 ESEM at 10 kV.

Phylogenetic analyses: The DNA sequences of specimens used in this study were compiled from previous publications on the group. We compared fragments of seven genes, four mitochondrial and two nuclear: 3' end of cytochrome c oxidase subunit (*cox1*); 5' end of the large ribosomal unit plus the Leucine transfer plus the 3' end of NADH dehydrogenase subunit 1 (*rrnL+trnL+nad1*); 5' end of the small ribosomal unit, 18S rRNA (SSU); and an internal fragment of the large ribosomal unit, 28S rRNA (LSU). The sequences were aligned using MAFFT online v.7 with the Q-INS-i algorithm [36]. Maximum likelihood analyses were performed with a data matrix combined with RAxML GUI [37, 38], with four partitions corresponding to the fragments *cox1*, *rrnL + trnL + nad1*, SSU and LSU, with the evolution model GTR + I + G and the default values for the other parameters [39].

The tree was rooted using *Catops picipes* (Fabricius, 1787), a representative of the Cholevini, another tribe of Leiodidae [40].

Statistics: The analyses were run on the raw measurements, the size-corrected and the phylogeny-controlled size-corrected residuals. For size-correction, the raw measurements were log₁₀-transformed and regressed against the log₁₀-transformed body lengths. The resulting residuals were used in the further analyses as size-corrected variables.

The raw and size-corrected measurements were checked for parametric test assumptions (data normality and equality of variances), and parametric one-way Anova and non-parametric Kruskal-Wallis tests were carried out accordingly for each measurement. We estimated the significance of the divergence of each measurement between sighted and

blind, and epigean and hypogean groups. To further explore significant differences between their interactions we grouped specimens as sighted epigean, blind epigean and blind hypogean and repeated the same tests. To account for multiple group comparisons Bonferroni corrected pairwise tests were used. The number of permutations for one-way Anovas was set to 10000 for every analysis. All tests were performed in the PAST software package [41].

In addition to the residual approach, we also performed one-way Ancovas in SPSS v.21 (IBM Corp., 2012) for assessing the effects of the specimen size on the measurements. We included log-transformed body size as a covariate and other log-transformed measurements as dependent variables for each level of grouping (sighted / blind; hypogean / epigean; sighted epigean / blind epigean / blind hypogean). To account for multiple group comparisons Bonferroni corrected pairwise tests were used.

To assess the influence of different life modes and ecology under control for phylogenetic effects, we ran phylogenetic Anovas using 'phylanova' function in the 'phytools' R software package [42]. For this analysis we used a reduced dataset (29 species) as not all species were included in the available phylogenetic tree. The raw data of all statistical results is provided in supplementary table 5 and 6.

Results

The antennae of all studied species are composed of scapus, pedicellus and 9 flagellomeres (Fig. 1A). Among the studied 38 species, compound eyes were present in 10, 28 were blind, 15 were epigean, and 23 hypogean. The body length of the beetles with eyes was on average $2709.08 (\pm 368.64) \mu\text{m}$, while the blind ones were $2915.68 (\pm 215.79) \mu\text{m}$ long (Fig. 2B; detailed values for every species in supplementary table 2). Hypogean species were on average larger ($3209.67 \pm 206.37 \mu\text{m}$) than epigean ones ($2327.16 \pm 304.04 \mu\text{m}$) (Fig. 2C).

The result of the phylogenetic analyses is provided in supplementary figure 1. Although carried out with a reduced number of species, the overall topology and the supported nodes obtained are in accordance with previous works (e.g. [31, 43, 44]). The Leptodirini are recovered monophyletic, with *Platycholeus* sp. as sister to the rest of the tribe, as already suggested previously [40].

The combined area of the flagellomeres V-VIII varied between $3\,947.03 \mu\text{m}^2$ and $129\,167.56 \mu\text{m}^2$ in the studied beetles (detailed values for every species in supplementary table 3). In the species with eyes it was on average $67\,833.49 (\pm 17923.88) \mu\text{m}^2$, in the blind ones $116\,574.31 (\pm 21\,306.78) \mu\text{m}^2$, in the epigean ones $55\,240.36 (\pm 12\,729.14) \mu\text{m}^2$ and in the hypogean ones $135\,383.05 (\pm 24\,238.91) \mu\text{m}^2$. Details on the individual segments can be found in supplementary table 3. In the uncorrected raw data, we found significant differences

in the area between the epigean and hypogean ($p=0.001$; Fig. 2A) and the blind hypogean and blind epigean species, respectively ($p=0.00194$; Fig. 2A), but not between the blind / sighted or the sighted epigean / blind epigean and sighted epigean / blind hypogean taxa. After size correction, there were significant differences between the blind and sighted ($p=0.007$; Fig. 2A), the hypogean and epigean ($p=0.033$; Fig. 2A), and the blind hypogean and sighted epigean groups ($p=0.04803$; Fig. 2A) (supplementary table 5). After size and phylogenetic corrections, no significant values were found in any of the studied groups. The same applies to the individual studied segments, except that differences between hypogean and epigean groups did not apply to the size-corrected measurements of flagellomeres VI and VIII. The differences between sighted epigean and blind hypogean groups for segment V raw measurements were significant, while size-corrected measurements for the same groups were not significant for segments VII and VIII (supplementary table 5).

The combined length of the flagellomeres V-VIII varied between 118.03 μm and 215.74 μm in the studied beetles (detailed values for every species in supplementary table 4). In the species with eyes it was on average 285.56 (± 39.43) μm , in the blind ones 589.83 (± 86.66) μm , in the epigean ones 252.91 (± 29.42) μm , and in the hypogean ones 677.27 (± 96.21) μm^2 . Details about the individual segments can be found in supplementary table 3. In the uncorrected raw data, we found significant differences in all compared groups except for the sighted epigean / blind epigean couple (Fig. 2A; supplementary table 5). After size correction, there were significant differences between the blind and sighted ($p=0.0006$; Fig. 2A), hypogean / epigean ($p=0.00119$; Fig. 2A) and sighted epigean / blind hypogean taxa ($p=0.0013$; Fig. 2A). After size and phylogenetic corrections, there were only significant differences between hypogean and epigean couple ($p=0.0483$; Fig. 2A). Significances for the individual flagellomeres are found in supplementary table 5.

The total number of setae on all studied flagellomeres varied between 73 and 405 in the studied beetles (detailed values for each species in supplementary table 3). While furrowed setae were observed on all studied flagellomeres, the smooth type is only present on the distal ones. In the sighted species the total number of setae was on average 205.60 (± 34.39), in the blind ones 168.96 (± 11.85), in the epigean ones 176.67 (± 25.13) and the hypogean ones 179.87 (± 13.32). Our analyses found no significant correlation between any of the groups in any analyses (Fig. 2A), except for size-corrected measurements between blind and sighted and hypogean and epigean groups on flagellomere VIII. However, after phylogenetic correction these effects were not significant anymore (supplementary material 5). The studied species only had furrowed (sensilla chaetica sensu [26]) and smooth (sensilla basiconica sensu [26]) setae on the antennae. The only significant differences we found between the studied groups, if furrowed or smooth setae were analyzed separately, were for

furrowed setae on flagellomere VIII between sighted and blind beetles (supplementary material 5). However, after correction for phylogeny the latter was not significant any more.

The total density of all setae on flagellomeres V-VIII varied between 0.47 / 500 μm^2 and 5.82 / 500 μm^2 in the studied beetles (detailed values for every species in supplementary material 3). In species with eyes it was on average 3.81 (± 0.38) / 500 μm^2 , in the blind ones 2.21 (± 0.23) / 500 μm^2 (Fig. 2D), in the epigean ones 3.93 (± 0.29) / 500 μm^2 , and in the hypogean ones 1.78 (± 0.16) / 500 μm^2 (Fig. 2E). In the uncorrected raw data, we found significant differences between the epigean and hypogean species ($p=0.0001$; Fig. 2A), the blind / sighted ($p=0.0016$; Fig. 2A), the sighted epigean / blind hypogean ($p=0.0003$; Fig. 2A), and the blind hypogean / blind epigean taxa ($p=0.0003$; Fig. 2A). After size correction, there were significant differences between the blind and sighted groups ($p=0.000026$; Fig. 2A), hypogean and epigean groups ($p=0.0002$), and the sighted epigean / blind hypogean groups ($p=0.00005$; Fig. 2A). These differences also remained after size and phylogenetic corrections in all three groups ($p=0.0098$; 0.0269; 0.0339; Fig. 2A). The results for the density of all setae on the individual flagellomeres and for furrowed setae alone are presented in supplementary material 3 and 5.

The length of the furrowed setae of flagellomeres V-VIII varied between 29.94 μm and 203.87 μm in the studied beetles (detailed values for every species in supplementary material 3). In the sighted species it was on average 61.89 (± 7.02) μm , in the blind ones 101.96 (± 9.19) μm , in the epigean ones 57.86 (± 5.43) μm , and in the hypogean ones 113.30 (± 9.54) μm . In the uncorrected raw data, we found significant differences between the epigean and hypogean species ($p=0.000097$), the blind / sighted ($p=0.01291$), the sighted epigean / blind hypogean ($p=0.00525$), and the blind hypogean / blind epigean taxa ($p=0.00666$) (Fig. 2A; supplementary table 5). After size correction, there were significant differences between the blind and sighted groups ($p=0.00317$), the hypogean and epigean ($p=0.00327$) and the blind hypogean / sighted epigean taxa ($p=0.00522$) but not between the others (Fig. 2A). After size and phylogenetic corrections, no significant values were found in any of the groups.

The diameter of the furrowed setae ranged between 1.63 and 5.91 μm in the studied beetles (detailed values for every species in supplementary material 3). In the sighted species it was on average 2.75 (± 0.31) μm , in the blind ones 3.12 (± 0.20) μm , in the epigean ones 2.53 (± 0.22) μm , and in the hypogean ones 3.35 (± 0.22) μm . The only significant differences we found between the studied groups was in the uncorrected raw data between the hypogean / epigean ($p=0.00221$; Fig. 2A) and the blind hypogean / blind epigean taxa ($p=0.0041$; Fig. 2A).

The performed Ancova analyses were in full accordance with the described results for all studied species, except for the non-significance of size-corrected density of furrowed setae between sighted epigean and blind epigean groups. The results for individual flagellomeres and other variables can be seen in Supplementary table 6 (alternative results from residual based analyses are highlighted in green).

Discussion

Our results on setal patterns of leiodid beetles challenges several widely accepted hypotheses about the antennae and their sensorial equipment in blind or cave insects.

For example, it is widely accepted in textbooks (e.g. [2, 8, 10, 13-15, 19, 45, 46] and original studies (e.g. [24, 47]) that cave-dwelling or blind insects have more sensilla than sighted or epigean ones. Surprisingly, our results show that this does not apply to the studied leiodid species, as we did not find any significant differences between the different categories in inter-specific comparisons (Fig. 2A). This applies to the total number of sensilla but also to each of the two types found in the studied beetles, the furrowed and smooth ones [24]. The furrowed sensilla, which are addressed as sensilla chaetica, are considered to act as mechanical or contact chemical receptors, while the smooth ones (sensilla basiconica) usually have an olfactory function [21]. A similar observation was made for the isopod crustacean genus *Asellus* by Vandel (1964). The density of antennal setae turned out as the only studied trait where we found significant differences between studied categories (blind / sighted; hypogean / epigean; sighted epigean / blind hypogean) after accounting for size and phylogenetic position (Fig. 2A). However, whereas common interpretations and the available literature suggest that blind species have a denser composition of tactile or olfactory sensilla to compensate for the loss of vision (e.g. [10, 48], we found the exact opposite. The density of setae is lower in blind or hypogean species than in sighted or epigean ones (Fig. 2D, E). To our knowledge, the only study specifically addressing the density of antennal sensilla in blind or cave insects is the one of Juberthie [47] who finds that cave species have denser sensilla than epigean ones. A similar result was found in springtails [49, 50]. This is even more astonishing as the studied cave species are on average larger than the epigean ones (see above) and previous research on bumblebees has shown that larger individuals of this group also have denser arrangements of sensilla [51]. Freelance, et al. [52] could show that crepuscular insects do not have denser arrangements of antennal sensilla than day-light active ones, whereas the cornea lenses of their ommatidia were larger. In addition to these allometric factors, it was shown that also sociality, diet, sex and sensitivity to odors affect the density of antennal sensilla [53-55].

Another widespread assumption is that antennal sensilla are elongated in troglobitic species, compared those of epigean relatives [8-10, 14]. Our initial results suggested significant differences of the length of the furrowed sensilla in blind / sighted or epigean / hypogean species. However, after including body size and the phylogenetic placement in the evaluation, the significance of the values was not confirmed, which indicates that the differences can be explained by phylogenetic constraints in leiodid beetles (Fig. 2A). The same applies to the diameter of the furrowed setae, which does not differ between any of the studied groups, after it was corrected for size or size and phylogeny.

It is also common textbook knowledge that blind or cave species have longer antennae with an increased surface area compared to sighted and epigean species (e.g. [8-10, 13-16, 46]). This hypothesis is seemingly confirmed by our uncorrected raw data, where we found significant differences in the antennal surface area between hypogean and epigean (p: 0.001; Fig. 2A) and blind hypogean and blind epigean species (p: 0.00194; Fig. 2A). Likewise we found significant differences in the length of the measured flagellomeres for all studied categories except sighted epigean / blind epigean couples (Fig. 2A). However, after correction for body size and phylogenetic constraints (Fig. 2A) the only significant difference that remains is the length of the studied flagellomeres between hypogean and epigean beetles, which is supported with a very weak p value of 0.0483. This might be correlated with the different body length of the studied species: the hypogean species were significantly larger than the epigean/edaphic ones (Fig. 2C). Our results thus support the general observation that troglomorphic animals have an increased body size compared to epigean relatives (e.g. [10]). In the studied beetles, the observation of longer antennae of the hypogean beetles is thus affected by allometric patterns. Similar results were also found by Faille [56] for the trechine beetles genus *Aphaenops* and for the species *Speonomus hydrophilus* where the length of the antennae vary independently from the rest of the body [57]. Faille [56] could also show that there is a strong evolutionary pressure on individual flagellomeres. As we only measured selected flagellomeres (V-VIII), we cannot fully exclude that the other ones are elongated. However, our data clearly show that in the studied beetles this does not apply to the distal segments with their enhanced sensory equipment [33]. Our data thus suggest that the widely accepted textbook statements that all cave arthropods have elongated antennae or antennae with an increased surface area should be treated with great caution and treated on a case-by-case basis.

As outlined above, our study with distantly related leiodid beetles across several different genera demonstrates that the studied blind and cave-dwelling species do not have more or longer, but rather less dense antennal sensilla than their sighted and epigean relatives. It was shown in several studies that the sensitivity increases with the number of sensilla both

for olfactory [51, 58] and tactile sensors [33]. As Crouau & Crouau-Roy (1991) found no differences in the ultrastructure of the antennal sensilla between cave and epigeal beetles, we also have no reason to assume that a modified construction might result in more efficient sensilla. In conclusion, we assume that the sensorial perception via antennal sensilla is not improved in the studied blind or cave-dwelling species, compared to their sighted and epigeal relatives. As we did not study multiple individuals from different populations of the same species, we cannot account for differences within a single species. However, our study clearly contradicts the widely accepted hypothesis that all cave-dwelling species compensate for the loss of visual input with increased sensory capacity in the antennae.

Figures plates:

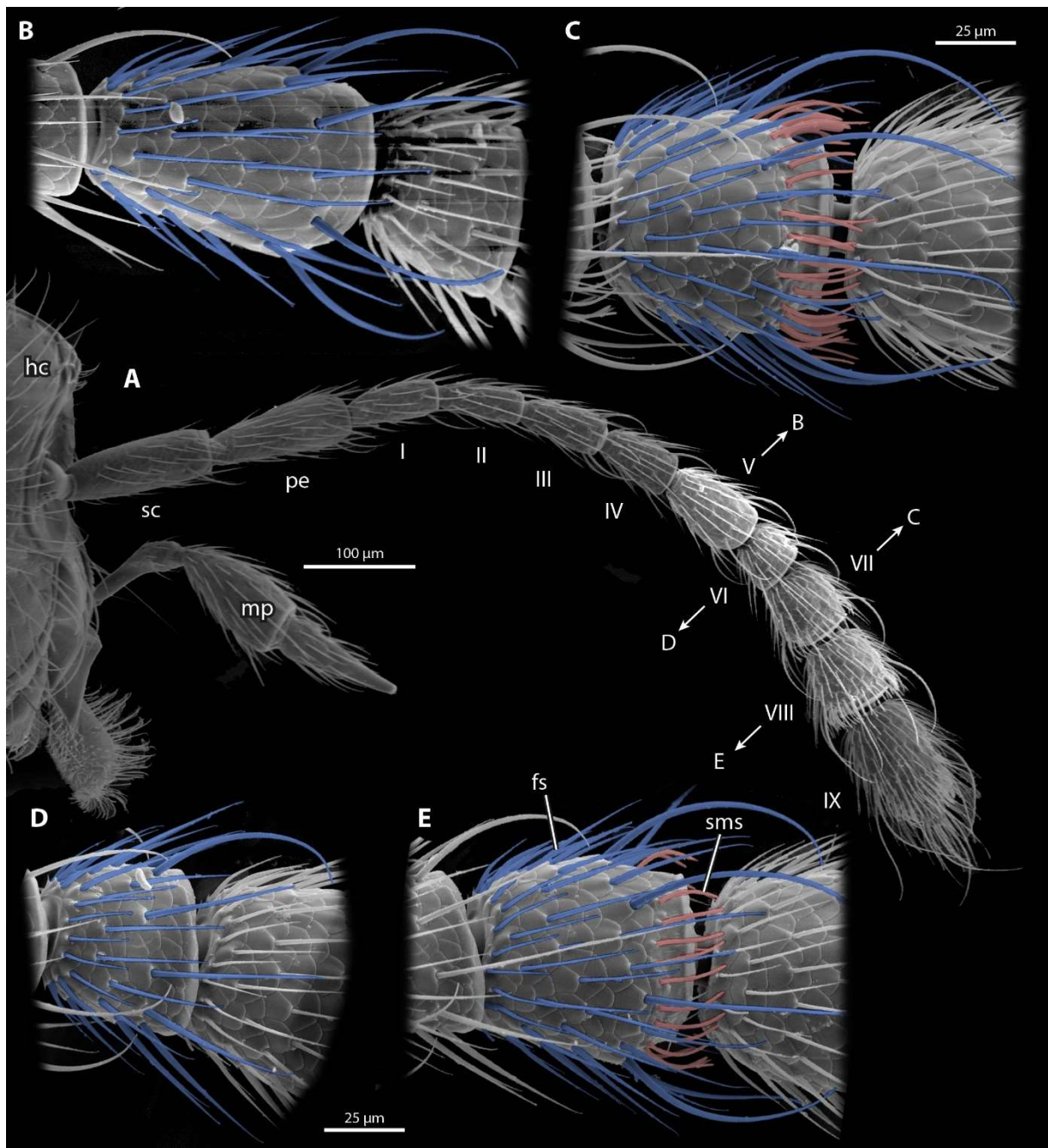


Fig. 1. Scanning electron micrographs of the antenna and the studied flagellomeres of *Adelopsella bosnica* (Reitter, 1884).

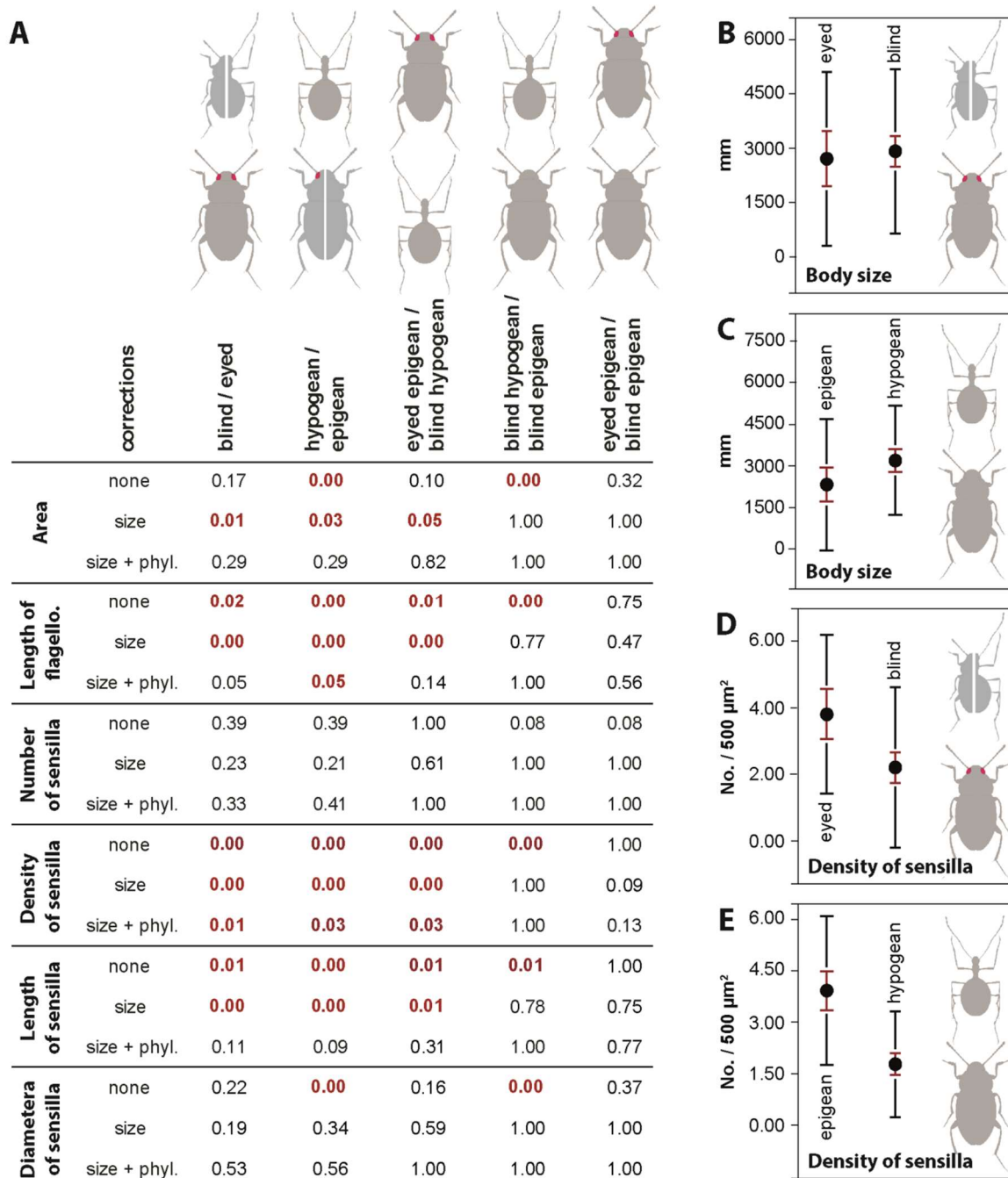


Fig. 2: Results of the statistical analyses for selected traits (raw data provided in Supplementary material 5). A) p-values for different traits with no correction (none), size correction (size) and size + phylogenetic correction (size + phyl.); Significant correlations in red and bold. B) mean body size between the studied sighted and blind species; C) mean

body size between the studied epigeal and hypogeal species; D) mean density of sensilla for the studied sighted and blind species; E) mean density of sensilla for the studied epigeal and hypogeal species. Standard error in red, standard deviation in black.

Acknowledgments

This work is dedicated to the late Ignacio Ribera, who had the original idea for this project. We would like to thank Juliane Vehof for help with image generation and the preparation of the beetle outlines in Fig. 2, David Hasselhoff for emotional support. All the collectors quoted in Supp Table 1, L. Deharveng (MNHN) for informations regarding the chaetotaxy of troglomorphic Collembola.

References

1. Gross, J.B., & Berning, D.J. (2012). *Cave evolution*. *eLS*, 1-13.
2. Romero, A. (2009). *Cave biology: Life in darkness*. Cambridge University Press, Cambridge.
3. Racovitza E. G. 1907. Essai sur les problèmes biospéologiques. *Archives de Zoologie Expérimentale et Générale*, 6, 371– 488.
4. Beale, A. D., Whitmore, D., & Moran, D. (2016). Life in a dark biosphere: a review of circadian physiology in “arrhythmic” environments. *Journal of Comparative Physiology B*, 186(8), 947-968.
5. Mammola, S. (2019). Finding answers in the dark: caves as models in ecology fifty years after Poulson and White. *Ecography*, 42(7), 1331-1351.
6. Protas, M.E., Hersey, C., Kochanek, D., Zhou, Y., Wilkens, H., Jeffery, W.R., Zon, L.I., Borowsky, R., & Tabin, C.J. (2006). Genetic analysis of cavefish reveals molecular convergence in the evolution of albinism. *Nature Genetics*, 38, 107-111.
7. Yoshizawa, M., Settle, A., Hermosura, M. C., Tuttle, L. J., Cetraro, N., Passow, C. N., & McGaugh, S. E. (2018). The evolution of a series of behavioral traits is associated with autism-risk genes in cavefish. *BMC Evolutionary Biology*, 18(1), 1-16.
8. Fišer, C. (2019). Adaptation: Morphological. In W. B. White, D. C. Culver, & T. Pian (eds), *Encyclopedia of caves* (third edition, pp. 33-39). Academic Press, London.
9. Moldovan, O. T. (2004). Adaptation: morphological (internal). In J. Gunn (ed) *Encyclopedia of caves and karst science* (pp 19–22). Fitzroy Dearborn, New York,
10. Howarth, F. G., & Moldovan, O. T. (2018). The ecological classification of cave animals and their adaptations. In O. T. Moldovan, L. Kováč, & S. Halse (eds.), *Cave ecology*, (pp. 41-67). Springer, Cham.

11. Christiansen, K. (1962). Proposition pour la classification des animaux cavernicoles. *Spelunca*, 2, 76-78.
12. Darwin C. R. (1859). *On the origin of species*. John Murray, London.
13. Gunn, J. (2004). *Encyclopedia of caves and karst science*. Taylor & Francis, New York.
14. Moldovan, O. T. (2012). Beetles. In W.B. White, & D. C. Culver (eds.), *Encyclopedia of caves* (second edition, pp. 54-62). Elsevier Academic Press, Amsterdam.
15. Moldovan, O. T., Kováč, L., & Halse, S. (2018). *Cave ecology*. Springer, Basel.
16. Crowson, R. A. (1981). *The biology of the Coleoptera*. Academic press, London.
17. Jeannel, R. (1911) Révision des Bathysciinae (Coléoptères, Silphides). Morphologie, distribution géographique, systématique. *Archives de Zoologie Expérimentale et Générale*, 47, 1–641.
18. Stork, N. E., McBroom, J., Gely, C., & Hamilton, A. J. (2015). New approaches narrow global species estimates for beetles, insects, and terrestrial arthropods. *Proceedings of the National Academy of Sciences*, 112(24), 7519-7523.
19. Trajano, E. (2012). Ecological classification of subterranean organisms. *Encyclopedia of caves* (second edition, pp. 275-277). Elsevier Academic Press, Amsterdam,.
20. Beutel, R. G., Friedrich F., Ge, S. Q. & Yang X. K. (2014). *Insect morphology and phylogeny: a textbook for students of entomology*. Walter de Gruyter, Berlin/Boston.
21. Hansson, B. S. (1999). *Insect Olfaction*. Springer, Berlin.
22. Zacharuk, R. (1985). Antennae and sensilla. In G. Kerkut & L. Gilbert (eds.), *Comprehensive insect physiology biochemistry and pharmacology. VI. Nervous system: sensory* (pp. 1-69) (Pergamon Press, London:).
23. Lucarelli, M., & Sbordoni, V. (1978). Humidity responses and the role of Hamann's organ of cavernicolous Bathysciinae (Coleoptera Catopidae). *International Journal of Speleology*, 9, 167–177.
24. Peck, S.B. (1977). An unusual sense receptor in internal antennal vesicles of *Ptomaphagus* (Coleoptera: Leiodidae). *The Canadian Entomologist*, 109, 81-86.
25. Buzilă, R., & Moldovan, O. (2000). Antennal receptors in two representatives of Leptodirinae (Coleoptera, Cholevidae): diversity and adaptations. *Evolution and Adaptation*, 6, 117-125.

-
26. Juberthie, C., & Massoud, Z. (1977). L'Équipement sensoriel de l'Antenne d'un Coléoptère troglobie, *Aphaenops crypticola* Linder (Coleoptera: Trechinae). *International Journal of Insect Morphology and Embryology*, 6, 147-160.
 27. Deharveng, L., & Bedos, A. (2018). Diversity of terrestrial invertebrates in subterranean habitats. In O. T. Moldovan, L., Kováč, & S. Halse (eds.) *Cave ecology* (pp. 107-172). Springer, Cham.
 28. Jeannel, R. (1926). Faune Cavernicole de la France, avec une Étude des Conditions d'Existence dans le Domaine Souterrain. Lechevalier, Paris.
 29. Faille, A. (2019). Beetles. In W. B. White, D. C. Culver, & T. Pian (eds.), *Encyclopedia of caves* (third edition, pp. 102-108). Academic Press, London.
 30. Balart-García, P., Cieslak, A., Escuer, P., Rozas, J., Ribera, I., & Fernández, R. (2021). Smelling in the dark: Phylogenomic insights into the chemosensory system of a subterranean beetle. *Molecular Ecology*, 30(11), 2573-2590.
 31. Cieslak, A., Fresneda, J., & Ribera, I. (2014). Life-history specialization was not an evolutionary dead-end in Pyrenean cave beetles. *Proceedings of the Royal Society B: Biological Sciences*, 281, 20132978.
 32. Friedrich, M., Chen, R., Daines, B., Bao, R., Caravas, J., Rai, P.K., Zagamajster, M., & Peck, S.B. (2011). Phototransduction and clock gene expression in the troglobiont beetle *Ptomaphagus hirtus* of Mammoth cave. *Journal of Experimental Biology*, 214, 3532-3541.
 33. Staudacher, E. M., Gebhardt, M., & Dürr, V. (2005). Antennal movements and mechanoreception: neurobiology of active tactile sensors. *Advances in Insect Physiology*, 32, 49-205.
 34. Schneeberg, K., Bauernfeind, R., & Pohl, H. (2017). Comparison of cleaning methods for delicate insect specimens for scanning electron microscopy. *Microscopy Research and Technique*, 80(11), 1199-1204.
 35. Pohl, H. (2010). A scanning electron microscopy specimen holder for viewing different angles of a single specimen. *Microscopy Research and Technique*, 73(12), 1073-1076.
 36. Katoh, K., & Standley, D. M. (2013). MAFFT multiple sequence alignment software version 7: improvements in performance and usability. *Molecular Biology and Evolution*, 30(4), 772-780.

37. Stamatakis, A. (2014). RAxML version 8: a tool for phylogenetic analysis and post-analysis of large phylogenies. *Bioinformatics*, 30(9), 1312-1313.
38. Silvestro, D., & Michalak, I. (2012). raxmlGUI: a graphical front-end for RAxML. *Organisms Diversity & Evolution*, 12(4), 335-337.
39. Stamatakis, A., Hoover, P., & Rougemont, J. (2008). A rapid bootstrap algorithm for the RAxML web servers. *Systematic Biology*, 57(5), 758-771.
40. Fresneda, J., Grebennikov, V.V. & Ribera, I. (2011) The phylogenetic and geographic limits of Leptodirini (Insecta: Coleoptera: Leiodidae: Cholevinae), with a description of *Sciaphyes shestakovi* sp.n. from the Russian Far East. *Arthropod Systematics & Phylogeny*, 69, 99–123.
41. Hammer, Ø., Harper, D. A., & Ryan, P. D. (2001). PAST: Paleontological statistics software package for education and data analysis. *Palaeontologia Electronica*, 4(1), 9.
42. Revell, L.J. (2012). Phytools: an R package for phylogenetic comparative biology (and other things). *Methods in Ecology and Evolution*, 3, 217-223.
43. Faille, A., Ribera, I., & Fresneda, J. (2016). On the genus *Aphaobius* Abeille de Perrin, 1878, with description of a new species from the mesovoid shallow substratum (MSS) of Austria (Coleoptera: Leiodidae: Cholevinae: Leptodirini). *Zootaxa*, 4169, 44-56.
44. Ribera, I., Fresneda, J., Bucur, R., Izquierdo, A., Vogler, A. P., Salgado, J. M., & Cieslak, A. (2010). Ancient origin of a Western Mediterranean radiation of subterranean beetles. *BMC Evolutionary Biology*, 10, 29.
45. Protas, M., & Jeffery, W. R. (2012). Evolution and development in cave animals: from fish to crustaceans. *Wiley Interdisciplinary Reviews: Developmental Biology*, 1(6), 823-845.
46. Chapman, R.F. (2013). S.J. Simpson, & A.E. Douglas (eds.) *The Insects: Structure & Function*, Cambridge University Press, Cambridge.
47. Juberthie, C., & Massoud, Z. (1980). Sur differents types d'organisation sensorielle antennaire chez les coléoptères Trechinae troglobies et description d'un type original de récepteur chez *Rakantrechus etoi*. *Mémoires de Biospéologie*, 7, 353–364.
48. Wilkens, H., Culver, D.C., & Humphreys, W.F. (2000). *Subterranean Ecosystems*, Elsevier, Amsterdam.

-
49. Deharveng, L. (1988). Collemboles cavernicoles. VII: *Pseudosinella bessoni* n. sp. et note sur l'évolution morphologique de la griffe chez les *Pseudosinella*. *Revue suisse de Zoologie*, 95(1), 203-208.
 50. Jantarit, S., Satasook, C., & Deharveng, L. (2019). *Coecobryasirindhornae* sp. n., the most highly troglomorphic Collembola in Southeast Asia (Collembola, Entomobryidae). *ZooKeys*, 824, 21-44.
 51. Spaethe, J., Brockmann, A., Halbig, C., & Tautz, J. (2007). Size determines antennal sensitivity and behavioral threshold to odors in bumblebee workers. *Naturwissenschaften*, 94(9), 733-739.
 52. Freelance, C. B., Tierney, S. M., Rodriguez, J., Stuart-Fox, D. M., Wong, B. B., & Elgar, M. A. (2021). The eyes have it: dim-light activity is associated with the morphology of eyes but not antennae across insect orders. *Biological Journal of the Linnean Society*, 134(2), 303-315.
 53. Gill, K. P., van Wilgenburg, E., Macmillan, D. L., & Elgar, M. A. (2013). Density of antennal sensilla influences efficacy of communication in a social insect. *American Naturalist*, 182(6), 834-840.
 54. Fialho, M. D. C. Q., Guss-Matiello, C. P., Zanuncio, J. C., Campos, L. A. O., & Serrão, J. E. (2014). A comparative study of the antennal sensilla in corbiculate bees. *Journal of Apicultural Research*, 53(3), 392-403.
 55. Polidori, C., Jorge, A., & Ornosá, C. (2020). Antennal morphology and sensillar equipment vary with pollen diet specialization in *Andrena* bees. *Arthropod Structure & Development*, 57, 100950.
 56. Faille, A. (2006). Endémisme et adaptation à la vie cavernicole chez les Trechinae pyrénéens (Coleoptera: Caraboidea): approches moléculaire et morphométrique. (Paris: Muséum national d'Histoire naturelle).
 57. Juberthie, C., Delay, B., and Ruffat, G. (1980). Variations biométriques entre différentes populations de *Speonomus hydrophilus* en relation avec leur situation géographique (Col. Bathysciinae). *Mémoires de Biospéologie*, 7, 249-266.
 58. Ochieng', S. A., & Hansson, B. S. (1999). Responses of olfactory receptor neurones to behaviourally important odours in gregarious and solitary desert locust, *Schistocerca gregaria*. *Physiological Entomology*, 24(1), 28-36.

4 Discussion

4.1 Entangled ecological classifications of subterranean animals

Ecological classifications of subterranean organisms have been developed since a very early stage of biospeological investigations (e.g. Schiødte 1849; Schiner 1854; Racovitza 1907). However, in practice it is often difficult to decide in which category a species belongs, especially when it comes to troglloxenes and troglrophiles (Howarth & Moldovan 2018). In addition, the concept of “troglobionts” (obligatory cave-dwelling inhabitants which complete the life cycle within a cave) is used by many scientists but could cause confusion due to two critical facts: (1) very few species are absolutely bound to the physical subterranean environment and (2) the degree of troglomorphy does not necessarily correspond to the strength of the “troglbiosis” (Sket 2008). More recently, Novak et al. (2012) proposed a binary system based on their investigations in Slovenia, with animals categorized into two groups: (1) the shallow subterranean fauna (in the upper 10 m of the subsurface), which consists of diverse organisms including randomly distributed non-trogllobites and soil-adapted “trogllobites”; (2) the deep subterranean fauna, which consists of cave-adapted trogllobites. In fact, both the earlier and the recent concepts are ambiguous in different ways.

4.1.1 Complexity of subterranean environment

The spaces beneath the surface of the earth can range from very large caves to extremely small fissures; moreover, they can be air-filled or filled with water (Culver & Pipan 2019). In fact, the most essential and constant shared feature of the underground is the absence of light. Apparently, understanding the biological role of the light is crucial for understanding challenges and consequences of adapting to dark environments (Friedrich 2019). Racoviță (1976) proposed that systems of joints and crevices in the rock around cave systems may provide important habitats for cave organisms, and that there might be more or less regular migration between such habitats and the caves. Instead of “cave ecosystem”, Rouch (1977) proposed that this is rather a complex “karst ecosystem”, which contains highly interconnected and diverse habitats within it (see also Simon 2019). Such habitats and also deep layers of soil are complete aphotic (Culver & Pipan 2019), with an atmospheric humidity near to saturation, and thus similar to conditions in caves (Vandel 1965). Aside from the absence of light and relatively constant environmental conditions, caves and related habitats can be variable in many ways. Ecosystems in tropical caves, for instance, can differ distinctly from their counterparts in temperate regions. The energy input can also vary considerably, and not all caves can be considered as strictly energy-poor

(Gunn 2004; Simon 2007). Taking into account the complexity and variability of subterranean environments, it becomes more and more apparent why it is so difficult to classify subterranean organisms in a meaningful way.

4.1.2 Subterranean species in different habitats

Beetles of the lightless underground are by no means restricted to caves, but many species occur in other types of subterranean habitats (Culver & Pipan 2019; Giachino & Vailati 2010). In this context is important to note that not all obligate cave-dwellers are troglomorphic, a phenomenon with different possible explanations: it is possible that these species are newcomers, or alternatively that the selective pressure was below a level required for structural transformation. On the other hand, not all troglomorphic organisms are subterranean, an option that attracted much less attention. It was suggested that this might be due to a reverse colonization of the epigeal environment by previously subterranean species (Culver 1982; Howarth & Moldovan 2018; Sket 2008). Some soil-dwelling species of Anillini (Carabidae) from western Australia with small or lacking eyes, for instance, were found in deep layers of soil (depth up to 60 m) (Baehr & Main 2016). In this context it should be noted that small species with short appendages from soil and other types of shallow subterranean habitats are often confused with obligate cave-dwellers, due to the absence of eyes and depigmentation (Culver & Pipan 2014). An example outside of Coleoptera and Insecta is the fully depigmented myriapod *Brachydesmus subterraneus* Heller (Diplopoda: Polydesmoidea), which is not strictly limited to caves but also inhabits soil (Sket 2008). Shared structural specializations (reduction of eyes and wings, and loss of pigmentation) of hypogean and endogean species clearly challenge the ecological classification of these organisms (Faille 2019). Moreover, seemingly typical troglobiontic beetles were also found in some artificial subterranean habitats, such as the carabid *Pseudanophthalmus*, collected in abandoned coal mines in Kentucky (U.S.A.) (Barr 1986). The history of artificial subterranean spaces is apparently not long enough for distinct structural transformations compared to epigeal ancestors, and scientists proposed that events of colonization achieved by troglobiontic species could be attributed to mine passageways following the intersection of natural voids (Slay & Bitting 2007). In the case of soil-dwellers, it is assumed that some euedaphic and epedaphic forms have developed distinctive structural adaptations linked with their specific environment, while fluent transitions between the two forms still occur in certain groups of soil arthropods (Eisenbeis & Wichard 1987). Additionally, even deep soil can be continuous with forest litter and other subterranean habitats, which makes it even more difficult

to assign species to one particular habitat type (Andújar & Grebennikov 2021). Elements of the subterranean fauna can also be linked with close relatives of the surface by structurally intermediate forms (Vandel 1965). It is also noteworthy that although shallow subterranean habitats have a close connection with the surface, some inhabitants of superficial substrates like leaf litter are apparently highly modified for subterranean life (Culver & Pipan 2008). Furthermore, listing some examples, Romero (2009) emphasized the difficulty to distinguish specific habitats of these organisms. He pointed out that some species of soil and interstitial habitats move between different environments, and also that some aquatic subterranean organisms can be found in both aquifers and springs.

These cases make the boundary among categories of subterranean species even more obscure. Apparently, it is still very challenging to set clear-cut lines among different categories of subterranean animals. Apparently, neither the specific properties of the habitat nor the degree of morphological specialization provides a fully reliable scheme.

4.2 Morphological modifications of subterranean beetles

Morphological features of arthropods are strongly linked with the function of the involved structures, especially in the contexts of feeding and locomotion (e.g. Koerner et al. 2012; Manton 1977; Matsumura et al. 2017; Hörnschemeyer et al. 2013). Crowson (1981) has stated that both endogean and cavernicolous beetles are similar in some ways, such as a low degree of mobility and high degree of geographical localization. Different shared morphological features of permanent cave-dwelling organisms have been recognized for a long time (see Vandel 1965), but the mechanisms behind distinct morphological changes are still under debate (Fišer 2019). The most frequently mentioned cave-related traits or “troglomorphies” are eyelessness, depigmentation and elongated appendages (Trontelj 2012). Instead of “gains” (elongation of the body, enlargement of the sensory organs, increased density or length of sensilla etc.), the “losses” (eyeless, winglessness, depigmentation, etc.) of subterranean animals have first fascinated biospeologists (see Culver & Pipan 2019; Howarth 2009). The leiodid *L. hochenwartii*, the very first-discovered cave beetle, is blind with elongated body and appendages, and the same condition was observed in many other troglobitic species of Leiodidae and also Carabidae (Faille 2009). Structural features considered as typical for cavernicolous beetles also occur in endogenous coleopteran species (Culver & Pipan 2019). Endogean beetles are the only group which could be considered as strictly subterranean, with typical specializations correlated with life in soil. Many of them show the following characteristics: photophobic behavior, depigmentation, eyes

partially reduced or absent, slender, elongated body form, shortening of the elytra, and reduction of the membranous hind wings. An example are soil-dwelling staphylinids of the subfamily Leptotyphlinae, living permanently in darkness, with a typical endogean body shape (see Fig. 172d in Eisenbeis & Wichard 1987), partially reduced eyes and lacking pigment (Coiffait 1958, 1959). Remarkably, in clear contrast to this specialized subfamily, distinct morphological adaptations to a permanent soil-dwelling lifestyle do not occur in other groups of staphylinids (Eisenbeis & Wichard 1987).

The interpretation of adaptations to various subterranean conditions is usually restricted to external features which can be easily observed. Detailed anatomical data are still scarce. However, rapid progress in the application of micro-CT and other techniques greatly improves the efficiency of acquiring high quality data on exo- and endoskeletal structures, muscles, and other internal soft parts of small animals (Friedrich et al. 2014; Wipfler et al. 2016). The following interpretations are based on detailed anatomical data obtained with a broad spectrum of techniques.

4.2.1 General shape and external and internal skeletal structures

Among the subterranean beetles examined, the most conspicuous change is the elongation of the head capsule, very distinct in the troglobitic *Sinaphaenops wangorum* Ueno et Ran (Carabidae) (Fig. 1a-c, Luo et al. 2018a) and also in *L. hohenwartii* (Leiodidae) (Fig. 8a, Luo et al. 2019b). Corresponding to the exoskeleton, the endoskeleton is also modified, notably with distinctly elongated gular ridge. However, the gular ridge of *S. wangorum* gradually obliterates anterior to the cephalic constriction, instead of reaching the postoccipital ridge as it is usually the case in carabids and other adephan beetle (Dressler & Beutel 2010). It is important to note that the elongation of the head is only present in the most advanced species, but not a universal feature among eyeless troglobitic beetles. In stark contrast to the abovementioned cases, the head of *Bathysciola ovata* (Kiesenwetter) (Leiodidae) is even transverse (Fig. 8b, Luo et al. 2019b). Besides, a distinct posterior constriction as present in *S. wangorum* is absent in many other species of Carabidae and Leiodidae (Jeannel 1926). The functional significance of this narrowed head region is still unclear.

Like the head, the thorax of advanced cave-dwelling beetles is also often elongated (Luo et al. 2018b). A distinctly modified body shape also occurs in some species of ground beetles which live in fissures of the ground or in deep soil. The postcephalic body tends to be narrower and also flattened compared to surface-dwelling relatives, and the prothorax is about as wide as the posterior body. The latter

feature could possibly reduce friction in the substrate and cause less obstruction when moving in a confined space. (Baehr & Main 2016; Forsythe 1987). In clear contrast to specialized cavernicolous members of Carabidae, subterranean species of Leiodidae do not necessarily show a trend towards elongation of body regions. It was pointed out by Culver & Pipan (2019) that soil-dwelling species of Leiodidae can even display a more compact body form, especially in the tribe Ptomaphagini (e.g. Peck 1973).

The shape of the middle body region of subterranean beetles is obviously affected by the loss of the flight organs and associated structures. Skeletal elements linked with the flight apparatus are largely reduced in all examined species of Carabidae, Leiodidae, and Pselaphinae with reduced wings (Luo et al. 2018b, 2019a, 2021b). Moreover, the skeletal elements of the pro- and pterothorax of the flightless myrmecophilous *C. testaceus* reach a maximum degree of compactness (Luo et al. 2021b). Even though these beetles live underground, this is very likely primarily linked with the association ants. The compactness of the thorax increases mechanical protection against the potentially aggressive hosts.

4.2.2 Compound eyes and nervous system

Compound eyes are usually highly efficient photoreceptive organs of insects and other groups of arthropods. Their presence is crucial for movements above ground, and also for detection of prey, suitable hosts, or predators (e.g. Beutel et al. 2014). At an early stage of study, the reduction or complete absence of eyes impressed scientists confronted with other “losses” of subterranean species of Coleoptera (see Culver & Pipan 2019; Rétaux & Casane 2013). Eigenmann (1909) and Poulson (1963) suggested that the degree of reduction of the eyes could be used as a clue to estimate the relative time of isolation of animals in caves. Fong et al. (1995) postulated that the reduced size of the light sense organs could be either considered as a result of directional selection or alternatively of neutral mutations. The species *S. wangorum* (Carabidae), *Troglocharinus ferreri* (Reitter) (Leiodidae), and *Claviger testaceus* Preyssler (Staphylinidae, Pselaphinae) are completely eyeless (Jałoszyński et al. 2020; Luo et al. 2018a, 2019b), whereas *Bergrothia saulcyi* (Reitter) (Pselaphinae), a species found in leaf litter and deeper soil layers, still has retained a vestige of the compound eyes (Luo et al. 2021a). Furthermore, regardless of the extent of specialization, the partial reduction or total absence of eyes in these cases was associated with the complete loss of the optic neuropils (Jałoszyński et al. 2020; Luo et al. 2018a, 2019b, 2021a). The same condition has been reported in other troglomorphic eyeless beetles (Ghaffar et al. 1984; Larsen

et al.; Packard 1888 1979), but the documentation of this feature is presently very insufficient.

Different degrees of reduction of eyes occur in various groups of animals. This is not restricted to subterranean species, but apparently obligatory and more obvious in animals living underground, especially in caves (Fong et al. 1995). Among various proposed mechanisms behind the reduction, the “energy-economy” hypothesis suggests that individuals with reduced eyes have a selective advantage (Fišer 2019), as the development and maintenance of useless visual organs structures cause high energetic cost (e.g. Moran 2015). In our comparative studies of pselaphine beetles, different degrees of eye reduction are documented: among the myrmecophiles, the compound eyes of the advanced *C. testaceus* are completely reduced including the optic lobes (Jałoszyński et al. 2020), whereas distinctly developed eyes are still present in *Diarctiger kubotai* Nomura (Jałoszyński et al. subm.); besides, even though both *B. saulcyi* and *Pselaphus heisei* Herbst living in leaf-litter, the former species possesses greatly reduced and vestigial compound eyes (Beutel et al. 2021) while the latter species have well-developed eyes (Luo et al. 2021a). Furthermore, the anatomical study in Luo et al. (2021a) confirmed that the vestigial compound eyes of *B. saulcyi* are non-functional, since the optic lobes with the optic neuropils are entirely lacking, and even a thin optic nerve is not preserved.

Even though some cave-dwelling dipteran larvae from Australia and New Zealand are capable to produce light (Meyer-Rochow 2007), nearly all subterranean organisms live in permanent complete darkness. Thus, acquisition of food and finding mating partners, and avoidance of competitors and predators must be accomplished without vision (Culver & Pipan 2019). Eyes are critical for surface-dwelling predacious carabid beetles to recognize and capture prey (Thiele 1977), the loss of sight and living in darkness does not seem to affect the success of the subterranean relatives.

It should be noted in this context that eyes are not the only photo-sensitive organs, and existence of extraocular photoreceptors is relatively widespread in the animal kingdom (Beutel et al. 2014; Yoshida 1979). For instance, two light-sensitive neurons were found on the abdomen of the Chinese swallowtail butterfly *Papilio xuthus* (Linnaeus) and were shown to be crucial for their copulation (Arikawa 1996). Furthermore, some eyeless organisms can in fact also be photosensitive (e.g. Plachetzki et al. 2012; Ullrich-Lüter et al. 2011). In a study on the nematode model organism *Caenorhabditis elegans* Maupas, light stimuli elicited negative phototaxis despite the lack of specialized light-sensing organs (Ward et al. 2008). The authors proposed that this is a mechanism for keeping them in a suitable

environment, i.e. soil, and is therefore important for their survival; additionally, a group of candidate photoreceptors were identified (Ward et al. 2008).

It can be assumed that reduction of the eyes always entails a drastic loss of visual perception. However, the photosensitivity of eyeless subterranean beetles is still poorly studied (Corbière-Tichané 1974; Friedrich et al. 2011; Langille et al. 2019). Corbière-Tichané (1974) has reported a sensory receptor located on the antennae of the larva of the eyeless cavernicole *Speophyes lucidulus* Delarouzee (Leiodidae, Leptodirini). Its fine structure and staining experiments suggested that photopigment may be present in this structure. In a study on the strongly cave-adapted *Ptomaphagus hirtus* (Tellkamp) (Leiodidae, Ptomagophagini), Friedrich et al. (2011) discovered the transcripts of all core members of the phototransduction protein machinery, and also showed that this species still shows phototactic response in behavioral tests. To test the degree of “blindness” of subterranean diving beetles, similar tests have been conducted with species of *Paroster* Sharp and *Limbodessus* Guignot in Australia (Langille et al. 2019).

4.2.3 Adaptations of antennae and sensilla patterns in Leiodidae

As major sensory organs of the head, antennae of epigean and subterranean insects are often modified. Elongation is an easily visible transformation common in cave beetles (Peck 1973), and it was often assumed that increased length is a compensation of the loss of the eyes (e.g. Yoshizawa et al. 2012). The elongation of antennae is distinct in the case of the highly specialized carabids and leiodids. In our studies, *S. wangorum* clearly shows this advanced specialization (Fig. 3 Luo et al. 2018a).

Types and the quantitative patterns of antennal and maxillary sensilla of cave beetles have been investigated in previous studies, and also the fine structure of Hamann’s organ in *L. hohenwartii* (Accordi & Sbordonni 1978; Juberthie & Massoud 1977; Nitzu & Juberthie 1996). It is often assumed that an increased number of sensory structures results in faster and more accurate orientation and food detection, and that the elaborated non-visual structures likely evolved in response to the combination of darkness and food scarcity (Fišer 2019). However, no distinct modification of the sensorial apparatus of the antennae was found in our investigations. In Study VIII, no significant variation of the number of sensilla was found among different ecological groups, and the density of sensilla was even lower in blind or hypogean species. Moreover, the length and diameter of the studied antennal sensilla of blind or hypogean species did not significantly differ from those of sighted or epigean ones (Luo et al. in prep.). The quantitative results

clearly refute widely accepted hypothesis about modified antennal sensillar patterns of subterranean beetles.

4.2.4 Mouthparts

The mouthparts are often more elongated in specialized troglobites compared to surface-living relatives (Fig. 5, 7, Luo et al. 2018a). This is apparently a common trait among cave-dwellers, at least in predacious species (Gunn 2004). In the case of the carabid *S. wangorum*, the mouthparts still follow a generalized coleopteran pattern, but are distinctly elongated (Luo et al. 2018a). It is conceivable that the elongation, especially of the mandibles, facilitates the seizure of prey in a dark environment. To adapt to a special aquatic dietary niche, a spoon-like structure of the mandibles of *Radziella styx* Casale & Jalžič, *Hadesia vasiceki* J. Müller and *Croatodirus bozicevici* Casale et al. (Cholevinae) is likely to stir the sediments and filter food particles (Moldovan et al. 2014). Although this specific modification of the mouthparts is limited to small group of subterranean beetles, it shows the potential to evolve structural modifications to increase the efficiency of food acquisition.

Whereas modifications of mouthparts are moderate in cave-dwelling species, with the general configuration largely maintained, profound changes were found in the myrmecophilous *C. testaceus*, for instance a highly unusual connection of the maxillae to the hypopharynx, and the formation of a uniquely transformed labium with a vestigial prementum (Jaloszynski et al. 2020). These transformations are clearly related with a close association with ants, and not with life in a lightless environment.

4.2.5 Reduction of the flight apparatus

Flight can be advantageous in different contexts. The ability of pterygote insects to invade the 3-dimensional space, especially plant surfaces, was arguably the most important trigger of diversification in the evolutionary history of Hexapoda (e.g. Beutel et al. 2017). Flight can for instance drastically improve the dispersal capacity and facilitates finding food sources, suitable habitats, or microhabitats, and also mating partners (Dudley & Pass 2018; Johnson 1969). Even though the membranous hind wings are usually covered by heavily sclerotized elytra in Carabidae and almost all other groups of beetles, many species have maintained a good flight performance and rely on the hind wings for dispersal, even over longer distance (Crowson 1981). Even though total loss or reduction of hind wings is not uncommon among surface-living carabids, and some species with largely retained

alae can be unable to fly, the ability to disperse by flight is apparently important for many ground beetles (Thiele 1977). Different patterns of wing reduction and flightlessness have evolved multiple times in pterygote insects (Roff 1990). These phenomena are related with latitude and altitude, and with specific habitats such as for instance deserts, mountains, the ocean surface, streams, pond margins (Fong et al. 1995). Furthermore, flightlessness of carabids is not necessarily due to the degeneration or loss of the hind wings and flight muscles, but in advanced cases also to a decreased size of the metatergum, a distinct simplification of this sclerite, loss of axillary sclerites, and rounded elytral humeri (Forsythe 1987). Whereas the partial or complete reduction of the hind wings and degeneration of flight muscles indicate relatively young cases of flightlessness and are often reversible, distinct modifications of sclerites linked with the flight apparatus are very likely irreversible and the result of older evolutionary transformations. Such advanced conditions, in addition to the reduction of the membranous wings and flight-related muscles, are now documented in the cave-dwelling *S. wangorum* (Carabidae) and *T. ferreri* (Leiodidae) (Luo et al. 2018b, 2019a). Flightlessness is not unique in subterranean insects but also present in many specialized environments groups such as deserts (Crowson 1981).

Two forms of non-functional wings were observed in the myrmecophilous pselaphine *C. testaceus*, and also largely reduced inter- and intrasegmental sutures and ridges, distinctly reduced skeletal elements linked with the flight apparatus. This clearly represents an advanced stage of reduction (Luo et al. 2021b). Even though this is likely linked with subterranean and myrmecophilous habits in the case *C. testaceus* and many other clavigerites, flight is reported in tropical ant-associated relatives, and also in other myrmecophiles, as for instance in Paussinae. In contrast to cave-dwellers, fully winged species with good flying abilities occur in myrmecophilous groups. This enables the respective species to colonize new ant nests more actively and easily, while flightless myrmecophilous beetles (e.g. in Staphylinidae) are transported by their ant hosts and show a higher degree of host specificity (Crowson 1981; Luo et al. 2021b).

4.2.6 Musculature

In the examined cave-dwelling species of Carabidae and Leiodidae, the modifications of the cephalic musculature were inconspicuous to almost neglectable. An unusual feature of the carabid *S. wangorum* is the presence of a single fiber extending from the posteroventral wall of the head capsule to the ventrolateral wall of the posterior pharynx (Luo et al. 2018a). However, it is presently unclear whether this also occurs in related subterranean carabids. This

condition is possibly correlated with the elongation of the posterior head capsule. Such an elongate ventral pharyngeal dilator is missing in the leiodid species examined (Beutel et al. 2021; Jałoszyński et al. 2020; Luo et al. 2019b, 2021a), despite of a moderate elongation of the head capsule.

In contrast to the large unmodified cephalic musculature of cave dwelling species of Carabidae and Leiodidae, a highly modified muscular system was observed in the Pselaphinae species (Jałoszyński et al. 2020). Along with the profound skeletal modifications, the muscles related with the mouthparts are distinctly simplified in *C. testaceus* (Jałoszyński et al. 2020). These modifications are very likely correlated with the modifications of the mouthparts and apparently adaptation to trophallaxis.

The pro- and mesothoracic musculature of the examined cave-dwelling beetles largely follows the normal pattern found in beetles (e.g. Larsén 1966). However, the obligatory loss of hind wings and the flight capacity results in the reduction of direct and indirect flight muscles in the metathorax (Luo et al. 2018b, 2019a), in a similar pattern as it also occurs in wingless species of the surface (Larsén 1966). Obviously correlated with the far-reaching reduction of the flight apparatus, metathoracic musculature also shows a high degree of reduction in the myrmecophilous *C. testaceus* (Luo et al. 2021b).

4.2.7 Other morphological features

As in the iconic leiodid *L. hohenwartii*, elongated legs are common cave-dwelling Carabidae and also occur in Leiodidae (e.g. Luo et al. 2018b). This constructive transformation increases the efficiency of locomotion and is one of the most common troglomorphic features (Fišer 2019). It is a characteristic of cavernicolous species living in more spacious environments. Not surprisingly this feature is usually absent in soil-dwelling species, as interspaces in soil are generally narrow. The walking speed of surface-living carabids can vary from 3.9 to 16.1 cm/s, allowing the faster species long range dispersal even without flight (Thiele 1977). As subterranean carabids usually live in relatively restricted spaces compared to their surface-dwelling relatives, long-range dispersal, even though it may be possible with long legs on principle, does not play a role anymore.

Although measurements are scarce (Lavoie et al. 2007; Vittori & Štrus 2014), a decrease of the cuticular thickness is considered as a typical feature of cave arthropods (e.g. Christiansen 2012; Faille 2019). Since a cave is an environment with consistent high humidity (Gunn 2004), the evaporative water loss is a minor problem for cave-dwelling animals (Vittori et al. 2017). The reduction of pigment

is another common troglomorphic feature (Christiansen 2012). It has been studied more intensively in aquatic organisms (e.g. Jeffery 2006; Protas et al. 2011), but remains rather poorly understood in terrestrial animals. In addition, even though cave-dwelling species are often larger than surface-dwelling relatives (Gunn 2004), it was found out that body sizes of subterranean diving beetles varied substantially from one community to the next (Vergnon et al. 2013).

4.2.8 Issues which remain unclear

Unlike common regressive troglomorphies like eyelessness and depigmentation, various constructive troglomorphies are taxon-specific (Fišer 2019). For example, cave-dwelling leiodids are categorized into four distinctive morphological groups (Moldovan et al. 2018). In contrast, cave-dwelling carabids evolved a more uniform body shape, much more elongated and slender than their surface relatives. Similar situations are also present in other groups of arthropods, such as for instance in the cave-dwelling crustacean genus *Niphargus* Dudich (Amphipoda), in which several morphological types evolved, each distinctly different from the other (Trontelj et al. 2012). Moreover, even the same species, like in *Asellus aquaticus* (Linnaeus), may display various morphological types (Konec et al. 2015). This may be a result of phylogenetic effects or linked with the specific microhabitats. At present, the mechanism behind this phenomenon remains insufficiently clarified (Fišer 2019). Molecular data suggest that different morphological types may be more closely associated to ecological conditions than linked with phylogenetic signal (Faille 2019). However, this may vary among different groups.

4.3 Effects of environmental factors on subterranean adaptation

4.3.1 Darkness

Even though environmental parameters (temperature, humidity, etc.) can vary in different cases, conditions in subterranean habitats are relatively constant compared to the epigeal environment (Eisenbeis & Wichard 1987; Culver & Pipan 2008). Moreover, the more or less complete absence of light is common to different subterranean habitats, and a critical factor in the context of morphological specializations of subterranean organisms (Culver & Pipan 2019; Fišer 2019).

Light is critical for animals in many different ways, affecting for instance development, reproduction, and circadian rhythms (Giese, 1964; Rowan 1938). In caves, darkness is apparently the most defining feature and a key driver of troglomorphic trait evolution (Simon 2019). On one hand, the absence of light directly results in the loss of vision-dependent means of allocating food and mating

partners; on the other hand, darkness provides an advantageous environment in terms of protection from predators, parasites, and extreme temperatures (Friedrich 2019). The absence of light makes compound eyes and other visual organs redundant, and correspondingly the regression or complete loss of eyes is a common and distinctive feature of animals in caves and other subterranean environments (Culver & Pipan 2019; Eisenbeis & Wichard 1987; Friedrich 2019; Gunn 2004). The dark environment can also favor elongation of appendages, notably sense organs like antennae and the walking legs (Friedrich 2019). However, this feature is not common in beetles living in soil or other interstitial microhabitats, which usually have short appendages as a result of limited space in their environment (Crowson 1981). The “gains” and “losses” of cave inhabitants are addressed as “constructive” and “regressive” troglomorphic traits, respectively: constructive changes (elongation of appendages, enlargement of sensory organs, etc.) bring fitness gains, whereas regressive modifications (eyelessness, depigmentation, etc.) benefit the animals by potentially reducing energy costs or risk of injury and inflammation (Friedrich 2019). Additionally, morphological modifications can be closely linked to behavioral modification, and thus potentially facilitate survival underground.

4.3.2 Food

The absence of light has a great influence on the energy input. The absence of photosynthesis as well as primary producers, drastically reduces the amount and variety of resources, even though flowing water, roots, and other media still transport energy into the caves for both aquatic and terrestrial organisms (Culver & Pipan 2019). The influx of energy mainly consists of dead organic matters from plants and animals, as well as feces, eggs, and cadavers of cave-dwelling animals such as bats and crickets (Simon 2019). Moreover, chemosynthetic microorganisms also provide nutrients and energy for the cave inhabitants (Crowson 1981; Engel 2007).

Despite of an existing variety of food sources, carnivorous habits and predators obviously play an important role in cave environment. Compared to their surface-dwelling relatives, cave-dwelling carabids tend to possess longer mandibles, and elongated heads and thoraces (see Luo et al. 2018a). In contrast, only highly specialized leiodid species have a slender body and their mandibles remain largely unmodified (see Luo et al. 2019a, b). These differences in subterranean evolution are apparently mainly linked with the feeding habits. Predacious carabids actively search their prey, even in narrow fissures of the cave walls, while scavenging leiodids feed on moist bat guano, carcasses, and various microorganisms (Majka &

Langor 2008; Peck 1977). In contrast to energy-poor cave and soil habitats, the nests of social insects are nutrient-rich, containing ant brood and collected and cultivated food. This provides many myrmecophilous beetles with a stable supply of food resources (Geiselhardt et al. 2007; Parmentier 2020). Being fed by the host ants like in highly modified species of the clavigerite Pselaphinae is an advanced and irreversible stage of myrmecophily.

4.3.3 Space

One of the most distinct differences between caves and other subterranean habitats like soil, sand and fissures are the available space for locomotion. Many cave animals are reportedly larger than their surface relatives, whereas animals dwelling in other subterranean habitats are often miniaturized (Friedrich 2019). To adapt to deep-soil habitats, endogean beetles do not only have to adjust to the degree of moisture, ventilation, and temperature, but also, very importantly, to the pore volume of the substrate (Crowson 1981; Eisenbeis & Wichard 1987). The very restricted space of the pre-existing crevices apparently corresponds to the shortened appendages of many soil-dwellers. Flightlessness, which also occurs in endogean beetles, likely depends on the depth of the preferred environment and to the capacity to move in vertical direction. While this is obligatory and irreversible in cave dwelling species, this is apparently not the case in soil dwelling beetles. Nevertheless, superficial subterranean habitats (MMS [Milieu Souterrain Superficiel], epikarst, seeps) can also hosts animals showing troglomorphy, even with elongated appendages in some cases. It is conceivable that these environments represent a potential stepping stone for colonizing deeper and more extreme environments (Culver & Pipan 2008; Friedrich 2019).

4.3.4 Other factors

Besides darkness and scarcity of food sources, the critical environmental factors in caves include low density of predators and competitors, constancy of the environment, and high humidity. These three characteristics actually are beneficial for the inhabitants and reduce the overall selective pressure (Trontelj 2012). In addition, the reduction or loss of the body pigmentation is likely made possible by the lack of biologically harmful UV light (Friedrich 2019).

4.3.5 Issues remained to be solved

Although more and more efforts have been made to study how environmental factors affect morphological traits of subterranean animals, nearly all experimental studies were based on cave-dwelling aquatic organisms (e.g. Culver et al. 2010; Delić et al. 2016; Kralj-Fišer et al. 2020). Presently, comparatively little is known on the effects on terrestrial groups. Furthermore, inhabitants living in other subterranean habitats are even much less explored.

4.4 Success of Coleoptera dwelling underground

Coleoptera represent the most successful radiation in Hexapoda in terms of described species (McKenna & Farrell 2009). Beetles of different groups colonized a plethora of different habitats: from dead trees or tree canopies to hot springs or tidal pools, and from high mountains to deserts (Crowson 1981). Considering the morphology of the adults, it is not surprising that they were also successfully colonizing various environments below the ground, and even became the most speciose group among troglobitic invertebrates (Decu 2004). A strongly armored body without exposed membranes and with elytra covering the membranous hind wings makes beetles predestined not only to move under bark (e.g. Archostemata), but also to live in leaf litter and to enter deeper levels of soil substrates and cracks.

4.4.1 Certain groups of beetles are more successful than others

As pointed out above, it is quite obvious why phytophagous or wood associated beetles are very rarely if ever found in deep soil or even caves. However, it is a more intriguing question why troglobiontic habits have mainly evolved in two non-related groups, Carabidae (especially in Trechini) and Leiodidae (Andújar & Grebennikov 2021; Faille 2019). In this context it is noteworthy that both families have distinctly different feeding habits (Culver & Pipan 2019), the former almost predominantly predacious, and the latter mostly mycetophagous or saprophagous. In Carabidae, species of the tribe Anillini are often found in soil and considered as endogean (Andújar & Grebennikov 2021). However, interestingly, the group is only poorly represented in caves in comparison to Trechini.

Since there are extremely limited plant resources in caves (Culver & Pipan 2019), it is not surprising that phytophagous beetles are extremely rare in the subterranean realm. Additionally, many beetles, for instance species of certain groups of Scarabaeidae, are decomposers of plant matters and often found in soil, but usually only as larval stages (Burgers & Raw 1967; Crowson 1981). Both Carabidae and Leiodidae successfully colonized different types of the

interconnected subterranean environments, which demonstrates their capability to disperse from leaf litter and superficial soil layers to deep soil and also caves. The structural modifications often lead to behavioral changes and might determine the success of underground colonization (Christiansen 1965). In contrast to the typical feeding behavior in the two families, some species are omnivores, as for instance *Poecilus cupreus* Linnaeus in Carabidae (see Charalabidis et al. 2019; Burgers & Raw 1967; Moldovan 2018), which allows them to take full advantage of the limited energy sources in the darkness and play an important role in the subterranean food chain. For instance, bat or bird guano and eggs of cave crickets provide organic food resources for both Carabidae and the saprophagous Leiodidae (Crowson 1981; Ferreira 2019; Kane & Poulson, 1976; Peck et al. 1989). Cave-dwelling carabid beetles are able to consume 90% of the eggs laid by cave crickets (Kane & Poulson 1976), and it was shown that the availability of this food source significantly affects the population dynamics of these cave beetles (Culver 1982). In some cases, morphological modifications are closely linked to the feeding habits, as for instance in *Cansiliella servadeii* Paoletti (Leptodirini, Leiodidae), a species in which hoe-shaped mandibles and spoon-shaped galeae optimize specialized semi-aquatic feeding (Casale et al. 2004; Dorigo et al. 2017).

Beetles living in soil are either predators or feeding on plant roots or decaying animals (for a summary of feeding habits of soil beetles also see Table VII in Burgers & Raw 1967). It was shown that species of *Catops* Paykull and *Ptomaphagus* Hellwig (Leiodidae) play a prominent part in the decomposition of carrion in soil substrate (Burgers & Raw 1967). The majority of soil-dwelling beetles inhabit the organic upper layer, and only certain species show distinct morphological modifications likely correlated with endogean life (Eisenbeis & Wichard 1987). In the case of Carabidae and Leiodidae, the respective feeding habits and the occurrence in various types of subterranean environments likely facilitates the invasion of caves. However, it remains unclear why other non-phytophagous coleopteran groups with highly diversified species only play a very marginal roles in the subterranean environment. For instance, staphylinid beetles also contain many species living in leaf-litter or even blind myrmecophilous ones. Nevertheless, they remain rare in the cave environment. Despite of the successful colonization of transitional zones, most subgroups of rove beetles did not become a distinct radiation in zones of extreme darkness. A noteworthy exception is the morphologically highly variable and speciose subfamily Pselaphinae. This group does not only contain numerous highly specialized myrmecophiles (e.g. Jałoszyński et al. 2020), but also a sizeable number of advanced cave-dwelling species.

In the case of myrmecophilous beetles, all relevant lineages contain taxa inhabiting soil and forest litter, which likely facilitates the evolution of an ant-

associated life style. However, the habitat type and also the diet are not the only factors potentially leading to myrmecophily (Parker 2016). Some beetles wandering near ant trails outside the nests show a “myrmecomorphic” morphological resemblance to their army ant hosts (Geiselhardt et al. 2007). The ant-like appearances can be viewed as a stepping stone towards myrmecophily, but may primarily protect the beetles against birds and other predators, which experienced stings of the ants host of Dorylinae (Hölldobler 1971). Similar to the cave-dwelling species, myrmecophilous coleopteran species are highly concentrated in certain lineages. In the megadiverse Carabidae, the tribe Paussini contains exclusively myrmecophilous beetles, while very few myrmecophilous species are found in other groups. In the similarly speciose Staphylinidae, the “APS” subfamilies (“Aleocharinae, Pselaphinae, Scydmaeninae”) contain the vast majority of myrmecophiles (Parker 2016).

4.4.2 Other subterranean insects

A. Diptera: Following Coleoptera, Diptera contains the second largest number of species living underground. However, subterranean flies are mostly non-troglobitic and the order contains only very few troglobites (Culver & Pipan 2019; Howarth 2009; Vandel 1965). Cave systems mainly provide suitable sites for hibernation and aestivation for species of Diptera, and thus play an important role of maintaining populations of this group (Kjærandsen 1993). Among the rare cases of troglobitic flies, it is noteworthy that both *Troglocladius hajdi* Andersen, Baranov & Hagenlund (Chironomidae) and *Spelobia tenebrarum* (Aldrich) (Sphaeroceridae) possess reduced eyes, but at the same time large wings, in stark contrast to subterranean beetles, where the losses are apparently closely correlated. However, in spite of being fully winged, *S. tenebrarum* is not considered as a good flier, and *T. hajdi* has never been observed flying so far (Andersen et al. 2016; Marshall & Peck 1985; Niemiller et al. 2019b). Furthermore, these flies live in soil during their larval development (Burgers & Raw 1967; Eisenbeis & Wichard 1987). Even though food uptake usually plays a minor role in adult dipterans, the larvae are very diverse in their feeding habits as it is also the case in beetles. Nevertheless, the two orders clearly evolved different ways of colonizing and using subterranean habitats. This is likely partly due to the different degree of importance of flight in their adult life, an essential feature in flies as the name suggests, and much less important in Coleoptera in comparison.

B. Hymenoptera: Ant species inhabit a great variety of terrestrial environments, including not only microhabitats like leaf litter or plant surfaces, but also underground (Wong & Guénard 2017). A disturbing case of a cave invasion is the

notorious red imported fire ant *Solenopsis invicta*, an obvious pest that can have devastating effects on cavernicolous faunas (Niemiller et al. 2019b; Reddell 2019). In spite of being often found in caves, most researchers consider their cavernicolous existence only as accidental (Ferreira 2019). Furthermore, cave-dwelling ants usually do not show morphological specializations like typical troglobites. Most of them still possess functional eyes and normally pigmented cuticle. Highly specialized cave-dwelling species remain mostly unknown in Formicidae (Wilson 1962). The almost complete absence of troglomorphic modifications in subterranean ants is possibly related to their lifestyle as social insects. It has been stated that cave-restricted ants would be unable to maintain a sufficiently large colony size (Wilson 1962).

C. Auchenorrhyncha: As a megadiverse suborder of phytophagous insects, Auchenorrhyncha (cicada, planthoppers etc.) do not seem like ideal candidates for adapting to life in caves. Nevertheless, remarkably, more than 70 troglobitic species are known from the Hawaiian Islands (Hoch & Howarth 1999). Cave-dwelling auchenorrhynchans feed on penetrated plant roots and still have extant surface-living relatives. These tropical non-relictual troglobites fit the pattern of adaptive radiation according to Howarth (1987). This also shows that different patterns and models may occur in tropical caves.

4.5 Conclusions and outlook

Beetles represent the most speciose subterranean radiation among all groups of animals (Faille 2019). Morphological features such as protective elytra and lacking exposed membranous areas make them predestined to penetrate from leaf litter into deeper soil layers and into systems of cracks. Such lightless environments were likely gateways to enter caves as extreme habitats, and also to specialized cryptic life styles like myrmecophily, which has evolved in different unrelated groups of beetles. Strong selective pressure in caves generally resulted in the correlated reductions of eyes and the flight organs, and also in depigmentation. Such regressive features can be accompanied by constructive modifications like elongation of legs, sensory appendages, and mouthparts (Moldovan 2012; Romero 2009; Faille 2019). Soil dwelling beetles usually maintain a certain flexibility with regard to their location, also in vertical direction. In contrast, a shift to life in caves is obviously irreversible, except for some forms living in the entrance zone. This also applies to beetles associated with ants. Far-reaching modifications like strongly reduced mouthparts tie these beetles irreversibly to their hosts.

Life in caves and other subterranean environments is obviously no option for the numerous phytophagous or wood-associated beetles, or only occurs in very rare

cases (e.g. species feeding on penetrated roots of plants or secondarily on fungi). What remains largely in the dark is why many ground-oriented groups, for instance many subgroups of Staphylinidae, did not evolve cavernicolous habits. Truly cave dwelling species are largely restricted to the predacious adepagan Carabidae and the polyphagan Leiodidae and Pselaphinae.

Despite of detailed morphological data provided in studies included in this dissertation, the knowledge of the anatomy of cave beetles is still highly fragmentary. An efficient working pipeline including different established and innovative techniques may lead to an improvement of this situation in the near future. Morphology-based studies should also include morphometric investigations of body shape, providing sound data in the context of cave adaptations. The application of these modern techniques will not only lead morphological research from two-dimensional visualization to three dimensions, but also make the process of quantitation of structural characters faster and more reliable. A major perspective is the exploration of the genetic background of phenotypic modifications. Evaluations of transcriptomes or genomes of cave dwelling species and epigeal relatives will likely yield important insights in the evolution of subterranean life. As many well-known statements on subterranean evolution were based on assumptions rather than solid evidence, many proposed hypotheses are still waiting to be tested in the future. To understand morphological transformations and adaptations of subterranean species, a combination of detailed morphological documentation, behavioral experiments, and functional and physiological investigations will be necessary. A broad methodological approach, a dense sampling of species, and a solid phylogenetic framework will likely make it possible to disentangle a complex network of evolutionary interactions between beetles of the underground and their environments.

5 Summary

Aims of the present study were: (1) a thorough morphological documentation of the head and thorax of selected representatives of two coleopteran families with subterranean species; (2) to analyze the effects of the environment based on comparisons of external and internal structural features of species from different specific habitats; (3) to evaluate antennal sensillar patterns to test the hypothesis that blind cave-dwelling species possess more extra-optic sensorial structures than their surface-dwelling relatives. The habitats of the selected species include caves, leaf-litter and deeper layers of soil, and ant nests.

By combining light microscopy, scanning electron microscopy, histological sections, micro-CT scanning and three-dimensional reconstructions, we conducted comparative morphological studies on 63 coleopteran species (Leiodidae and Staphylinidae). The anatomy of *Troglocharinus ferreri* (Reitter, 1908) (head and thorax), *Bergrothia saulcyi* (Reitter, 1877) (head), *Claviger testaceus* Preyssler, 1790 (head and thorax), *Diartiger kubotai* Nomura, 1997 (head), *Pselaphus heisei* Herbst, 1792 (head) was examined and documented in detail (Study I - VII). Skeletal structures, muscles, elements of the nervous systems and glands were studied and compared, and discussed in the context of evolutionary transformations linked with different subterranean environments.

Studies I and VI provide the first detailed anatomical documentations of the troglobitic leiodid *T. ferreri*. The head of *T. ferreri* displays distinct features linked with subterranean habits, including the complete loss of compound eyes, circumocular ridges and optic lobes. Comparing different species Leptodirini, two different trends were found in troglobitic representatives of this leiodid tribe. The head capsule of species in some genera is distinctly elongated, whereas representatives of other genera have broadened and more transverse heads. The body of *T. ferreri* is more elongated and slender compared to epigeal leiodids, with a largely unmodified prothorax. The pterothorax is greatly modified, with loss of the flight apparatus and strongly reduced flight-related muscles. The phenomenon of reduced muscles in *T. ferreri* is similar to what we previously found in the troglobitic carabid species *Sinaphaenops wangorum* Uéno & Ran, 1998.

The cephalic morphology of pselaphine species was studied in Studies II-V, including various species with different habitats such as leaf-litter and soil and ant nests. Study II provides the first thorough documentation of the head morphology of *C. testaceus*, which is a blind obligate myrmecophilous species. Highly modified mouthparts (e.g. unusual connection of the maxillae to the hypopharynx and a transformed labium with a vestigial prementum) were found, and many cephalic

muscles are reduced compared to the coleopteran groundplan and other staphylinoids. Species living in leaf-litter and/or soil substrate were studied in Study III and IV. *B. saulcyi* shows features adapted to deep-soil life. This flightless species has greatly reduced and non-functional eyes and long appendages. The study on the predacious *P. heisei*, a species with well-developed compound eyes, shows cephalic muscles likely very close the groundplan condition of Pselaphinae. The relatively unmodified morphological configuration in this case is linked with life in the upper soil layers combined with specialized carnivorous habits. Study V not only provides a detailed description of the head morphology of *D. kubotai*, but also a reconstruction of the phylogeny of the pselaphine supertribe Clavigeritae based on 155 morphological characters of the head. The thoracic morphology of *C. testaceus* was documented in Study VII, which provides detailed anatomical data for this flightless ant-associated species. Aside from features related to myrmecophilous habits (e.g. small body size, compact body and robust appendages), two differing patterns of advanced reduction of skeletal and muscular elements were found in both species with vestigial wings. Studies II-V show that the structural megadiversity of the successful staphylinid subfamily Pselaphinae reflects an extreme diversification of life habits, including for instance life in deep soil, caves or ant nests. Study VIII was focused on the morphology of antennal sensilla in Leiodidae, including species with or without eyes living in caves or in leaf-litter. The results show that the number, length and diameter of sensilla does not differ among different ecological groups, and that the density of sensilla is even lower in blind or hypogean species. This unambiguously refutes the common assumption that cave-dwellers compensate their blindness with an enriched array of sensilla.

Due to their strong mechanical protection, beetles were apparently predestined to invade subterranean environments. Our comparative evaluation suggests that leaf litter and more or less deep soil layers were likely not only steppingstones to life in deep systems of cracks and in true caves, but also environments potentially leading to highly specialized life styles like a close association with ants. To reveal different aspects of subterranean evolution in Coleoptera and other groups, further anatomical investigations with a broader sampling are required. This should include inhabitants of different specific environments. Morphological studies including geometric morphometrics should be combined with functional, behavioral and physiological investigations. Additionally, the exploration of the genetic background should have high priority. Carried out with a solid phylogenetic framework, this will likely reveal important mechanisms of adaptations to different subterranean environments.

6 Zusammenfassung

Ziele des vorliegenden Promotionprojekts waren: (1) gründliche Dokumentationen der Kopf- und Thoraxmorphologie mehrerer ausgewählter repräsentativer Coleoptera-Arten; (2) Analyse der Anpassungen an verschiedene Habitate auf der Grundlage vergleichender Studien der äußeren und inneren Morphologie zwischen Arten aus unterschiedlichen Habitaten; (3) ein Test der Hypothese nach der blinde Höhlenbewohner als Ausgleich für den Verlust von Augen mehr extraoptische Sinnesstrukturen besitzen als ihre an der Oberfläche lebenden Verwandten. Unter den ausgewählten Arten waren Bewohner von Höhlen, Laubstreu, Bodensubstrat, und Ameisennestern.

Durch die Kombination von Lichtmikroskopie, Rasterelektronenmikroskopie, histologischen Schnitten, Mikro-CT Scans und dreidimensionalen Rekonstruktionen führten wir vergleichende morphologische Studien an 63 Käferarten durch (Leiodidae und Staphylinidae). Dabei wurden innere und äußere Strukturen von *Troglocharinus ferreri* (Reitter, 1908) (Kopf und Thorax), *Bergrothia saulcyi* (Reitter, 1877) (Kopf), *Claviger testaceus* Preyssler, 1790 (Kopf und Thorax), *Diartiger kubotai* Nomura, 1997 (Kopf), *Pselaphus heisei* Herbst 1792 (Kopf) im Detail untersucht und dokumentiert (Studie I-VII). Skelettstrukturen, Muskeln, Elemente des Nervensystems und Drüsen wurden dokumentiert und im Hinblick auf die übergeordneten Fragestellungen diskutiert.

Die Studien I und VI liefern die ersten gründlichen morphologischen Dokumentationen des troglobitischen Leiodiden *T. ferreri*. Der Kopf dieser Art weist Merkmale auf, die klar mit der unterirdischen Lebensweise verbunden sind, einschließlich des vollständigen Verlusts von Facettenaugen, zirkumokulären Leisten und optischen Loben. Im Vergleich verschiedener Leptodirini-Arten wurden bei troglobitischen Vertretern dieser Tribus zwei verschiedene Tendenzen gefunden. Arten einiger Gattungen weisen eine deutlich verlängerte Kopfkapsel auf, während Arten anderer Gattungen sich durch verbreiterte und eher transversale Köpfe auszeichnen. Der Körper von *T. ferreri* ist im Vergleich zu epigäischen Leiodiden länglicher und schlanker, bei einem weitgehend unveränderten Prothorax. Der Pterothorax ist stark abgewandelt, mit dem Verlust des Flugapparates und einer stark reduzierten Flugmuskulatur. Das Phänomen der reduzierten Muskulatur bei *T. ferreri* ähnelt dem, was vorher bei der troglobitischen Carabidenart *Sinaphaenops wangorum* Uéno & Ran, 1998 festgestellt wurde.

Die Morphologie von Vertretern der Pselaphinae wurde in den Studien II-V untersucht, mit einem Fokus auf Arten, die in Laubstreu, mehr oder weniger tiefem Bodensubstrat oder Ameisennestern leben. Studie II ist die erste gründliche

Dokumentation der Kopfmorphologie von *Claviger testaceus*, einer augenlosen obligat myrmekophilen Spezies. Es wurden stark modifizierte Mundwerkzeuge (z.B. ungewöhnliche Verbindung der Mandibel mit dem Hypopharynx und ein stark modifiziertes Labium mit einem rudimentären Prämentum) gefunden, und viele Kopfmuskeln waren im Vergleich zum Coleopteren-Grundplan und anderen Staphylinoiden reduziert. In Laubstreu und Bodensubstrat lebende Arten wurden in Studien III und IV untersucht. *Bergrothia saulcyi* zeigt Merkmale, die Anpassungen an das Leben in tieferen Bodenschichten darstellen. Diese flugunfähige Art hat stark reduzierte und nicht funktionsfähige Augen sowie lange Körperanhänge. Bei der in Laubstreu lebenden räuberischen Art *Pselaphus heisei* sind gut entwickelte Facettenaugen vorhanden, und die gut entwickelte Kopfmuskulatur entspricht wahrscheinlich weitgehend dem Grundplan der Pselaphinae. Die extreme strukturelle Vielfalt der Pselaphinae reflektiert eine enorme ökologische Vielseitigkeit, inklusive starker Spezialisierungen wie dem Leben in tiefen Bodenschichten, Höhlen und Ameisennestern. Studie V liefert nicht nur eine detaillierte Beschreibung der Kopfmorphologie von *Diartiger kubotai*, sondern auch eine Rekonstruktion der Phylogenie der Clavigeritae und der gesamten Pselaphinae, basierend auf 155 morphologischen Merkmalen des Kopfes. Die thorakale Morphologie von *C. testaceus* wurde in Studie VII dokumentiert. Abgesehen von Merkmalen, die mit der myrmekophilen Lebensweise zusammenhängen (z. B. kleine Körpergröße, kompakter Körper und robuste Anhängsel) wurden zwei unterschiedliche Formen der Flügelreduktion festgestellt und deutliche Reduktionen der Skelett- und Muskelelemente. Studie VIII behandelt die Morphologie der Antennensensillen von Leiodiden, unter Berücksichtigung von Arten bei denen Augen vorhanden sind oder fehlen und die in Höhlen oder in Laubstreu leben. Die Ergebnisse zeigen, dass sich Anzahl, Länge und Durchmesser der Sensillen zwischen verschiedenen ökologischen Gruppen nicht unterscheiden und die Dichte der Sensillen bei blinden oder hypogäischen Arten sogar geringer ist. Unsere Ergebnisse widerlegen die verbreitete Annahme, dass Höhlenbewohner das Fehlen von Licht als Reiz mit einer erweiterten Ausstattung von Sensillen kompensieren.

Mit ihrem starken mechanischen Schutz sind Käfer offensichtlich dafür prädestiniert in unterirdische Lebensräume einzudringen. Unsere vergleichende Auswertung legt nahe, dass die Laubstreu- und mehr oder weniger tiefe Bodenschichten Trittsteine für Übergänge zum Leben in tiefen Spaltensystemen und Höhlen waren, und auch zu hochgradig spezialisierten Lebensweisen wie einer engen Bindung an Ameisen.

Um verschiedene evolutive Aspekte einer unerirdischen Lebensweise bei Käfern und anderen Gruppen zu ergründen, sind zunächst weitere anatomische

Untersuchungen mit einer breiteren Auswahl von Taxa erforderlich. Dabei sollten Bewohner unterschiedlicher unterirdischer Lebensräume berücksichtigt werden. Morphologie inklusive geometrischer Morphometrie sollte mit funktionellen und physiologischen Untersuchungen und mit Verhaltensstudien kombiniert werden. Zusätzlich sollte die Erforschung des genetischen Hintergrunds hohe Priorität haben. Mit einer soliden phylogenetischen Grundlage werden sich daraus wahrscheinlich wichtige Erkenntnisse zu Mechanismen der Anpassung an verschiedene unterirdische Habitate ergeben.

7 References

- Abeille de Perrin, E. (1904). Description d'un Coléoptère hypogé français. *Bulletin de la Société Entomologique de France*, 9(15), 226-228.
- Accordi, F., & Sbordoni, V. (1978). The fine-structure of Hamann's organ in *Leptodirus hohlenwarti*, a highly specialized cave Bathysciinae (Coleoptera, Catopidae). *International Journal of Speleology*, 9(2), 153–165.
- Andersen, T., Baranov, V., Hagenlund, L. K., Ivković, M., Kvifte, G. M., & Pavlek, M. (2016). Blind flight? A new troglobiotic orthoclad (Diptera, Chironomidae) from the Lukina Jama–Trojama cave in Croatia. *PloS One*, 11(4), e0152884.
- Andújar, C., & Grebennikov, V. V. (2021). Endogean beetles (Coleoptera) of Madagascar: deep soil sampling and illustrated overview. *Zootaxa*, 4963(2), 317–334.
- Andújar, C., Pérez-González, S., Arribas, P., Zaballos, J. P., Vogler, A. P., & Ribera, I. (2017). Speciation below ground: Tempo and mode of diversification in a radiation of endogean ground beetles. *Molecular Ecology*, 26(21), 6053-6070.
- Arikawa, K., Suyama, D., & Fujii, T. (1996). Light on butterfly mating. *Nature*, 382, 119-119.
- Baehr, M., & Main, D. (2016). New genera and species of subterranean anilline Bembidiini from the Pilbara, northwestern Australia (Insecta: Coleoptera: Carabidae: Bembidiini: Anillina). *Records of the Western Australian Museum*, 31(2), 59-89.
- Bardgett, R. (2005). *The biology of soil: a community and ecosystem approach*. Oxford University Press, Oxford.
- Barr, T. C. (1968). Cave ecology and the evolution of troglobites. In T. Dobzhansky, M. K. Hecht, & W. C. Steere (eds.), *Evolutionary biology* (pp. 35-102). Springer, Boston, Massachusetts.
- Barr, T. C. (1986). An eyeless subterranean beetle (*Pseudanophthalmus*) from a Kentucky coal mine (Coleoptera: Carabidae: Trechinae). *Psyche*, 93(1-2), 47-50.
- Belkaceme, T. (1991). Skelet und Muskulatur des Kopfes und Thorax von *Noterus laevis* Sturm: ein Beitrag zur Morphologie und Phylogenie der Noteridae (Coleoptera: Adephaga). *Stuttgarter Beiträge zur Naturkunde Serie A (Biologie)*, 462, 1–94.

- Beutel, R. G., Friedrich F., Ge, S. Q. & Yang X. K. (2014). *Insect morphology and phylogeny: a textbook for students of entomology*. Walter de Gruyter, Berlin/Boston.
- Beutel, R. G., Luo, X. Z., Yavorskaya, M. I., & Jałoszyński, P. (2021). Structural megadiversity in leaf litter predators-the head anatomy of *Pselaphus heisei* (Pselaphinae, Staphylinidae, Coleoptera). *Arthropod Systematics & Phylogeny*, *79*, 443.
- Beutel, R.G., Yavorskaya, M., Mashimo, Y., Fukui, M. & Meusemann, K. (2017). The phylogeny of Hexapoda (Arthropoda) and the evolution of megadiversity. *Proceedings of the Arthropodan Embryological Society of Japan*, *51*, 1–15.
- Burgers, A. & Raw, F. (1967). *Soil biology*. Academic Press, London.
- Casale, A., Vigna Taglianti, A., & Juberthie C. (1998). Coleoptera Carabidae. In C. Juberthie, & V. Decu (eds), *Encyclopaedia Biospeologica, Tome 2* (pp. 1047–1081). Société Internationale de Biospéologie, Moulis-Bucarest.
- Casale, A., Giachino, P. M., & Jalžić, B. (2004). Three new species and one new genus of ultraspecialized cave dwelling Leptodirinae from Croatia (Coleoptera, Cholevidae). *Natura Croatica*, *13*(4), 301-317.
- Charalabidis, A., Dechaume-Moncharmont, F. X., Carbonne, B., Bohan, D. A., & Petit, S. (2019). Diversity of foraging strategies and responses to predator interference in seed-eating carabid beetles. *Basic and Applied Ecology*, *36*, 13-24.
- Christiansen, K. A. (1962). Proposition pour la classification des animaux cavernicoles. *Spelunca*, *2*, 76-78.
- Christiansen, K. A. (1965). Behavior and form in the evolution of cave Collembola. *Evolution*, *19*(4), 529-537.
- Christiansen K. A. (2012) Morphological adaptation. In W.B. White, & D.C. Culver (eds.), *Encyclopedia of caves* (pp. 517-528). Elsevier-Academic Press, Amsterdam
- Coiffait, H. (1958). Contribution á la connaissance des Coléoptères du sol. *Vie et milieu, suppl.* *7*, 1-204
- Coiffait, H. (1959). Monographie des Leptotyphlites (Col. Staphylinidae). *Revue Française d'Entomologie*, *26*(4), 237-437.
- Corbière-Tichané, G. (1974). Sur la présence possible d'un pigment visuel dans un récepteur sensoriel de l'antenne d'un coléoptère cavernicole *Speophyes lucidulus* Delar.(Bathysciinae). *Vision Research*, *14*(9), 819-822.

- Crowson, R. A. (1981). *The biology of the Coleoptera*. Academic press, London.
- Culver, D. C. (1982). *Cave life*. Harvard University Press, Cambridge, Massachusetts.
- Culver, D. C., & Pipan, T. (2008). Superficial subterranean habitats—gateway to the subterranean realm. *Cave and Karst Science*, 35(1-2), 5-12.
- Culver, D. C., & Pipan, T. (2014). *Shallow subterranean habitats. Ecology, evolution, and conservation*. Oxford University Press, Oxford.
- Culver, D. C., & Pipan, T. (2019). *The biology of caves and other subterranean habitats (Second edition)*. Oxford, Oxford University Press.
- Culver, D. C., Holsinger, J. R., Christman, M. C., & Pipan, T. (2010). Morphological differences among eyeless amphipods in the genus *Stygobromus* dwelling in different subterranean habitats. *Journal of Crustacean Biology*, 30(1), 68-74.
- Culver, D. C., Kane, T. C., & Fong, D. W. (1995). *Adaptation and natural selection in caves*. Harvard University Press, Cambridge, Massachusetts.
- Danielopol, D. L., & Rouch, R. (2012). Invasion, active versus passive. In W.B. White, & D. C. Culver (eds.), *Encyclopedia of caves* (second edition, pp. 404-409). Elsevier-Academic Press, Amsterdam.
- Darwin C. R. (1859). *On the origin of species*. John Murray, London.
- Decu, V. (2004). Insecta: Coleoptera (Beetles). In J. Gunn (ed.), *Encyclopedia of caves and karst science* (pp. 965-974). Fitzroy Dearborn, New York.
- Decu, V., & Juberthie, C. (1998). Coléoptères (généralités et synthèse). In: C. Juberthie, & V. Decu (eds.), *Encyclopaedia Biospeologica, Tome 2* (pp. 1047–1081). Société Internationale de Biospéologie, Moulis-Bucarest.
- Deharveng, L., & Bedos, A. (2018). Diversity of terrestrial invertebrates in subterranean habitats. In O. T. Moldovan, L. Kováč, & S. Halse (eds.), *Cave ecology* (pp. 107-172). Springer, Cham.
- Delić, T., Trontelj, P., Zakšek, V., & Fišer, C. (2016). Biotic and abiotic determinants of appendage length evolution in a cave amphipod. *Journal of Zoology*, 299(1), 42-50.
- Deuve, T., & Tian, M. Y. (2014). Un nouveau Trechini aphénopsien dans l'ouest du Guizhou (Coleoptera, Caraboidea). *Bulletin de la Société entomologique de France*, 119(3), 319-322.
- Dorigo, L., Squartini, A., Toniello, V., Dreon, A. L., Pamio, A., Concina, G., Simonutti, V., Ruzzier, E., Perreau, M., Engel, A.S., Gavinelli, F., Martinez-

- Sañudo, I. Mazzon, L. & Paoletti, M. G. (2017). Cave hygropetric beetles and their feeding behaviour, a comparative study of *Cansiliella servadeii* and *Hadesia asamo* (Coleoptera, Leiodidae, Cholevinae, Leptodirini). *Acta Carsologica*, 46(2-3), 317-328.
- Dressler, C., & Beutel, R. G. (2010). The morphology and evolution of the adult head of Adephaga (Insecta: Coleoptera). *Arthropod Systematics & Phylogeny*, 68(2), 239-287.
- Dudley, R., & Pass, G. (2018). Wings and powered flight: Core novelties in insect evolution. *Arthropod Structure & Development*, 47(4), 319-448.
- Eberhard, S. M., & Howarth, F. G. (2021). Undara lava cave fauna in tropical Queensland with an annotated list of Australian subterranean biodiversity Hotspots. *Diversity*, 13(7), 326.
- Eigenmann, C.H. (1909). *Cave vertebrates of America. A study in degenerative evolution*. Carnegie Institution of Washington, Washington DC.
- Eisenbeis, G., & Wichard, W. (1987). *Atlas on the biology of soil arthropods*. Springer-Verlag, Berlin.
- Endler, J. A. (1986). *Natural selection in the wild*. Princeton University Press, Princeton, New Jersey.
- Engel, A. S. (2007). Observations on the biodiversity of sulfidic karst habitats. *Journal of Cave and Karst Studies*, 69(1), 187-206.
- Erwin, T. L. (1979) A review of the natural history and evolution of ectoparasitoid relationships in Carabid beetles. In T. L. Erwin, G. E. Ball, D. R. Whitehead, & A. L. Halpern (eds.), *Carabid beetles: their evolution, natural history, and classification* (pp. 479–484). Dr. W. Junk Publishers, The Hague.
- Faille, A. (2019). Beetles. In W. B. White, D. C. Culver, & T. Pipan (eds.), *Encyclopedia of caves* (third edition, pp. 102-108). Elsevier-Academic Press, Amsterdam.
- Faille, A., & Deharveng, L. (2021). The Coume Ouarnède system, a hotspot of subterranean biodiversity in Pyrenées (France). *Diversity*, 13(9), 419.
- Faille, A., Casale, A., Balke, M., & Ribera, I. (2013). A molecular phylogeny of Alpine subterranean Trechini (Coleoptera: Carabidae). *BMC Evolutionary Biology*, 13(1), 1-16.
- Faille, A., Ribera, I., Deharveng, L., Bourdeau, C., Garnery, L., Quéinnec, E., & Deuve, T. (2010). A molecular phylogeny shows the single origin of the

- Pyrenean subterranean Trechini ground beetles (Coleoptera: Carabidae). *Molecular Phylogenetics and Evolution*, 54(1), 97-106.
- Faille, A., Tänzler, R., & Toussaint, E. F. (2015). On the way to speciation: shedding light on the karstic phylogeography of the microendemic cave beetle *Aphaenops cerberus* in the Pyrenees. *Journal of Heredity*, 106(6), 692-699.
- Ferreira, R. L. (2019). Guano communities. In W. B. White, D. C. Culver, & T. Pipan (eds), *Encyclopedia of caves* (third edition, pp. 474-484). Elsevier-Academic Press, Amsterdam.
- Fišer, C. (2019). Adaptation: Morphological. In W. B. White, D. C. Culver, & T. Pipan (eds), *Encyclopedia of caves* (third edition, pp. 33-39). Elsevier-Academic Press, Amsterdam.
- Fong, D. W., Kane, T. C., & Culver, D. C. (1995). Vestigialization and loss of nonfunctional characters. *Annual Review of Ecology and Systematics*, 26(1), 249-268.
- Forsythe, T. G. (1987). The relationship between body form and habit in some Carabidae (Coleoptera). *Journal of Zoology*, 211(4), 643-666.
- Friedrich, F., & Beutel, R. G. (2008). The thorax of *Zorotypus* (Hexapoda, Zoraptera) and a new nomenclature for the musculature of Neoptera. *Arthropod Structure & Development*, 37, 29–54.
- Friedrich, F., Farrell, B. D., & Beutel, R. G. (2009). The thoracic morphology of Archostemata and the relationships of the extant suborders of Coleoptera (Hexapoda). *Cladistics*, 25, 1–37.
- Friedrich, F., Matsumura, Y., Pohl, H., Bai, M., Hörnschemeyer, T., & Beutel, R. G. (2014). Insect morphology in the age of phylogenomics: innovative techniques and its future role in systematics. *Entomological Science*, 17(1), 1-24.
- Friedrich, M. (2019). Adaptation to darkness. In W. B. White, D. C. Culver, & T. Pipan (eds), *Encyclopedia of caves* (third edition, pp. 16-23). Elsevier-Academic Press, Amsterdam.
- Friedrich, M., Chen, R., Daines, B., Bao, R., Caravas, J., Rai, P. K., Zagmajster, M., & Peck, S. B. (2011). Phototransduction and clock gene expression in the troglobiont beetle *Ptomaphagus hirtus* of Mammoth cave. *Journal of Experimental Biology*, 214(21), 3532-3541.

- Geiselhardt, S. F., Peschke, K., & Nagel, P. (2007). A review of myrmecophily in ant nest beetles (Coleoptera: Carabidae: Paussinae) linking early observations with recent findings. *Naturwissenschaften*, *94*(11), 871-894.
- Ghaffar, H., Larsen, J. R., Booth, G. M., & Perkes, R. (1984). General morphology of the brain of the blind cave beetle, *Neaphaenops tellkampfi* Erichson (Coleoptera, Carabidae). *International Journal of Insect Morphology & Embryology*, *13*(5-6), 357-371.
- Giachino, P.M. & Vailati, D. (2010). *The subterranean environment. Hypogean life, concepts and collecting techniques. L'ambiente sotterraneo. Vita ipogea, concetti e tecniche di raccolta.* WBA Handbooks 3. World Biodiversity Association, Verona.
- Giese, A. C. (1964). *Photophysiology, volume II: action of light on animals and microorganisms; photobiochemical mechanisms; bioluminescence.* Academic Press, New York and London.
- Gunn, J. (2004). *Encyclopedia of caves and karst science.* Taylor & Francis, New York.
- Hermann, H. R. (1979). *Social insects, volume 1.* Academic Press, New York.
- Hoch, H., & Howarth, F. G. (1999). Multiple cave invasions by species of the planthopper genus *Oliarus* in Hawaii (Homoptera: Fulgoroidea: Cixiidae). *Zoological Journal of the Linnean Society*, *127*(4), 453-475
- Hölldobler, B. (1971). Communication between ants and their guests. *Scientific American*, *224*(3), 86-95.
- Holsinger, J. R. (2012). Vicariance and dispersalist biogeography. In W.B. White & D.C. Culver, (eds.), *Encyclopedia of caves* (second edition, pp. 849-858). Elsevier-Academic Press, Amsterdam.
- Hörnschemeyer, T., Bond, J., Young, P. G., & Deans, A. (2013). Analysis of the functional morphology of mouthparts of the beetle *Priacma serrata*, and a discussion of possible food sources. *Journal of Insect Science*, *13*(1), 126.
- Howarth, F. G. (1987). The evolution of non-relictual tropical troglobites. *International Journal of Speleology*, *16*(1), 1-16.
- Howarth, F. G. (2009). Cave insects. In V. H. Resh, & R. T. Cardé (eds.), *Encyclopedia of insects* (second edition, pp. 139-143). Academic Press, Burlington, Massachusetts.

- Howarth, F. G., & Moldovan, O. T. (2018). The ecological classification of cave animals and their adaptations. In O. T. Moldovan, L. Kováč, & S. Halse (eds.), *Cave ecology*, (pp. 41-67). Springer, Cham.
- Huang, S., Wei, G., Wang, H., Liu, W., Bedos, A., Deharveng, L., & Tian, M. (2021). Ganxiao Dong: a hotspot of cave biodiversity in northern Guangxi, China. *Diversity*, *13*(8), 355.
- Humphreys, W. F. (2008). Rising from Down Under: developments in subterranean biodiversity in Australia from a groundwater fauna perspective. *Invertebrate Systematics*, *22*(2), 85-101.
- Jałoszyński, P., Luo, X. Z., & Beutel, R. G. (2020). Profound head modifications in *Claviger testaceus* (Pselaphinae, Staphylinidae, Coleoptera) facilitate integration into communities of ants. *Journal of Morphology*, *281*(9), 1072-1085.
- Jeannel, R. (1926). Monographie des Trechinae. Morphologie comparée et distribution géographique d'un groupe de coléoptères (Première livraison). *L' Abeille*, *32*, 221–550.
- Jeffery, W. R. (2001). Cavefish as a model system in evolutionary developmental biology. *Developmental Biology*, *231*(1), 1-12.
- Jeffery, W. R. (2006). Regressive evolution of pigmentation in the cavefish *Astyanax*. *Israel Journal of Ecology & Evolution*, *52*(3-4), 405-422.
- Jeffery, W. R. (2019). *Astyanax mexicanus*: a vertebrate model for evolution, adaptation, and development in caves. In W. B. White, D. C. Culver, & T. Pipan (eds), *Encyclopedia of caves* (third edition, pp. 85-93). Elsevier-Academic Press, Amsterdam.
- Johnson, C. G. (1969). *Migration and dispersal of insects by flight*. Methuen, London.
- Joseph, G. (1882). Systematisches Verzeichnis der in den Tropfsteingrotten von Krain einheimischen Arthropoden nebst Diagnosen der vom Verfasser entdeckten und bisher noch nicht beschriebenen Arten. *Berliner Entomologische Zeitschrift*, *26*, 1–50.
- Juberthie, C., & Massoud, Z. (1977). L'équipement sensoriel de l'antenne d'un coléoptère troglobie, *Aphaenops cryticola* Linder (Coleoptera: Trechinae). *International Journal of Insect Morphology & Embryology*, *6*(3–4), 147–160.
- Kane, T. C., & Poulson, T. L. (1976). Foraging by cave beetles: spatial and temporal heterogeneity of prey. *Ecology*, *57*(4), 793-800.

- Kjærandsen, J. (1993). Diptera in mines and other cave systems in southern Norway. *Entomologica Fennica*, 4(3), 151-160.
- Koerner, L., Gorb, S. N., & Betz, O. (2012). Functional morphology and adhesive performance of the stick-capture apparatus of the rove beetles *Stenus* spp. (Coleoptera, Staphylinidae). *Zoology*, 115(2), 117-127.
- Konec, M., Prevorčnik, S., Sarbu, S. M., Verovnik, R., & Trontelj, P. (2015). Parallels between two geographically and ecologically disparate cave invasions by the same species, *Asellus aquaticus* (Isopoda, Crustacea). *Journal of Evolutionary Biology*, 28(4), 864-875.
- Kralj-Fišer, S., Premate, E., Copilaș-Ciocianu, D., Volk, T., Fišer, Ž., Balázs, G., Herczeg, G. & Fišer, C. (2020). The interplay between habitat use, morphology and locomotion in subterranean crustaceans of the genus *Niphargus*. *Zoology*, 139, 125742.
- Langille, B. L., Hyde, J., Saint, K. M., Bradford, T. M., Stringer, D. N., Tierney, S. M., Humphreys, W. F. Austin, A. D. & Cooper, S. J. (2021). Evidence for speciation underground in diving beetles (Dytiscidae) from a subterranean archipelago. *Evolution*, 75(1), 166-175.
- Langille, B. L., Tierney, S. M., Austin, A. D., Humphreys, W. F., & Cooper, S. J. (2019). How blind are they? Phototactic responses in stygobiont diving beetles (Coleoptera: Dytiscidae) from calcrete aquifers of Western Australia. *Austral Entomology*, 58(2), 425-431.
- Larsen, J. R., Booth, G., Perks, R., & Gundersen, R. (1979). Optic neuropiles absent in cave beetle *Glacivicola bathyscioides* (Coleoptera, Leiodidae). *Transactions of the American Microscopical Society*, 98(3), 461–464.
- Larsén, O. (1966). On the morphology and function of locomotor organs of the Gyridae and other Coleoptera. *Opuscula Entomologica Supplementum*, 30, 1–241.
- Lavoie, K. H., Helf, K. L., & Poulson, T. L. (2007). The biology and ecology of North American cave crickets. *Journal of Cave and Karst Studies*, 69(1), 114-134.
- Liu, W., & Wynne, J. J. (2019). Cave millipede diversity with the description of six new species from Guangxi, China. *Subterranean Biology*, 30, 57.
- Luo, X. Z., Antunes-Carvalho, C., Ribera, I., & Beutel, R. G. (2019a). The thoracic morphology of the troglobiontic cholevine species *Troglocharinus ferreri* (Coleoptera, Leiodidae). *Arthropod Structure & Development*, 53, 100900.
- Luo, X. Z., Antunes-Carvalho, C., Wipfler, B., Ribera, I., & Beutel, R. G. (2019b). The cephalic morphology of the troglobiontic cholevine species

- Troglocharinus ferreri* (Coleoptera, Leiodidae). *Journal of Morphology*, 280(8), 1207-1221.
- Luo, X. Z., Hlaváč, P., Jałoszyński, P., & Beutel, R. G. (2021a). In the twilight zone—The head morphology of *Bergrothia saulcyi* (Pselaphinae, Staphylinidae, Coleoptera), a beetle with adaptations to endogean life but living in leaf litter. *Journal of Morphology*, 282(8), 1170-1187.
- Luo, X. Z., Jałoszyński, P., Stoessel, A., & Beutel, R. G. (2021b). The specialized thoracic skeletomuscular system of the myrmecophile *Claviger testaceus* (Pselaphinae, Staphylinidae, Coleoptera). *Organisms Diversity & Evolution*, 21, 317–335.
- Luo, X. Z., Wipfler, B., Ribera, I., Liang, H. B., Tian, M. Y., Ge, S. Q., & Beutel, R. G. (2018a). The cephalic morphology of free-living and cave-dwelling species of trechine ground beetles from China (Coleoptera, Carabidae). *Organisms Diversity & Evolution*, 18(1), 125-142.
- Luo, X. Z., Wipfler, B., Ribera, I., Liang, H. B., Tian, M. Y., Ge, S. Q., & Beutel, R. G. (2018b). The thoracic morphology of cave-dwelling and free-living ground beetles from China (Coleoptera, Carabidae, Trechinae). *Arthropod Structure & Development*, 47(6), 662-674.
- Majka, C. G., & Langor, D. (2008). The Leiodidae (Coleoptera) of Atlantic Canada: new records, faunal composition, and zoogeography. *Zookeys*, 2, 357-402.
- Manton, S. M. (1977). *The Arthropoda, habits, functional morphology and evolution*. Clarendon Press, Oxford.
- Marshall, S. A., & Peck, S. B. (1985). The origin and relationships of *Spelobia tenebrarum* (Aldrich), a troglobitic, eastern North American, sphaerocerid fly. *The Canadian Entomologist*, 117(8), 1013-1015.
- Matsumura, Y., Michels, J., Appel, E., & Gorb, S. N. (2017). Functional morphology and evolution of the hyper-elongated intromittent organ in *Cassida* leaf beetles (Coleoptera: Chrysomelidae: Cassidinae). *Zoology*, 120, 1-14.
- McKenna, D.D. & Farrell, B.D. (2009) Beetles (Coleoptera). S.B. Hedges & S. Kumar (eds.), *The timetree of life* (pp. 278–289). Oxford University Press, Oxford.
- Meyer-Rochow, V. B. (2007). Glowworms: a review of *Arachnocampa* spp. and kin. *Luminescence: the Journal of Biological and Chemical Luminescence*, 22(3), 251-265.
- Moldovan, O. T. (2012). Beetles. In W.B. White, & D. C. Culver (eds.), *Encyclopedia of caves* (second edition, pp. 54-62). Elsevier-Academic Press, Amsterdam.

- Moldovan, O. T. (2018). An overview on the aquatic cave fauna. In O. T. Moldovan, L. Kováč, & S. Halse (eds.), *Cave ecology* (pp. 173-194). Springer, Cham.
- Moldovan, O. T., Jalzic, B., & Erichsen, E. G. I. L. (2004). Adaptation of the mouthparts in some subterranean Cholevinae (Coleoptera, Leiodidae). *Natura Croatica*, *13*(1), 1-18.
- Moldovan, O. T., Kováč, L., & Halse, S. (2018). *Cave ecology*. Springer, Basel.
- Moran, D., Softley, R., & Warrant, E. J. (2015). The energetic cost of vision and the evolution of eyeless Mexican cavefish. *Science Advances*, *1*(8), e1500363.
- Mynhardt, G. (2013). Declassifying myrmecophily in the Coleoptera to promote the study of ant-beetle symbioses. *Psyche*, *2013*, 696401.
- Nagel, P. (1979). Aspects of the evolution of myrmecophilous adaptations in Paussinae (Coleoptera, Carabidae). In P. J. Den Boer, H. U. Thiele, & F. Weber (eds.), *On the evolution of behaviour in carabid beetles*. (pp. 15–34). Landbouwhogeschool Wageningen, the Netherlands.
- Niemiller, M. L., Bichuette, M. E., Chakrabarty, P., Fenolio, D. B., Gluesenkamp, A. G., Soares, D., & Zhao, Y. (2019a). Cavefishes. In W. B. White, D. C. Culver, & T. Pipan (eds), *Encyclopedia of caves* (third edition, pp. 227-236). Elsevier-Academic Press, Amsterdam.
- Niemiller, M. L., Helf, K., & Toomey, R. S. (2021). Mammoth Cave: a hotspot of subterranean biodiversity in the United States. *Diversity*, *13*(8), 373.
- Niemiller, M. L., Taylor, S. J., Slay, M. E., & Hobbs III, H. H. (2019b). Biodiversity in the United States and Canada. In W. B. White, D. C. Culver, & T. Pipan (eds), *Encyclopedia of caves* (third edition, pp. 163-176). Elsevier-Academic Press, Amsterdam.
- Nitzu, E., & Juberthie, C. (1996). Changement dans l'équipement sensoriel des antennes et des palpes maxillaires en fonction de l'habitat chez les Coléoptères Clivininae (Scaritidae). *Mémoires de Biospéologie*, *23*, 91–102.
- Novak, T., Perc, M., Lipovšek, S., & Janžekovič, F. (2012). Duality of terrestrial subterranean fauna. *International Journal of Speleology*, *41*(2), 181-188.
- Packard, A. S. (1888). The cave fauna of North America, with remarks in the anatomy of brain and the origin of blind species. *Memoirs of the National Academy of Sciences*, *4*, 1–156.
- Parker, J. (2016). Myrmecophily in beetles (Coleoptera): evolutionary patterns and biological mechanisms. *Myrmecological News*, *22*, 65-108.

- Parmentier, T. (2020) Guests of Social Insects. In C. Starr (ed.), *Encyclopedia of social insects* (pp. 1-15). Springer, Cham.
- Peck, S. B. (1973). A systematic revision and the evolutionary biology of the *Ptomaphagus* (*Adelops*) beetles of North America (Coleoptera; Leiodidae, Catopinae), with emphasis on cave-inhabiting species. *Museum of Comparative Zoology Bulletin*, 145, 29-162.
- Peck, S. B. (1977). A review of the distribution and biology of the small carrion beetle, *Prionochoeta opaca* of North America. (Coleoptera; Leiodidae; Catopinae). *Psyche*, 84(3-4), 299-307.
- Peck, S. B., Kukalová-Peck, J., & Bordón, C. (1989). Beetles (Coleoptera) of an oil-bird cave: Cueva del Guácharo, Venezuela. *The Coleopterists' Bulletin*, 43(2), 151-156.
- Pellegrini, T. G., & Ferreira, R. L. (2011). *Coarazuphium tapiaguassu* (Coleoptera: Carabidae: Zuphiini), a new Brazilian troglobitic beetle, with ultrastructural analysis and ecological considerations. *Zootaxa*, 3116(1), 47-58.
- Plachetzki, D. C., Fong, C. R., & Oakley, T. H. (2012). Cnidocyte discharge is regulated by light and opsin-mediated phototransduction. *BMC Biology*, 10, 17.
- Pohl, H. (2010). A scanning electron microscopy specimen holder for viewing different angles of a single specimen. *Microscopy Research and Technique*, 73(12), 1073-1076.
- Polak, S. (2005). Importance of discovery of the first cave beetle *Leptodirus hochenwartii* Schmidt, 1832. *Endins*, 28, 71-80.
- Poulson, T. L. (1963). Cave adaptation in amblyopsid fishes. *American Midland Naturalist*, 70, 257-290.
- Poulson, T. L., & White, W. B. (1969). The cave environment. *Science*, 165(3897), 971-981.
- Protas, M. E., Trontelj, P., & Patel, N. H. (2011). Genetic basis of eye and pigment loss in the cave crustacean, *Asellus aquaticus*. *Proceedings of the National Academy of Sciences*, 108(14), 5702-5707.
- Protas, M., Conrad, M., Gross, J. B., Tabin, C., & Borowsky, R. (2007). Regressive evolution in the Mexican cave tetra, *Astyanax mexicanus*. *Current Biology*, 17(5), 452-454.

- Racoviță, G. (1976). La phénomène de migration chez les Coléoptères cavernicoles. *Travaux de l'Institut de Spéologie "Emil Racovitza", 15*, 103-111.
- Racovitza E. G. (1907). Essai sur les problèmes biospéologiques. *Archives de Zoologie Expérimentale et Générale, 6*, 371– 488.
- Reddell, J. R. (2019). Spiders and related groups. In W. B. White, D. C. Culver, & T. Pipan (eds.), *Encyclopedia of caves* (third edition, pp. 1018-1030). Elsevier-Academic Press, Amsterdam.
- Rétaux, S., & Casane, D. (2013). Evolution of eye development in the darkness of caves: adaptation, drift, or both? *EvoDevo, 4*(1), 1-12.
- Ribera, I., Fresneda, J., Bucur, R., Izquierdo, A., Vogler, A. P., Salgado, J. M., & Cieslak, A. (2010). Ancient origin of a Western Mediterranean radiation of subterranean beetles. *BMC Evolutionary Biology, 10*, 29.
- Roff, D. A. (1990). The evolution of flightlessness in insects. *Ecological Monographs, 60*(4), 389-421.
- Rohner, N., Jarosz, D. F., Kowalko, J. E., Yoshizawa, M., Jeffery, W. R., Borowsky, R. L., Lindquist, S., & Tabin, C. J. (2013). Cryptic variation in morphological evolution: HSP90 as a capacitor for loss of eyes in cavefish. *Science, 342*(6164), 1372-1375.
- Romero, A. (2009). *Cave biology: life in darkness*. Cambridge University Press, Cambridge.
- Rouch, R. (1977). Considérations sur l'écosystème karstique. *Comptes Rendus de l'Académie des Sciences, Paris, 284*, 1101–1103.
- Rowan, W. (1938). Light and seasonal reproduction in animals. *Biological Reviews, 13*(4), 374-401.
- Rusdea, E. (1994). Population dynamics of *Laemostenus schreibersi* (Carabidae) in a cave in Carinthia (Austria). In K. Desender, M. Dufrêne, M. Loreau, M.L. Luff & J.P Maelfait (eds.), *Carabid beetles: ecology and evolution* (pp. 207-212). Kluwer Academic Publishers, Dordrecht.
- Sánchez-Fernández, D., Rizzo, V., Cieslak, A., Faille, A., Fresneda, J., & Ribera, I. (2016). Thermal niche estimators and the capability of poor dispersal species to cope with climate change. *Scientific Reports, 6*(1), 1-8.
- Schiner, J. R. (1854). Fauna der Adelsberger- Lueger-und Magdalenen-Grotte. In A. Schmidl (ed.), *Grotten und Höhlen von Adelsberg, Lueg, Planina und Laas* (pp. 231-272). Braunmüller, Wien.

- Schiødte, J. C. (1849). Bidrag til den underjordiske Fauna. *Vidensk. Selsk. Skr.*, 5
Række naturvidenskabelig Og Mathematisk Afdeling, 2, 1–39.
- Schneeberg, K., Bauernfeind, R., & Pohl, H. (2017). Comparison of cleaning methods for delicate insect specimens for scanning electron microscopy. *Microscopy Research and Technique*, 80(11), 1199-1204.
- Simon, K. S. (2019). Cave ecosystems. In W. B. White, D. C. Culver, & T. Pipan (eds), *Encyclopedia of caves* (third edition, pp. 223-226). Elsevier-Academic Press, Amsterdam.
- Simon, K. S., Pipan, T., & Culver, D. C. (2007). A conceptual model of the flow and distribution of organic carbon in caves. *Journal of Cave and Karst Studies*, 69(2), 279-284
- Sket, B. (2004). Subterranean habitats. In J. Gunn (ed.), *Encyclopedia of cave and karst science* (pp. 1519-1523). Fitzroy Dearborn, New York.
- Sket, B. (2008). Can we agree on an ecological classification of subterranean animals?. *Journal of Natural History*, 42(21-22), 1549-1563.
- Slay, M. E., & Bitting, C. J. (2008). Is a mine a terrible thing to waste? Additional subterranean habitats for troglobitic fauna and other cavernicoles in the Ozarks. In W. R. Elliott (ed.), *Proceedings of the 2007 national cave and karst management symposium*, (pp. 89-95). St. Louis, USA.
- Tercafs, R., & Brouwir, C. (1991). Population size of Pyrenean troglobiont coleopters (*Speonomus* species) in a cave in Belgium. *International Journal of Speleology*, 20(1), 3.
- Thiele, H. U. (1977). *Carabid beetles in their environments: a study on habitat selection by adaptations in physiology and behaviour*. Springer, Berlin, Heidelberg, New York.
- Tian, M., Huang, S., & Wang, D. (2017). Discovery of a most remarkable cave-specialized trechine beetle from southern China (Coleoptera, Carabidae, Trechinae). *Zookeys*, 725, 37-47.
- Trontelj, P. (2012). Natural selection. In W.B. White, & D.C. Culver (eds.), *Encyclopedia of caves* (pp. 517-528). Elsevier-Academic Press, Amsterdam.
- Trontelj, P., Blejcek, A., & Fišer, C. (2012). Ecomorphological convergence of cave communities. *Evolution*, 66(12), 3852-3865.
- Ullrich-Lüter, E. M., Dupont, S., Arboleda, E., Hausen, H., & Arnone, M. I. (2011). Unique system of photoreceptors in sea urchin tube feet. *Proceedings of the National Academy of Sciences*, 108(20), 8367-8372.

- Vandel, A (1965). *Biospeleology: The biology of cavernicolous animals*. Pergamon Press, Oxford.
- Vergnon, R., Leijs, R., van Nes, E. H., & Scheffer, M. (2013). Repeated parallel evolution reveals limiting similarity in subterranean diving beetles. *The American Naturalist*, 182(1), 67-75.
- Viré, A. (1904). La biospéologie. *Comptes rendus de la Académie des Sciences du Paris*, 139, 826-828.
- Vittori, M., & Štrus, J. (2014). The integument in troglobitic and epigeal woodlice (Isopoda: Oniscidea): a comparative ultrastructural study. *Zoomorphology*, 133(4), 391-403.
- Vittori, M., Tušek-Žnidarič, M., & Štrus, J. (2017). Exoskeletal cuticle of cavernicolous and epigeal terrestrial isopods: a review and perspectives. *Arthropod Structure & Development*, 46(1), 96-107.
- v. Kéler, S. (1963). *Entomologisches Wörterbuch*. Akademie Verlag, Berlin.
- Ward, A., Liu, J., Feng, Z., & Xu, X. S. (2008). Light-sensitive neurons and channels mediate phototaxis in *C. elegans*. *Nature Neuroscience*, 11(8), 916-922.
- Watts, C. H. S., & Humphreys, W. F. (2009). Fourteen new Dytiscidae (Coleoptera) of the genera *Limbodessus* Guignot, *Paroster* Sharp, and *Exocelina* Broun from underground waters in Australia. *Transactions of the Royal Society of South Australia*, 133(1), 62-107.
- Wheeler, W. M. (1910). *Ants, their structure, development and behavior*, Columbia University Press, New York.
- White, W. B., & Culver, D. C. (2019). Cave, definition of. In W. B. White, D. C. Culver, & T. Pipan (eds), *Encyclopedia of caves* (third edition, pp. 255-259). Elsevier-Academic Press, Amsterdam.
- Wilson, E. O. (1962). The Trinidad cave ant *Erebomyrma* (= *Spelaeomyrmex*) *urichi* (Wheeler), with a comment on cavernicolous ants in general. *Psyche*, 69(2), 62-72.
- Wipfler, B., Machida, R., Müller, B., & Beutel, R. G. (2011). On the head morphology of Grylloblattodea (Insecta) and the systematic position of the order, with a new nomenclature for the head muscles of Dicondylia. *Systematic Entomology*, 36, 241–266.
- Wipfler, B., Pohl, H., Yavorskaya, M. I., & Beutel, R. G. (2016). A review of methods for analysing insect structures—the role of morphology in the age of phylogenomics. *Current Opinion in Insect Science*, 18, 60-68.

- Wong M.K.L., & Guénard B. (2017). Subterranean ants: summary and perspectives on field sampling methods, with notes on diversity and ecology (Hymenoptera: Formicidae). *Myrmecological News*, 25, 1-16
- Yamamoto, Y., & Jeffery, W. R. (2000). Central role for the lens in cave fish eye degeneration. *Science*, 289(5479), 631-633.
- Yamamoto, Y., Stock, D. W., & Jeffery, W. R. (2004). Hedgehog signalling controls eye degeneration in blind cavefish. *Nature*, 431(7010), 844-847.
- Yang, W. (1983). Xu Xiake's contribution to the study of karst caves in the ancient history of China. *Carsologica Sinica*, 2(2), 137-145.
- Yoshida, M. (1979). Extraocular photoreception. In H. Autrum (ed.) *Handbook of sensory physiology*, (pp. 581 –640). Springer, New York.
- Yoshizawa, M., Yamamoto, Y., O'Quin, K. E., & Jeffery, W. R. (2012). Evolution of an adaptive behavior and its sensory receptors promotes eye regression in blind cavefish. *BMC Biology*, 10(1), 1-16.

8 Appendixes

Supporting materials of Studies III (Luo et al. 2021a) and IV (Beutel et al. 2021) can be found on the official websites of the publications.

Study III: <https://onlinelibrary.wiley.com/doi/full/10.1002/jmor.21361>

Study IV: <https://arthropod-systematics.arphahub.com/article/68352/list/5/>

Studies V and VIII are unpublished, the materials can be found at:

<https://upload.unijena.de/data/61b7191a0005c8.69387260/Studies%20V%20and%20VIII-supporting%20information.zip>

Supporting materials of Studies II and VII are provided in the present section.

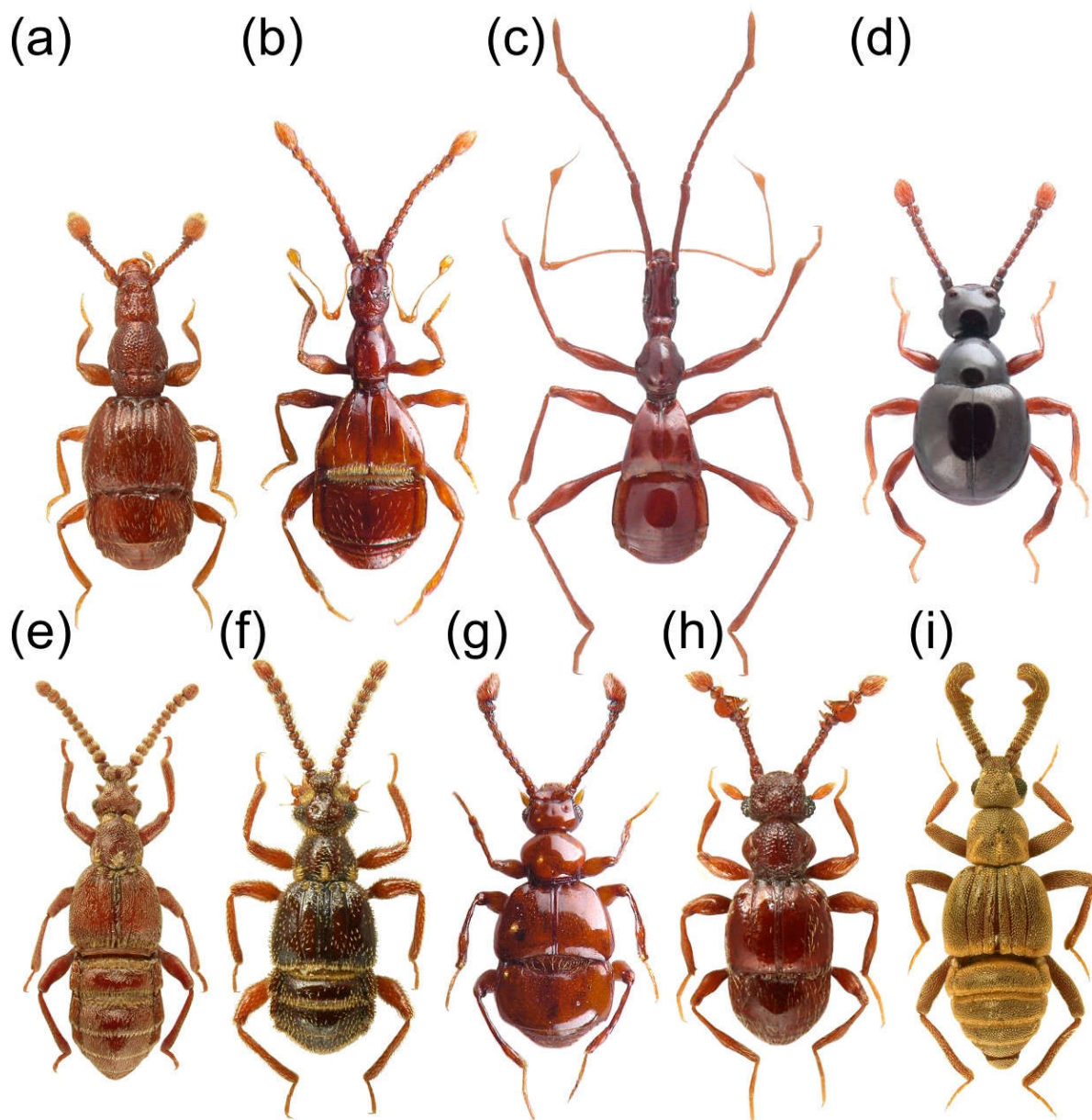


FIGURE S1 Diversity of non-Clavigeritae pselaphines; selected examples. (a) *Philoscotus longulus* Sawada (Japan); (b) *Pselaphogenius orientalis* Besuchet (Japan); (c) Pselaphini, genus indet. (New Caledonia); (d) *Eupines* sp. (New Caledonia); (e) *Chennium bituberculatum* Latreille (Ukraine); (f) *Centrotoma prodiga* Sharp (Japan); (g) *Batraxis splendida* Nomura (Jeannel); (h) *Trisinus galloisi* (Jeannel) (Japan); (i) *Apharinodes papageno* Nomura (Japan).

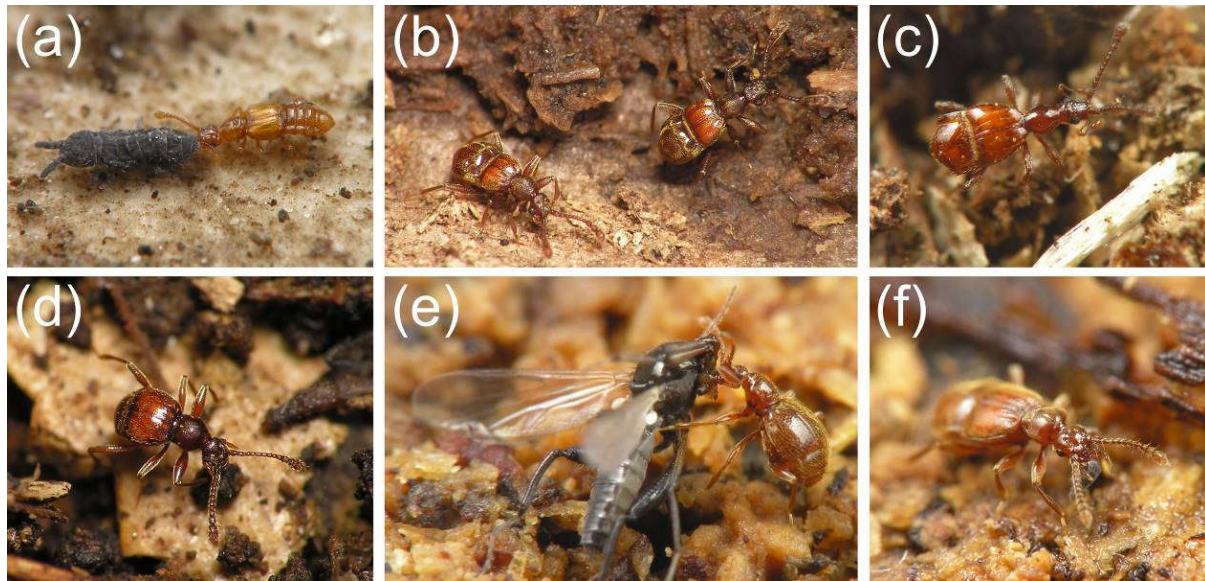


FIGURE S2 Diversity of non-Clavigeritae pselaphines; living beetles. (a) *Euplectus* sp. (Poland) attacking a springtail; (b) *Raphitreus speratus* (Sharp) (Japan); (c) *Pselaphus heisei* Herbst (Poland); (d) *Triomicrus* sp. (Japan); (e) *Briaxis* sp. (Poland) feeding on a dead fly; (f) *Trichonyx sulcicollis* (Reichenbach) (Poland), feeding on springtail.

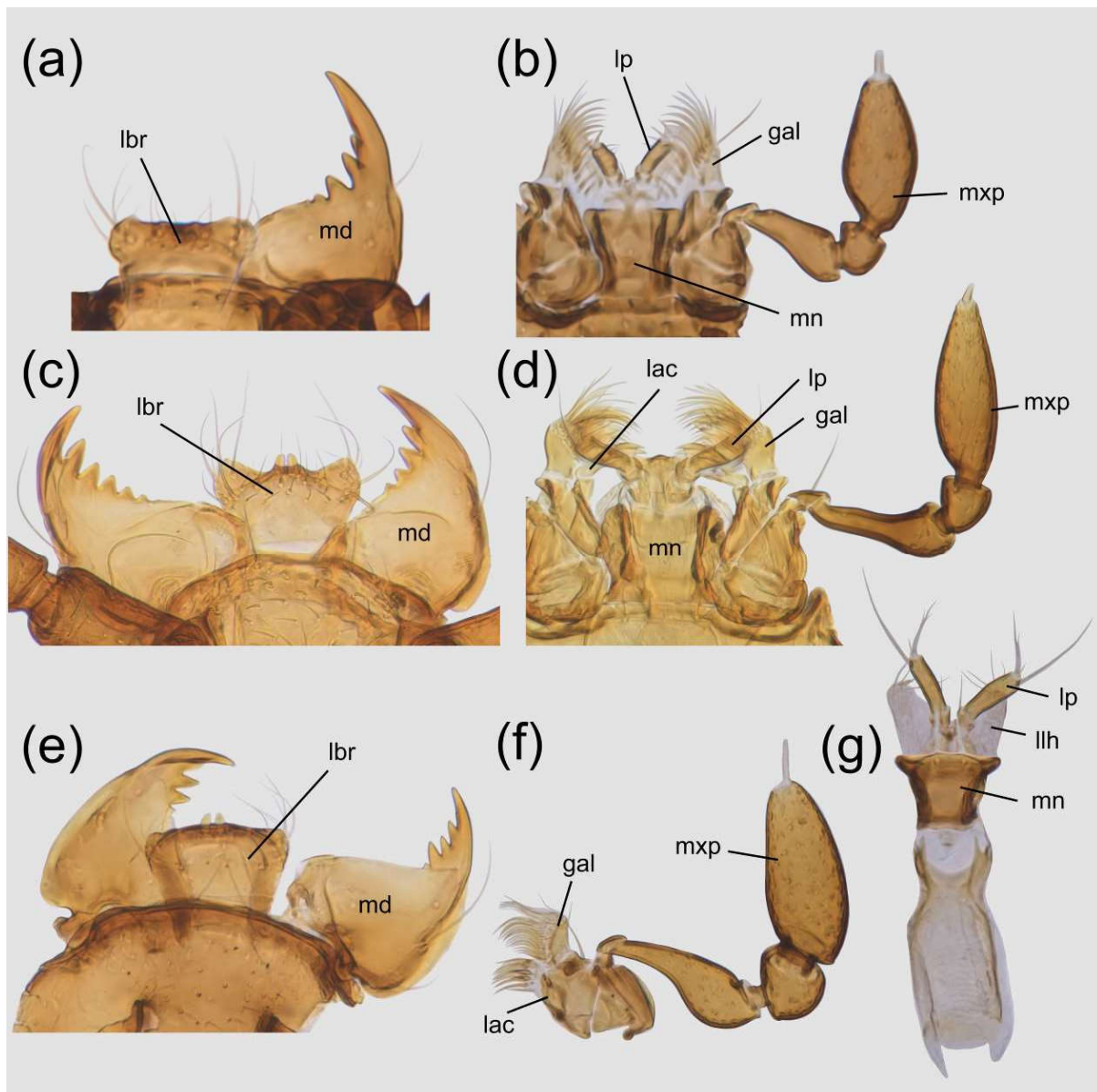


FIGURE S3 Examples of dissected mouthparts in free-living European pselaphines. (a, b) *Euplectus karstenii* (Reichenbach); (c, d) *Trichonyx sulcicollis* (Reichenbach); (e–g) *Brachygluta fossulata* (Reichenbach). Abbreviations: gal, galea; lac, lacinia; lbr, labrum; llh, lateral lobe of hypopharynx; lp, labial palp; md, mandible; mn, mentum; mxp, maxillary palp.

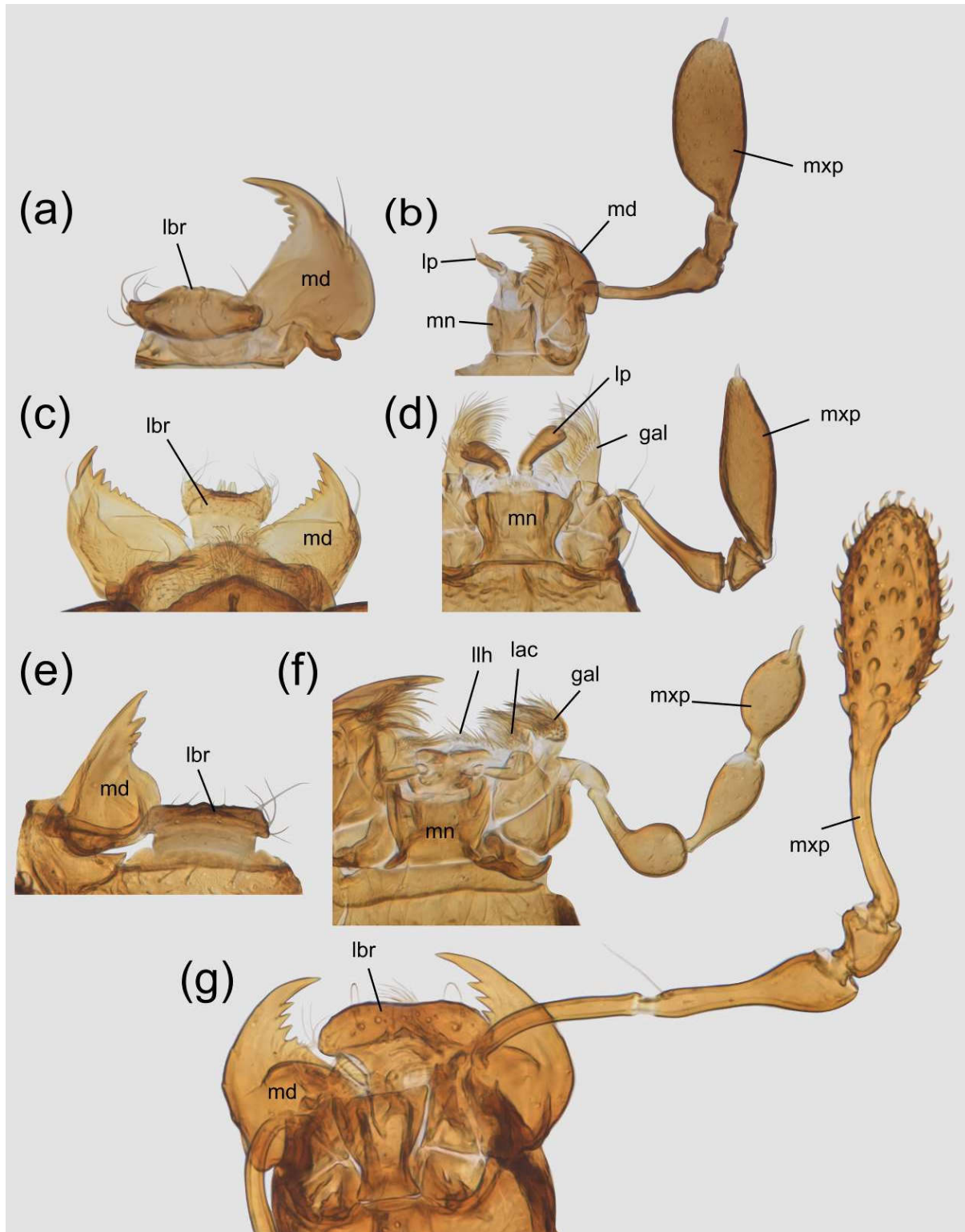


FIGURE S4 Examples of dissected mouthparts in free-living European pselaphines. (a, b) *Bryaxis bulbifer* (Reichenbach); (c, d) *Batrisodes venustus* (Reichenbach); (e–f) *Tyrus mucronatus* (Panzer); (g) *Pselaphus heisei* Herbst. Abbreviations: gal, galea; lac, lacinia; lbr, labrum; llh, lateral lobe of hypopharynx; lp, labial palp; md, mandible; mn, mentum; mxp, maxillary palp.

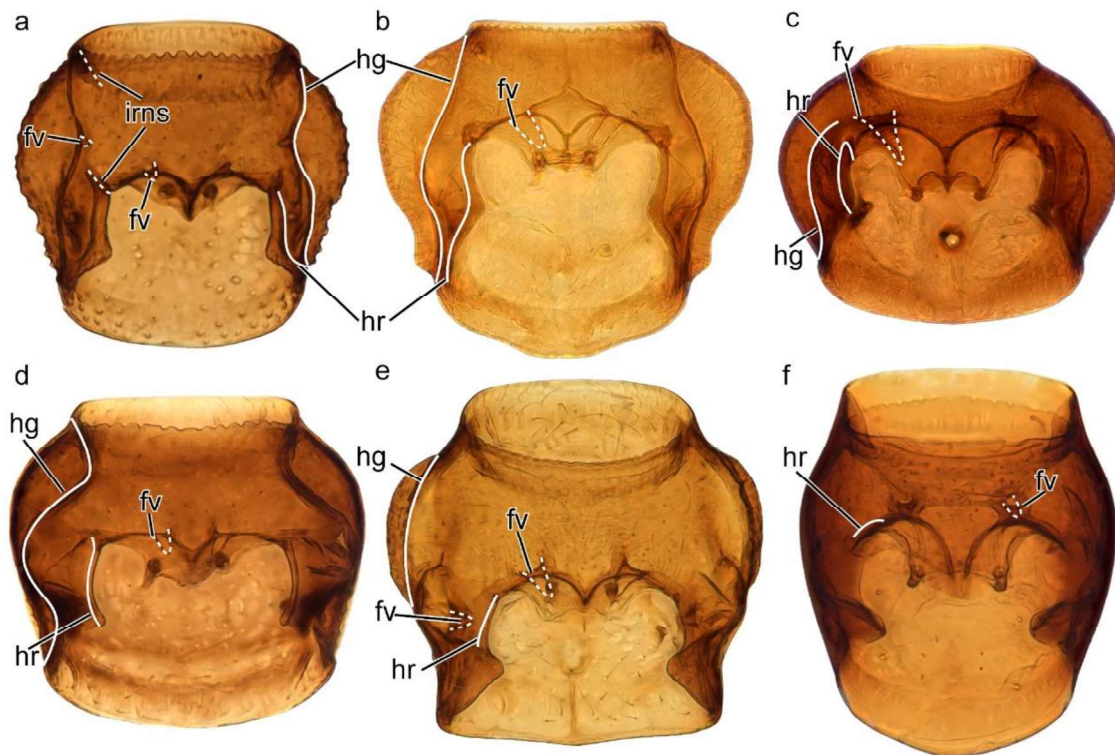


Fig. S1. Prothorax in ventral view of (a) *Euplectus karstenii* (Euplectitae: Euplectini); (b) *Trichonyx sulcicollis* (Euplectitae: Trichonychini); (c) *Brachyglura fossulata* (Goniaceritae: Brachyglutini); (d) *Bryaxis bulbifer* (Goniaceritae: Bythinini); (e) *Batrisodes venustus* (Batrisitae: Batrisini); (f) *Pselaphus heisei* (Pselaphitae: Pselaphini). Abbreviations: fv, fovea; hg, hypomeral groove; hr, hypomeral ridge; irns, internalized rudiments of notosternal suture.

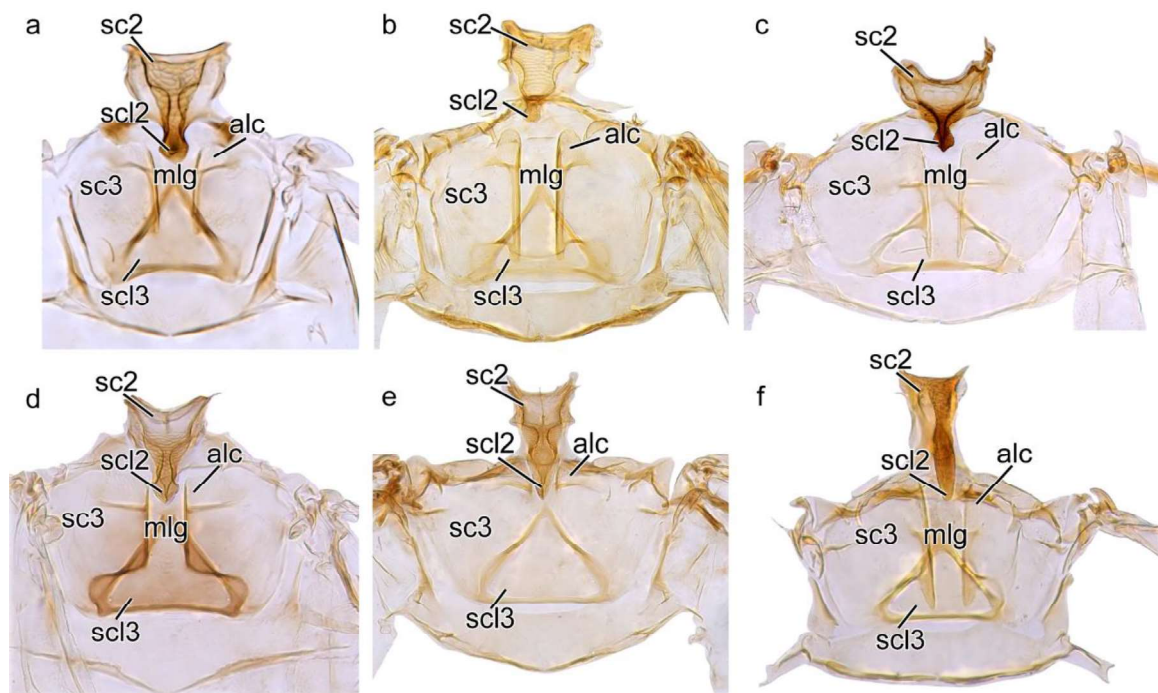


Fig. S2. Pterothorax in dorsal view of (a)-(f) (species order are same as Fig. S1).
Abbreviations: alc, alacrista; mlg, median longitudinal groove; sc2/3, meso-/metascutum; scl2/3, meso-/metascutellum.

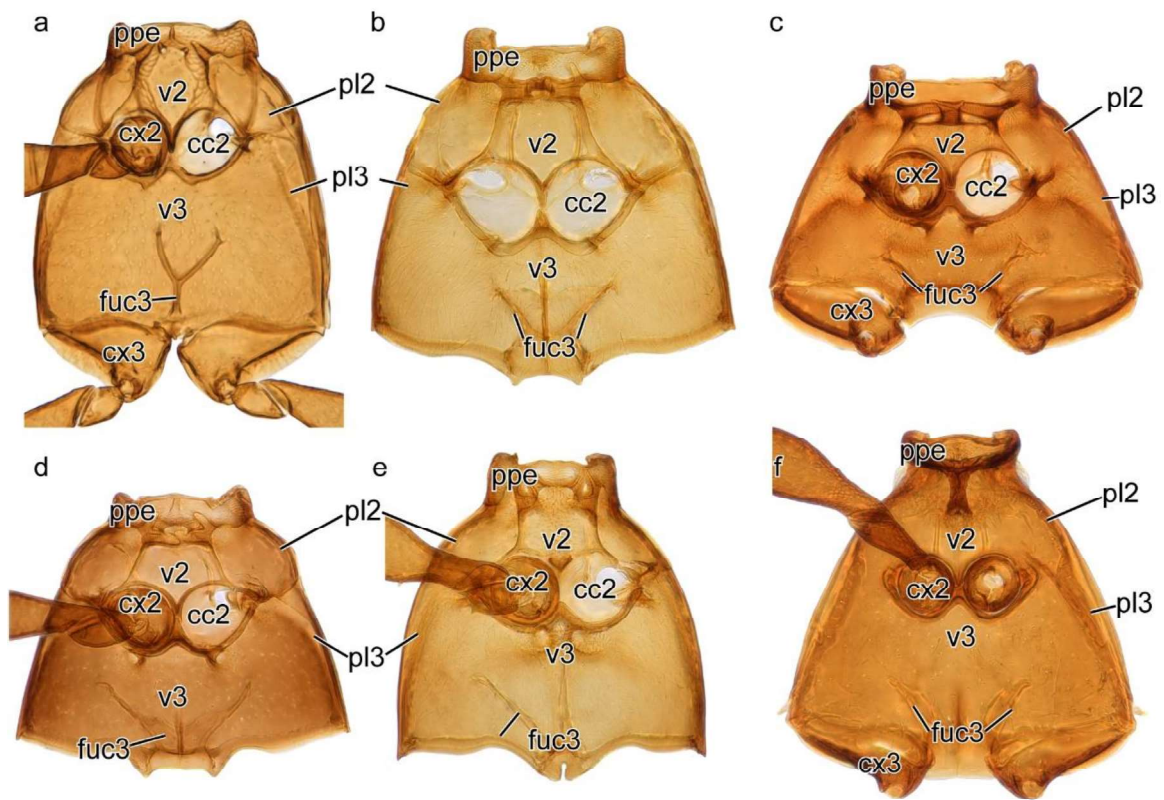


Fig. S3. Pterothorax in ventral view of species (a)-(f) (species order are same as Fig. S1). Abbreviations: cc2, meso-metacoxal cavity; cx2/3, meso-/metacoxa; fu3, metafurca; pl2/3, meso-/metapleuron; ppe, prepectus.

9 Acknowledgements

It is finally the time to express my gratitude to the enormous kindnesses I received in the last four years.

First and foremost, I would like to say “Thank you” to my supervisors Prof. Dr. Rolf Beutel (FSU, Jena) and Dr. Ignacio Ribera (IBE, Barcelona). Both of them are wise, hard-working, warm-hearted, humble, generous, serious in the labs and humorous in the bars. As a result, the thought of “How lucky I have been to have you two together on my side?” has jumped into my head more than once.

Vielen Dank, Rolf. Thank you for agreeing to supervise my PhD thesis back in 2017 and stay at the position till the very end. You are like a magic magnet, and your charisma and personality obviously attracted many talented and passionate people to our attic. It must have been tough for you to accept and tolerant my countless weaknesses, thank you for holding up there. Thanks for coming to talk to me that often and keeping your office door always open to me. I have to admit that I felt nervous every time when I received your comments of my manuscript, because I knew it will end up be very colorful with all your efforts. Anyway, I appreciate all the training I got in the research group, which has helped me to become a better researcher. Aside from being the most important advisor of my academic career, thank you for sharing many memorable moments outside of the lab with me. Our trip to Erzgebirge, many lovely evenings at Grünowski, and the way you laugh will not be forgettable as well.

Muchas gracias, Ignacio. Thank for you providing the chance to me to visit your lab. I truly wished I could write “this dissertation is dedicated to late Dr. Ignacio Ribera” in this section, but I had realized that you might expect some work with better quality. I will try to work on the projects you have left us, and probably get more meaningful job done. By the way, some e-mails you sent me are still starred, and sometimes I like to read through them and see what I could do in the future. The tragedy of losing you indeed leaded me to a very deep cave, and I did not successfully adapt to that darkness like our cave-dwelling beetles. However, more than just “fortunately”, Rolf and Beny chose to intervene and later bear the burden of my troubles, which they apparently did not have to. I doubt they were doing this for keeping themselves fit, since Rolf does weigh-lifting regularly and Beny’s shoulders are often occupied by Leo and Freddy.

Merci, Beny. Thanks for supporting me both scientifically and non-scientifically. Even though we did not see each other that often, I am very grateful to the fact that I could ask for help when I was in trouble and share my ups and downs when

I visited Bonn. The irreplaceable support you have provided during my PhD study is definitely more than what a colleague would have done. I appreciate that.

The present dissertation could not be completed without our collaborators from different institutions: Dr. Paweł Jałoszyński, Dr. Caio Antunes-Carvalho, Dr Arnaud Faille, Dr. Mariam Gabelaia, Peter Hlaváč, Javier Fresnada. Thank you for your valuable help. I have learned a lot from you and would like to work with you more often. Many thanks also to all the researchers listed in the literature references, who collected the beetles, conducted the experiments, wrote the excellent papers. It was a pleasure to share the passion with you.

The colleagues at Phyletisches Museum have made the work atmosphere very pleasant and homelike. PD Dr. Hans Pohl guided me to our laboratory facilities and has always been helpful when there were technical issues. I would also like to extend thanks to Adrian, Kenny, Daniel, Margarita, Michael, Brendon, Noriko, Bernd, and Sabrina who shared the roof with me. The two short stays at the lab of water and cave beetles (IBE) in Barcelona gave the chance to know some warmhearted and lovely researchers: Adrián, Pau, Alfonso, Lídia, Mattia, Leo, Héctor, Anabela and other colleagues. During my stays in Bonn, Juliane was always very kind and helpful, thank you for your help.

It is also worthwhile to note that sport has made some essential and positive influences in the last four years. I had lots of good experience in Jena with the trainers and players from the Hochschulsport courses. Many thanks to everyone who helped me to improve my German and English language skills, especially Milano, the Augsburgger who is living in the Netherlands, who kindly corrected my grammar, enriched my vocabulary, and shared funny things with a stranger.

Besides, I would like to thank my family and friends back in China. It was a pity that sometimes I could only share my joy with you by modern communication technology, but it truly helped the interaction. I am so glad that the distance of 8000 kilometers has not weakened but even strengthened our connection. I want to express special gratitude to my late grandpa, who was my best friend for the first 22 years in my life. He has been and will always be my “Kraftquelle”.

Thanks to China Scholar Council, which awarded me the scholarship (No. 201708440281) for my PhD study.

I know I say “Thank you” a lot, but I mean it every time. It was fun, thanks for your companionship.

10 Curriculum Vitae

[This part intentionally left blank]

11 Ehrenwörtliche Erklärung

Ich erkläre hiermit, dass mir die Promotionsordnung der Fakultät für Biowissenschaften der Friedrich-Schiller-Universität bekannt ist. Die vorliegende Dissertationsschrift wurde selbstständig, ohne die Hilfe Dritter und ohne Benutzung anderer als der angegebenen Hilfsmittel angefertigt. Die aus anderen Quellen direkt oder indirekt übernommenen Daten und Konzepte sind unter Angabe der Quellen gekennzeichnet. Alle Personen die Beiträge zum Material, zur Auswertung dieses oder zur Herstellung der Manuskripte geleistet haben sind jeweils als Autoren aufgeführt:

Prof. Dr. Rolf G. Beutel¹, Dr. Ignacio Ribera², Dr. Benjamin Wipfler³, Dr. Paweł Jałoszyński⁴, Dr. Caio Antunes-Carvalho⁵, Dr. Mariam Gabelaia³, Dr. Arnaud Faille⁶, Dr. Alexander Stoessel^{1, 7}, Dr. Margarita I. Yavorskaya⁸, Peter Hlaváč⁹

¹ Institut für Zoologie und Evolutionsforschung, Friedrich-Schiller-Universität Jena

² Institute of Evolutionary Biology (CSIC-Universitat Pompeu Fabra)

³ Zoologisches Forschungsmuseum Alexander Koenig

⁴ Museum of Natural History, University of Wrocław

⁵ Departamento de Biologia Geral, Instituto de Biologia, Universidade Federal Fluminense

⁶ Department of Entomology, Stuttgart State Museum of Natural History

⁷ Department of Archaeogenetics, Max Planck Institute for the Science of Human History

⁸ Institut für Evolution und Ökologie, Universität Tübingen

⁹ Department of Entomology, National Museum, Natural History Museum, Prague

Die Hilfe des Promotionsberaters wurde nicht in Anspruch genommen und es wurden Dritten weder mittelbar noch unmittelbar durch geldwerte Leistungen für Arbeiten entlohnt die im Zusammenhang mit dem Inhalt dieser Dissertation stehen. Die Dissertationsschrift wurde nicht bereits zuvor als Prüfungsarbeit für eine Staatliche oder andere wissenschaftliche Prüfung eingereicht.

Ort, Datum: _____

Signatur: _____